Proceedings
of the
6th American
Water Jet Conference

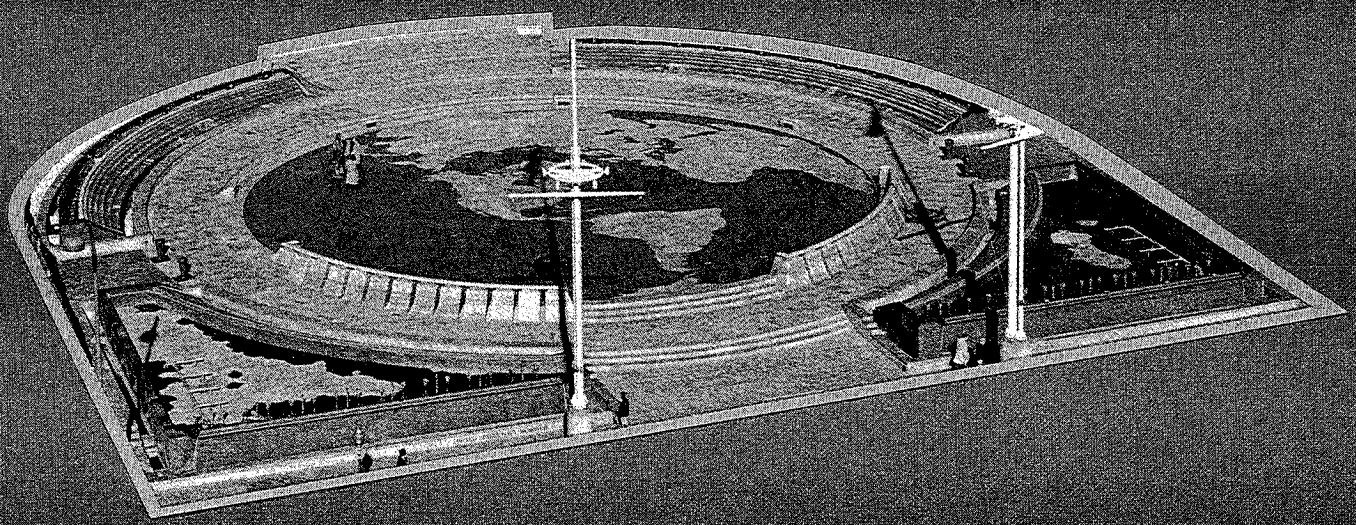

August 24-27, 1991

Houston, Texas

Edited by Thomas J. Labus

Proceedings
of the
6th American
Water Jet Conference

August 24-27, 1991
Houston, Texas

Edited by

Thomas J. Labus

Published by the

Water Jet Technology Association

The editors, sponsors or the organizers are not responsible for statements or opinions made in the papers printed in this proceedings.

Cover Photograph: Naval War Memorial located in Washington, D.C. The globe on the granite floor of the memorial was carved using water jets.

ISBN 1-880342-00-6

Copies obtainable from:

Water Jet Technology Association
818 Olive Street – Suite 918
St. Louis, MO 63101
USA
Telephone: (314)241-1445
Fax: (314)241-1449

Price: $90.00 (payable in advance)

FOREWORD

Water jet technology is undergoing rapid growth. A myriad of materials are cut routinely by jets, including paper products, textiles, building materials, rubber, fiberglass, plastics, composites, food, metal, ceramics, glass, and rocks. This list expands daily as people apply the unique properties of fluid jets to industrial problems.

I am confident that many new applications for fluid jet cutting will be discovered. The world of jet cutting is very young and, thus, has all the vigor, enthusiasm, and potential of youth.

The Water Jet Technology Association proudly presents these proceedings with the expectation that they will convey to the reader a sense of the power and potential of water jet technology.

GEORGE A. SAVANICK
President
Water Jet Technology Association

The success of this conference can be attributed to the cooperative efforts of people dedicated to sharing their knowledge and information in fluid jet technology. I would like to express my thanks to the members of the Organizing Committee for their valuable suggestions, and to A. Conn for organizing the Contractors Session. The international participation is due in no small part to the efforts of the international advisors, and in particular M. Vijay. My thanks go to the authors for their efforts in sharing their knowledge in the written papers and oral presentations, and to the session chairmen for the smooth running of the sessions. The firms which exhibited and participated in the technical tours deserve recognition for their willingness to support the technology and share their knowledge. **Supporters** of this conference deserve special acknowledgement of their continued commitment to fluid jet technology.

Many people at D. Birenbaum & Associates contributed to the organization and detailed running of the conference. I would personally like to thank Ms. L. Hampton for her efforts especially in the publication of these *Proceedings*. Fruitful discussions with M. Birenbaum provided direction and focus for specific areas in this and future meetings.

A willingness to share information is at the heart of this conference, and is essential to the future growth of the technology.

T.J. LABUS
Editor & Conference Chairperson

ORGANIZING COMMITTEE

Thomas J. Labus (Chairperson)
Scire Corporation
Fontana, WI

Andrew F. Conn
Conn Consulting, Inc.
Baltimore, MD

Dr. Mohamed Hashish
Quest Integrated, Inc.
Kent, WA

George Rankin
Aqua-Dyne, Inc.
Houston, TX

Dr. George Savanick
Bureau of Mines
Minneapolis, MN

Damon C. Schroter
Ingersoll-Rand Company
Baxter Springs, KS

Forrest Shook
NLB Corporation
Wixom, MI

Evette Steele
Supreme Technologies, Inc.
Lebanon, OH

Dr. David Summers
University of Missouri-Rolla
Rolla, MO

Dr. Mohan Vijay
Institute of Mechanical Engineering
Ottawa, Ontario

Dr. Fun-Den Wang
Colorado School of Mining
Golden, CO

John Wolgamott
StoneAge, Inc.
Durango, CO

INTERNATIONAL ADVISORS

Australia:	*John Link* Melbourne, Victoria
Austria:	*Dr. -Ing. H. Peters* Ternitz, Austria
China:	*Dr. Cheng Dazhong* Xuzhou, Jiangsu
Czechoslovakia:	*Dr. J. Noskievic* Ostrava, Czechoslovakia
England:	*D.H. Saunder* Bedford, England
France:	*Dr. E. Deliac* Pau Cedex, France
Germany:	*Hans P. Rink* Talheim, Federal Republic of Germany
Hungary:	*Dr. S. Toth* Debrecen, Hungary
India:	*M.F. Engineer* Bombay, India
Italy:	*Prof. Dr. Ing. R. Ciccu* Cagliari, Italy
Japan:	*Hiroshi Sugino* Toyoma, Japan
Malaysia:	*Mohamad Aslan* Kuala Lumpur, Malaysia
New Zealand:	*M.J. Simpson* Christchurch, New Zealand
Poland:	*Dr. Eng. A. Kalukiewicz* Krakow, Poland
Singapore:	*Dr. J.S.T. Cheung* Singapore, Republic of Singapore
Sweden:	*B. Grinndal* Stockholm, Sweden
U.S.S.R.	*Dr. G.A. Atanov* Donetsk, U.S.S.R

TABLE OF CONTENTS

Session V: High Pressure Equipment and Systems

Pages

Session VI: Abrasive Jets - Fluid Mechanics and Nozzle Design

Session VII: Construction, Non-Manufacturing Applications

Session VIII: Novel Jets and Applications - I

Session IX: Novel Jets and Applications - II

Pages

Session X: Direct Pumping of Abrasive Suspension Jets: Basics and Applications

Contractors Session

Poster Session

Supported by

Aqua-Dyne Inc., Houston, Texas, USA

Dowell-Schlumberger, Houston, Texas, USA

Flow International Corp., Kent Washington, USA

International Society of Water Jet Technology, Ottawa, Canada

Toyo Glass Machinery Co., Ltd., Yokohama, Japan

6th American Water Jet Conference
August 24 - 27, 1991: Houston, Texas

PHOTOELASTIC INVESTIGATION OF JET PIERCING PROCESS

M. Ramulu, H. Yeh, K.P. Wong, S.P. Raju

Department of Mechanical Engineering, FU-10
University of Washington
Seattle, WA 98195

ABSTRACT

An experimental investigation was conducted to study the material removal in pure water and abrasive water-jet piercing process in a birefringent polymer material. A two dimensional dynamic photoelasticity method was utilized to record the photoelastic stress patterns associated with jet piercing and identify the jet-material interfacial stress field. A comparative study of material removal mechanisms with pure waterjet and abrasive waterjet impacting and piercing showed that the waterjet contributes to the macro-cracking and scooping action of the material whereas an abrasive waterjet contributes to micro-crack nucleation, and micro-machining followed by erosion.

Organized and Sponsored by the Water Jet Technology Association.

1.0 INTRODUCTION

Waterjets have been widely used in a variety of industrial and mining applications which include cutting of rock, concrete, wood, plastics, and coal. Recently waterjets have emerged as a novel tool to fiber-reinforced composites machining, food processing and in medicine and surgery. The process of waterjet cutting involves accelerating water to very high velocities and aiming a collimated jet at the target. An abrasive waterjet on the other hand has abrasive particles entrained in a high pressure fluid which act as random point-chipping tools upon impacting the target material. A considerable amount of research has been reported in the literature on pure and abrasive waterjet impacting and cutting. See for example, Bowden & Brunton[1961], Brunton[1960], Daniel et al[1974], and Hashish[1988]. But very few studies relating to the material removal mechanism or the material failure process during the jet impingement process have been found to date.. The exact roles played by the individual phases of the eroding medium is also yet unknown. The present study utilizes a two dimensional photoelastic method to investigate the jet piercing by pure and abrasive waterjets. An attempt is also made to study the material behavior and the stress associated with the jet penetration process due to the impact of a pure and abrasive waterjet and their roles in material removal is discussed.

2.0 Experimental Setup and Procedure

High pressure abrasive waterjet system utilized in the present study consists of a powerjet model 20 -35 high pressure abrasive waterjet system, an abrasive waterjet nozzle, a hopper to transfer the abrasive and a workpiece assembly to hold the machinable specimens. The high pressure waterjet system used in our experiments was capable of generating pressures upto 240 MPa, at an exit water flow rate of 2.50 liters/min. The high pressure hose from the system is connected to an abrasive waterjet nozzle which has a 0.33 mm jewel orifice and a 1.16 mm diameter carbide nozzle. The abrasive waterjet table was used to accommodate the circular polariscope with minimal obstruction. Glass sheets placed upright on the top of table acted as shields to protect the polariscope from being damaged by the splashing abrasive particles. A 100 mm dia circular polariscope mounted on the boom of the waterjet pedestal facilitated the capturing of the isochromatic fringe patterns. A light field setting was used throughout the experiments. An annealed sheet of polycarbonate, 3.2 mm thick sandwiched and epoxied between two sheets of plexiglass is used as a 2-dimensional photoelastic model in our analysis. Experiments were performed on two types of specimens viz., notched and unnotched. A high speed photographic system was configured to enable the capture of the rapidly changing stress fields accompanying the changes in the depth in the jet piercing process. Figure 1 shows the overview of the experimental setup and the high speed photographic system used in the investigation is shown schematically in figure 2 Details of the experimental setup and high speed camera system can be found in Wong[1991].

Dynamic photoelastic experiments were conducted on both notched and unnotched specimens for various supply pressures, with and without abrasives, and the photoelastic fringe patterns were recorded for a jet exposure time of 1 second. From the photoelastic record at the base of the pierced holes, the variation of the depth of cut with time was evaluated. The largest fringe order was obtained through a numerical extrapolation from a semi-log plot of the radius of the fringe vs the fringe order and the maximum shear stress at the impact zone was ascertained using the stress-optic law. A comparative study of the type of crack nucleation phenomenon involved, and the nature of stress field induced in the presence of a notch and without a notch was made. Scanning electron microscopy was utilized not only to assess damage which may have occurred during the abrasive waterjet drilling process but also used to examine the material removal mechanism involved in the piercing process.

3.0 Results and Discussion

3.1 Pure Waterjet

Figures 3(a) to 5(a) show the typical dynamic photoelastic fringe pattern associated with the impingement of a pure waterjet on the unnotched workpiece material for varying supply pressures. Waterjet-upon-impact generated dilatational waves and its influence can be seen in the first frame of each experiment as ill-defined semi-circle gray fringes and these influences disappeared in the rest of the frames. The magnitude of the maximum shear stress developed in the vicinity of impact zone depends on the value of the supply pressure used. The high state of stress generated at the impact zone resulted in immediate jet penetration, cratering and macro-cracking in the workpiece material. Continued flow of the jet produced quasi-static pressurization of the initial crater and this resulted in the opening of the cracks and in the enlargement of craters. Examination of the photoelastic record shows that crack extension and opening is accompanied by a pressure relief around the crater. A high supply pressure of 240 MPa produced sharper cracks and the growth rate of these cracks was higher under high supply pressure conditions.

The results for the case of a very low pressure, however showed some interesting features. For a pressure of 110 MPa, the jet didn't penetrate into the material but an extremely shallow crater was observed on the surface. As soon as jet impacts the material, there is only a normal pressure due to the fluid, in action and as time proceeds a quasi-static pressure distribution due to the spreading of the jet is observed. The stress field generated in the material is due to a shear force resulting in a typical shear stress fringe pattern as depicted in the figure 5(a) at a jet exposure time of 0.875 seconds. The photoelastic records associated with a notched specimen of radius of curvature varying from 0.98 to 1.2 mm are shown in figures 3(b) to 5(b) for various supply pressures. As observed before, the cracking was always associated with a high supply pressure but however with a difference. The presence of a notch combined with applied jet pressure generated a state of stress that was most conducive for crack initiation and propagation due to a high stress concentration at the notch. This high stress concentration resulted in multiple macro-crack generation and penetration of the jet. As the jet flow continued the crack opening became longer and the cracks coalesced in comparison with unnotched specimens. Unlike the previous case of unnotched specimens, the stress fields associated with cracks were initially under a tension mode and changed to a mixed mode (i.e. tension and shear) loading condition later. However when the crack growth decreased or was arrested, the stress field associated with these cracks was always a pure shear or mode II stress as can be seen in figure 4(b). There was neither jet penetration nor cracking observed at low pressures even in presence of a notch. This leads one to conclude that there exists a threshold pressure below which there is no effect of the pure waterjet on the material and this is in accordance with the findings of other investigators. This feature was true for both notched and unnotched specimens. However at high pressures, cratering and material removal mechanisms involves the process of macro-cracking and scooping of the material from within the inside resulting in a wider crater with time.

Figures 6 and 7 shows the depth of penetration and maximum shear stress with respect to time corresponding to the photoelastic records shown in figures 3 to 5. As expected we find that the stress field decays with the penetration depth of the jet. The crater depth was almost 1 to 1.5 times the jet diameters. The maximum shear stress fields associated with notched specimens were higher than the unnotched specimens in spite of the existence of multiple cracks. The crater depth increased with the supply pressure as well as the jet exposure time.

3.2 Abrasive Waterjet

Figure 8 shows the typical photoelastic records of the dynamic fringe pattern of abrasive waterjet recorded in unnotched specimens using abrasive garnet of size #80, at a flow rate 5 g/s under a supply pressure of 240 MPa. Photoelastic records shown in Figures 9(a) and (b) were generated using notched and unnotched specimens. Abrasive garnet of size #50, at a flow rate 11 g/s, under the jet pressure of 110 MPa was used. Abrasive waterjet in both these cases produced almost immediate penetration and material removal in the polycarbonate workpiece. At the onset of impact, in all cases one observes an initial crack which is akin to the one observed in a pure waterjet impact process. These showed initial cracks are due to a pure water impact during the initial stages of the process. With the lapse of time however, the oncoming abrasive waterjet stream upon impact causes simultaneous fracture and erosion of the specimen, as a result of which the initial crack gets chipped and forms into a conical hole. Figure 10 shows the change in the penetration depth with the jet exposure time. The depth of penetration was clearly a function of the supplied pressure, the abrasive size and its flow rate. Maximum shear stress associated with jet piercing was not calculated due to localized and unchanging stress fields, because the abrasive waterjet impact time was extremely short and also because there was a quick release of stress due to cracking followed by erosion. Unlike waterjet, the abrasive waterjet process operates on a microscopic level and hence a scanning electron microscope was used to examine the pierced holes.

Pierced holes in polycarbonate specimen were sectioned with standard fly cutting techniques on a milling table, and polished with a rouge polishing compound. The cross-section was then coated with a thin film of gold-paladium (sputtered) prior to examination under a scanning electron microscope (SEM). Typical SEM micrographs of a hole pierced at 240 MPa with #80, and #50 garnet sizes and at an abrasive flow rate of 5.5 g/s and 30.78 g/s respectively are shown in figures 11(a) and (b). SEM revealed numerous microcracks at the bottom of the sectioned holes. No plastic deformation was observed on the damaged surfaces indicating a highly localized material removal process at a very rapid rate and therefore the loading stress was not transferred to the entire specimen. Material removal is a result of the continual bombardment and invasive penetration of the abrasive particles on the material surface creating microcracks. At the bottom of both the holes, numerous cracks averaging about a quarter of the nominal impacting abrasive size (~180 μm) were observed. Aided by pressurized water entering the cracks, which caused hydrowedging, Mazurkiewicz[1978], the incoming abrasive particles shattered the crack-weakened surfaces. Material was thus removed and the process repeated itself. Plowing marks, similar to those reported by Hutchings [1979], were also observed in the bored holes. The highly localized brittle cracked zone could explain the fact that no residual stresses were observed after the material was machined. The ability of abrasive waterjet to produce extremely localized microcracks in brittle material, during the material removal process would explain why abrasive waterjets can contour-cut very brittle materials like annealed glass.

4.0 CONCLUSIONS

1. The photoelastic method was successfully utilized to study the stress field associated with the pure and abrasive waterjet impacting and piercing process.

2. Pure waterjets exhibited macro-cracks and the cutting action was uneven compared to the abrasive waterjet. Abrasive waterjets are hence very efficient because the abrasive particles and the fluid medium provide the necessary activation energy to bring about microcracking and these particles act alongside with the fluid particles in eroding the surface.

3. The operating stresses involved in the abrasive waterjet piercing process were found to be highly localized and no residual stresses were found on the polycarbonate material.

4. SEM examination of the cross-sectional profile of abrasive waterjet pierced specimens revealed microcracks at the bottom of the holes. This suggests that the incessant bombardment of abrasive waterjet created crack nucleation sites with crack growth abetted by the hydro-wedging action of the incoming jet. Microcrack weakening of the jet-material interface precedes material removal.

5.0 Acknowledgements

We sincerely appreciate the financial support of the National Science Foundation through the Presidential Young Investigators Award, Grant Number MSS-895864.

6.0 References

1. Bowden, F. P., and Brunton, J. H., "The Deformation of Solids by Liquid Impact at Supersonic Speeds", Proceedings of the Royal Society of London, A 263, pp 433-450, Oct. 1961.

2. Brunton, J. H., "The High Speed Photography of Liquid/Solid Impact", Proceedings of the Fifth International Congress on High Speed Photography, Paper N-3, Washington D. C., USA, Oct. 22nd, 1960.

3. Daniel, I. M., Rowlands, R. E., Labus, T. J., "Photoelastic Study of Water Jet Impact", Proceedings of the Second International Symposium on Jet Cutting Technology, Paper A1, Cambridge, England, Apr. 2nd-4th, 1974.

4. Hashish, M.,"Visualization of the Abrasive Waterjet Cutting Process", Experimental Mechanics, Vol. 28, N. 2, pp 159-169, 1988.

5. Hutchings, I.M., "Mechanism of the Erosion of Metals by Solid Particles", Erosion: Prevention and Useful Application, ASTM STP 664, W.F. Alder,Ed., American Society for Testing and Materials, pp 59-76, 1979.

6. Li, H. Y., Geskin, E. S., Chen, W. L., "Investigation of Forces Exerted by an Abrasive Water Jet on a Workpiece", Proceedings of the Fifth American Water Jet Conference, Toronto, Canada, pp 69-77, Aug. 29th-31st, 1989.

7. Mazurkiewicz, M., Sebastian, Z., Galecki, G., "Analysis of the Mechanism of Interaction between High-Pressure Water Jet and the Material being cut", Proceedings of the Fourth International Symposium on Jet Cutting Technology, Canterbury, England, Apr. 12th-14th, 1978.

8. Ramulu, M., Wong, K.P., "Preliminary Investigation of Abrasive Waterjet Piercing Process by Dynamic Photoelasticity", International Journal of Waterjet Technology, 1991 (in print).

9. Wong, K.P., "Photoelastic Investigation of Abrasive Waterjet Machining", Master thesis, Department of Mechanical Engineering, University of Washington, Seattle, 1991.

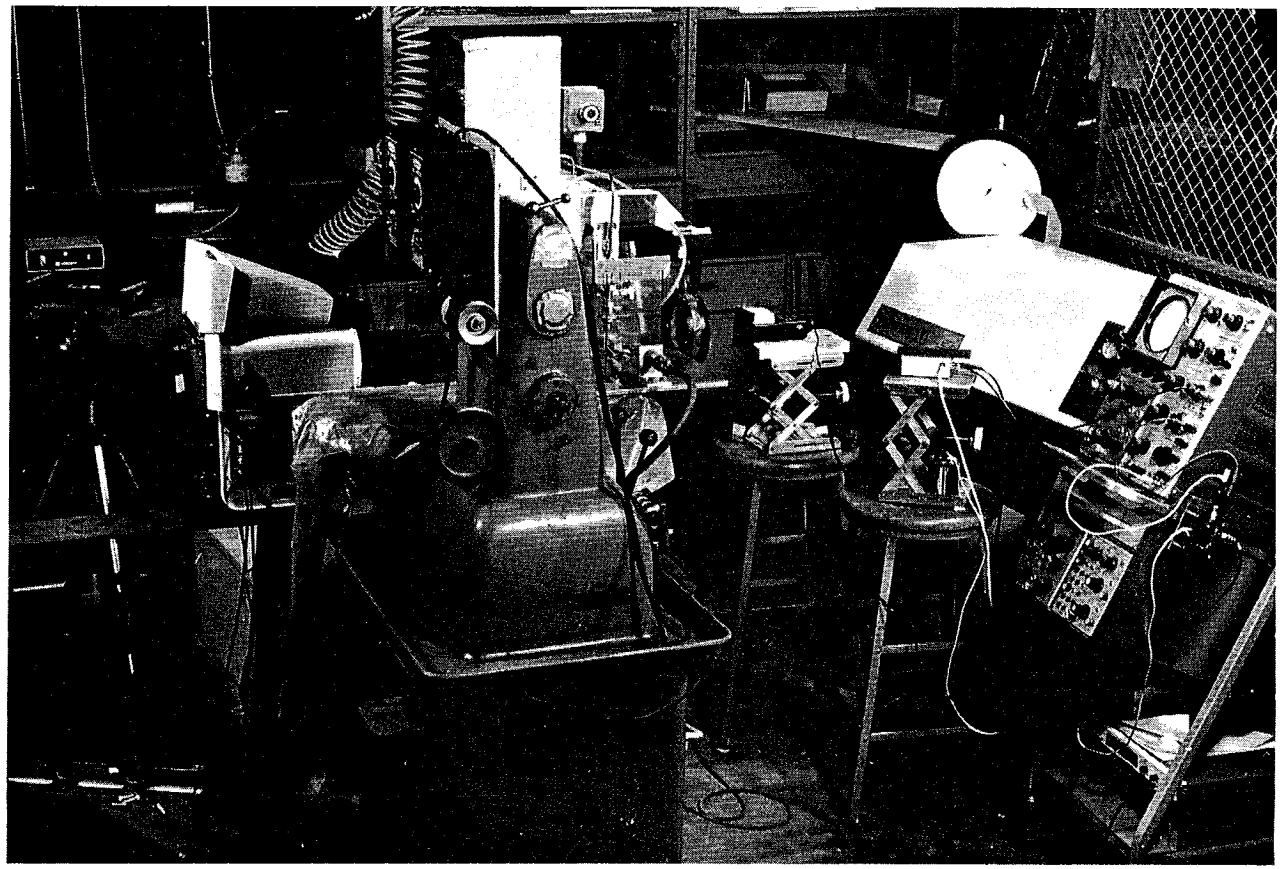

Figure 1. The photoelastic abrasive waterjet experimental setup.

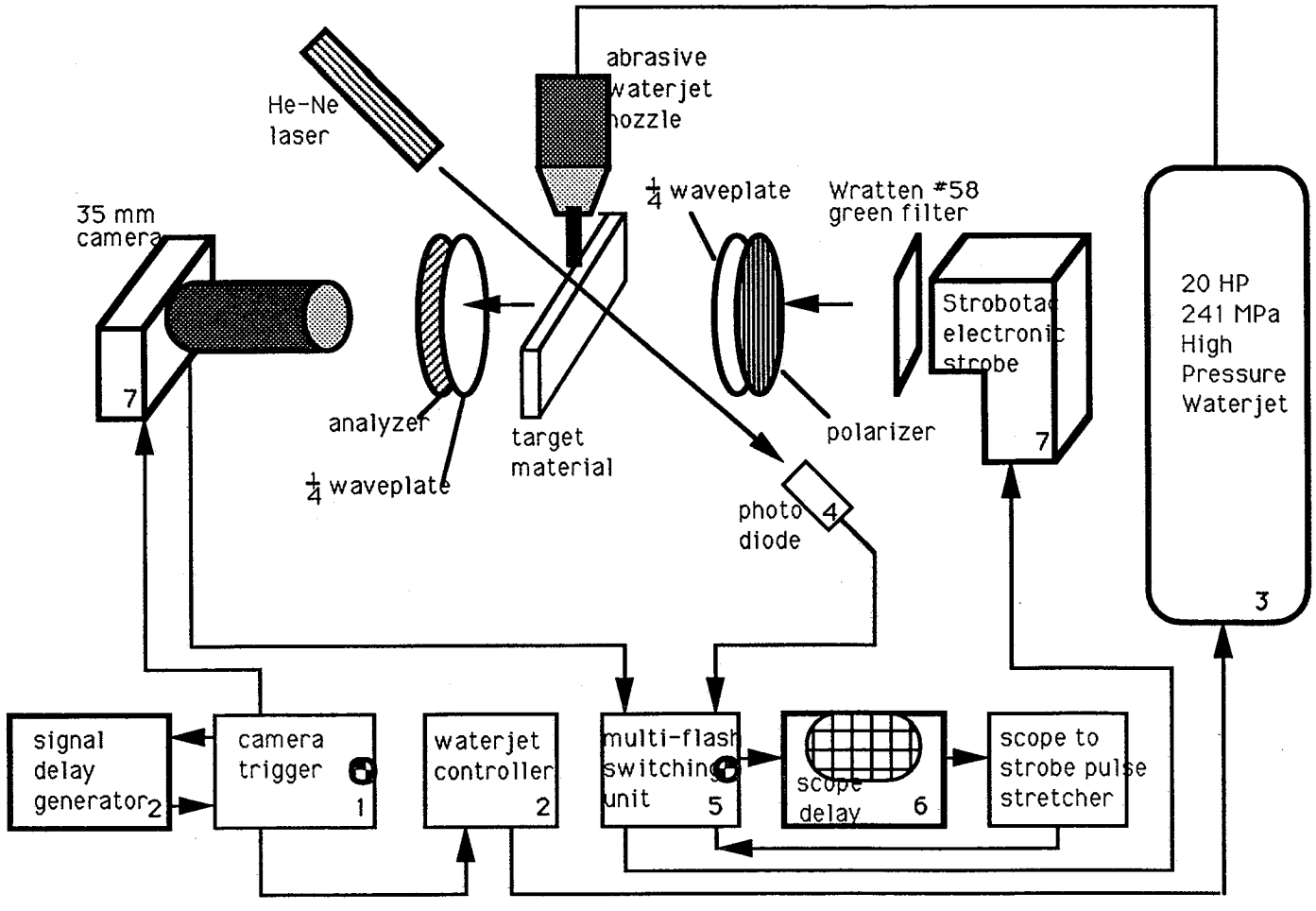

Figure 2. Schematic diagram of the high speed camera system.

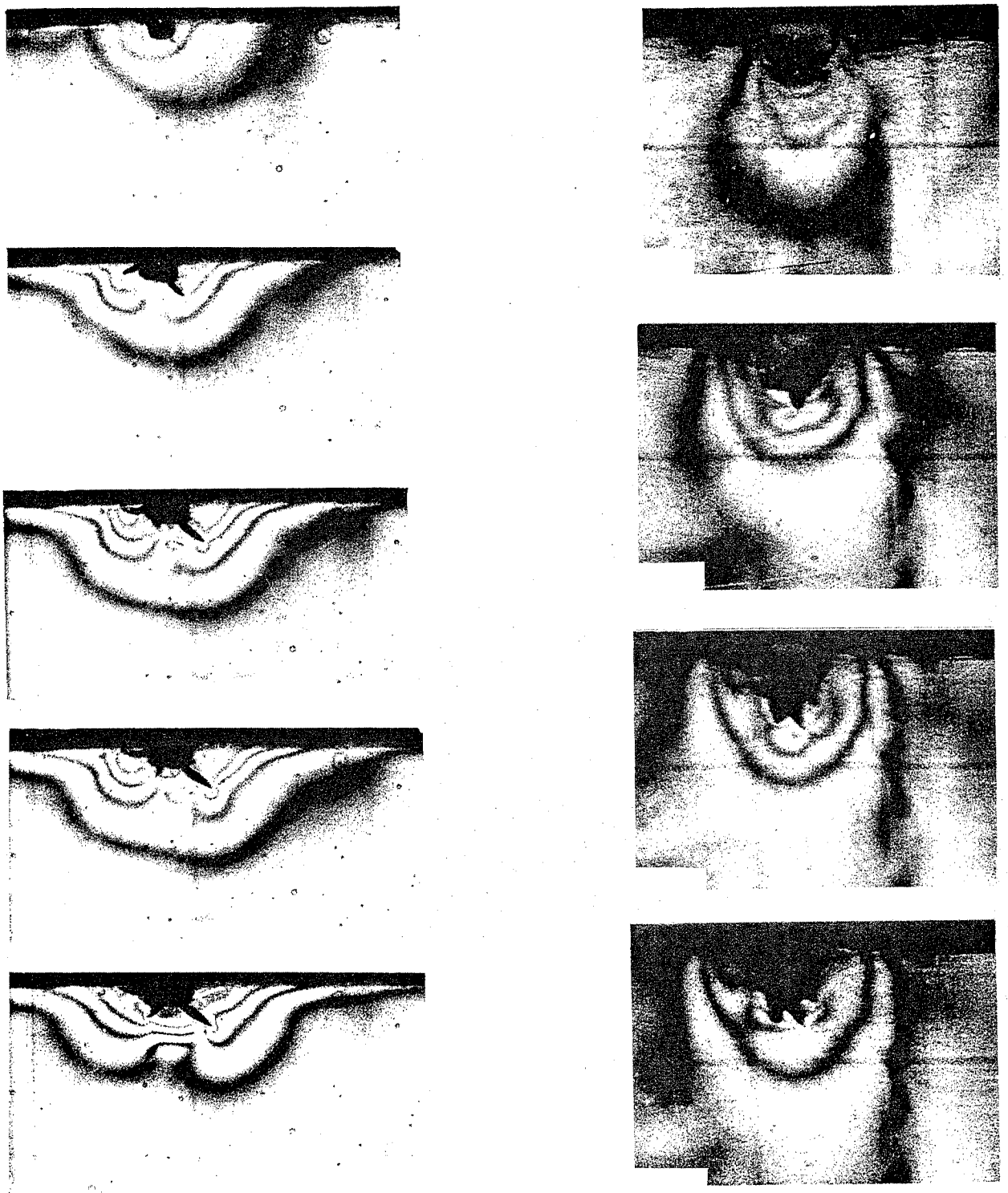

(a) Without notch

(b) with notch

Figure 3 Typical dynamic photoelastic records of the pure waterjet impact at a supplied pressure 240 MPa on the specimen. Standoff distance: 6mm, notch depth: 1.52 mm, radius: 0.98 mm.

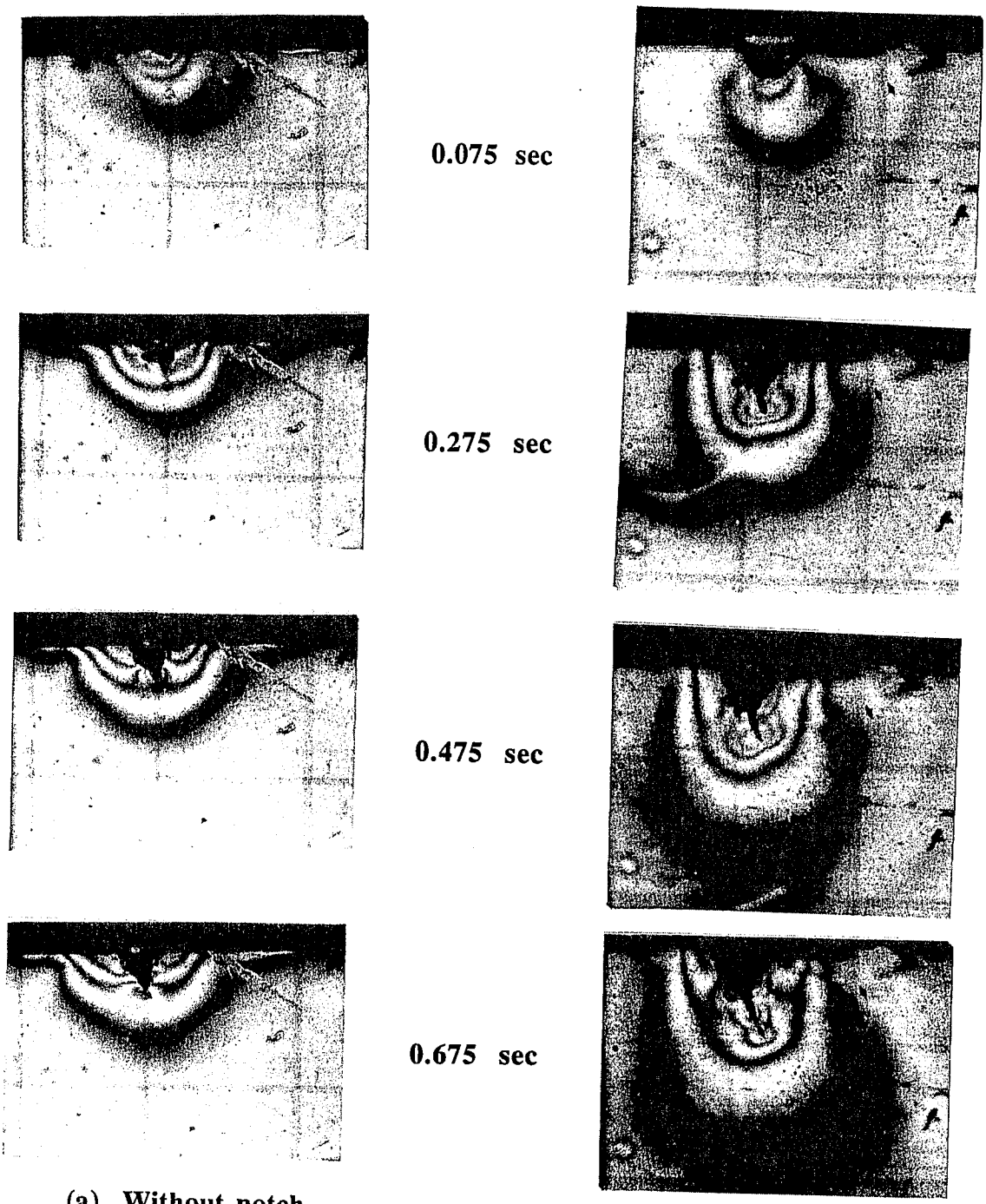

Figure 4 Typical dynamic photoelastic records of the pure waterjet impact at a supplied pressure 220 MPa on the specimen. Standoff distance: 6 mm, notch depth: 1.55 mm, radius: 1.19 mm.

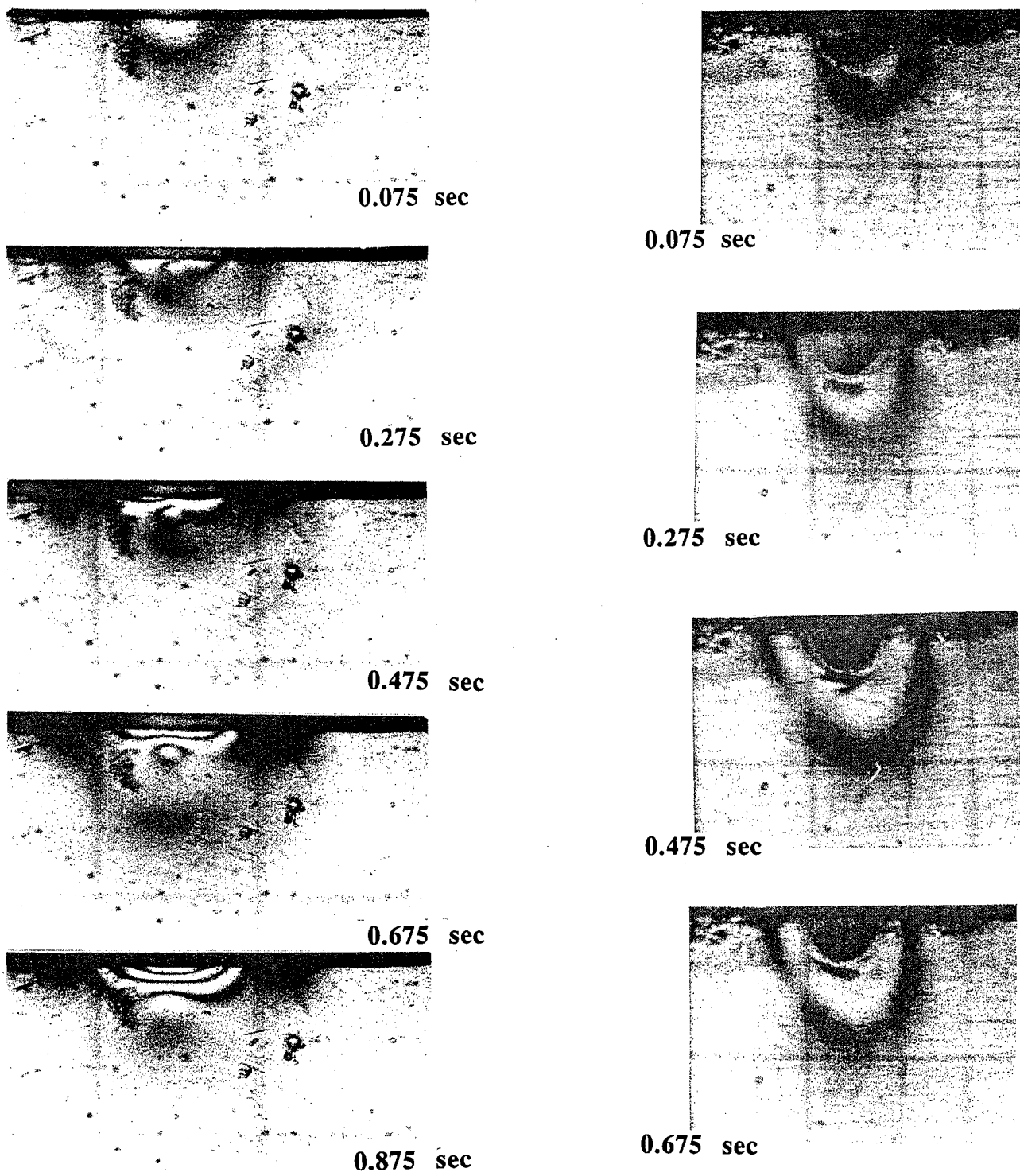

Figure 5 **Typical dynamic photoelastic records of the pure waterjet impact at a supplied pressure 110 MPa on the specimen. Standoff distance: 6mm, notch depth: 1.23 mm, radius: 1.13 mm.**

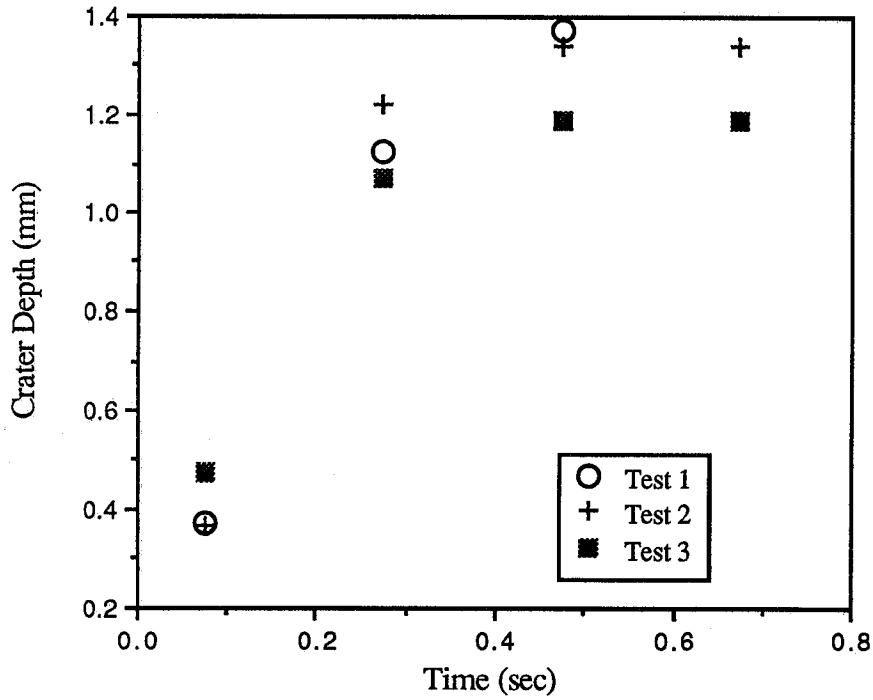

(a) Crater Depth vs. Time

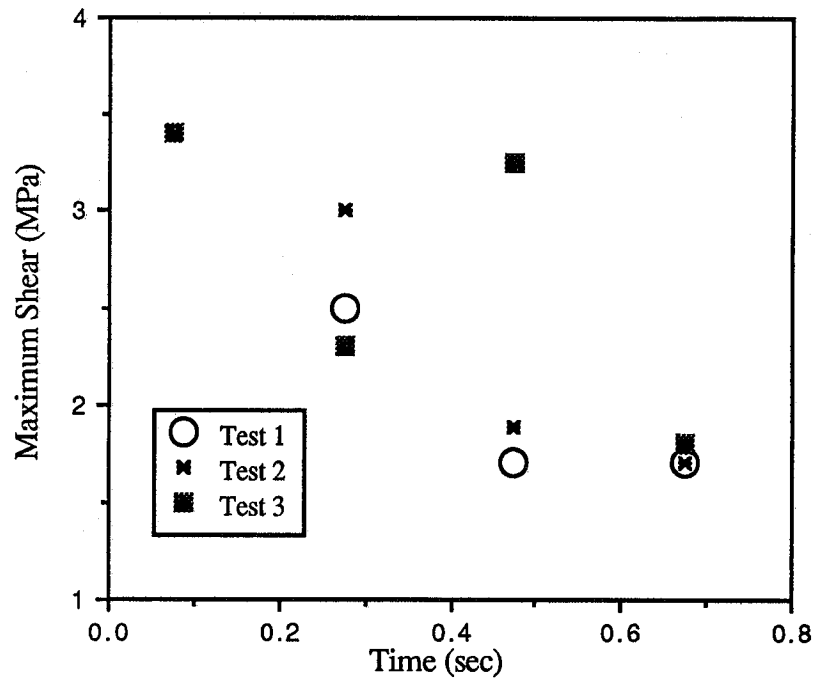

(b) Maximum Shear vs. Time

Figure 6 **Jet penetration depth, and maximum shear stress as a function of jet exposure time at a supply pressure 220 MPa, on the specimen without notch.**

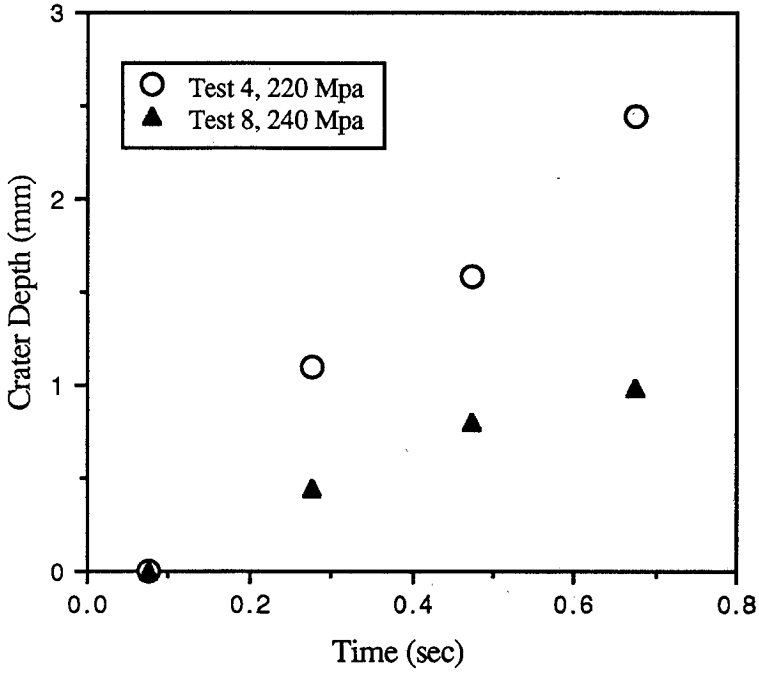

(a) Crater Depth vs. Time

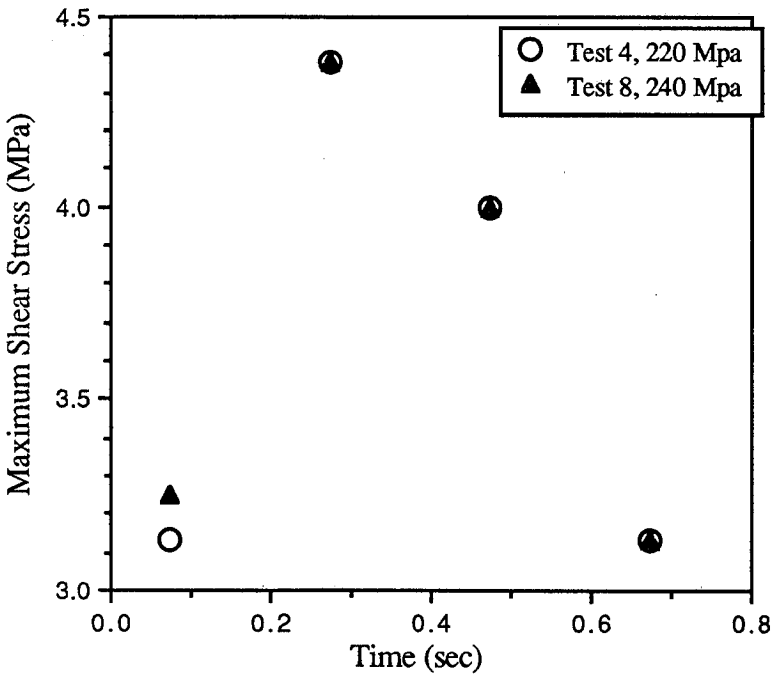

(b) Maximum Shear Stress vs. Time

Figure 7. Jet penetration depth, and maximum shear stress as a function of jet exposure time on the notched specimens.

0.075 sec

0.275 sec

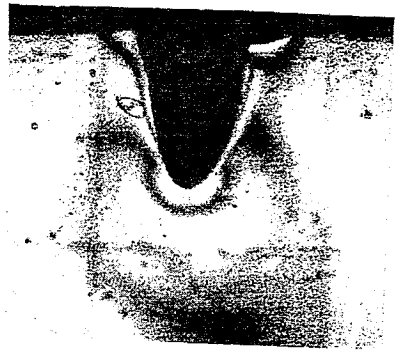

0.475 sec

0.675 sec

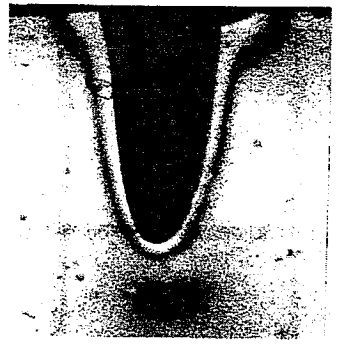

0.875 sec

Figure 8 **Typical dynamic photoelastic records of the abrasive waterjet impact at supplied pressure 240 MPa, garnet abrasive #80, abrasive flow rate 5 g/s, without notch.**

First impact

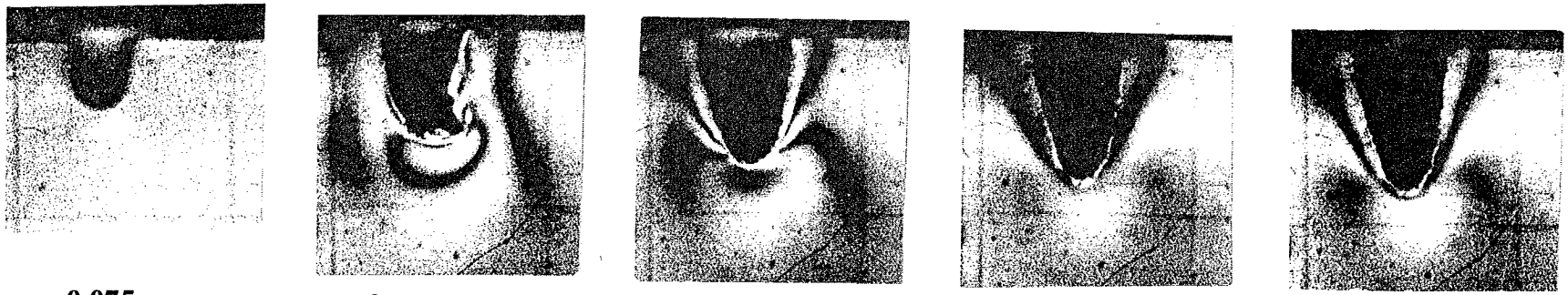

Second impact

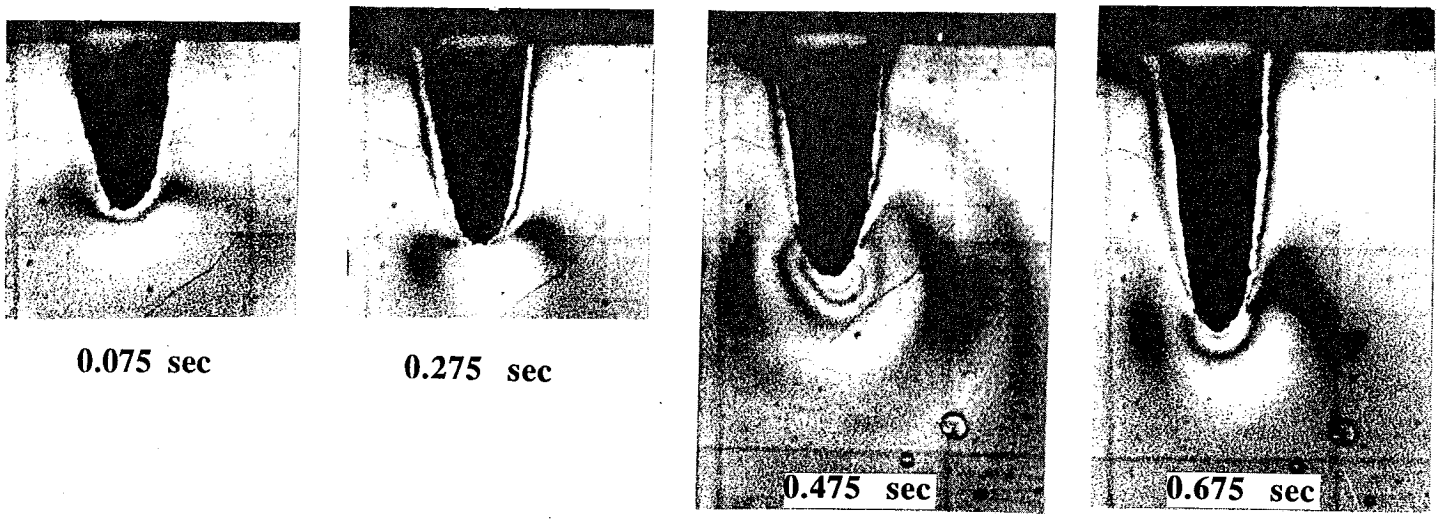

Figure 9.a Typical dynamic photoelastic records of the abrasive waterjet impact at supplied pressure 110 MPa, garnet abrasive #50, abrasive flow rate 11 g/s, with notch depth 1.67 mm, radius: 0.67 mm.

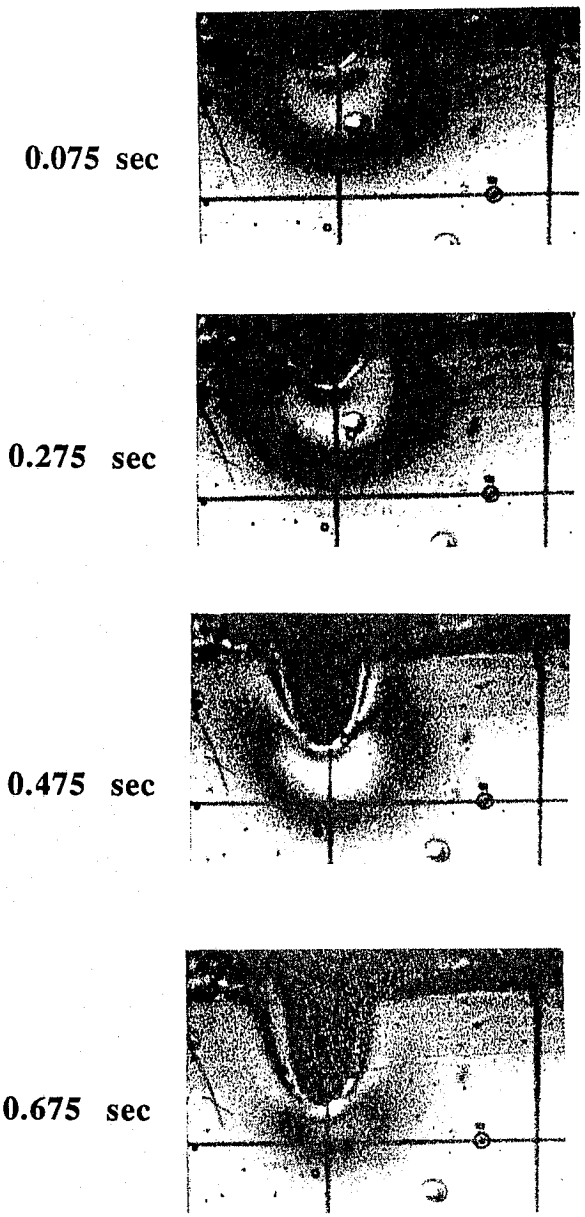

Figure 9.b **Typical dynamic photoelastic records of the abrasive waterjet impact at supplied pressure 110 MPa, garnet abrasive #50, abrasive flow rate 11 g/s, without notch .**

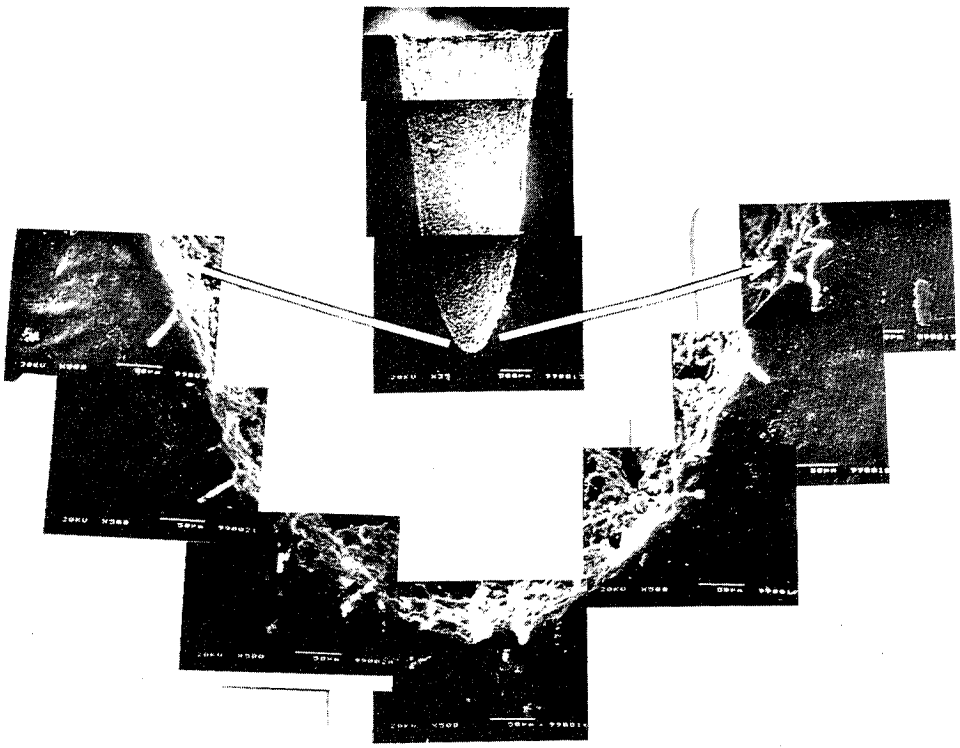

(a) 240 MPa, garnet size #80, flow rate 5.53 g/s

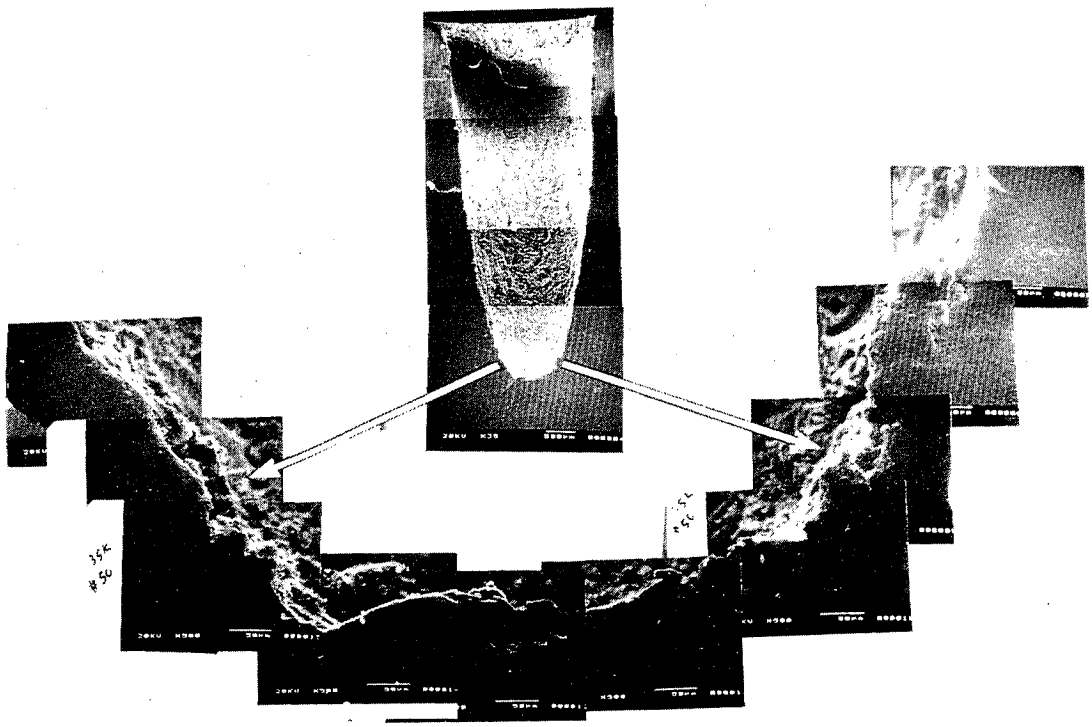

(b) 240 MPa, garnet size #50, flow rate 30.78 g/s

Figure 10. SEM pictures for abrasive waterjet piercing processes

6th American Water Jet Conference
August 24 - 27, 1991: Houston, Texas

Paper **2**

Characterization Of Material Removal In The Course Of Abrasive Waterjet Machining

F. Hu, Y. Yang, E.S. Geskin, Y.Chung
New Jersey Institute of Technology, Newark, USA

ABSTRACT

The objective of this work was to develop a practical technique for predicting the geometry of the surfaces generated in the course of abrasive waterjet machining. The experimental procedure involved the generation of grooves on the grounded surface of aluminum samples and the subsequent determination of the groove dimensions.

Charts relating the process conditions and the results of machining were constructed. The operational conditions were characterized by Particles Distribution Density (PDD), determined as a ratio between the mass flowrate of abrasive particles and the traverse rate. It was found that for fixed conditions of jet formation the rate of material removal is directly proportional to PDD. The coefficient of proportionality, however, is a function of process conditions.

In order to improve the prediction technique, process conditions were represented by the Energy Distribution Density (EDD) which was determined as the available energy of the jet delivered to a unit length of the generated groove. It was found that there is a strong correlation between the depth of the groove and EDD. The regression equation relating EDD with the depth of machining can be used for predicting the machining results.

Organized and Sponsored by the Water Jet Technology Association.

1.0 INTRODUCTION

The material removal by AWJ results from the actions of impinging particles and water. As the first approximation, we can consider water flow only as particles accelerators and reduce the process analysis to the study of the interaction between particles and a workpiece.

Material destruction by the impinging particles has been investigated by a number of authors (Finnie, Bitter, Hashish, Kim). It has been found that erosion weight or volume loss per individual particle collision is the function of the particle kinetic energy. Also, it was suggested that the total material removal by the impinging particles can be determined by the equation:

$$\text{Erosion loss} = kmv^n \qquad (1)$$

The values of k and n are determined by process conditions. It was found that material removal by the impinging particles depends on the ductility of the workpiece material, angle of attack, size, and flowrate of particles. According to the experimental data obtained, the value of n can exceed or be less than 2. Thus, equation (1) was modified for each particular case of material erosion. The presented paper concerns itself with this type of modification for optimal conditions of AWJ machining.

Previous work (Geskin) has demonstrated that at a comparatively low abrasive flowrate the depth of the jet penetration is proportional to the number of particles. The objective of the presented paper is to determine the range of machining conditions when such proportionality exists.

In the course of the performed experiments AWJ was used to generate a series of grooves on the surface of aluminum samples. The grooves were formed at different operational conditions and the details of their geometry were determined. The acquired information was used to construct charts relating the depth of jet penetration with complex variables, characterizing the number of particles and particles energy per unit of the groove length. The constructed charts demonstrate the existence of the linear relationship between the depth of jet penetration and constructed complex variables for a wide range of operational conditions.

2.0 EXPERIMENTAL PROCEDURE

The 5-axes waterjet machining cell "Streamline" was used to generate grooves on the aluminum 6061-T6 samples. The samples had the form of a parallelepiped with dimension of 254 mm X 127 mm X 25.4 mm (10"X5"X1"). The process variables included the particles size (50, 80, and 220 mesh), particles flowrate (86.5-284.5 g/min), traverse rate (1.8-30.3 mm/s), diameters of the water nozzle (0.21, 0.25 and 0.30 mm) and focusing tube (0.836, 1.165 and 1.565 mm) and number of passes (1-4). The experiments were carried out at the stand-off distance of 2.5 mm and the water pressure of 320 MPa. The Barton Mines garnet was used as an abrasive material.

The process conditions were characterized by complex parameters representing the mass of impinging particles (Particles Distribution Density or PDD) or particles energy (Energy Distribution Density or EDD) per unit of the length of a generated groove. These new variables characterized the intensity of energy supply to the surface of a workpiece and were determined by equations

$$PDD = Ma/U \tag{2}$$

and

$$EDD = 0.5 \cdot V_a^2 \cdot PDD \tag{3}$$

The value of v is determined by the equation (Chen):

$$Va = Vsw\left(1 - 0.267\left(\frac{Qa}{Qw}\right)^a\right) \tag{4}$$

where $a = 2.557\left(\frac{D_n}{D_t^2}\right)$ and $Qw = b\sqrt{P}$

The coefficient b is determined in the course of calibration.

In several cases the values of velocities determined by equation (4) also were measured by using a Laser Transit Anemometer (LTA). The results of the measurements validated the use of equation (4).

Equation (3) determines the kinetic energy of impinging particles. However, our current study of the mechanics of material destruction by AWJ has shown that the water also has a substantial contribution to this destruction. Thus, the available energy of the flow, rather than the kinetic energy of the particles, should be used to describe AWJ-workpiece interaction generally.

In our experiments the results of machining were evaluated by the depth of the jet penetration, the volume of material removed, and the width of the generated groove. This evaluation involved the

formation of the database representing the coordinates of scanned points of the generated surface. These coordinates were determined by the use of a computerized optical microscope called the "Videometrix". The use of the acquired database which determined the groove characteristics is shown in Fig 1.

The experimental results were presented in the form of charts that related PDD and EDD with the measured characteristics of the groove geometry. These charts show the effects of the various measurable parameters on the surface generation.

3.0 EFFECT OF PDD ON MATERIAL REMOVAL

Figs. 2 and 3 show the effect of the total amount of abrasive particles delivered by identical conditions and the results of machining. Machining was carried out at the same PDD and different amounts of abrasive were delivered due to the difference in the number of passes. The constructed charts show that both depth of the penetration and the volume removed are directly proportional to the amount of impinging particles. The presented charts demonstrate that for a given set of operational conditions the results of material removal are determined by PDD.

The effects of the change of process parameters (particles flow rate, diameters of the water nozzle and focusing tube) on the relationship between PDD and material removal is shown in Figs 4–9. The grooves generation on the aluminum surface was investigated at PDD = 0.06 – 0.5 g/mm. At PDD < 0.06g/mm no groove was formed. At PDD > 0.5 g/mm the depth of the groove became too big to carry the Vidiometrix measurements.

The presented charts show that the depth of penetration and the amount of material removed remains proportional to PDD for all ranges of tested operational conditions. The coefficient of proportionality, however, changed. The value of this coefficient increased as the particles velocity grew. The relationship between a process variable and the velocity determined by equation (4) enabled us to predict the effect of a variable in question on material removal. As it follows from the constructed charts and equation (4), the depth of penetration increased with the increase of abrasive flowrate and nozzle diameter. When the diameter of the focusing tube is reduced the depth of penetration also increases.

4.0 THE USE OF EDD FOR PROCESS CHARACTERIZATION

Charts (Figs. 2–9) show that the results of machining depend on PDD and particles velocity. Thus, the process description can be improved by the use of EDD as a characteristic variable. The relation between EDD and the depth of penetration is shown in Fig 10. This chart integrates the description of material removal for a wide range of operational conditions. The relationship between EDD and h can be represented by a straight line. However, scattering of the experimental points around this line is substantial.

It is possible, however, to identify three groups of experimental points, determined by a specific combination of the water nozzle and the focusing tube. The charts representing these groups (Figs. 11–13) show a comparatively strong correlation between the depth of penetration and EDD.

Preliminary study of the acquired experimental data has shown that probably the difference in material removal by AWJ generated by various nozzle combination is due to the difference in energy dissipation (exergy loss) during water–particles mixing, specifically particles destruction in the course of mixing.

5.0 CONCLUSION

The proportionality between h and EDD has shown that material removal by an impinging particle is proportional to the particle's kinetic energy and that the groove generation is caused by the superposition of the actions of individual particles. This simple model can be used as the first approximation of the mechanism of AWJ machining.

The linearity of the relationship between EDD and h enable us to use this process characteristic for control of AWJ machining. If the region of process linearity is determined and the particles velocity can be evaluated, the construction of a chart, representing material removal, becomes practical. If the information about particles velocity is not readily available, PDD rather than EDD must be used for process prediction. As it follows from the constructed charts, such prediction should be limited to conditions when the process variables determining the particles velocity (diameters of the nozzle and focusing tube, size and flowrate of particles etc.) are specified.

The charts presented in this paper were constructed for comparatively shallow machining of aluminum. The further development of the prediction technique will involve the characterization of the surface generation in the course of machining of aluminum, steel, glass, and some other materials at a much wider range of process variables. More accurate prediction of particles velocity also is needed to improve the evaluation of EDD.

ACKNOWLEDGEMENTS

The authors gratefully acknowledge the support of NSF under grant #DMC8810639 "Fundamental Study of Abrasive Waterjet".

REFERENCES

1. Bitter, J.G.A., "A Study of Erosion Phenomena- Part I," Wear, Vol. 6, pp. 5-21, 1963.

2. Bitter, J.G.A., "A Study of Erosion Phenomena- Part II," Wear, Vol. 6, pp. 169-190, 1963.

3. Chen, W.L., Geskin, E.S., "Correlation Between Particle Velocity and Condition of Abrasive Waterjet Formation," Proceedings of 6th Waterjet Technology Conference, Houston, August 1991.

4. Finnie, I., Levy A. and McFadden, D.H., "Fundamental Mechanisms of Erosive wear of Ductile Metals by Solid Particles," Erosion: Prevention and Useful Applications, ASTM STP 664, pp. 36-58, 1979.

5. Geskin, E.S., Chen, W.L., Chen, S.S., Hu, f., Khan, M.E.U., Kim, S., Singh, P., Ferguson, R., "Investigation of Anatomy of Abrasive Waterjet," Proceedings of 5th Waterjet Technology Conference, pp. 217-231, Toronto, August 1989.

6. Hashish, M., "A Modeling Study of Metal Cutting with Abrasive Waterjets," Journal of Engineering Material and Technology, Vol. 106, pp. 88-100, Jan. 1984.

7. Zeng,J. and Kim, T.J., "A study of a Brittle Erosion Mechanism Applied to Abrasive Waterjet Processes," Proceedings of 10th International Symposium on Jet Cutting Technology, B1, Amsterdam, November 1990.

NOMENCLATURE

a,b,k,n	=	constant
Do	=	Waterjet sapphire nozzle diameter (mm)
Dt	=	Abrasive focusing tube diameter (mm)
EDD	=	Energy distribution density = the amount of kinetic energy of particles per unit length of the generated kerf (J/cm)
h	=	Depth of generated kerf (mm)
PDD	=	Particles distribution density = mass of abrasive particles suppled per unit of length of the generated kerf (g/cm)
Ma	=	Mass flowrate of a abrasive particles (g/cm)
P	=	Water pressure (MPA)
Qa	=	Volumetric flow rate of abrasive particles (cm3/min)
Qw	=	Volumetric flow rate of water (g/min)
Sa	=	Abrasive particles' size (mesh)
U	=	Traverse rate (mm/min)
V	=	Volume of material removed per 1 cm of the generated kerf (cm3)
Va	=	Abrasive particles velocity (m/sec)
Vsw	=	Sapphire nozzle waterjet velocity (m/sec)
W	=	Width of the generated kerf (mm)

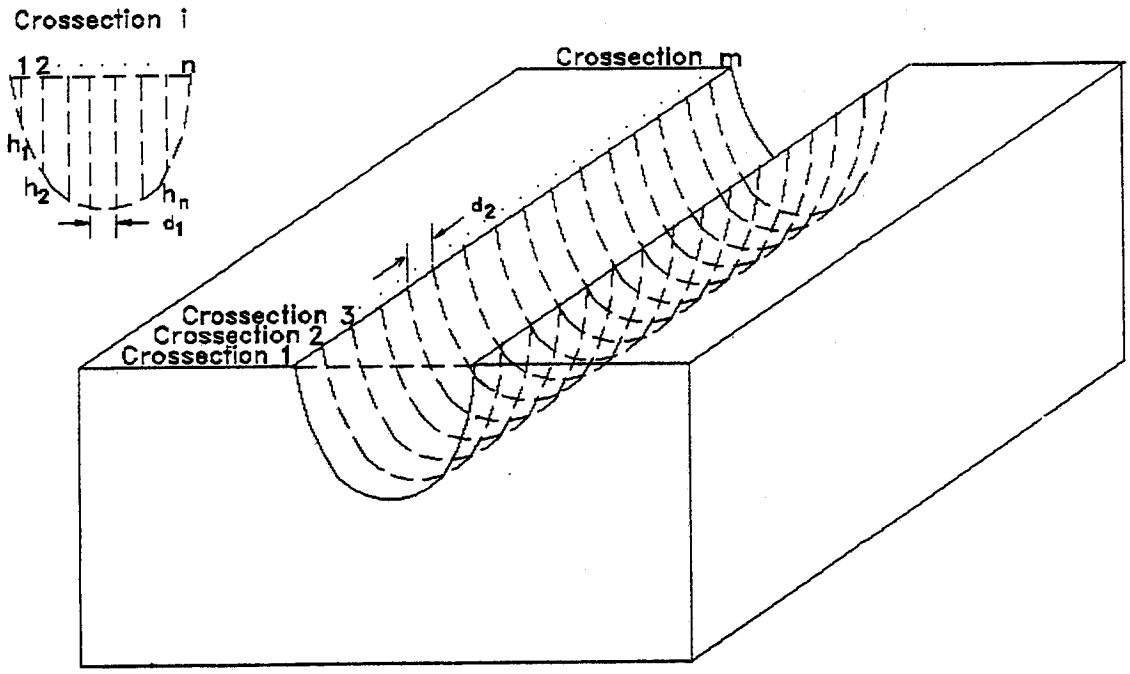

Area of crossection i : $A_i = d_1 \times (h_1 + h_2 + \cdots\cdots + h_n)$

Volume removed : $V = d_2 \times (A_1 + A_2 + \cdots\cdots + A_m)$

Fig.1 Schematic of data acquisition in the course of the study of groove geometry.

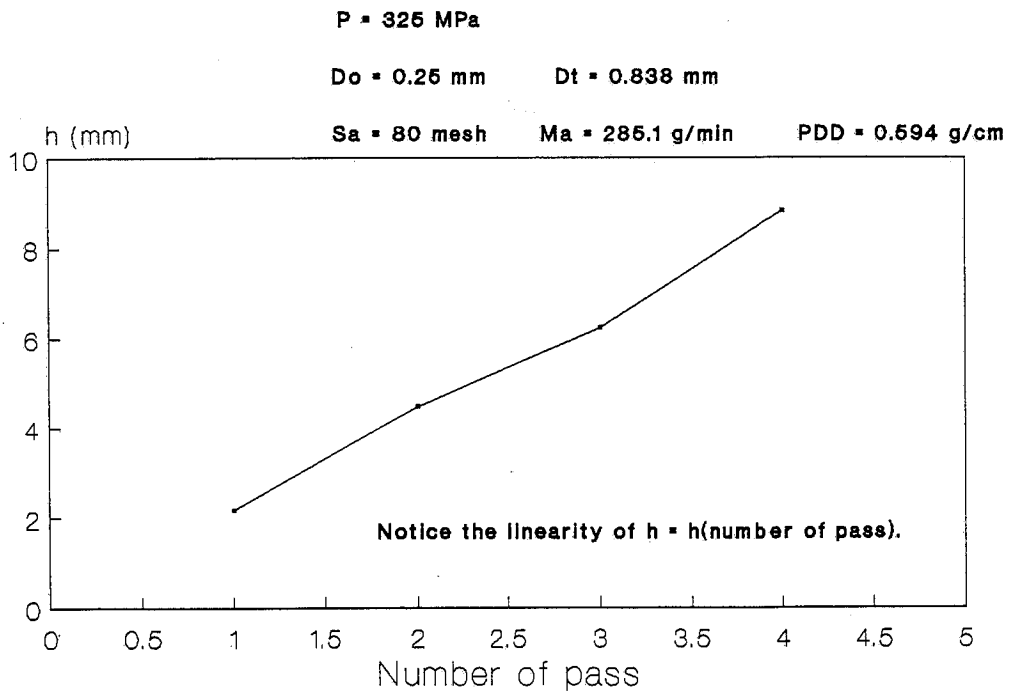

Fig. 2 Relationship between h and number of pass.

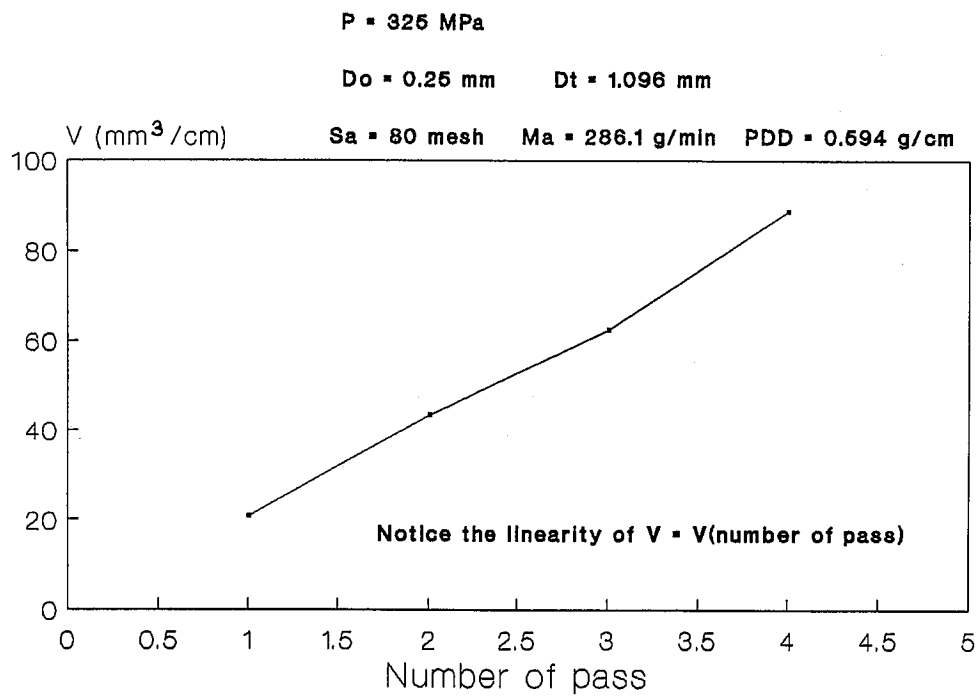

Fig. 3 Relationship between V and number of pass.

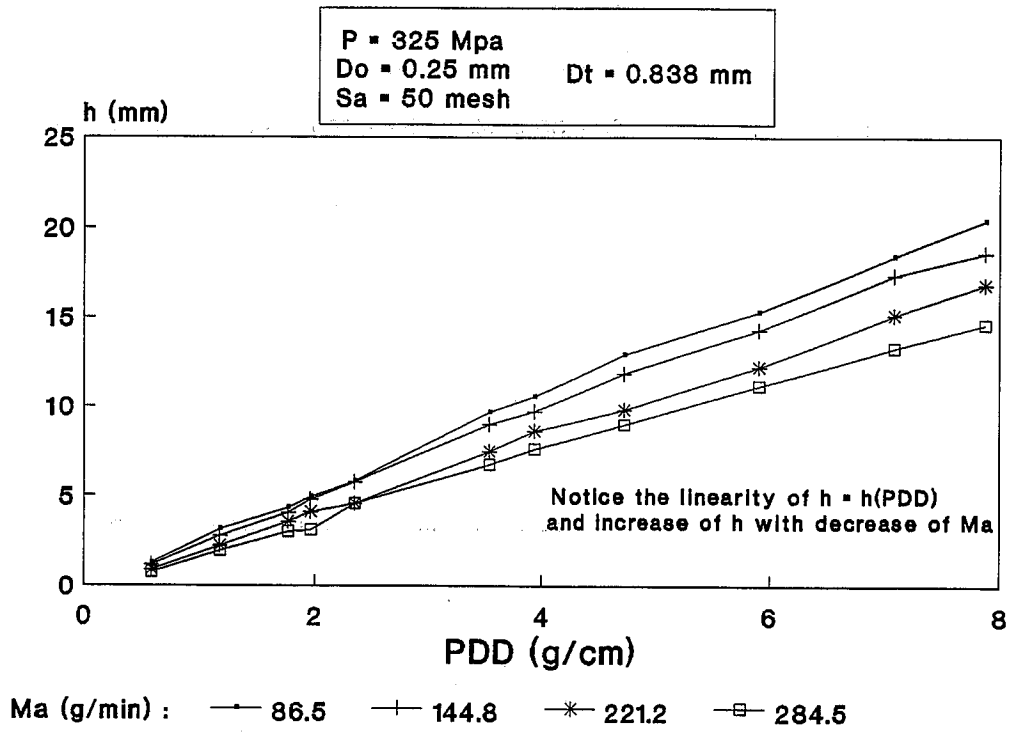

Fig. 4 Relationship between PDD, Ma and h.

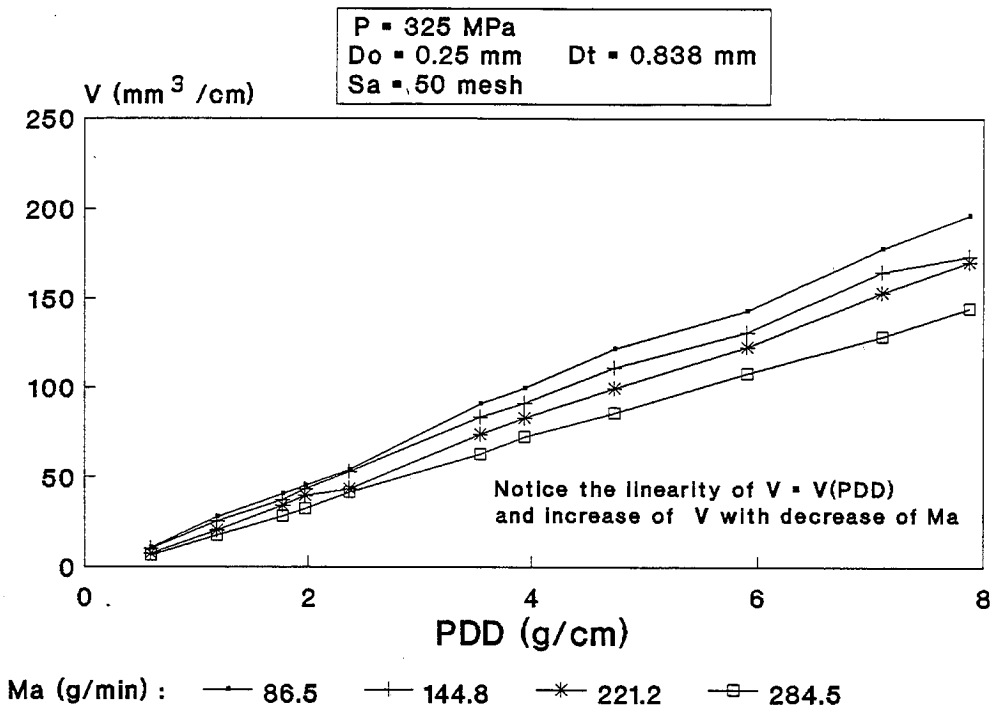

Fig. 5 Relationship between PDD, Ma and V.

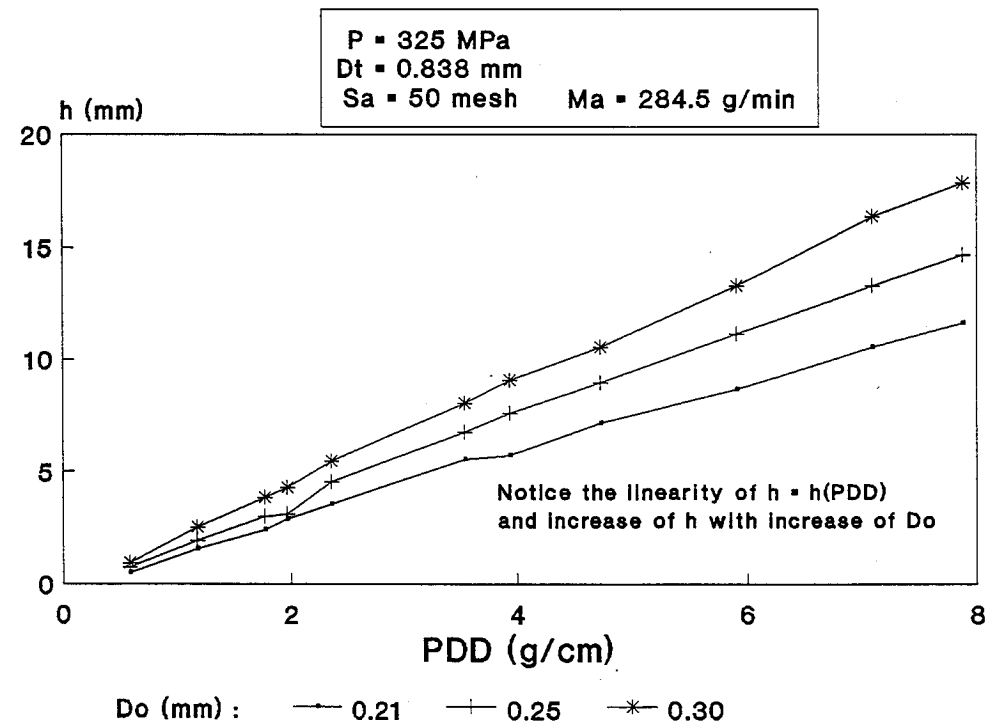

Fig. 6 Relationship between PDD, Do and h.

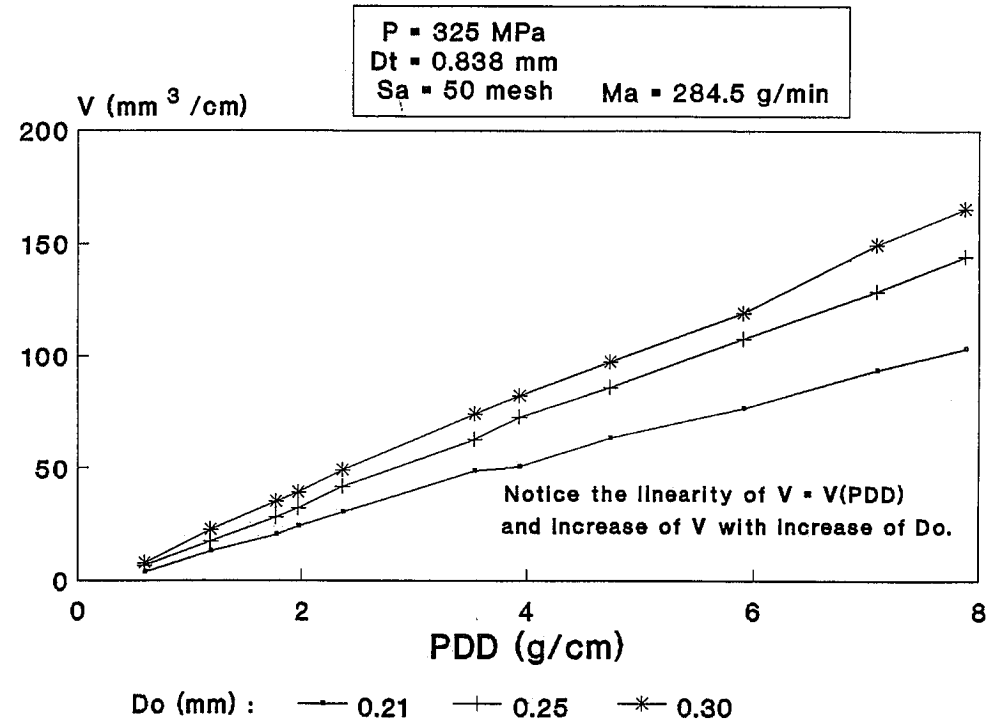

Fig. 7 Relationship between PDD, Do and V.

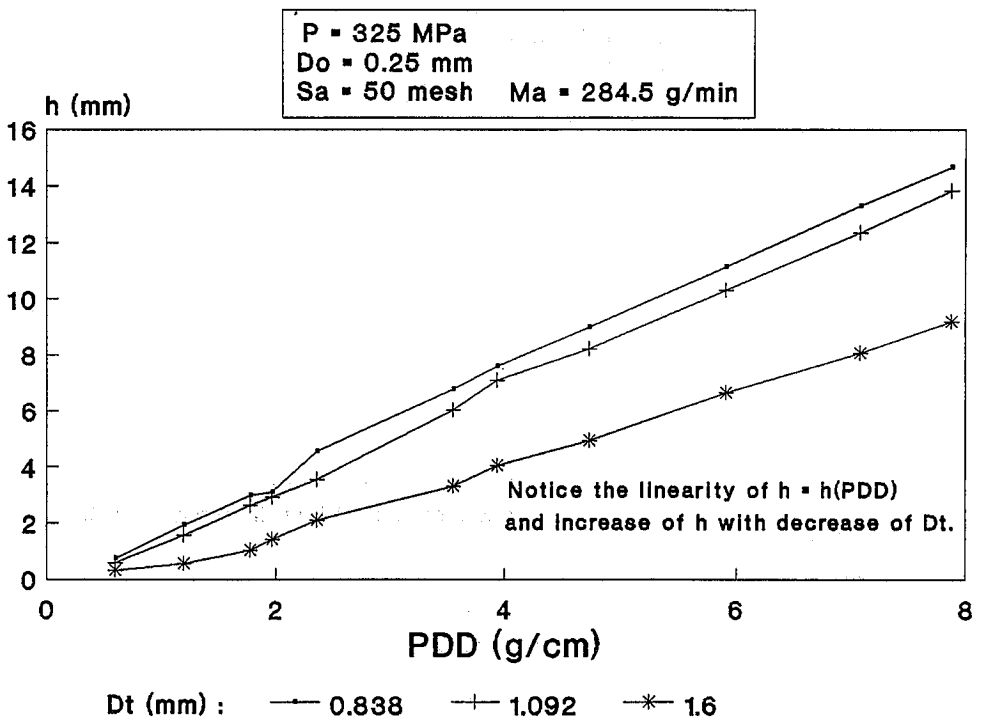

Fig. 8 Relationship between PDD, Dt and h.

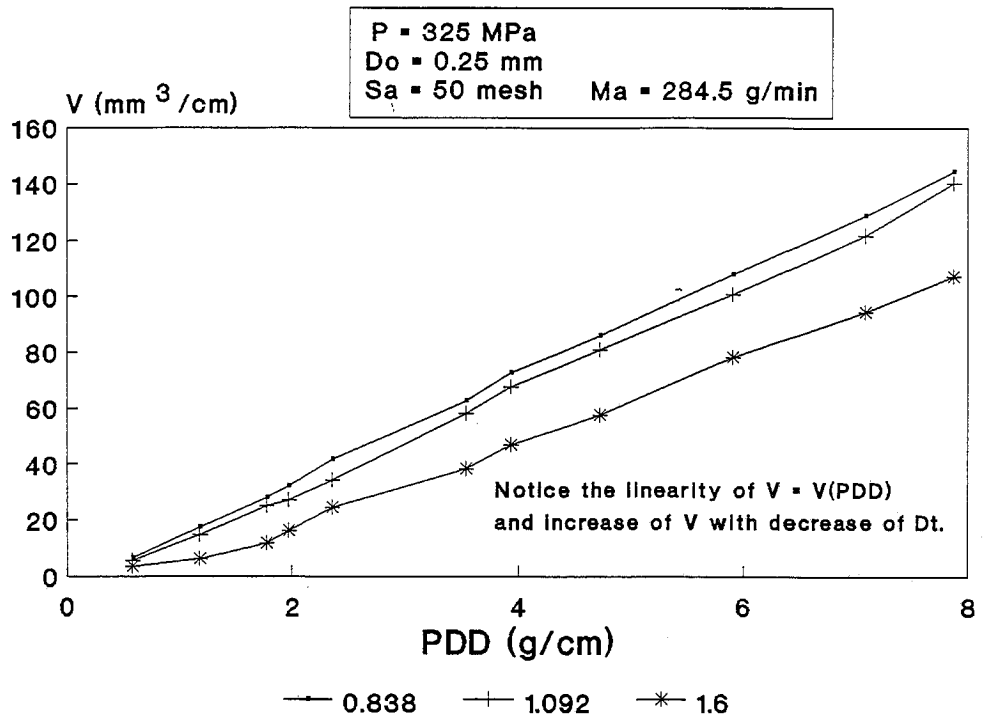

Fig. 9 Relationship between PDD, Dt and V

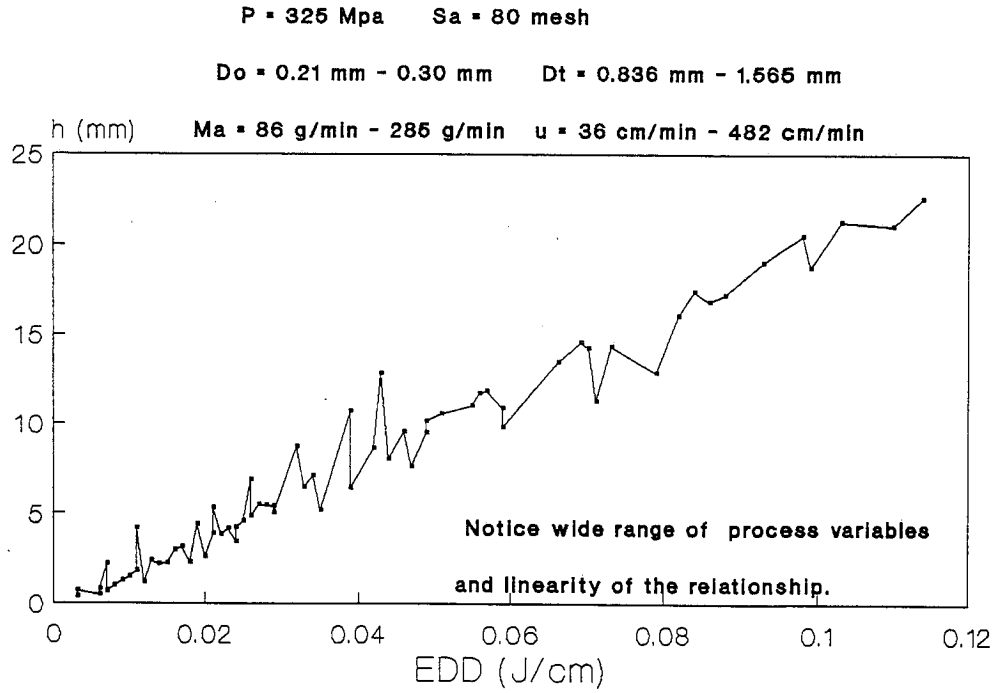

Fig. 10 Effect of EDD on h

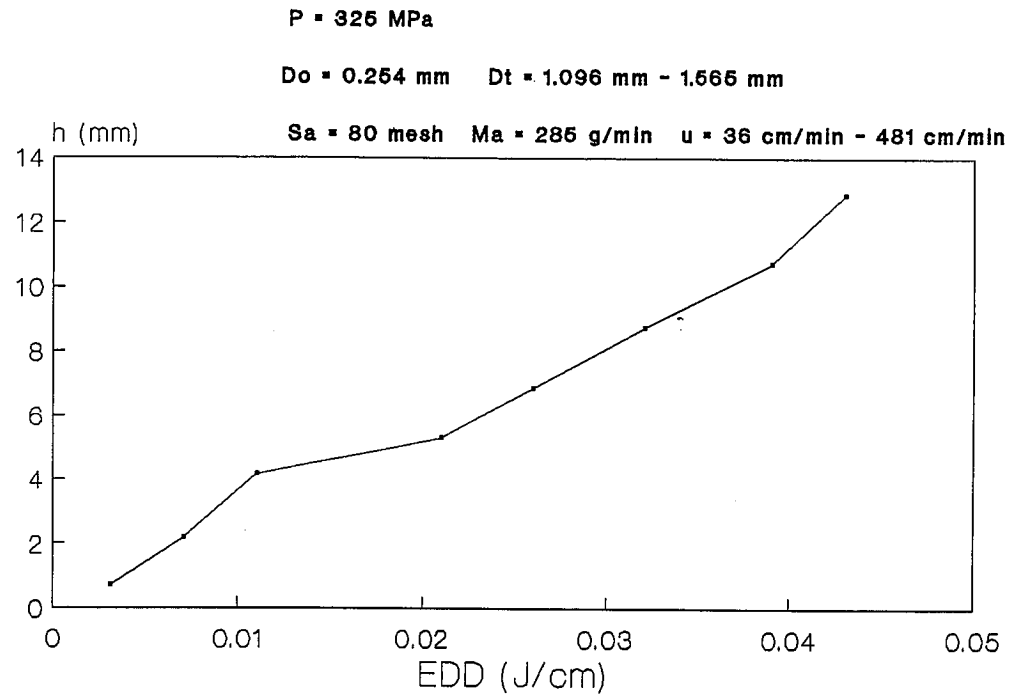

Fig. 11 Effect of EDD on h. The group of "upper" part.

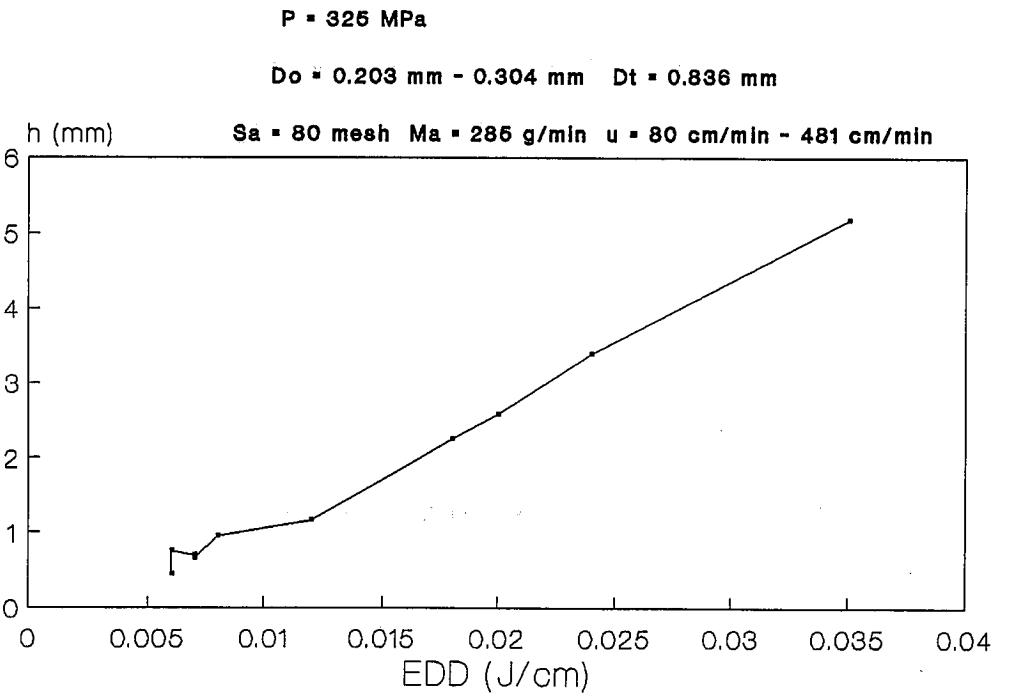

Fig. 12 Effect of EDD on h. The group of "lower" part.

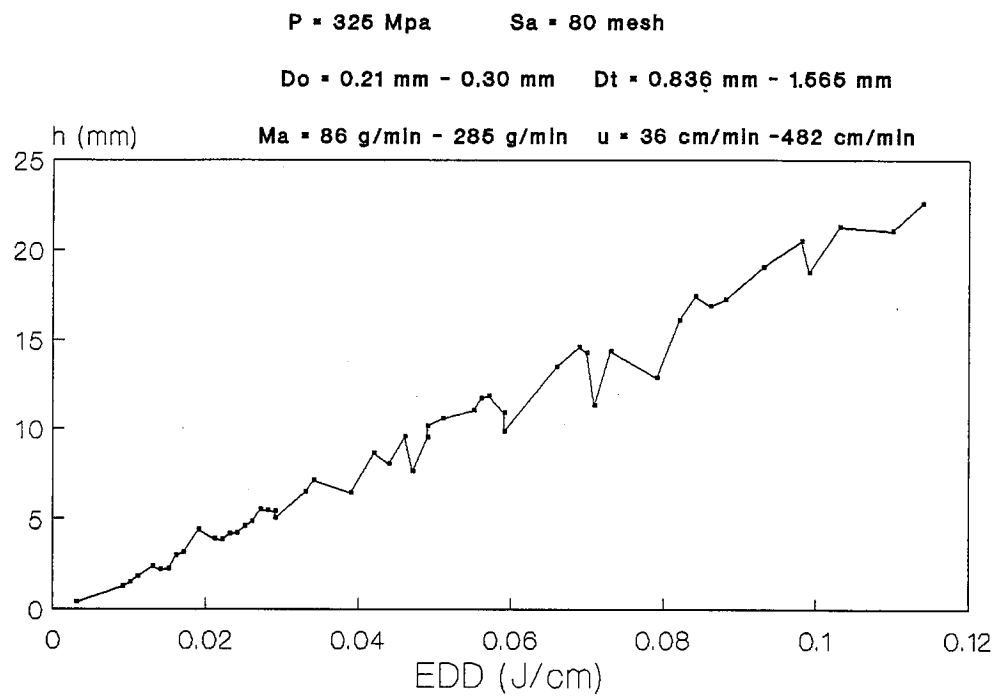

Fig. 13 Effect of EDD on h. The group of "middle" part.

6th American Water Jet Conference
August 24 - 27, 1991: Houston, Texas

Paper **3**

PREDICTION EQUATIONS FOR DEPTH OF CUT MADE BY ABRASIVE WATER JET

S.Matsui, H.Matsumura, Y.Ikemoto, Y.Kumon and H.Shimizu
KAWASAKI HEAVY INDUSTRIES, Ltd. Kobe, Japan

ABSTRACT

An experimental investigation to examine the relationship between mechanical properties and the cutting characteristics of materials cut by abrasive water jet are reported in this paper. After several materials that have different mechanical properties were cut by abrasive water jet with several traverse speeds, the depth of cut of each material was measured.

Considering the relations between the obtained data and the mechanical properties, it was found that a rate of kerf area generation was suitable to present cutting characteristic of the material and that it could be predicted by the mechanical properties of the material. Furthermore, prediction equations estimating the rate of kerf area generation of materials were obtained.

1.0 INTRODUCTION

In abrasive water jet cutting, cutting characteristics (such as depth of cut, cutting speed, roughness of cut surface) of materials are strongly affected by the material properties. Recently, many kinds of new materials are required to be cut for industrial use, however in such a case, the cutting conditions are often determined by trial and error. Therefore, if the prediction equation of material's depth of cut is obtained, it is very useful to estimate the cutting characteristics of the materials that have never been cut by abrasive water jet. There are relatively many papers presenting the relations between water jet conditions and the cutting characteristics[1-6] but there are few papers concerning the influence of the mechanical properties[7].

To define the relationship between the cutting characteristics and the mechanical properties of the materials, experiments of abrasive water jet cutting for several kinds of materials that have different mechanical properties were conducted. Prediction equations for material's depth of cut were also considered.

2.0 EXPERIMENT

A schematic diagram of abrasive water jet cutting equipment used in this study is shown in Fig.1. Its high pressure pump is an intensifier type. The maximum pressure is 392(MPa) and maximum water flow rate is 3.3 (1/min). An abrasive supply unit is a self entrained type using a light vacuum generating around the jet. Abrasive flow rate can be varied with an oriffice set below an abrasive hopper. Abrasive nozzle is moved by a 2-axis numerical controller.

Table 1 shows test materials used in this study and their mechanical properties. Test materials were selected so that they had widely different mechanical properties. Figures of test specimens are shown in Fig.2. Test specimens made of ductile materials such as steels were machined to the wedge-shaped figure(left side of the Fig.2), but block type test specimens (right side of Fig.2) were used for brittle materials as it was rather hard to obtain and to machine them. The data of material's depth of cut were obtained by measuring the section indicated 'Depth of Cut' in the Fig.2. In brittle materials, the average data obtained from a few points by using a measuring pin were adopted for the depth of cut.

Cutting conditions were as follows;

Pressure	:250(MPa)
Water nozzle diameter	:0.33(mm)
Abrasive nozzle diameter	:1.2(mm)
Abrasive	:Garnet sand
Abrasive flow rate	:0.43(kg/min)
Stand off distance	:2(mm)

Under a fixed cutting condition mentioned above, test specimenns made of ductile and brittle materials were cut at several traverse speeds which were varied from 2 to 1000(mm/min). After that, the test specimen's depth of cut were mesured and the cut surfaces of some materials were observed by SEM.

3.0 RESULTS

Fig.3 show the relation between the depth of cut and traverse speed obtained by this experiment. In Fig.3, white marks present ductile materials such as steels, and solid marks present brittle materials such as alumina. The depth of cut of such materials had a tendency to declease uniformly according to the inclease of traverse speeds, but at a certain traverse speed, it varied widely due to the kind of materials. The largest depths were in sodaglass and stones(marble and granite) and aluminum alloy(A5083-O), and then steels(304 stainless steel etc.), alumina, cemented carbide, silicon nitride were followed in order. The depth of cut of sodaglass was about 1000 times as large as that of cemented carbide.

Cut surface observation of some kinds of materials after abrasive water jet cutting by SEM were conducted. Fig.4 is the cut surface photographs of mild steel(JIS-SM41), which is almost same as mild steel(JIS-SS41), sodaglass and alumina(92%). On mild steel(JIS-SM41), scraped marks were observed, which were supposed to be formed by plastic flow of the material. On the other hand, there were small cracks here and there on soda glass and alumina, which were supposed to be caused by micro cracking on cutting. After these observations, it was presumed that there might be different cutting mechanizms between ductile materials and brittle materials.

4.0 DISCUSSION

On discussing the relation between cutting characteristics and mechanical properties of materials, a rate of kerf area generation(Ȧ) was adopted as a parameter presentng cutting characteristic instead of depth of cut. This is because the material's depth of cut was strongly affected by the traverse speed, then it could not be determined uniquely. Here, a rate of kerf area generation(Ȧ) is defined as a product of traverse speed and the depth of cut of materials. and it presents the area which can be cut per unit time. A rate of kerf area generation is used as an indication of machinability in a field of laser or discharge machining[8] because it has almost constant value for a material, and it is independent of the material's thickness or cutting speed. Fig.5 and Fig.6 show the relation between a rate of kerf area generation and a traverse speed on each material. In the case that a traverse speed was not too slow or too high for the materials,therate of kerf area generation showed almost constant value for the materials independent of the traverse speeds. Therefore it was found that a rate kerf area generation was suitable to present a cutting characteristics of materials. The little deviated values from constant values seemed to be caused by another reasons such as nozzle matters.

The relation between a rate of kerf area generation and the mechanical properties of materials are discussed. First,the relation between Vickers Hardness, H(Hv) and a rate of kerf area generation is shown in Fig.7. Here, Vickers Hardness was picked because it was most useful mechanical properties of materials. This graph shows that there is some correlation between them and a rate of kerf area generation had a tendency to decrease according to a rise of hardness. There was relatively a good correlation between them on brittle

materials, however on ductile materials, the correlation is not so good, hence it was impossible to predict a rate of kerf area generation by only hardness. So further dicussion about other material parameters which are suitable to predict a rate of kerf generation was carried out.

Fig.8 shows the rate of kerf area generations which were arranged by material parameter $F(=\sigma_u^2/2E)$(MPa). Here, σ_u(MPa) presents a tensile stress, E(MPa) presents Young's modulus of materials and material parameter F is a modulus of fracture . A modulus of fracture F is thought to present an elastic energy of material fracture in a 1-axis tensile test by considering its physical meaning. It can not be said that there is a good correlation between a rate of kerf area generation and a modulus of fracture F in all kinds of materials. However, in brittle materials except for stones such as marble, that is, soda glass, alumina, cemented carbide and silicon nitride, a rate of kerf area generation showed a good correlation with a modulus of fracture F. Therefore in brittle materials, it is reasonable to predict the rate of kerf area generation by a modulus of fracture F. In ductile materials such as steels, a good correlation was not observed. The reason of this is considered that a modulus of fracture F does not involve the plastic energy terms which is required for ductile materials to fracture. Stones, that is, marble and granite had different tendencies compared with other brittle materials. In stones, there are many latent cracks and these will drop the tensile strength, however, they are considered not to affect the rate of kerf area generation on an abrasive water jet cutting. Therefore, the modulus of fracture F of stones would have small values against the rate of kerf area generation and deviate from the correlation line.

Fig.9 shows the relation between a rate of kerf generation and a material parameter $(\sigma_u+\sigma_y)\cdot\varepsilon/2$(MPa) in ductile materials. Here, σ_u(MPa) is a tensile stress, σ_y(MPa) is a yield stress(or proof stress) ε(%) is an elongation, and the term $(\sigma_u+\sigma_y)\cdot\varepsilon/2$ presents a value of (Flow Stress)*(Elongation). A material parameter $(\sigma_u+\sigma_y)\cdot\varepsilon/2$ showed a good correlation with a rate of kerf area generation. As a value of (Flow stress)*(Elongation) can be presumed an energy used in a plastic deformation of a ductile material during a 1-axis tensile test. It is supposed that plastic deformation energy is the most correlative parameter to water jet cutting of ductile materials.

Fig.10 shows the relation between a rate of kerf area generation and a material parameter $H\cdot\varepsilon$ in ductile materials. Here, H(Hv) is a Vickers Hardness, ε(%) is an elongation, and $H\cdot\varepsilon$ is a material parameter which was found experimentally as a correlative. $H\cdot\varepsilon$ is also regarded as a correlative value to plastic deformation energy of ductile materials by cosidering its physical meaning. $H\cdot\varepsilon$ wouldmore correlate with the rate of kerf area generation than hardness H only. It can be said from this graph that a rate of kerf area generation of ductile materials is determined uniquely by the $H\cdot\varepsilon$. In ductile materials such as steels, hardness is nearly proportional to the flow stress, therefore the good correlation can be explainable as well as the parameter (Flow Stress)*(Elongation). Thus, both the material parameter (Flow Stress)*(Elongation), that is, $(\sigma_u+\sigma_y)\cdot\varepsilon/2$, and $H\cdot\varepsilon$ were found to be useful as parameters to estimate the rate of kerf

area generation of ductile materials well. However, the parameter $H \cdot \varepsilon$ is more convenient for industrial use.

The material parameters obtained in this study were different values on ductile and brittle materials, respectively. However, these parameters can be explained as the same one presenting approximate values of fracture energy that are required for materials in 1-axis tensile test. Fig.11 shows a schematic diagram of absorbed energy of material on fracture. An upperside of Fig.11 shows a $\sigma-\varepsilon$ curve of material in general, and the absorbed energy is presented as a shaded area. The absorbed energy is generally divided into an elastic area (1) and plastic area (2). In brittle materials, the $\sigma-\varepsilon$ curve is approximated to the left-side of Fig.11, and its fracture energy is presented as $(\sigma_u \cdot \varepsilon/2)=(\sigma_u^2/2E)$ because the plastic deformation can be ignored. This value is equal to a modulus of fracture F, mentioned above. On the other hand, in ductile materials, the $\sigma-\varepsilon$ curve is approximated to the right-side of Fig.11 because the elastic area is relatively small compared with the plastic area in general. Therefore, fracture energy can be presented as $(\sigma_u+\sigma_y) \cdot \varepsilon/2$ by using the flow stress, $(\sigma_u+\sigma_y)/2$. Thus, the material parameters, $(\sigma_u+\sigma_y) \cdot \varepsilon/2$, $H \cdot \varepsilon$ in ductile materials and $(\sigma_u^2/2E)$ in brittle materials turned out to be almost equal to the fracture energy of materials on 1-axis tensile test. Therefore a fracture energy of materials is the most influencing factor to the cutting characteristic of materials on water jet cutting.

Prediction equations for a rate of kerf generation by using $(H \cdot \varepsilon)$ and $(\sigma_u+\sigma_y) \cdot \varepsilon/2$ in ductile materials and $(\sigma_u^2/2E)$ in brittle materials are found as follows (from Fig.8,9,and10);

$\dot{A}=10^{4.74}(H \cdot \varepsilon)^{-0.67}$ (Ductile Materials)

$\dot{A}=10^{4.98}((\sigma_u+\sigma_y) \cdot \varepsilon/2)^{-0.64}$ (Ductile Materials)

$\dot{A}=10^{0.91}(\sigma_u^2/2E)^{-1.97}$ (Brittle Materials, except Stones)

Here, $\dot{A}$:the rate of kerf area generation (mm^2/min)
ε :elongation(%)
σ_u:tensile stress(MPa)
σ_y:yield stress(MPa)

From these equations, a rate of kerf area generation of materials can be predicted conveniently. These equations will be useful on estimating the cutting properties of materials that have never been cut by an abrasive water jet.

As there are many factors which affect the water jet cutting mechanizm, more precise equations considering the micro cutting phenomina will be investigated and a equation which is applicable to both ductile and brittle materials will be discussed after this.

5.0 CONCLUSION

The results obtained from this study can be summarized as follows;
1) It was supposed that there seemed to be different cutting phenomina (fracture mechanizms) between ductile and brittle materials from the results of some SEM observation at cut surfaces.
2) In the ductile materials, a parameter $H \cdot \varepsilon$ and a plastic deformation energy, that is, $(\sigma_u+\sigma_y) \cdot \varepsilon/2$ had a good correlation with a rate of kerf area generation.
3) In the brittle materials, a parameter $\sigma_u^2/2E$ had a good correla-

tion with a rate of kerf area generation.

REFERENCE

1) S.Matsui, H.Matsumura, Y.Ikemoto, K.Tsujita and H.Shimizu,"High precision cutting method for metallic materials by abrasive waterjet",Proceedings of 10th International Symposium on Jet Cutting Technology", Amsterdam, BHRA, October,1990
2) H.Matsumura, Y.Ikemoto, H.Shimizu,"Development and application of waterjet cutting technology," WELDING TECHNIQUE,November, 1988, pp89-98
3) S.Matsui, H.Matsumura, Y.Ikemoto, Y.Kumon, H.Shimizu, M.Kiyoshige, T.Okada and K.Tsujita,"Development and Application of Water-jet Cutting Technology", KAWASAKI TECHNICAL REVIEW Vol. 108, 1991,pp51-58
4) Hashish, M.,"A Model for Abrasive-Waterjet(AWJ) Machining," Transactions of the ASME, Vol.111, April 1989, pp.154-162
5) Hashish, M.,"A Modeling Study of Metal Cutting With Abrasive Waterjets," Transaction of the ASME, Vol. 106, Jan. 1984, pp.88-100
6) H.Blickwedel, N.S.Guo, H.Haferkamp, H.Louis,"Prediction of abrasive jet cutting performance and quality," Proceedings of 10th International Symposium on Jet Cutting Technology. Ocotber 1990
7) D.C.Hunt, T.J.Kim and J.G.Sylvia,"A parametric study of abrasive waterjet processes by piercing experiment," Proceedings of 8th International Symposium on Jet Cutting Technology, BHRA, England September 1986, pp.287-295
8) New Engineering Review of Cuttng p429

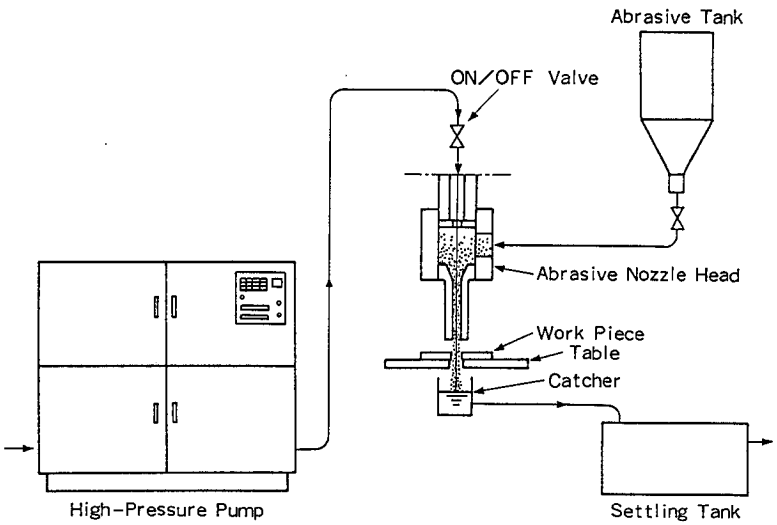

Fig.1 Experimental equipment

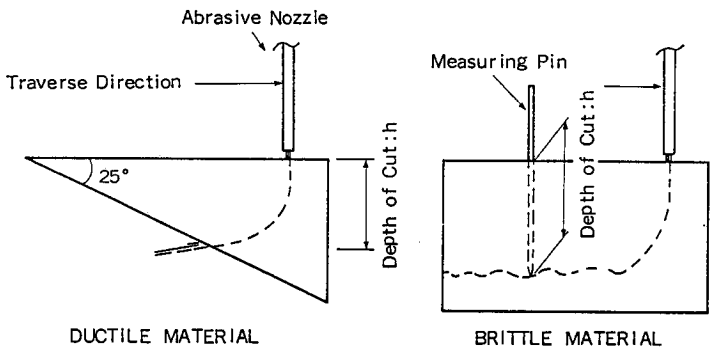

Fig.2 Test specimen

Table 1 Mechanical properties

	Materials	Vickers Hardness (Hv)	Elongation (%)	Tensile Strength (MPa)	Yield Strength (MPa)	Modulus of Elasticity (GPa)
Ductile Materials	Mild Steel (JIS-SS41)	160	37	441	284	206
	304 Stainless Steel	167	63	617	255	196
	HT90	290	25	880	844	206
	A5083-O	84	24	304	147	69
	Ti-6Al-4V	350	14	980	911	114
Brittle Materials	Soda Glass	535	–	49 ※	–	74
	Granite	(285)	–	(10)	–	55
	Marble	140	–	(4)	–	49
	Alumina	1050	–	343 ※	–	343
	Cemented Carbide	1950	–	980 ※	–	598
	Silicon Nitride	1200	–	784 ※	–	294

※ Data of transverse rupture stress

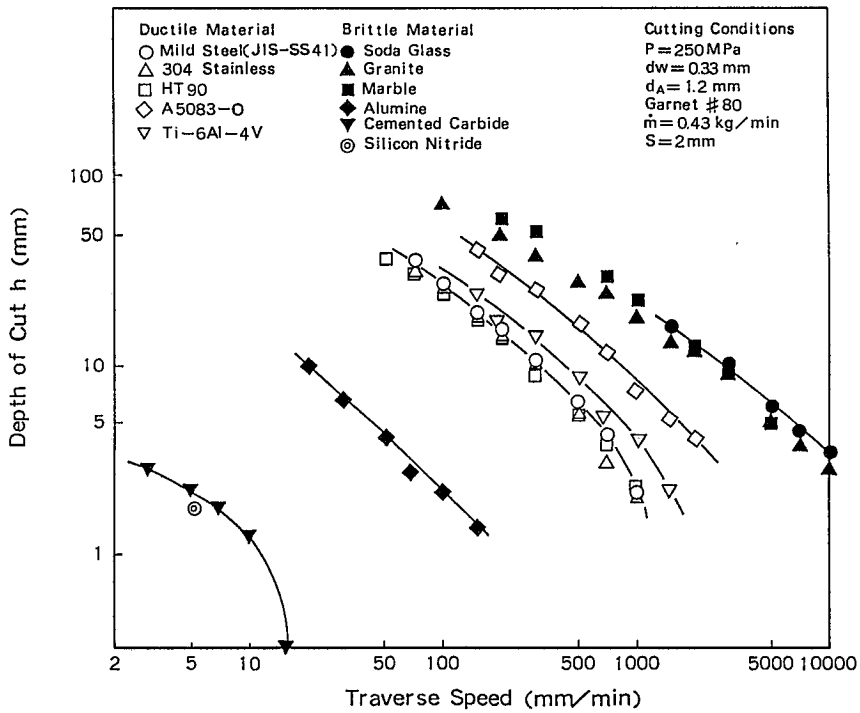

Fig.3 Relation between traverse speed and depth of cut

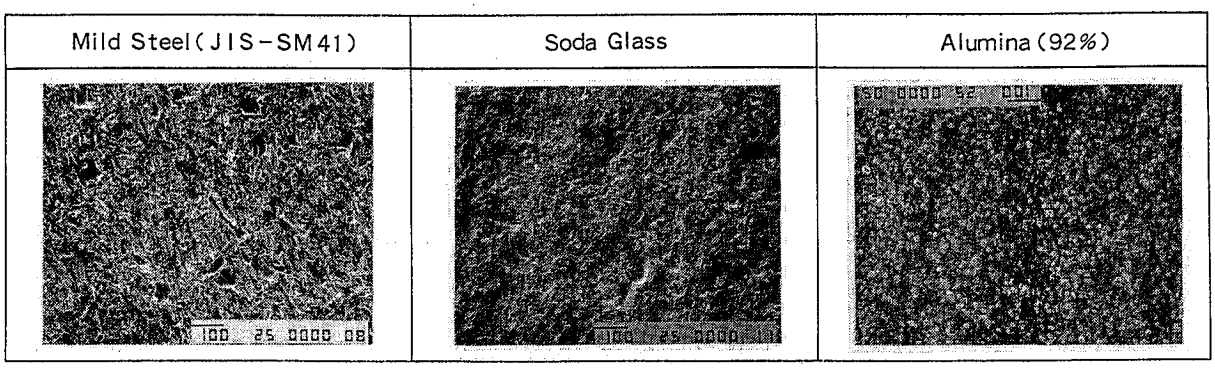

Fig.4 Observation of cut surfaces by SEM

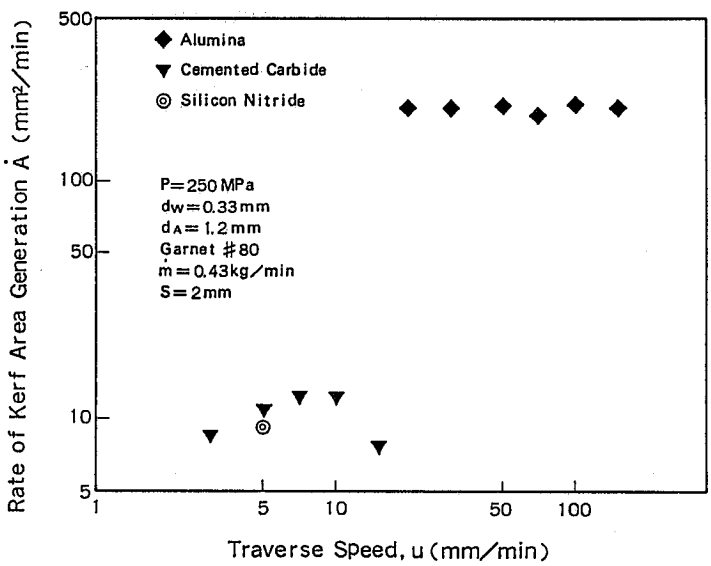

Fig.5 Relation between traverse speed and Ȧ (1)

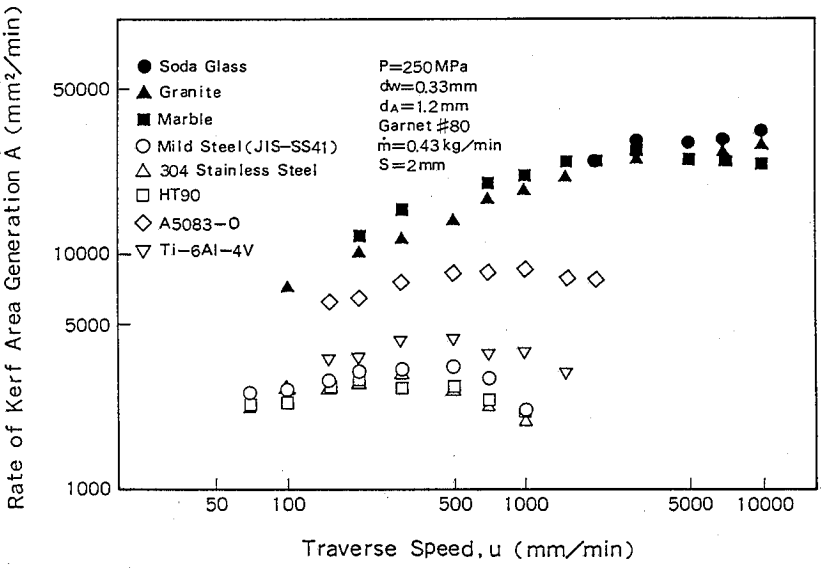

Fig.6 Relation between traverse speed and Ȧ (2)

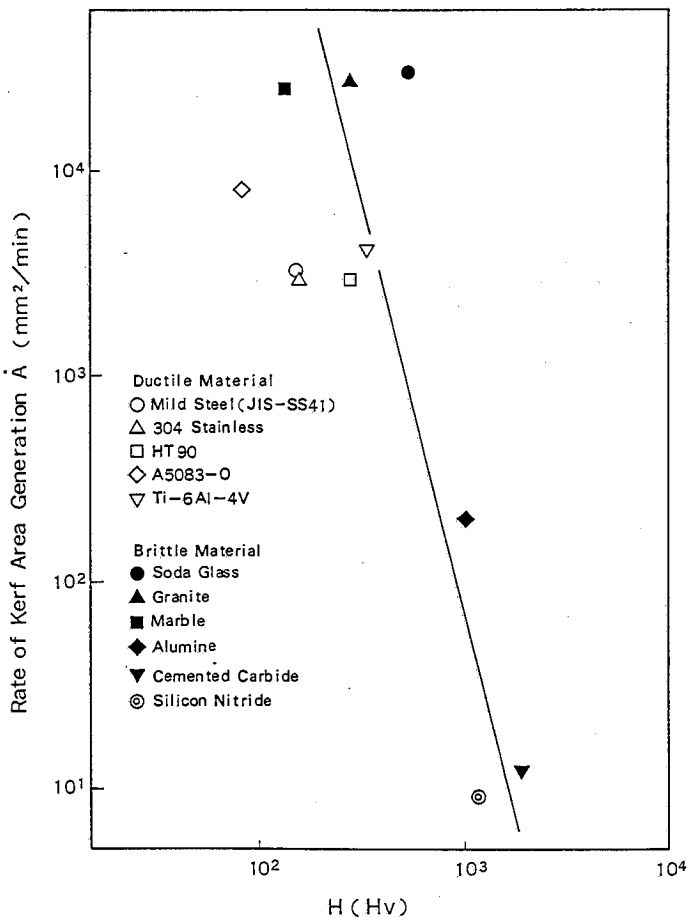

Fig.7 Relation between hardness (Hv) and A

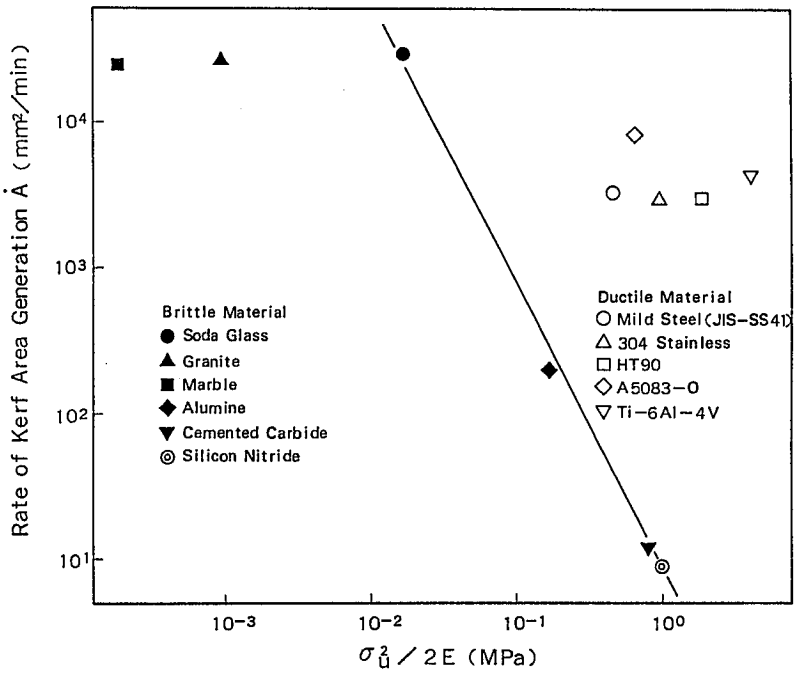

Fig.8 Relation between modulus of fracture and Ȧ

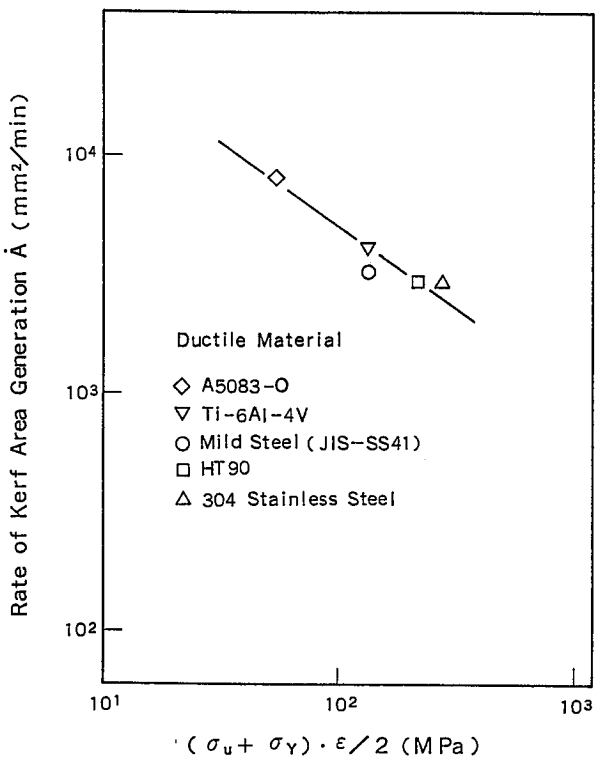

Fig.9 Relation between plastic deformation energy and Ȧ

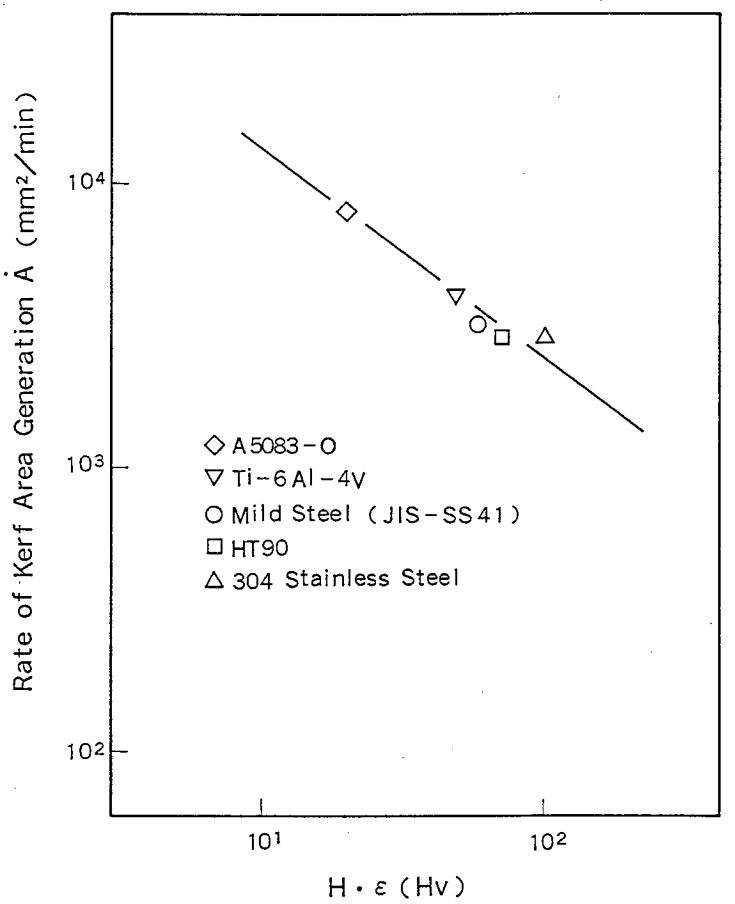

Fig.10 Relation between H・ε and Ȧ

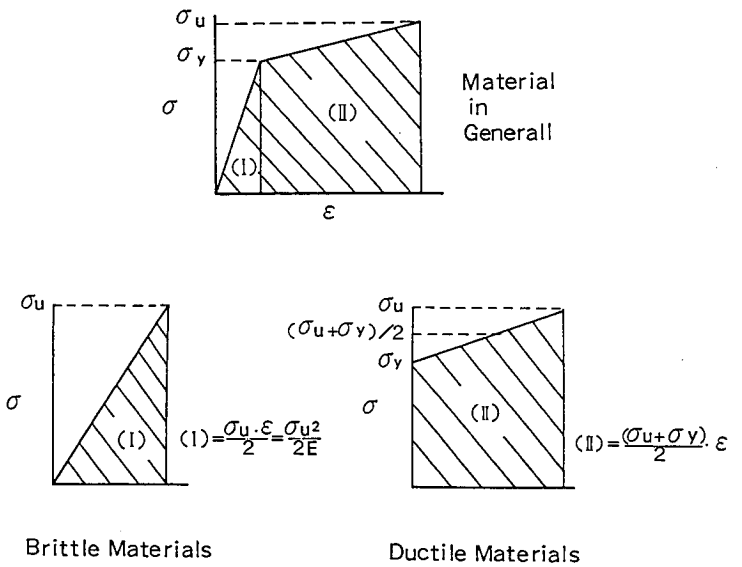

Fig.11 Schematic diagrams of absorbed energy on fracture

6th American Water Jet Conference
August 24 - 27, 1991: Houston, Texas Paper 4

A Study of a Leading Edge Profile for a Slot Formed During Hydro-Abrasive Cutting

Dr. M. Mazurkiewicz
University of Missouri-Rolla
Rock Mechanics & Explosives Research Center
Rolla, MO 65401, USA

ABSTRACT

Performance of the high pressure hydro-abrasive jet is examined from the point of view the rate of material removal by a single abrasive particle. The abrasive particle's interference with a sample material and leading edge of the cutting slot formation is discussed and a calculation is presented.

Organized and Sponsored by the Water Jet Technology Association.

1.0 INTRODUCTION

High pressure hydro-abrasive jets have demonstrated their cutting ability for various materials and are well accepted by a variety of different industries. The outstanding performance of recently developed cutting tools are well received, but the physics of the process is not yet understood.

The rate of material removal during cutting by hydro-abrasive jet is the summation of the microchips separated from the material being cut by each single abrasive particle colliding with the workpiece. The number of particles involved in the cutting process, the kinetic energy gained during the particle ejection, particle distribution in the jet cross section as well as abrasive material properties, particle size and geometry are the most vital parameters which need to be taken into consideration to predict the cutting result. The mechanical properties of the workpiece, traverse speed, stand-off distance, jet angle, and number of passes are also important in determination of the cutting results. Theoretically, it is a very complicated task.

Among the many parameters influencing cutting performance, the design parameters of the cutting head are also important and are not yet optimized. The cutting head design has an important influence on the acceleration of abrasive particles, the level of particle disintegration during ejection (Galecki) as well as particle distribution (Mazurkiewicz, 1987) in the jet cross section.

Analysis is required to understand the interaction of the abrasive particles with the workpiece. The stream of solid particles has received considerable attention in the past (Finnie, 1958; Finnie, 1972, Finnie, et. al., 1972; Finnie, et. al., 1967) and the prime motivation for erosion studies was the severe erosive wear that occurred in the equipment in many applications. From the hydro-abrasive cutting technology point of view, there is interest in creating the conditions where the erosion is as intensive as possible. The most basic equation established so far predicts that the volume removed by a rigid grain cutting into a ductile surface is essentially:

$$V = \frac{M\,U^2}{p}\,f(\alpha) \qquad (1)$$

where V is the volume removed from the surface, M the mass of eroding particles, U the particle velocity, p the horizontal component of flow pressure between the particle and the surface, and $f(\alpha)$ a function of the angle of impact measured from the surface to the particle velocity vector. According to this study, the volume removed is generally proportional to the mass of eroding particles and depends strongly on particle velocity. The velocity exponent ranges from 2.05 to 2.44 in different metals.

The particle's size does not have an influence on rigid particles, provided it is greater than 100 microns. The most impressive feature is that the variation of volume removal is a function of the impinging angle. The influence of impinging angle on the material erosion is demonstrated in Figure 1 for ductile and brittle materials. The erosion peak for ductile materials is in the range of 15 to 20 degrees, and for brittle materials, the peak is observed at approximately 90 degrees.

2.0 FINNIE'S CUTTING ANALYSIS

The following assumptions represent the single grain cutting analysis (Finnie, 1958; Finnie, 1972, Finnie, et. al., 1972; Finnie, et. al., 1967) for the configuration presented in Figure 2.

1. Material is attacked and removed by rigid particles which do not fracture during collision.

2. There is no initial rotation of the particles, which represents rather average conditions, i.e. $\Phi_o = 0$.

3. The ratio of the vertical force to the horizontal force during cutting is taken as a constant K. By analogy to the grinding and scratching tests, a reasonable value is K = 2.

4. A constant plastic flow pressure exists during cutting and its horizontal component is denoted by p.

5. Based on metal cutting and scratching observation, the depth over which metal contacts the particle is taken as twice the depth of cut, i.e., $\Psi = L/Y_T = 2$. This is the condition required to form a chip.

6. The volume removed is the product of the area swept out by the particle edge with the width b, i.e.

$$\text{Volume} = b \int Y_T \, dX_T = b \int_{}^{t_c} Y_T \, \dot{X}_T \, dt \qquad (2)$$

where dt is the time at which cutting ceases and the dot denotes differentiation with respect to the time t.

7. A final assumption is that because the depth of cut is small compared with the particle size, the vertical and horizontal forces on the particle are taken to be located at its tip. This assumption leads to an equation of motion in the X, Z, and Φ directions and the volume removal determined.

Based on the above assumption, and taking the origin of coordinates at the particle center of gravity and referring to Figure 2, an equation of motion was written as follows:

$$m \ddot{y} + p K \Psi b y = 0$$

$$m \ddot{x} + p \Psi b y = 0$$

$$I \ddot{\phi} + p \Psi b r y = 0 \qquad (3)$$

where m, I and r are the mass, moment of inertia, and distance from the center to the edge of the particle, p is the constant horizontal component of the contact stress. In the second quantity of each equation, we have taken $Y_T = y$ and in the third equation the vertical component of the moment applied to the particle is neglected. In the third equation, r is largely compared to y as indicated by experiment.

Equation (3) solved for boundary conditions resulted in

$$y = \{(V \sin \alpha)/\beta\} \sin \beta t$$

$$x = \{(V \sin \alpha)/\beta K\} \sin \beta t + (V \cos \alpha t) - \{(V \sin \alpha)/K\} t$$

$$\phi = \{(m r V \sin \alpha)/\beta K I\} [\sin \beta t - \beta t] + \dot{\phi}_o t \qquad (4)$$

where $b = \sqrt{p \Psi b K/m}$. V is the particle velocity, ϕ its angle of impingement, and $\dot{\phi}_o = 0$ at $t = 0$.

Finnie's analysis finally leads to the following equations:

$$W = (\rho/\Psi p) MV^2/2 (\sin 2\alpha - 3 \sin^2\alpha); \alpha \leq 18.5^\circ \qquad (5)$$

$$W = (\rho/\Psi p) MV^2/6 \cos^2\alpha; \alpha \geq 18.5^\circ \qquad (6)$$

The influence of K on the angle for maximum erosion is not significant. For K = 1.3, 2.0, 2.5, the corresponding maximum erosion occurs at approximately 13, 15, 17, 20 degrees. These results compare quite well with the experimental results for carbon steel, copper, and aluminum when silicon carbide particles were used.

The analysis predicts a weight loss proportional to the square of the particle velocity. Figure 3 shows the weight loss as a function of particle velocity for 46 mesh silicon carbide particles eroding annealed SAE 1020 steel. A curve corresponding to $W \quad V^2$ gives a reasonable fit to the data for the range of the velocities shown.

3.0 NUMERICAL PREDICTIONS OF THE WEIGHT LOSS

Equations (5) and (6) predict the weight loss of a surface eroded by grains for K = 2. In practice, we would expect this to overestimate the weight loss as some grains will strike on flat faces, unable to cut, others will fracture instead of cutting, and still others may strike rebounding grains. This reservation was

suggested by reduction of the predicted erosion by 50%, The ratio $\Psi = L/Y_T$ (see Fig. 2) is also an unknown quantity, but by analogy to the metal cutting experiments, a reasonable value is about 2. Taking these assumptions into equation (5), it was found that the volume (W/ρ) removed at angles of about 20 degrees is:

$$W/\rho = 0.1\ (M\ V^2/2)\ 1/p \qquad (7)$$

This means that about 10% of the particle kinetic energy divided by the horizontal component of the stress on the face of the abrasive grains, gives the volume removed. The quantity p, which was assumed to be constant, is related in some way to the plastic flow stress of the material. It is expected that the flow stress in erosion to be considerably greater than that obtained in conventional tension or hardness test.

4.0 THE EFFECT OF PARTICLE ROTATION

Initial rotation of the grain was easily incorporated into the analysis. For such a situation, erosion will now occur and the attack angle will be 90 degrees. In Figure 4, the result of assuming an "omega" distribution for initial rotation is shown (Finnie, 1972). The angle at which maximum erosion occurs is slightly higher than for a nonrotating particle.

5.0 PARTICLE SIZE

One of the most intriguing aspects of erosion is that the mass of the sample removed by a particular mass of the abrasive particles is not dependent on the particle size, if the particle size is bigger than 100 microns. For particle size below this size, erosion is less and less efficient as the particle size is decreased (Sheldon). The physical reason for this effect is not clear. It might be that the fragmentation of larger particles leads to more efficient cutting than occurs with smaller particles, that the geometry of the cutting process changes when smaller particles are used, that the grain size of the metal eroded is a factor, and possibly oxide coating on the metal erodes too.

6.0 PARTICLE SHAPE AND STRENGTH

The analysis of ductile erosion presented (Tilly) is based on rigid abrasive particles that do not fracture during cutting. While most of the work was carried out with angular silicon carbide grains, the same tests carried out with rather more "blocky" aluminum oxide grains gave very similar results. The analysis could be extended to rigid particles of other shapes, again excluding fracture of the particle, by selecting appropriate K and I. It was proven, from experimental work (Tilly), that particle shape and strength play a role in erosion and in particular, it was seen that the fracture of the particle may drastically change the shape of the curve of volume removal as a function of angle.

7.0 EROSION BY THE STREAM OF SOLID PARTICLES

The results of the experimental work (Neilson) for the erosive action of a particle-laden gas stream on the specimen material indicate that the relation between the erosion and the attack angle have the same character as for the single grain test reported in the literature. For example, in Figure 5, erosion versus attack angle data are presented for aluminum eroded by 210 micron aluminum oxide particles at 129.3 m/s. It can be noticed that the maximum erosion occurred in the same angle range as was reported earlier for single grain tests.

Little effect of particle concentration on erosion has been reported. No satisfactory explanation for this phenomenon has yet been presented.

The results of single particle erosion tests reported in the literature and partially presented above is an excellent base for better understanding the mechanism of high pressure hydro-abrasive jet cutting. The data generated during single grain tests needs to be carefully adopted, due to a rather significant difference in collision velocity in the single grain test and high pressure hydro-abrasive jet cutting. As was previously noted, the volume removed is the function of the collision velocity, and the effect of particle shattering, and the secondary erosion thus produced, can be significantly higher at increased velocity. Also the maximum depth of cut by a single grain could be higher at increased velocity.

8.0 HYDRO-ABRASIVE JET CUTTING MECHANISM

To incorporate the results generated for single grain collision, for hydro-abrasive jet cutting model explanation, first of all, the basic analysis needs to be conducted to establish the range of angles in which the abrasive particles carried by the hydro-abrasive jet are striking the leading edge of the gap being cut. The actual variation in angle depends on the nozzle characteristics and on interaction of the particle and fluid stream outside the nozzle. It was observed in practice (Finnie, 1958; Finnie, 1972; Finnie, et. al., 1972) that the distribution of particle angles leaving the nozzle, is extremely small. The extreme variation was approximately $\pm$ 3 degrees. However, rebounding grains may deflect arriving grains and lead to erosion at a variety of angles. It is certain that grain/sample interaction is not organized and uniform. In average hydro-abrasive cutting conditions, the sample surface is attacked by the stream of particles with such a small clearance distance that chain collisions are unavoidable.

A schematic picture of the event is presented in Figure 6, showing the position of the single grain colliding with the gap leading edge. According to the direction in which grain is moving and its velocity, and the sample traverse rate, the contour of the gap leading edge can be predicted and the grain attack angle estimated. This angle varies along the gap contour. The small attack angle is observed in the top of the specimen and, when the grain energy is not high enough to cut through, this angle increases significantly

up to 90 degrees. For cutting thin plates through, the observed angle should be in the narrow range of the small angle.

Different attack angles mean a different mass of material separated from the sample. So, material removal effectiveness of defined jet parameters and specified traverse rates is a function of the distance from the nozzle to the sample top surface. Standoff distance is also important because the stream of grains spreads and intra-stream collisions diminish the kinetic energy of individual grains.

Abrasive particle interference with sample material can be in the few different kinematic schemes presented in Table I. Abrasive particle rotation during collision with material is possible but the weight loss angle relation (see Fig. 4) for a single grain is not significant and the main volume removed is due to the nonrotating particles. It is very hard to predict which model is dominant or what combination of such models really exists. It is also difficult to verify the models experimentally.

Based on the abrasive particle spacing in the hydro-abrasive jet calculation (Mazurkiewicz, 1989), analysis can be conducted on the jet and single abrasive particle performance for most typical cutting conditions. For that reason, a schematic of particle orientation during cutting was prepared (Fig. 7). For calculation, the following was assumed, jet generating pressure 138 MPa, water nozzle diameter 0.35 mm, Idaho garnet mesh no. 36, with feed rate of 910 g/min, which corresponds to particle average size 425 microns. The material selected was aluminum and the sample traverse speed was 5 mm/sec. For an abrasive nozzle diameter of 1.5 mm, the expected abrasive jet velocity is about 200 m/sec.

Assuming that all the particles are the same size and spaced uniformly (Mazurkiewicz, 1989), and that all of the particles colliding with the workpiece separate a microchip, material removal weight shows very close results to the calculation performed according to the Finnie's equation.

For the data presented, the above calculation shows that 3.30 columns of abrasive particles are taking part in removing material. For one second of operation, as many as 925,666 particles collide with the material and the material removed, calculated for the traverse rate (5 mm/sec) was a 83.83 mm^3. The average depth of cut performed by a single grain is 0.2 microns and the weight of a single chip is 0.244 10^{-6} g.

The step-by-step calculation is shown in Table II.

9.0 LEADING CUTTING EDGE PROFILE

The instantaneous leading edge of the cutting profile formed by a hydro-abrasive water jet for particular operational parameters is a result of material microchipping out from the workpiece. Following the geometric change of the leading profile affords an understanding of the mechanism of the material removal from the

cutting zone. Work performed so far conducted at the Rock Mechanics and Explosives Research Center is described below.

The operational cutting parameters applied to 38 mm thick aluminum plate were varied in these tests; the pressure generated jet 210 MPa and 280 MPa, traverse speed steady - 50 mm/min and the abrasive feed rate - 208, 368, 372, 550, 1112, and 1140 g/min. The generated cutting cross sections were measured and equations were established. Examination of these profiles revealed several results (see Fig. 8) which are quite understandable from the single abrasive grain work point of view. First, the leading profile gets flatter as the pressure of the jet increases (compare plots #2 and #1, #3 and #4, #6 and #5) for a set traverse speed and abrasive rate. The cutting profile was expected to become flatter as the abrasive rate increased for a set of pressure and traverse speed (see plot #2, #3, #6, and #7, #8, #9, and #1, #4, #5). This expectation was proved for lower abrasive feed rate. For high feed rate, such as the level of 1112 g/min and 1140 g/min, the profile became more curved (see plot #6 and #5). These results can be interpreted that the number of the abrasive grains supplied into the jet is too high and the mutual disturbance is significant. This makes a cutting profile more typical of low abrasive feed rates. It is illustrated by tests #6 and #5.

10.0 CONCLUSIONS AND REMARKS

Based on the approach described in this paper, the following conclusions and suggestions can be formulated:

* Based on the average particle size, its average velocity, average attack angle for given geometrical jet parameters, material size, traverse rate and its specific plastic flow pressure, it is possible to calculate the weight loss with reasonable agreement to Finnie's equation.

* Material removal by single abrasive grain depends very strongly on the attack angle. Even a small attack angle increase (up to 18.5 deg) causes a significant increase in material removal rate.

* The leading cutting gap profile is a good source of information for operational parameters evaluation. This needs further study with respect to the abrasive particle attack angle.

* Material removal by the hydro-abrasive jet mechanism is very complicated and requires more attention in optimization work. Special attention should be devoted to the measurement of particle velocity. This is the strongest parameter, on which the cutting effect depends.

ACKNOWLEDGEMENTS

I would like to take the opportunity to thank my students, Mr. Kenneth Nicholas and Mr. Joseph Rapp for conducting a series of tests relating to the effect of jet deflection.

REFERENCES

1. Finnie, I., "Some Observation on the Erosion of Ductile Metals", Wear, 19, (1972), Elsevier.

2. Finnie, I., "The Mechanism of Erosion of Ductile Metals", Proceedings of the Third U.S. National Congress of Applied Mechanics, Brown University, Providence, R.I., June 1958.

3. Finnie, I., Wolak, J., Kabil, Y., "Erosion of Metals by Solid Particles", ASTM Journal of Materials, September 1967, Vol. 2, No. 3.

4. Finnie, I., McFadden, D.H., "On the Velocity Dependence of the Erosion of Ductile Metals by Solid Particles at Low Angles of Incidence", Wear, 48, (1972), Elsevier.

5. Galecki, G., Mazurkiewicz, M., Jordan, R., "Abrasive Grains Disintegration Effect During Jet Ejection", International Water Jet Symposium, Beijing, China, September 1987.

6. Mazurkiewicz, M., "Single Abrasive Particle and High Pressure Hydro-Abrasive Jet Performance Study", SME International Conference and Exposition, May 1989, Detroit, MI.

7. Mazurkiewicz, M., Olko, P., Jordan, R., "Abrasive Particle Distribution in High Pressure Hydro-abrasive Jet", International Water Jet Symposium, Beijing, China, September 1987.

8. Neilson, J.H., Gilchrist, A., "Erosion by a Stream of Solid Particles", Wear, 11, (1968), pp 111-122.

9. Sheldon, G.L., Finnie, I., Trans. ASTME, 83B, (1966), pp 387-392.

10. Tilly, G.P., Wear, 14, (1969), pp 241-248.

NOMENCLATURE

α^{o} - angle of impingement
v - volume removed from the surface
M - mass of the ending particle
U - the particle velocity
W - weight
b - particle edge with
ρ - density
m - mass
I - moment of inertia
r - distance from the center of the edge
K - ratio of the vertical force to the horizontal force
p - plastic flow
y_T - depth of cut
L - depth of the metal contact with the particle

Table I. Possible interaction between single abrasive particle and the leading edge gap.

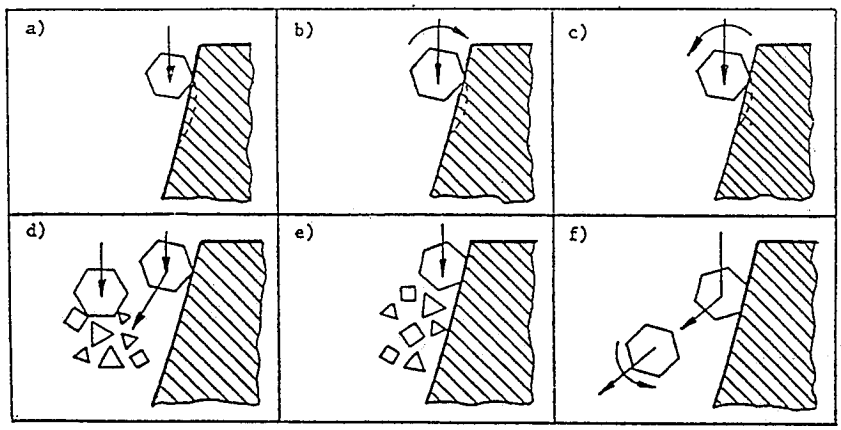

a) traversing, non-rotating particle separating chip from the sample
b) traversing and clockwise rotating particle separating chip from sample
c) traversing and counter clockwise rotating particle separating chip from sample
d) rebounding particle struck by the oncoming particle
e) particle crushed on sample surface, possible chip separation
f) rebounding particle and imposed rotation

TABLE II. Material removal by single abrasive grain, calculation procedure.

1. Cutting conditions:

d	-	jet diameter - 1.5 mm
v_t	-	traverse rate - 5 mm/s
t	-	workpiece thickness - 10 mm
v_a	-	abrasive particle velocity - 200 m/s
d_a	-	abrasive particle average diameter for garnet mesh no. 36 - 425 microns
l_a	-	spacing between particles - 288 microns[10]
material :		aluminum - $\rho = 2.7$ g/cm^3
p	-	aluminum plastic flow - 1,380 MPa

2. Abrasive particles spacing

$$l = d_a + l_a$$

$$l = 0.425 + 0.288 = \mathbf{0.713}\ \text{mm}$$

3. Number of columns formed by abrasive particles on the half of the front jet periphery (see Fig. 7)

$$n_v = \frac{\pi \cdot d}{2l} = \frac{\pi \cdot 1.5}{2 \cdot 0.713} = \mathbf{3.30}$$

4. Number of particles in a column for one second cut

$$n_h = \frac{v_a}{l} = \frac{200{,}000}{0.713} = \mathbf{280{,}505}$$

5. Volume of material eroded during one second action (see Fig.7)

$$V_c = [(d \cdot s_t) + \frac{\pi \cdot d^2}{4} \cdot \frac{1}{2}] \cdot t$$

$$V_c = [(1.5 \cdot 5) + \frac{\pi \cdot 1.5^2}{4} \cdot \frac{1}{2}] \cdot 10 = 83.83 \text{ mm}^3$$

6. Number of the grains involved in the volume (83.83 mm^3) eroding process

$$n = n_v \cdot n_h = 3.30 \cdot 280{,}505 = \mathbf{925{,}666} \text{ grains}$$

7. Volume eroded by single grain

$$V_g = \frac{V_c}{n} = \frac{83.83}{925{,}666} = \mathbf{9.056 \cdot 10^{-5}} \text{ mm}^3/\text{grain}$$

8. Weight eroded by single grain

$$W = V_g \cdot \rho = 9.056 \cdot 10^{-5} \cdot 2.7 \cdot 10^{-3} = \mathbf{0.244 \cdot 10^{-6}} \text{ g}$$

9. Weight eroded by single grain calculated according to equation (5)

$$W = \left(\frac{\rho}{\Psi \cdot p}\right) \cdot \frac{M \cdot V^2}{2} \cdot (\sin 2\alpha - 3 \sin 2\alpha)$$

for average attack angle assumed $\alpha = 0.5^0, 1.0^0, 2.0^0, 3.0^0$, $\Psi = 2$, and single grain weight $1.5274 \cdot 10^{-4}$ g[10],

$W_{\alpha = 0.5^0} = \mathbf{0.515 \cdot 10^{-6}}$ g
$W_{\alpha = 1.0^0} = \mathbf{0.935 \cdot 10^{-6}}$ g
$W_{\alpha = 2.0^0} = \mathbf{1.648 \cdot 10^{-6}}$ g
$W_{\alpha = 3.0^0} = \mathbf{2.144 \cdot 10^{-6}}$ g

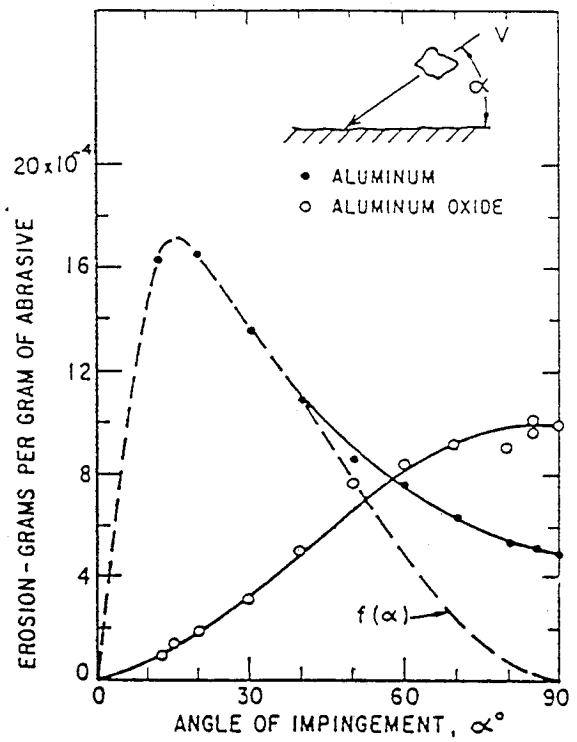

Figure 1. Weight removed by erosion as function of angle of impingement for 1100-0 aluminum and high density aluminum oxide.

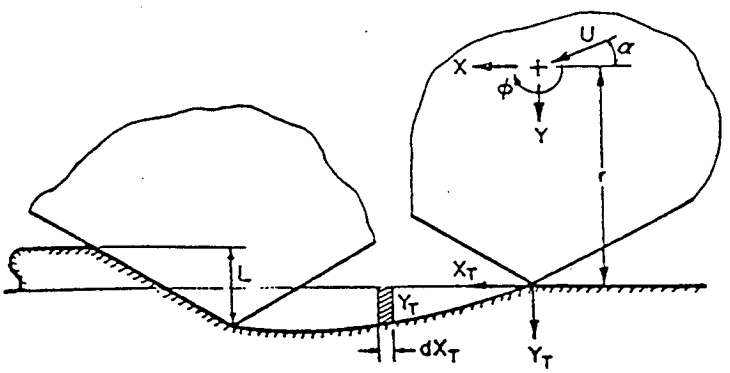

Figure 2. An idealized two-dimensional model of a rigid grain cutting into a ductile metal.

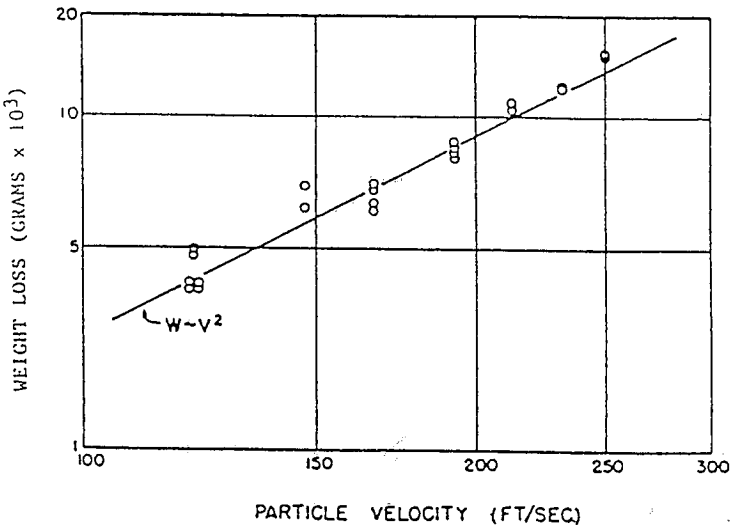

Figure 3. Weight loss of annealed SAE 1020 steel as a function of particle velocity. Abrasive, 20 grams 46 mesh silicon carbide; angle, 20°.

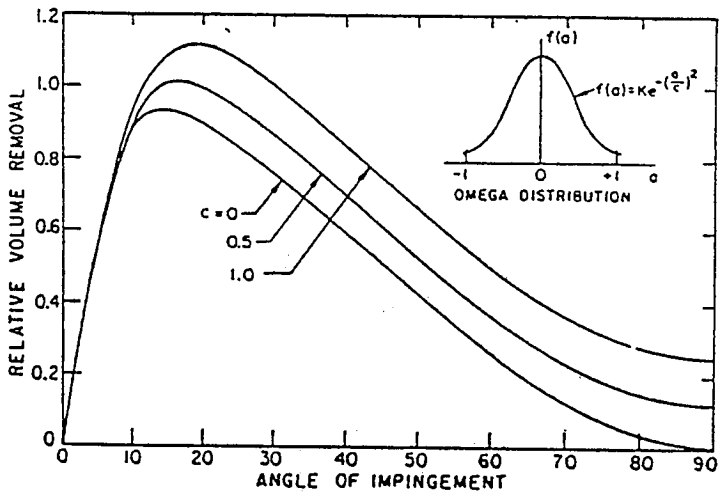

Figure 4. Influence of rotation on weight loss-angle relation. The assumed distribution for the dimensionless rotation parameter $a = \phi_o r/U$ is also shown.

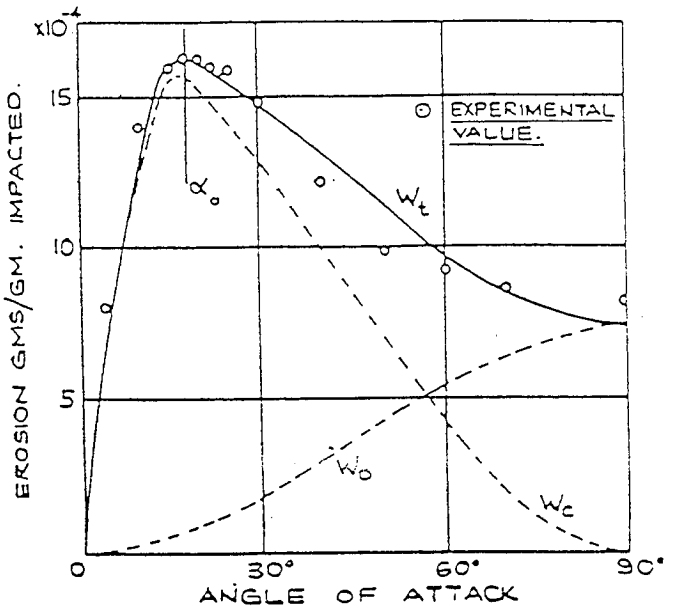

Figure 5. Erosion vs. angle of attack characteristic for aluminium eroded by 210 μ aluminium particles at 129.3 m/sec.

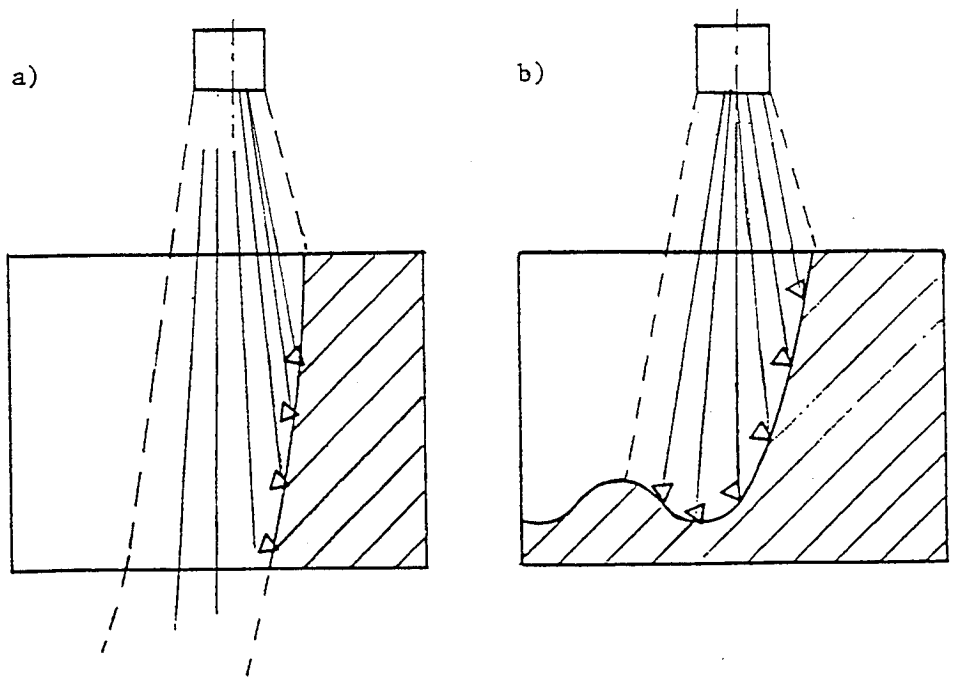

Figure 6. Expected collision angle between single grains and leading of the gap. a) able to cut through b) no able to cut through.

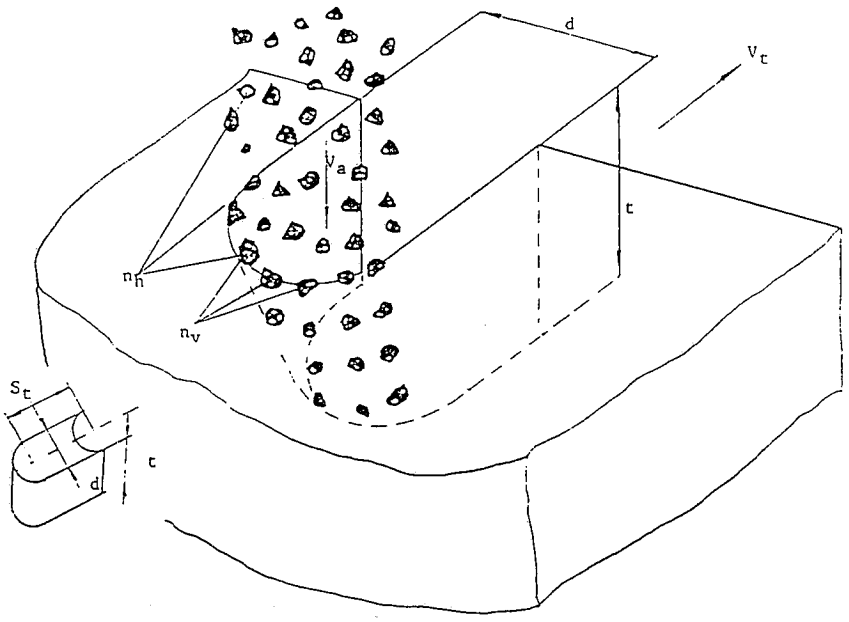

Figure 7. Schematic diagram of the hydro-abrasive jet interaction with material.

- d - jet diameter
- t - material thickness
- V_t - workpiece traverse rate
- S_t - workpiece displacement in one second
- n_h - number of particles in one column
- n_v - number of columns involved in cuttin;

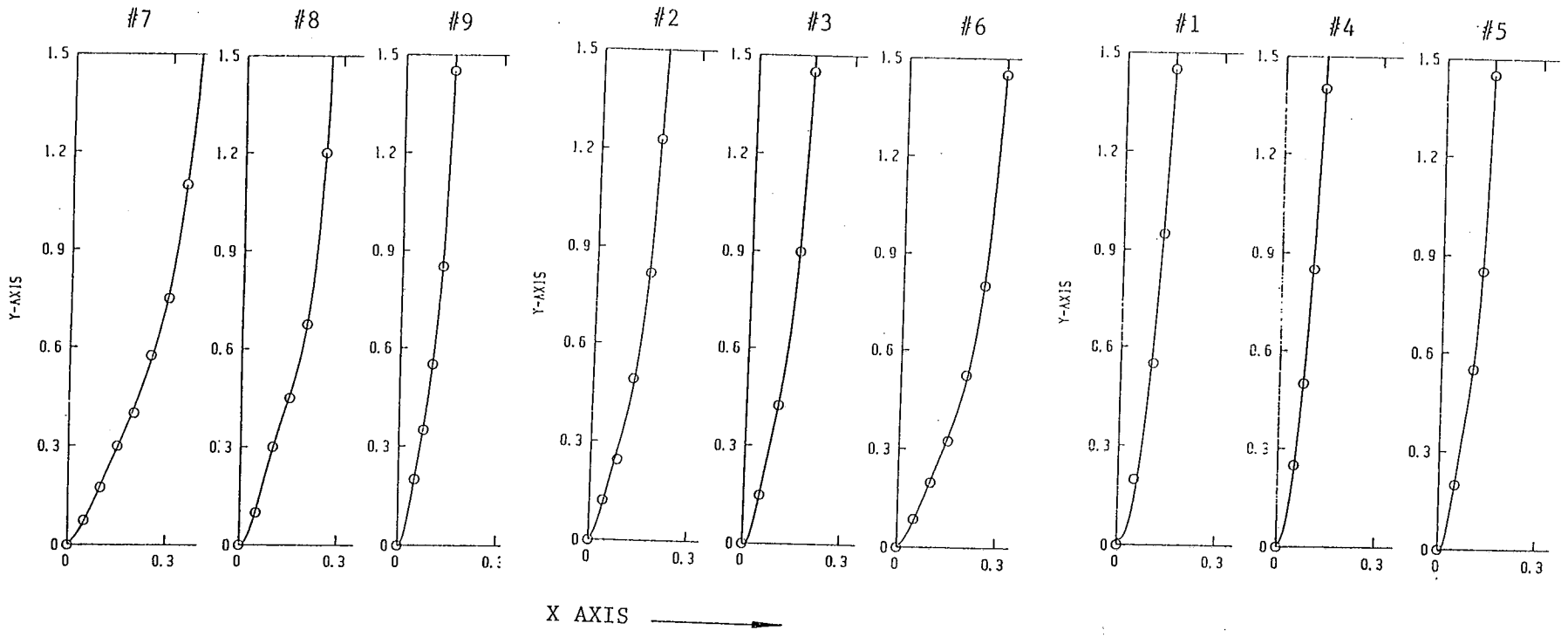

Pressure: MPa	280	280	280	210	210	210	280	280	280
Abrasive Feed Rate: g/min	368	550	1140	208	372	1112	208	372	1112

Figure 8. Leading edge profile formed during hydro-abrasive cutting of aluminum sample 1.5 inches thick for indicated parameters. Traverse rate: 2 ipm; Abrasive: garnet mesh #60; Nozzle combination: 0.011/0.038.

Abstract for
6th American Water Jet Conference
August 24-27, 1991
Houston, Texas

EFFECT OF TARGET MATERIAL IN ABRASIVE WATERJET TURNING

Mohamed Hashish
Senior Research Scientist

Ajmal Ansari
Research Scientist

QUEST Integrated, Inc.
Kent, Washington 98032

An experimental investigation to determine the influence of target (specimen) material on turning by abrasive waterjet was conducted. The materials that were tested include 6061 aluminum, 642 aluminum-bronze, 304 stainless steel, 15-5 stainless steel, magnesium boron carbide, aluminum silicon carbide, magnesium silicon carbide, iron-tungsten carbide, zirconia, and Rene'41. The effects of depth of cut and traverse speed on volume removal rate are presented. Some results relating to dependence of volume removal rate on abrasive mass flow rate are also included. Significant mechanical properties that influence the volume removal rate of the target material in abrasive waterjet turning are identified to help in formulating an erosion resistance parameter that will be useful for predictive and modeling purposes.

Organized and Sponsored by the Water Jet Technology Association.

6th American Water Jet Conference
August 24 - 27, 1991: Houston, Texas Paper **6**

An Advanced System for Rock Tunneling – Results from a Field Experiment

Michael Hood, Xiaohong Li, and Peter Salditt
University of California, Berkeley

Geoffrey Knight
Mining and Construction Technologies, Inc.

ABSTRACT

Results are presented from an ongoing field experiment that is being conducted at a tungsten mine in the Sierra Nevada mountains in California. The purpose of this experiment is to demonstrate the benefits of a novel design of full-scale, boom-type tunneling machine and to show that this novel system can cut effectively and economically in hard rock formations.

A principal, and a key, feature of this cutting system is the use of moderate pressure water jets to assist the drag bit cutting tools. Jet assisted cutting is not new but, in the past, difficulty has been experienced in reproducing in the field the substantial benefits of this cutting method that are observed when experiments are conducted in the laboratory. One popular suggestion for this discrepency is that the tool velocity on most practical rock excavation machines is much higher than the tool velocities employed during the laboratory experiments and that, somehow, this accounts for the reduced benefits of jet assisted cutting on field machines. Other workers have suggested that in most of the field experiments conducted to date, inadequate attention has been paid both to the position(s) of the jet(s) with respect to the cutting tool, and to the need to increase the jet power proportionally with the increase in tool velocity.

The current field trials program sets out to resolve these questions. The results show that when attention is paid to proper jet placement and when appropriate values for jet pressure and jet flow rate are employed the benefits of jet assisted cutting on full-scale mining and tunneling machines are dramatic. Not only are the forces acting on the tools reduced substantially but the cooling effect of the jets greatly reduces tool wear. This combination of reduced forces and wear enable drag bits to be used to cut much stronger rock.

1. INTRODUCTION

1.1 Previous work with Jet Assisted Cutting

In this cutting method one or more water jets at moderate pressure (35-150 MPa) are directed immediately adjacent to a mechanical tool during the rock cutting operation. When appropriate jets are employed in this manner they serve to continuously flush away the crushed rock from the region adjacent to and beneath the cutting tool (Figure 1). This enables the tool to bear directly against the intact rock surface; this has the effect of reducing the tool forces necessary to induce fracture of the rock. Many research workers have demonstrated these tool force reductions in laboratory experiments (Hood, 1976; Ropchan, 1980; Dubugnon, 1981; Fenn, 1985). These jets also serve to cool the tool (Hood, 1978; Nienhaus *et al.*, 1986) and this has the effect of substantially increasing tool life by reducing tool wear (Anon., 1982; Morris and Harrison, 1985; Morris and MacAndrew, 1986). Other advantages claimed for this jet assisted cutting method include dramatic reductions in dust at the working face and substantial reductions in frictional sparking.

Since these benefits should lead to both increased productivity and improved health and safety one might have expected that this cutting method would have found widespread acceptance by industry. This has not happened. Although attempts have been made to install water jet assisted cutting systems on commercial excavation machines these, generally, have not succeeded in reproducing the main benefit of reducing tool forces. Today the commonly accepted view is that low pressure (10-20 MPa) water jets are useful for dust suppression and perhaps even for enhancing tool life but the moderate pressure systems are inadequate to reduce tool forces on full-scale production machines. The explanation for the discrepancy between the laboratory and the field results is attributed to the higher cutting tool velocities and the higher depths of cut taken by the tools on the field machines.

This conclusion, that the main benefits of jet assisted cutting necessarily are lost at high cutting tool velocities and high cut depths, is controversial. If it could be shown that jet assisted cutting can be effective in reducing tool forces on full-scale production machines then this technology would enhance the performance of all rock cutting machines and drills. This, however, is not the main benefit that would be realized from the successful development of this cutting technology. If the levels of tool force reduction observed in the laboratory experiments could be reproduced in the field then this would lead to the development a new generation of machines capable of excavating in rock that currently has to be mined by the traditional drill-and-blast method. These machines would find markets in surface and underground mining and in tunneling.

2. EXPERIMENTS

2.1 Objectives

1. To test the hypothesis that if proper attention is paid to the position of the water jets with respect to the rock:tool interface and if the levels of jet power are increased appropriately to compensate for (i) increases in the depth of cut taken by the cutting tool and (ii) increases in tool velocity, then the benefits of substantial reductions in tool forces are preserved.
2. To demonstrate that a purpose-designed, rigid, rock cutting test rig equipped with an appropriate water jet system to assist the cutting operation is capable of extending significantly the range of rocks that can be cut economically with a drag bit machine.

2.2 Apparatus

The test rig being used for these trials is shown in Figure 2. It is a boom-type machine capable of excavating a tunnel 5 m high and 4.3 m wide. It is fitted with a cutter head 0.9 m in diameter (bit tip to bit tip) and this head is powered through a mechanical gearbox with a 112 kW electric motor. The gearbox has a two speed drive giving the tool cutting velocities of 0.78 and 1.41 m/s. The test rig is skid mounted and has a mass of 40 t. During the cutting operation the rig is anchored in the tunnel between the hanging and footwall with a roof canopy that is activated hydraulically. Unlike a conventional roadheader this test rig has four hydraulic rams attached to the cutter boom (Figure 2). These serve to stabilize the boom during the cutting operation. The cutter head is fitted with 17 drag bits. Five of these bits, on the nose of the head, are conventional point-attack picks. These are used primarily for sumping. The remaining twelve bits are patented, jet assisted cutting tools. Two moderate pressure (70 MPa) water pumps provide water to the bits. The total water jet power to the cutter head is 140 kW.

2.3 Instrumentation

The rig is fully instrumented. Data from the sensors on the rig is taken to a computer located in an instrument shed adjacent to the test rig in the mine (Figure 3). Measurements that are made during the cutting operation include:

1. The power to the cutter motor. This information is used to calculate the average torque at the cutter head.
2. The pressures in the hydraulic rams attached to the boom. This data is used to calculate the average thrust force on the cutter head.
3. The angular position of the cutter head. This information is required to calculate the thrust on the head.
4. The pressure of the water jets. This information, together with a knowledge of the numbers and sizes of the water jet nozzles on the head, is used to calculate the flow rate of the jets and hence the jet power.
5. A telemetry system has been purchased and it is planned to strain gauge on the the cutting tools and use this telemetry system to monitor the three orthogonal force components acting on an individual tool during the cutting process.

2.4 Procedure

Before cutting tests are commenced the rock face is mapped. Six methods are used to evaluate the nature, the strength, and the competence of the rock:

1. The hardness of the rock minerals is determined using a knife scratch test. This test determines whether the Moh's hardness is greater than or less than 5.2.
2. The indentation hardness of the rock is determined using a Schmidt hammer.
3. The compressive and tensile strengths of the rock are determined from cores samples. These samples are drilled at strategic points in the face.
4. The mineralogy is determined using thin sections. These sections are made from chip samples taken from the face.
5. The presence or absence of calcium carbonate in the rock is determined by observing whether the rock effervesces when drops of dilute hydrochloric acid are poured onto the face.
6. The rock competence is determined by mapping the face for fractures prior to each cutting operation.

First the cutter head is sumped into the face to a predetermined depth so that a known number of tools are engaged in cutting the rock. The instrumented cuts then are made by shearing the cutter head through a horizon in the face where the rock conditions are fairly homogeneous. Before the instrumented cut is made the desired pressure for the water jets is set at the two high pressure pumps. The desired water jet flow rate at this operating pressure is obtained by appropriate adjustment of the number and diameter of the water jet nozzles.

2.5 The Rock

The rock face that is being cut is located in a contact metamorphic zone and it consists of a mixture of medium strength (60-120 MPa) marble and very strong (170-240 MPa), highly abrasive hornfels.

3. RESULTS

The results obtained to date in these trials are dramatic. Initially we attempted to sump the cutter head into the hornfels with the point-attack bits. These attempts resulted in immediate failure of the bits with no visible damage caused to the rock face. These five sumping, point-attack bits are not jet assisted but cooling to these bits was provided by low pressure, high volume flow through a 30 mm diameter water hose. Despite the high flow rate of this water cooling stream these bits failed by melting in less than one minute. It is possible to sump the head with these non-jet assisted bits in the weaker layers of the marble, however even in this rock the cutting rate needs to be kept very low in order to prevent causing damage to the bits.

Once the head has been sumped the vast majority of the rock is excavated in the shearing cuts and this is machined mostly by the jet assisted cutting tools. Provided that adequate power is delivered to the individual cutting tools we experience no difficulty in cutting the competent marble. Consistently we are able to achieve a depth of cut per revolution of the cutter head of 60 mm in marble. Furthermore, we are able to cut the strong abrasive

hornfels but more slowly, typically using a 5 mm cut depth. The use of drag bits in rock this strong and abrasive is unprecedented.

4. CONCLUSIONS

The program, to date, has been successful in that both of the original objectives have been met. We have demonstrated that a system of water jet assisted cutting can successfully be employed on full-scale mining systems and produce substantial reductions in tool forces, as well as the other benefits of improved tool life and elimination of dust and frictional sparking, when appropriate attention is paid to the position(s) and the power of the water jets.

We conclude that the technology now exists to extend the range of rocks that can be cut with drag bit machines from the present limit of rocks with a uniaxial compressive strength, C_0, of 80 MPa to those with a value of C_0 of approximately 170 MPa. This technological advance is made possible though a combination of an appropriate water jet system to assist the cutting operation and a cutting machine with a rigid drive to the cutter head, capable of taking deep, widely-spaced cuts at low rotational cutting speeds.

5. ACKNOWLEDGEMENT

These field trials are funded by the California Department of Commerce, under the California Competitive Technology program, and by Mining and Construction Technologies, Inc..

6. REFERENCES

Anonymous, Field trials with a 10,000 psi prototype system,*Seminar on Water Jet Assisted Roadheaders for Rock Excavation,* sponsored by the U.S. Dept. of Energy and the U.K. Natl. Coal Board, Pittsburgh, PA, May 26-27, 1982.

Dubugnon, O., An experimental study of water assisted drag bit cutting of rocks, *Proceedings of the 1st U.S. Waterjet Symposium,* Golden, CO, April, 1981, II-4.1-II-4.11.

Fenn, O., The use of water jets to enhance the performance of free rolling cutters in hard rock, D. Eng. thesis, Rand Africaans University, South Africa, 1985.

Hood, M., Cutting strong rock with a drag bit assisted by high pressure water jets, *Journal of the South African Institution of Mining and Metallurgy,* 1976, 77, **4**, 79-90.

Hood, M., A study of methods to improve the performance of drag bits used to cut hard rock, Ph.D. thesis, University of the Witwatersrand, South Africa, 1978.

Morris, A.H. and Harrison, W., Significant advance in cutting ability - roadheaders, *Proceedings Rapid Excavation and Tunneling Conference,* New York, NY, June 16-20, 1985, **1**, 317-340.

Morris, C.J. and MacAndrew, K.M., A laboratory study of high pressure water jet assisted cutting, *Proceedings of the 8th International Symposium on Jet Cutting Technology,* Durham, England, September 2-11, 1986, 1-8.

Nienhaus, K., Weigelt, H. and Thimons, E.D., The development of a water-jet-assisted shearer loader, *Proceedings of the 8th International Symposium on Jet Cutting Technology,* Durham, England, September 2-11, 1986, 79-92.

Ropchan, D., Wang, F.D. and Wolgamott, J., Application of waterjet assisted drag bit and pick cutter for the cutting of coal measure rocks, Final Technical Report to the U.S. Dept. of Energy, Contract No. ET-77-a-01-9082, April 1980.

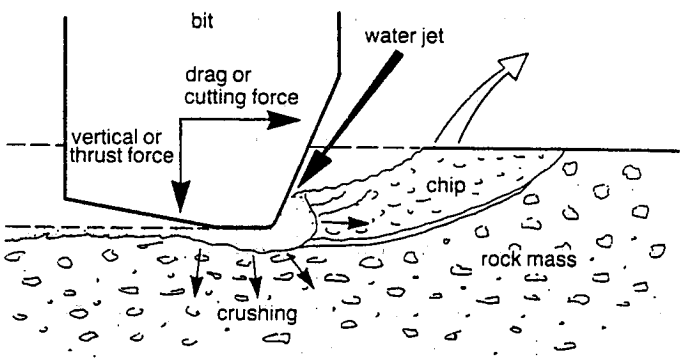

Figure 1 The synergistic rock cutting action of a water jet assisting a drag bit (*from* Dubugnon, 1981)

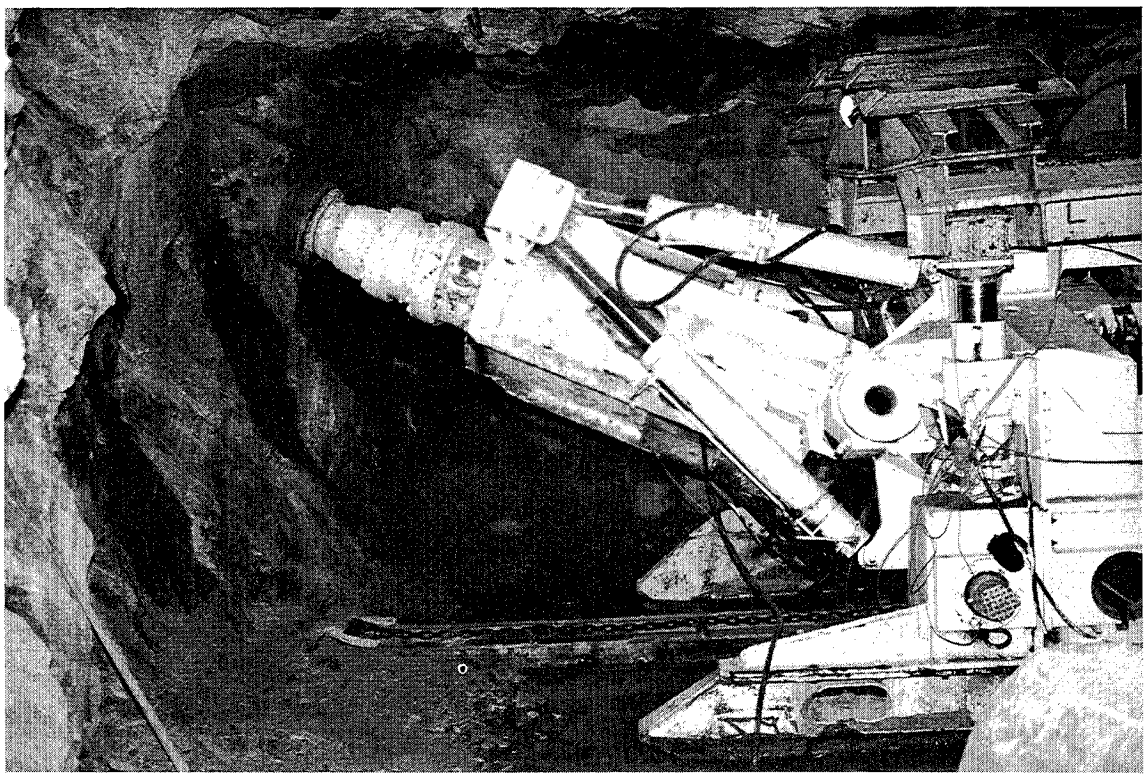

Figure 2 The rock cutting test rig

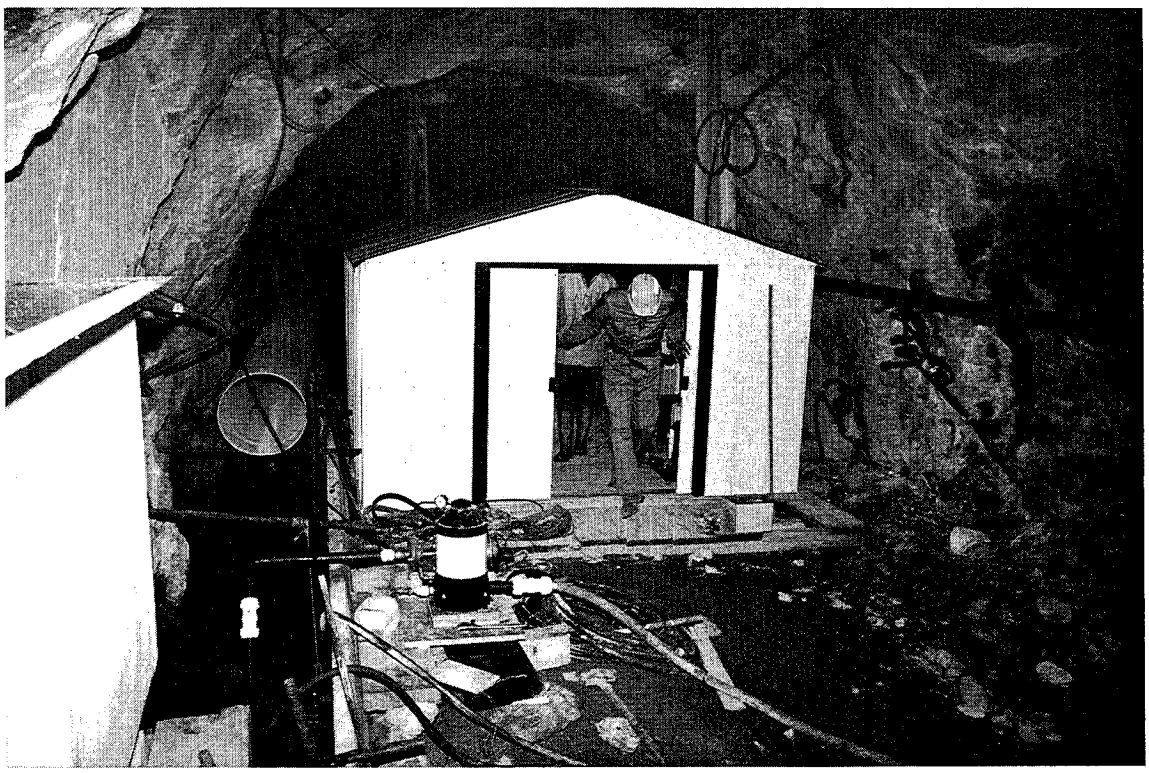

Figure 3 The instrument shed housing the computer

6th American Water Jet Conference
August 24 - 27, 1991: Houston, Texas

Paper 7

JET POWER OPTIMIZATION IN GRANITE KERFING USING OSCILLATING NOZZLES

A. Bortolussi, R. Ciccu, Wan-Mo Kim, P.P. Manca, G. Massacci

Department of Mining and Mineral Engineering
Mineral Science Study Centre
University of Cagliari, Italy

ABSTRACT

The paper deals with the problem of assessing the equipment performance requirements and the optimum setting of operational variables for driving deep kerfs in granite rocks by means of high velocity oscillating water jets. To this end systematic cutting tests have been carried out on samples of a medium-grained grey granite, under variable experimental conditions (pumping pressure, nozzle diameter, traverse velocity and oscillation frequence). Cutting results are evaluated in terms of rate of exposure and specific energy. The reasons underlaying the most favourable combination of operational variables are discussed in the light of the fundamental knowledge of rock erosion mechanisms.

Organized and Sponsored by the Water Jet Technology Association.

1.0 INTRODUCTION

In granite quarries sawmill blocks are presently being recovered by resorting to drill-based techniques, using decoupled explosive charges for the primary and secondary cuts and wedges for the subsequent block shaping and squaring operations. Flame cutting is often used for the bench opening slots, sometimes replaced, albeit rarely, by the method of overlapping drillholes.
Such a solution is generally preferred due to its inherent simplicity, flexibility, reliability and cost effectiveness.
However it is little accurate, thus entailing a considerable reduction of the block pay-volume due to shape irregularities. Therefore, overall quarry recovery can also be remarkably affected.
The faulty rock-saving capability of traditional technologies becomes more and more important as long as the unit worth of the material increases until a break-even point is reached, depending on stone block recovery, where the lower cost of quarrying is offset by the economic detriment brought about by the loss of valuable material.
It ensues that cheap and rude technologies are still favoured only in the case of low-yield quarries where stone having a minor market value is produced, whereas advanced and precise technologies, though more expensive, should be opted for in the case of high-priced material, especially if extracted with high recovery levels.
Actually diamond wire, already widely adopted for cutting softer marble, became a winning competitor versus flame in modern granite quarries, and threatening the yet very popular explosive splitting, provided that substitution is technically feasible and justified on economic grounds.
In such a situation, the prospects of water jet appear promising in those cases where the advantages of driving precision cuts into the rock with negligible material damage are exploited to a larger extent, i.e. in the case of valuble material extracted from high-yield stone bodies.
A suitable combination of water jet with diamond wire can be envisaged for the granite quarries of the future (Bortolussi), under the growing pressure exerted by the market, demanding fine-shaped blocks and better performing materials, as well as by the environment protection regulations, imposing less disturbing and land preserving methods.
In deep kerfing of rocks using high velocity water jets, cutting rate depends very much on the way by which water power is applied to the rock.
The problem of assessing the geometric and operational conditions for optimum jet cutting performance is quite difficult to solve on account of the many variables involved (number of jets, pressure and water rate, power distribution among jets, impact angle of each jet, kind of movement and velocity of the nozzle head and so on).
Moreover, cutting results are strongly affected by the characteristics of the rock (mineral composition, grain size, microfracturation pattern, mechanical strenght and deformability features).
In stone quarrying, jet power optimization represents the necessary condition for the industrial application of water jet technology. Yet it is expensive with respect to the other available technologies, due to the high cost incidence of energy on the unit cut area.
To the end of casting some more light on the subject, work is in

progress at the University of Cagliari using a pumping system capable of providing a water rate of 54 l/min under a pressure of 240 MPa, integrated with a lance driving structure able to reproduce the different kinds of movement suitable for deep kerfing (translating, rotating or oscillating jets).

2.0 MECHANISM OF ROCK EROSION

The process of rock excavation using water jets has been thoroughly studied throughout the world both theoretically and experimentally (Agus, Erdmann-Jesnitzer, Labus, Summers).
However the well known models proposed so far, though very helpful for understanding the basic mechanisms underlying erosion phenomena, are practically unsuitable as predictive tools of general validity, owing to the extreme variability of rock features, whose complexity cannot esily be described by simple and readily available parameters.
Concerning granite, it seems clear that rock breaks up under the action of a water jet according to a two-phase process, having some interesting analogies, though at a much smaller scale, with explosive blasting. Firstly the rock is finely crushed in the immediate vicinity of the impingement point as the consequence of the very high compressive stresses, either static and dynamic, imparted by the jet. Then the surrounding rock is broken into coarser fragments, as the result of the propagation of preexisting or newly formed discontinuities according to its minero-petrographic and micromechanical features. Failure essentially results from tensile stresses (Agus).
The extent of each phase and thence the overall damage produced eventually depend on the suitable matching between jet and rock properties. It is likely that stronger and compact rocks would require faster jets to initiate the fractures (first phase enhanced), whereas weaker and porous rocks are excavated more efficiently using slower jets.
If this is true (further experiments are needed to confirm the assumption) maybe jet velocity can be tuned to a easily measurable compactness-related property of the rock, like for instance sound velocity.
As regards jet power, it is a widely acknowledged fact that the excavation rate (volume removed per unit time) is proportionally affected (Labus). Therefore, for a given pressure, it should be expected that greater damage is progressively obtained as water rate increases (specific energy remaining constant) on condition that jet power is suitably distributed and efficiently applied to the rock, similarly to the loading of explosive among the drillholes in bench blasting.
Moreover, larger rock burdens can be demolished by a jet with a given power in the case of weaker or intensively microfractured rocks than in the case of sound rocks. Kerf geometry itself, and in particular the presence and location of free faces, may therefore assume a decisive importance.
Concerning rock properties, granularity characteristics often play a major role, of controversial opinion, based on heterogeneous experimental findings, seems to exist among the water jet experts. It seems reasonable to assume that smaller grain size is a favourable factor if intergranular bonds are weak, as it happens for partially

weathered or tectonically stressed brittle materials. Whereas the opposite may hold in the case of strong intergranular bonds, characterized by high fracture energy.

3.0 EXPERIMENTAL PLAN

In the light of the above, a suitable collection of systematic testing data was deemed necessary in order to assess the influence of the various operational conditions on cutting results, as the starting step of a reserch program intended to demostrate the industrial feasibility of water jet technology in Sardinian granite quarries.
Tests aimed at evaluating the feasibility of deep kerfing, consisted in driving a slot into the rock samples, wide enough to allow lance penetration.
The oscillating twin-jet solution was here adopted due to its inherent simplicity. Rotating and translating jets will be tested later on the same material and operating conditions in order to elucidate the respective advantages.
The experimental program embraced 54 kerfing tests, each one consisting of 5 passes of the simulated twin-jet lance. The factorial plan was conceived for studying the combined effect of the 4 chief variables:

- pumping pressure;
- water rate;
- oscillation frequency;
- traverse velocity.

The range of each variable was selected on the basis of previous experience on the same granite. In particular, the setting values for pressure (100, 150 and 200 MPa), nozzle diameter (0.7 and 1.25 mm) and traverse velocity (1.5, 3.0 and 4.5 m/min) were adopted independent of each other. Oscillation frequency was matched to traverse velocity on condition that the pitch of ensuing jet trajectory at the kerf center line (5.0, 7.5 and 10.0 mm) was smaller, equal or larger than the average grain size of the material (single crystals or clusters).

4.0 FACILITIES

The high-pressure jet generation system used in the experiments consists of a three piston, one stage Hammelmann pump model HDP 330, capable of supplying up to 52 l/min of water through two nozzles under a pressure of 250 MPa. Primary energy source is a Diesel engine giving better operational flexibility than the electric counterpart over the wide range of settings required by the experimental plan.
Sample movement beneath the jet is obtained by means of a hydraulic driven carrying table.
The water jet lance is held in the working position by a clamping device to which the oscillating movement is transmitted through a connecting rod/crank mechanism actuated by a frequency-controlled electric motor.
The lance head is provided with a single central nozzle: the twin-

jet operation is reproduced by simply resorting to crossed passages over the sample.
A general view of the experimental set up is shown by the photograph of Figure 1.

5.0 MATERIAL

The granite used for the kerfing experiments comes from the Fiore quarry, in the Buddusò district (Sardinia), and is commercially known as "Pearl Grey" due to the typical translucent appearance of quartz and feldspar, while plagioclase is opaque milky white.
The granite is essentially isotropic in texture and has a holocrystal hypidiomorphic, uneven-grained structure. Mineral composition is 31 % quartz, 38% feldspar, 24.5% plagioclase and 6.5% biotite. Average crystal size is 2.9 mm (with 0.51 relative standard deviation) for quartz, 3.8 mm (0.28) for feldspar, 1.7 mm (0.36) for plagioclase and 1.4 mm (0.34) for mica.
In particular, quartz occurs in xenomorphous zones with marked undulating extinction, often polycrystal with uneven boundaries and sutures between the grains as well as in smaller subidiomorphic or rounded crystals, frequently hosted inside feldspar. The quartz crystals generally display intense intra- and intergranular microfractures involving also the adjacent feldspar crystals and, though much less commonly, plagioclase.
The K-feldspar consists of orthoclase and predominating microcline occurring in large xenomorphous grains, at times clearly interstitial. Both orthoclase and microcline are normally microperthitic; inter-and intra-granular fractures are frequently observed, often filled with sericite.
The plagioclase, composed essentially of oligoclase, occurs in the form of idio- or subidiomorphic prisms with more or less marked zonings and frequent albite edges. Plagioclase crystals tend to be clustered together with ill-defined contours.
The mica consists of biotite, for the most part in idiomorphic grains, isolated or more commonly in clusters, sometimes strongly chloritized.
The fabric features of the granite tested are shown by the photograph of Figure 2.
Presently blocks are quarried using a combination of flame torching (opening slot), diamond wire sawing (bench slicing), explosive splitting (underhand cut) and wedging (final block shaping). Considerable interest is addressed to water jet as a possible substitute of flame and of explosive splitting.

6.0 COMPUTER SIMULATION

The locus of jet impingement points and the corresponding displacement velocity as a function of time have been studied by computer simulation for the various experimental conditions.
The plot of a typical path (two crossed passes) of the jet intercept at the original sample surface is represented in Figure 2, superimposed to the polished surface of the granite. The distance between tracks is of the same order of magnitude as the average size of rock granularity.
The modulus of jet velocity against time for three different

oscillation frequencies is shown by the diagram of Figure 3.
The oscillation cycle is slightly asymmetric due to the umbalanced forth/back stroke of the lance driving mechanism.
Velocity is higher roughly at the center line of the kerf; therefore somewhat deeper erosion should be expected near both kerf walls, where jet action time is accordingly longer. However rock is there more confined thus eventually offsetting the advantage. The prevalence of either effect may depend on the operating conditions as well as on the particular microstructural features of the rock, as it will be discussed later.

7.0 TESTS

Experiments have been carried out changing one variable at a time (pressure, nozzle diameter, traverse velocity and oscillation frequency) according to a factorial plan including a total of 54 tests.
Cube-shaped samples, 15 cm by edge, were obtained from the same rock block using a diamond saw, thus securing uniformity of minero-petrographic characteristics.
Each experiment consisted of 10 alternating passages of the jet over the sample, thus reproducing the effect of 5 one-way passages of a twin-nozzle lance.
In particular, the jet was directed at an angle of 22° from the vertical line against the upper face of the test cube laying horizontally on the carrier table. After each forward passage the sample was rotated 180° while maintaining the same lance setting, so as to cross the previous path at a -22° angle from the vertical with random phase shifting.
Stand-off distance, initially set at 20 times the nozzle diameter, was maintained unchanged during the test.
To study the effect of rock anisotropy, the various faces of the sample were used for the kerfing experiments, so as to cross the planes of preferential splitting at different angles.
At times some major hidden fractures crossing the entire sample became evident if traversed by the kerf, giving rise to anomalous excavation. That part of the slot was obviously excluded from volume measurements.
Nor were taken into consideration those parts at both ends of the slot (and sometimes at the kerf lips) where major spalling occurred.
Oscillation amplitude was set at 4 cm for all tests. However tapered kerfs were generally obtained due to the progressive increase of the stand-off distance after each passage. Besides that, the excavation was progressively poorer near the kerf walls due to the particular lance manipulation device adopted.

7.0 RESULTS AND DISCUSSION

Kerfs obtained under varying experimental conditions were inspected in order to assess the effect of jet excavation.
Only the central part of the kerf was taken into consideration, excluding the 3-5 cm end parts affected by considerable spalling.
Excavated volume was measured by pouring freely flowing classified dry sand into the kerf space delimited at both end sides by mastic

plugs.
Kerf bottom depth was measured corresponding to the longitudinal center line and to two selected cross sections at 1/3 distance from either end, using a comb-like profilograph provided with adjustable needles.
Kerfs were also inspected in order to put into evidence the differential effect produced by the jet on each mineral component.
Kerf shape is likely to be influenced by the kind of load applied by the jet. Indeed it seems that higher pressure favours a better excavation at both the kerf sides, where the rock is more confined, whereas higher flowrate produces a more efficient erosion at the centre, exploiting the free faces represented by the traverse step created at each oscillation of the jet and by the kerf bottom itself.
Again an interesting analogy with multiple row bench blasting using delayed blastholes can be observed.
Actually, two substantially different cross profiles were obtained at the kerf bottom: either concave or convex according to cases.
Microscopic examination revealed that the fact is strongly influenced by the textural features of the granite at hand which was found to be slightly anisotropic for the presence of oriented "hair-like" microfractures across the crystals, especially quartz.
In particular the convex kerf bottom profile (higher depth at the wall foot) was generally obtained when the kerf was driven parallel to the planes of microfractures whereas the concave profile was achieved on perpendicularity condition.
It was also found that kerf surface roughness depends mainly on pressure, in agreement with the results obtained elsewhere: (Hilaris, Raether). Higher pressures give smoother walls and a rougher bottom and vice versa. In fact jet action on individual crystals becomes more selective when impinging normally on the target surface, the more as pressure increases (Agus). Generally protuberances correspond to plagioclase or feldspar crystals, craters to quartz.
The reason why tapered kerfs were obtained working at high jet power, besides the effect of increased stand-off distance as cutting proceeded (the lance was not penetrated into the kerf after each passage), can also be explained by the fact that lance oscillation movement occurred on a cylindrical surface, depriving the jet of a lateral component perpendicular to the wall, thus producing poorer excavation and consequently a gradual reduction of kerf width.
This drawback can be minimized in the case of a lance with diverging nozzles oscillating (or rotating) on its own axis, which represents the best solution for industrial application (Reichman, Labus).
The technical results achieved with the kerfing experiments are represented in Tables I, II and III, where net cutting rate, average depth of cut and specific energy are given for the various experimental conditions. Data for the 15 Hz frequency are incomplete due to vibrations which caused a dynamic unbalance of the lance driving system thus rendering very difficult the control of setting point.
As regards cutting rate it emerges that unsatisfactory results are obtained with the 0.7 mm nozzle, whatever the pressure, whereas the performance of 1.25 mm nozzles is generally good even at a pressure as low as 100 MPa.
For a given diameter and pressure, cutting rate increases with traverse speed showing that the peak point would be reached far

beyond 7.5 cm/s.
The effect of oscillation frequency seems negligible, though it appears that moderate oscillation, from 3 to 8 Hz depending on traverse velocity, is optimum. The fact that better results are achieved when frequency is appropriately tuned to traverse velocity is thus confirmed (Labus). The reason maybe stands in the suitable matching between oscillation pitch and grain size of the rock, taking into account that intergranular contacts can be considered as weakness points to fracture propagation caused by the jet. The average value of cutting rate over oscillation frequency with the 1.25 mm nozle is plotted in figure 4 as a function of traverse speed for different pumping pressures.
Concerning the average incremental kerf depth, the favourable effect of pressure is clearly evident. The peak value of depth per passage against pressure is reached first for the 0.7 mm than for the for the 1.25 mm nozzle. In both cases depth decreases as traverse velocity increases, as expected.
As well known to water jet experts (Hashish), depth is sensitive to traverse speed, gradually diminishing as the lance is moved faster, though the effect is more marked for the smaller nozzles. For the 1.25 mm nozzle jet penetration is deeper at the intermediate oscillation frequency, whereas this does not happen for the smaller diameters. The curves giving the depth per passage achieved at variable traverse speed with the 1.25 mm jet are shown in Figure 5.
Specific energy lends itself to some interesting considerations. Experimental data point out that values achieved with the 1.25 mm nozzles are almost constant irrespective of pressure, meaning that waterjet efficiency is satisfactory even at moderate pressures, provided that enough hydraulic power is applied (Figure 6). On the other hand energy efficiency is strongly influenced by flowrate.
Actually, strong evidence exists about the importance of maintaninig the overall power concentrated in few jets instead of dispersing it among many jets with the attempt to achieve a more uniform application of the hydraulic load to the rock. Indeed cutting rate achieved with two 1.25 mm nozzles bearing a jet power of 190 kW is 2 to 4 times the cutting rate achievable with four 0.7 mm nozzles bearing roughly the same power.

8.0 CONCLUSIONS

On the basis of the experimental results so far achieved the following conclusions can be drawn:

- Water jet is a feasible technology for driving deep kerfs in granite rocks provided that enough power is applied. In fact net cutting rates higher than 2.5 m^2/h (representing the break-even point against flame torching) can be achieved even with relatively moderate pressure (100 MPa) using adequate flowrates.
- For satisfactory performance to be achieved (high cutting rate with low specific energy) it is advisable that jet power is distributed among few nozzles with larger diameter; otherwise efficiency deteriorates.
- Cutting may be facilitated if the kerf is driven parallel to the easier splittability planes of the rock, though this is is not a major restriction to the efficient use of water jet.
- Rock excavation with water jets presents very interesting

analogies, though at a much smaller scale, with bench blasting: the effect of pressure corresponds to the detonation velocity of the explosive while water rate corresponds to the charge per unit volume of rock. Excavation with water jets can be envisaged as a two-phase process: a direct stressing of the rock produced by trains of compressive/tensile shock waves travelling inside the rock toward the available free faces (kerf surface and rock discontinuities), followed by fragmentation as a result of fracture propagation at the expense of the residual energy of the jet penetrating into the existing discontinuities. Oscillation velocity plays the role of delay between blastholes and oscillation pitch that of rock burden between rows.

ACKNOWLEDGEMENTS. This research was carried out according to the programs of MURST and CNR with the financial support of the Ente Minerario Sardo (EMSa) through a research contract. Granite samples have been provided by Mr. S. Fiore.

REFERENCES

1. Agus M., Bortolussi A., Ciccu R., Manca P.P., Massacci G., Bosu M.: Jet Impingements Tests on Mineral Crystals, Proc. 1st Asian Conf. on Recent Advances in Jetting Technology, Singapore (1991), pp 1-9.
2. Bortolussi A., Ciccu R., Manca P.P., Massacci G.: Granite Quarrying with Water Jets: a Viable Technique?, Proc. 5th American Water Jet Conf., Toronto, (1989) pp 49-58.
3. Erdmann Jesnitzer F., Louis H., Wiedemeier J.: Rock Excavation with High Speed Water Jets; a wiew on drilling and cutting results of rock materials in relation to their fracture machanical behaviour, Proc. 5th Int. Symp. on Jet Cutting Technology, Hanover (1980), pp 229-236.
4. Hashish M: Critical and Optimum Traverse Rates in Jet Cutting, US Water Jet Symp., Golden (1981) pp 1-14.
5. Hawrilewicz B.M., Vijay M.M., Remisz J., Paquette N.: Design and Testing of a Rock slotter for Mining and Quarrying Applications, Proc. 9th Int. Symp. on Jet Cutting Technology, Sendai (1988), pp 377-386.
6. Hilaris J.A., Bortz S.A.: Quarrying Granite and Marble using High Pressure Water Jet, Proc. 5th Int. Symp. on Jet Cuttting Technology, Hanover (1980), pp 229-236.
7. Labus T.J.: Energy Requirements for Rock Penetration by Water Jets, Proc. 3rd Int Symp. on Jet Cutting Technology, Chicago (1976) pp 29-40.
8. Raether R.J., Robinson R.G., Summers D.A.: Use of High Pressure Water Jet for Cutting Granite, Proc. 2nd US Water Jet Conf., Rolla (1983), pp 203-207.
9. Reichman J.M., Cheung J.B.: An Oscillating Water Jet Deep-Kerfing Technique, Int. J. Rock Mech. Min. Sci., 154 (1978), pp 135-144.
10. Labus T.J.: Material Excavation using Rotating Water Jets, Proc. 7th Int. Symp. on Jet Cutting Technology, Ottawa (1984), pp 504-516.
11. Summers D.A.: A Review of Water Jet Excavation Research, 26th US Symp. on Rock Mechanics, Rapid City (1985), pp 895-903.

12. Summers D.A., Yao J., Yazicy S.: Basic Consideration in Water Jet Cutting, Proc. 1st Asian Conf. on Recent Advances in Jetting Technology, Singapore (1991), pp 93-100.
13. Vijay M.M., Grattan-Bellew P.E., Brierley W.H.: An Experimental Investigation on Drilling and Deep Slotting of Hard Rocks using High Pressure Water Jets, Proc. 7th Int. Symp. on Jet Cutting Technology, Ottawa (1984), pp 419-438.

NOMENCLATURE

d = Nozzle diameter (mm)
P = Pumping Pressure (MPa)
Q = Water Flowrate (dm^3/min)
V = Traverse Velocity (cm/s)
f = Oscillation frequency (Hz)
W = Jet Power (kW)
R = Cutting Rate (m^2/h)
E = Specific Energy (kJ/cm^3)
h = Average kerf depth (cm)

Table I. Cutting Rate R (m^2/h) on "Pearl Grey" granite (Sardinia) using oscillating jets.

P (MPa)		100		150		200	
d (mm)		0.70	1.25	0.70	1.25	0.70	1.25
V (cm/s)	f (Hz)						
2.5	1.7	0.08	0.56	0.37	0.76	0.49	0.98
	2.5	0.05	0.54	0.19	0.98	0.26	1.25
	5.0	0.04	0.34	0.18	0.78	0.22	1.04
5.0	3.3	0.05	0.44	0.39	1.15	0.51	1.91
	5.0	0.03	0.75	0.36	1.27	0.40	1.77
	10.0	0.06	0.65	0.15	1.14	0.29	1.69
7.5	5.0	0.03	0.52	0.16	1.40	0.33	2.80
	7.5	0.09	0.49	0.25	1.85	0.28	2.78
	15.0	-	-	-	0.95	-	2.24

Table II. Average Depth per passage (mm) in deep kerfing of "Pearl Grey" granite (Sardinia) using oscillating jets.

P (MPa)		100		150		200	
d (mm)		0.70	1.25	0.70	1.25	0.70	1.25
V (cm/s)	f (Hz)						
2.5	1.7	0.43	3.12	2.04	4.21	2.71	5.47
	2.5	0.27	3.01	1.06	5.46	1.42	6.97
	5.0	0.24	1.92	1.01	4.34	1.25	5.74
5.0	3.3	0.15	1.22	1.08	3.20	1.42	5.29
	5.0	0.07	2.08	1.00	3.52	1.12	4.92
	7.5	0.17	1.79	0.43	3.16	0.80	4.70
7.5	5.0	0.06	0.96	0.30	2.60	0.60	5.18
	7.5	0.16	0.91	0.47	3.42	0.52	5.15
	15.0	-	-	-	1.77	-	4.15

Table III. Specific Energy (kJ/cm^3) in deep kerfing of "Pearl Grey" granite (Sardinia) using oscillating jets.

P (MPa)		100		150		200	
d (mm)		0.70	1.25	0.70	1.25	0.70	1.25
V (cm/s)	f (Hz)						
2.5	1.7	23.2	10.4	9.3	14.2	10.7	16.8
	2.5	37.6	10.8	17.8	10.9	20.4	13.2
	5.0	41.6	17.0	18.6	13.8	23.2	16.0
5.0	3.3	33.6	13.3	8.7	9.3	10.2	8.7
	5.0	70.4	7.8	9.5	8.5	12.9	9.4
	7.5	29.4	9.1	22.1	9.5	18.0	9.8
7.5	5.0	58.9	11.3	20.8	7.7	16.0	5.9
	7.5	20.8	12.0	13.5	5.8	18.4	6.0
	15.0	-	-	-	11.3	-	7.4

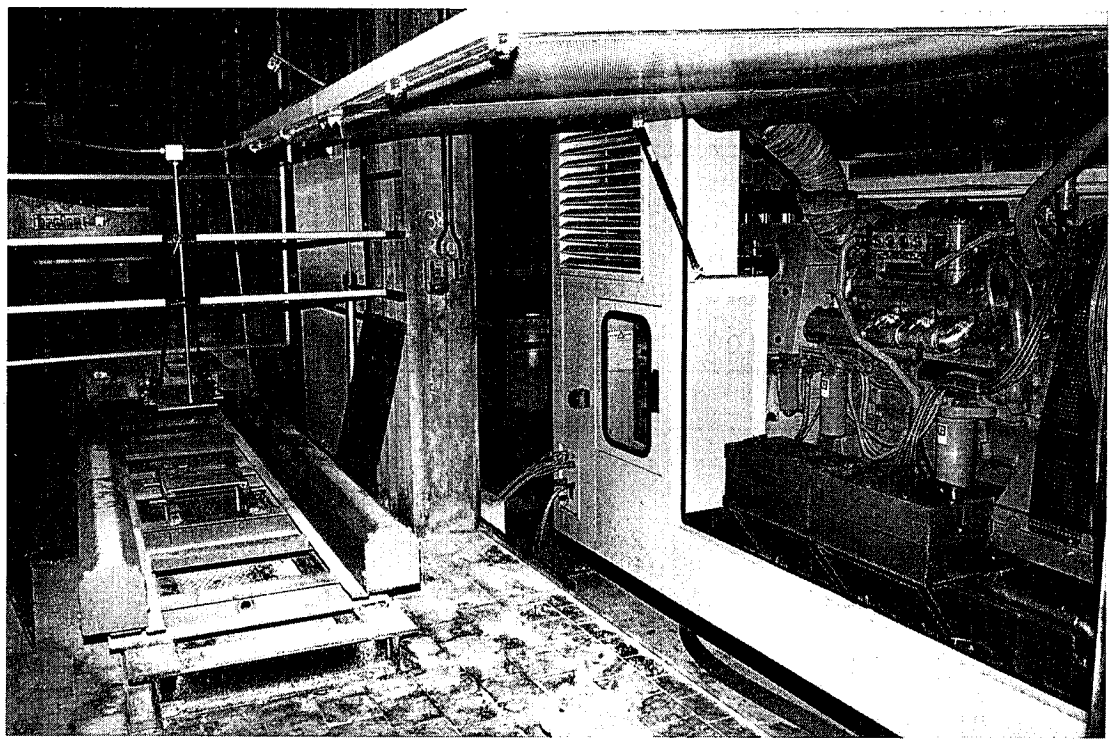

Figure 1. General view of the facilities used for the granite kerfing experiments at the University of Cagliari.

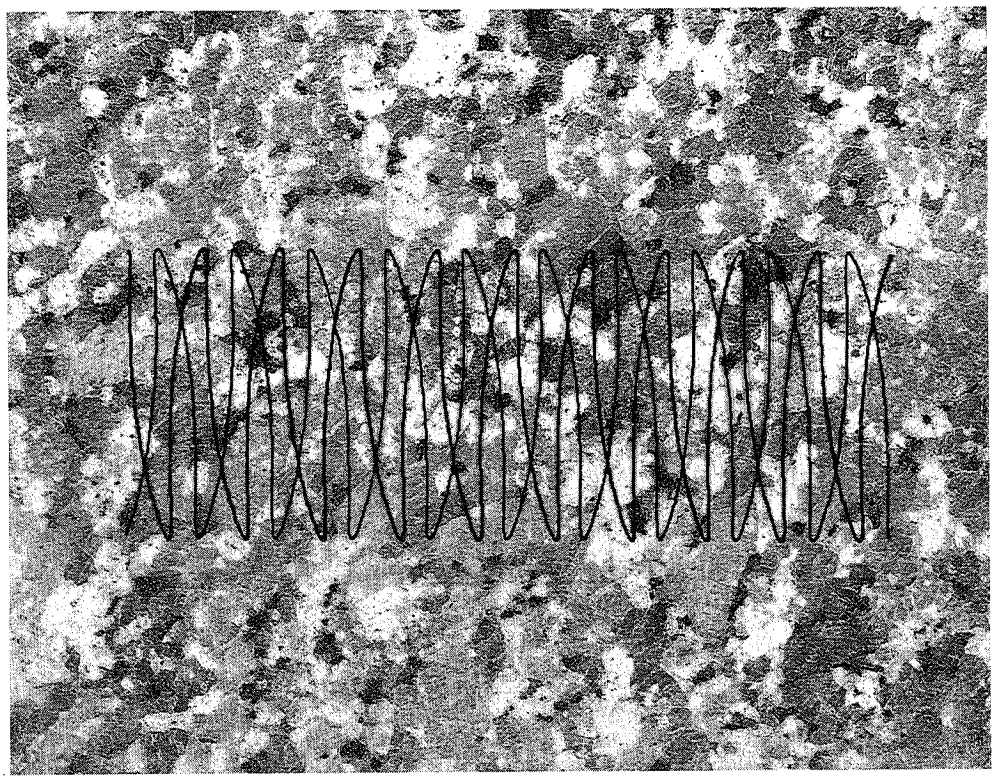

Figure 2. Twin jet tracks on the sample surface. Traverse velocity: 5.0 cm/s; oscillation frequency: 5 Hz

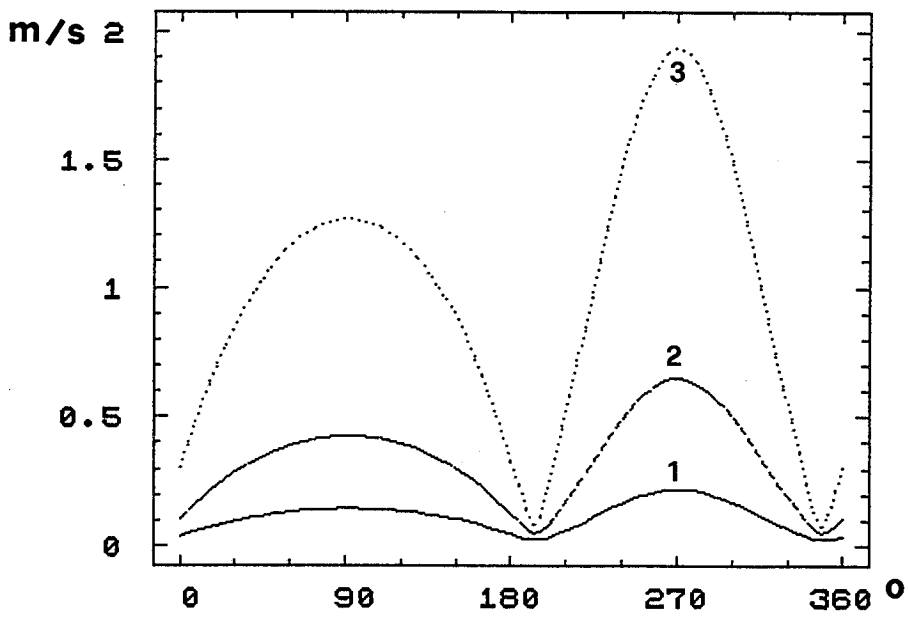

Figure 3. Modulus of oscillation velocity as a function of phase angle.
1 - V = 2.5 cm/s; f = 1.7 Hz
2 - V = 5.0 cm/s; f = 5.0 Hz
3 - V = 7.5 cm/s; f = 15.0 Hz

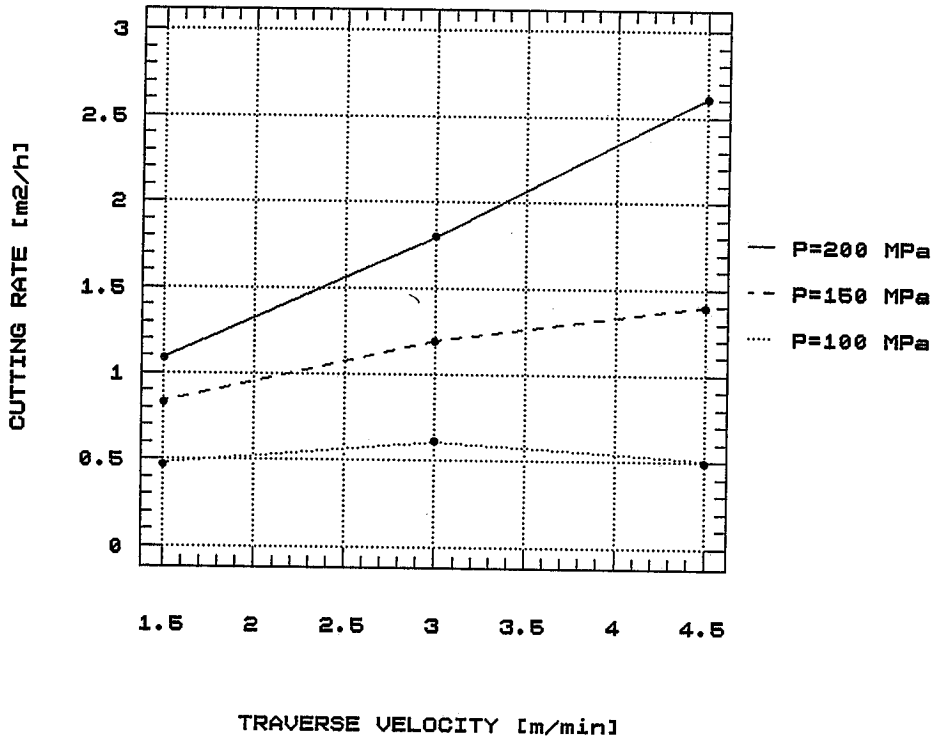

Figure 4 . Cutting rate as a function of traverse velocity

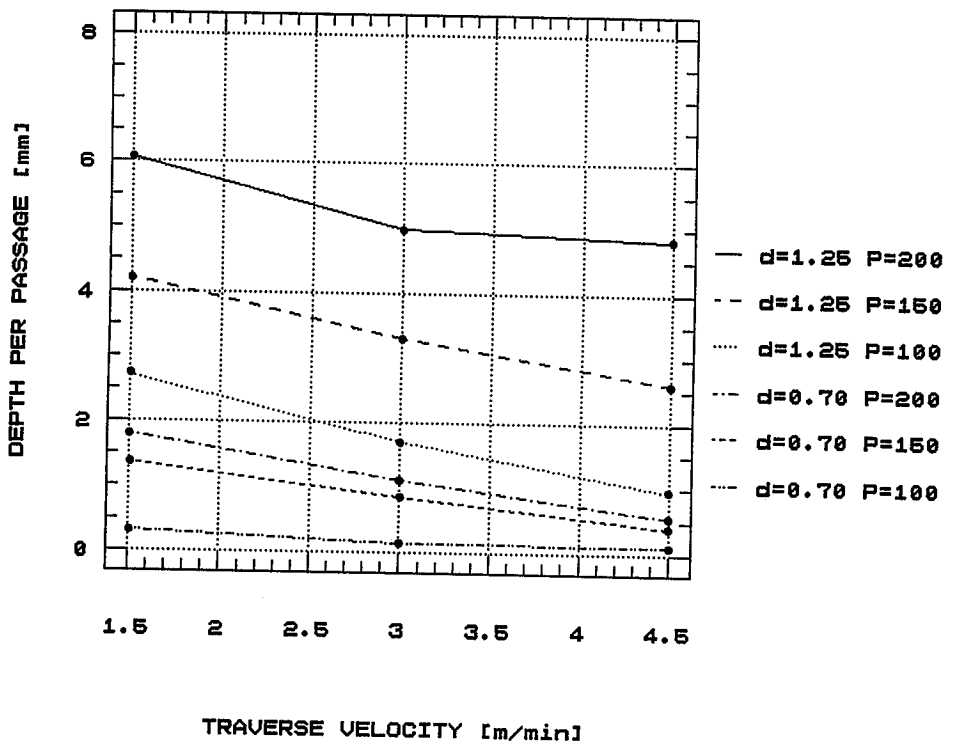

Figure 5. Average depth per passage h against traverse velocity.

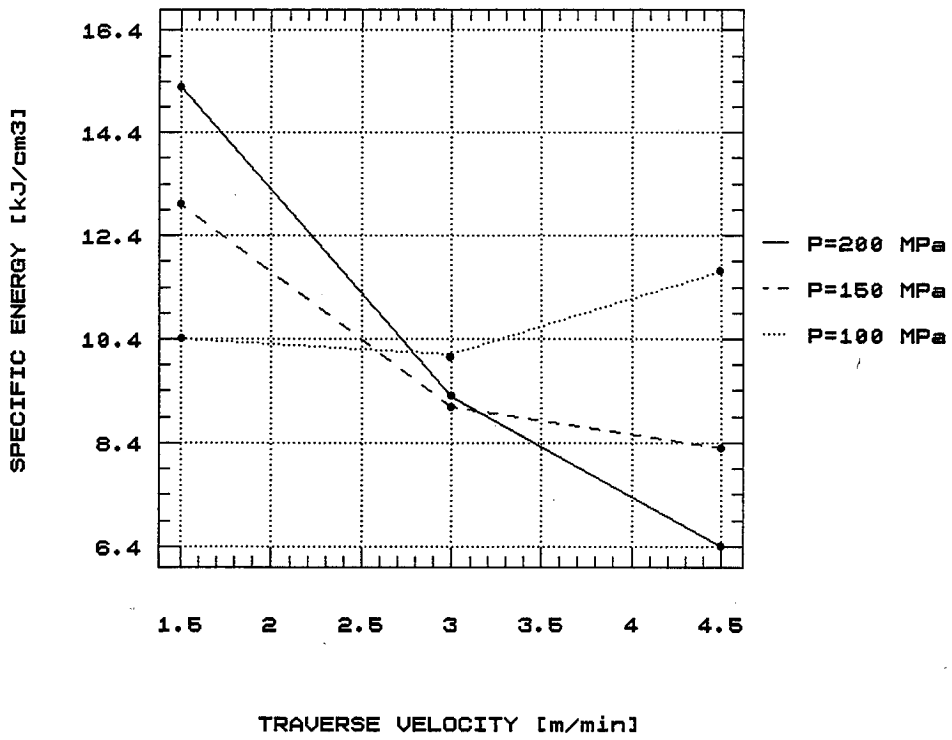

Figure 6. Specific Energy as a function of traverse velocity.

6th American Water Jet Conference
August 24 - 27, 1991: Houston, Texas

Paper 8

Test On Walls Of A Railway Tunnel And Samples Of Concrete And Blocks Of Rocks With High Pressure Water Jet Equipment For Outdoor Applications In Czechoslovakia

J. Vašek, J. Foldyna
Mining Institute Of The Czechoslovak Academy Of Sciences, Ostrava, Czechoslovakia
J. Novák
PTV Ltd., Prague, Czechoslovakia

ABSTRACT

An extensive range of tests of the efficiency of high pressure water jetting have been performed in Čremošné (Slovakia). The experiments have been performed both at a tunnel test site and field laboratory. The high pressure water jet was tested in a tunnel as a tool for joints cleaning, tunnel face cleaning, cutting through the tunnel wall and removing the layer of weathered concrete. The experiments in the field laboratory were aimed at cutting of different types of concrete samples using abrasive water jet and blocks of rock using both abrasive and rotating water jets.

1.0 INTRODUCTION

The Mining Institute Ostrava in co-operation with the Railway Construction Brno, MENET Průhonice and Phoenix Co. Praha realized an extensive range of field tests in Čremošné tunnel and field laboratory using high pressure equipment Flow Systems, which were lent by the firm Flow Europe GmbH (W.Germany). Experiments were mainly aimed at verification and demonstration of the possibilities and efficiency of high pressure water jets in tunnel maintenance. High pressure water jets were tested in Čremošné tunnel as a tool for some operations of the tunnel wall rejointing technology.

The range of experiments in tunnel was completed by tests of concrete and rock cutting in the field laboratory situated near the tunnel for the Railway Construction Brno, Metrostav Prague, Czech Stone Industry and many others.

2.0 RAILWAY TUNNELS MAINTENANCE AND REDEVELOPMENT

Considering that the Czechoslovak railways had been laid down largely in the second half of 19th century and present-day form was reached roughly forty years ago, redevelopment and maintenance of the tunnels have gained increasing significance for trouble-free operation of the Czechoslovak railway traffic. It concerns also the Čremošné tunnel situated in the middle of Slovakia on the railway line between Žilina and Banská Bystrica towns.

Due to the activity of underground water (mostly under pressure) which is mineralised possibly also with deleterious effects, the function of the original tunnel drainage is impaired continuously. Draining elements are clogged or dissolved alternatively, their function is damaged and percolations take place in the tunnel wall (Fig. 1). These percolations restrict the train traffic, especially in winter time when ice formations are created, and make railway electrification impossible.

In this case the aim of maintenance is to make a good tunnel wall as efficient as possible. In addition to the drainage wells and grouting in the rock massif, draining interventions have to be carried out in the tunnel face (Fig. 2).

In Čremošné tunnel the wall maintenance of the first 350 m from tunnel mouth had been carried out by means of the present-day technology until the water jet test took place. The present-day technology includes following operations :

- cleaning of the tunnel wall face from dirts and disintegrated material by means of sand blasting and subsequent washing (danger of silicosis)
- removing of the old joints fillings by means of pneumatic jackhammers (danger of silicosis and vasoneurosis) and filling of joints with a new material the water-tightness of which is based on the expansibility of special cement composition
- breakings for diverters in the tunnel wall by means of contour drilling and manual breaking, blasting or disintegrating by inexplosive compounds
- removing the layer of weathered concrete from the concrete lining by means of pneumatic jackhammers (danger of silicosis and vasoneurosis), installation of steel nets and a new concrete layer.

The present-day operations are time-consuming, laborious and health endangering. Therefore we had to take into consideration the technology allowing to accelerate these operations and to improve the working conditions. Technology of high pressure water jetting was found to be the most suitable for this purpose.

3.0 PROBLEMS SOLVED IN THE FIELD LABORATORY

In addition to the tests aimed at evaluation of the applicability of high pressure water jet technology in tunnel maintenance, a series of other tests were included in the experimental program. This part of the experimental program was performed in the field laboratory which was situated nearby the tunnel.

The aim of the tests in the field laboratory were to demonstrate that abrasive water jet is able to cut different types of concrete and rocks and to evaluate the cutting power of the jet. For this purpose different concrete samples were prepared by the Railway Constructin Brno and Metrostav Prague and rock samples by the Dimensioned Stone Industry. Specified requirements for cuting were set by all of them.

In addition to abrasive water jet cutting tests on rock samples tests were performed by rotating water jets.

4.0 EXPERIMENTAL EQUIPMENT

The high pressure water jet was generated by high pressure pump JETPAC™ 1003-13-02, specially designed for outdoor aplications. The pump was equipped with three pressure intensifiers with max. operating pressure 235 MPa and max. water flow rate 17.0 1/min. This

pump, driven by 99 kW diesel turbo engine, was placed on the platform wagon. The high pressure water distribution to individual working tools was performed by high pressure flexible hoses. Following working tools were used during the tests in tunnel :
- JETLANCE™ - hand-held tool equipped with rotating head for two, four or eight nozzles
- JETWAND™ - hand-held tool equipped with single nozzle head
- Universal cutting system Model 6400 - system for abrasive water jet cutting, consisting of abrasive water jet cutting head and hydraulically driven unit for cutting head movement above the material to be cut.

The platform wagon was also equipped with water tank (8 m^3 volume) and hydraulic system supplying water under pressure aprox. 0.5 MPa for high pressure pump. In addition the platform wagon was equipped with lamps providing sufficient ilumination of the working site in tunnel.

The persons working with hand-held tools had to be provided with water resistant protective clothing and gloves, helmets and protective shields.

In addition to the equipment used in the tunnel, the field laboratory was equipped with copying table Gloortronic adjusted for abrasive water jet cutting, having traverse speeds ranging from 1,2 to 300 mm/min. This manipulator was used for cutting straight and curved cuts in concrete and rock samples.

5.0 EXPERIMENTAL RESULTS

5.1 Tests in tunnel

The tests were performed at the tunnel test site of the length of aproximately 20 m (situated 500 m from the tunnel mouth) which was chosen by experts from the Railway Construction Brno as the working site with the most difficult conditions.

5.1.1 Removing of old joints filling (Fig. 3)

The hand-held tool JETLANCE™ equipped with rotating head for two nozzles was used for tests of removing of the old joints filling. Cement mortar was removed from 10 - 40 mm wide joints in tunnel wall up to the requested depth of 100 mm. During the tests the longitudinal performance, i.e. the length of cleaned joints achieved per hour, was measured. The longitudinal performance obtained was 17

m/hour, which represented aprox. nine times greater performance compared with that of the pneumatic jackhammer.

5.1.2 Tunnel wall face cleaning

The hand-held tool JETLANCE™ was used for tests of cleaning of the tunnel wall face. At the begining the tool was equipped with a rotating head with eight nozzles for cleaning, after that a rotating head with two nozzles for joints filling removing. The reason for this was that the operation could be combined (Fig. 4). The area performance, i.e. cleaned area of tunnel wall face per hour, was measured during the tests. The area performance was 39 m^2/hour, which represented approx. eleven times greater performance compared with sand blasting and subsequent washing.

5.1.3 Cutting of slots for diverter's breaking (Fig. 5)

These tests were aimed at the testing of the possibility of replacing the contour drilling by cutting of parallel slots through the tunnel wall which would allow diverter's breaking. Slots were cut by abrasive water jet by means of Universal cutting system Model 6400. Quartz sand with maximum grain size 1.2 mm was used as abrasive material. The cuts through granite wall and through concrete (300 mm thickness) were realized. The longitudinal performance, i.e. the length of the slot of the required depth per hour, was measured during tests. The longitudinal performance was 1,5 m/hour, which represented aprox. three times greater performance compared with contour drilling.

5.1.4 Removing of the layer of weathered concrete

The hand-held tools JETWAND™ and JETLANCE™ equipped with rotating head for two and four nozzles were used for tests of removing the layer of weathered concrete from the concrete lining. The layer of weathered concrete was removed up to the depth of 100 mm. The area performance, i.e. area of removed layer of weathered concrete per hour, was measured during the tests. The greatest area performance was obtained with JETLANCE™ equipped with rotating head for two nozzles. This performance was 1,4 m^2/hour, which represented aprox. four times greater performance compared with present-day technology (pneumatic jackhammer).

5.2 Tests in the field laboratory

5.2.1 Cutting of concrete

The company "Railway Construction" Brno prepared 12 different samples of building materials for tests of abrasive jet cutting of concrete in the field laboratory. All concrete samples were made according to the class B 20 (Czechoslovak State No. 73 2400). Concrete mixture recipe and its mechanical properties are given in Table I. Detailed descriptions and schematic drawing of samples are presented in Fig. 6.

Abrasive jet cuts in concrete samples included straight sections and curves of different radii and all samples were cut trough by single pass of the jet. Cutting parameters and results of concrete cutting are given in Table II.

5.2.2 Cutting of armoured concrete segments

The company Metrostav Prague supplied armoured concrete segments 55N and BN for tests of abrasive water jet cutting. The 55N segments are used for supporting underground lines and the BN segments are for supporting underground stations.

Concrete charcteristics, basic mechanical properties and diagrammatic schemes for both types of segments are given in table III and Figures 7 and 8, respectively.

During the tests, an opening was cut in the 55N segment and part of the BN segment was halved by single pass of the jet. Cutting parameters and results of concrete segments are given in table II (below line).

All the tests of concrete cutting by abrasive water jet were performed by means of the cutting head of the Universal cutting system Model 6400 and copying table Gloortronic as a manipulator of the cutting head.

5.2.3 Cutting of rocks samples

In addition to the abrasive jet cutting of concrete samples we performed tests on samples of sandstone, granite, travertine and marble supplied by the Dimensioned Stone Industry. Tests were made using either the cutting head of the Universal cutting system Model 6400 and the copying table Gloortronic as a manipulator for abrasive

jet cuts or the Jetlance™ with two rotating water jets (at 10° angles to the axis of rotation) and the Universal cutting system Model 6400 as a manipulator for rotating water jet cuts. The abrasive water jet served for halving the rock samples by single pass of the jet, the rotating water jets were used to make deep cuts using multiple passes of the rotating jets.

Physical and mechanical properties of the rock samples are presented in Table IV. Cutting parameters and results of abrasive jet cutting of rock samples are summarized in Table V, rotating jets cutting in Table VI.

It is to be noticed that cutting performance of rotating water jet cutting was much higher when traverse speed increased from aproximately 100 mm/min to 600 mm/min. In additon the cutting performance of rotating water jet cutting was much higher when tests were performed in sandstone in comparison with abrasive water jet cutting even at lower operating water pressure and smaller water nozzle diameter.

6.0 CONCLUSIONS

Tests of the application of high pressure water jets as a new technology for tunnel maintenance, usually performed by hand-held tools, proved to have 3 to 11 times greater performance of individual operations compared with present-day technology. Results obtained during the tests in Čremošné tunnel confirmed the acceptability and profitableness of high pressure water jets in tunnel maintenance.

Using of properly designed and remotely controlled manipulator may even increase the performance of high pressure water jets. In addition, the operator may control the manipulator from soundproof and dustproof cabine which would considerably increase the safety of work.

Concrete and rock cutting results serve also as a basic knowledge for expanding the high pressure water jet cutting technology in the field applications in Czechoslovakia.

More than 200 specialists from many Czechoslovak enterprises, from the U.S.S.R. and Bulgaria visited Čremošné tunnel test site and field laboratory during the last days of our experimental program.

ACKNOWLEDGEMENTS

The authors wish to thank to the Flow Internatinal Corp. (Kent, U.S.A.) and to the Flow Europe GmbH. (Darmstadt, Germany) for lending the high pressure equipment JetPac. Special thanks to Dr. Michael Pao and Dr. Uwe Ehlbeck.

REFERENCES :

1. Jeřábek, Z.: "Technical possibilities to use high pressure water jet for tunnel maintenance at czechoslovak railways" (in Czech) Proceedings from colloquy Using of high pressure water jet in tunnel civil engineering, Čremošné, May 1989

2. Jeřábek, Z.: "Evaluation of the high-pressure water jet technology in the Railway Civil Engineering Enterprise Brno of the Railway Constructions and Installations Group" (in Czech) Proceedings Mining Geomechanics 89, Ostrava, 1989, pp. 426-436

3. Vašek J., Foldyna J., Hlaváč L.: "Testing of high pressure water jet equipment in outdoor application (tunnel Čremošné)" Report of Mining Institute, Ostrava, 1989

4. Vašek J., Foldyna J., Jeřábek Z., Momber A.: "Die Anwendung von Hochdruckwasserstrahlen bei der Instandhaltung von Eisenbahntunneln" Bauplanung-Bautechnik, 44 Jg., Heft 3, März 1990, pp. 111-113.

NOMENCLATURE

a - abrasive grain size [mm]
da - abrasive nozzle diameter [mm]
dw - water nozzle diameter [mm]
h - depth of cut (sample thickness) [mm]
n - number of water nozzles
p - operating water pressure (caltulated from oil pressure measured in primary circle of the pump) [MPa]
v - traverse speed [mm/min]
P - cutting performance (P = h.v) [m^2/hour]
Pa - area performance [m^2/hour]
Pl - longitudinal performance [m/hour]
Qa - abrasive flow rate [kg/min]

Table I. Concrete mixture recipe and mechanical properties

	1 m^3
cement SPC 325	315 kg
sand 0-4 mm	740 kg
gravel	1100 kg
water	175 l
total specific weight	2340 kg/m^3
strength of concrete (cube)	20 MPa
tensile strength of concrete	1.4 MPa

Table II. Results of abrasive water jet cutting of concrete samples

Sample	h	p	dw	da	Abrasive	a	Qa	v	P
No.1	300	220	0.81	3.2	quartz sand	0.40	1.59	16.0	0.288
No.2	150	235	0.64	2.3	quartz sand	0.40	0.54	22.1	0.199
No.3	300	220	0.81	2.3	quartz sand	0.40	1.98	74.8	1.346
No.4	150	220	0.81	2.3	quartz sand	0.40	1.98	260.0	2.340
No.5	300	220	0.81	3.2	quartz sand	1.20	1.50	33.0	0.594
No.6	150	207	0.97	3.2	quartz sand	1.20	1.93	93.4	0.841
No.7	300	220	0.81	3.2	quartz sand	1.20	1.50	45.8	0.824
No.8	150	207	0.97	3.2	quartz sand	1.20	1.93	140.0	1.260
No.9	300	220	0.81	3.2	quartz sand	1.20	1.50	92.8	1.670
No.10	150	207	0.97	3.2	quartz sand	1.20	1.93	248.0	2.232
No.11	300	207	0.97	3.2	quartz sand	1.20	1.93	43.6	0.785
No.12	150	207	0.97	3.2	quartz sand	1.20	1.93	73.2	0.659
55N	200	207	0.97	3.2	quartz sand	1.20	1.93	22.0	0.264
BN	250	207	0.97	3.2	quartz sand	1.20	1.93	22.0	0.264
BN	500	207	0.97	3.2	quartz sand	1.20	1.93	3.5	0.104

Table III. Concrete charcteristic and basic mechanical properties for 55N and BN segments

		55N segment	BN segment
		1 m^3	1 m^3
cement sulfares 325		470 kg	550 kg
sand	0 - 8 mm	805 kg	775 kg
gravel	4 - 8 mm	215 kg	210 kg
	16 -22 mm	780 kg	740 kg
water		171 l	167 l
cube strength		35 MPa	45 MPa
tensile strength		1,9 MPa	2,2 MPa

Table IV. Physical and mechanical properties of rock samples

rock	volume weight [kg/m^3]	porosity (real) [%]	compresive strength [MPa]	tensile strength [MPa]
sandstone Božanov sample 1	2 189	16.84	42.5	3.4
marble Supíkovice sample 2	2 714	0.48	82	11.4
granite Černá voda sample 3	2 610	1.32	160	16.2
travertine Spiš sample 4	2 425	-	89	7.9

Table V. Results of abrasive water jet cutting of rock samples

Rock	h	p	dw	da	Abrasive	a	Qa	v	P
granite	420	227	0.76	3.2	quartz sand	1.20	1.93	7.0	0.175
marble	510	220	0.81	3.2	quartz sand	1.20	1.50	3.0	0.092
sandstone	275	220	0.81	2.3	quartz sand	0.40	1.98	16.0	0.264
travertine	500	227	0.76	3.2	quartz sand	1.20	1.93	11.3	0.339

Table VI. Results of rotating water jets cutting of rock samples

Rock	p	dw	n	v	h	P
granite	207	0.64	2	640	5.0	0.192
granite	207	0.64	2	102	10.0	0.061
marble	207	0.64	2	680	7.0	0.286
sandstone	207	0.64	2	630	31.7	1.198
sandstone	207	0.64	2	640	31.0	1.190
travertine	207	0.64	2	110	4.0	0.026

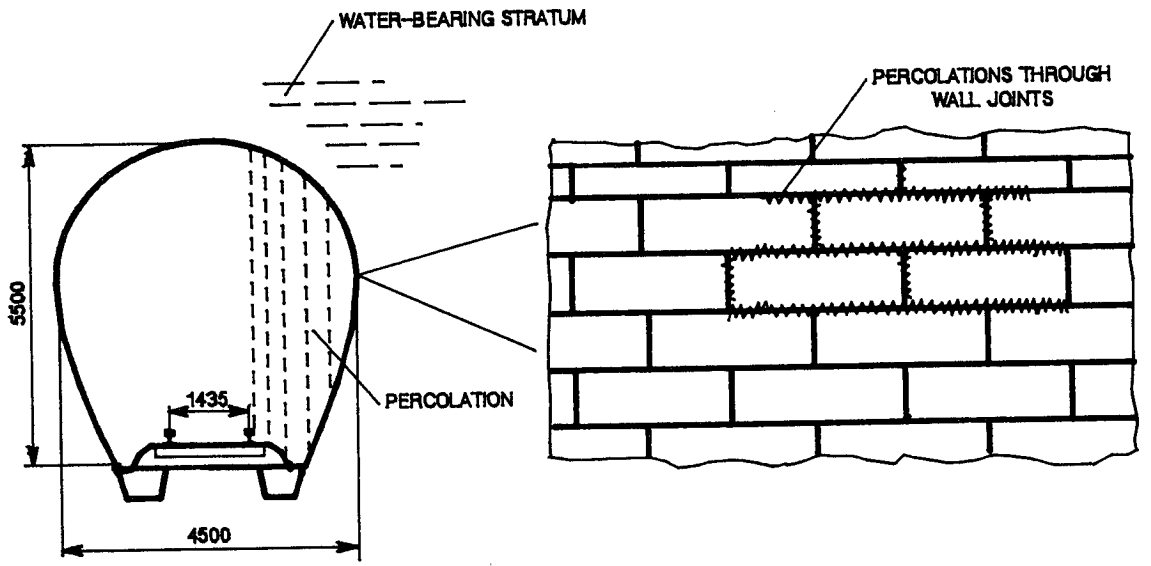

Figure 1. Scheme of percolations through wall joints

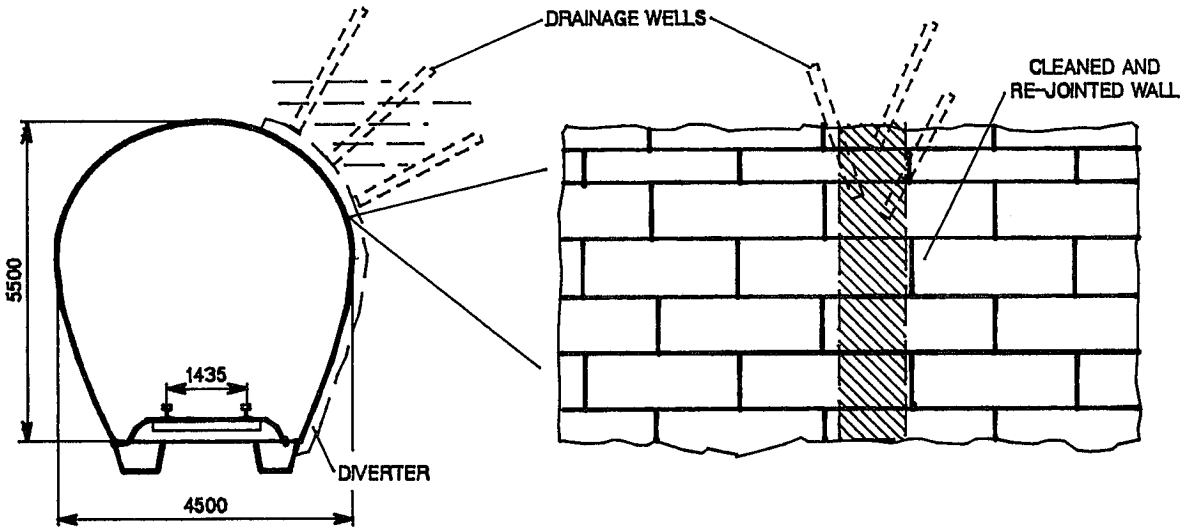

Figure 2. Scheme of maintenance intervention

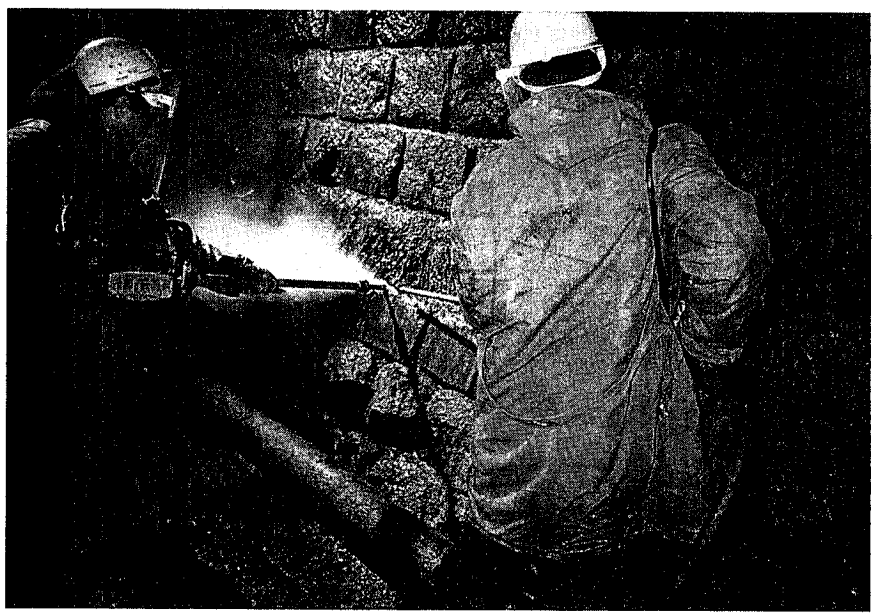

Figure 3. Removing of the old joints filling using JETLANCE™

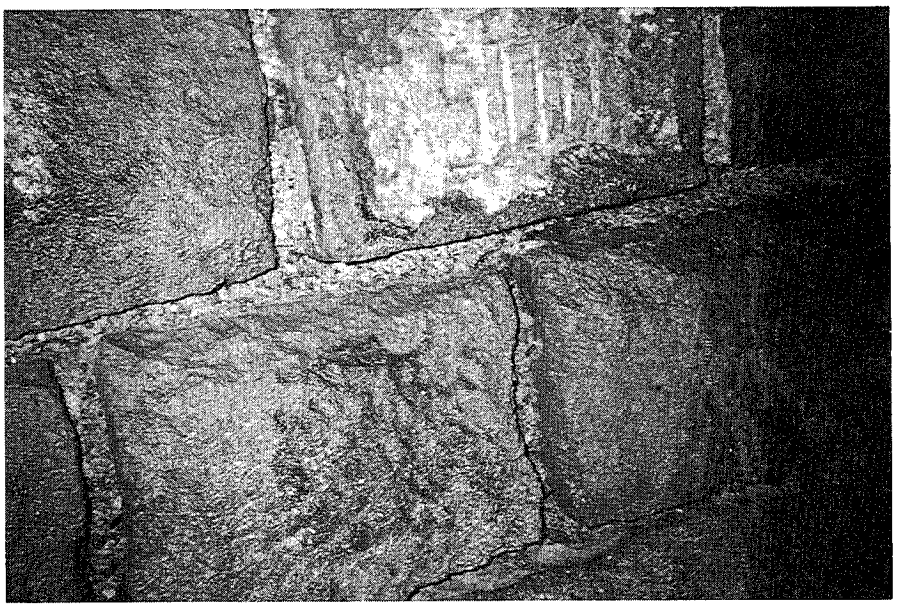

Figure 4. Tunnel wall after cleaning and removing of joints filling

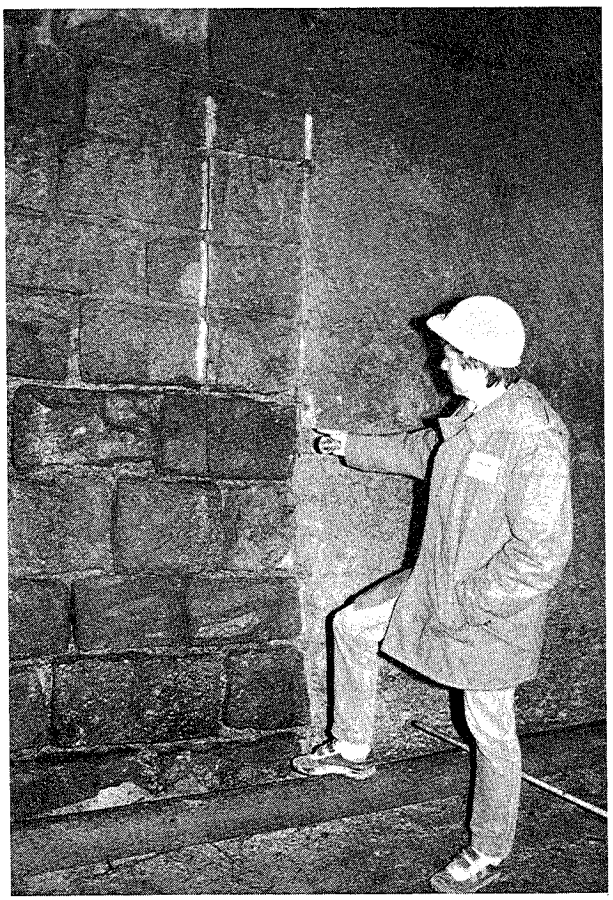

Figure 5. Cuts of slots for diverters breaking

	Sample dimensions: 1,0x0,5x0,3 [m]		Sample dimensions: 1,0x0,5x0,15 [m]
1.	Concrete armoured with steel bars of diameter of 28 mm 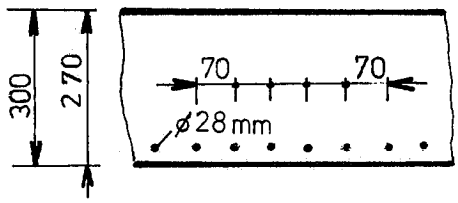	2.	Concrete armoured with steel bars of diameter 14 mm 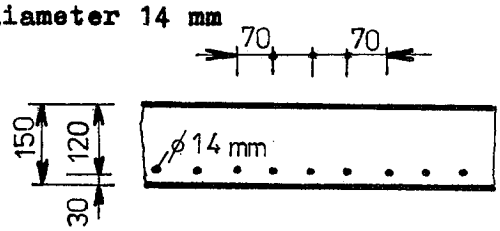
3.	Monolithic concrete, not armoured	4.	Monolithic concrete, not armoured
5.	Shotcrete armoured with mettalic meshes 100 x 100 x 6 [mm] 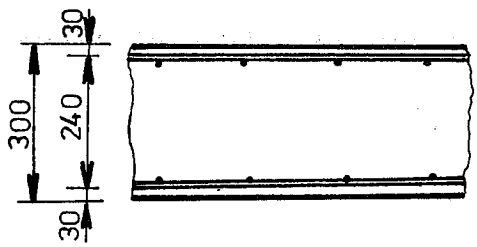	6.	Shotcrete armoured with mettalic meshes 100 x 100 x 6 [mm] 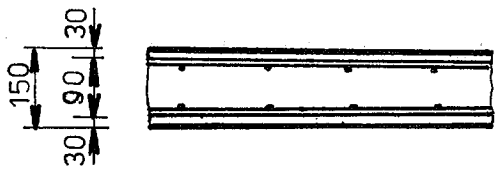
7.	Shotcrete, not armoured	8.	Shotcrete, not armoured
9.	Monolithic concrete with inbuilt wood (spruce boards 100/20, length 450 mm) 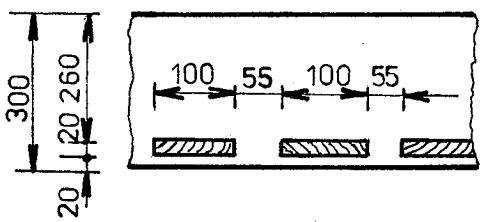	10.	Monolithic concrete with inbuilt wood (spruce boards 100/20, length 450 mm) 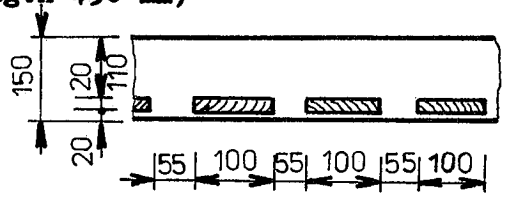
11.	Monolithic concrete with addition of cut wires (length of 20 mm, diameter of 0,4 mm) - 5 % of total weight of the cement	12.	Monolithic concrete with addition of cut wires (length of 20 mm, diameter of 0,4 mm) - 5 % of total weight of the cement

Figure 6. Diagrammatic drawings and descriptions of concrete samples

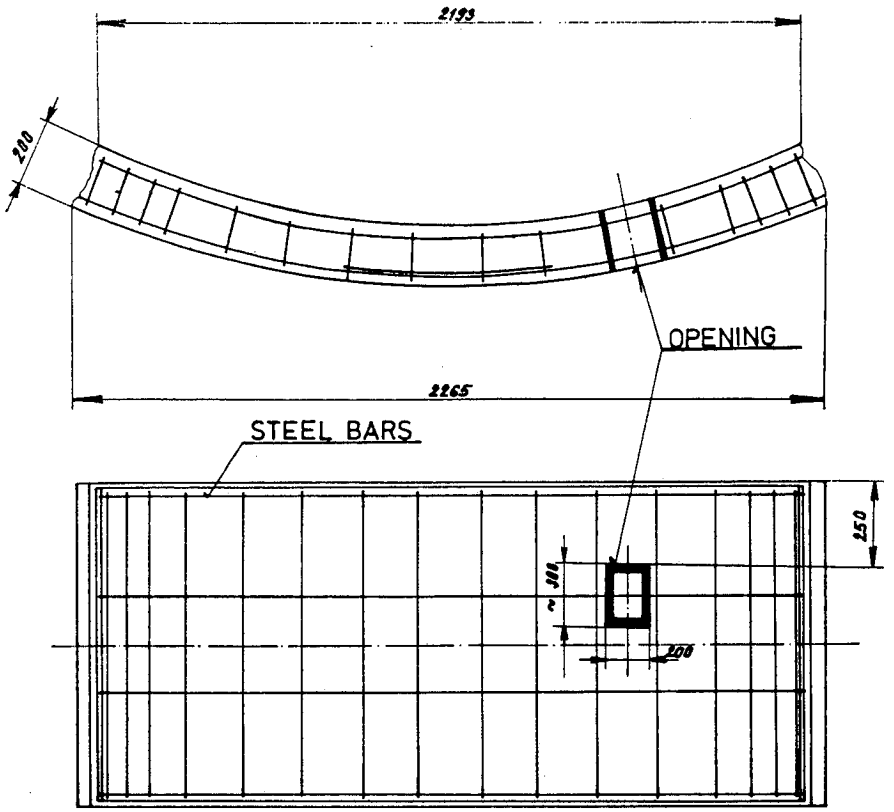

Figure 7. Diagrammatic scheme of the 55N segment

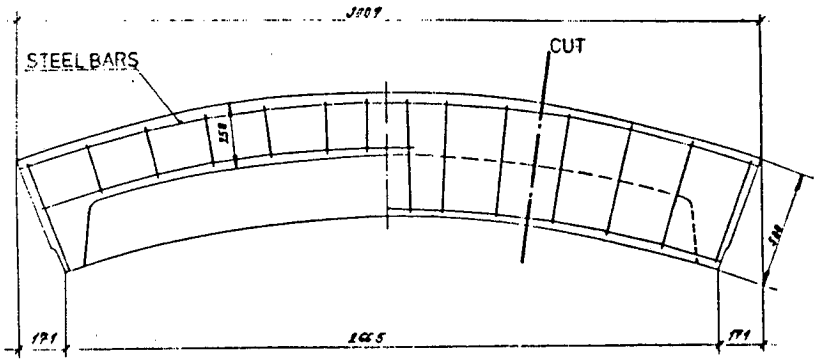

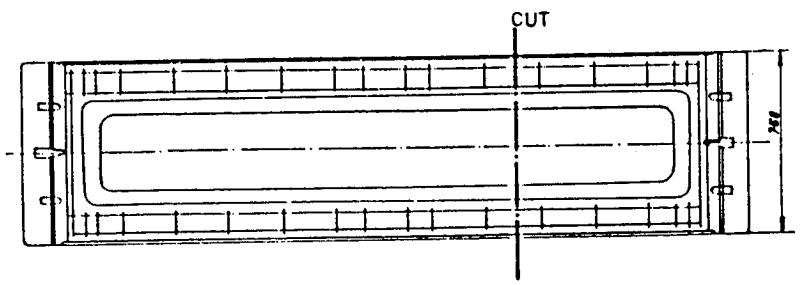

Figure 8. Diagrammatic scheme of the BN segment

6th American Water Jet Conference
August 24 - 27, 1991: Houston, Texas Paper 9

THE IMPULSIVE WATER JETTER IS A QUALITATIVELY NEW MACHINE FOR ROCK BREAKING

Gennady Atanov
Donetsk State University, UkSSR

Abstract

The advantages of the impulsive hydrodynamic method of rock breaking by means of impulsive high speed water jet are shown in comparison with the traditional methods.

There are results of the impulsive water jetter investigations and the ways of increasing its efficiecy.

Organized and Sponsored by the Water Jet Technology Association.

1. The problem of hard rocks breaking.

The demand for industrial application of raw materials is growing with every year. To get them it is necessary to break different rocks among which hard and very hard rocks make up considerable part. The main and often the only method of breaking them is the drilling-and-blasting method. However, it is insufficiently productive and uneconomic and is hazardous for workers' health especially in underground mines. It is also dangerous for ecology. There are some mining and geological conditions under which mechanical rock breaking appears to be ineffective due to the rock hardness and its high abrasivity. Lumps of hard rocks are broken by pneumo-hydrolic strikers still they themselves break down rapidly because of high shock loading. The drilling-and-blasting method cannot often be used either through the impossibility to provide the safe conditions (for example gaseous rocks, seismically dangerous zones) and therefore minerals cannot be mined by it. Besides the abovementioned methods of rocks breaking have practically exhausted reserves of productivity.

Productivity of labour in mining industry can be considerably increased only by applying the new approaches to the development of mining technology. The possible technologies based on different principles for instance ultrasonics, lazers etc. have been investigated lately.

2. The impulsive hydrodynamic method of rock breaking. The impulsive water jetter.

The hydromechanization proved to be a highly productive method for breaking rocks. A new qualitative stage of it is the application of the impulsive liquid jets. The impulsive principle

allowed to create powerful installations (up to some hundreds of megawatt) and made it possible to get the liquid jet speeds up to some kilometres per second. No rock in Nature can withstand a blow of such a jet. The application of the impulsive jet became the basis of the new method - the impulsive hydrodynamic method.

There are some ways of producing the impulsive jets: the cumulative effect, the inercial principle, the electrohydraulic effect and others (1,2). The extrusive effect when water is outsed through the aperture is realized in the impulsive water jetter (IWJ). Figure 1 shows the scheme of the traditional IWJ. It consists of the following main parts: gas receiver - 1, heavy piston -2, barrel -3, nozzle -4. The principle of its operation is the following: the piston, having been accelerated to the definite speed along some distance from its extreme left position under the action of the compressed gas in the receiver closes the barrel filled with water. As a result of this acceleration the piston acquires great kinetic energy which is transformed into water internal energy, the water pressure increasing and it is ejected from the nozzle at a high speed. Thus the shot of some milliseconds duration takes place. Before the following shot the piston must return to the extreme left position and this can be done in different ways.

The principal role here is played by the compressibility of water. The IWJ shot time if of short duration, it considerably exceeds the characteristic time of the process i.e. the propagation time of disturbance from the piston to the nozzle. Therefore the individual disturbance (including the shock wave arising at the piston blow against water) changes negligibly the

parameters and they can be averaged throughout the barrel volume and can be described in the quasi-stationary approach. The mathematical model of the shot - the internal ballistics system of equations - is the system of the ordinary differential equations.

The curve 1 (Figure 2) shows the typical water pressure dependence in the barrel on time. The pressure value can attain several hundreds of megapascal and it is limited only by the strength of the installations (3).

The hydrodynamic problems may be divided into three groups:

1) the problems of internal ballistics, i.e. the investigations of the processes occuring inside the IWJ;

2) the problems of the exterior ballistics, i.e. the investigations of the jet motion and its transformations in the air;

3) the problem of jet interaction with an obstacle.

All these problems belong to the sphere of gas dynamics and therefore they are to be solved by taking the water compressibility into account (4). The Donetsk State University plays the leading role in hydrodynamic investigations of the impulsive jets. The internal ballistics is the most developed field there. The theoretical basis for calculating the impulsive installations has been created and acceptable accuracy of the theory has been experimentally proved (3,5).

The process of rock breaking by the impulsive jets has been studied least of all. And though much consideration was given to this problem the breaking criteria have hot been determined yet, the connection between the parameters characterizing the internal ballistics of the installations and the jet breaking ability has not been found out.

3. The results of the impulsive water jetter investigations.

The greatest number of the investigations on rock breaking have been carried out with the IWJ. It is more studied among the impulsive hydrodynamic installations taking into account both its design and its physics processes.

The most systematic reseaches of this problem have been carried out by Dongiprouglemash Institute (Donetsk, UkSSR) (6-9). This Institute has designed a heading combine of a new type (Figure 3) on the basis of the IWJ mounted on the rock-loading machine. Its total mass is about 20,000 kg, the mass of the IWJ is 2,600 kg. At the initial gas pressure of 4 MPa in the receiver, the maximum water pressure is about 450 MPa. The nozzle outlet diameter is equal to 10.5 mm, the flow rate is from 2 to 3 m^3/h and the jet frequency is up to 12 shots per min. The operational power of the combine is 160 kWt.

The following table contains some characteristics of this heading combine and of different pneumohydrolic strikeres.

Table

Parameters	Country, Firm, Type	FRG, Krupp, HM 2200	Finland, Rammer, S-86	UkSSR, Dongiprouglemash, IV-5
The shock energy, kJ		-	8.2	100
The mass, kg		3800	3460	2600
The necessity of dust suppression		yes	yes	no

The heading combine was tested in the underground mine for driving the main roadway. The cross section area of the roading was 12.3 m^2. The face consisted of the following types of rocks : sandstone near the roof (hardness after Prof. Protodiakonov: f=6), aleurolite near the floor (f=4) and a coal seam with pirite inclusions (f=9) between them. A 130 m length of the roading was driven with 1,560 m^3 rock breaking and 175,000 shots were made for this work. The maximum driving speed was 1 m/shift, the breaking efficiency of sandstone, aleurolite and coal being 8,20 and 51 dm^3 per shot respectively. The results of the tests obtained allow us to think of a serial production of this machine for the full-fase of f=8 breaking with speed of 120 m/month. Besides the IWJ for the rocks with f=10 has been calculated on the basis of their results (10).

The IWJ has been applied on the mechanical heading combine as a supplementary breaking device (11). Such combine has several advantages. Owing to the operation of the two breaking devices together the combine's productivity grows. Moreover this combine can been used for breaking the more hard rocks because the jet action weakens the face in general. It is important that the combine autonomy increases essentially if there are the great hardness rock inclusions which cannot be broken by the mechanical device. In this case there is no necessity in high productivity of the combine and the inclusions can be broken only by the jet for which the rocks with the hardness of f=12-13 are quite accessibile.

The same IWJ was used for breaking the 600 mm thick reinforced concrete wall during the construction of the Dnieper Electric

Power Station - 2. The breaking efficiency was 1.5 m^3/h and it did not practically depend on the fitting (20 mm diameter bar and 150x 150 mm reinforcing fabric mech) (Figure 4). The dam spillway of 40-years cure concrete was battered by the IWJ with the efficiency of 0.5-0.6 m^3/h which is 2-3 times more than that of the powder rock breaker.

The sandstone lumps (f=12;1100x1200x1500 mm) were broken by 4-5 shots for 35-40 sec. The mounting of the machine for breaking the next lump took 60-80 sec (Figure 5,a,b). The efficiency was 50-60 m^3/h.

In the process of the IWJ investigation many difficulties have been successfully solved, many important technical solution have been found. All this enables to increase the reliability, to decrease essentially the mass of the IWJ and to provide its proper automatic operation.

About 100,000 shot have been achieved by IWJ without its repairing, this enabling the IWJ application in technological process demanding continuous operation and high efficiency.

The principal IWJ parameters which can be obtained are:

The IWJ energy, kJ	20	60	100
The nozzle outlet diameter, mm	5	7	10
The thrown out water mass, kg	0,5	0,8	1,0
The gas pressure in the receiver, MPa	7	7	7
The piston disperse distance, m	0,3	0,4	0,525
The shot frequency, min^{-1}	30	25	20
The IWJ length no more, m	1,2	2,0	2,5
The IWJ mass no more, kg	700	1500	2200
The maximum water pressure,MPa	120	350	550

A new autonomous installation with a wide range of possibilities is worked out in Donetsk State University (Figure 6). It is created on the basis of an excavator with hydraulic drive that allowed through its oil station to provide the automatic work of the IWJ.

4. The impulsive water jetter advantages.

Summarizing the results of the considered and other tests we can say that the application of the IWJ for rock breaking has the following advantages:

1) high efficiency and low power capacity;

2) no cutting tool is needed. This saves the expenses for its manufacture, sharpening and change;

3) no contact of the impulsive hydrodynamic machine with rock face and for the reason there is no great load on it;

4) small dimension and light weight of the machine;

5) high mobility of the machine and the posibility of its application for auxiliary operation (making drain grooves and holes for the support legs ets.);

6) simplicity in mechanization and automatization of the work especially for underground mining;

7) ability of breaking rocks of high hardness and of any abrasiveness;

8) improvement of labour and safety conditions.

The last item is especially important for underground works. A heading Machine with a mechanical breaking device produces much rock dust during its operation and even if special dust removal devices are applied the dust content in air can be 5 times as much of the maximum limit. It results in silicosis, a serious disease

of miners, which is a social disaster for a large number of countries. When the above described IWJ worked in the underground mine the dust content was 6 mg/m^3 that did not exceed the maximum limit. It is explained by jet watering of the rock fase. At the same time the consumed quantity of water is so neglibigle that it cannot cause catarrhal diseases and rheumatism which are characteristic for conventional hydraulic method.

The experiments on utilizing the impulsive jets and the theoretical analysis allow us to suggest that the fields of applying the impulsive hydrodynamic breaking method in oremining and civil engineering are practically unlimited. It can be successfully used as it has been already mentioned for driving the main roadway including tunnels; for coal cutting; for cutting slots in advance in the mine to exlude sudden outbursts; for cleaning mud stuck to the walls of bunkers and mine cars; for breaking reinforced concrete foundations; for loosening the frozen soils; for ice-breaking; for breaking oversizes and profilling roadbed on rocky bases; for rock excavation; for knocking rigid cores out of castings; for stripping of obstructions with earthquakes and slashing and so on.

5. The ways of increasing the impulsive water jetter efficiency.

We want to stress the important fact - the possibility of the IWJ destructive force essential increase. To understand this it is necessary to analyze the processes connected with jet motion. Because of strongly expressed nonstationarity of the process the dynamic jet pressure on the nozzle outlet, in general, is lower than the pressure in the barrel. Both pressures can be considered the same only for the quasi-stationary proce s ses. The necessary

conditions enabling to do this, have been described in paper (12). But the jet speed differs greatly from the outlet speed. Due to this fact the jet pressure is variable and different from its value on the nozzle outlet.

The physics of the process is the following (13). As it is seen from Figure 2 (curve 1) the time dependence of the water pressure in the barrel is of bell character, the dependence of outlet speed being identical. The result is that at the initial stage of the shot while pressure is increasing the outlet speed becomes greater, the behind particles moving faster than the preceding ones. Therefore the initial particles of the jet are thrown about and behind ones are impeded, the speed of the head of the jet being increased, due to the more rapid particles which penetrate into it but this speed remains less than the outlet speed. The speed of the head of the jet is maximum when the more rapid particles outleting from the nozzle at maximum pressure (P_m) penetrate into it.

When the pressure and consequently the jet speed decrease the jet becomes uncompact, tears away from the nozzle and it is impeded by air. The outlet speed and the distance at which it attains its maximum are increasing with the P_m. This distance is 180-240 bores of the nozzle. The dependences of the maximum outlet speed (curve 1) and of the maximum speed of the head of the jet (curve 2) on P_m for some cases are shown in Figure 7.

Quantitatively the described effect is estimated by the pressure factor k_p which is defined as the squared ratio of the maximum jet speed to the maximum outlet speed. From the above given considerations it is clear that $k_p<1$. The curve 3 (Figure 7) gives

its dependence on P_m. The decrease of k_p with the increase of P_m is explained by the fact that in this case the speed of the pressure growth dp/dt increases, the described processes being intensified. One can see that the dynamic pressure of the jet is practically two times lower than that of the water in the barrel but this circumstance is not considered at the estimation of the destruction. The existing approach assumes the equality of the pressures.

6. The increase of impulsive water jetter effectiveness in the framework of the traditional scheme.

From above it follows that one of the directions of the IWJ efficiency increase is to raise the pressure factor. This can be done by different methods. Some k_p increase can be obtained in the framework of the used IWJ with the piston but the radical way is to use the traditional IWJ schemes allowing to control the shot. At the beginning we shall describe some ways of k_p increase for the used IWJ.

The first way can be called two-stage as gas energy is passed to water at two doses (14) (Figure 8). Technically it is achieved by a freely moving striker inside the hollow piston m2. In the speeding up process the striker is pressed to the back piston wall then having hit water the piston is impeded, the striker being not affected by the impedance, and it moves to the front piston wall in its relative motion.

The striker does not influence the process in this stage of the shot. Its influence begins when it reaches the front piston wall and hits it. There is the same situation as at the beginning of the shot, the striker passes its energy to water, the energy of

which being increased. In this scheme the calculation of the necessary striker shift l is principal as just this shift defines the hit moment and hence the character of the process. The curve 2 (Figure 2) corresponds to the two-stage shot for the same initial conditions as in the traditional shot (curve 1). Here the striker comes into operation in the stage of the pressure descrease and restores it to its maximum.

The essence of the second k_p increase method is illustrated by Figure 9 (14). Here there is also a striker -3 and a piston -1 but the striker is placed on the spring -2. Thus at the beginning of the shot water receives not all the energy given by the piston, part of it being accumulated by the spring. When at the final stage of the shot the pressure begins to decrease the accumulated energy is passed to water. It is possible to control the shot properties to some extent changing the spring toughness. The curve 3 (Figure 2)demonstrates approximate P(t) dependence for this scheme.

Thus two circumstances further the k_p increase: the speed decrease of the pressure growth and the increase of the high pressure action time.

7. The optimal shot control.

Though both considered and other methods for the IWJ traditional scheme allow to rise the shot efficiency but they do not give the solution of the problem in principle. It can be received only by means of the IWJ traditional scheme, the main condition being the presence of some beforehand given function on which the shot parameters depend. The necessary properties of the shot are provided by the special choice of this function. Such functions are called controling.

At first we shall consider the so called revolver IWJ scheme in which the necessary for shot energy is stored by the rotating revolver (15)(Figure 10). The revolver has a lug -2 of a definite form. Having been untwisted to the definite speed, the revolver through the lug contacts with the piston -3 locking the barrel -4 and moves it into it. This is the shot.

The principal moment here is that the lug form can be different and it is possible to set the problem of the choice of such form which could provide the necessary demands to the shot. The IWJ traditional scheme has no such an opportunity.

The above described jet properties allow to draw the conclusion that if the water pressure in the barrel remains constant the pressure factor will be equal to 1. And besides the destruction efficiency will be the higher the longer the state at which $k_p=1$ will last. The analysis with the wave process taken into account shows that the best form of the pressure impulse is not rectangular, as it can appear on the face of it, but such a form when the pressure is growing for some time.

The shot process of the revolver IWJ is described at the same approaches as they are in traditional IWJ, its mathematical model representing the system of the ordinary differential equations. The control problem is solved by the variational methods.

The results of the calculations for one of the variants of the IWJ are illustrated by Figure11. Curve 1 represents the lug height (its form) as the function of the turn angle $h=h(\varphi)$ and curve 2 shows the pressure impulse obtained for this form. The essence of this control is that at the initial stage of the shot the pressure must rapidly grow and therefore h increases greately and

after that the h growth slows down to stabilize the pressure. The strengthening of the h growth at the final stage is explained by the necessity to compensate the pressure decr e ase taking place because of water eject. The control and the angle of the turn are divided by their maximum values.

It is very important that the control problem allows to get not only the definite character but also the necessary quantity of the water pressure in the barrel.

The control shot is also allowable by the powder IWJ (16). Here the water is outsted by the combustion products of the powder the pressure of which can be very great. The controling function here is the combustion surface of the powder, depending on the time and being defined both by the shot parameters and by the charge geometry.

Figure 12 shows the solution results of one of the controling problems the purpose of which was to get the constant shot pressure 300 MPa. The touch curves correspond to the shot with the above described demands (1- the pressure, 2- the combustion surface; the combustion surface and the time are divided by their maximum values). Here the time for achievement the stationary regime is greater than that for the revolver IWJ. This is explained by the facts that, firstly, the definite part of the blast chamber is occupied by gas and its compression requires some time, secondly, gas compression is accompained by water oust and, consequently, by the increase of its volume. The law of the pressure change being characterized by the higher pressure at the initial stage allows to decrease the time for achieving the stationary regime.

In Donetsk State University there is a software allowing to calculate and to optimize the internal ballistics processes for the IWJ of the different schemes and the motion of the jets. There are also the systems for experimental investigations of the IWJ.

References

1. Atanov, G.A. 1987: The hydroimpulsive installation for breaking of the mining rocks (Гидроимпульсные установки для разрушения горных пород). Kiev, Visha shcola (In Russia).
2. Atanov, G.. and A.I.Petrakov 1983: Impulsive hydrodynamic method of rock breaking. Proc. 6th International Conference on Erosion by Liquid and Solid Impackt (September, Cambridge, England). Editors J.Field, N.Comey. Paper 32: 1-8.
3. Atanov, G.A. 1982: Interior ballistics of impulsive water jet. Proc. 6th International Symposium on Jet Cutting Technology (April, Guildford, England). Editor BHRA. England. Paper C5: 141-159.
4. Atanov, G.A. and Yu.D.Ukrainskiy 1979: Experimental investigation internal ballistics of the impulsive water jetter (Экспериментальное исследование внутренней баллистики импульсного водомета). Izv. Acad. Nauk SSSR, Mech. of Fluid and Gas, *N* 3 (In Russian).
5. Petracov, A.I. 1975: The impulsive water jet for breaking of the mining rocks (Импульсные водометы для разрушения горных пород). The Coal of Ukrainian, *N* 3 (In Russian).
6. Petrakov, A.I., M.M.Golitenko and O.D.Krivorotko 1972: The rock breaking of the highhead impulsive water jets (Разрушение пород высоконапорными водяными струями). The Coal, *N* 3 (In Russian).
7. Petrakov, A.I. and O.D.Krivorotko 1982: Breaking the mining rock of the impulsive jets (Разрушение горных пород импульсными струями). The Coal, *N* 3 (In Russian).
8. Petrakov, A.I. and O.D.Krivorotko 1978: Some experiense in

developing mining roadways using experimental heading machine with pulsed water jets. Proc. 4th International Symposium on Jet Cutting Technology (Aprel, Canterbury, England). Editor BHRA. England. Paper J3: 23-36.

9. Atanov, G.A., O.D.Krivorotko and Yu.A.Pilipenko 1989: The calculation of the impulsive water jetters principal parameters for opening mining driving (Расчет основных параметров импульсных водометов для проходки шахтных выработок). Izv. VUZov SSSR, Mining magazine, *N* 12 (In Russian).
10. Krivorotko, O.D., Yu.V.Moskovchenko and Yu.A.Pilipenko 1988: The Results of the mine tests a hydromechanical combine for breaking of the hard mining rocks (Результаты шахтных испытаний гидромеханического комбайна для разрушения крепких горных пород). In col. Mechanization of the process of production in the coal mines of Donbass. Donetsk, Donetsk Coal Institute (In Russian.
11. Atanov, G.A. 1975: The calculation of the impulsive water jetter shot with the wave processes (Расчет выстрела импульсного водомета с учетом волновых процессов). Izv. VUZov SSSR, Energetics, *N* 3 (In Russian).
12. Atanov, G.A. and B.I.Beshevly 1987: About the motion peculiarity of the impulsive water jetter jet (Об особенностях движения струи импульсного водомета). In col. Aerodynamic of unstationary processes. Tomsk, Tomsk State University (In Russian).
13. Patent document USSR *N* 1170146, 12/1982, IPC^4 E21C 45/00.
14. Patent document USSR *N* 1065603, 4/1982, IPC^3 E21C 45/00.

15. Atanov, G.A. and V.V.Kokin 1989: The impulsive water jetter with revolver accumulator of energy (Импульсный водомет с маховиковым накопителем энергии). Second All-Union Conference on the Revolver Accumulator of Energy (September, Jitomir, UkSSR) (In Russian).
16. Patent FRG 2907759, 2/1979, IPC^3 B05B 3/02.

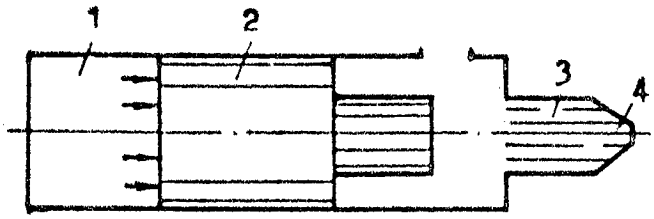

Figure 1
The impulsive water jetter scheme.

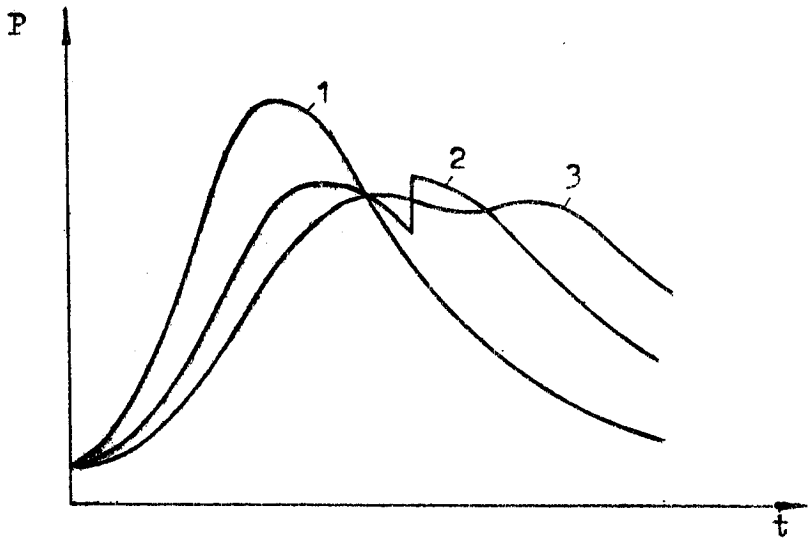

Figure 2
The water pressure impulse in the barrel.

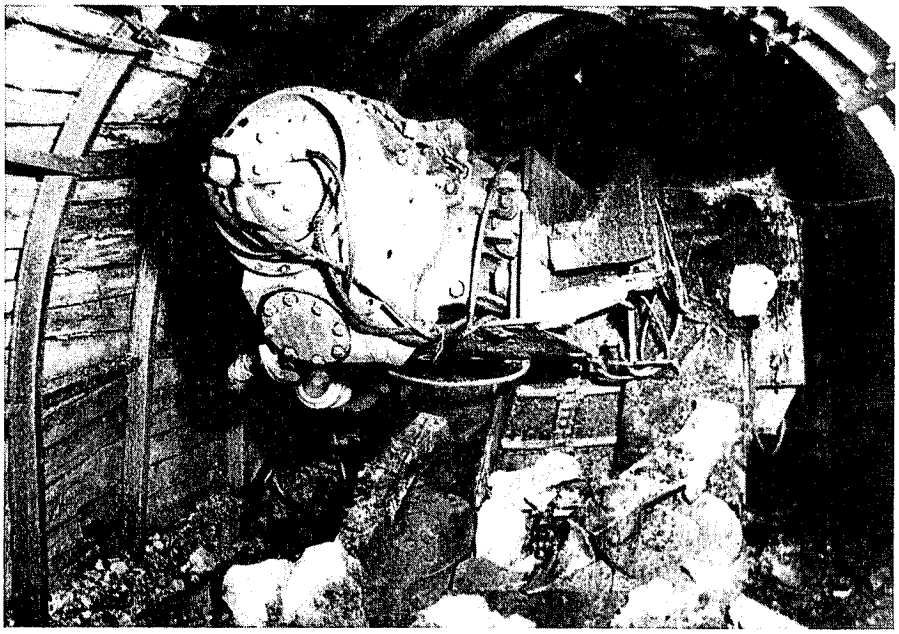

Figure 3
The heading combined with the impulsive water jetter.

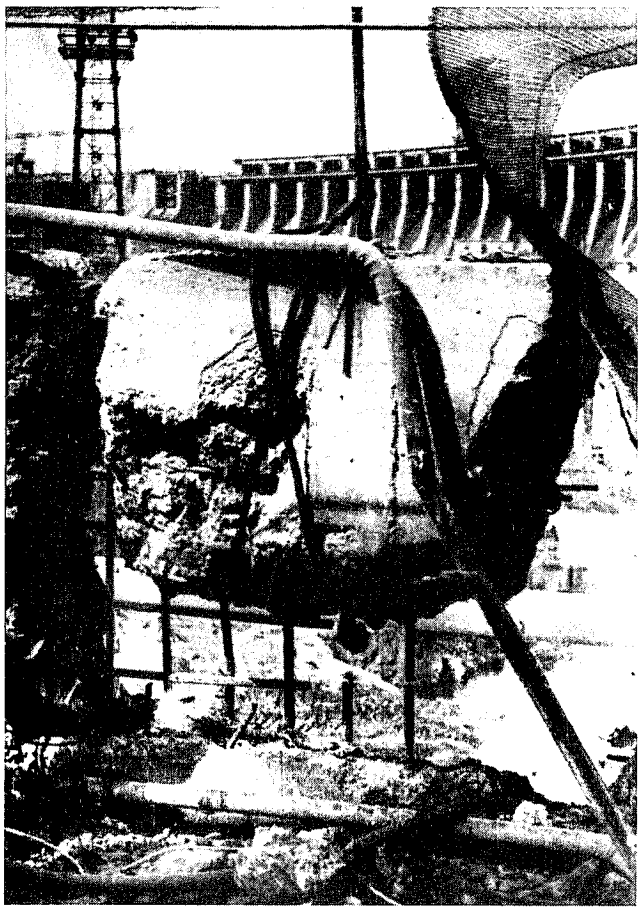

Figure 4
Breaking of the reinforced concrete.

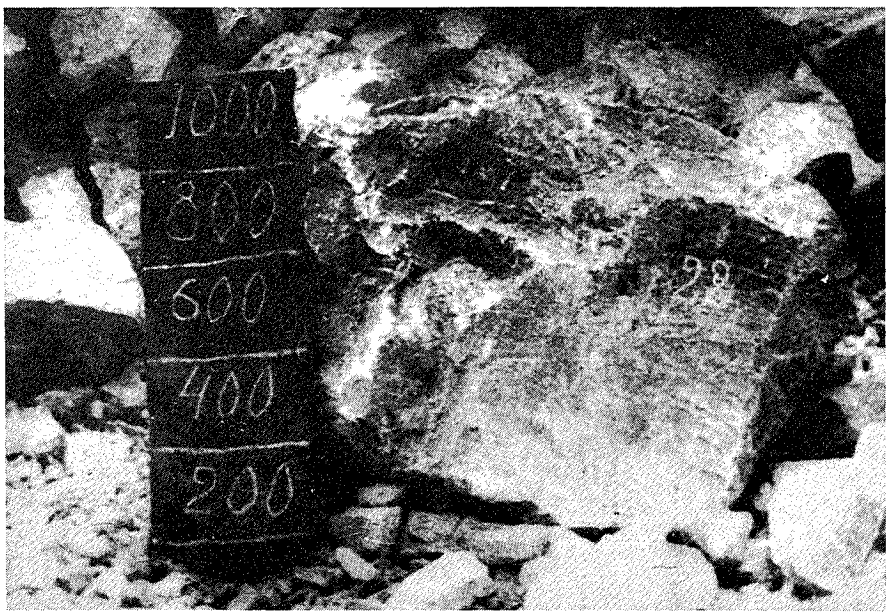

Figure 5a
Breaking of the sandstone lump – before breaking.

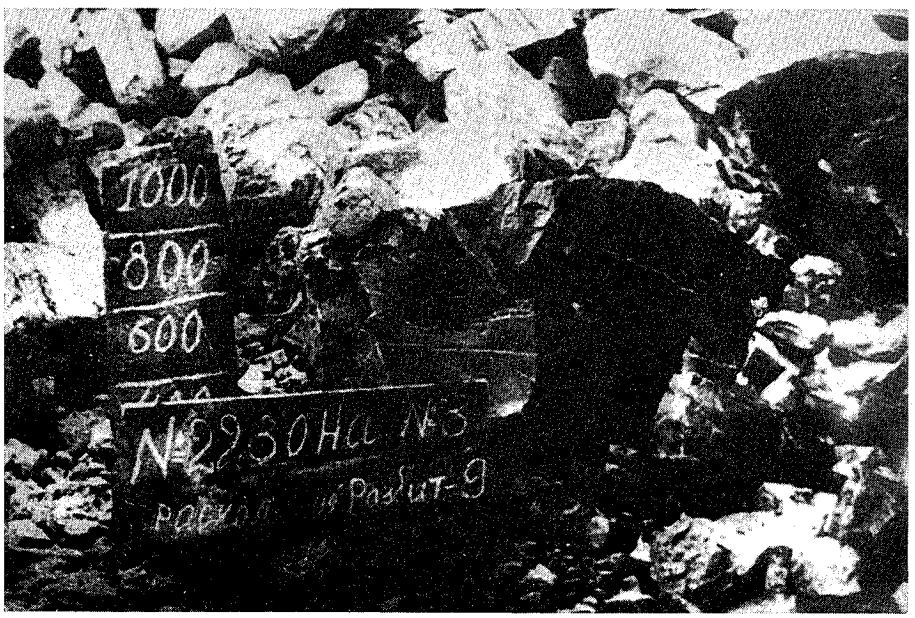

Figure 5b
Breaking of the sandstone lump – after 9 shots.

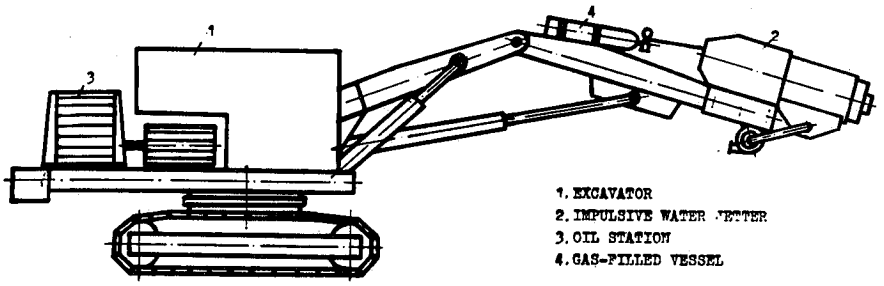

Figure 6
The autonomous machine with the impulsive water jetter.

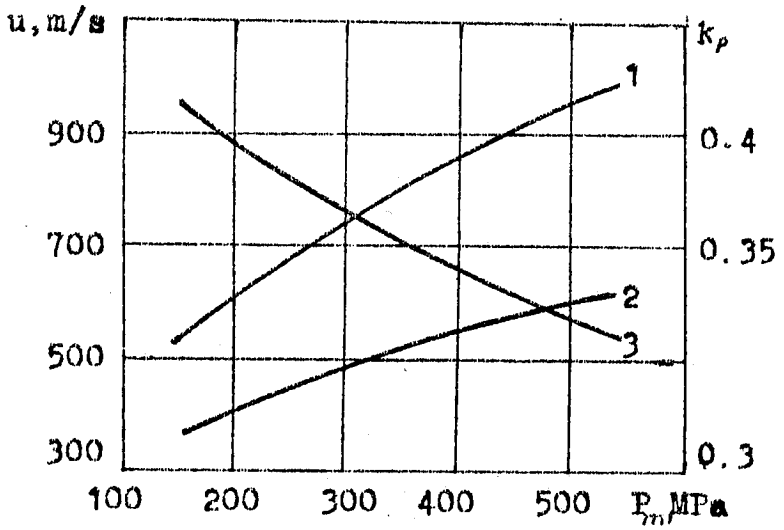

Figure 7
The investigation results of the impulsive water jetter jets motion.

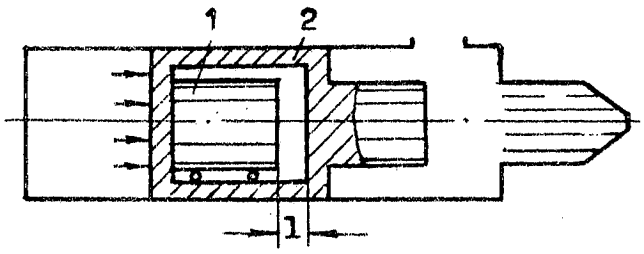

Figure 8
The impulsive water jetter scheme with a freely moving striker.

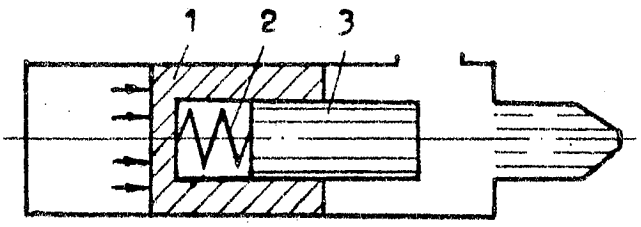

Figure 9
The impulsive water jetter scheme with a striker placed on the spring.

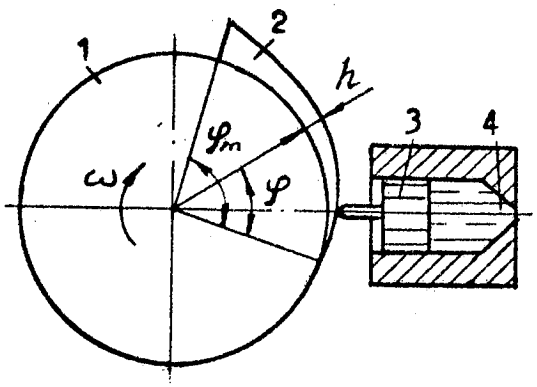

Figure 10
The revolver impulsive water jetter scheme.

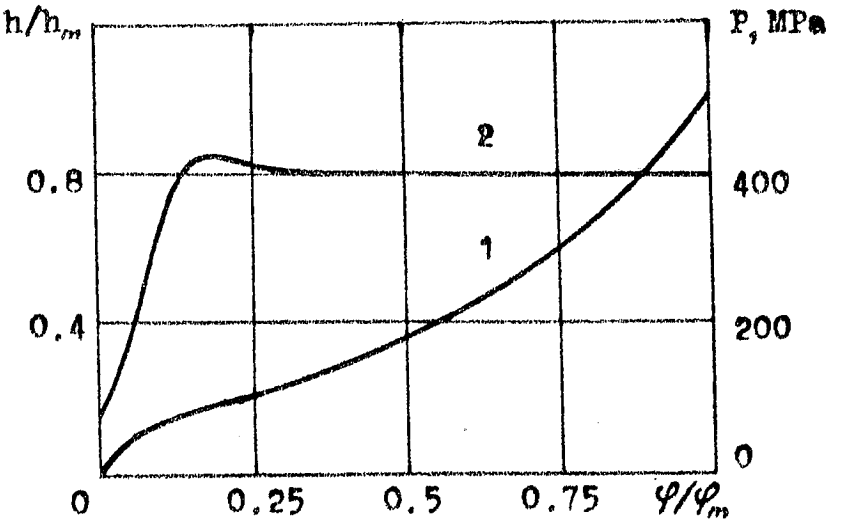

Figure 11
The results of the calculations for the revolver impulsive water jetter.

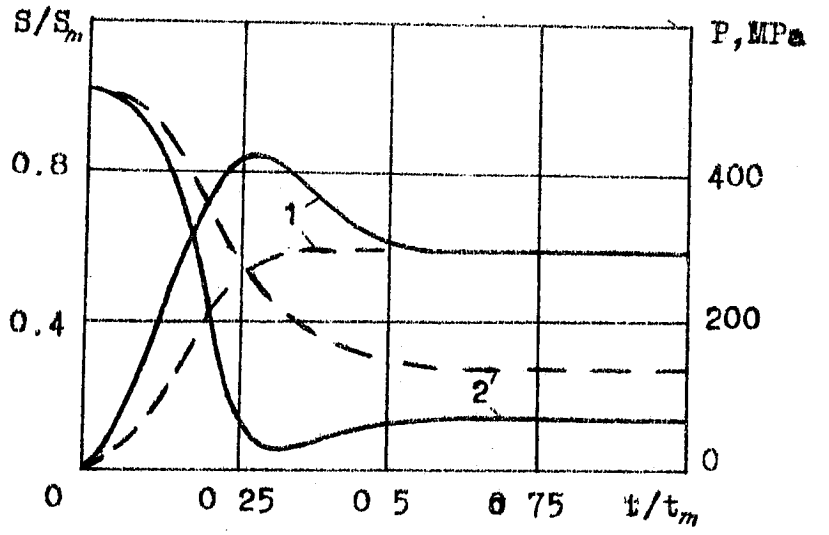

Figure 12
The results of the calculations for the powder impulsive water jetter.

6th American Water Jet Conference
August 24 - 27, 1991: Houston, Texas

Paper **10**

High Precision Cutting Method For Metallic Materials By Abrasive Waterjet

S. Matsui, H. Matsumura, Y. Ikemoto, and H. Shimizu
Kawasaki Heavy Industries,Ltd.
Kobe, Japan

I. Takada
Tokyo Electric Power Company
Tokyo, Japan

ABSTRACT

Experimental investigations were conducted to develop a precision cutting method for metallic materials by abrasive waterjet(AWJ). Accuracy and quality of cut were examined with respect to the width of kerfs, the taper angle of cut surfaces, and the roughness, etc. The effects of traverse speed and material thickness on the accuracy and quality of cut were investigated in detail. The effects of wear of abrasive nozzles on them were also considered. As the results of this study, it was shown that AWJ could be successfully applied for precision cutting of metallic materials surpassing the conventional precision cutting processes.

Organized and Sponsored by the Water Jet Technology Association.

1.0 INTRODUCTION

AWJ cutting is increasingly being used in various industrial fields as a cutting method for metallic materials because it leaves no heat-affected-zone and no thermal distortion and can easily machine difficult-to-machine materials such as titanium, Inconel and tool steels, etc., and also can cut them at the speed which is about ten times faster than that of conventional precision cutting processes such as wire electrical discharge machining. In these fields, net-shape or near-net-shape cutting is required, with much higher accuracy (within 0.1mm) than that for cutting concrete structures and FRPs.

However, only few papers concerned with accuracy and properties of AWJ cutting have been reported at present[1),2)]. And there is a little stock of knowledge and data available for the precision cutting with AWJ.

This paper describes the accuracy and properties of AWJ cutting in type 304 austenite stainless steel plates, and a method to make AWJ cutting edges more precise.

2.0 EXPERIMENTAL EQUIPMENT AND METHOD

An experimental instrument used in this study is an AWJ cutting table combined with a 2-axis numerical controller. Figure 1 shows an appearance of the instrument.

A high pressure pump is an intensifier type. Its maximum pressure is 392MPa and the maximum water flow rate is 3.3ℓ/min. An abrasive supplying unit is a self entrained type using a light vacuum generating around the jet. Abrasive flow rate can be varied with an orifice set below an abrasive hopper.

Stabilities of traverse speed, pressure, and abrasive flow rate are good enough for the present examination.

Type 304 stainless steel (SUS304), a popular structural steel, was used in this study. Thicknesses of specimens were 10mm, 20mm and 48mm. To examine the quality of AWJ cutting edge, cuts were made in these specimens varying the traverse speed.

Cutting conditions were as follows:

Specimen	: Type 304 stainless steel plates ($10mm^t$, $20mm^t$, $48mm^t$)
Pressure	: 245MPa
Water nozzle diameter	: ϕ0.33mm
Abrasive nozzle diameter	: ϕ1.2mm
Abrasive	: Garnet sand #80
Abrasive flow rate	: 0.4kg/min
Traverse speed	: 3-100mm/min
Stand-off distance	: 2mm

After cutting, various geometrical parameters concerned with the accuracy of cutting such as surface roughness, taper angle, straightness, drag, etc. were measured. Another cutting experiment using wedge-shaped specimens shown in Fig.2 was also carried out to obtain the relationship between traverse speed and depth of cut.

In this study, thickness and cutting speed were selected as main parameters, although cutting performance can be affected by many parameters[3),4)]. This is because that cutting parameters except for these two parameters might not be usually varied much drastically in practical use of AWJ.

The reasons of selecting type 304 stainless steel as a experimental material is that this shows intermediate cutting characteristics among metallic materials[5)] and it can not be rusted.

3.0 RESULTS AND DISCUSSIONS

3.1 DEPTH OF CUT

Figure 3 shows the relation between the depth of cut and the traverse speed. The depth of cut represents the maximum thickness to be cut through at a given traverse speed. Each value of the depth of cut was obtained by averaging two cutting data, since it slightly scattered by spiking. In the range of this study, there is a linear relationship of -1 gradient between the two parameters on the log-log plots.

3.2 KERF WIDTH

Figure 4 shows the relations between the traverse speed and kerf width at the both sides of the specimens. Values of kerf width were measured at the inner points by 0.5mm from the both surfaces of the specimen. As shown in this figure, the kerf width at both sides decreases linearly with an increase in traverse speed on the semi-log plots.

The kerf width at the lower side decreases consistently with an increase in thickness of plates. On the other hand, the upper kerf width does not change with an increase in plate thickness.

There is a same linear relationship between traverse speed and upper kerf width. This relationship is useful to compensate the kerf width automatically with NC devices. The kerf width at the upper side is nearly equal to the diameter of the abrasive nozzle. But it slightly decreases with increasing traverse speed.

The kerf width at the upper side is also affected by nozzle wear. Therefore, in high precision cutting, it is necessary to correct the increase of the kerf width with time elapsed or to use a newly developed long-life nozzle.

3.3 INCLINATION OF CUT SURFACE

The difference between upper and lower kerf widths results in the inclination of cut surface. The width at the lower side is larger than that at the upper side at relatively slow traverse speed as shown in Fig.4. On the contrary in the range of higher traverse speed, the width at the lower side is smaller than that at the upper side.

At both high and low traverse speed, the inclination of the cut surface is produced. In middle speed, there is a proper cutting

speed that makes the width of the upper and lower side nearly equal. This cutting speed is in the range of 1/10 to 1/20 of the maximum cutting speed shown in Fig.3 for each thickness. This means that obtaining a kerf without inclination needs to use very slow cutting speed. It is not an efficient manner for AWJ cutting. Compensating the inclination of kerfs with a control of the nozzle attitude can make cutting speed several times faster than the conventional manner without the nozzle control.

Change of the kerf width and the inclination of kerf with traverse speed as mentioned above, is explained qualitatively as follows:

AWJ after being expelled from the nozzle tends to spread in nature. This causes the spreading at the lower kerf at slow cutting speed, because the jet has excessive energy enough to erode materials around it. On the other hand, in the range of relatively high cutting speed, since there is not enough time for spread parts of AWJ to remove the material at the lower section of the specimen, the kerf width at the lower side decreases.

Figure 5 shows the relations between the inclination of kerf and the traverse speed for each thickness. The inclinations of kerf were calculated from the values of kerf width by assuming symmetry of the kerfs. In the figure, open marks represent the kerf inclination and solid marks represent the inclination angle of kerfs. The relationships between the inclination and the cutting speed for each thickness are shown on different lines. The inclination increases consistently with the cutting speed. The relations between the inclination angle and the cutting speed for each thickness are plotted on almost the same line in the graph.

3.4 STRAIGHTNESS OF KERF

Figure 6 and Fig.7 indicate profiles of kerf edge in 20mm and 48mm thick plates, respectively to investigate straightness of kerf. The profiles were calculated from the kerf width assuming that the kerf is symmetric. The kerf width increases in the middle of thickness at low cutting speed. This means that there is a dent in the kerf. On the other hand, the profile of kerf shows an S-shaped line in a range of higher cutting speed and the portion corresponding to the dent moves to upper side. The changes of the kerf profile with cutting speed are identical for both 20mm and 48mm thick plates.

Figure 8 shows straightness which calculated from the profile. The straightness represents the maximum distance between the cut surface and a base line connecting both ends of the profile. As shown in the figure, the straightness is best in a range of middle cutting speed for the 48mm thick plate. And the straightness is worse at lower and higher cutting speed. But, for both 10mm and 20mm thick plates, the tendency mentioned above is not clear. However, from Fig.6, Fig.7, and Fig.8, it may be said that the profile and straightness of kerf is a function of maximum cutting speed.

If the straightness does not meet the accuracy requirements, the merit of compensating the inclination would be lost. But the results of this experiment shows that the values of the straightness are usually within 5/100mm and good enough for the accuracy requirements

for most AWJ cutting.

3.5 DRAG

Figure 9 shows the profiles of drag line for some traverse speeds. Values of drag for different thicknesses are plotted against the distance from upper surface. For each thickness, the drag at the same speed were plotted on the same circle. This shows that the profile of drag line are approximated to a circle whose center is on the upper surface of the plate.

Figure 10 shows the radius of drag line calculated from the values of drag. The relationship between the radius of drag line and the traverse speed is approximately linear on the log-log plots.

Dimensional error of cutting caused by the drag is schematically illustrated in Fig.11. Figure 12 shows the estimated dimensional error for cutting a circle of 20mm diameter in the plates of some thicknesses. The dimensional error (Δ) for cutting a curved line can be calculated using the measured value of drag in linear cutting by the following equation:

$$\Delta = \sqrt{(R + W/2)^2 + \delta^2} - (R + W/2)$$

Where, R is radius of cutting line, W is kerf width, δ is drag of cut.

As shown in the figure, the error remarkably increases with the cutting speed and the thickness of plate to be cut. Since the cutting error enlarges with a decrease in radius of cutting line, extremely slow cutting speeds compared to the maximum cutting speed for given thickness have to be used for high precision cutting with AWJ. To check the equation, an experimental datum is plotted in the figure. It agrees well with the calculated value. This means that the equation can be used to estimate the dimensional error of cut. The dimensional error caused by the drag can be compensated with proper advance angles of the nozzle.

Figure 13 shows cutting samples indicating the effect of the drag on dimensional error. Figure 14 shows a precision cutting method compensating the width, the inclination of kerf and the drag of cut. Figure 15 shows application samples of the precision cutting method.

3.6 SURFACE ROUGHNESS

Figure 16 shows the surface roughness of cut in a 48mm thick plate. Locations of the measurement were three, the sections distant by 0.5mm from the upper and lower surfaces of the specimen and the middle section of the thickness.

The surface roughness at the upper and middle sections is about 25μm to 30μm in R_{max}. And they do not change remarkably with the cutting speed. The values of the roughness at these sections seem to mainly depend on particle size of the garnet sand used as abrasive.

The surface roughness at the lower section increases remarkably with cutting speed by value approximately 25μm to 250μm. The reason for

this is considered as follows:

In cutting action by AWJ, the upper and middle sections of the specimen are directly attacked by abrasive particles. Since the abrasive particles consume little kinetic energy before removing materials, the cutting action is very steady. On the other hand, at the lower section of the specimen, since the cutting action becomes cyclic producing striations on the cut surface, this section has relatively bad surface roughness.

Figure 17 shows the relationship between the surface roughness at lower section and the normalized cutting speed which is defined as the ratio of the cutting speed (u) to the maximum cutting speed (u_{max}) for each thickness. This figure shows that the surface roughness can be expressed by the normalized cutting speed within some deviations.

In this figure, cutting speed to obtain the value of surface roughness within 0.1mm is shown to be about $0.3u_{max}$ to $0.4u_{max}$. Although, for a quality cut to obtain the vertical kerfs with AWJ, about $0.1u_{max}$ is usually used as a cutting speed. Therefore, a precision cutting method proposed here with nozzle position and attitude control can make the quality cut several times faster than the conventional AWJ cutting, without a remarkable increase in surface roughness.

4.0 CONCLUSIONS

The results obtained from this study can be summarized as follows:

(1)The Width, the inclination, and the drag of cut for each thickness can be expressed as a function of the cutting speed.

(2)The maximum surface roughness of kerf and the straightness for various thicknesses can be expressed as a function of the normalized cutting speed with the maximum cutting speed for each thickness.

(3)The straightness of cut is usually within 5/100mm and good enough for most applications of precision AWJ cutting.

(4)The maximum traverse speed to obtain surface roughness within 0.1mm is about $0.3u_{max}$ to $0.4u_{max}$.

(5)By compensating the width, the inclination of kerf and the drag of cut with the combination of nozzle position and attitude control, high precision and efficiency cutting can be obtained.

REFERENCES

1) Y.Sugino et al. : THE PRESENT OF WATERJET CUTTING, Joitec,P134-140, Vol.5, No.3 (1989) (in Japanese)
2) D.K.M.Tan : A MODEL FOR THE SURFACE FINISH IN ABRASIVE WATERJET CUTTING, Proc. of the 8th International Symposium on Jet Cutting Technology, BHRA, P309-314 (1986)
3) M.Hashish : ASPECTS OF ABRASIVE-WATERJET PERFORMANCE OPTIMIZATION, Proc. of the 8th International Symposium on Jet Cutting Technology, BHRA, P297-308 (1986)

4) M.Kiyoshige et al. : A STUDY OF ABRASIVE WATERJET CUTTING USING SLURRIED ABRASIVES, Proc. of the 9th International Symposium on Jet Cutting Technology, BHRA, P61-73 (1988)
5) S.Matsui et al. : CURRENT APPLICATIONS OF ABRASIVE WATERJET (AWJ) CUTTING FOR MANUFACTURING INDUSTRIES, Proc. of the 5th Internation al Symposium of the Japan Welding Society, P225-230 (1990)

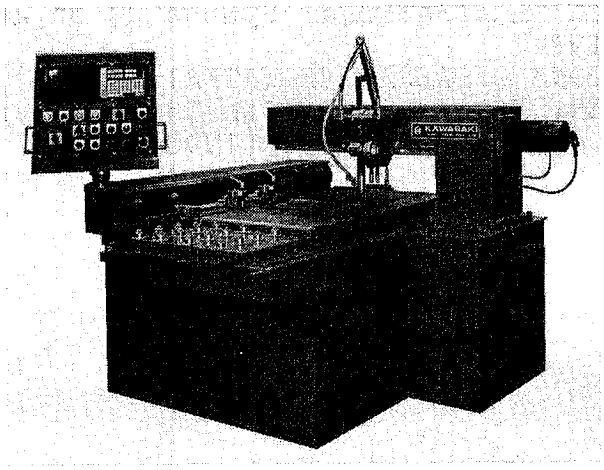

Fig.1 Cutting equipment

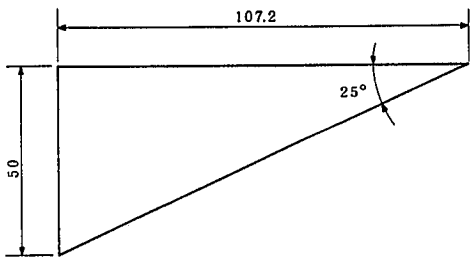

Fig.2 Tapered specimen
(for determination of maximum depth of cut)

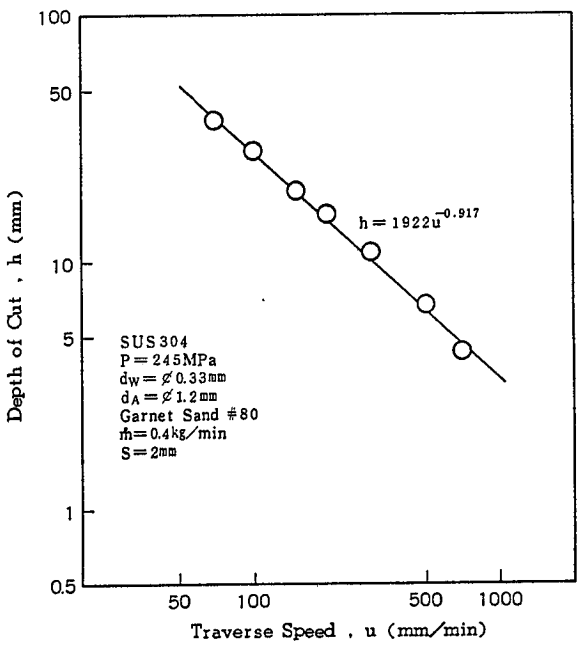

Fig.3 Relation between depth of cut and traverse speed

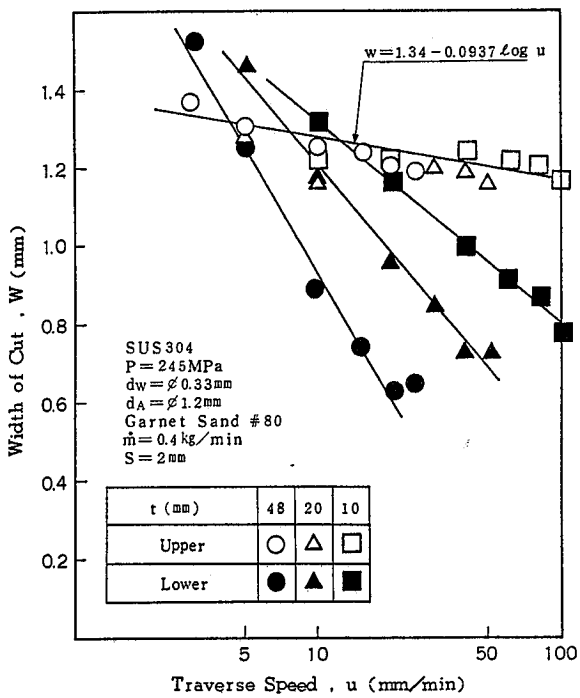

Fig.4 Relation between width of cut and traverse speed

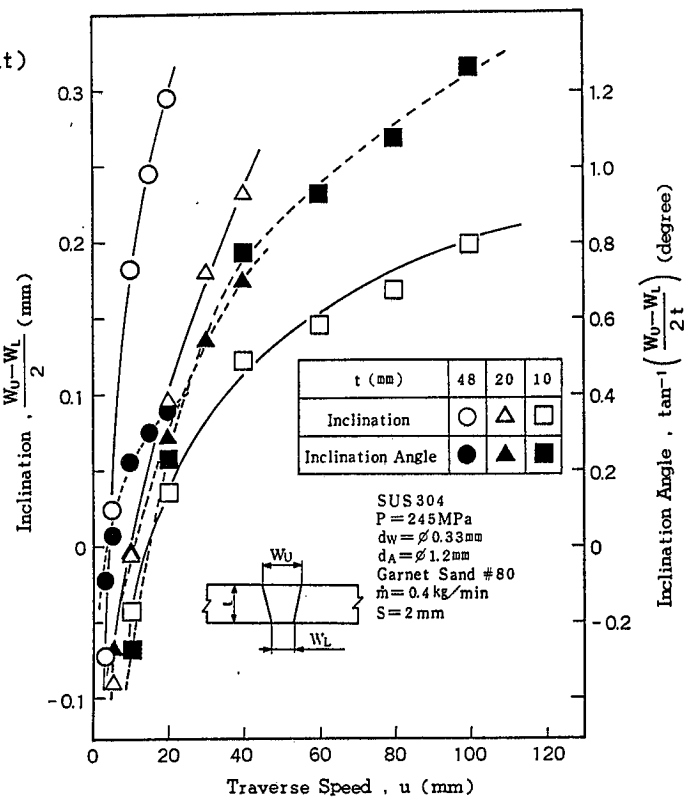

Fig.5 Relation between inclination angle and traverse speed

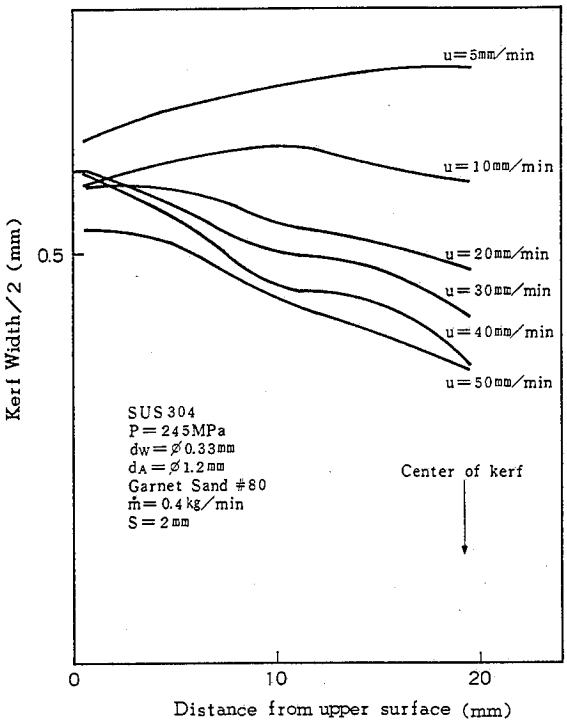

Fig.6 Kerf profile (t=20mm)

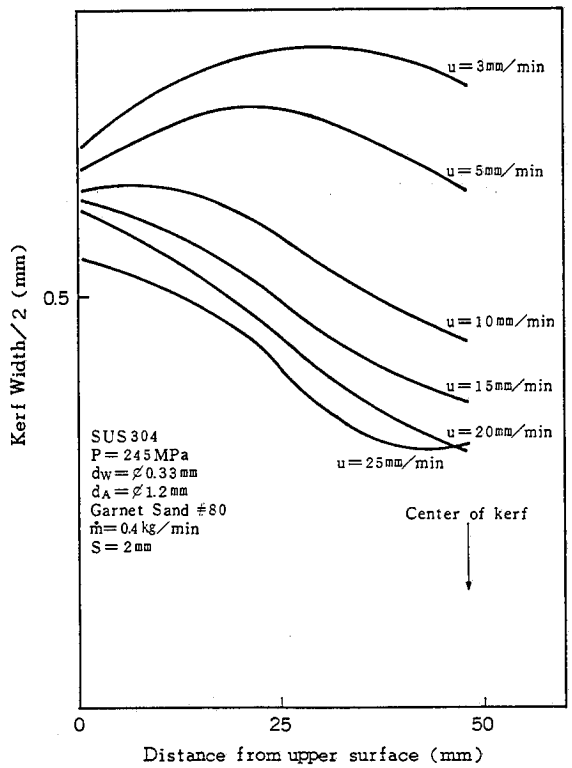

Fig.7 Kerf profile (t=48mm)

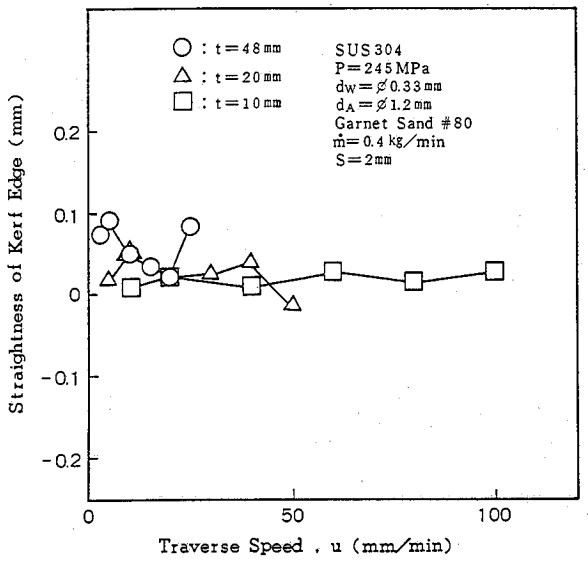

Fig.8 Relation between straightness of kerf edge and traverse speed

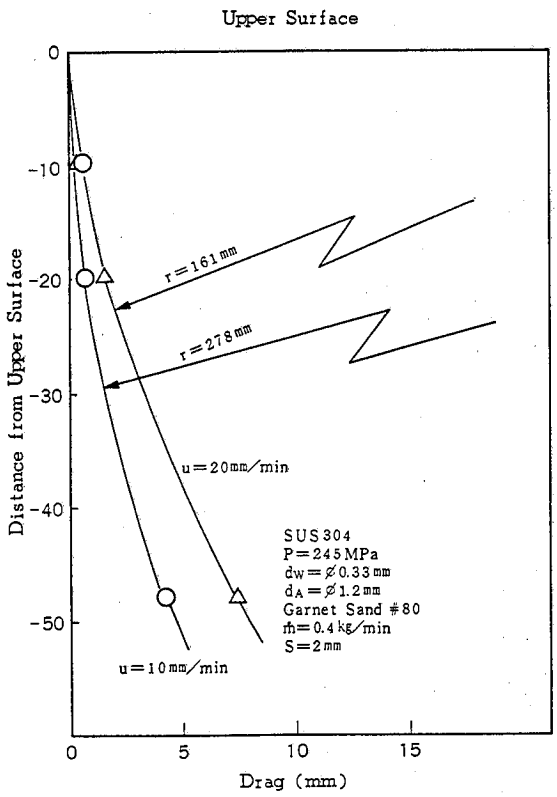

Fig.9 Profile of drgline

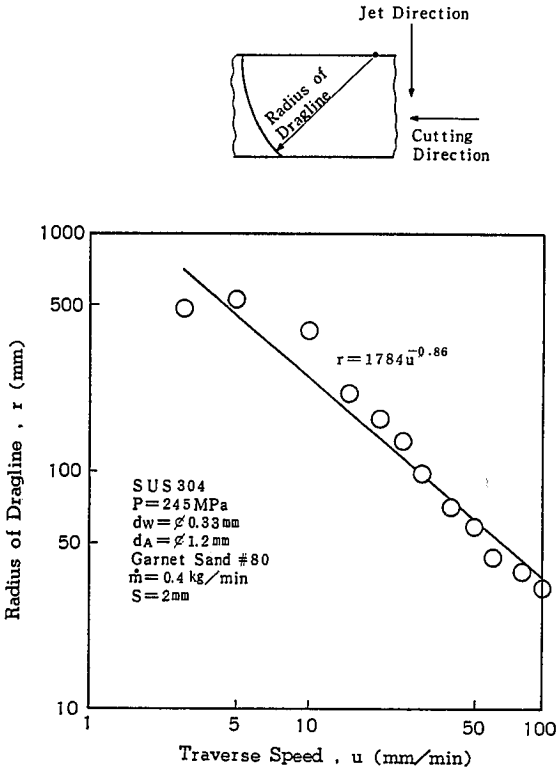

Fig.10 Relation between radius of dragline and traverse speed

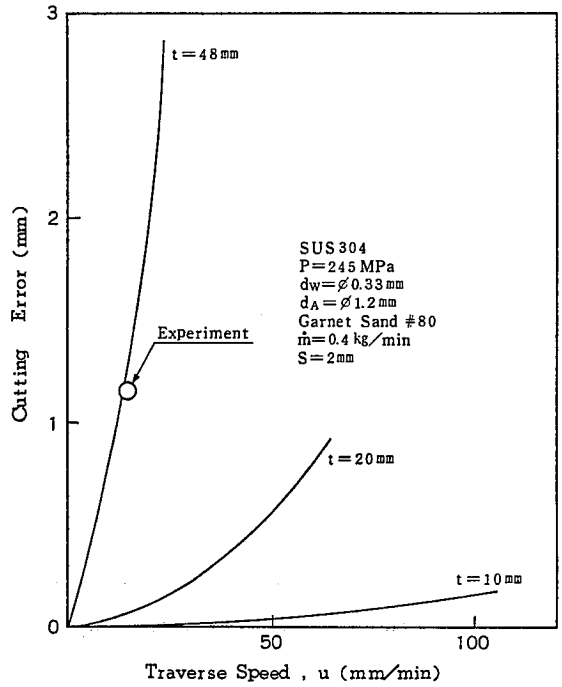

Fig.12 Estimated and measured cutting error caused by drag

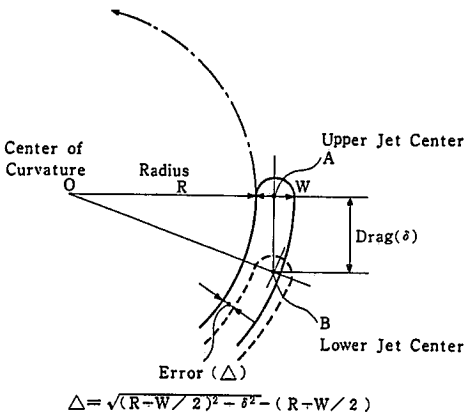

Fig.11 Schematic representation of cutting error

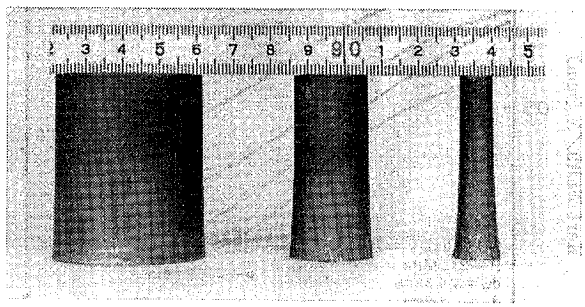

(a) R=20mm (b) R=10mm (c) R=5mm

SUS304
P=245MPa
dw=ø0.33mm
dA=ø1.2mm

Garnet Sand #80
ṁ=0.4 kg/min
s=2mm
u=15mm/min

Fig.13 Cutting samples showing cutting error caused by drag

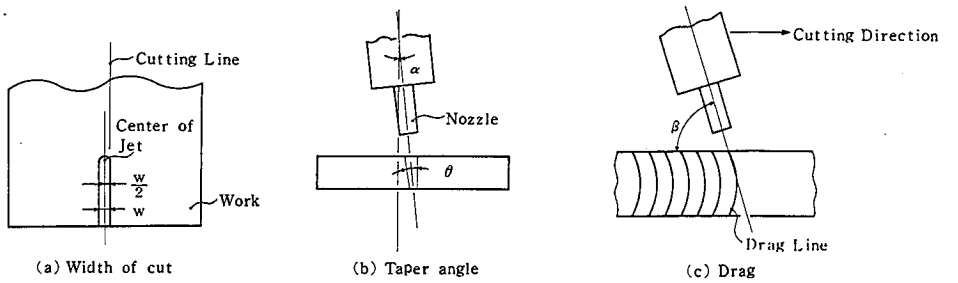

Fig.14 Compensation methods for cutting error

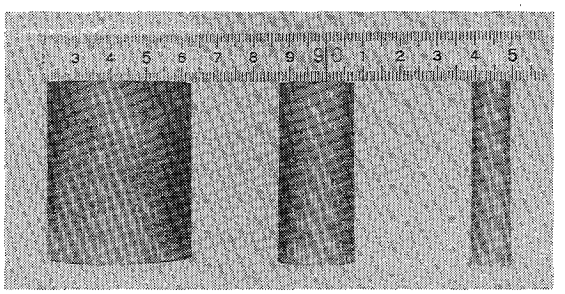

(a) R=20mm (b) R=10mm (c) R=5mm

SUS304 Garnet Sand #80
P=245MPa ṁ=0.4kg/min
d_W=⌀0.33mm s=2mm
d_A=⌀1.2mm u=15mm/min

Fig.15 Cutting samples showing the results of combined compensation for taper angle and drag by position and attitude controlle (t=48mm)

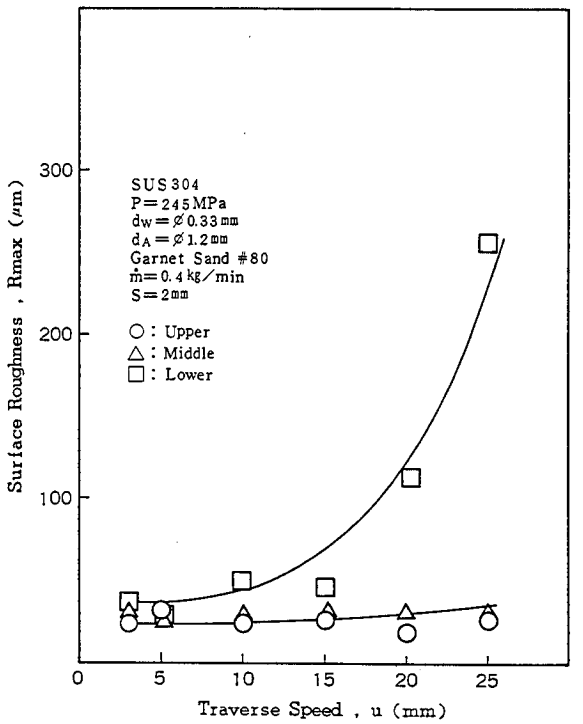

Fig.16 Relation between surface roughness and traverse speed (t=48mm)

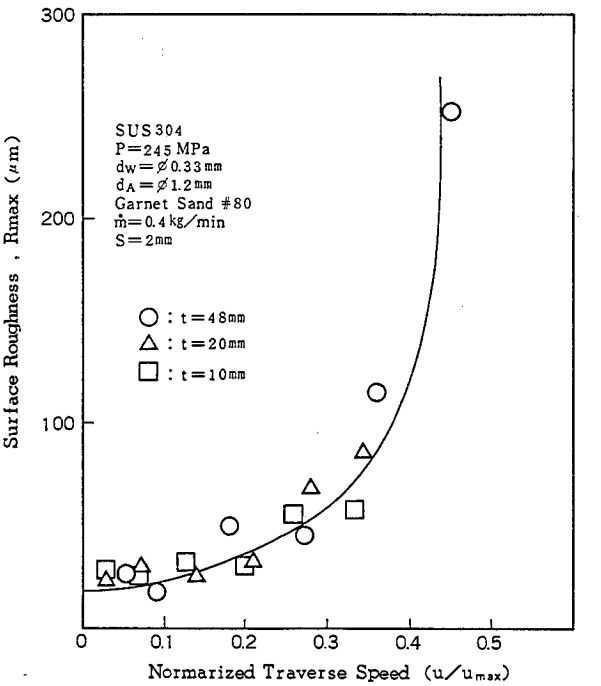

Fig.17 Relation between surface roughness and normarized traverse speed

6th American Water Jet Conference
August 24 - 27, 1991: Houston, Texas Paper **11**

Comprehensive Evaluation Of Abrasive Waterjet Cut Surface Quality

Pawan J. Singh, Wei-Long Chen and Jose Munoz
Advanced Development Center
Ingersoll-Rand Waterjet Cutting Systems
Baxter Springs, Kansas, U.S.A.

ABSTRACT

An intensive experimental study was conducted to investigate the relationship between surface finish of abrasive waterjet cut surface and associated cutting process parameters. A surface analyzer with laser stylus was used to measure the roughness of surfaces cut from various materials, including aluminum, glass, steel and neoprene rubber. The process parameters employed in the experiment were 1). cutting speed 2). abrasive mass flow rate 3). size of water orifice 4). size of abrasive mixing tube 5). size abrasive garnet 6). water pressure. The roughness was measured at different depths of cut sample. The cut surface was evaluated by SEM to study surface topography. The results of this study can not only help a user to select the "best" process parameters to fit his need, but they also provide important information in understanding the cutting mechanism associated with the abrasive waterjet cutting process.

1. INTRODUCTION

With an expanding realm of abrasive waterjet cutting (AWJ) applications, much attention is now focused on the cutting process and quality of the cut surface. The material removed by AWJ is an erosion process, resulting from the impact of abrasive particles entrained in the AWJ. This process has been studied and reported in [1]. For ductile materials, the erosion process consists of a cutting wear process and a deformation wear process, providing two different surface finish zones. In the cutting wear process, the abrasive particles strike the target surface at a shallow angle and produce a relative smooth surface finish. As the depth increases, the deformation wear mode dominates and striations begin to appear on the bottom of the surface.

The dual roughness zone is typical of beam-type cutting processes, be it laser, plasma or abrasive waterjet. In these processes, the cutting is relatively smooth and surface characteristics statistically homogeneous, until the beam loses a significant amount of energy in material removal. Then, the beam begins to bend towards the previously cut slot to exit, and the angle of attack becomes steeper, which also changes the material removal mechanism. In abrasive waterjet and for

ductile materials, this mechanism changes from cutting shear of atomic boundaries to deformation shear. The deformation wear process is more efficient in material removal [1] and it helps in cutting thicker materials than would otherwise be possible . However, with increasing thickness, the particle beam broadens considerably and is incapable of uniform, continuous cutting. The cutting on the bottom of the thick material then takes place through intermittently variable material removal, resulting in striations. The depth of these striations, and therefore surface roughness, increases with material thickness until, finally, separation stops.

The striations are seen in all materials, ductile or brittle, metal or plastic, and are likely caused by cutting beam instability, excited by bending the beam, which gets stronger with cutting depth. From this discussion, it is clear that striations can only be eliminated by extension of the cutting wear zone, which can be achieved by adjustment of various cutting parameters such as reduction in cutting speed or increase in abrasive flow rate. A complete understanding of cut surface characteristics cannot be achieved without examining the relationship between surface quality and important cutting parameters. That is the thrust of this paper.

This study goes beyond earlier attempts [2-6] to cover a comprehensive envelope of materials and cutting parameters, including:

- Water pressure
- Orifice diameter
- Abrasive focusing tube diameter (or carbide tube)
- Abrasive size
- Cutting speed
- Abrasive mass flow rate
- Materials: aluminum, steel, glass, rubber

2. EXPERIMENTAL SETUP AND PROCEDURE

The AWJ system used in this study consisted of Streamline II 40S intensifier, HS-2000 CNC cutting station and Alignable Hydroabrasive Nozzle Assembly, all manufactured by Ingersoll-Rand Company and shown in Figures 1 and 2. The intensifier is rated at 414 MPa (60,000 psi). HS-2000 has a rated accuracy of +/- 0.254mm (0.01 inch) in each axis full span and speed range of 2.5-5080 mm/min (0.1-200 ipm). For cutting tests, the material sample is fixed while the cutting head moves at specified speeds. The abrasive is gravity fed to the nozzle over a very short distance by a vibrating abrasive meter. The meter was calibrated before each series of tests.

Figure 3 shows the sample geometry and dimensions. All samples are cut with a fixed stand-off distance of 2mm (0.08 inch). With these wedge-shaped samples, the effect of material thickness, a critical parameter, on surface quality can be

observed in one cut for all thicknesses from 12.7mm (0.5 inch) to 25.4mm (1 inch). At least two cuts are made for each test and if any significant variation is observed between the first two cuts, a third or a fourth cut is made. Test data reported here is an arithmetic average of the data obtained from each cut.

2.1 MEASUREMENT SETUP

An optical non-contact laser stylus surface analyzer (Model RM600) manufactured by Rodenstock Company was used to measure surface characteristics of the AWJ cut surface. The surface measuring system is equipped with three major components:

- optical distance sensor
- traverse table
- evaluation and display computer

As depicted in Figure 4, the optical distance sensor works with an infrared laser whose beam is focused on the surface of the sample. The light spot with a diameter of 2 microns is imaged onto a focus detector in the sensor. If the distance to the measuring surface changes, then the detector sends a control signal to move the lens until the laser beam again focuses exactly on the sample surface. As the focus distance is constant, the movements of the lens correspond exactly to the contour profile of the measuring surface. The measured values are transmitted to a computer to calculate and display surface roughness. The measurement setup is shown in Figure 5.

The sensor is motor driven along a specified path at a user-selected speed. Measurement rate depends on the degree of variation of surface height. Key specifications for the instrument are as follows:

Roughness Measurement Range:	$\pm$ 300 μm
Measurement Resolution:	200 nm
Measurement Linearity:	0.3%
Measurement Rate:	Depends on surface roughness. Minimum 5 measurements/sec for very rough surfaces. Normal rate 500 measurements/ sec
Minimum Reflectivity:	1 to 2%
Traverse Speed:	max. 0.5 mm/sec
Traverse Range:	max. 60 mm
Absolute Error:	< 0.3% of measuring range

The recorded data is analyzed and displayed graphically with the aid of a dedicated software package. The analysis produces various means of evaluation of surface characteristics such as average roughness, rms roughness, maximum peak-to-peak roughness, skewness and waviness. The raw data can be digitally

filtered at specified cut-off frequencies before analysis. For this analysis, the data was filtered as to be compatible with a mechanical stylus of 0.1 mm in diameter.

The laser analyzer offers several advantages over the common mechanical stylus. Chief among them is the absence of contact between the measuring device and the measured surface. Other advantages include higher resolution and accuracy, better repeatability, and greater reliability in use. The main disadvantage is that the laser sensor is less sensitive on darker surfaces due to their poor reflectivity. This sensitivity can be enhanced by coating the surface with thin high-reflectivity coatings, but at the risk of some loss of accuracy. In our tests, black rubber was sprinkled with corn starch baby powder and excess dusted off to increase instrument sensitivity.

2.2 TEST PROCEDURE

The laser analyzer was first checked for accuracy by testing a standard surface of known roughness, and for repeatability by taking multiple readings over a specified traverse. For both cases, the variation was less than 2% of the average reading. On the standard surface, the difference between laser analyzer and mechanical stylus measurements was less than 1% of the specified roughness.

The significance of roughness variation in horizontal direction was investigated first. Three roughness data were taken on each side of the cut surface at a specified depth of cut. These measurements were repeated for various depths and the data was regressed with a second degree polynomial. The regression curve is shown in Figure 6 for one case of cutting aluminum. It shows that the roughness scattering at the same depth of cut is not significant. The same conclusions is also reported in [3].

The roughness measurements at each depth are randomly distributed but the variance is nearly uniform in the cutting wear zone as shown in Figure 6a. The variance becomes much larger in the deformation wear zone, where the striations sharply increase the absolute value of roughness [Figure 6b]. It is also apparent from Figure 6 that sample thickness had little influence on vertical roughness profile, for while the sample thickness varied along the cut direction, the roughness at a constant depth was nearly the same at any point along the cut.

Figure 7 shows roughness profiles and their spectra at five depths, from 3.2mm (0.125 in.) to 15.9mm (0.625 in.), for an aluminum sample. From these profiles, cutting wear and deformation wear zones can be clearly identified since roughness characteristics in these two regions vary substantially. In the cutting wear region at the top, roughness profile is more random, with a broad distribution of spectral harmonics. To the contrary, in the deformation wear zone at the bottom, roughness

is characterized by cyclic peaks and valleys and the spectral distribution is concentrated in a narrow range. In between these two zones, there is a transition zone in which roughness characteristics gradually change from one type to the other. Another roughness characteristic for ductile materials is the presence of occasional high peaks or valleys in the surface profile. At such locations, it is likely that stray particles may have hit the surface at larger angles of attack and cut deeper into the surface, even occasionally embedding themselves. An example of such embedment is shown in the SEM photograph of Figure 8.

Spectral analysis is a good starting tool to examine the origin, and prediction of striation amplitude and frequencies. In Figure 7b, the horizontal scale represents wave number, not frequency as is typical of most spectra plots. However, the frequency can be easily derived by multiplying cutting speed with the wave number. Inverse of the wave number gives wave length, a measure of spacing between striations. The vertical scale is a relative measure of amplitude. From Figure 7, it is clear that striations become more cyclic and well defined as the cut depth increases. In our analysis, we could not directly relate main spectral frequency to obvious cutting parameters such as cutting speed or pressure pulsation frequency generated by pump movement. This is a fertile area for research.

3 TEST PARAMETERS

Test parameters were selected within the scope of practical application. For example, all tests except these involving orifice or focus tube diameter variation were run with 0.25mm (0.010 in.) orifice bore and 0.76mm (0.030 in.) focusing tube bore, a common combination used in many abrasive field applications. In addition, to avoid quality variation among orifices and focusing tubes, the same orifice and focusing tube are used in each experiment.

Following parameters were varied and roughness data for each recorded and analyzed:

a. water pressure: 172, 207, 276, and 345 MPa (25, 30, 40 and 50 ksi)
b. orifice size: 0.18, 0.25, 0.3 and 0.36 mm (0.007, 0.010, 0.012 and 0.014 inch)
c. focusing tube size : 0.56, 0.76 and 1.1 mm (0.022, 0.03 and 0.043 inch)
d. garnet size: mesh 80, 120 and 220
e. cutting speed: 25, 63.5, 127, 191 and 254 mm/min (1, 2.5, 5, 7.5 and 10 ipm)
f. abrasive mass flow rate: 227, 340, 454, 567 and 680 g/min (0.5, 0.75, 1.0, 1.25 and 1.5 lb/min)
g. materials: aluminum (T6061-T6511), mild steel glass, rubber.

Excluding variations in one particular parameter, the following parameter values were used as base values.

Abrasive material:	Barton mines garnet
Abrasive particle size:	mesh 80
Abrasive mass flow rate:	227 g/min (0.5 lb/min.)
Water pressure:	345 MPa (50,000 psi)
Orifice bore:	0.25mm (0.01 in.)
Focusing tube bore:	0.76mm (0.03 in.)
Focusing tube length:	50.8 mm (2 in.)
Attack angle:	0 degrees (vertical jet)
Stand off distance:	2mm (0.08in.)
Number of passes:	1

4. EXPERIMENTAL RESULTS

While the measured data allowed complete analysis of surface characteristics, only average roughness data (Ra) is reported here for conciseness. Ra provides a good comparative measure of surface roughness, although it averages out any salient departures from a normal pattern. The measurement results are based on an average of single measurement at each depth on at least two samples. The error estimate (2σ) is $\pm$ 0.254 microns (10 μin.).

4.1 INFLUENCE OF WATER PRESSURE

Figure 9 shows the relationship between water pressure and surface finish at different depths of cut. The results indicate better surface finish is obtained on the top part of cut surface when lower water pressure is used. Abrasive mass flow rate is held constant at 227 g/min (0.5 lb/min) for all pressures. It may appear counterintuitive to expect better finish at lower pressures, although it is so only in a relatively narrow zone; however, the surface finish depends on particle velocity and number of particles striking a certain surface zone, among many other factors. Lower velocity particles do less damage to the surface but lose energy quickly and the resulting depth of cut and extent of cutting wear zone are lower. Also, when more particles strike a target, some of the particles remove the material and other particles finish the surface.

Figure 9 also shows that the extent of cutting wear region, somewhat arbitrarily defined by a break in the roughness slope, is proportional to water pressure. The SEM pictures of surface cut at 172 MPa (25 ksi) and 276 MPa (40 ksi) are shown in Figure 10. The surface finish is relatively homogeneous. Darker spots in Figure 10b are indicative of stray particles striking the material at steeper angle and creating small burrows.

4.2 INFLUENCE OF SAPPHIRE ORIFICE SIZE

The results of orifice size effect are shown in Figure 11. For a specified size of focusing tube, 0.76mm (0.030 in.) I.D. in this case, larger size of water orifice does not provide better quality of surface finish. A proper selection of size ratio between orifice and focusing tube is essential to obtain better cutting results [6,8]. For 0.76mm (0.030 in.) focusing tube, 0.25mm (0.010 in.) or 0.3mm (0.012 in.) orifice is best suited for optimal surface finish. It should be noted, however, the difference in roughness is not very large. While larger orifice implies higher water flow and intensifier power, cutting rate and finish are largely dependent on abrasive flow rate which has been kept fixed in this experiment.

4.3 INFLUENCE OF FOCUSING TUBE SIZE

For 0.25mm (0.010 in.) orifice, the best surface finish is achieved with 0.56mm (0.022 in.) bore focusing tube as shown in Figure 12. The finish is comparable with 0.76mm (0.030 in.) and 1.1mm (0.043 in.) bore tubes. Smaller bores concentrate abrasive jet to a narrower cross-section, improve mixing and reduce kerf width. However, they also require very careful alignment, high-quality focusing tube and optimal focusing tube length to reduce mixing losses and abrasive degeneration to finer particles.

4.4 INFLUENCE OF ABRASIVE PARTICLE SIZE

An abrasive with smaller mesh number has a larger average value of particle size and fewer particles per unit weight. Many studies [1,6] have shown larger particles cut faster because of higher particle inertia. However, the surface finish is rougher in the cutting wear zone although the zone itself is considerably extended. Figure 13 shows while best finish is achieved with mesh 220 garnet in a narrow region near the top, the finish gets substantially rougher beyond 3.8 mm (0.15 in.) depth. In the range of cut depth shown in Figure 13, mesh 120 garnet strikes the best balance between surface finish and cutting performance.

4.5 INFLUENCE OF CUTTING SPEED

Cutting speed has the most influence on surface finish, primarily by extending the cutting wear zone. At lower speeds, more particles strike a unit cut surface, thus extending cutting depth, and refinishing and smoothing already-cut surface. Obviously, this improvement comes at the expense of reduced output. Thus, in practice, the selection of proper cutting speed is the most important parameter. Figure 14 shows the relationship between cutting speed and surface finish. At 254 mm/min (10 ipm), cutting wear zone is very narrow and the finish gets rapidly worse with cut depth. On the other hand, surface finish remains virtually unchanged with cut depth at speeds below 63.5 mm/min (2.5 ipm.) An interesting observation here is the

roughness decreases slightly with cutting depth, in the cutting wear zone, and then rises, creating a trough-shaped curve. The decrease, however, is relatively minor.

4.6 INFLUENCE OF ABRASIVE MASS FLOW RATE

Figure 15 shows the influence of abrasive mass flow rate, from 227 g/min (0.5 lb/min) to 567 g/min (1.25 lb/min), on roughness. The roughness decreases with increase in mass flow rate, but much of the improvement lies in the deformation wear or striation zone. It results from improved cutting capability and increase in maximum cut depth with higher abrasive loading. Other studies [6] have shown that there is an optimum abrasive loading beyond which cutting performance begins to decline. Figure 15 indicates a direct relationship between improved performance and lower roughness, provided other parameters such as abrasive type and mesh size are held constant.

4.7 INFLUENCE OF MATERIAL TYPE

Besides aluminum, selected tests were run on three materials - mild steel, glass, high-grade neoprene rubber - with very different material properties. Steel has higher hardness and shear strength but is less ductile. Glass is brittle and some investigators [1] have proposed an entirely different cutting mechanism based on crack propagation. Rubber is highly elastic and has a low shear modulus. Despite these inherent disparities in material structure and properties, all of them exhibit the same pattern of cut surface topography, marked by a smooth zone on the top and depending on the cut depth a striated zone on the bottom.

Figure 16 shows influence of abrasive size on roughness at a relatively low speed of 25.4 mm/min (1 ipm). Roughness characteristics are very similar to those for aluminum, albeit at a higher speed, 254 mm/min (10 ipm), as shown in Figure 13. One major difference is that unlike aluminum where the best possible finish hovered around 3.8 microns (150 μin), an excellent finish of less than 1.27 microns (50 μin) can be obtained with steel in the top region. Steel is less ductile than aluminum and material plastic flow during erosion wear is less pronounced than that in aluminum, which results in smoother surface.

Figures 17a and 17b show roughness as a function of cut depth and abrasive size for 340 g/min (0.75lb/min) and 227 g/min (0.50 lb/min) abrasive flow rate respectively. The pattern of roughness variation is similar in those two figures as well as similar to pattern for steel and aluminum. Rough zone, above 6.35 microns (250 μin), is characterized by clearly distinguishable striations. Higher abrasive loading produces a slightly better finish as well as larger smooth zone at the top.

The picture is not much different for neoprene rubber, as evidenced by Figure 18, where the lower speed is shown to produce smoother finish. Once again, the surface is characterized by two-zone roughness pattern.

5. DISCUSSION

An extensive experimental study has been conducted to investigate relationship between surface finish and AWJ operational parameters. A few observations are worthy of special attention. First, the surface roughness does not asymptotically increase with depth of cut in the cutting wear zone, and, in fact, may slightly decrease before turning around and increasing again. Initially, this trend was attributed to possible experimental error and the data was repeated and rechecked. In addition, SEM micrographs were prepared and examined [Figure 19]. Both investigations verified that the observed trend was indeed accurate. We hypothesize that the slight improvement arises from increased disintegration of larger particles to finer particles with cut depth which improve the finish. Additional investigation is needed to prove this hypothesis.

Second, surface finish for certain materials can actually be improved by reducing water pressure but at the cost of reduced productivity through lower cutting speed. For ductile materials, higher water pressure and therefore higher particle velocity and kinetic energy have greater potential of creating rough spots of accumulated plastic flow.

Third, the best way of assuring good finish throughout the cut region is to reduce cutting speed, which extends the smooth region and improves surface finish through repeated particle impacts. Since reduced cutting speed also means lower productivity, a balance needs to be struck between desired finish and best cutting speed to achieve that finish.

Fourth, irrespective of the type of material, surface topography is characterized by two regions, one statistically homogeneous (smooth) region and the other marked by striations. The amplitude of striations depends on cut depth, abrasive loading and many other parameters. Generally, better the cutting performance, lower the amplitude at a given depth of cut. The frequency of striations has some relationship with abrasive jet diameter and cutting speed but these relationships are not clear enough to formulate a predictive equation.

As indicated earlier, the two-region topography is produced by all beam-type cutting devices. It is likely caused by dynamic instabilities of the beam, resulting from upstream influence of transition at the end of smooth region where the beam does not have enough energy to penetrate the rest of the material without deflection. For abrasive jets, jet bending and cyclicity have been observed with a high-speed camera and reported in [1,9]. However, empirical evidence would indicate that abrasive

particle density also varies cyclically in the striation zone and particle clusters form and disappear in this unstable zone. These clusters have higher energy density and can penetrate the material providing easier exit for the jet. Even beyond the limit of full penetration depth of cut, these clusters can create intermittent holes through the material as is normally observed for very thick materials or for cutting at above-normal speeds.

Fifth, parameters that improve cutting performance improve surface finish in the striation zone by reducing the extent of such zone. In the smooth zone, the quality of finish depends on abrasive size, particle velocity and material type.

In practice, surface finish cannot be discussed independently of optimization criteria. We assume the user wants to minimize total cutting cost. The user may specify a certain minimum roughness, but beyond that, selection of optimum cutting parameters will depend on cost components, both variable or fixed. If fixed component is relatively high, focus will be on achieving high cutting rate through the use of high abrasive flow rate and a larger orifice. If variable costs are relatively high, lower abrasive flow rate and cutting speed may be desirable. This comprehensive study provides some guidelines in selection of these parameters, particularly for aluminum.

While the surface finish of AWJ cut parts is critical for high-precision applications, so is kerf profile. The kerf width on the top surface is close to abrasive jet diameter. However, the kerf width on the bottom surface depends again on the cutting mechanism. In the cutting wear zone, the kerf width on the bottom is larger than that on the top due to jet spreading. However, in the striation-dominated deformation wear zone, the kerf width, while not uniform is on the average narrower than the top kerf [7]. In practice, for high-precision applications, kerf variation from top to bottom is required to be nearly zero, while for many other applications, the kerf taper or surface roughness is not significant since the cut surface undergoes another finishing process. This study has focused on surface finish characteristics only.

6. CONCLUSIONS

Following conclusions are supported by this study:

- The operational parameters that lead to better cutting performance also extend the cutting wear region.
- The striations, when they occur at the bottom of cut surface, determine the surface finish.
- Optimization of cutting parameters can improve surface finish.
- Better surface finish in the cutting wear zone does not always guarantee better surface finish in the deformation wear zone.

o Selection of lower cutting speed is the only parameter, among all parameters evaluated here, which provides significant improved surface finish in both wear zones.
o All materials tested here exhibited a two-region surface topography and cut surface finish characteristics were similar regardless of material properties.

7. ACKNOWLEDGMENT

The authors thank I-R management for their support, and their permission to publish these results.

8. REFERENCES

1. Hashish, M., 1984, "On the Modeling of Abrasive-Waterjet Cutting", Proceedings of the 7th International Symposium on Jet Cutting Technology, Ottawa, Canada, Paper E1, p.p. 249-265.
2. Tan, D.K.M., 1986, "A Model for the Surface Finish in Abrasive Waterjet Cutting", Proceedings of 8th International Symposium on Jet Cutting Technology, Durham, England, Paper 31.
3. Hunt, D.C., Burnham, C.D. and Kim T.J., 1987, "Surface Finish Characterization in Machining Advanced Ceramics by Abrasive Waterjet", Proceedings of 4th U.S. Waterjet Conference, Berkeley, California, U.S.A., p.p. 169-174.
4. Burnham, C.D. and Kim, T.J., 1989, "Statistical Characterization of Surface Finish Produced by a High Pressure Abrasive Waterjet", Proceedings of 5th American Waterjet Conference, Toronto, Canada, paper 16, p.p. 165-175.
5. Blickwedel, H., et al, 1990, "Prediction of Abrasive Jet Cutting Efficiency and Quality", Proceedings of 10th International Symposium on Jet Cutting Technology, Amsterdam, Paper L2.
6. Hashish, M., 1982, "Steel Cutting with Abrasive Water Jets", Proceedings of 6th International Symposium on Jet Cutting Technology, University of Surrey, U.K., Paper K3.
7. Matsui, S. Matsumura, H., Ikemoto, Y., Tsukita, K., and Shimizu, H., 1990, "High Precision Cutting Method for Metallic Materials by Abrasive Waterjet", Proceedings of 10th International Symposium on Jet Cutting Technology", Amsterdam, Paper G3
8. Chen, W.L. and Geskin, E.S., 1990, "Measurement of the Velocity of Abrasive Waterjet by the Use of Laser Transit Anemometer", Proceedings of 10th International Symposium on Jet Cutting Technology, Amsterdam, Paper B4.
9. Geskin, E.S., Chen, W.L. et al, 1989, "Investigation of Anatomy of an Abrasive Waterjet", Proceedings of 5th American Water Jet Conference, Toronto, Canada, paper 21, p.p. 217-230.
10. Evan, A. G., 1979, "Impact Damage Mechanism: Solid Projectiles", Erosion, ed C. M. Preece, Academic Press

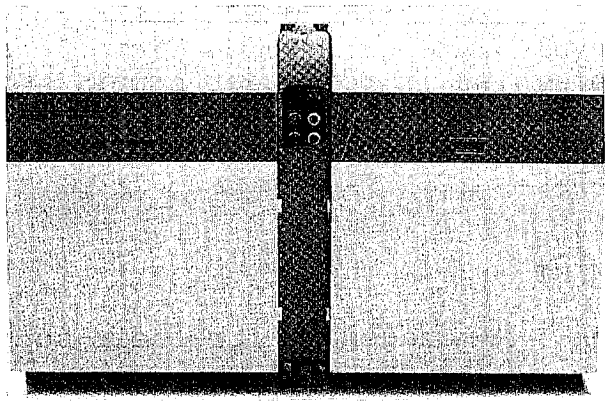

Figure 1: Ingersoll-Rand 40S Intensifier Pump (40 HP)

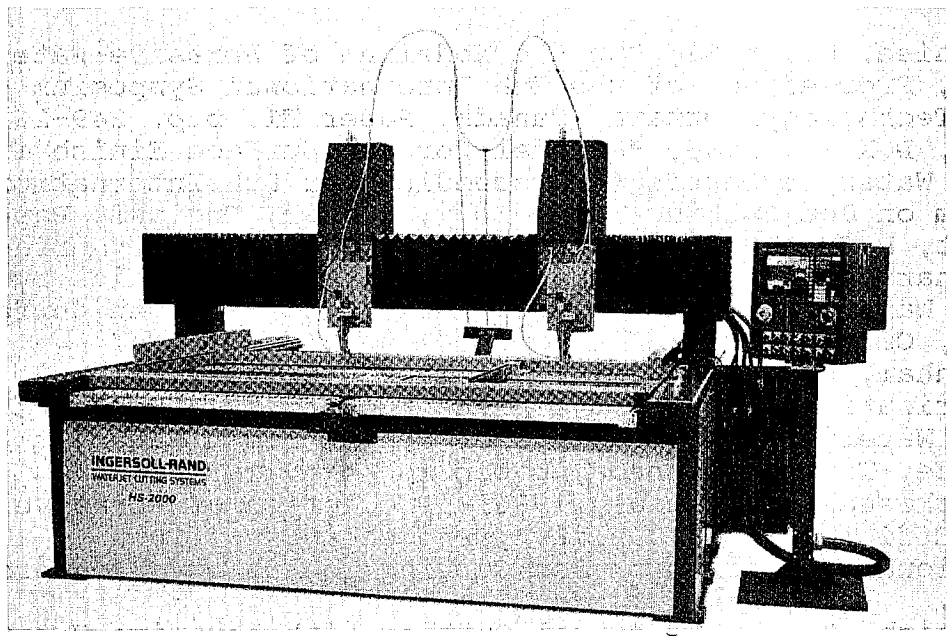

Figure 2: Ingersoll-Rand HS-2000 CNC Cutting Station and Hydroabrasive Nozzle Assembly

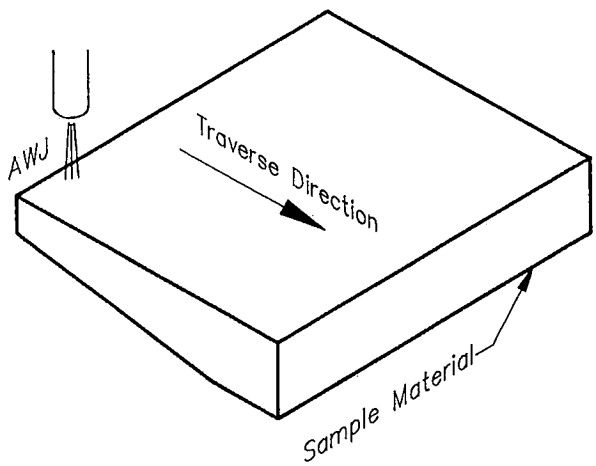

Figure 3: Sketch of Sample Configuration and Cut Direction

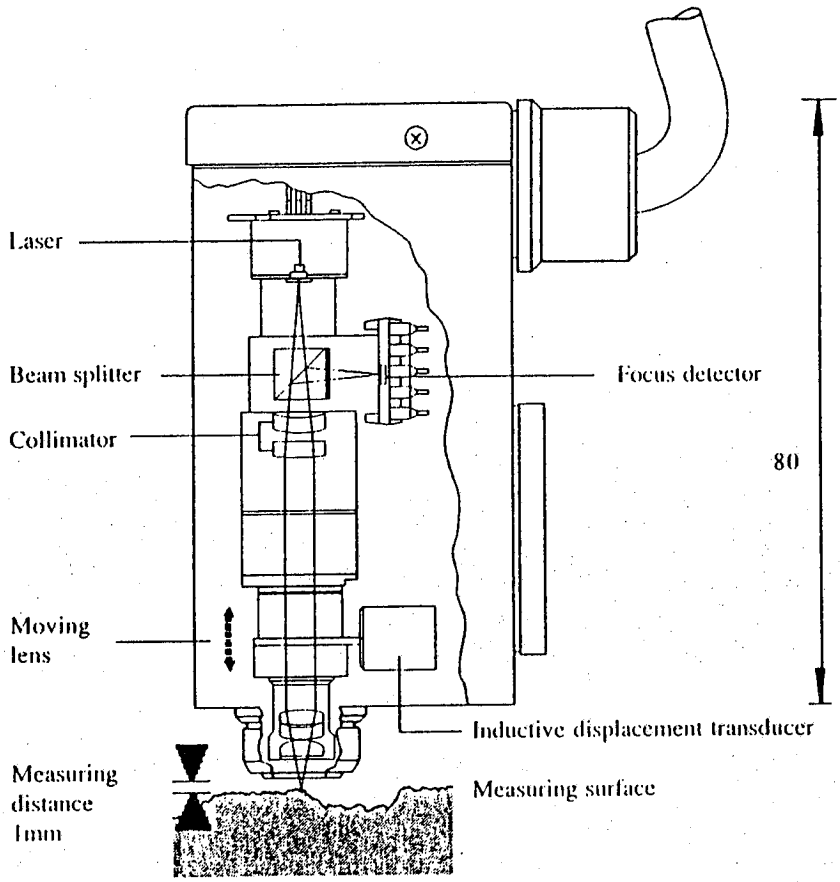

Figure 4: Schematic of Laser Sensor Function Principle

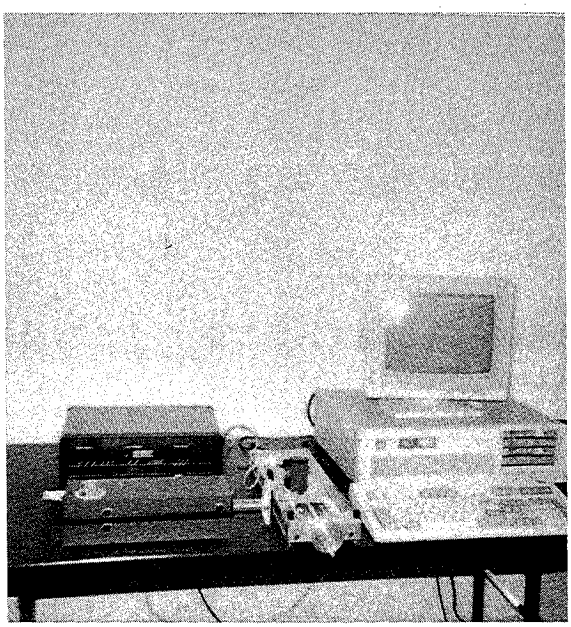

Figure 5: Setup of Measurement System

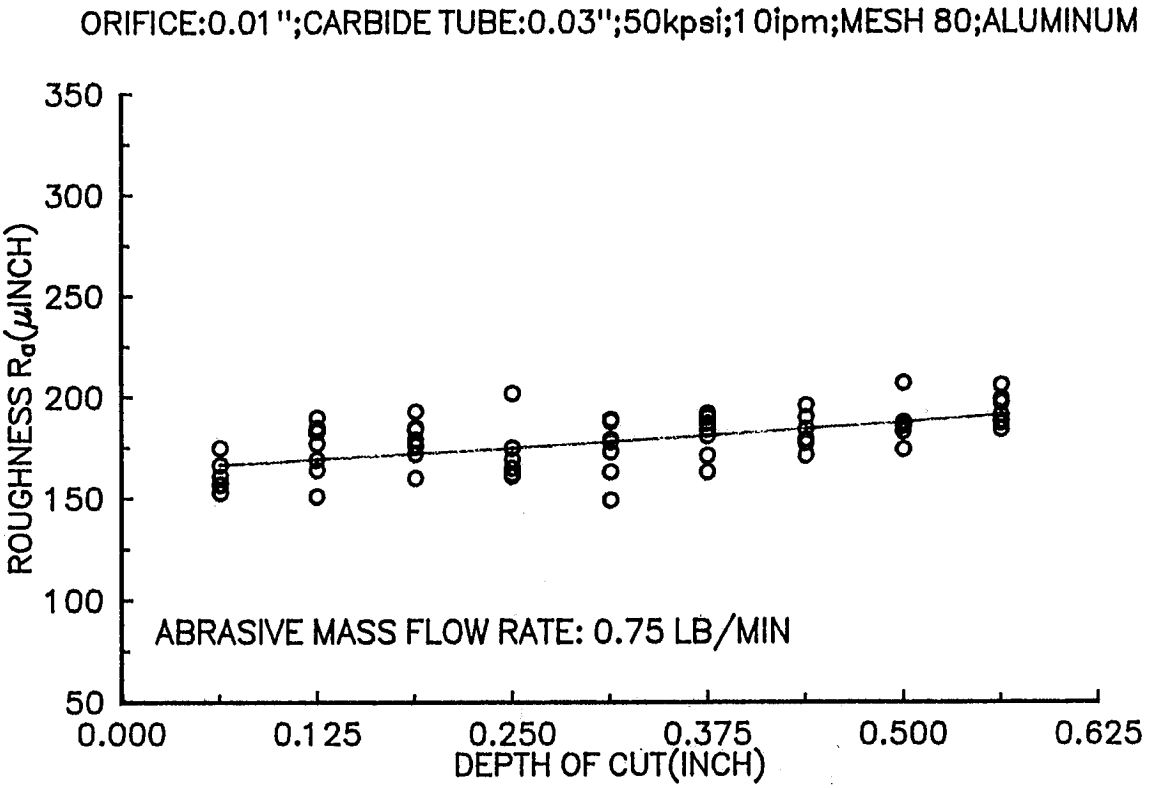

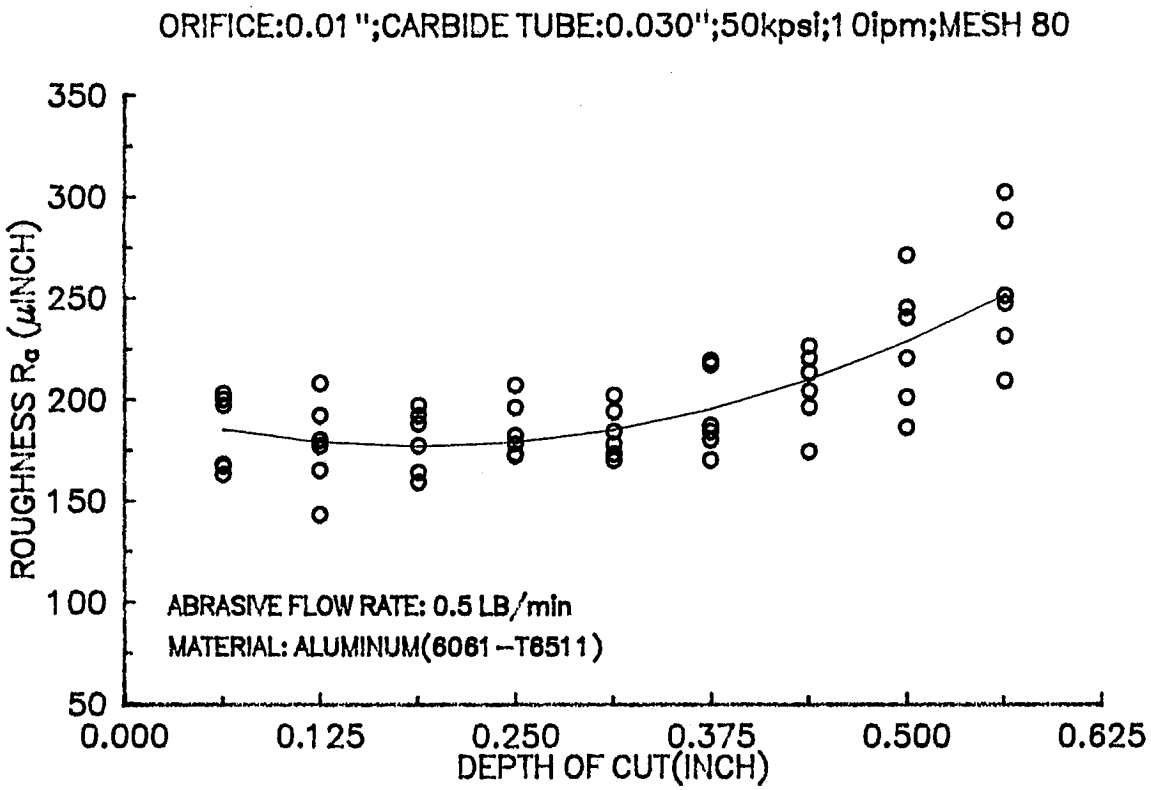

Figures 6a (top) and 6b (bottom): Roughness Variation Along Traverse Direction at Various Depths of Cut. Abrasive Mass Flow Rate is 0.75 lb/min in 6a) and 0.5 lb/min in 6b).

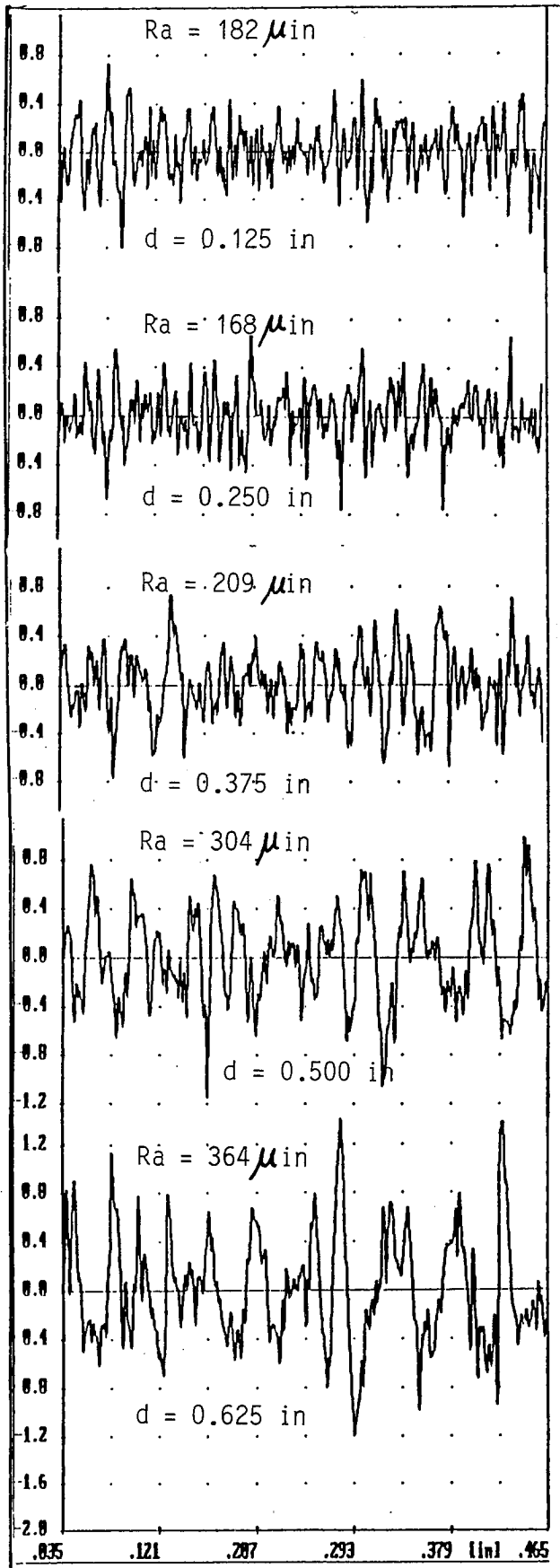

Figure 7a

Cutting Wear

Transition Zone

Deformation Wear Zone

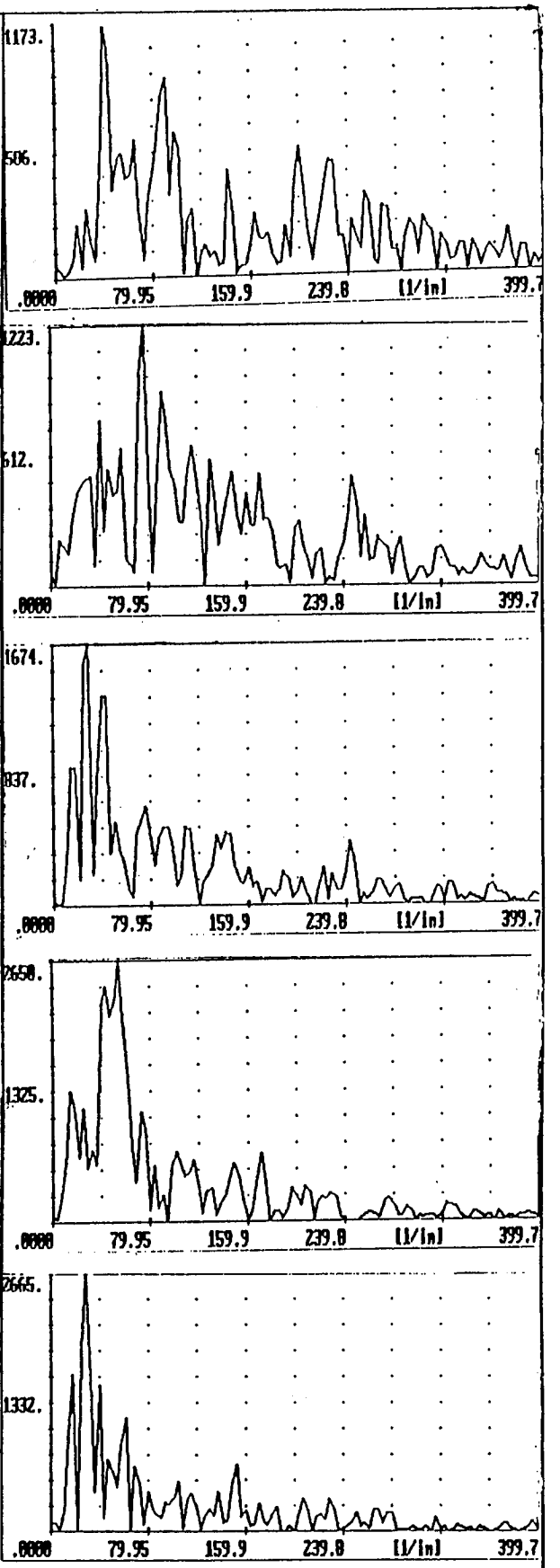

Figure 7b

Figure 7: Roughness Profiles (7a) and their Spectra (7b) at Various Depts of Cut for Aluminum. d defines the depth of cut.

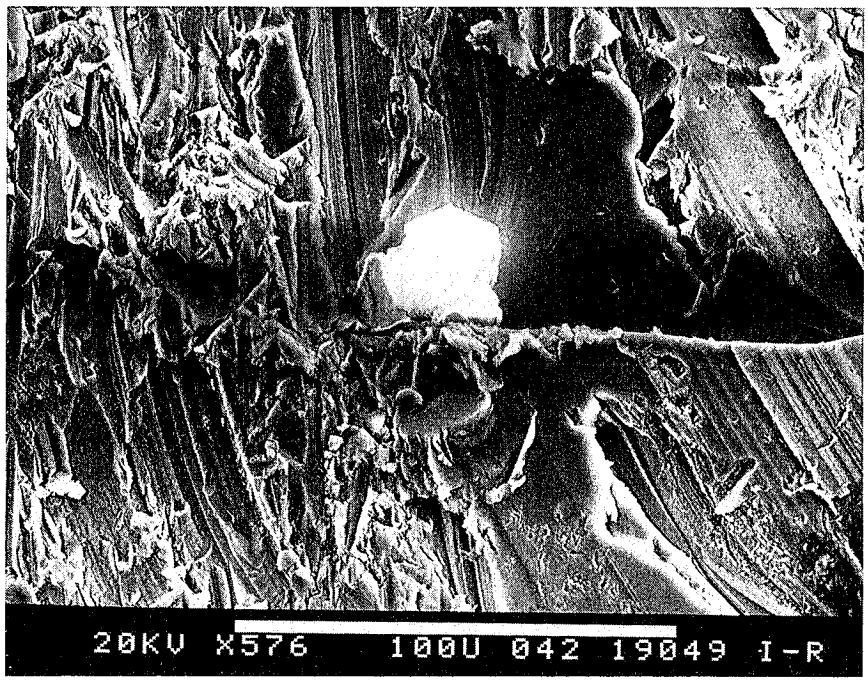

Figure 8: Embedded Garnet Particle in Aluminum Sample

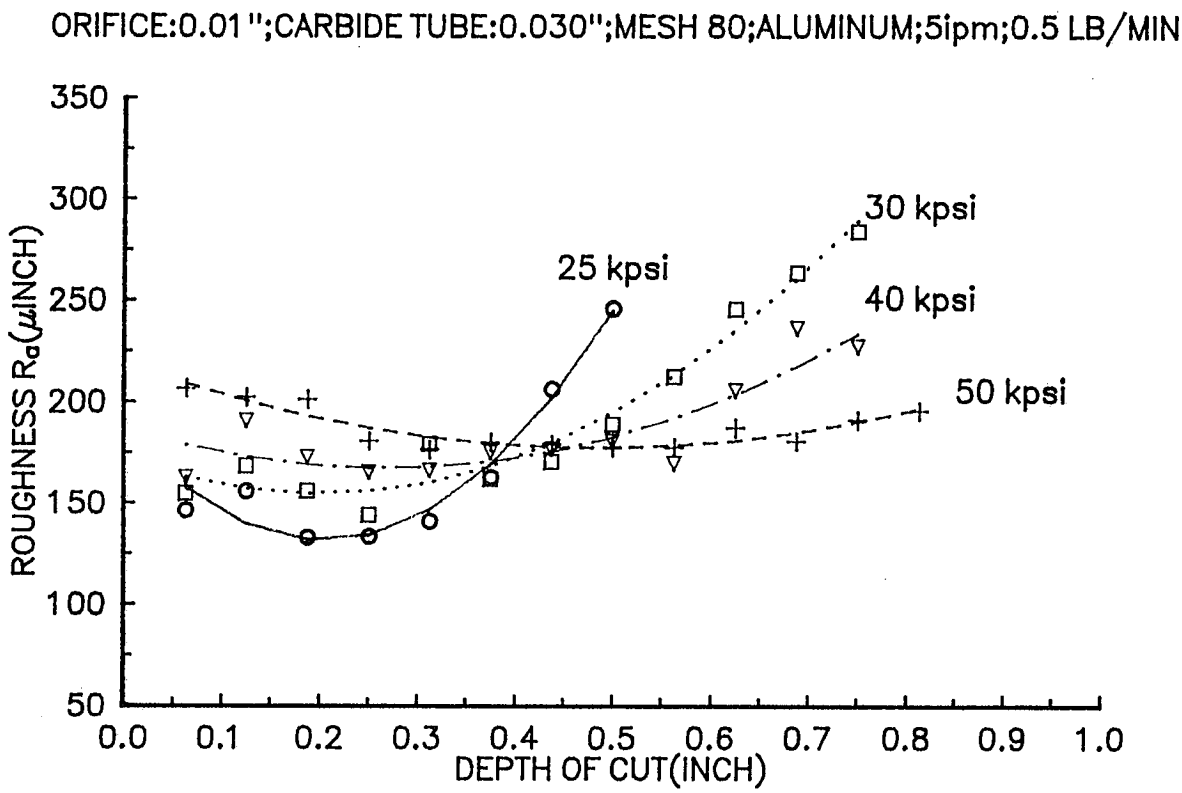

Figure 9: Effect of Water Pressure on Roughness

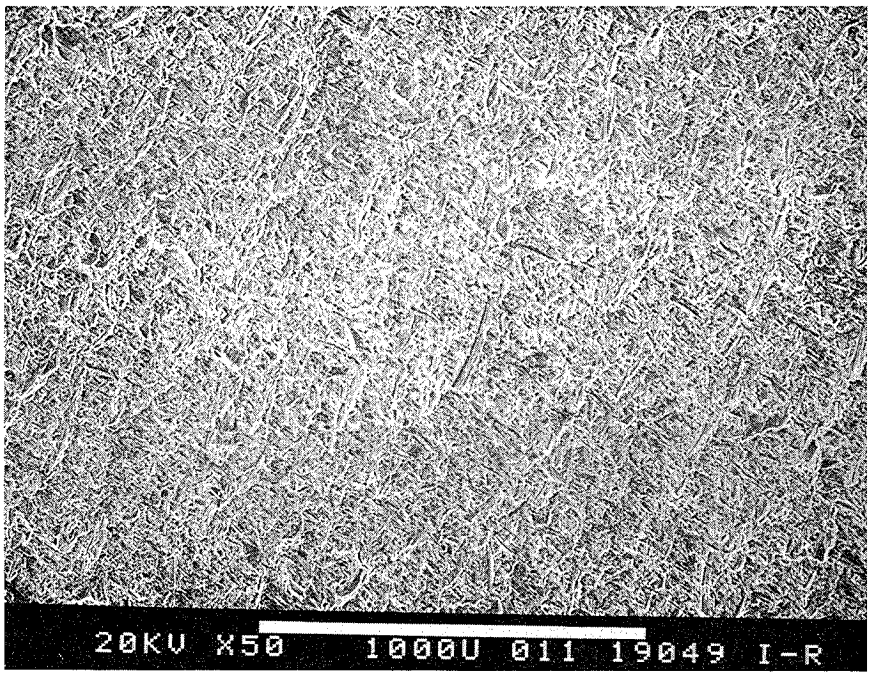

Figure 10a: SEM Micrograph. 25 ksi; Aluminum Specimen; Mesh 80; 5 ipm; 0.5 lb/min; Orifice: 0.01:; Focusing Tube: 0.03"; 1/8" Below Top

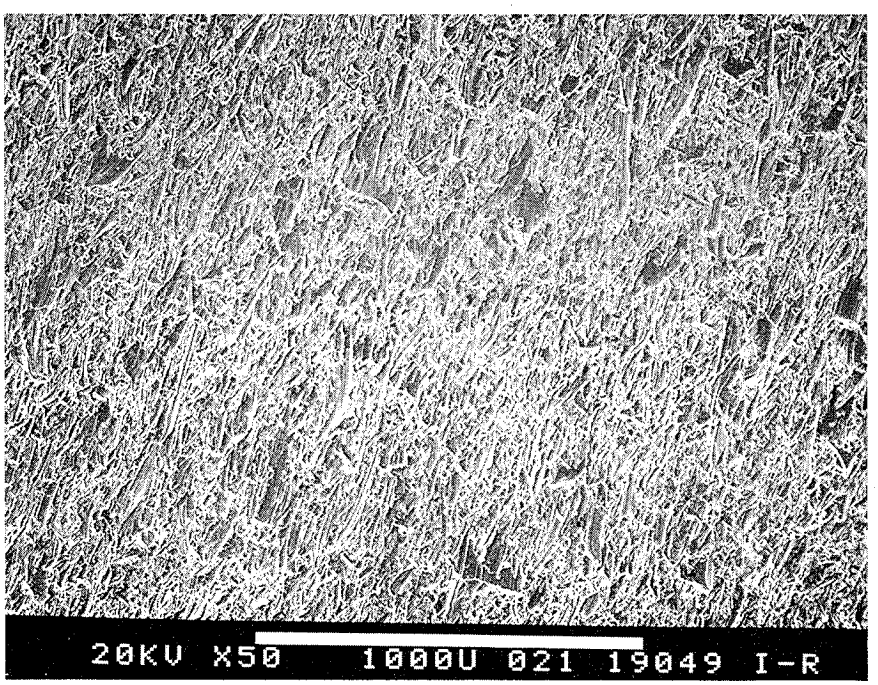

Figure 10b: SEM Micrograph. 40 ksi; Aluminum Specimen; Mesh 80; 5 ipm; 0.5 lb/min; Orifice: 0.01"; Focusing Tube: 0.03"; 1/8" Below Top

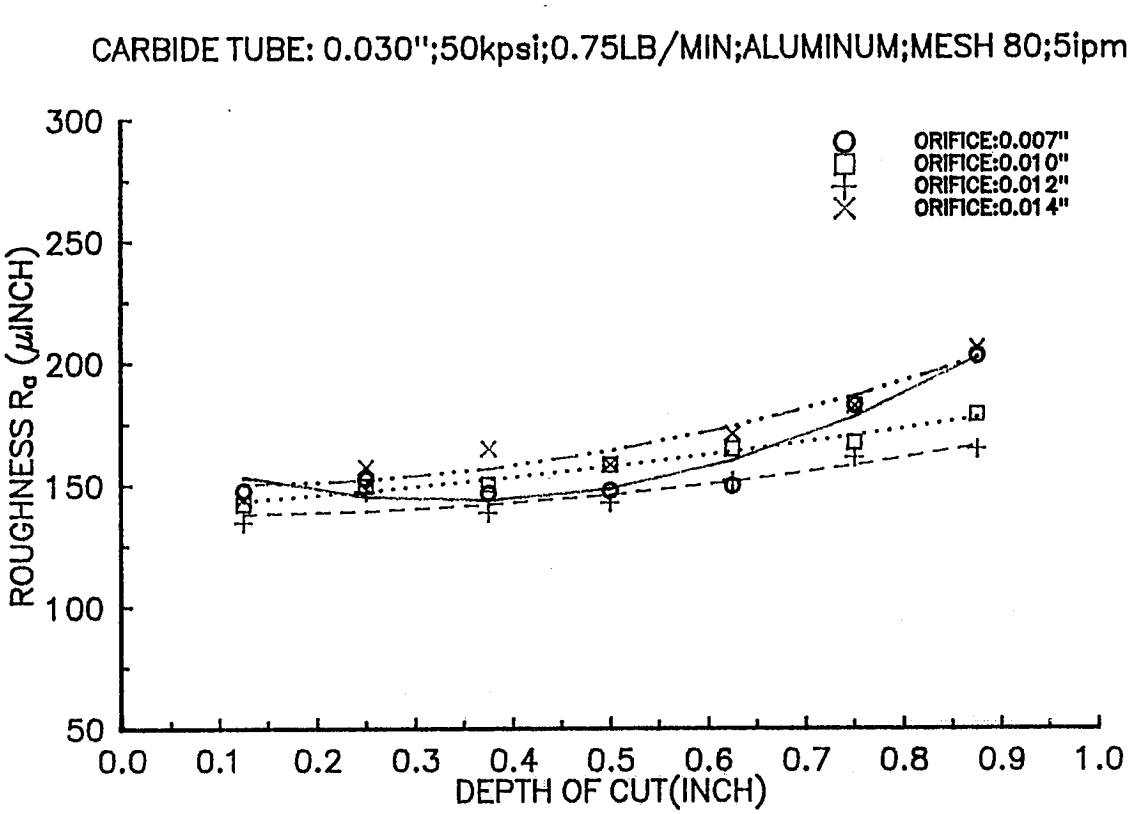

Figure 11: Effect of Orifice Size on Roughness

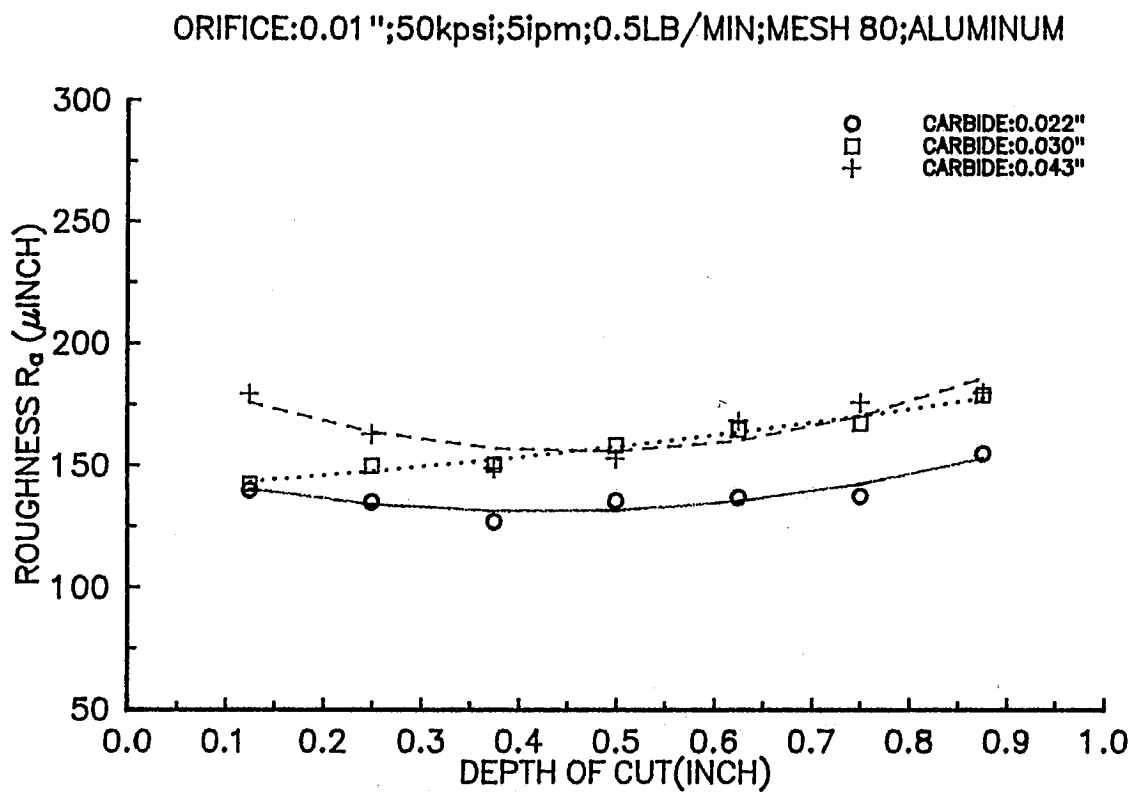

Figure 12: Effect of Focusing Tube Size on Roughness

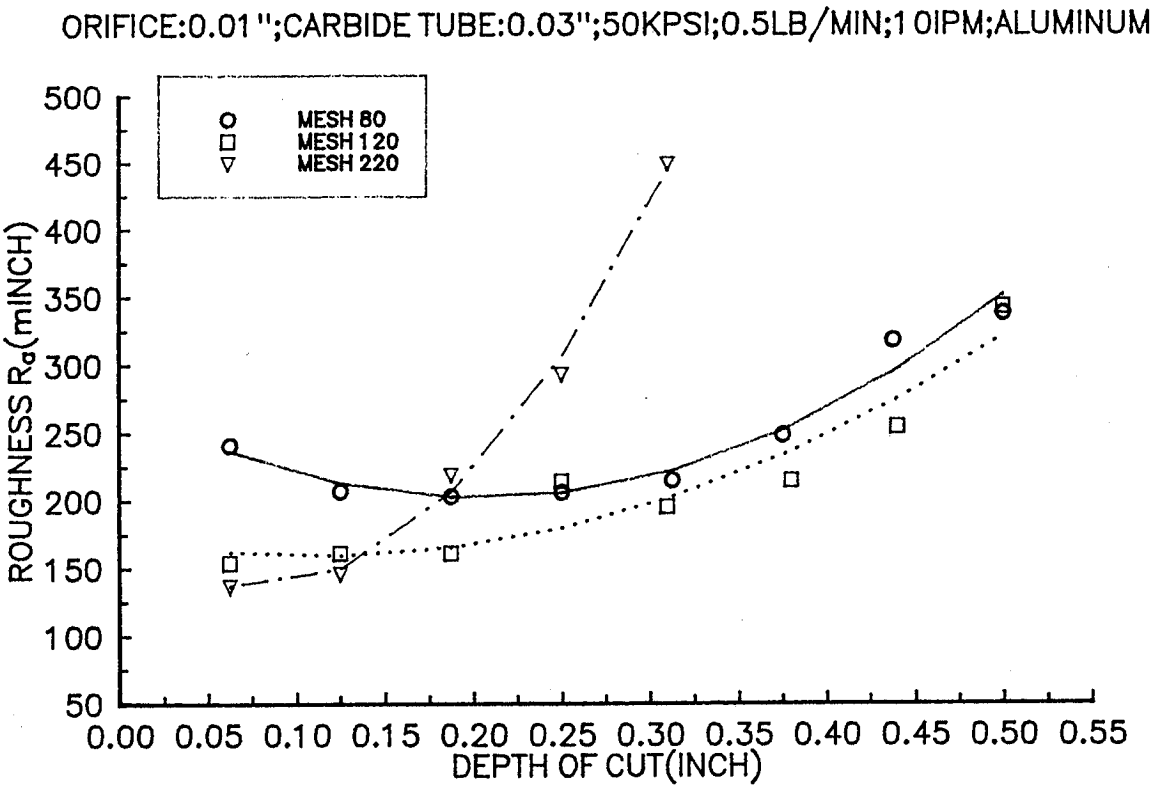

Figure 13: Effect of Abrasive Particle Size on Roughness

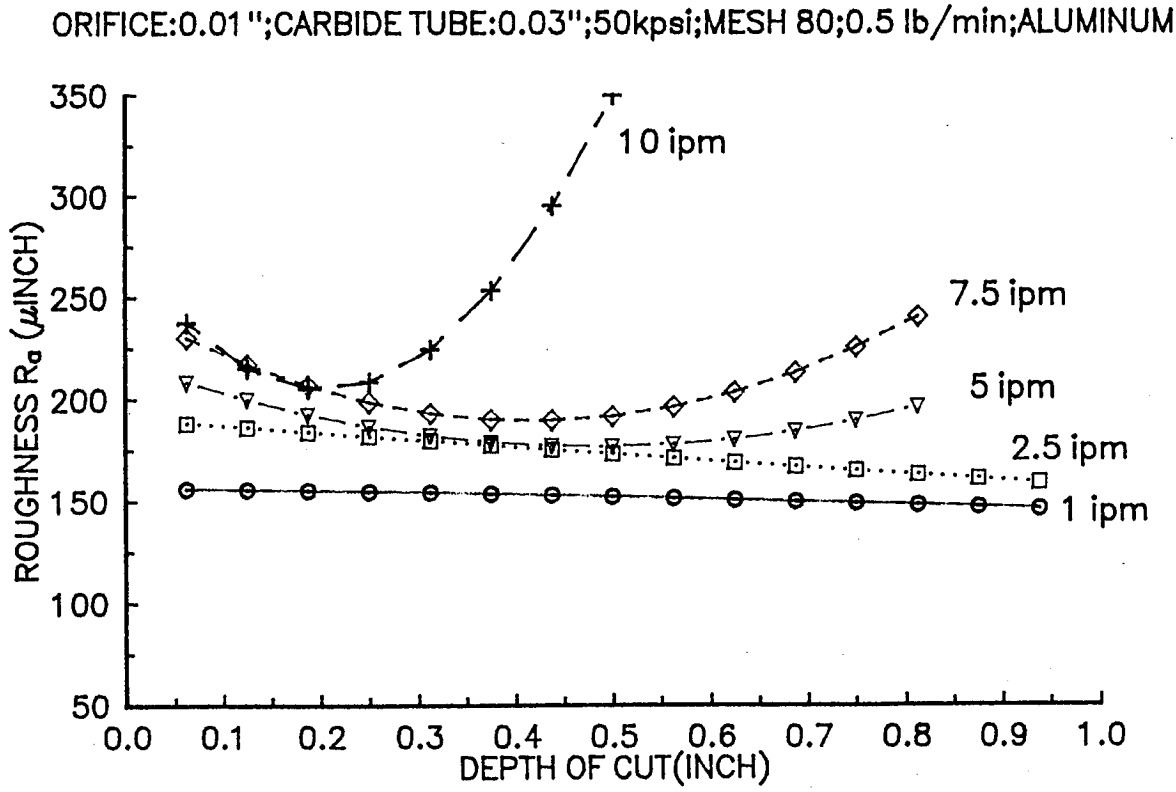

Figure 14: Effect of Cutting Speed on Roughness

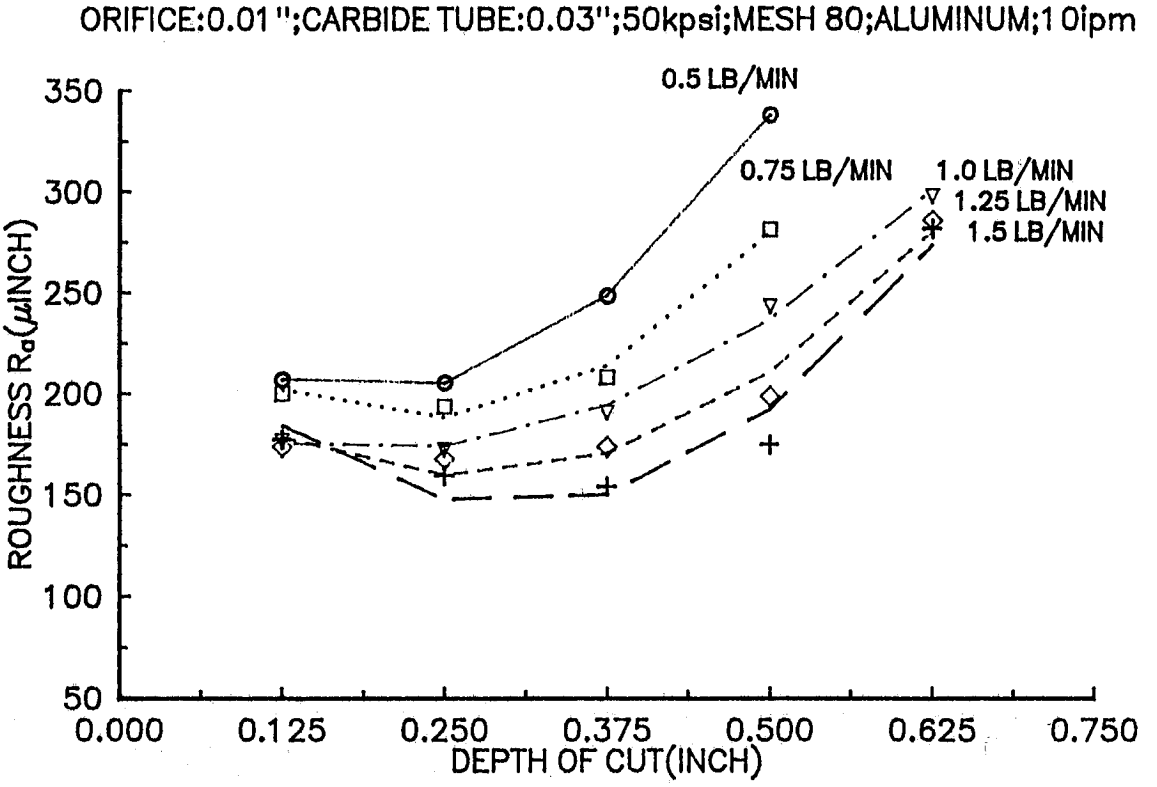

Figure 15: Effect of Abrasive Flow Rate on Roughness

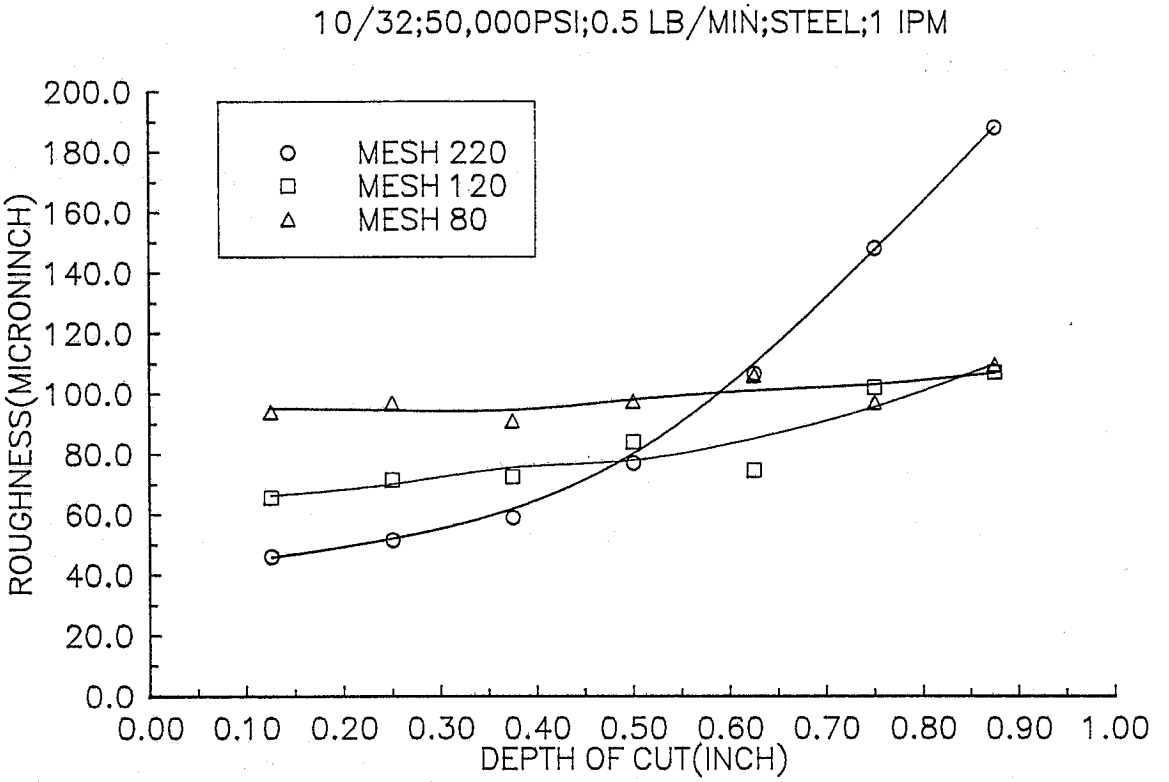

Figure 16: Effect of Abrasive Particle Size on Roughness.
Mild Steel Sample

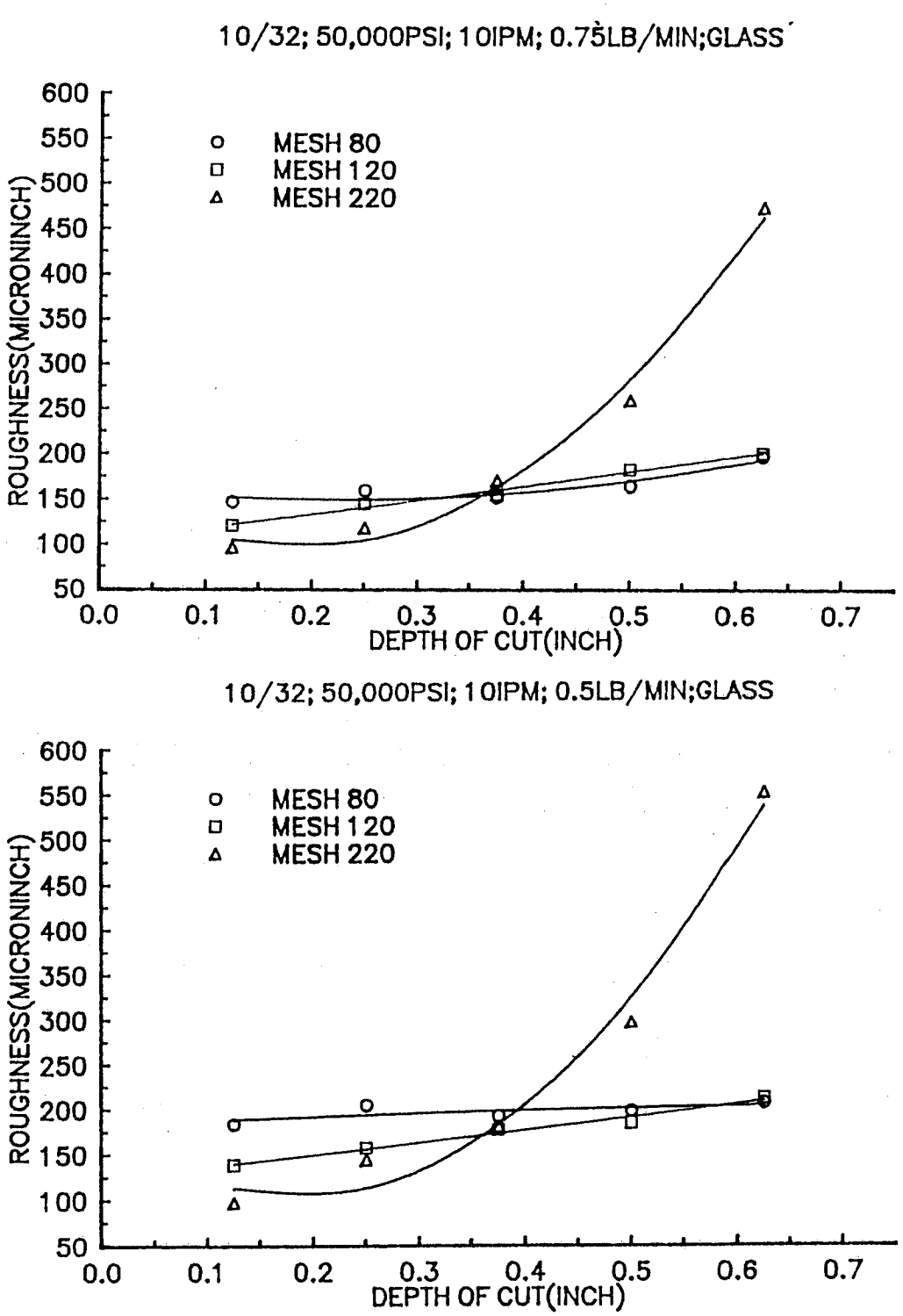

Figures 17a (top) and 17b (bottom):
Influence of Abrasive Particle Size on Roughness.
Glass Sample. Abrasive Mass Flow Rate is 0.75 lb/min
in 17a) and 0.5 lb/min in 17b)

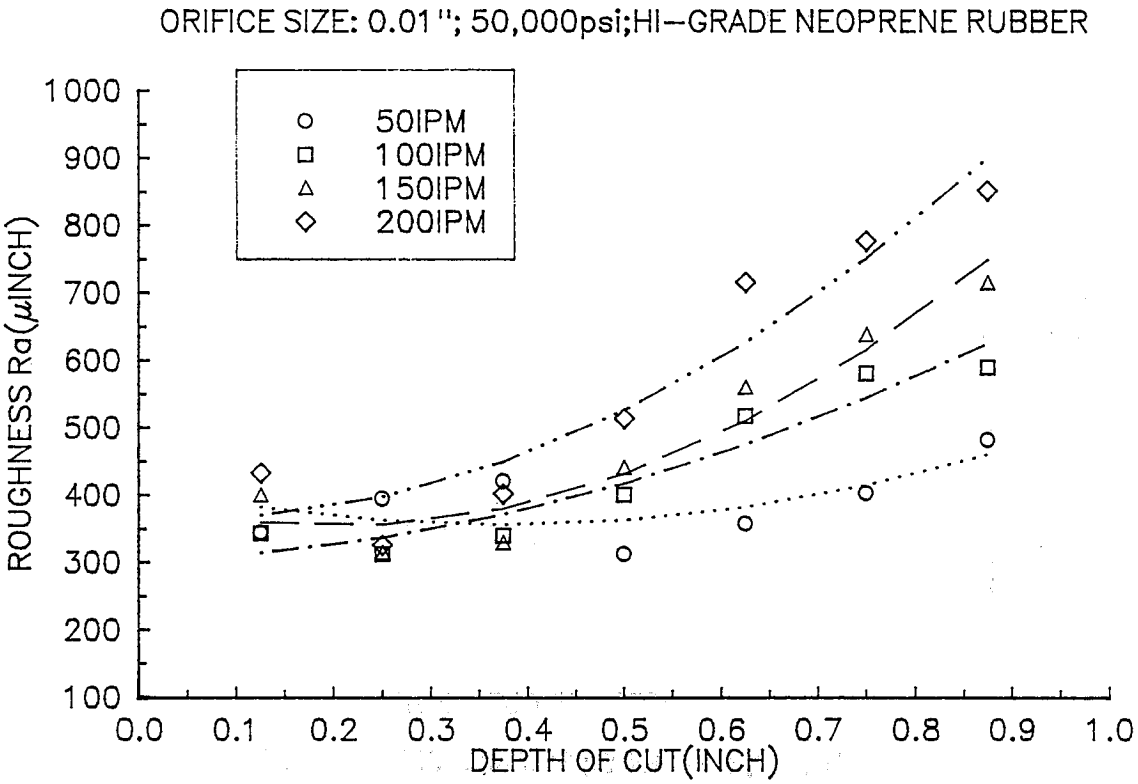

Figure 18: Influence of Cutting Speed on Roughness.

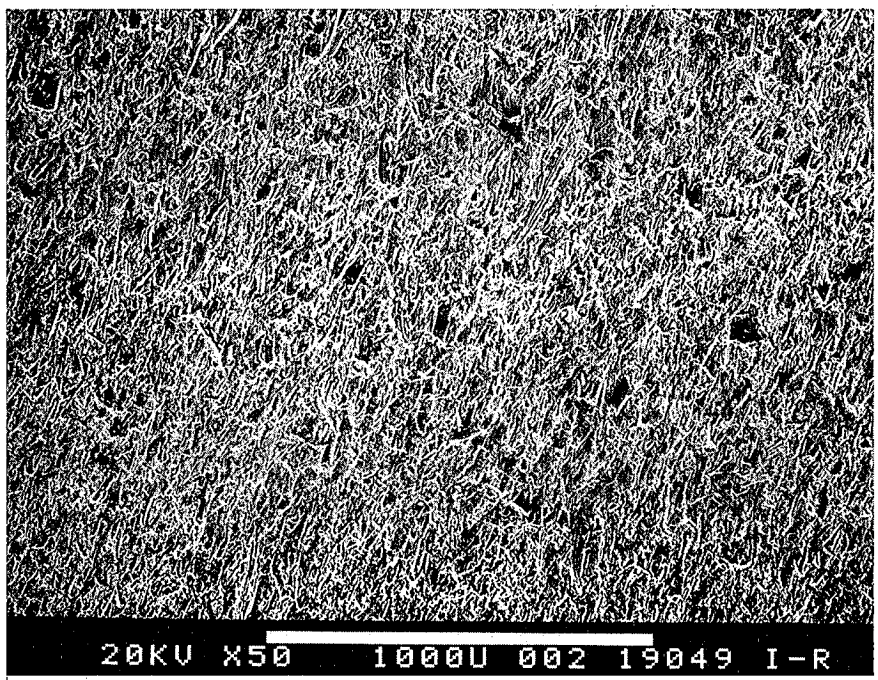

Figure 19a: SEM Micrograph. 50 ksi; Aluminum Specimen; Mesh 80; 5 ipm; 0.5 lb/min; Orifice: 0.01 in.; Focusing Tube: 0.03 in; 0.125 in Below Top

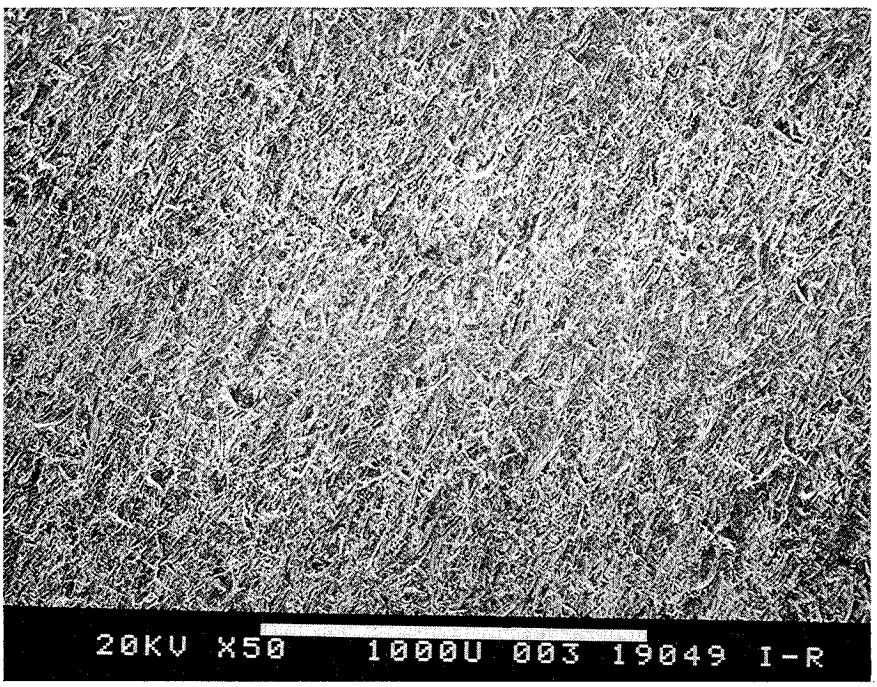

Figure 19b: SEM Micrograph. 50 ksi; Aluminum Specimen; Mesh 80; 5 ipm; 0.5 lb/min; Orifice: 0.01 in; Focusing Tube: 0.03 in; 0.250 in Below Top

6th American Water Jet Conference
August 24 - 27, 1991: Houston, Texas Paper 12

CHARACTERIZATION OF ENERGY DISSIPATION PHENOMENON IN ABRASIVE WATERJET CUTTING

Jiyue Zeng, Richard Heines and Thomas J. Kim
Waterjet Research Laboratory
Department of Mechanical Engineering
University of Rhode Island
Kingston, RI 02881

ABSTRACT

An experimental study was conducted to investigate the energy dissipation phenomenon associated with the abrasive waterjet cutting. In abrasive waterjet process, as the jet stream penetrates deeper into the material, the stream dissipates energy thereby reducing the cutting efficiency. The pronounced effect of energy dissipation can be observed by the tapered edge in kerf cut and curved striation marks at the lower portion of the cut surface. To quantify the energy dissipation phenomenon in abrasive waterjet cutting applications, a series of cutting experiments was conducted. The curvatures of striation marks and the exit angles of jet stream were measured in terms of several waterjet process parameters. It was found that the striation marks can be characterized as a parabola in cutting depth coordinate. The cutting efficiency was expressed in terms of the slope of striation curves, which was used as a process control parameter.

Organized and Sponsored by the Water Jet Technology Association.

1.0 INTRODUCTION

The surface finish produced by abrasive waterjet (AWJ) machining varies as a function of the cutting depth of a workpiece. The most pronounced characteristics of the AWJ machined surface is the development of striation marks which transpire below a region with relatively smooth surface finish as shown in Figure 1. The zone separating these two regions is defined as the transition zone by Kim, et. al. [1,2,3] in their studies on the surface finish characterization in AWJ machining. This type of inconsistency in surface roughness distribution is a unique characteristic of an AWJ process as well as any high energy beam cutting processes. Several studies by Hashish [4,5] have ascertained the material removal mechanisms in an AWJ cutting process, which quantify the material removal in two different stages. The mechanism of AWJ cutting process generally depends on the process parameters and the workpiece geometry, namely the thickness. In the first stage the abrasive particles strike the surface at a shallow angle producing a relatively smooth surface. The material removal phenomenon associated with this stage is called the cutting wear mechanism. The secondary region, displaying unsteady cutting with striation marks as shown in Figure 1, is called the deformation wear zone. This secondary penetration process is primarily responsible for the striation marks at the bottom of the kerf. The material removal is controlled by erosive wear due to particles impacting at large angles of attack.

The controllability of an AWJ process for achieving acceptable dimension tolerance and quality of the surface finish is essential in precision machining applications. Variation of the kerf width in cutting depth direction (taper) and the curved striation marks on the kerf walls are directly related to the dissipation of jet stream energy. Since the intrinsic nature of energy dissipation phenomenon in AWJ processes cannot be completely eliminated, a better understanding of the energy dissipation mechanism is essential for controlling the AWJ process in precision machining applications.

The purpose of this study is to characterize the energy dissipation phenomenon in the abrasive waterjet process and discuss the feasibility of controlling the process parameters to enhance the accuracy as well as the quality of AWJ machined components.

2.0 CHARACTERIZATION OF THE ENERGY DISSIPATION PHENOMENON

As the AWJ cutting efficiency decreases, visible striation marks trailing opposite to the cutting head traverse direction are usually observed. One of the interesting phenomena observed during the cutting experiments of a variety of workpiece materials was the similarity of striation patterns regardless of the different cutting conditions. To quantify this observation, a series of cutting tests was conducted using four different types of materials representing both ductile and brittle categories. These materials with different thickness were cut by varying the cutting parameters as shown in Table 1. The striation marks were etched and plotted in Figure 2 in terms of the deviation, referred to the depth coordinate and the depth in the workpiece. For a qualitative comparison of these curves, each curve was normalized with respect to the workpiece thickness (X_{max}) in the X direction and the maximum deviation (Y_{max}) in the Y direction, and plotted linearly

and logarithmically in Figure 3 (a) & (b), respectively. Interestingly, all of these curves line up closely to a curve of parabola. Curve-fitting the data with parabolas yield the correlation coefficients between 0.990 and 0.999. The curve-fitted equations and the corresponding correlation coefficients are listed in Table 2. Therefore, the striation marks can be characterized in terms of a simple functional expression as:

$$y = a(x-b)^2+c \qquad (1)$$

where:

y = horizontal deviation of the curve
x = depth in the workpiece
a,b,c = coefficients to be determined

This type of generalization can be used as a first approximation for quantifying the geometric nature of the striation. It is noticed that the curve-fitted expression (1) for striation curves is not applicable in the neighborhood of the top of workpiece, where y should vanish at $x = 0$. A better curve-fitting can be achieved by combining a straight line for $0 \leq x < b$ and equation (1) for $x \geq b$ if the mathematical expression in this region is needed. Since the energy dissipation phenomenon is insignificant for small values of x, equation (1) was used in this study. For a group of preset waterjet cutting parameters, the striation curves are parallel as shown in Figures 1 and 4. Therefore, a continuous cutting process can be modelled as a curve (parabola) moving in the y direction with a constant speed of u. For a given traverse time period of Δt, the striation curve shifts a distance of Δy as shown in Figure 4. At a given location on the curve, the perpendicular distance between the curve 1 and 2 is defined as the local removal thickness Δh, which can be expressed by:

$$\Delta h = \Delta y \cos\alpha = \frac{\Delta y}{\sqrt{1+\tan^2\alpha}} \qquad (2)$$

where α is the angle of slope of the striation curves, which can be determined from equation (1):

$$\tan\alpha = y' = 2a(x-b) \qquad (3)$$

The one-dimensional material removal rate can be defined as:

$$M = \lim_{\Delta t \to 0} \frac{\Delta h}{\Delta t} = \frac{dh}{dt} \qquad (4)$$

and the one-dimensional displacement rate as:

$$u = \lim_{\Delta t \to 0} \frac{\Delta y}{\Delta t} = \frac{dy}{dt} \qquad (5)$$

From equations (2), (4), and (5), one can obtain a relation between the material removal rate M and the displacement rate u by:

$$\frac{M}{u} = \cos\alpha \qquad (6)$$

From equations (3) and (6):

$$\frac{M}{u} = \frac{1}{\sqrt{1+4a^2(x-b)^2}} \qquad (7)$$

The linear displacement rate u is the traverse rate of the jet stream and is an input parameter. The linear material removal rate M is an output parameter, dependent on the water pressure and flow rate, abrasive type and flow rate, mixing efficiency, target material properties as well as the dissipating mechanisms along the jet stream path. The ratio M/u represents the cutting efficiency at the localized zone. Equation (6) & (7) explicitly indicate the trend that the cutting efficiency decreases as the angle of slope α or the depth x increases. When the cutting efficiency is reduced to a certain degree, the abrasive entrained jet stream becomes unstable and a striation mark starts to develop. The cutting efficiency eventually reaches a critical point at which the jet stream significantly loses its cutting power and is "kicked-back" by the target material. This critical point is associated with the maximum cutting depth for a given cutting condition.

3.0 CRITICAL JET EXIT ANGLE AND CONTROLLABILITY OF AWJ CUTTING QUALITY

Since the least cutting efficiency occurs at the jet stream exit, i.e., at the bottom of the workpiece, if this cutting efficiency can be predicted and controlled, quality control of the AWJ process will become feasible. Equation (6) indicates that the cutting efficiency depends solely on the angle of the slope of the striation curve. This angle at the jet exit is visible and measurable during the cutting process as shown in Figure 5. Therefore, if the exit angle is monitored during the cutting process and used as a feedback control

signal to adjust the cutting parameters, the preset requirements such as the cutting depth or the surface roughness can be precisely attained. For rough cutting applications with no concerns on the quality of surface finish, the maximum attainable cutting speed is usually desirable. In this case, by simply monitoring the exit angle of the jet stream at the bottom of the workpiece by an optical sensor or scanner, one can maintain the exit angle below the theoretically predicted value by adjusting the traverse speed. This approach would allow one to achieve the maximum cutting speed while minimizing the risk of potentially hazardous "jet stream kick-backs." The jet exit angle at which a "kick-back" phenomenon occurs is defined as the critical exit angle, α_c. Based on a series of cutting tests, it was derived that the value of the critical exit angle α_c approximately remain constant regardless of the variation of cutting parameters or type of workpiece materials.

To verify this hypothesis, a series of cutting experiments by abrasive waterjet was conducted. Five different test materials, Aluminum 6061-T6, Polypropylene, Plexiglass, 901 Tool Steel and White Marble, were chosen to include a group of materials from both ductile and brittle categories. In addition to material properties, the cutting process was also tested by varying waterjet parameters such as: cutting speed, water pressure, abrasive flow rate, orifice/nozzle size, workpiece thickness, and abrasive type and size. The traverse speed was chosen to be the major controlling parameter. For each of the three materials, Aluminum 6061-T6, Polypropylene and White Marble, four sets of cutting tests were conducted. In each set of cutting tests, one of the four parameters, water pressure, abrasive flow rate, orifice/nozzle size, and workpiece thickness, was varied while the others were held constant. The values of these parameters are listed in Table 3.

For each test cut, the cutting speed was started at zero and then increased gradually until the critical point of deflection (kick-back) was reached. At this point, the cutting speed was immediately decreased slightly until the cutting was resumed. Several photos were taken of the exiting jet with a camera equipped with a telephoto lens and positioned just far enough from the cutting area to avoid the cloud of water vapor and dust created during the cutting process. A pressurized air nozzle was also positioned near the cutting area so as to disperse this cloud and increase the clarity of the photographs. The critical jet exit angle can be measured directly from these pictures as shown in Figure 5. This method serves only as an indication of the feasibility of monitoring the exit angle during the cutting process. For the purpose of analysis a simpler method for obtaining the exit angle was used by simply etching the cut surface onto a piece of paper and then measuring the angle from the etching as shown in Figure 6. The resulting values of the critical jet exit angle are listed in Table 3 and plotted in Figures 7 - 12.

From Figures 7 - 11, it appears that the only parameter which exhibits a significant trend in its relationship with the critical exit angle is the workpiece thickness (see Figure 11). The curves in Figures 7 through 10 shows that the critical angles for the majority of the samples lie in a band between fifteen and twenty-five degrees. This can be seen more clearly in Figure 12, which is a plot of all the data obtained from the 38 mm thick workpieces. The mean value and the standard deviation of these data were found to be:

Mean Value:	20.4 degrees
Standard Deviation:	4.08 degrees

The measurement inaccuracy might be the cause of this deviation since the values of the exit angle were measured when the cutting speed had been reduced for a small, but varying amount from the critical point. The instability of the critical cutting condition should be another important factor which makes the jet exit angle fluctuate. Nevertheless, the above general trends can be explained analytically.

Previous studies [6] show the existence of a qualitative relation between the material removal rate and most of the cutting parameters. That is, increasing the water pressure P, abrasive flow rate $\dot{m}$ will enhance the material removal rate while higher values of material properties F and workpiece thickness H tend to reduce the material removal rate. It was also found that the accumulated length of the striation curve, S, is more directly related to the local material removal rate than the workpiece thickness. A qualitative relation is hence established to be:

$$M = K \frac{P^{n1}\dot{m}^{n2}}{F^{n3}S^{n4}} \qquad (8)$$

where K, n1, n2, n3, and n4 are constants to be determined.

Combining equations (6) and (8) leads to the following relation:

$$\cos\alpha_c = K \frac{P^{n1}\dot{m}^{n2}}{uF^{n3}S^{n4}} \qquad (9)$$

Now the phenomena observed in Figures 7 through 11 can be explained analytically with equation (9). In Figure 7, the increase in water pressure P was balanced by an increase in traverse rate u while the other parameters remain unchanged. Therefore, the critical exit angle α_c remains constant, according to equation (9). In Figure 8, since the variation of the orifice/nozzle size was mainly affecting the width of the kerf being cut and had the least effect on the cutting efficiency, α_c was unaffected. In Figure 9 the increased abrasive flow rate $\dot{m}$ was balanced by the increased traverse rate u, and in Figure 10, the increased material erosion resistance F was balanced by the reduced traverse rate u. They all lead to a constant α_c. However, the situation of increased workpiece thickness (Figure 11) is more complicated. Since the jet parameters (P and $\dot{m}$) and the workpiece material (F) were unchanged, the jet cutting power, or the material removal rate, was the same regardless of the variation of workpiece thickness and traverse rate. From the point of view of energy dissipation, it is obvious that two jets with identical cutting power tend to go through the same length (S) on the jet stream path before the critical point of kick-

back is reached. To attain the same value of S on two workpieces with different thickness, the striation curve on the thinner workpiece has to posses a larger curvature. This has been an observed fact on the specimen used in Figure 11. This can also be justified from the curve-fitted equations in Table 2. The trend of decreased workpiece thickness is associated with the trend of increased "a", where "a" is referred to equation (1), and an increased "a" means a larger curvature for a parabola. Since an increased workpiece thickness (H), was associated with a reduced traverse rate u, but an unchanged S, as assumed above, the value of α_c tends to decrease, according to equation (9). It may be argued that the actual lengths of curves S are different for the workpieces with different thickness (thinner one having a smaller curve length), which contradicts the assumption above. However, if imaging that a striation curve with a large curvature will form an extensional thin section on the bottom of the workpiece, which will not be able to retain because of the large pressure acting on it, the assumption of unchanged S can still be justified.

Equation (9) simply shows a possible functional relationship among the major parameters based on Figures 7 - 11. More experiments should be conducted to quantitatively determine the exact relation between the critical jet exit angle and the workpiece thickness.

The scheme for automatic control of a rough cut (i.e., regardless of surface finish) can be described as follows: (1) The water pressure, abrasive type and size, abrasive flow rate, nozzle size are preset by other considerations such as nozzle wear, cost, cutting cycle, etc.; (2) The information of the workpiece thickness (exact or estimate) are fed into a computer to determine the critical value of the jet exit angle; (3) The manipulator arm, which is connected to the control system and used to perform the traverse motion of the jet, is initially set still and then speeded up gradually; (4) An optical sensor is used to monitor the jet angle and continuously feed back the signal of the angle to the control system; (5) The control system will then compare the angle to the critical value, and in sequence send off controlling signal to the manipulator to speed up or slow down the cutting speed so as to keep the jet exit angle below the critical value and therefore avoid the risk of kick-back.

Similar schemes can be applied to control the surface quality of the AWJ cuts as long as the critical value of jet exit angle corresponding to the required surface finish is determined.

Matsui, et. al. [7] proposed a compensation method for reducing the taper and striation by inclining the AWJ nozzle for a certain angle. If the value of the nozzle inclination angle is related to the critical jet exit angle, the proposed compensation method will be more efficient.

4.0 CONCLUSIONS

(1) The striation marks on the abrasive jet cut surface can be characterized by a parabola.

(2) The cutting efficiency depends solely on the slope of the striation curve.
(3) The critical jet exit angle at the condition of kick-back decreases as the workpiece thickness increases while its dependence on the other parameters is insignificant.
(4) It is feasible to use the jet exit angle as a control parameter for rough cutting applications to maximize the cutting speed while avoiding the risk of hazardous kick-back of the jet.

REFERENCES

1. Hunt, C.D., Kim, T.J., and Reuber, M., "Surface Finish Optimization for Abrasive Waterjet Cutting," presented at the 9th International Symposium on Jet Cutting Technology, the BHRA Conference Proceedings, Sendai, Japan, October, 1988.

2. Hunt, D.C., Burnham, C.D. and Kim, T.J., "Surface Finish Characterization in Machining Advanced Ceramics by Abrasive Waterjet," presented at the 4th U.S. Waterjet Conference, Conference Proceedings, August 1987.

3. Burnahm, C.D. and Kim, T.J., "Statistical Characterization of Surface Finish Produced by Abrasive Waterjet," presented at The 5th American Waterjet Symposium, the symposium proceedings, Toronto, Canada, August 1989.

4. Hashish, M., "Steel Cutting with Abrasive Waterjet," proceedings of the 6th International Symposium in Jet Cutting Technology, BHRA Fluid Engineering, April 1982, pp. 465-487.

5. Hashish, M., "A Modeling Study of Metal Cutting with Abrasive-Waterjets," ASME Journal of Engineering Materials and Technology, Vol. 106, No. 1, Jan. 1984, pp 89-100.

6. Zeng, J. and Kim, T., "The Machinability of Porous Materials by a High Pressure Abrasive Waterjet," proceedings of the Winter Annual Meeting of ASME, San Francisco, U.S.A. Dec. 10-15, 1989.

7. Matsui, S., Matsumura, H., Ikamoto, Y., Tsukita, K., Shimizu, H., "High Precision Cutting Method For Metallic Materials by Abrasive Waterjet," proceedings of 10th International Symposium on Jet Cutting Technology, Amsterdam, Oct. 31-Nov. 2, 1990.

NOMENCLATURE

a,b,c = Curve-fitted coefficients
F = Erosion resistance of workpiece
K = Proportional constant
M = One-dimensional material removal rate
$\dot{m}$ = Abrasive flow rate
n_1, n_2, n_3, n_4 = Constants

P = Water pressure
S = Length of striation curve
t = Time
u = Traverse rate
x = Depth in the workpiece
y = Horizontal deviation of striation curves
α = Angle of slope of striation curves
α_c = Critical jet exit angle
Δh = Removal thickness measured perpendicularly to striation curves
Δt = Given traverse time period
Δy = Displacement measured parallel to the jet traverse direction
$\bar{u}$ = Mean value
σ = Standard deviation

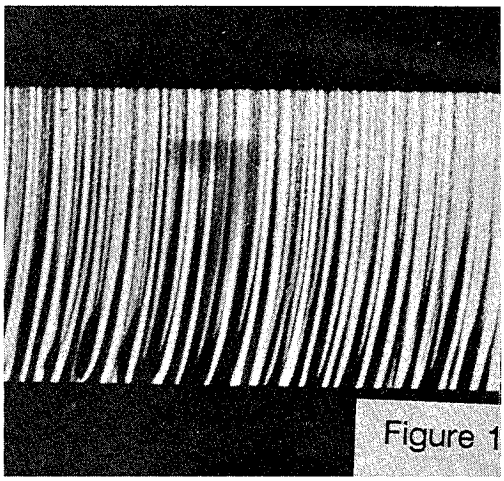

(a)on 6061-T6 Aluminum

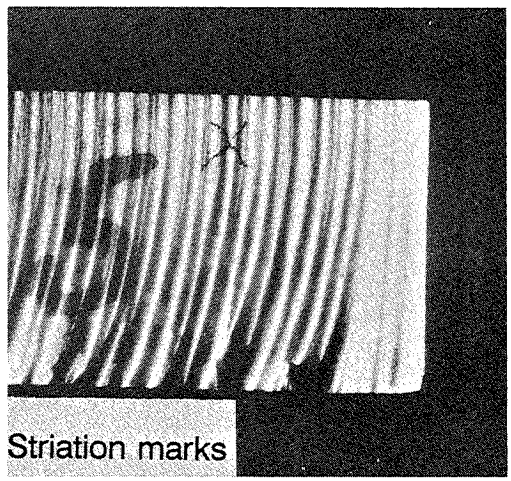

(b) on White Marble

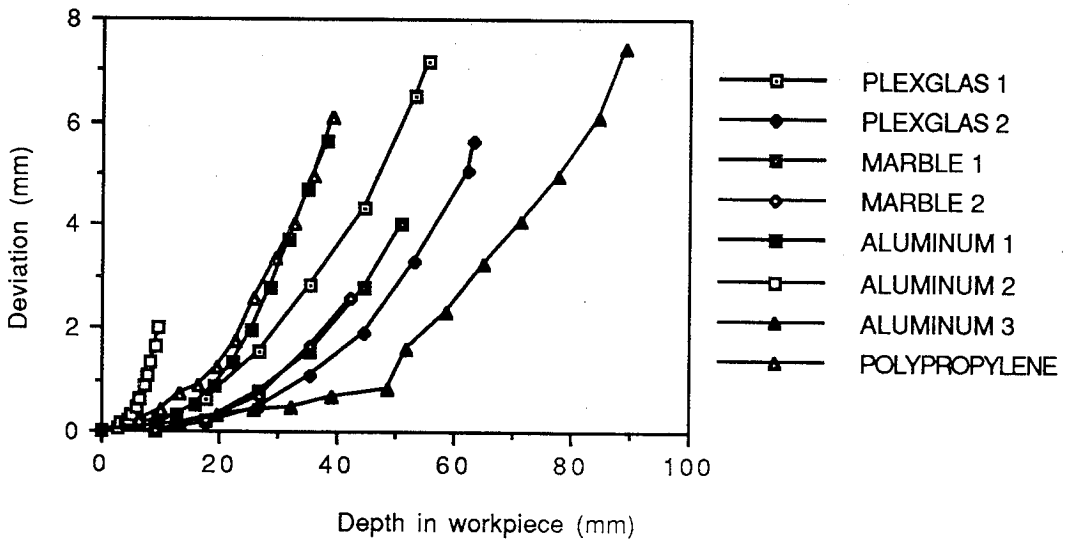

Figure 2 Striation Curves

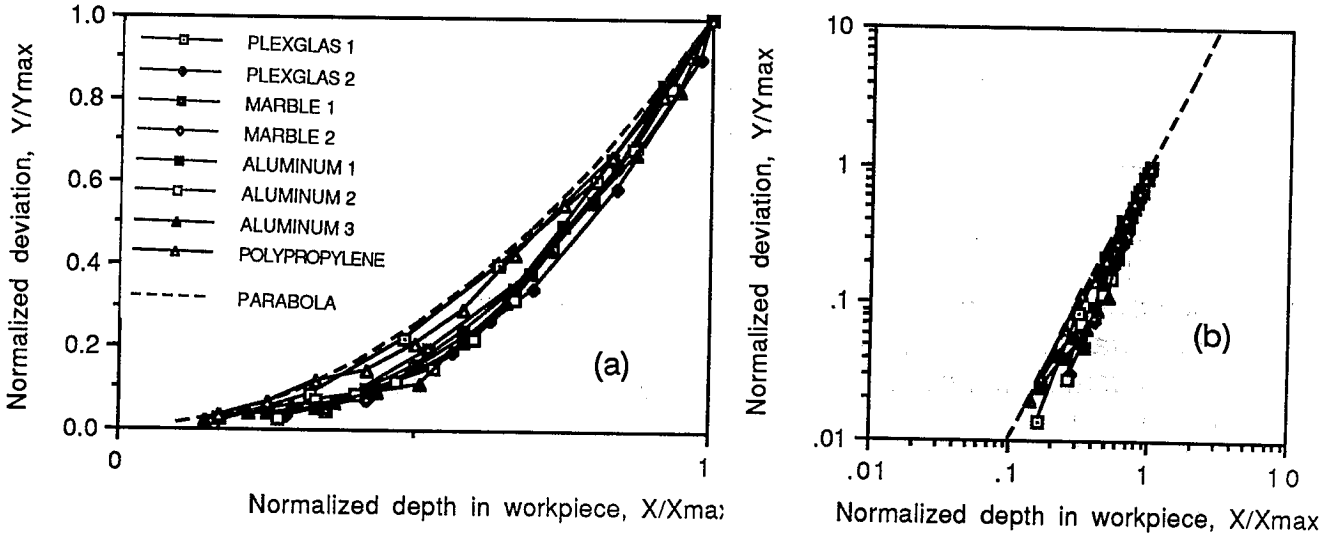

Figure 3 Normalized striation curves

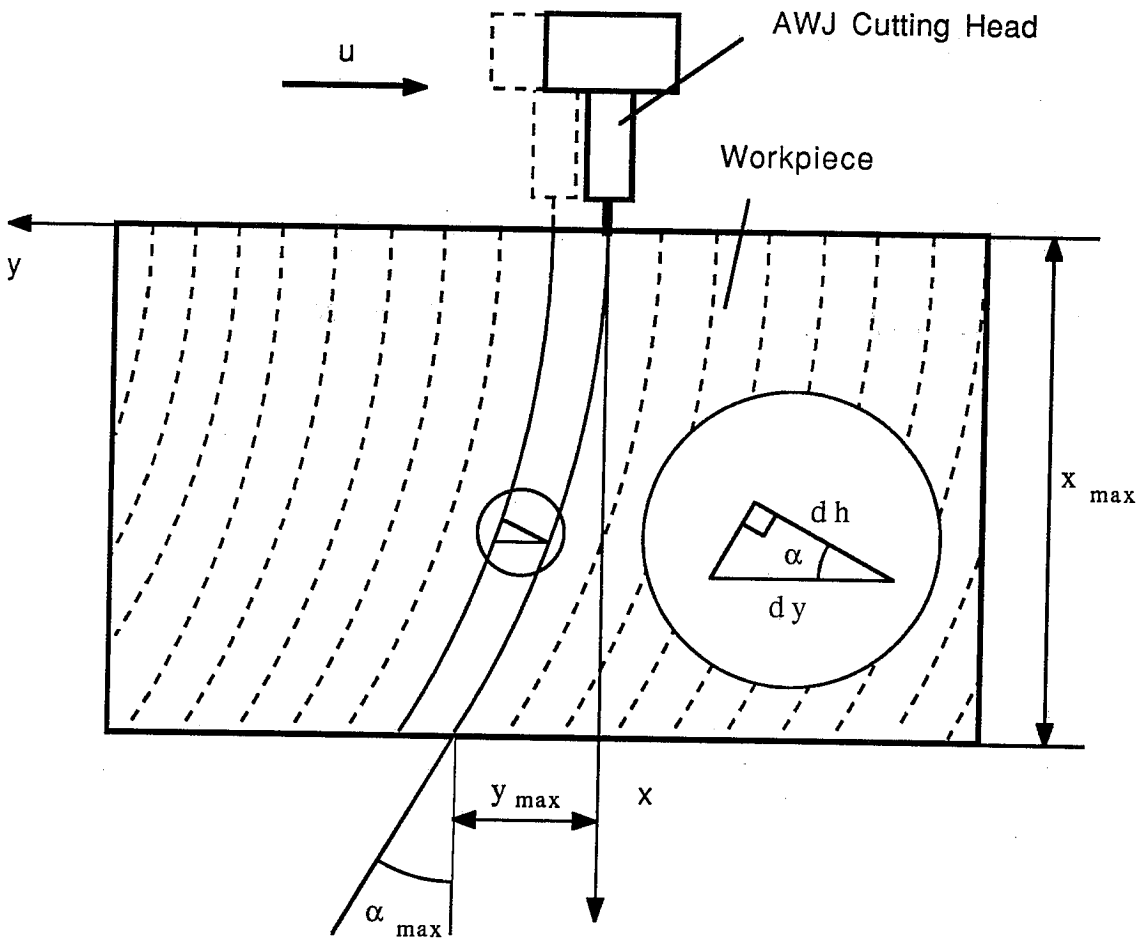

Figure 4 Characteristics of striation curves

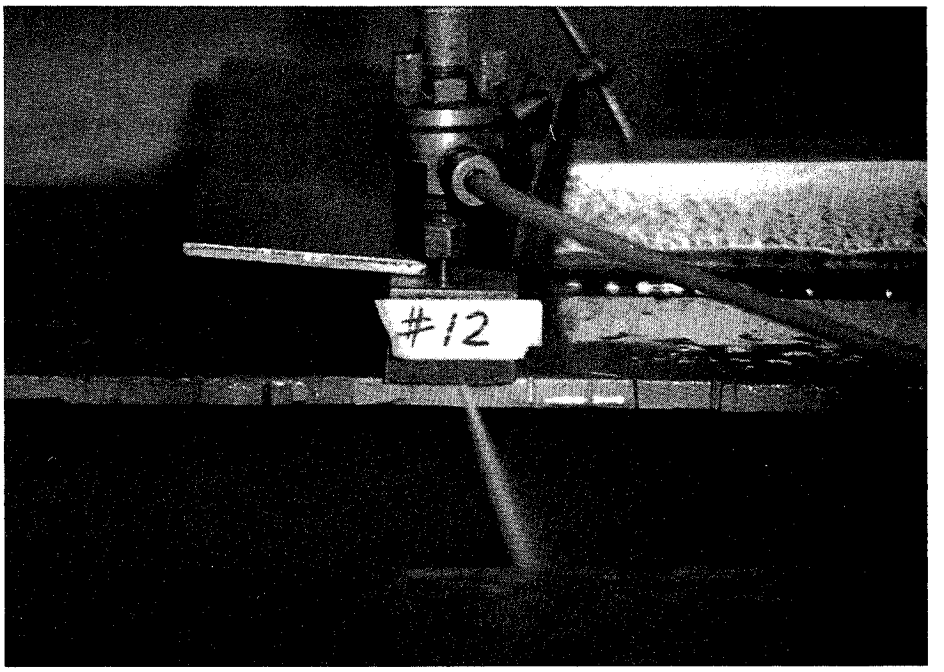

Figure 5 Jet exit angle is visible and measurable during the cutting process

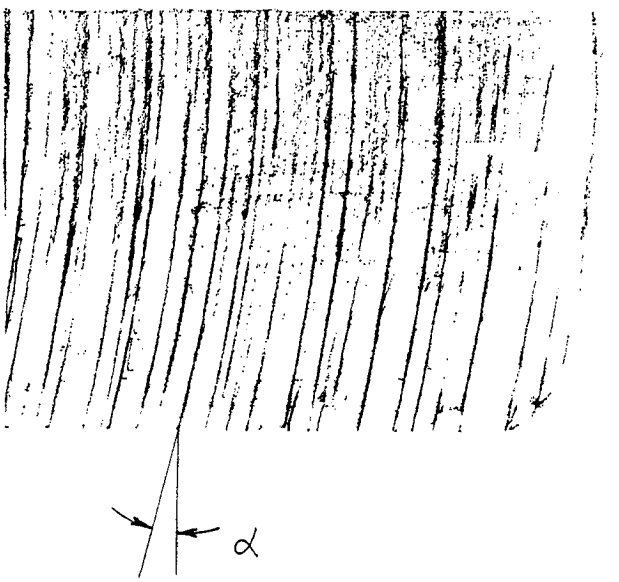

Figure 6 Critical jet exit angle measured from the etching of a cut surface

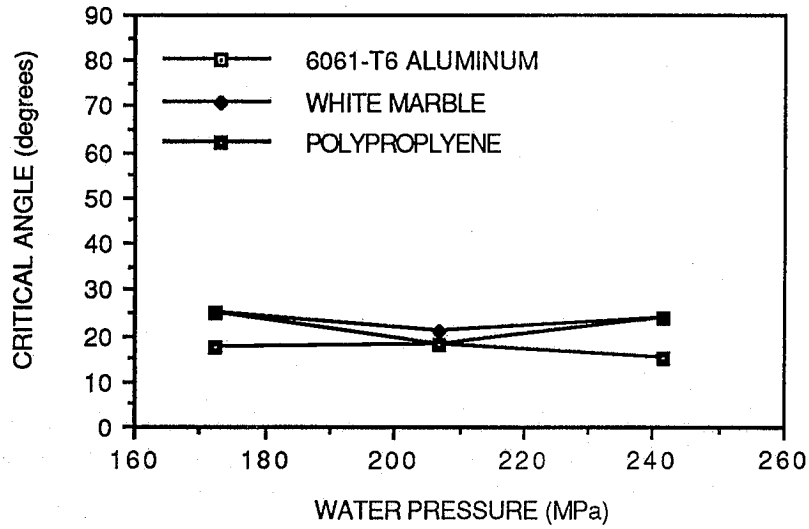

Figure 7 Effect of water pressure on the critical jet exit angle

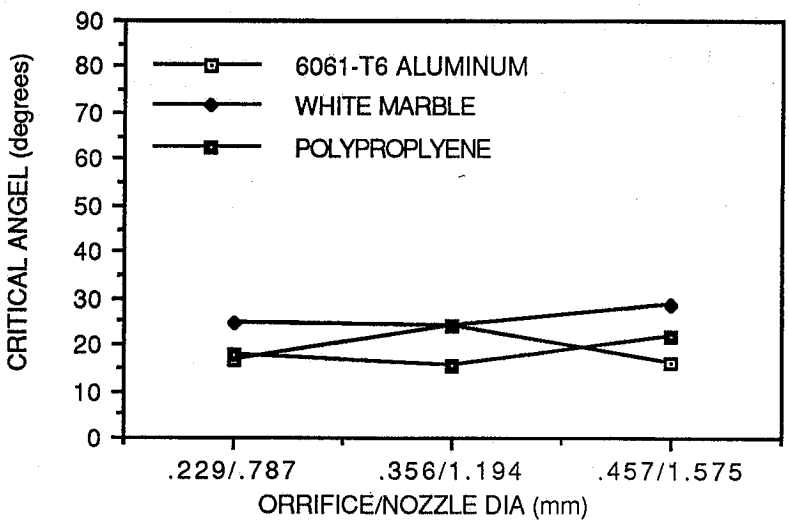

Figure 8 Effect of orifice/nozzle size on the critical jet exit angle

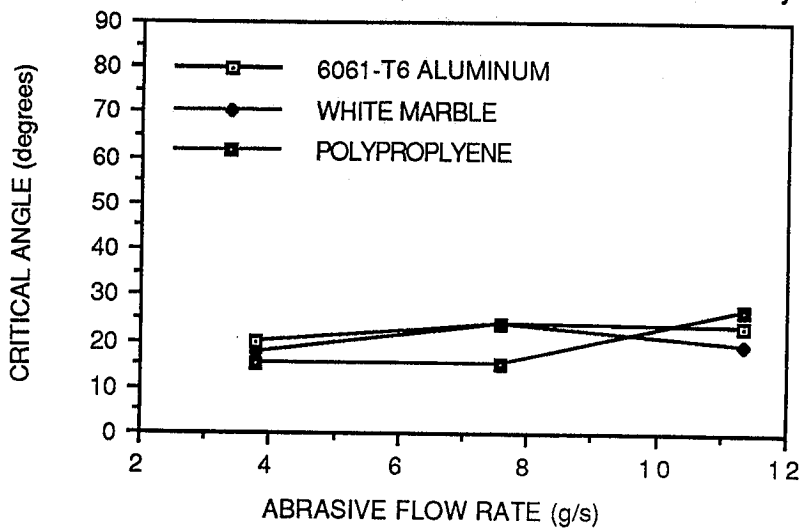

Figure 9 Effect of abrasive flow rate on the critical jet exit angle

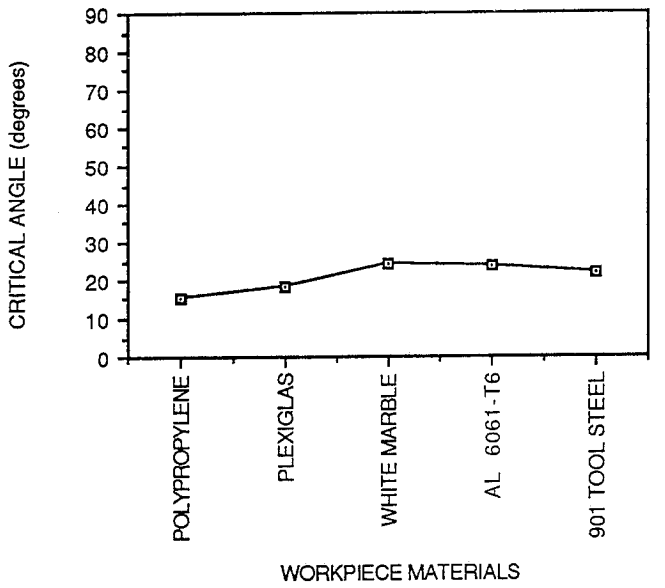

Figure 10 Effect of workpiece material on the critical jet exit angle

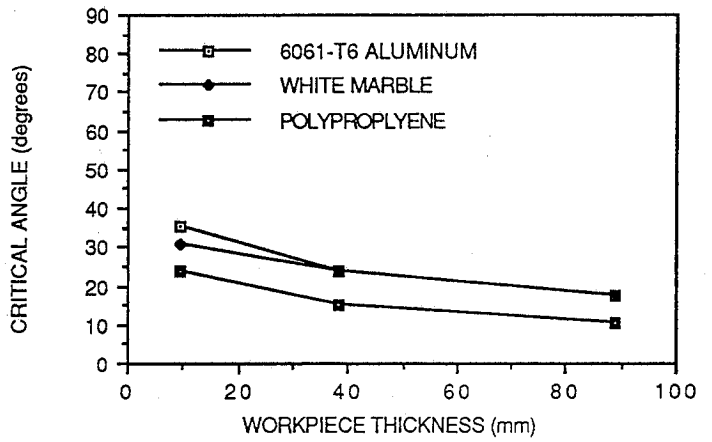

Figure 11 Effect of workpiece thickness on the critical jet exit angle

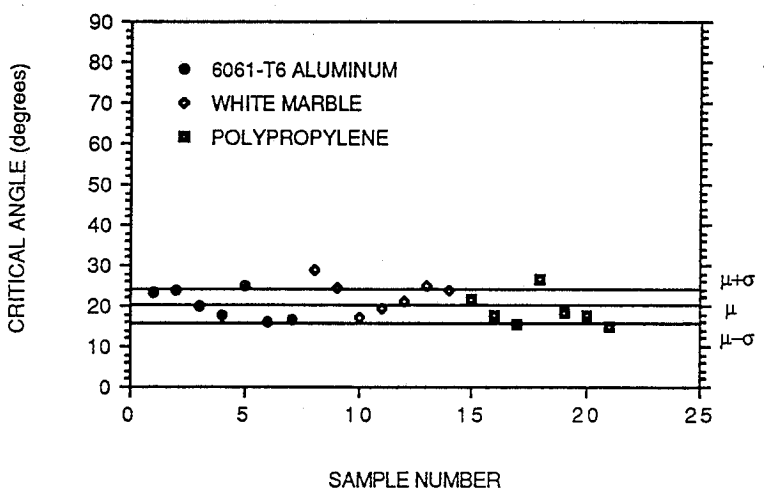

Figure 12 Critical jet exit angles for 38 mm thick workpiece

Table 1 Cutting test parameters

SAMPLE LABLE	THICK-NESS (mm)	WATER PRESSURE (Mpa)	ORIFICE/ NOZZLE SIZE (mm / mm)	ABRASIVE TYPE AND MESH NO.	ABRASIVE FLOW RATE (g/s)	STAND-OFF DISTANCE (mm)	CUTTING SPEED (mm/s)
Plexiglas 1	55.35	241	.457/1.168	Barton # 80	11.4	1.5	2.5
Plexiglas 2	63.36		.457/1.168	IGE Maine Garnet # 60	11.4		1.0
Marble 1	51.06		.457/1.168		11.4		1.0
Marble 2	42.44		.457/1.168		11.4		1.0
Al 6061-T6 1	38.2		.356/1.168	Barton Garnet # 80	11.4		1.5
Al 6061-T6 2	9.67		.356/1.168		7.6		10.5
Al 6061-T6 3	89.3		.356/1.168		7.6		0.4
Polypropylene	39.1		.356/1.168		7.6		5.25

Table 2 Curve-fitting data of striation marks

CURVE LABLE	CURVE-FITTED EQUATION	COEFFICIENT OF CORRELATION R^2
PLexiglas 1	$Y = 2.489 \times 10^{-3} (X - 2.069)^2 - 0.0032$	0.999
Plexiglas 2	$Y = 2.038 \times 10^{-3} (X - 11.51)^2 - 0.1037$	0.994
Marble 1	$Y = 2.112 \times 10^{-3} (X - 7.311)^2 - 0.0629$	0.998
Marble 2	$Y = 2.115 \times 10^{-3} (X - 7.023)^2 - 0.0692$	0.998
Aluminum 1	$Y = 5.414 \times 10^{-3} (X - 5.806)^2 - 0.0157$	0.997
Aluminum 2	$Y = 3.072 \times 10^{-2} (X - 1.657)^2 - 0.0259$	0.995
Aluminum 3	$Y = 1.352 \times 10^{-3} (X - 16.60)^2 - 0.0069$	0.990
Polypropylene	$Y = 4.444 \times 10^{-3} (X - 2.495)^2 + 0.0654$	0.998

Table 3 Cutting test parameters and the critical jet exit angles

SAMPLE MATERIAL	THICK-NESS (mm)	WATER PRESSURE (Mpa)	ORIFICE/ NOZZLE SIZE (mm / mm)	ABRASIVE FLOW RATE (g/s)	STAND-OFF DISTANCE (mm)	CUTTING SPEED (mm/s)	CRITICAL JET EXIT ANGLE (degrees)
Al 6061-T6	38.1	241	.356/1.168	7.6	1.5	2.0	23.8
Plexiglas						3.5	18.3
Polypropylene						5.25	15.2
901 Tool Steel						0.2	21.8
White Marble						3.75	24.0
Al 6061-T6	9.5	241	.356/1.168	7.6		10.5	35.4
	38.1					2.0	23.8
	88.9					0.4	17.2
	38.1	172	.356/1.168	7.6		1.3	25.0
		207				1.6	17.8
		241				2.0	23.8
	38.1	241	.229/.787	7.6		0.7	16.5
			.356/1.168			2.0	23.8
			.457/1.575			1.6	16.0
	38.1	241	.356/1.168	3.8		1.6	19.8
				7.6		2.0	23.8
				11.4		1.5	23.5
Polypropylene	9.5	241	.356/1.168	7.6		27.0	23.7
	38.1					5.25	15.2
	88.9					0.5	10.2
	38.1	172	.356/1.168	7.6		2.5	17.6
		207				3.0	18.1
		241				5.25	15.2
	38.1	241	.229/.787	7.6		2.7	17.5
			.356/1.168			5.25	15.2
			.457/1.575			7.0	21.9
	38.1	241	.356/1.168	3.8		3.0	15.3
				7.6		5.25	15.2
				11.4		4.5	26.9
White Marble	9.5	241	.356/1.168	7.6		24.0	30.7
	38.1					3.75	24.0
	88.9					1.0	17.6
	38.1	172	.356/1.168	7.6		2.3	24.9
		207				2.5	21.0
		241				3.75	24.0
	38.1	241	.229/.787	7.6		2.0	24.4
			.356/1.168			3.75	24.0
			.457/1.575			3.0	28.9
	38.1	241	.356/1.168	3.8		2.0	17.2
				7.6		3.75	24.0
				11.4		3.5	19.2

6th American Water Jet Conference
August 24 - 27, 1991: Houston, Texas Paper 13

Abstract

Precision Machining with Abrasive-Waterjets

by

Mohamed Hashish
Senior Research Scientist
QUEST Integrated, Inc.
(Formerly Flow Research, Inc.)

for

6th American Waterjet Technology Conference
August 24-27, 1991, Westin Galleria
Houston, Texas

This paper presents recent and current research efforts on precision multi-dimensional machining with abrasive waterjets. A number of machining operations will be presented through which the precision limits and their most influencing factors will be discussed. For example, hole drilling (0.02 to 0.1 inch diameter) with 0.001 inch accuracy can be achieved. However, the control strategy was found to be dependent on the diameter range. The effects of the dynamic jet parameters (pressure, traverse rate, and abrasive flow rate) on the accuracy and repeatability of hole geometry results are presented for metals and composites. Turning of complex shapes such as helixes and threads is also addressed. Methods of controlling the turned diameter and its surface morphology are discussed with numerical examples. Examples of three-dimensional machining operations which include cutting, turning, drilling, and milling are addressed to illustrate the operational requirements of advanced machining centers.

Organized and Sponsored by the Water Jet Technology Association.

6th American Water Jet Conference
August 24 - 27, 1991: Houston, Texas Paper 14

AN ABRASIVE JET BOREHOLE MINER

George A. Savanick
Bureau of Mines, U.S. Department of the Interior
Minneapolis, Minnesota 55417-3099, USA

ABSTRACT

The Bureau of Mines has designed, built and tested an abrasive jet borehole miner for hard rock. It integrates an abrasive jet cutter with a downhole slurry pump and is in the form of an assembly that is suspended in a well and is rotated by a turntable at the well head.

This device generates a 68.9 MN/m^2, 75.7 Lpm (10,000-psi, 20-gpm) collimated jet containing 7.26 kg/min (16 lb/min) of abrasive. This jet erodes the rock in the borehole wall and forms a slurry. The addition of the abrasive greatly enhances the erosive power of a 68.9 MN/m^2, 75.7 Lpm (10,000-psi, 20-gpm) jet of water without abrasives. The slurry is pumped to the surface by a downhole eductor.

The abrasive jet borehole miner was tested in a simulated well in the laboratory and in a taconite mine. Samples of charcoal granite, Duluth gabbro, and Sioux quartzite were cut and the cuttings pumped in the laboratory. Taconite was cut and pumped from a borehole in an open pit mine.

1.0 INTRODUCTION

Borehole mining, also known as slurry mining, is a process in which a tool incorporating a water-jet cutting system and a downhole slurry pumping system are used to mine ore through a single borehole drilled from the surface to the buried ore. Water jets from the mining tool erode the ore and form a slurry. The slurry flows into the inlet of a pump in the base of the tool. The slurry is lifted to the surface where it can be transferred by a pipeline to a processing plant.

The first patent for a tool that used water jets to fragment rock adjacent to a borehole and a down-hole slurry pump to lift the broken ore to the surface was issued to Clayton (1932). Patents on similar borehole mining tools were issued to Aston (1950), Quick (1955), Fly (1964), Pfefferle (1969), Wenneborg (1973), Archibald (1974), and Brunelle (1977).

Fly's apparatus was built and used to excavate sandstones, limestones, and shales to a maximum depth of 106.7 m (350 ft). The apparatus described in the Wenneborg patent was built by the FMC Corp. and tested in eastern North Carolina. The apparatus described in the Archibald patent was built by Marconaflo, Inc., and used to mine uraniferous sandstones and tar sands.

In 1974, the Bureau of Mines contracted with Flow Industries to design, fabricate, and test a borehole mining tool. This tool was used to mine coal in Washington, uraniferous sandstone in Wyoming, oil sands in California, and phosphate in Florida (Savanick, 1978). In 1978, Flow Industries, Inc. built another borehole mining tool similar to the Bureau's machine, but with some notable design changes. This second tool differs from the Bureau tool in that the cutting nozzle can be moved vertically independently from the remainder of the tool. This permits water-jet cutting to be performed anywhere along the length of the borehole while the slurry pump remains at the base of the borehole where the slurry density is highest. This tool was used to mine phosphate in Florida and oil sands in Alberta on an experimental basis.

All of these borehole miners have used a water jet to slurrify the ore. These machines have been used to mine only soft rocks, such as coal, sandstone, or phosphate ore, because unaided water jets are capable of disaggregating only soft rocks. The purpose of this paper is to describe a new type of borehole miner, an abrasive jet borehole miner, which extends the borehole mining technique to hard rocks by using an abrasive jet cutter.

2.0 DESIGN

The abrasive jet borehole miner, shown schematically in figures 1a-1b integrates an abrasive jet cutter with a downhole slurry pump. It is in the form of an assembly that is suspended in a well and is rotated by a turntable at the wellhead. This assembly consists of a bundle of four pipes. Pipe 1 supplies pressurized water 68.9 MN/m^2, 75.7 Lpm (10,000 psi, 20 gpm) to an 1.98-mm (0.078-inch-diameter) nozzle in a cutting head (figs. 2,3), pipe 2 supplies abrasive to a mixing chamber downstream of the nozzle, pipe 3 supplies water to a nozzle in a downhole eductor used as a slurry pump, and pipe 4 is the outlet for the downhole slurry pump.

The device works as follows: A water jet issues from nozzle 5 (fig. 3) into mixing chamber 7, causing a pressure drop therein by the venturi effect. This pressure drop induces abrasive to flow from pipe 2 into mixing chamber 7 where the abrasive is entrained into the water jet, thereby creating an abrasive jet. The abrasive jet passes through collimating pipe 8 where the abrasives are accelerated. The abrasive jet exits the collimating pipe and impacts the ore in the borehole wall.

The 68.9 MN/m^2, 75.7 Lpm (10,000-psi, 20-gpm) abrasive jet erodes the hard rock in the borehole wall and forms a slurry. The addition of the abrasive greatly enhances the erosive power over that possessed by a 68.9 MN/m^2, 75.7 Lpm (10,000-psi, 20-gpm) jet of water without abrasives.

The slurry is induced to flow into the inlet of eductor 11 (figs. 1a and 1b). This eductor operates by the venturi effect caused by the flow of a water jet 4.13 MN/m^2, 151.4 Lpm (600 psi, 40 gpm) from nozzle 6 into mixing section 9, and diffuser 10, of eductor 11. The slurry is mixed with the water jet in section 9 and lifted to the surface through pipe 4 after being slurried and pressurized in diffuser 10.

The position of the slurry pump 11 is fixed at the base of the pipe bundle. The abrasive jet cutter (fig. 3) composed of nozzle 5, mixing chamber 7 and collimating pipe 8 can be moved vertically in a notch between pipes 3 and 4. This allows the abrasive jet to be placed anywhere along the length of the borehole while the slurry pump stays at the base of the borehole, ready to accept cuttings which fall in the borehole. The entire assembly can be oscillated 360° both clockwise and counterclockwise by a turntable mounted over the borehole where it provides rotation and oscillating movement to the abrasive jet borehole miner, which passes through the rotary turntable. This table is driven with a DC electric motor which provides rotation speeds in the range of 0 to 20 rpm. The turntable is fitted with limit switches which provide an oscillating turntable motion adjustable from 0 to 360°. The turntable also allows for vertical movement of the entire mining tool or for the cutting jet separately.

An interval is cut in the borehole wall as follows. The oscillation of the turntable trips a limit switch, causing a screw feed to operate, thereby lifting the abrasive jet cutter 8 a distance of 6 mm in the well. This motion causes a corresponding cut to be made in the adjacent rock. This sequence of actions is repeated until the desired volume is excavated.

3.0 LABORATORY TESTS

A simulated well for testing the abrasive jet borehole miner was built at the Farmington High-Energy Test Site of the Bureau of Mines. The well consists of a 15.14-cm (6-inch-diameter) well casing extending from the ground surface through a hole in the ceiling of an underground laboratory and terminating a steel box (fig. 4). An abrasive jet issuing from the borehole miner suspended in the casing cuts a rock sample in the steel box. The box can accommodate rocks as large as .22m^3 (8 ft^3). Cuttings enter a downhole slurry pump and are lifted to the surface where they are collected in a hopper. Lifts as high as 15.2 mm (50 ft) are possible in this facility.

Samples of charcoal granite, Duluth gabbro, and Sioux quartzite were cut and the cuttings were pumped to the surface. Chambers were cut in these samples (figs. 5,6) with the aid of the device described above in the last paragraph under "Design" which permitted the abrasive jet to be moved vertically a fraction of an inch after being traversed horizontally on the rock face. This device avoided the creation of ridges in the rock which deflect the jet and cause low-efficiency cutting.

The potential use of the borehole miner as an in-situ leaching well completion device was demonstrated by slotting steel casing (fig. 7) and cutting the chambers in hard rock.

Table I gives the cutting rate with a static abrasive jet. Table II gives the cutting rate attained with a traversing abrasive jet. Note that the cutting rates are small, thus precluding the use of the abrasive jet borehole miner as a bulk mining tool. It is better used in specialized applications such as taking a sample or chambering of boreholes.

Table I. - Cutting of a hole with a 68.9 MN/m^2, 75.7 Lpm (10,000-psi, 20-gpm) static abrasive jet. Red Flint abrasive (45-55 mesh); standoff distance 1.5 cm (0.6 inch).

Material	Compressive strength, MN/m^2 (psi)	Entrainment rate, kg/m (lb/min)	Volume removed, cm^3	Cutting	
				Time, min	Rate, cm^3/min
Sioux quartzite.	503.3 (73,000)	6.16 (13.6)	3.5	0.5	7.0
Charcoal granite...	279.9 (40,600)	7.44 (16.4)	6.0	0.5	12.0
Steel casing.....		6.16 (13.6)	1.3	0.86	1.5

Table II. - Slot cutting with a 68.9 MN/m^2, 75.7 Lpm (10,000-psi, 20-gpm) traversing abrasive jet. Red Flint abrasive (45-55 mesh); standoff distance 1.27 cm (0.5-in).

Rock	Compressive strength, MN/m^2 (psi)	Entrainment rate of abrasive, kg/min (lb/min)	Volume removed, cm^3	Cutting	
				Time, min	Rate, cm^3/min
Sioux quartzite	503.3 (73,000)	6.16 (13.6)	539	5.0	107.8
Charcoal granite	279.9 (40,600)	7.44 (16.4)	412	4.38	94.1
	279.9 (40,600)	7.44 (16.4)	1,026	11.7	87.7
	279.9 (40,600)	7.44 (16.4)	781	10.76	72.6
	279.9 (40,600)	7.44 (16.4)	621	10.0	62.1
Steel casing.....		6.16 (13.6)	2.0	3.17	0.7

4.0 FIELD TEST

The prototype abrasive jet borehole miner was field tested at Inland Steel Co.'s Minorca Mine at Virginia, MN. The borehole miner was suspended (fig. 8) in a 3.04-cm (12-inch-diameter) borehole in a bench of taconite. A 68.9 MN/m^2, 75.7 Lpm (10,000-psi, 20-gpm) abrasive jet containing 7.26 kg/min (16 lb/min) of silica sand (45-55 mesh) was used to cut a cavity in the taconite at the base of the borehole. The cuttings were pumped 12.19 m (40 ft) to the surface with a slurry pump incorporated into the borehole miner.

The production rate was not measured because of the impossibility of measuring either the volume of the cavity cut or the volume of the cuttings lifted to the surface.

5.0 CONCLUSIONS

1. A collimated abrasive jet cutter can be combined with a jet slurry pump to produce an abrasive jet borehole miner capable of extracting hard rock remotely from the surface through a 15.24-cm (6-inch-diameter) vertical borehole.

2. This abrasive jet borehole miner is capable of excavating the hardest rock and can cut holes in steel casing.

3. This miner can use any abrasive.

4. This miner excavates limited volumes of hard rock from the sidewall of the borehole. It is not intended to be used as a bulk miner. Instead, it is designed for such applications as sampling or creating chambers in the borehole. It can also be used as a steel casing perforator.

6.0 REFERENCES

1. Archibald, W. R., "Underground Mining System," U.S. Patent No. 3,797,590, Mar. 19, 1974.

2. Aston, C. P. T., "Jet Mining and Excavation," U.S. Patent No. 2,518,591, Aug. 15, 1950.

3. Brunelle, P. R., "Subterranean Drilling and Slurry Mining," U.S. Patent No. 4,059,166, Nov. 22, 1977.

4. Clayton, E. E., "Process and Apparatus for Mining," U.S. Patent No. 1,851,565, Mar. 29, 1932.

5. Fly, A. B., "Hydraulic Jet Under-Reaming Process," U.S. Patent No. 3,155,177, Nov. 3, 1964.

6. Pfefferle, G. H., "Apparatus for and Method of Mining A Subterranean Ore Deposit," U.S. Patent No. 3,439,953, Apr. 22, 1969.

7. Quick, T. E., "Method and Apparatus for Hydraulic Reaming of Oil Wells," U.S. Patent No. 2,720,381, Oct. 11, 1955.

8. Savanick, G. A., "Borehole (Slurry) Mining of Coal, Uraniferous Sandstone, Oil Sands and Phosphate Ore," Bureau of Mines, RI 9101.

9. Wenneborg, W. Z., "Method for Subterranean Drilling and Mining," U.S. Patent No. 3,730,593, May 1, 1973.

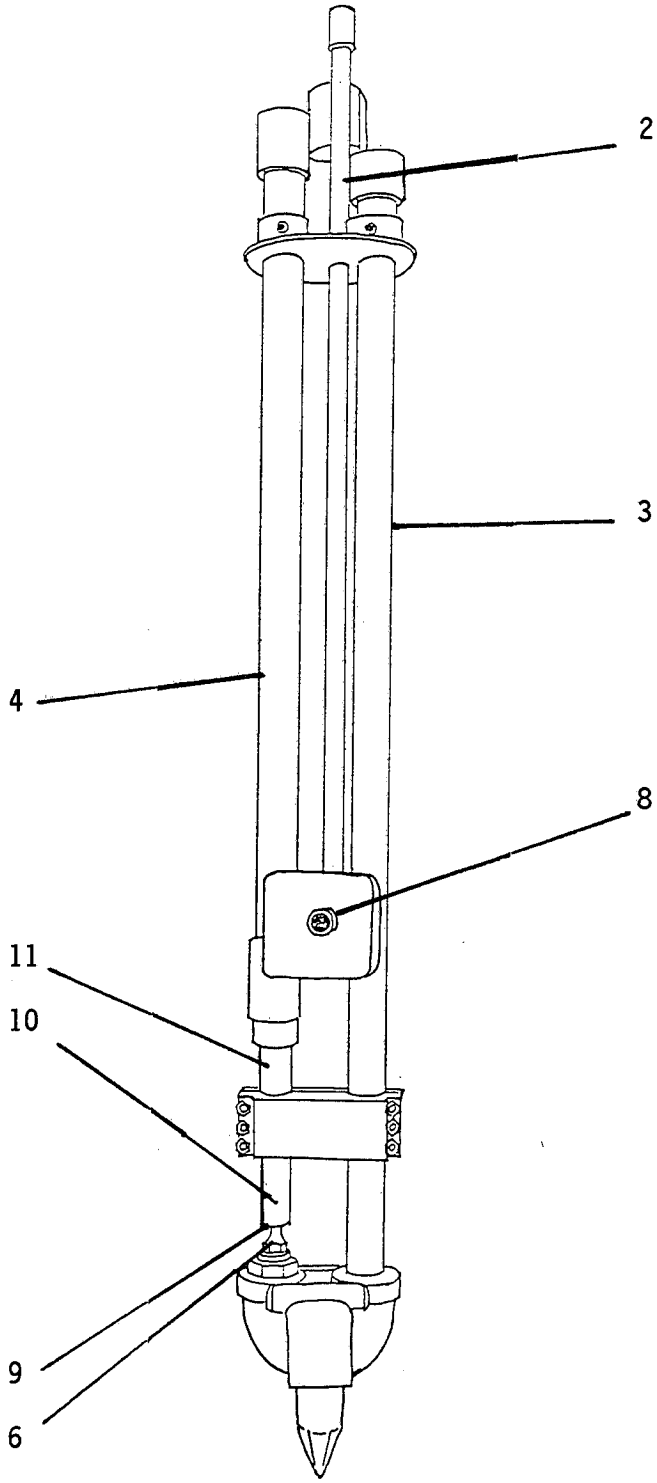

KEY
2 = Abrasive supply pipe
3 = Eductor water supply pipe
4 = Slurry pump outlet pipe
6 = Eductor nozzle
8 = Abrasive collimating pipe
9 = Eductor mixing section
10 = Eductor diffuser
11 = Eductor

Figure 1a. - Schematic Drawing of the Abrasive Jet Borehole Miner (Front View).

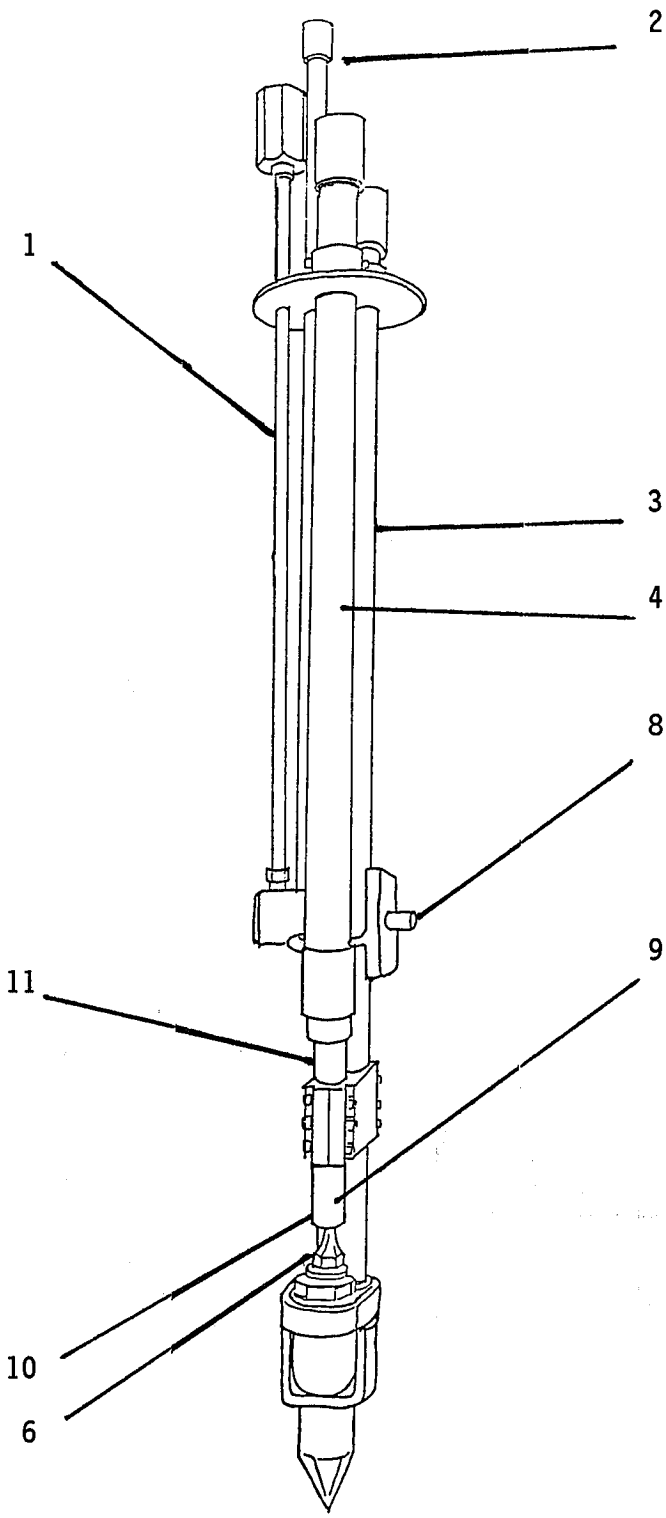

KEY
1 = Water supply pipe for jet cutter
2 = Abrasive supply pipe
3 = Eductor water supply pipe
4 = Slurry pump outlet pipe
6 = Eductor nozzle
8 = Collimating pipe
9 = Nozzle mixing section
10 = Eductor diffuser
11 = Slurry pump

Figure 1b. - Schematic Drawing of the Abrasive Jet Borehole Miner (Side View).

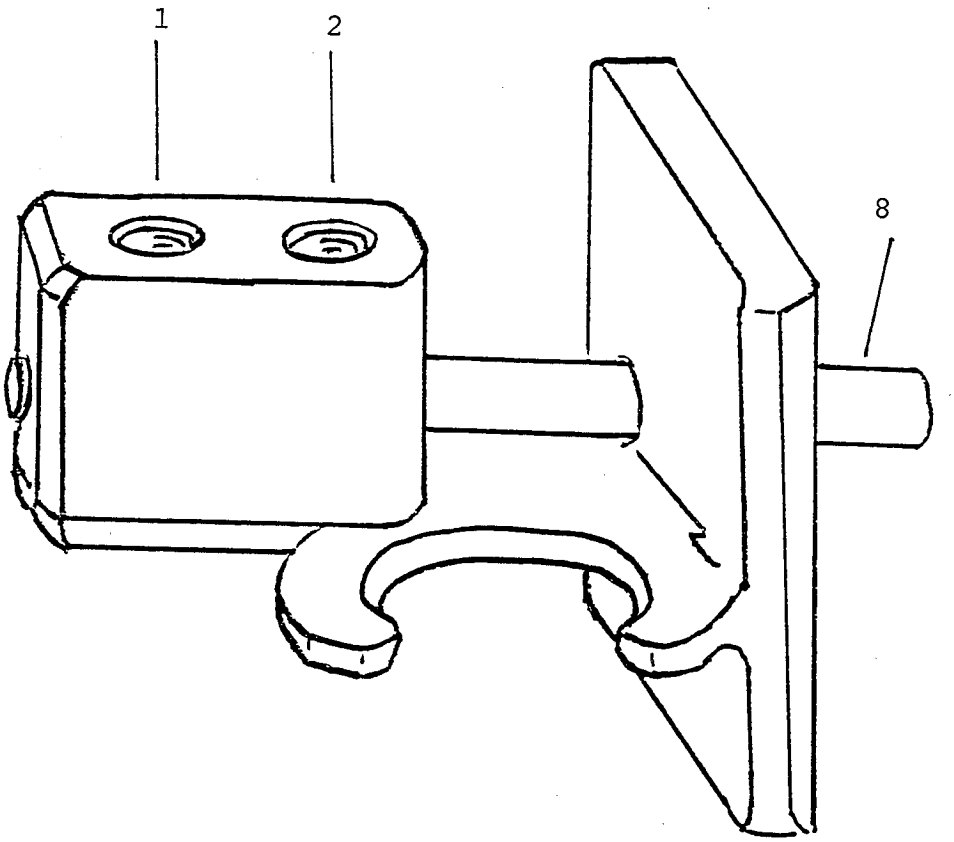

Figure 2. - Schematic Drawing of Abrasive Jet Cutter.

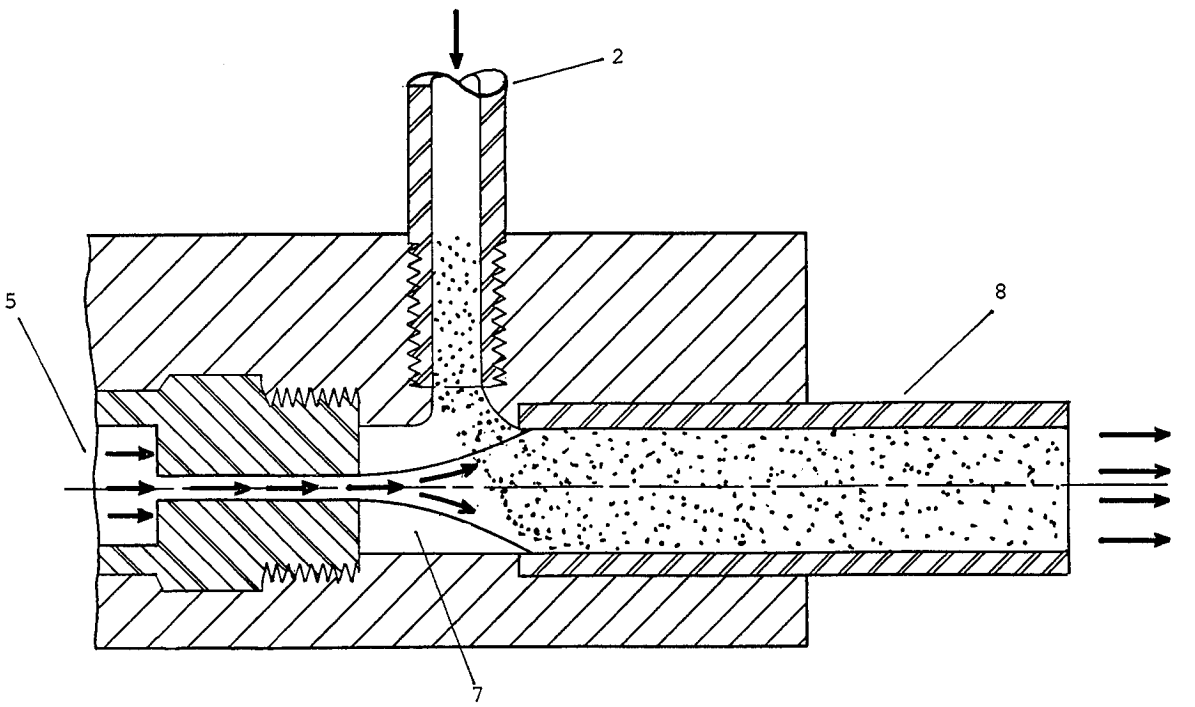

Figure 3. - Cutaway View of Abrasive Jet Cutter.

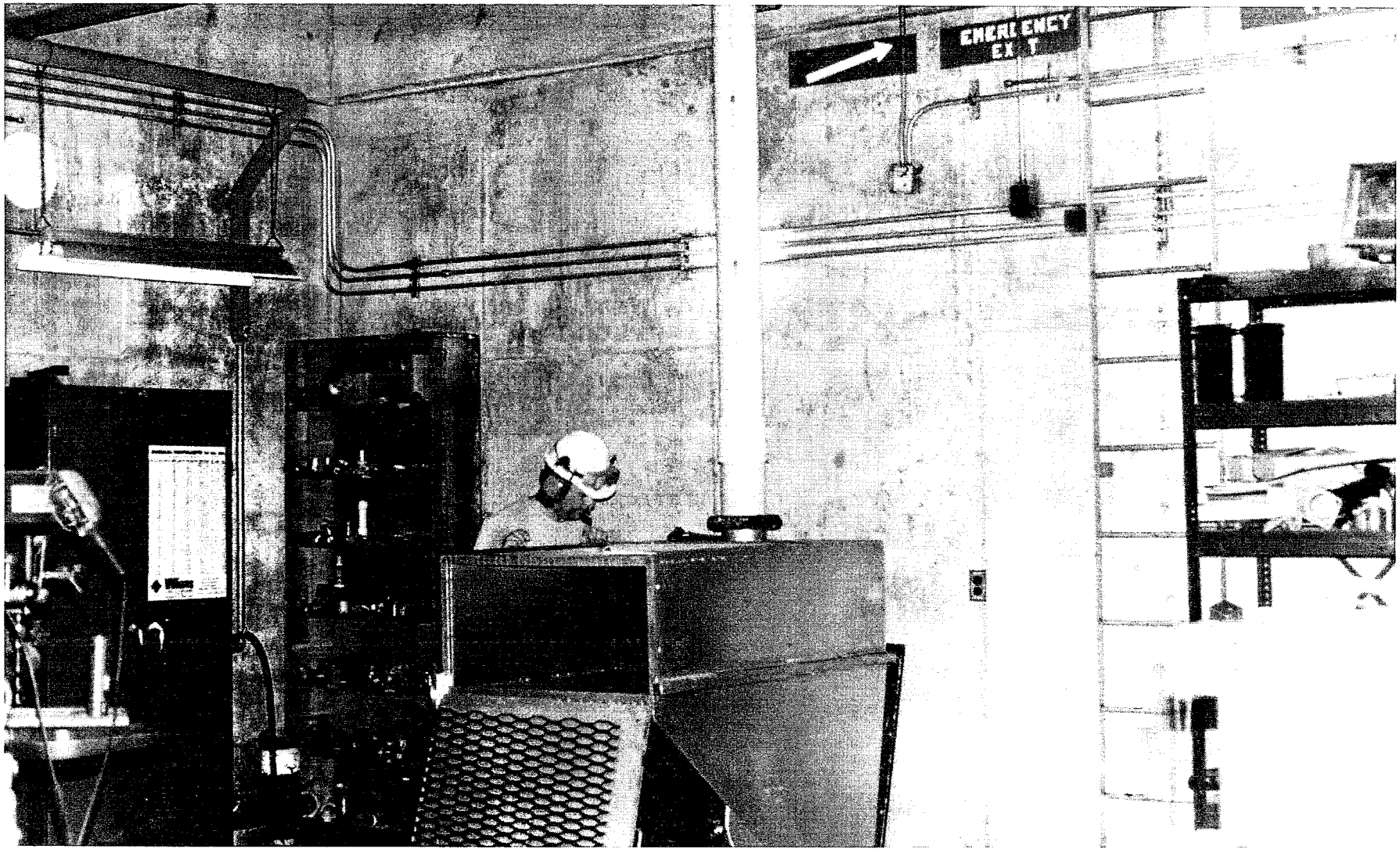

Figure 4. - Simulated Well.

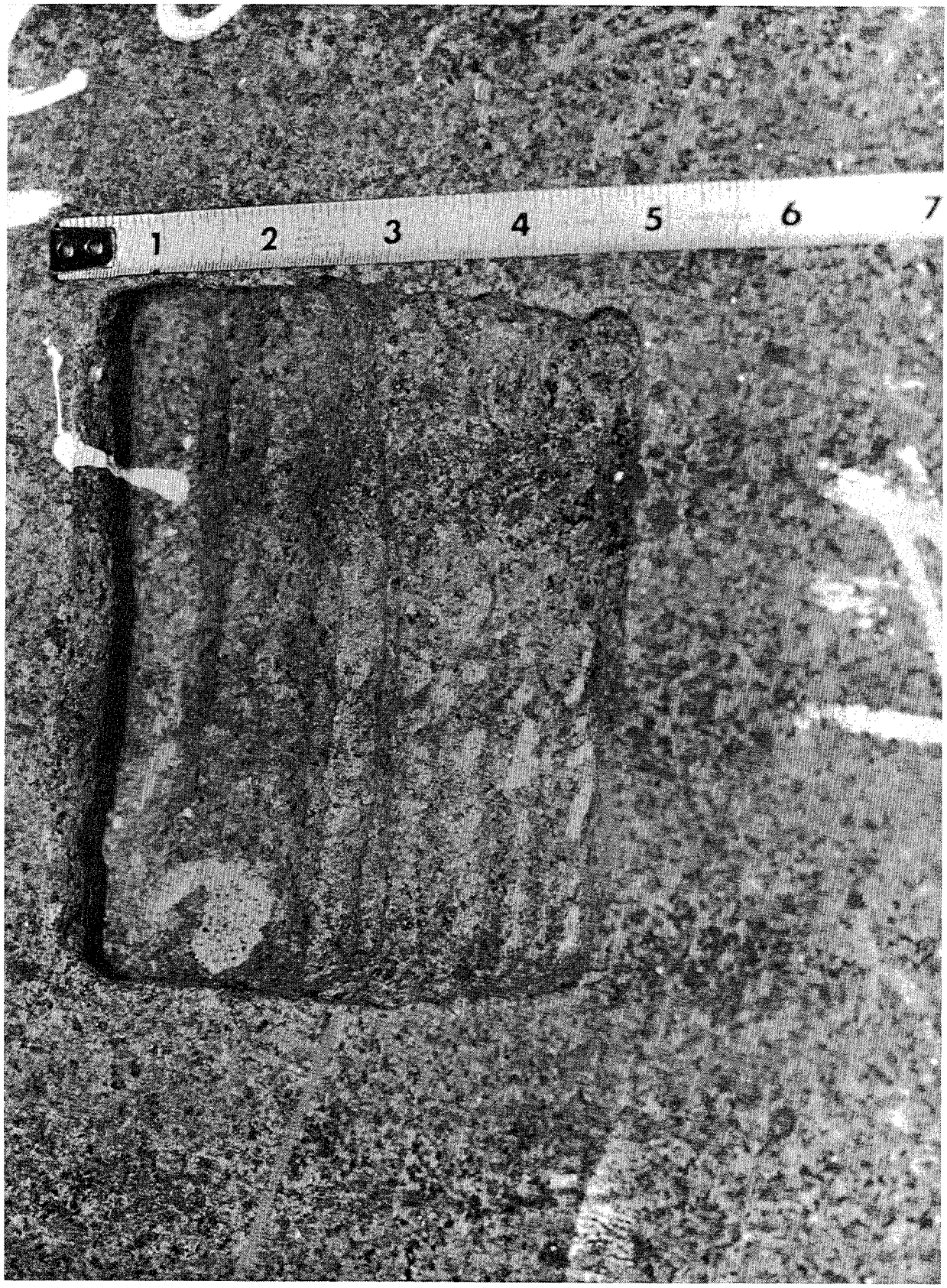

Figure 5. - Chambers Cut in Block of Charcoal Granite.

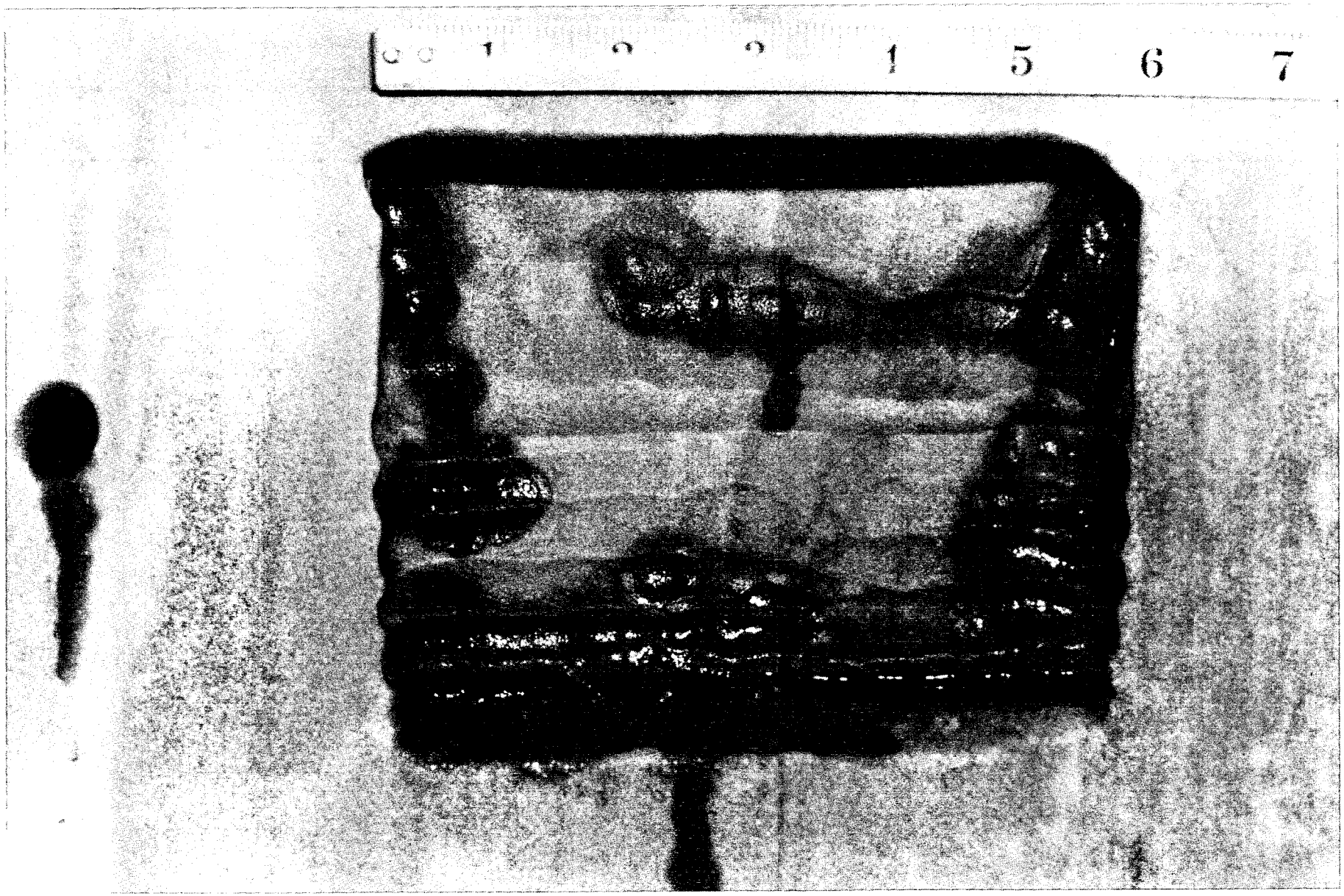

Figure 6. - Chamber Cut in Block of Sioux Quartzite.

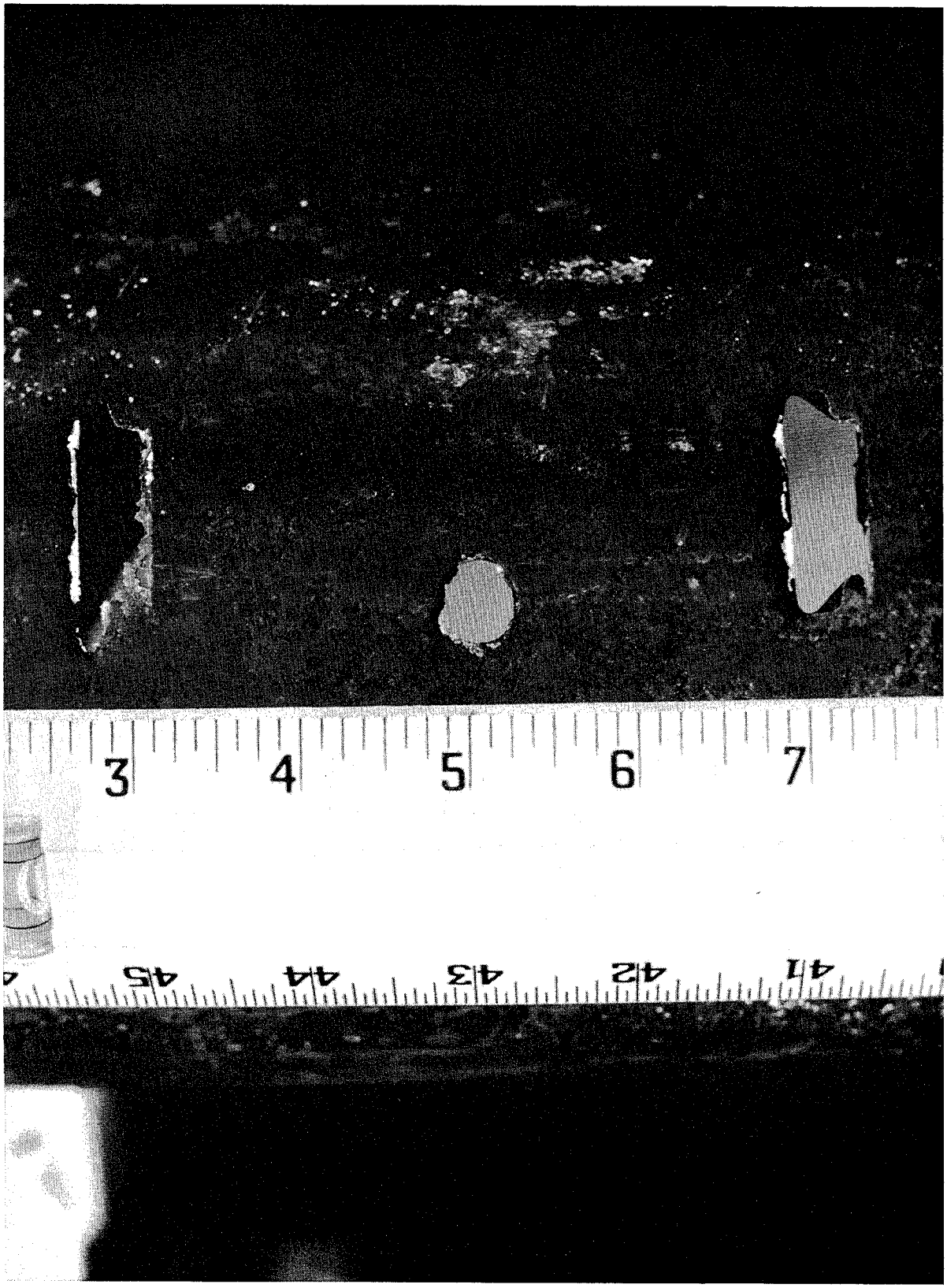

Figure 7. - Perforation in a Steel Pipe.

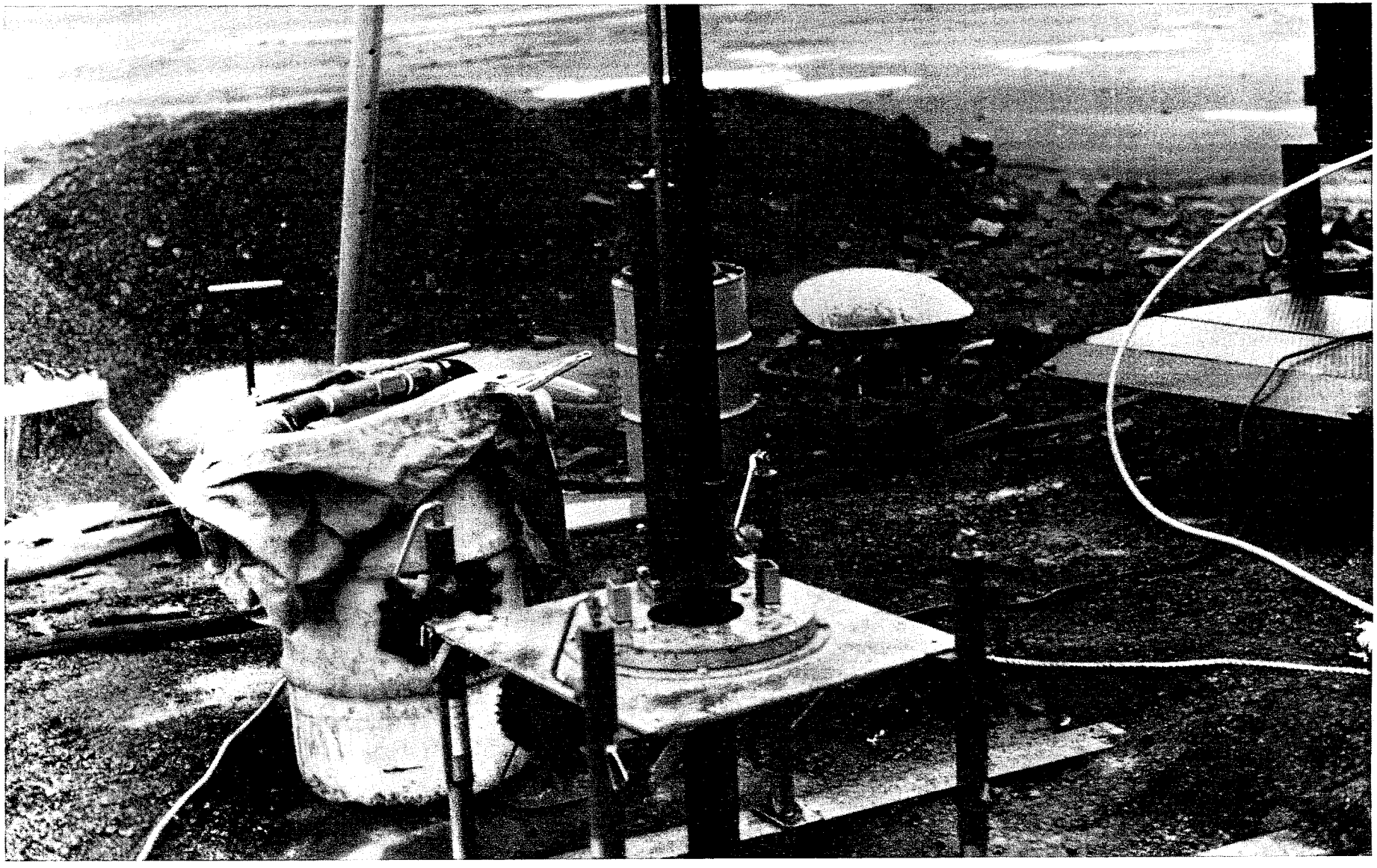

Figure 8. - Borehole Miner Suspended in Borehole at Minorca.

6th American Water Jet Conference
August 24 - 27, 1991: Houston, Texas Paper 15

Comparison of the Performance of High-Speed Abrasive-Entrained Cavitating and Plain Water Jets for Selective Mining Applications

M.M. Vijay
Combustion and Fluids Engineering Laboratory
Institute of Mechanical Engineering
National Research Council of Canada
Ottawa, Ontario, Canada, K1A 0R6

ABSTRACT

This investigation was concerned with the potential of the high-speed abrasive-entrained, cavitating and plain water jets for selective mining of metal-bearing rock minerals, by slotting along the seams or fragmentation within the ore zone. Limited number of tests were conducted in the laboratory on slotting of metal-bearing and non-metal-bearing (muck or waste) rock samples supplied by the mines in Northern Ontario, Canada. The range of independent variables investigated were as follows:

Nozzle pressure	= 69 - 138 Mpa
Hydraulic power	= 29 - 82 kW
Standoff distance	= 1.3 - 10.2 cm
Traverse speed	= 0.5 - 1.5 cm/s
Abrasive feed rate	= 0.23 - 0.45 kg/min

Tests with cavitating jets, issuing from a simple conical entry and from a centre-body nozzle, were conducted under submerged conditions. The nozzle diameter was held constant at 1.20 mm for all the tests.

The conclusion from this preliminary and limited investigation was that all three types of high-speed water jets have a good potential for selective mining of metal bearing rock material, although more work is required to optimize the nozzle systems. Within the range of variables investigated, the jets had virtually no effect on the non-metal-bearing rock samples. Based on this preliminary work, recommendations for implementing water jet techniques for selective mining are put forward.

Organized and Sponsored by the Water Jet Technology Association.

1.0 INTRODUCTION

Often, as shown in Fig. 1, the metal bearing minerals occur in veins or bands in rock formations in the mines. The common practice of extracting such minerals involves drilling and blasting over a certain area of the rock mass. The economics of the method depends on the nature of the formation (for example, hard or soft) and the degree of enrichment of the ore minerals. If the enrichment is low or moderate, the process of separating the ore minerals from the waste material becomes time consuming, labour intensive and hence expensive. Therefore, there is an incentive to seek alternative competitive technologies for extracting metal bearing minerals from such mines. The aim of the work reported in this paper was to investigate the feasibility of using water jets for selectively removing the ore veins, leaving the waste material (muck) intact which then could be blasted out and removed from the mines.

A total of 165 linear slotting tests with non-rotating abrasive-entrained, cavitating and pure water jets were conducted in the laboratory on metal bearing and non-metal bearing rock samples supplied by the mines in Northern Ontario, Canada. The range of variables investigated, believed to satisfy the requirements of the mining companies, was as follows:

- **Nozzle pressure = 69 (± 2.5%) - 138 (± 1.2%), MPa**
- **Hydraulic power = 29 (± 6%) - 82 (± 4%), kW**
- **Standoff distance = 1.3 (± 4%) - 10.2 (± 0.5%), cm**
- **Traverse speed = 0.5 (± 3.5%) - 1.5 (± 5%), cm/s**
- **Abrasive feed rate = 0.23 - 0.45 (± 3%), kg/min**

It is shown, despite the limited extent of experimental results, that all three of types of jets have a good potential for selective mining of metal bearing minerals. Based on this preliminary investigation, strategies for implementing the water jet techniques for selective mining are suggested.

2.0 EXPERIMENTAL FACILITY

The existing facility in the laboratory for drilling and slotting of rocks with rotating high speed water jets was employed in the present investigation (Vijay, 1984; Vijay, 1989). It consisted essentially of a high pressure pump (Indescor, 138 MPa and 76 litre/min), a rotating device, a traverse trolley and a set of nozzles. Nozzles for producing pure water, abrasive-entrained and cavitating jets are shown in Fig. 2. The nozzle diameter (D) was 1.20 (± 1%) mm for all the tests, which met the requirement of 82 kW at the maximum operating pressure of 138 MPa, assuming a nozzle discharge coefficient of 0.95. Tests with cavitating water jets were conducted under submerged conditions in a plexiglass tank (Fig. 2D), using a simple conical entry nozzle (Fig. 2A) and an existing centre-body nozzle (Fig. 2C). Extensive work has been conducted in the laboratory on the structural and eroding characteristics of cavitating water jets produced by a variety of nozzles (Szymczak, 1987 & Vijay, 1990). For example, Fig. 3A shows the formation of vaporous cavitation bubbles in the mixing layers of a high speed submerged jet issuing from a conical entry nozzle at a relatively high cavitation number (σ) of 0.0127 [nozzle pressure (P) = 1.1 MPa]. The appearance of the cavitating jet issuing from a centre-body nozzle at a cavitation number of 0.00604 (P = 6.9 MPa) is shown in Fig. 3B. It is clear from these

illustrations that profuse cavitation will occur in the range of nozzle pressures (69 to 138 MPa) investigated (for details, see Vijay, 1987 and Vijay, 1990).

Tests using abrasive-entrained water jets were conducted with the abrasive entraining device depicted in Fig. 2B. As discussed by Vijay (1989) and others (for example, Hashish, 1989, and Labus, 1989), apart from the operating variables, a number of geometric parameters influence the formation of a well-mixed abrasive-entrained water jet. Although no attempt was made to optimize the device, observations of the erosion of the twin-orifice nozzles (Vijay, 1989) indicated that the device produced a well-mixed slurry jet. Smooth flow of the abrasives through the annular gap (Fig. 2B) was achieved by mixing the particles with small amount of water in the hopper and rotating the device at about 100 RPM. Tests were conducted with single orifice nozzles, not with the twin-orifice nozzles as depicted in Fig. 2B. Nozzles and the tubing for accelerating the abrasives were fabricated from aluminum oxide (hard ceramic).

3.0 TEST MATERIALS

Three large, irregularly shaped rock samples were obtained from the mining companies, one of which consisted of waste (non-ore-bearing) material. In order to acquire statistically significant results, the blocks were cut into slices, as shown for example in Fig. 4, about 16 to 17 cm in thickness and they were not embedded in concrete. No attempts were made to measure their properties or to analyze their composition, although these have significant effects on the cutting performance (see Grattan-Bellew, 1986 and Vijay, 1984, 1985, 1989 and 1991). However, the following information was supplied by the mining companies.

MASSIVE SULPHIDE (ore-bearing rock): Major minerals of this rock material are: chalcopyrite, cubanite, pentlandite, millerite, pyrrhotite and bornite. Accessory minerals include galena, altaite, hessite, magnetite, native silver, gold, parkerite, chalcocite, mackinawite and sphalerite. A number of platinum group minerals, bismuthides and tellurides are also present as extremely small grains. Magnitudes of some of the measured physical properties are:

- Density = 4499 kg/m^3 (Standard deviation = 137)
- Uniaxial compressive strength = 167 MN/m^2 (Standard deviation = 31)
- Cohesion = 21 MN/m^2
- Uniaxial tensile strength = 8 MN/m^2
- Friction angle = 47°
- Young's modulus = 68 X 10^3 MN/m^2
- Poisson's ratio = 0.20

INTERMEDIATE GNEISS (non-ore-bearing rock): Major minerals of this rock material are: quartz, plagioclase, andesine and orthopyroxene. Clinopyroxene, euhedral apatite, traces of zircon, grains of titaniferous magnetite and ilmenite are also present. The content of mafic minerals is between 40 to 60 percent. Magnitudes of some of the measured physical properties are:

- Density = 2831 kg/m^3 (Standard deviation = 90)

- Uniaxial compressive strength = 276 MN/m^2 (Standard deviation = 90)
- Cohesion = 62 MN/m^2
- Uniaxial tensile strength = 20 MN/m^2 (Standard deviation = 2)
- Friction angle = 51°
- Young's modulus = 78 X 10^3 MN/m^2 (Standard deviation = 17 X 10^3)
- Poisson's ratio = 0.28 (Standard deviation = 0.06)

4.0 EXPERIMENTAL PROCEDURE

The experimental procedure was quite simple. Once the operating variables (P, S, V and ma) were set at the desired values, the rock sample was traversed under the jet. After each pass, the nature of the slot and any other pertinent information, such as nozzle wear (qualitative observation and measurement of the orifice diameter), was noted; several measurements of depths and widths of the slot were taken. This procedure was followed until either a desired depth of the cut was achieved or the rock sample was completely penetrated or prematurely fractured.

To assess the applicability of the water jet technique for selective mining, three parameters were considered, namely, total depth of the cut or the depth of cut per pass (h^*); specific kerfing energy (Ea), and in the case of abrasive-entrained water jets, the life of the erodible components. Widths of the slots were used only for qualitative assessment. Specific kerfing energy is defined as the energy spent per unit surface area generated by the cutting tool. Its magnitude was calculated in two ways, as given by equations 1 and 2 below:

$$Ea = nHp/Vh^* \quad (1)$$

where:

nHp = total power input in n passes
h^* = total depth of cut after n passes
V = Traverse speed of the nozzle

or

$$Ea = Hp/V[h^*_{(n+1)} - h^*_n] \quad (2)$$

where:

$h^*_{(n+1)}$ = depth of cut after (n+1) passes

and

h^*_n = depth of cut after n passes

The depth of cut (h^*) in these equations is the mean of the measurements taken along the length of the slot. The errors in the estimated values of specific kerfing energy were in the range of 5 to 20 percent, depending on the errors in the measured values of the operating variables and the depths of cut, which ranged from 1 to 10 percent.

In the case of cavitating water jets, due to premature fragmentation and also lack of the rock samples, only few tests were conducted. Also, since generally the depths cuts were very small in the non-ore-bearing rock samples, experimental work on these samples was deliberately limited.

5.0 PRESENTATION OF RESULTS

Qualitative appearance of the slots made in the samples are shown in Fig. 4. These are included in order to highlight the distinct features of the cuts made by the three different types of jets. Experimental results are plotted in Figures 5 to 11. In Figures 5 to 9, the magnitudes of the mean depths of the slots are plotted as a function of the nozzle pressure (Fig. 5), traverse speed of the nozzle (Fig. 6), standoff distance (Fig. 7), the ratio of abrasive feed rate to the water feed rate (Fig. 8), and the pass number (Fig. 9). A distinction between the cumulative depth and the depth per pass is clearly indicated in Fig. 9. The magnitudes of the specific kerfing energy, an important parameter for evaluating the potential of the water jet technique, are plotted in Figures 10 and 11. To avoid cluttering the plots with overlapping data, only those showing the trends are plotted in the figures, except Fig. 11. Here all data are plotted, but the overlapping does not show the individual points. Due to the limited scope of the investigation and also lack of the rock samples, gaps do exist in the plots. Nevertheless, the results are statistically significant to make appropriate evaluation of the performance of water jet techniques for selective mining applications. It should also be stated that the data points are joined by lines only to indicate the trends.

6.0 DISCUSSION

Qualitative Observations:

It is clear from Figs. 4A and B that it was quite difficult to cut, at the operating conditions investigated, the non-ore-bearing rock material, even with the abrasive-entrained water jets. Extensive work done previously in the laboratory has shown that this type of rock is almost impermeable because of its ultra-fine grain structure, and therefore difficult to cut (see Vijay, 1989). Whether the magnitude of cohesion (it is almost 3 times that of ore-bearing rock; it should be remarked here that the author is not certain how this parameter is defined and measured by the mining companies) has any effect on cuttability with water jets is not clear at this time. Surface spalling was predominant in slotting with plain water jets.

The appearance of the slots in the ore-bearing samples cut with the plain, abrasive-entrained and the cavitating water jets is illustrated in Figs. 4C, D, E and F respectively. Both plain and abrasive-entrained water jets made well-defined slots in the samples, although occasional spalling and lines of fractures (see Fig. 4C) did occur during some tests. It should be noted that for the same operating conditions, abrasive-entrained water jets made wider slots than plain water jets (Figs. 4C and D; Vijay 1989). The rock samples fragmented quite frequently during testing with cavitating water jets (Figs. 4E and F) and as such, it was not possible to measure accurately the depths or the widths of the slots. It should be emphasized that although spalling or premature fragmentation may not be desirable in certain applications, in the case of mining, be it selective or otherwise, they contribute significantly to the material removal rate and hence to the overall efficiency of the water jet technique.

Observations from the Quantitative Results:

Figure 5: The effect of pressure on the mean depth of cut, achieved in a single pass, at a constant traverse speed of 0.508 cm/s and a standoff distance of 1.27 cm is indicated in this figure. It can be seen that the depths of cut in the waste material are quite small compared to the ore-bearing samples. Adding abrasives to the water did not make any difference to these samples (see also Figs. 7 & 8). In terms of the

depths of cut, performance of naturally cavitating water jets was no better than the plain water jets. The term 'natural cavitation' is used here to indicate that any high-speed water jet will cavitate under submerged conditions (Fig. 3A, see also Szymczak, 1987 and Vijay 1989). Cavitation is a complex phenomenon, and the mechanism of interaction between the cavitation bubbles and the rock-like material is not well understood. Furthermore, cavitation bubbles generated within and around the jets submerged in a large tank of water are distributed randomly (Fig. 3) and are not focused to impinge directly on the target material where the cut is required. These randomly distributed bubbles implode randomly at several locations on the rock sample, probably contributing to the excessive fractures observed during testing (Figs. 4E & F). Therefore, although cavitating water jets did not make deep cuts in the samples, they did facilitate removal of appreciable amounts of rock material by fragmentation. In this regard, a more appropriate performance parameter is the specific energy based on the volume of material removed, which was not measured in the investigation. From this standpoint, further work with cavitating water jets is highly recommended.

The plot (Fig. 5) shows, with the exception of the data pertaining to cavitating jets, that the depths of cut increase linearly with the pressure. It is apparent that abrasive-entrained water jets cut deeper slots in the ore-bearing rocks than pure water jets. The gain in the depth of penetration is a function of both the pressure and the abrasive feed rate (see also Fig. 8). Increasing the abrasive feed rate appears to have more beneficial effect on the depth of cut at the lower than the higher pressure. For instance, the depth of cut increased by almost a factor of 3 at 69 MPa compared to a factor of only 1.6 at 138 MPa, when the abrasive feed rate was increased from zero to 0.454 kg/min. This is probably due to the fact that since the nozzle diameter was kept constant, as the pressure was increased, the water flow rate also increased, diluting the concentration of abrasives (r = abrasive feed rate/water feed rate) in the jet. As discussed below, the concentration, not the absolute amount of abrasives, is more important for examining the effect of increasing the amount of abrasives in the jet. Another interesting observation from this figure is that the trend of the data seems to indicate that whereas the slope (dh^*/dP) for the abrasive-entrained water jets either remains constant or increases with pressure, for pure water jets it decreases. In other words, when cutting with plain water jets, increasing the pressure indiscriminately results in diminishing returns in the depth of cut.

Figure 6: This plot shows the effect of the traverse speed on the depth of cut. For both abrasive-entrained and plain water jets, the depth of cut decreases, as anticipated, as the traverse speed is increased. However, since the traverse speed and the specific kerfing energy are inversely related [eq. (1)], the specification of an appropriate traverse speed should be based on the magnitude of the specific kerfing energy (see Fig. 10).

Figure 7: The influence of the standoff distance on the depth of cut is indicated in this figure. In principle this effect should be a function of the type of jet. For instance, for abrasive-entrained water jets, the acceleration of the particles (to the speed of the jet) may or may not continue beyond the nozzle exit, resulting in the observed increase or decrease in the depth of cut. The situation is more complex, as already explained, for cavitating water jets. The effect of standoff distance is not only related to the formation, growth and collapse of the bubbles, but also to the ventilation of the bubbles when the jet is not confined or focused. In the present case, as the jets emerged in a tank of water, the bubbles simply dispersed when the standoff distance was increased resulting in reduced depths of cut. The most significant observation from this plot is that, for plain and abrasive-entrained water jets, the depth of cut is fairly insensitive to standoff distance up to 7.6 cm. This

is quite encouraging because it gives some degree of freedom in designing nozzle systems to deal with uneven or highly irregular surfaces in the mines. The shallow depths of cut and the scatter in the data for non-ore-bearing rocks should be noted.

Figure 8: In the previous three figures, the effect of abrasives was indicated by using the absolute amount of abrasives introduced into the high-speed water jet. To truly measure the effect of increasing the amount of abrasives, the concentration of the abrasives, as mentioned above, is the more important parameter. This figure does show what happens to the depth of cut when the concentration is increased at a given pressure. The trend of the data appears to indicate that the depth of cut levels of at some value of the concentration. This is probably due to, among other factors (see Labus, 1989), the choking effect in the mixing chamber and the ceramic tubing, the dimensions of which were not changed to accommodate larger amounts of abrasives. These factors have an important bearing in designing viable systems.

Figure 9: The cutting ability of the plain and abrasive-entrained water jets in succeeding passes over the same path of cut is depicted in this figure. For comparison, the cumulative depth achieved after n passes are also plotted. With the exception of one set of data, the pressure was held constant at 69 MPa. Since all the variables are held constant, the depth of cut in the (n+1)th pass depends on two factors: (i) how the slot in the nth pass affects the jet and (ii) what type rock structure the jet encounters. If the rock properties vary from layer to layer, then it is not possible to predict how deep the cuts will be in the successive passes, and some scatter in the data is to be expected. If the rock fabric is uniform and homogeneous, then for plain water jets, the depths of the cuts should gradually decrease from pass to pass because of the loss of power in the jet owing to friction, and the cumulative depth should reach a limit, as confirmed by the data. For abrasive water jets, generally the same observations should hold. However, it is possible for the slot in the nth pass to behave as a collimator or an accelerator for the abrasive particles, nullifying the effect of friction to some extent. Consequently, the abrasive-entrained water jet might retain its cutting ability to greater depths than the plain water jet, once again borne out by the results. At the higher pressure of 103.5 MPa, the cumulative depth of cut after the 2nd pass is quite impressive. Therefore, abrasive-entrained water jet offers definite advantages in situations where it is not possible to adjust readily standoff distances.

Figures 10A and B: The potential of the water jet techniques for processing the rock material was examined above in terms of the directly observable variables. In some applications where energy considerations are secondary to the problem at hand, this approach to assess the potential of the technique is acceptable. However, for continuous commercial applications, energy considerations become important. The useful parameters in this regard are the specific kerfing energy [eqs. (1) & (2)] or the specific energy based on the volume removal rate.

In these figures, specific kerfing energy is plotted as a function of the standoff distance, although the effect of other variables can be easily seen. It is clear that slotting of non-ore-bearing rocks with plain or abrasive-entrained water jets is highly inefficient compared to ore-bearing rock material. It is important to keep this in mind in evaluating the techniques for selective mining applications. The magnitudes of the specific kerfing energies achieved for ore-bearing samples are within the range of 5×10^3 to 2×10^4 J/cm^2, which compare favourably with the results previously obtained in the laboratory or in the field and also with some of the conventional techniques, such as the flame jet technique (Hawrylewicz, 1988 and Vijay, 1989). The trends of the data indicate that it is possible to reduce these magnitudes even further by optimizing the nozzle designs and the operating variables.

The figures also show that specific kerfing energy increases slightly or remains fairly constant with the standoff distance for both plain and abrasive-entrained jets. It was seen earlier in Fig. 5 that the depth of cut increased with pressure. From the standpoint of energy, however, increasing the pressure had an adverse effect on the performance. This implies that the gain in the depth of cut was not adequate enough to compensate for the increased amount of energy. Fig. 10B brings out clearly the effect the traverse speed has on the specific energy. Although the depth of cut decreases as the traverse speed is increased from 0.508 to 1.524 cm/s (see Fig. 6), specific energy values decrease significantly. Theoretically, at some value of the traverse speed, which will vary with the pressure, the magnitude of the specific energy should become minimum (Vijay, 1984). This will be the optimum traverse speed, and from the standpoint of mining applications, it will be worthwhile to find its magnitude. Finally, the data clearly indicate that the performance of abrasive-entrained water jets is significantly better than that of plain water jets (specific kerfing energy values could not be measured in the tests with cavitating jets).

Figure 11: The influence of multipass cutting on specific energy is depicted in this figure. The dotted lines show the specific energy calculated for each successive pass and the solid lines, based on the cumulative depth of cut after n passes. Since the total power input is constant in each pass, the magnitude of the specific energy depends on the depth of cut achieved in that pass (Fig. 9). The scatter and the fluctuations in the results for each successive pass is obviously due to the scatter in the depths of cuts discussed previously. However, magnitudes of specific energies based on cumulative depths of cut, up to about four passes, appear either to remain constant, or increase only slightly. This is particularly so in cutting with abrasive-entrained water jets. Therefore, if the objective is to cut as deep a slot as possible, at a fixed standoff distance and a given set of operating conditions, then multipass cutting is obviously the choice.

Assessment of the Techniques for Selective Mining: The viability of the water jet techniques depends on whether the ore-bearing veins contain any traces of waste material, and if so, how they are imbedded in the veins. It is seen in the results presented above that it is extremely difficult to cut the waste material with all the three types of water jets. Therefore, if the veins are completely separated from the waste body, then water jets can preferentially remove the useful ores, leaving the waste body intact which can then be blasted out and removed. If, on the other hand, their concentrations in the veins are low, it is relatively easy to displace them (without cutting) with the carbide-tipped nozzles (Vijay, 1989 & 1991). However, full exploitation of the techniques requires a prior knowledge of the disposition of the veins below the surface. In the case of the abrasive-entrained water jets, the life of the erodible components, viz., the mixing chamber, the ceramic tubing and the nozzle is a major consideration. In the present investigation, the life of these components was of the order of three hours, although the maximum abrasive feed rate was only 0.454 kg/min. This certainly is not satisfactory if the technique is to be adopted for continuous mining operations.

One possible procedure is illustrated in Fig. 12. This involves slitting along the seams by drilling a series of holes and spreading the fractures between consecutive holes with the jets emerging in the direction of the seams (Fig. 12A). Preliminary results obtained in the laboratory on a block of hard black granite (Fig. 12B), using plain rotating water jets for drilling and twin stationary jets for fracturing, seem to support this method of extraction (Vijay, 1989). However, further work in the laboratory on large mining samples (or small samples confined in a matrix of concrete) and, in situ in the field is required to establish the economic viability of the method.

7.0 CONCLUSIONS

The conclusions from this preliminary and limited scope of the investigation are as follows:

* Selective mining of ore-bearing minerals by slotting with high-speed abrasive-entrained, cavitating and plain water jets appears technically feasible. However, further work is required to optimize the nozzle systems.

* Slotting performance of abrasive-entrained water jets was superior, on the average by 50 percent, to that of cavitating or plain water jets.

* Cavitating water jets appear to have excellent potential for fragmenting the ore zone. This offers the possibility of mining the ore minerals by chipping followed suction.

* The maximum depth of cut achieved with the abrasive-entrained water jet was in excess of 16 cm, achieved after two passes. The minimum value of the specific energy was 4.5×10^3 J/cm^2.

8.0 RECOMMENDATIONS FOR FUTURE WORK

The experimental results have clearly indicated that all three types of jets have a good potential for selective mining of ore minerals. Although the depths of cuts achieved with the abrasive-entrained water jets were better than those of the cavitating or plain water jets, depth alone is not an important factor. Spalling and fragmentation which frequently occurred in cutting with the cavitating or plain water jets contribute, in addition to the simplicity of the systems, to the overall material removal rate. The performance of the plain water jets can probably be improved by increasing the hydraulic power in the jet rather than the pressure. As far as the cavitating jets are concerned, the problem of making them to work effectively at large standoff distances in air remains to be solved. Artificial submergence of the jets is a possibility and is worth investigating. Field trials are highly recommended.

9.0 ACKNOWLEDGMENTS

The author is grateful to Mr. N. Paquette and Mr. O. McMullin, Combustion and Fluids Engineering Laboratory, for conducting the experimental work in the laboratory.

10.0 REFERENCES

1. Grattan-Bellew, P.E., and M.M. Vijay, Influence of Physical Properties of Rock on Rate of Penetration of a Water Jet Drill, Canadian Mineralogist, Vol. 24, No. 2, pp. 323-328, 1986.

2. Hashish, M., The Potential of an Ultrahigh-Pressure Waterjet Rock Drill, Paper No. 32, Proc. 5th American Water Jet Conference, Toronto, Canada, Ed: M.M. Vijay and G.A. Savanick, National Research Council of Canada and Water Jet Technology Association (U.S.A), pp. 321-332, 1989.

3. Hawrylewicz, B.M., M.M. Vijay, J. Remisz and N. Paquette, Design and Testing of a Rock Slotter for Mining and Quarrying Applications, Paper G4, Proc. 9th Int. Symp. on Jet Cutting Technology, Ed: P.A. Wood, BHRA, England, pp. 377-386, 1988.

4. Labus, T.J., K.F. Neusen, D.G. Albert and T.J. Gores, Factors Influencing the

Abrasive Mixing Process, Paper No. 20, Proc. 5th American Water Jet Conference, Toronto, Canada, Ed: M.M. Vijay and G.A. Savanick, National Research Council of Canada and Water Jet Technology Association (U.S.A), pp. 205-215, 1989.

5. Szymczak, M., S. Tavoularis, A. Fahim and M.M. Vijay, Flow Visualization of High Speed Water Jets, Proc. 4th U.S. Water Jet Conference, Berkeley, California, U.S.A., Ed: M. Hood and D. Dornfeld, The American Society of Mechanical Engineers, New York, U.S.A, pp. 43-50, 1987.

6. Vijay, M.M., P.E. Grattan-Bellew and W.H. Brierley, An Experimental Investigation of Drilling and Deep Slotting of Hard Rocks with Rotating High Pressure Water Jets, Paper H2, Proc. 7th Int. Symp. on Jet Cutting Technology, Ed: G.A. Watts and J.E.A. Stanbury, BHRA, England, pp. 419-438, 1984.

7. Vijay, M.M., and P.E. Grattan-Bellew, An Assessment of Rotating High Pressure Water Jets for Drilling and Slotting of Hard Ore Bearing Rocks, Proc. 3rd U.S. Water Jet Conference, Pittsburgh, Pennsylvania, U.S.A., Ed: N. Styler, Water Jet Technology Association, U.S.A., pp. 231-247, 1985.

8. Vijay, M.M., Some Aspects of High Speed Cavitating Water Jets, Proc. Int. Water Jet Symposium, Beijing, China, Ed: Fun-Den Wang, Colorado School of Mines, Golden, Colorado, U.S.A., pp. 2-59-74, 1987.

9. Vijay, M.M., Evaluation of Abrasive-Entrained Water Jets for Slotting of Hard Rocks, Paper No. 33, Proc. 5th American Water Jet Conference, Toronto, Canada, Ed: M.M. Vijay and G.A. Savanick, National Research Council of Canada and Water Jet Technology Association (U.S.A), pp. 333-342, 1989.

10. Vijay, M.M., and W. Yan, Water Jet Cutting Techniques for Processing of Hard Rock Material, Int. J. Surface Mining, Vol. 3, No. 2, pp. 59-70, 1989.

11. Vijay, M.M., C. Zou and S. Tavoularis, Study of the Characteristics of Cavitating Water Jets by Photography and Erosion, Paper F2, Proc. 10th Int. Symp. on Jet Cutting Technology, BHR Group Ltd., England, 1990.

12. Vijay, M.M., The Influence of Properties of Rocks on Nozzle Design for Drilling and Slotting with Water Jets [Keynote Paper], Proc. 1st Asian Conference on Recent Advances in Jetting Technology, Singapore, Ed: J.S.Y. Tan, CI-Premier Pte. Ltd., 150 Orchard Road, #07-14, Orchard Plaza, Singapore 0923, pp. 108-128, 1991.

11.0 NOMENCLATURE

d	Diameter of the centre-body in the nozzle, mm
D	Diameter of the nozzle, mm
Ea	Specific kerfing energy, J/cm^2
h^*	Depth of slot per pass or after a number of passes, cm
Hp	Total power input, essentially hydraulic power, kW
ma	Abrasive feed rate, kg/min
mw	Water flow rate from the nozzle, kg/min
n,N	Pass number and the rotational speed
P	Nozzle pressure, MPa
r	Abrasive feed rate/Water flow rate
S	Standoff distance, cm
V	Traverse speed of the nozzle, cm/s
α	Nozzle entry angle, deg

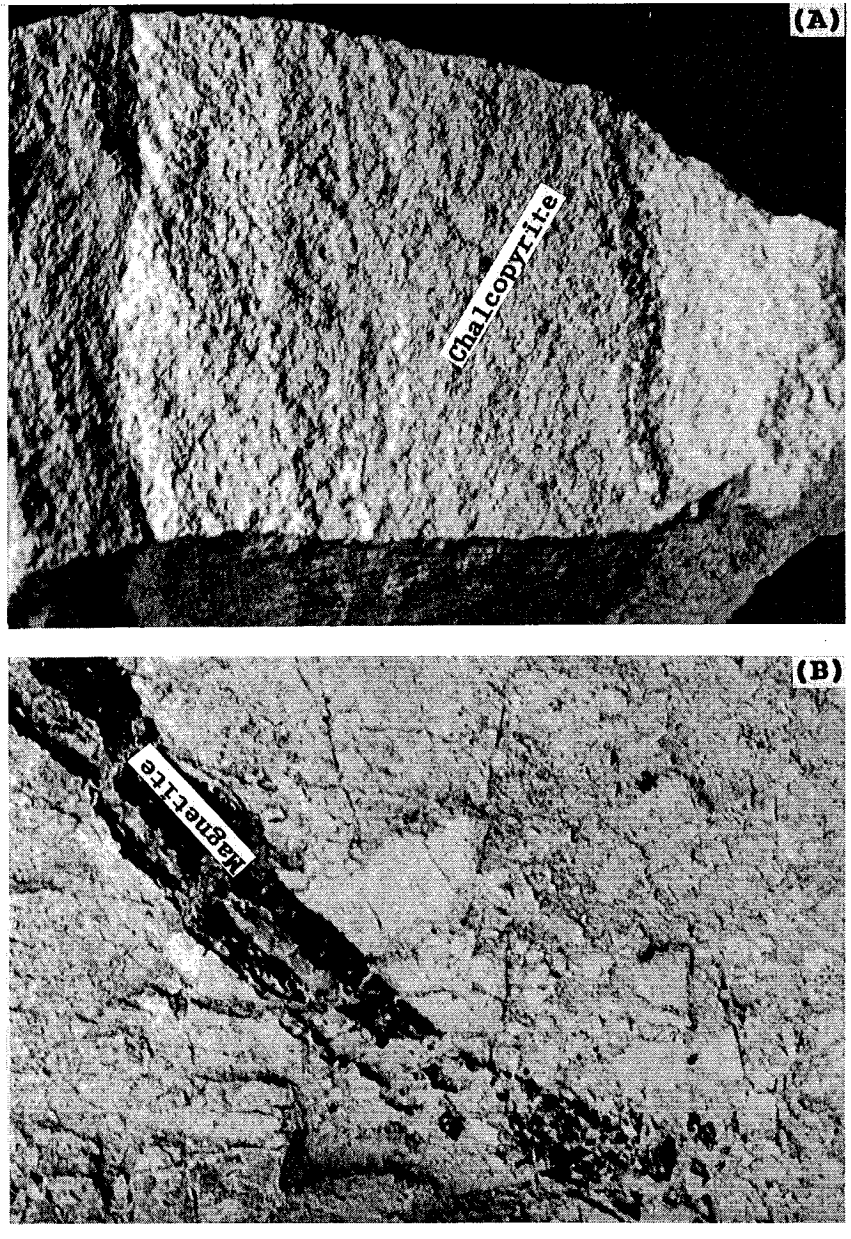

Fig. 1 Rock formations showing the metal bearing veins. (A) Chalcopyrite (B) Magnetite

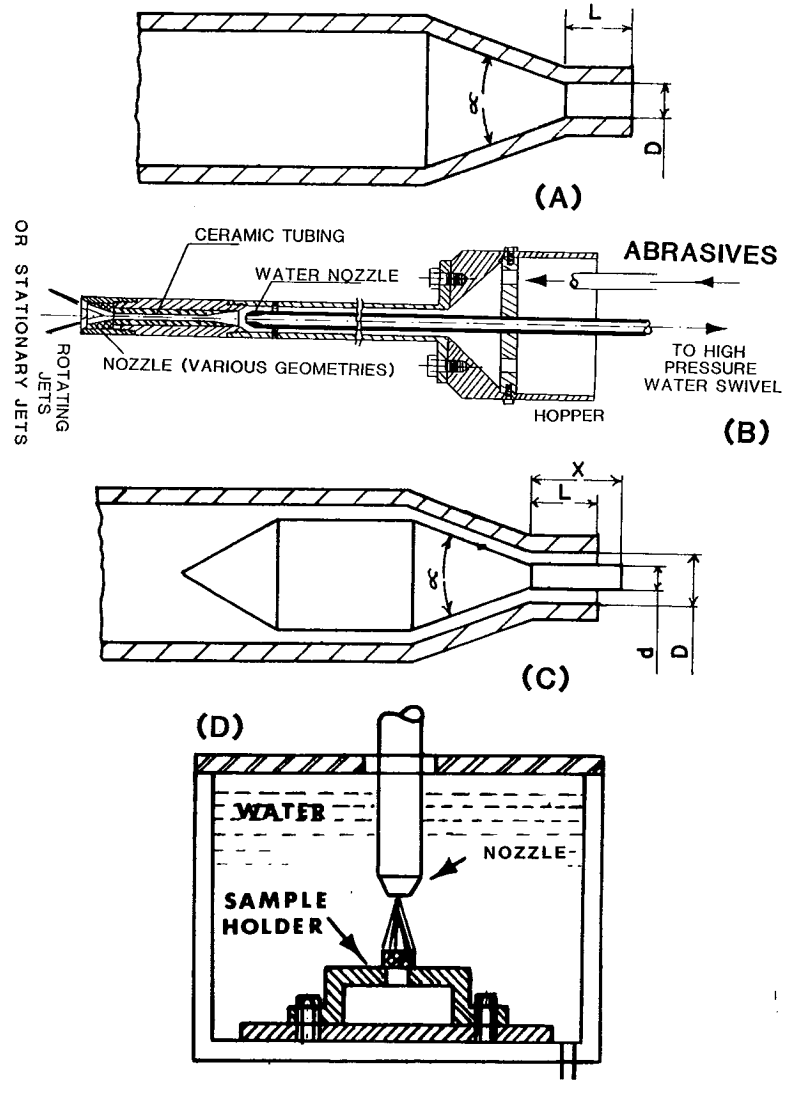

Fig. 2 Nozzle systems: (A) Conical, (B) Abrasive-entraining, (C) Centre-body and (D) Plexiglass tank for submerged testing

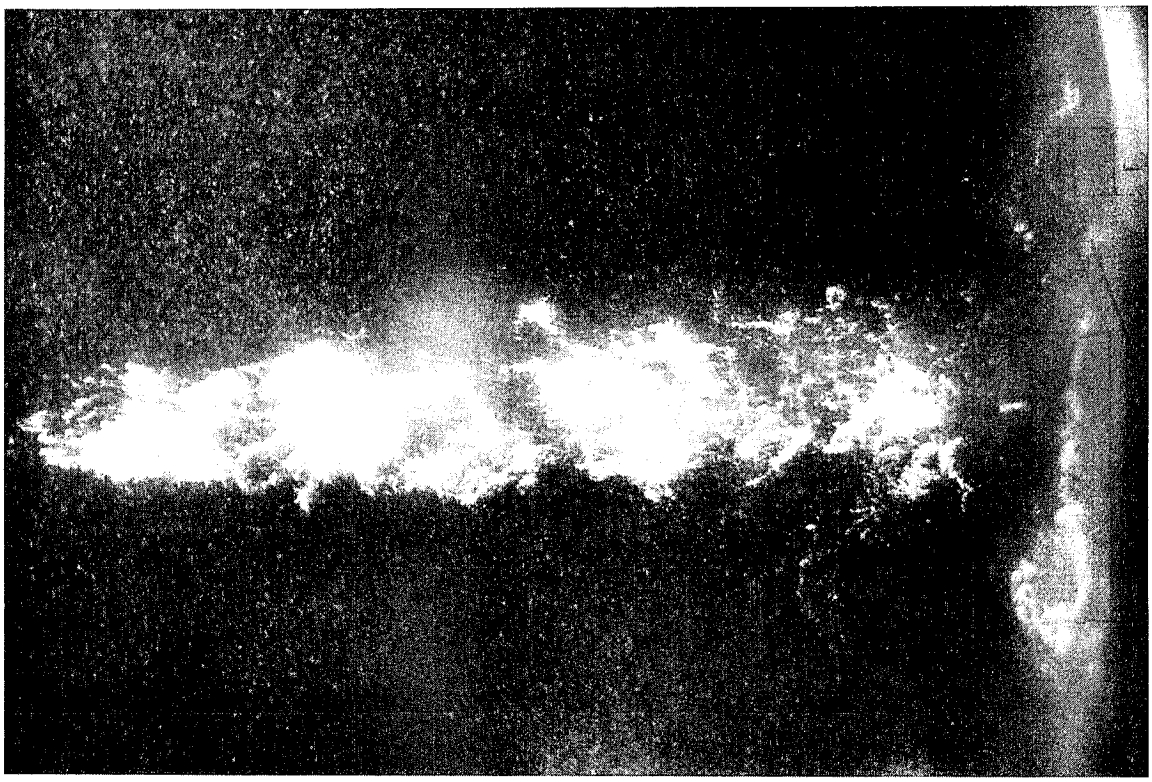

Fig. 3A Appearance of a submerged cavitating water jet emerging from a conical entry nozzle and impinging on a target of aluminum Nozzle pressure = 1.1 MPa, Cavitation number = 0.0127 (Vijay, 1990)

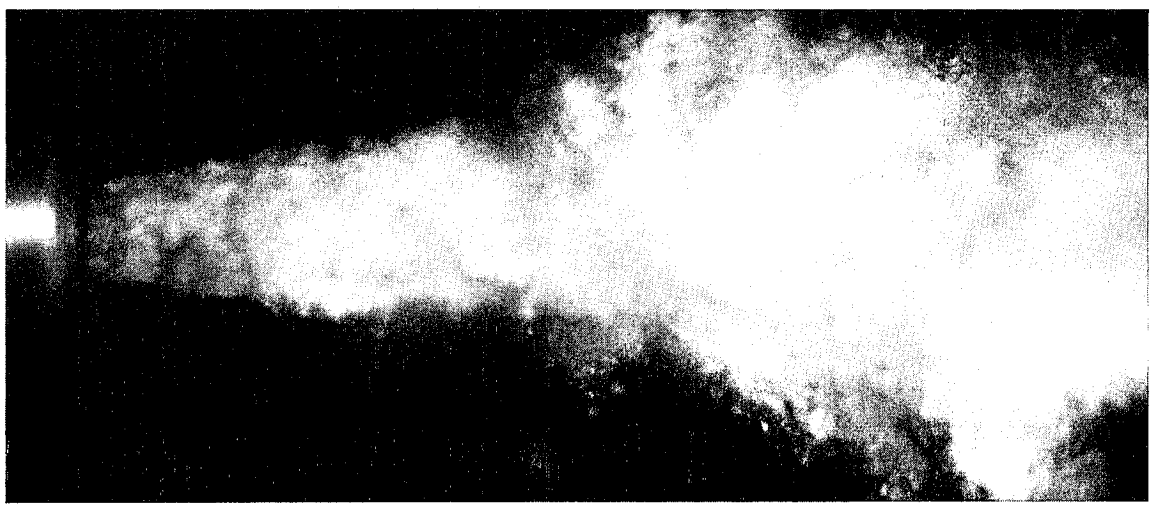

Fig. 3B Appearance of a submerged cavitating water jet emerging from a centre-body nozzle. Nozzle pressure = 6.9 MPa, Cavitation number = 0.00604 Magnification = 6 (Vijay, 1990)

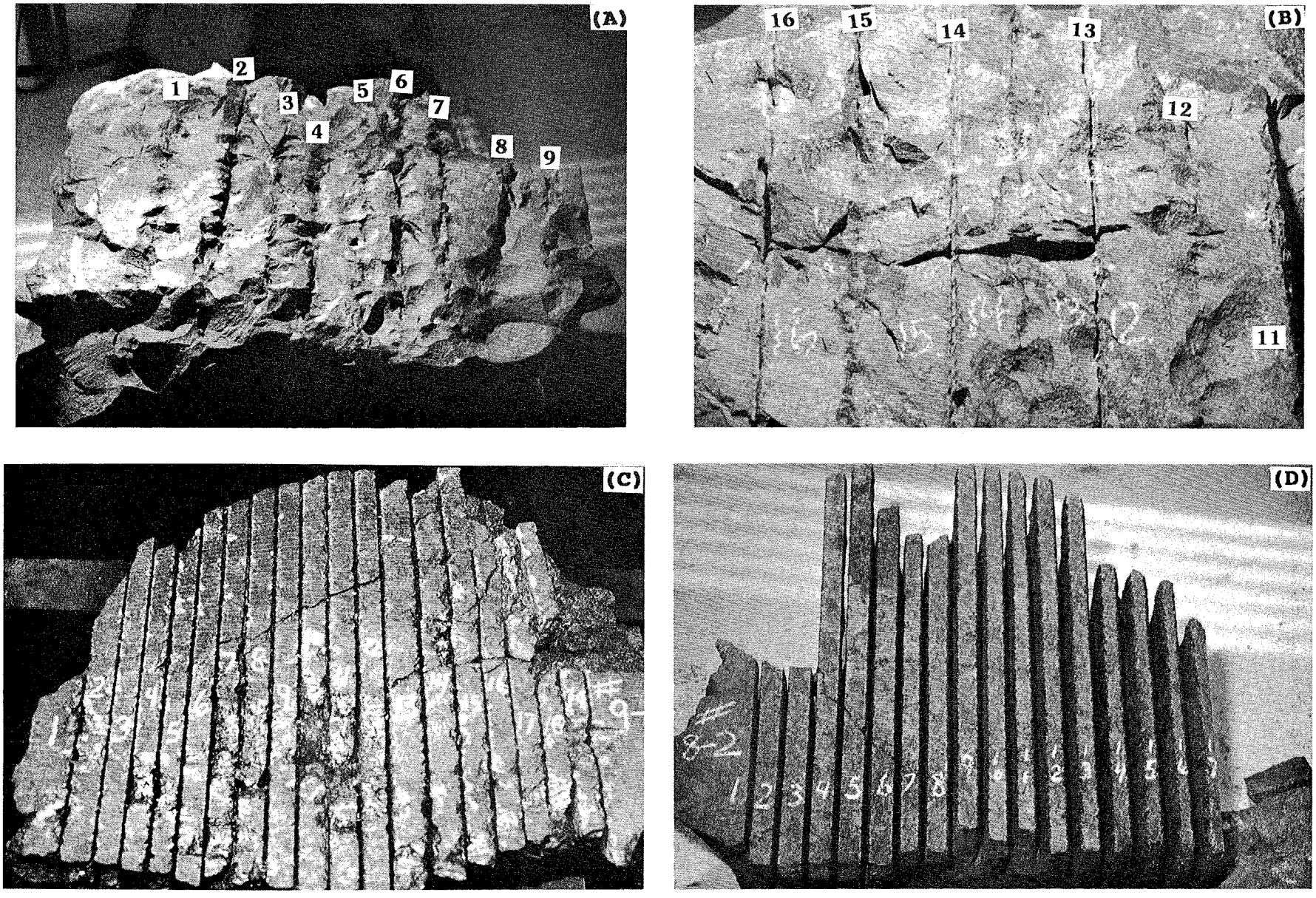

Fig. 4 Appearance of the slots made in non-ore-bearing and ore-bearing rock samples. Plain water jets (A & C); Abrasive-entrained water jets [(B, slots 12, 14 & 15), and (D)]

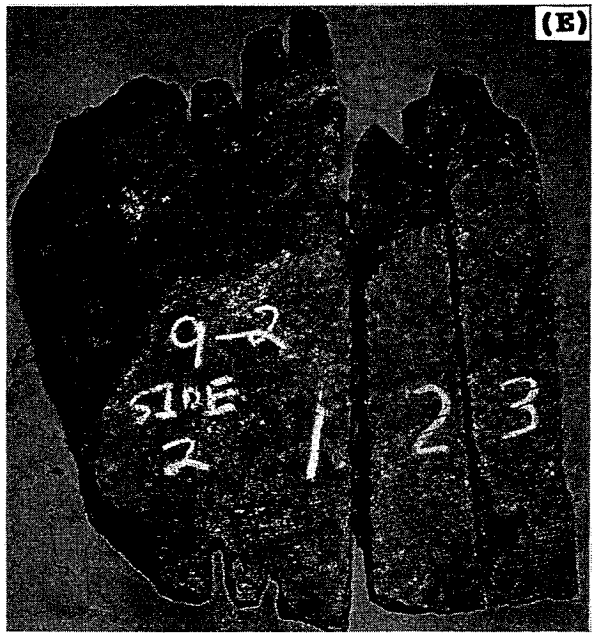

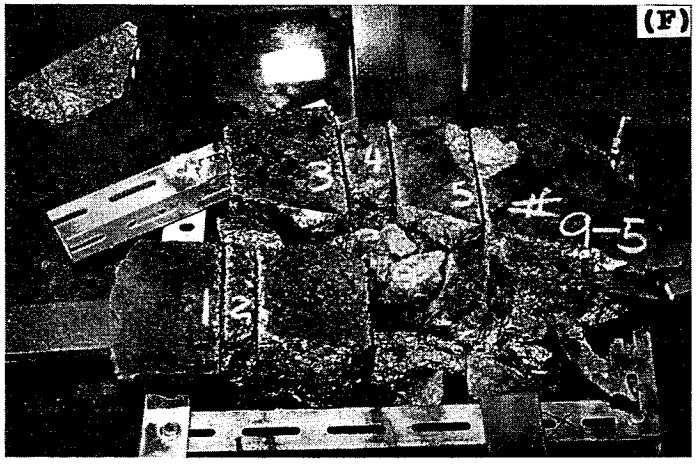

Fig. 4 Continued (E & F).
Appearance of the slots made in ore-bearing samples with submerged cavitating water jets.

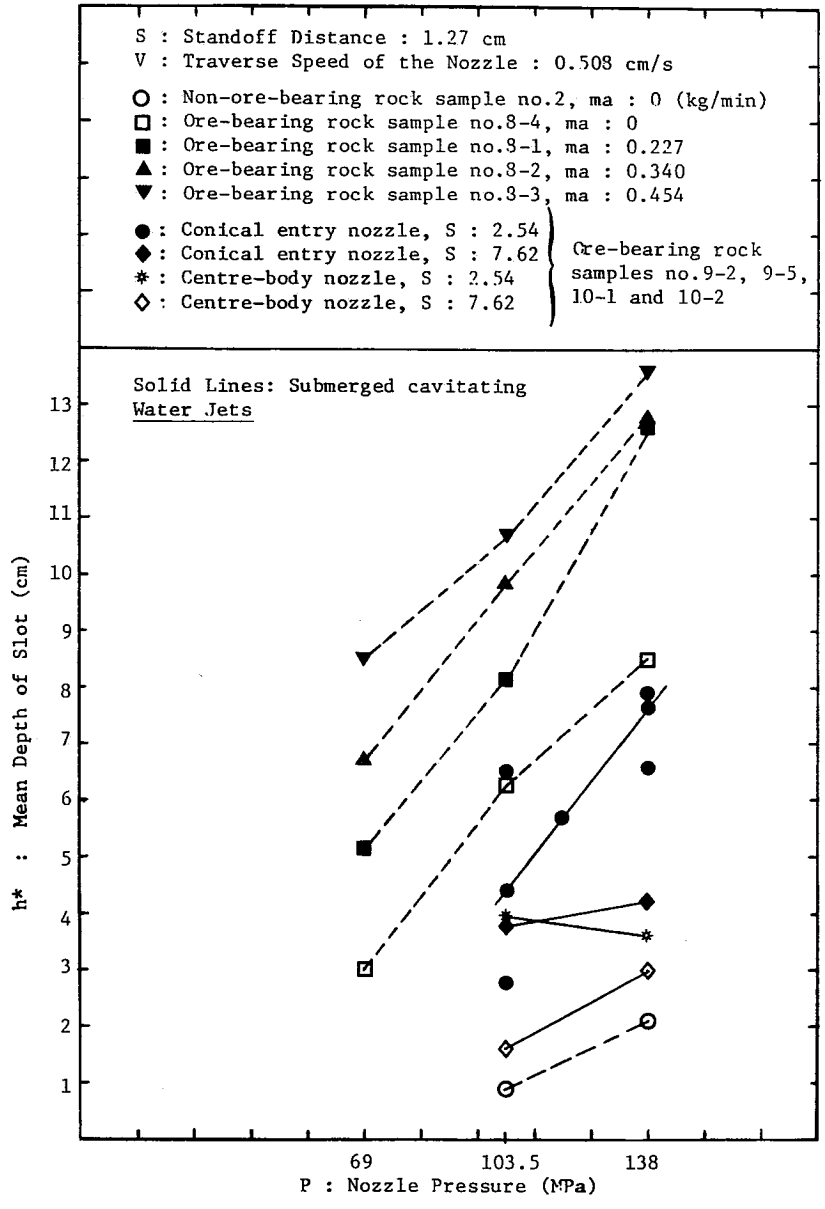

Fig. 5 Plot of mean depths of slots (h^*) against nozzle pressure (P)

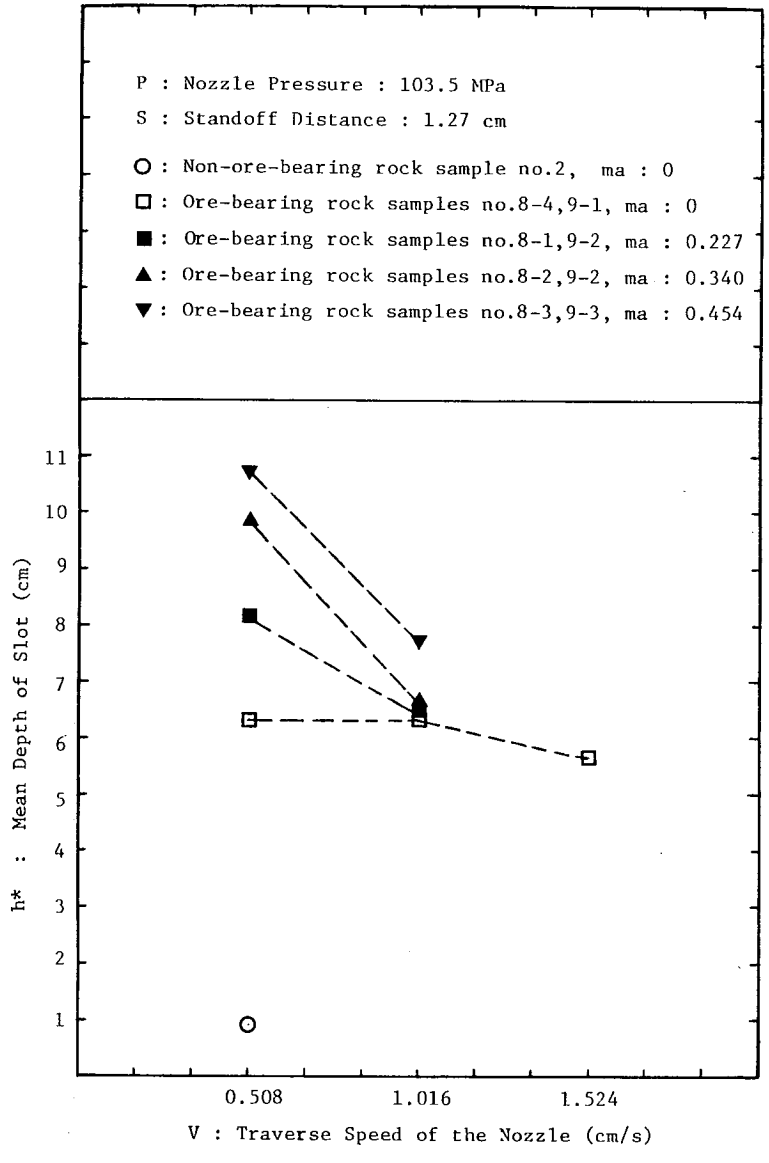

Fig. 6 Plot of mean depths of slots (h*) against traverse speed of the nozzle (V)

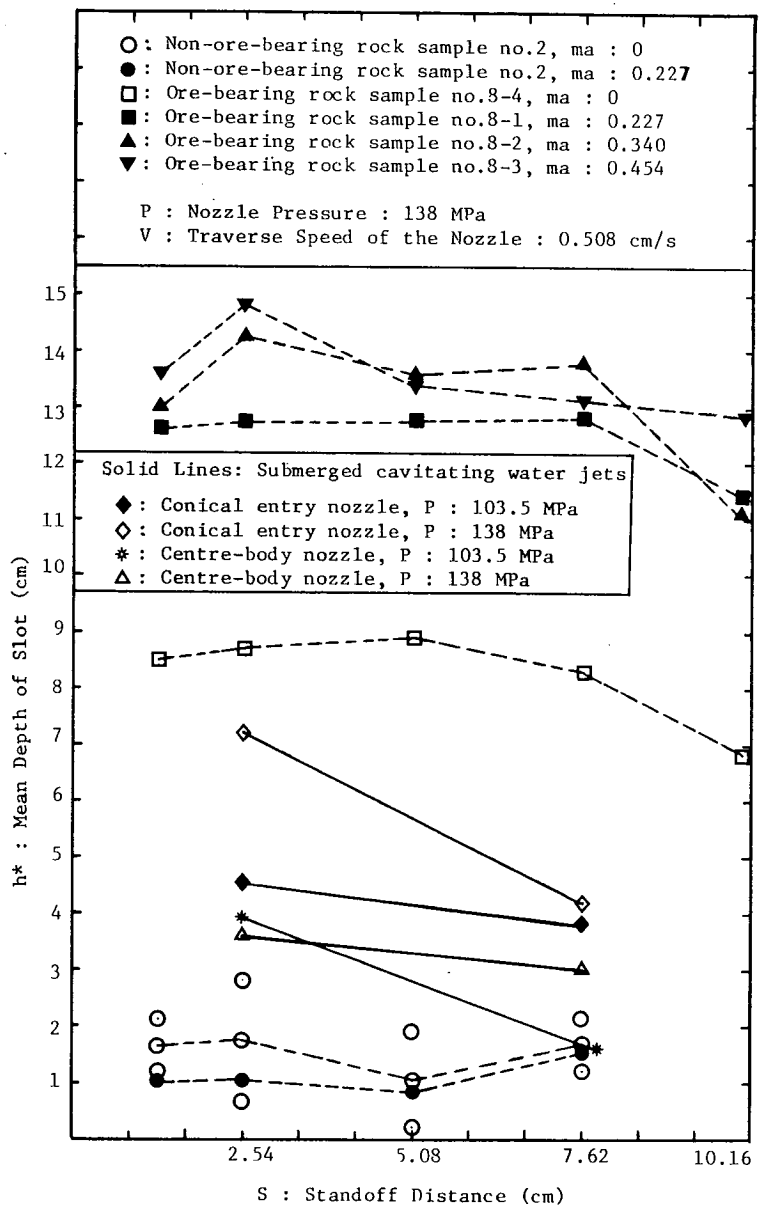

Fig. 7 Plot of mean depths of slots (h*) against standoff distance (S)

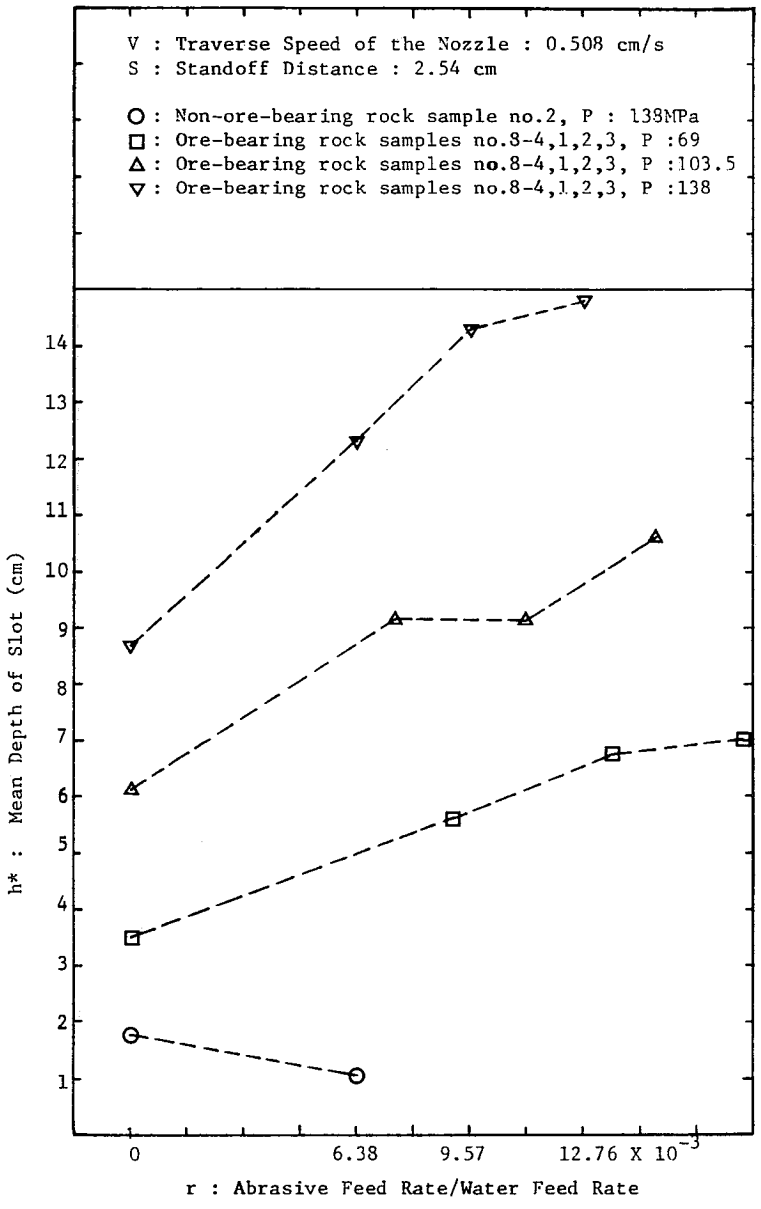

Fig. 8 Plot of mean depths of slots (h*) against r = Abrasive feed rate/Water feed rate

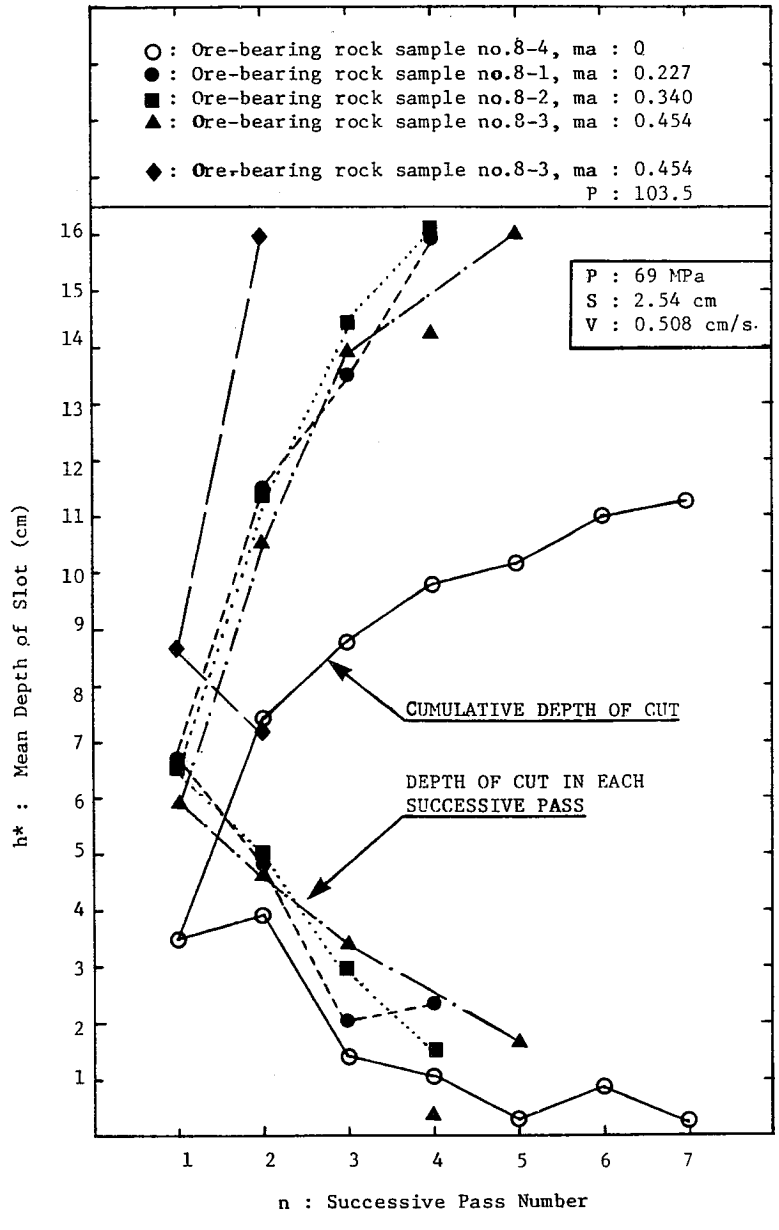

Fig. 9 Plot of mean depths of slots (h*) against the pass numbers (n)

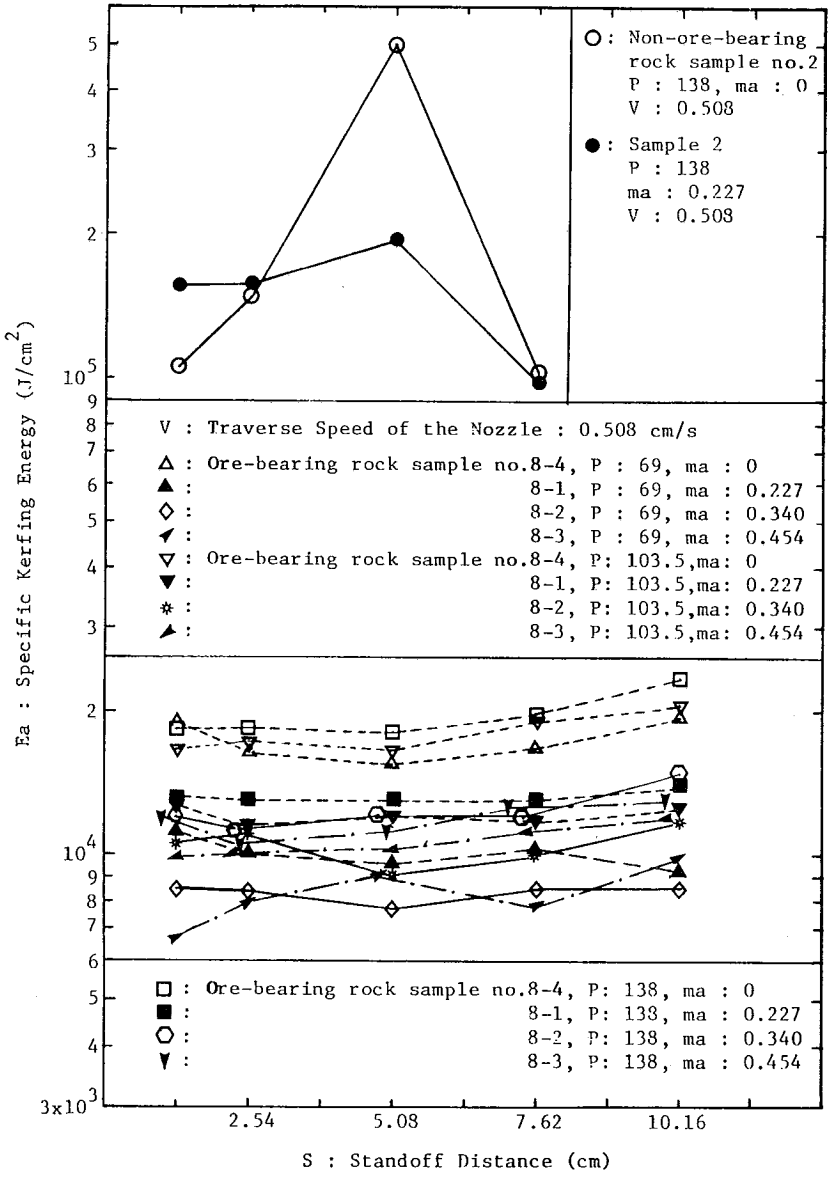

Fig. 10A Plot of specific kerfing energy (Ea) against standoff distance (S)

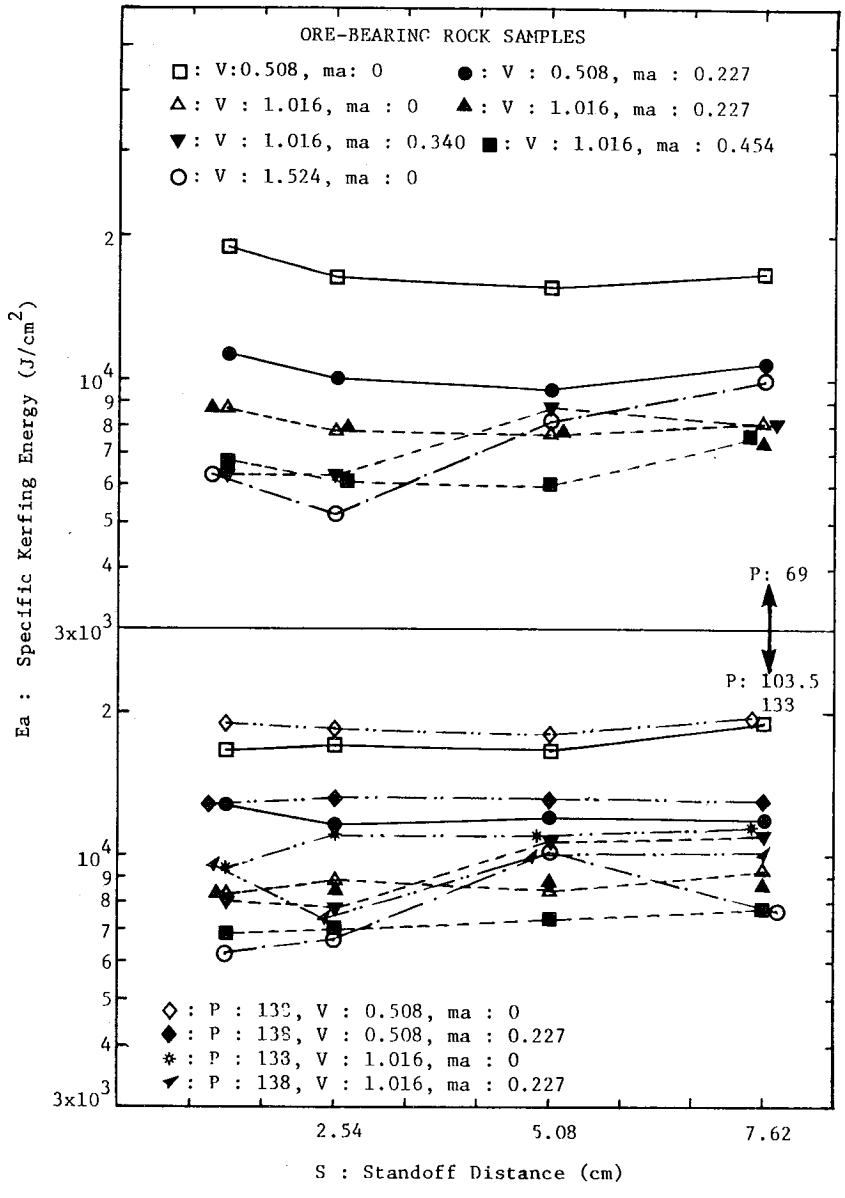

Fig. 10B Plot of specific kerfing energy (Ea) against standoff distance (S)

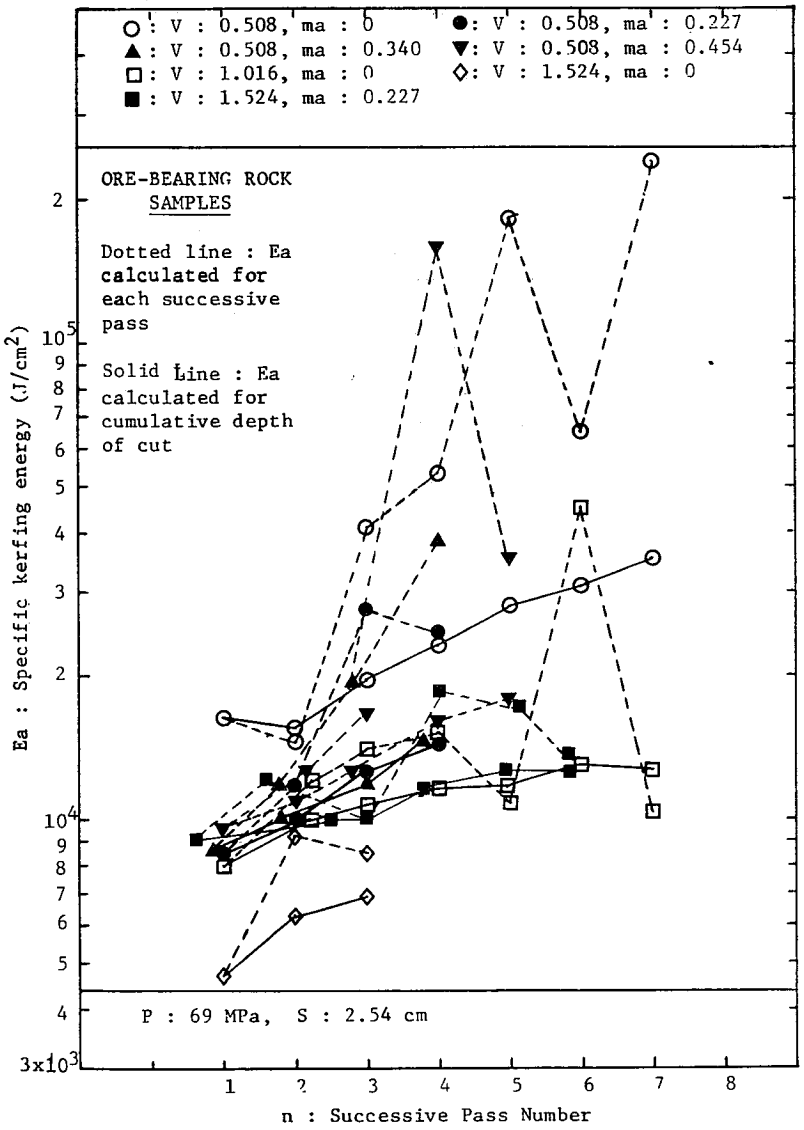

Fig. 11 Plot of specific kerfing energy (Ea) against the pass number (n)

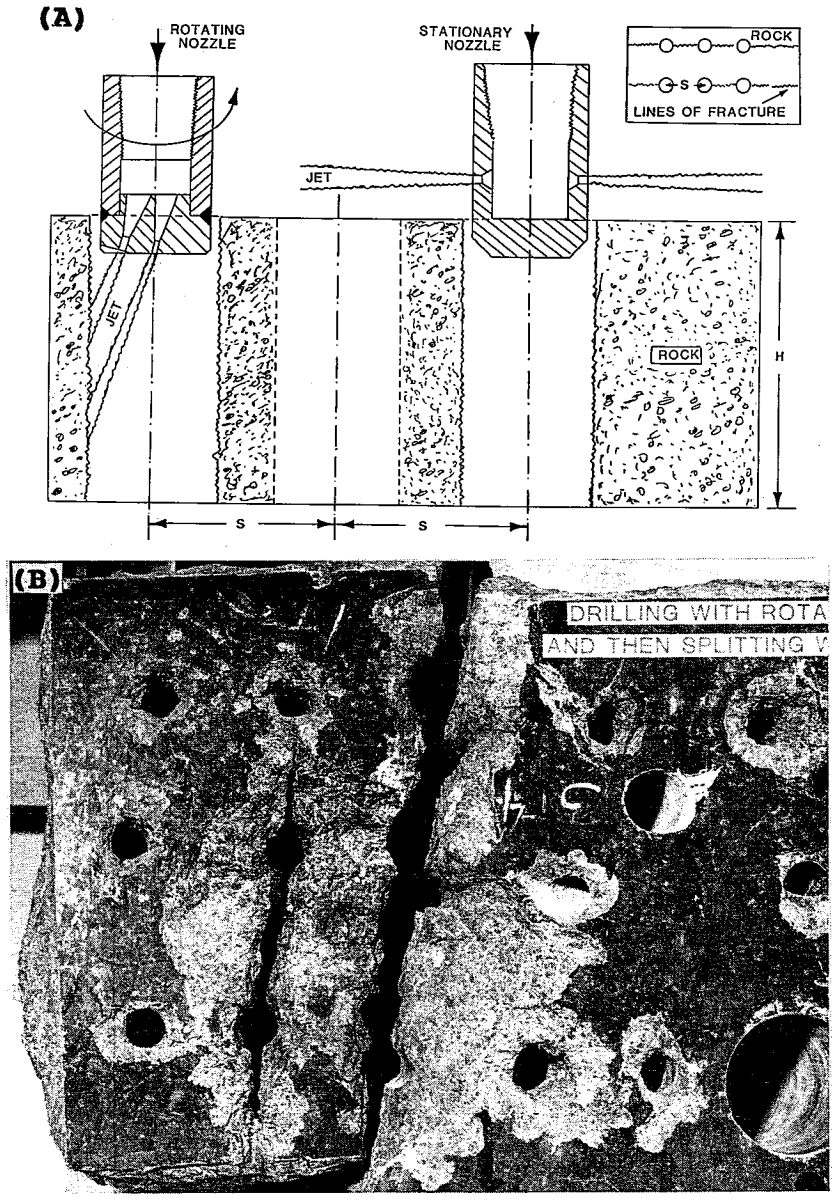

Fig. 12 A possible technique for selective mining of ore-bearing rock samples: (A) Drilling and splitting along the seams, as shown on black granite in (B).

6th American Water Jet Conference
August 24 - 27, 1991: Houston, Texas Paper **16**

A High Pressure Waterjet System For Inseam Longhole Drilling In Coal

P. Kennerley
The University Of Queensland-Brisbane, Australia

R. Phillips
Capricorn Coal Management-Middlemount, Australia

G.D. Just
Department of Resource Industries-Brisbane, Australia

D.A. Summers
University of Missouri-Rolla, USA

ABSTRACT

The underground coal mining industry needs more effective methods for drilling longholes in coalseams for methane drainage and inseam exploration. Present techniques are costly and limited in length and directional control by the cutting process which requires contact between the bit and the coalseam. Early trials using high pressure waterjets to drill holes in coalseams indicated the cutting process had the potential to provide a more efficient drilling technique. A research program proposal was subsequently submitted by Capricorn Coal Management, the operators of German Creek Mine, to the National Energy Research, Development and Demonstration Council (NERDDC) for funding to develop a high pressure waterjet longhole drilling system. Relevant operating parameters of the technique were determined using a prototype model developed from laboratory and small scale field tests. Extensive large scale field tests resulted in the development of a longhole system used to drill holes over 200m in length. Pump pressures of 650bar and flowrates of 160 litres per minute maintained an average penetration rate of 1m/min. Directional control of the holes was easier than conventional drilling techniques. Bit wear and downhole capital risk were substantially reduced. Modifications are currently underway to extend the capability of the system to 500m and beyond.

Organized and Sponsored by the Water Jet Technology Association.

1.0 INTRODUCTION

Methane Drainage

Coal seams may contain high quantities of seam gas usually comprised of methane and/or carbon dioxide. High gas levels pose safety problems in underground mines in the form of instantaneous gas outbursts and explosions. The Coal Mining Acts have limits on the maximum air concentration for both of these gases and as a consequence mine production can be slowed if the gas levels exceed the statutory limits. Production is stopped at this time until the levels of gas can be reduced by the action of the ventilation. In Queensland men must be withdrawn if the carbon dioxide level exceeds 0.5% and all electrical equipment must be shutdown if methane concentration exceeds 1.25%.

Gas concentration in the working place can be reduced if the seam gas is predrained by drilling holes in the coal and allowing them to vent the gas. In high production underground mines where longwall mining is practised the procedure typically involves drilling 80mm diameter holes across the longwall block (an area of isolated coal usually about 2km long and 200m wide) extending beyond the proposed development headings on the opposite side, a distance of about 250m. This system will drain the gas from the block in approximately 100 days by using vacuum assist and reduce the coal gas content down to an acceptable level. Delays to development were significantly reduced in the German Creek Mines Central Colliery 305 longwall panel recently when cross block in seam drainage using vacuum assist in the German Creek Seam was used. The effectiveness of this drainage method however would have been accelerated with better controlled drilling methods.

A more efficient method for draining longwall blocks uses longer holes, in excess of 500m, drilled into the block and parallel with the direction of the development roadways. These holes can be left to drain without vacuum assist for considerably longer periods if mine scheduling allows. Substantially fewer parallel longholes are required to achieve the same effect as the cross block holes. The increased length of these holes however makes them correspondingly more difficult to drill.

Seam Exploration

Longholes are also used for seam exploration to assist in mine planning. At the German Creek Mine holes have been drilled from existing open cut highwalls for distances of up to 800m down dip for the purpose of geological structure investigation. Obstructions to seam continuity were noted by changes in penetration rate and observation of drill cuttings. Use of this technique enabled several dykes of thickness from 0.1 to 2.0m to be mapped in an area of coal designated for future longwall mining.

Longhole Drilling Equipment and Techniques

All of these drilling applications use conventional drilling methods of either standard rotating rod string with tungsten drag or Polycrystalline Diamond (PCD) bits or a static rod string and water driven turbine down the hole motor (DHM) fitted also with either tungsten drag or PCD bit. A six button PCD bit costing A$3,000 may typically last 1500m in coal before refurbishing at a cost of A$240 per button. Five to seven refurbishes are usually possible before the bit is discarded. Tungsten drag bits are cheaper, A$800 but typically require sharpening after 300m in coal. The life of both bit types is substantially reduced if the bit wanders into the seam roof or floor. For gas drainage the principle objective is to maintain the bit within the coalseam. This is generally the objective also for seam exploration.

When using a conventional rotating rod string bit guidance within the seam is achieved by varying both bit rotation and thrust. Increasing thrust and lowering rotation forces the bit up and by reversing that combination the bit trajectory will fall in relation to the seam profile. It is exceptionally difficult, if not impossible, to control the azimuth of the bit. At the German Creek Mine rotary drilled holes invariably wandered to the right, with reference to the hole collar, within 60 to 100m from the collar. Holes generally straightened on a bearing most probably controlled by seam

structure after 250m. The bit frequently dived into the floor of the seam in the first 60m often causing the hole to be abandoned.

Much greater control can be achieved by using a DHM which is located in front of a non magnetic copper beryllium drill collar used for hole surveying purposes. The DHM has a bent sub or kick off at the distal end. The amount of the bend can vary from 0.75 degrees up to 4.0 degrees. The rods are pushed into the hole using a hydraulically operated and controlled drilling unit. The bit tip is guided in the seam by conducting regular down hole surveys using various techniques that employ photographic cameras or continuous readout "measure while drilling" (MWD) electronic survey tools. This system enables both trajectory and azimuth to be controlled.

Down hole motor drilling systems are expensive, require costly rebuilds and skilled operators. A typical DHM costs in excess of A$40,000 with rebuild cost of A$4,500 after 100 hours use. MWD survey units cost in excess of A$150,000. Although pumpdown photographic single shot cameras are much cheaper they can be unreliable and cost valuable drilling time. The cost of non magnetic copper beryllium drillrod is about A$1000/m. Typically 6 to 9m are used to shield the compass inside the pump down survey tool from the magnetic effect of the drillstring.

Both conventional in seam drilling techniques continue to be used with qualified success at the German Creek Mine. However as mining in Australia is forced into deeper reserves, correspondingly higher seam gas contents will be encountered. This will place additional pressure on existing longhole drilling techniques to become more efficient to ensure coal production does not fall below economically acceptable levels. The development of a high pressure waterjet operated downhole drilling system was identified as a means of significantly reducing the cost and improving the effectiveness of longhole drilling. This led to the planning of a major research project to investigate the potential of the technique.

2.0 RESEARCH PROJECT PLANNING

Field trials using high pressure waterjets to drill holes in coalseams were first carried out some 15 years ago, (Summers et al, 1979). Hole lengths up to 15m were drilled at an average drillrate of 1.2m/min using a nozzle fixed to a rotating drill pipe. These tests were a precursor to the development of a system for drilling horizontal holes from the bottom of vertical well bores. The results of these trials indicated that the non contact nature of the drilling process had the potential to provide a superior drilling technique. The benefits included faster drillrates, less thrust required by the drillrig, reduced bit wear, straighter holes, hole chambering and the potential to self steer. Despite the initial success achieved with the technique subsequent attempts to drill longer holes were hampered by feed, steering and cuttings removal problems that restricted lengths to 40m, (Becker and Schmidt, 1983), (Hackel, 1984).

As a result of a visit to The University of Queensland in 1987 by Summers a research proposal for grant funds was submitted to the National Energy Research, Development and Demonstration Council (NERDDC) by Capricorn Coal Management, the operators of the German Creek Mine, to develop a high pressure waterjet drilling system for drilling longholes in coalseams for methane drainage and inseam exploration. The proposal involved a three stage research program over a period of forty two months involving personnel from the German Creek Mine, The University of Queensland and the University of Missouri-Rolla. Grant funds were subsequently awarded on a staged basis with project work commencing in July 1988.

Stage 1 of the project incorporated a review of available technology to establish basic design parameters and develop a prototype working model. Existing technology was to be used wherever possible to expediate the development process. The basic operating paramaters of the system were established through laboratory tests carried out at The University of Queensland Experimental Mine (UQEM) followed by short field trials in the nearby Ipswich Coalfield. More comprehensive field trials were carried out at the German Creek Mine in the Bowen Basin of central Queensland. The aim

of this stage of the project was to develop a prototype model capable of drilling holes to 30m in length. These investigations formed part of a Masters program of research by Kennerley (1990).

Stage 2 involved the design, fabrication and testing of a longhole drilling system capable of drilling holes to 300m in length. This required the design of drill rods capable of withstanding operating pressures of up to 700bar to suit a conventional longhole drillrig and intermittent pump down single shot survey tool. The survey tool was required to allow the steering capability of the system to be fully evaluated.

Stage 3 of the project was planned to refine and upgrade the system into a practical working model capable of drilling very long holes to a length of at least 500m. This length was equivalent to the width of two longwall panels and gate roads. The potential to drill through harder rock sections at lower pressures by the injection of abrasives into the waterjet would also be investigated.

3.0 PROTOTYPE MODEL DEVELOPMENT

Initial Test Program

Stage 1 commenced with preliminary drill trials at The UQEM. The purpose of these trials was to become familiar with high pressure waterjet technology and procedures and to establish basic design parameters. To make the trials as authentic as possible the holes were drilled into a block of artificial coal or "coalcrete" made from a mixture of coal, cement and water. The Stoneage SA 2100 Waterjet Assisted Rotary Rock Drill was used to carry out the tests. The results obtained from these tests provided sufficient encouragement to attempt a field trial with the equipment at a nearby colliery.

Field tests in the Four Foot Seam beneath a highwall at Rhondda Colliery in the Ipswich Coalfield produced holes similar in size to the holes drilled in the coalcrete, about 35mm. In contrast however the size of the drill cuttings were much larger. This caused blockages in the hole that made it impossible to drill beyond lengths of more than 1m.

Subsequent trials were carried out with the Hammelmann RD 45 self rotating, high pressure waterjet nozzle. This nozzle drilled a hole that left sufficient room to flush the larger cuttings. Penetration rates of up to 4m/min confirmed the potential of the technique for cutting coal. The maximum hole length drilled was 4m. The absence of central or converging face jets proved troublesome in the banded sections of the coalseam. This problem was overcome by the addition of a central jet in the nozzle. Tests with the Hammelmann nozzle however were eventually discontinued due to bearing sealing problems.

These preliminary trials were instrumental in highlighting some fundamental differences between conventional and high pressure waterjet cutting processes in coal. The most significant findings were.

(a) High pressure waterjet drilling produces a large range of cuttings. The cuttings vary in size from fines to large blocky units. The successful application of the waterjet technique in coal would therefore require a nozzle that could minimize the size of the cuttings to prevent removal problems from occurring.

(b) Coal could be drilled with waterjets at relatively low pressures. Pressures as low as 200bar were sufficient to drill holes in coal with the Hammelmann nozzle. This meant it was not necessary to use nozzles with particularily powerful waterjets.

(c) High pressure waterjet drilling produces a substantially rougher wall profile, squarish rather than round. This could cause cutting removal problems in longholes.

(d) Continuous, uninterrupted operation with a self rotating nozzle required a nozzle with an effective seal that would prevent fine coal cuttings from clogging the bearings.

Woma FR Series Nozzles

The Woma FR series of high pressure, self rotating nozzles were designed to clean and cut through solid build up inside pipes. Therefore the conditions in which these nozzles operated suggested that they would be suitable for drilling holes in coalseams. Tests in the German Creek Seam beneath the highwall in Pit C at the German Creek Mine confirmed this expectation. At a pump pressure of 750bar the FR22 nozzle drilled 80mm holes to 10m in length at an average penetration rate of 1m/min. At this length the 70 litres per minute of water flowing from the four 1mm jet inserts was not sufficient to maintain effective cuttings removal and blockages resulted. Reducing the penetration rate to 0.3m/min permitted the holes to be extended to 20m in length until once again blockages prevented further drilling.

The addition of four 1mm parallel backward facing or "retro" jets behind the nozzle increased the flowrate through the system. This prevented further blockages from occurring. Holes up to 38m in length were then drilled using the FR22 and retro jets attached to 12mm high pressure hose. No auxillary feed was required as the thrust of the retro jets was sufficient to maintain a penetration rate of 1m/min over this distance. The holes were abandoned when the cuttings indicated that the nozzle was drilling in the floor of the seam. Drilling in the floor of the seam slowed the penetration rate to less than 0.1m/min. Hole surveys taken after drilling was completed confirmed that each hole had dipped towards the seam floor.

The manner in which the holes tended to dip appeared to be due to the floppy nature of the drillstring and preferential cutting in the bottom section of the hole. To overcome these problems the high pressure hose was replaced with EW drillrod used for conventional drilling underground. The rod couplings were modified to seal at high pressure. To prevent the hole being undercut as it advanced the nozzle was raised to the centre of the hole using a length of bent EW rod behind the nozzle, Figure 1 . Holes up to 52m in length were successfully drilled with a 1m section of rod bent at an angle of 1 degree and facing 12 o'clock. This was the maximum length possible using the experimental drillrig developed for the tests. Post drilling hole surveys indicated that the holes were heading towards the seam roof. The surveys also indicated a tendency for the holes to drift to the North East, towards the direction of the primary cleat.

4.0 LONGHOLE SYSTEM DEVELOPMENT

The principal objective of the second stage of the project was to develop a system capable of drilling holes to 300m in length. To achieve this it was proposed to combine the prototype system developed during stage 1 with conventional underground longhole drill rigs and intermittent survey techniques. This phase of the project therefore required the transformation of an essentially experimental drill system to a full scale longhole drilling operation. Control over the size of the hole and effective cuttings removal were identified as the most important factors that would influence the success of the operations. The parameters that influenced these two factors were.

(a) nozzle design
(b) pump pressure
(c) penetration rate
(d) variation in seam properties
(e) design of the drillstring and downhole assembly

Significance Of Hole Size

In contrast to conventional drilling techniques where the hole size is fixed by the diameter of the drill bit the size of the hole drilled with high pressure waterjets can vary during the drilling operations according to changes in pump pressure, penetration rate and seam properties. Given the stop start nature of conventional longhole drilling operations this makes the task of controlling hole size more difficult using a high pressure waterjet cutting process. It is necessary however to maintain a relatively uniform hole size during the drilling operations to ensure inhole flow velocities remain high enough for effective cuttings removal. Significant enlargements or "hole chambering" will cause the cuttings to settle in the hole which could lead to the drillstring becoming jammed. The size of the cuttings itself is also important. Jamming or hydraulic lock will occur around the drillstring if the cuttings are too large to be removed from the hole or cannot be prevented from collecting at a narrow section of the hole. Nozzle design is therefore critical to the success of the drilling operations.

Effect of Pressure on Hole Size

To be competitive with conventional DHM drilling techniques a penetration rate of 1m/min was required. This had been achieved drilling 80mm holes at a pump pressure of 750bar with the FR22 nozzle. However larger holes were now required to accomodate the downhole survey equipment. Initial trials were subsequently carried out with the larger FR47. To establish the effect changes in pump pressure during drilling operations would have on the size of the hole and subsequent cuttings a series of short 2m holes were drilled into the German Creek Seam at a constant penetration rate of 1m/min.

Figure 2 highlights the results of the tests. As expected the results showed a steady increase in the size of the hole as the pump pressure was increased. The results also indicated that changes in pressure would have a significant effect on hole size. However these values reflect local conditions only. The effect of overburden confining pressure underground substantially reduces the permeability of the coalseam from that of the test site, which had been exposed to weathering and affected by blasting from the mining operations. Thus the longholes drilled from the test site would narrow until they reached the seam area outside the influence of these external factors. The reduction in seam permeability would therefore be advantageous as the drilling operations would become less sensitive to changes in pressure.

Effect of Pressure on Cutting Size

Cutting samples taken from the holes to establish the size range and the effect of pressure changes upon this range were analysed using standard laboratory sieve techniques. Figure 3 shows the relationship between cummulative weight percent of each size. The size of the cuttings ranged from +16mm to -0.125mm. Although the effect of overburden confining pressure underground would be expected to reduce these measured values, they would still be considerably larger than those produced using conventional drilling techniques which typically vary no more than 1 to 2mm. Removing all of the cuttings from the hole was therefore going to be difficult to achieve without some form of mechanical assistance. Therefore because complete cuttings removal was not possible then the holes needed to be large enough to permit the larger cuttings to settle without affecting the drilling operations. The addition of the retro jets behind the nozzle would assist this process by propelling the cuttings from the back of the hole. Due to the differences in mass a separation process would occur that could produce a more even distribution of the cuttings inside the hole.

Significantly the median size did not vary substantially throughout the tests, from 2 to 5mm. This indicated it would be possible to vary pump pressure during drilling operations with the FR47 without adversely affecting the size of the cuttings. Thus the results obtained from the short hole trials with the FR47 provided sufficient encouragement to suggest that with careful control of drilling operations the nozzle could be used for drilling longholes.

Drillstring and Downhole Assembly

Special high pressure drillrods were designed for the longhole trials. These rods were made to conform to the handling requirements of conventional underground drillrigs. The drillrods were 56mm in diameter with a 40mm diameter bore. The bore of the drillrods was controlled by the diameter of the pump down survey tool used to measure the direction of the hole. A short length of high pressure rod was made into a retro unit for cuttings removal. Non magnetic, austenetic stainless steel survey rods were also manufactured to shield the compass inside the survey tool from the magnetic effects of the drillstring. These rods were placed in the drillstring ahead of the drillrods. The non magnetic section of the drillstring contained the locating sub or "muleshoe" for the survey tool.

Earlier survey results indicated that steering correction would be required to prevent the holes from deviating. Hole direction would be controlled by orienting a bent sub between 12 and 6 o'clock. The degree of correction would be based on the results of the hole surveys. A 1m length of rod bent an angle of 1 degree centralized the FR47 in a 100 to 110mm hole. This hole size would provide sufficient clearance for the nozzle, drillstring and larger cuttings in the hole.

5.0 LONGHOLE DRILL TRIALS

Equipment

A Kempe U4-450 conventional underground drillrig with a remote control console was used to carry out the longhole trials in the German Creek Seam beneath the highwall in Pit C, Figure 4. A Hammelmann 280kW (375hp) triplex pump with 45mm diameter plungers driven by a 230kW (300hp) Volvo motor supplied 180 litres per minute of water at a pressure of 650 bar to 205 litres per minute at 560 bar. A remote control foot gun enabled the drillrig operator to retain control of the pump pressure during drilling operations. A high pressure water swivel attached to the drillrods was used for rod rotation when adding rods to the drillstring and adjusting the position of the bent sub. Because the nozzle was self rotating rod rotation was not required during drilling.

Results

To compensate for the effects of overburden confining pressure the first longhole was drilled using a pump pressure of 650bar. The flowrate through the system was approximately 160 litres per minute. The performance of the system was very encouraging as the hole reached a length of 123m, exhausting the supply of drillrod, at an average penetration rate of 1m/min. Surveys were carried out at regular intervals to compare the accuracy of the technique to conventional longhole drilling. Directional control with the bent sub maintained the hole within a 0.5m target zone in the upper half of the seam, Figure 5. Minimal steering corrections were required to achieve this level of accuracy. A branched hole was also drilled from the mother hole to a distance of 52m. No cuttings removal problems were encountered during the drilling operations.

A second longhole was later drilled to 225m in length. This hole successfully drilled through an intrusive dyke, some 2m in width, 46m from the drill site. Again no problems were encountered with cuttings removal. Problems with the survey equipment however restricted the maximum length of survey to 140m. Thus the last 85m of the hole were drilled "blind" without the assistance of survey information. This made it difficult to maintain the hole in the seam and a lot of time was spent drilling through the coal/stone interface of the seam boundary. This slowed the penetration rate to 0.5m/min. The hole was eventually abandoned when the system pressure dropped to 400bar, the result of two damaged jet inserts in the retro unit.

Discussions

The longhole trials proved that the high pressure waterjet cutting process was a viable alternative for drilling longholes in coalseams. The most notable features of the system were.

(a) A reduction in downhole capital risk. A typical conventional downhole assembly consisting of a PCD bit, DHM and copper beryllium drillrod costs A$50,000. The corresponding cost of the FR47 and stainless steel drillrod was less than A$10,000.

(b) A reduction in bit wear. The FR47 showed little sign of wear after 300m of drilling through coal and stone. In comparison a tungsten drag bit would need sharpening after drilling 300m, this would require the withdrawal of the drillstring from the hole. A PCD bit would also begin to exhibit signs of wear.

(c) The performance of the drill provided sufficient encouragement to suggest that with additional refinements the system will require less surveys to maintain control of the hole direction. Any marginal improvements in control of hole direction has the potential to significantly improve productivity when pump down survey equipment is used.

6.0 FUTURE MODIFICATIONS

Stage 3 of the project is currently in progress to extend hole lengths to 500m. This involves hardening the system to operate more effectively in a full scale longhole drilling operation. The major modifications under investigation are.

(a) The development of a new nozzle to increase the penetration rate of the system. Mechanically assisted waterjet cutting is also being considered to enable the system to drill through harder rock such as the seam roof and floor, faults and dykes. The possibility of enhancing the cutting potential of the waterjets with abrasives is currently under investigation.

(b) An additional 500m of drillrod are being made from stronger, harder steel to prevent thread gall that resulted from the rod handling operations.

(c) Changes to the pump down survey equipment are required due to the pressure build up ahead of the probe caused by water bypassing the probe during the pump down operation. This problem was partially resolved in the longhole trials by sealing the back of the probe with pump buckets. A more suitable seal is currently being investigated which involves the adaptation of pipeline pigs. A downhole flow controlled dump valve assembly is also currently under development at The University of Queensland. The long term aim of the project is to adapt MWD survey equipment to the system to reduce drilling downtime that results from the pump down survey operations.

7.0 CONCLUSIONS

Results of an extensive program of field tests have demonstrated the successful development of a high pressure waterjet longhole drilling system for coalseams. The basic design of the system incorporates modified technology and processes from conventional longhole drilling and the waterjetting industry. The non contact nature of the drilling process confirmed the following features.

(a) improved control of the drilling operations
(b) substantial reduction in bit wear
(c) lower capital risk downhole
(d) improved productivity rates

Modifications are currently in progress to extend the capability of the system to 500m and beyond.

ACKNOWLEDGEMENTS

The development of the waterjet longhole drilling system would not have been possible without the financial support of NERDDC and the committment from Capricorn Coal Management to undertake the project and schedule the extensive program of field trials into the daily mine operations. The many individual contributions made by the staff and personnel of the German Creek Mine, The UQEM, Strata Drilling, SIMTARS and the various contracted pump operators are gratefully appreciated.

REFERENCES

1. Becker, H, and Schmidt, B H, "Drilling Boreholes In Coalmines Using High Pressure Water", Second US Waterjet Conference, pp179-182, 1983.

2. Hackel, B, Private communique to Mr Jellicoe of Woma Australia, 1984.

3. Kennerley, P, "Development of a High Pressure Waterjet Drilling System For Coalseams", Masters Thesis in Mining Engineering, The University of Queensland, 1990.

4. Summers, D A, Barker C R, and Keith, M D, "Waterjet Drilling Of Horizontal Holes In Coal", AIME Annual Conference, 1979.

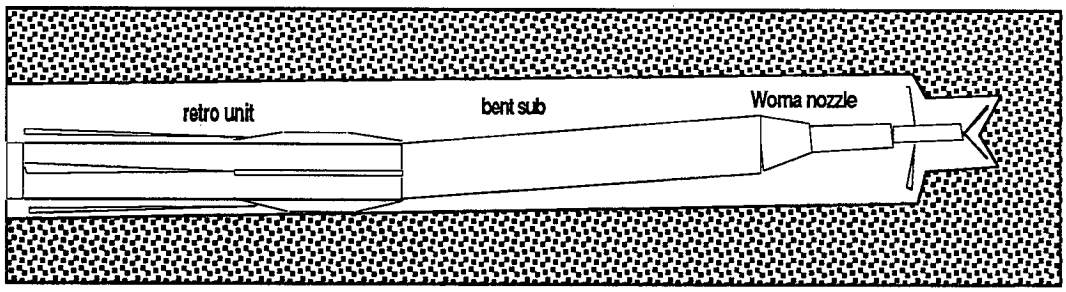

Figure 1 Prototype Downhole Assembly

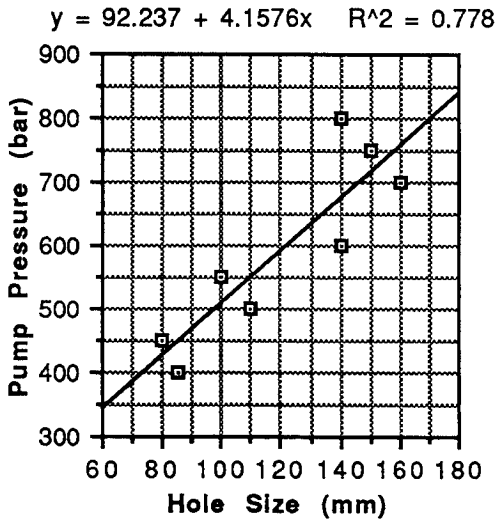

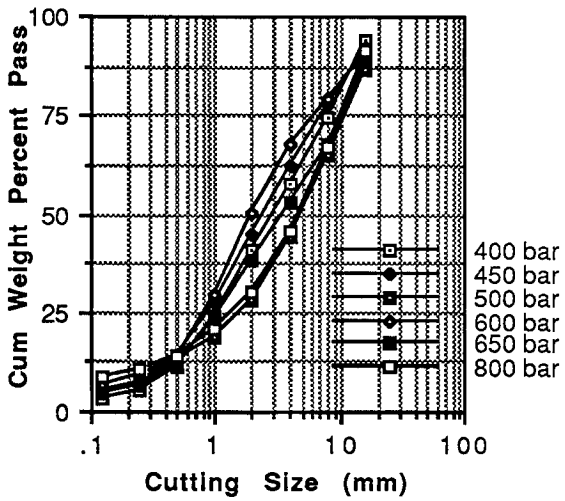

Figure 2 Effect of Pressure on Hole Size

Figure 3 Effect of Pressure on Cutting Size

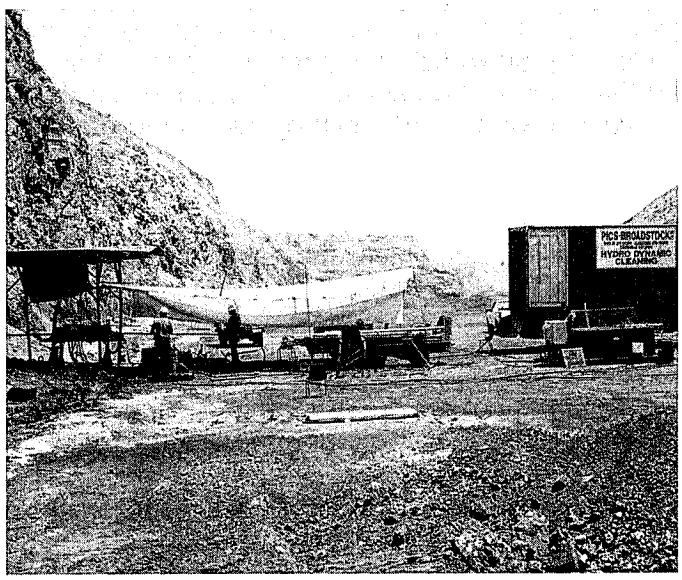

Figure 4 Drill Site Pit C

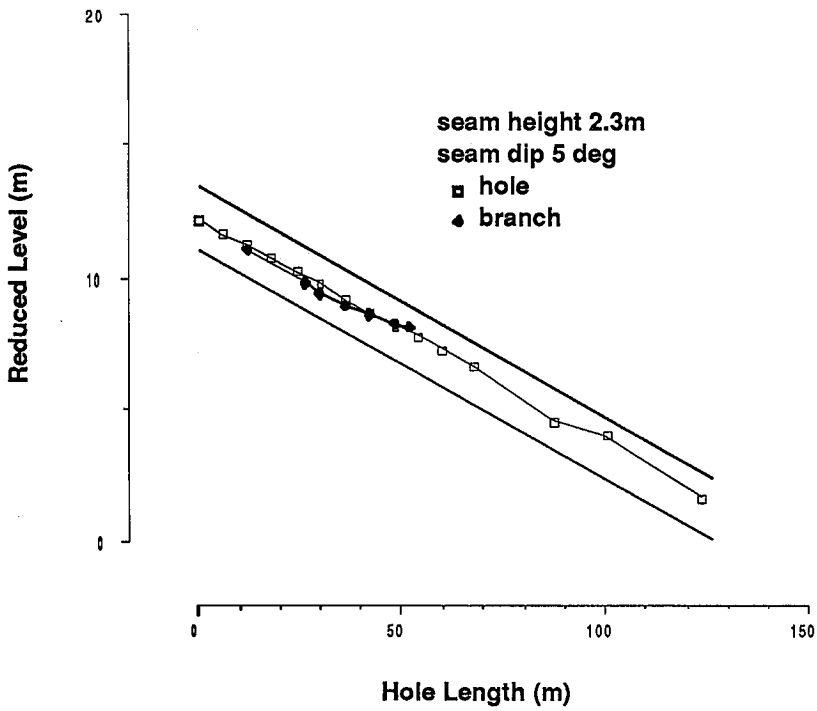

Figure 5 Hole Trajectory

6th American Water Jet Conference
August 24 - 27, 1991: Houston, Texas Paper 17

The Development of an Inexpensive, Accurate and User Friendly Water Jet Motion Control Cutting Machine

CHRISTIAN M. OLSEN
Boeing Commercial Airplane Group, 777 Program
Seattle, Washington, USA

AND

ROBERT H. TODD
Manufacturing Engineering & Engineering Technology Dept.,
Brigham Young University
Provo, Utah, USA

ABSTRACT

During the 1990-91 school year, seven senior engineering students developed a 4 ft. by 6 ft. 3-axis, abrasive water jet motion control cutting machine and control system. This machine was built as part of a new course in Integrated Product and Process Design developed at Brigham Young University. This new course comprises a joint effort between the Manufacturing Engineering and Technology Department and the Department of Mechanical Engineering. This paper describes the efforts of this student team, the machine components in detail, and unique attributes of the machine.

The machine is user friendly, accurate, and relatively inexpensive. Off the shelf components were utilized wherever possible. Project activities described in this paper include the writing of a functional specification using results from a quality function deployment analysis, concept generation and selection, preliminary and detailed design (including robustness design), process design, and assembly of the machine itself.

This machine will be used for manufacturing development activities associated with BYU's Advanced Composites Manufacturing Engineering Center and its associated Consortium of over thirty companies. The machine will also be used in activities associated with BYU's new undergraduate and graduate programs in Manufacturing Engineering.

Organized and Sponsored by the Water Jet Technology Association.

1.0 INTRODUCTION

Water-jet cutting is a relatively new technology, but due to the many advantages it offers, it is quickly gaining wide acceptance and experiencing much industrial use. For these reasons, it is desired that the technology be further introduced to the university level for study. Unfortunately, water-jet machines are very expensive (1), well beyond the reach of most universities and many companies. Brigham Young University (BYU) has come up with a solution to this problem by enlisting the talents of several senior mechancial and manufacturing engineering students and making a substantial donation for machine components. The students, during a year long senior capstone course entitled "Integrated Product & Process Design," have designed and produced a water-jet cutting machine that is relatively inexpensive, capable of high accuracy and repeatability tolerances, robust in design, computer controlled, and very user friendly. The user friendliness results from a unique control system based on a 486 personal computer and high level robotics software.

This paper briefly describes the design processes taught within the course, emphasizing the importance of the customer wants throughout the development of the machine. It then presents the attributes of the final design, discussing both the design advantages and their direct relationship to original customer wants.

2.0 CUTTING MACHINE DEVELOPMENT

Brigham Young University had specific wants from a water jet cutting machine. The university wanted a machine that was very accurate and repeatable, a machine that was robust, a machine that was safe to operate, a machine that was easy to use and maintain, a relatively inexpensive machine, and a machine that could adapt to future needs of the university.

2.1 Concept Generation & Evaluation

From these customer wants technical functional specifications were developed (See Table 1) and used as target values during the evaluation of concepts. Many concepts were generated and then analyzed using Quality Function Deployment (QFD). QFD Capture (2), using a computerized weighting defined by customer wants, enabled comparisons between the concepts generated. These comparisons clearly eliminated inferior concepts and helped the engineering team focus upon those concepts that most optimally met customer wants. The resulting final concept and subsequent design consisted of those attributes found in Table 2.

2.2 Design & Fabrication

Preliminary design was accomplished utilizing a CAD solid modeler (CATIA) to check for overall dimensionality and interference of major components. Detailed design was done using AutoCAD Release 10. Additional hours were spent contacting product vendors and experts in the field of water jet cutting such as Frank Romeo of Romeo Engineering (3) and Gary Hulsey of the University of Texas at Arlington (4).

The actual fabrication of the cutting machine was done in part by the Brigham Young University Research Machine Shop and the students themselves. Production involved fabrication of the structures and carriages, machining of critical surfaces, assembly of the carriage components, precision leveling of the slides and carriages, fabrication of component devices, installation of component devices, wiring of the controller hardware, installation of the high-pressure system, software encoding, and overall debugging.

3.0 BYU'S WATER JET CUTTING MACHINE

The final machine, as seen in Figure 1, is composed of many components that may be broken down into 6 main categories. These categories include the machine structures, the unique controller, the motion transmitting devices, the high-pressure system, the water containment devices, and the site facilities.

3.1 Structures

Main Framework - The main framework, the principal support of the machine, was fabricated from mild carbon steel with overall dimensions of 97" long by 62" wide by 72" tall (See Figure 2). To achieve a rigid, robust structure four 8-inch box-beam columns with wall thicknesses of 1/2 inch were used as corner supports and 4-inch box-beams with a 1/4 inch wall thickness were used laterally. Inaccuracies caused by vibration transmission through the structure were reduced by bolting the structure to the shop floor and filling each 8-inch column with pea-gravel. To reduce tolerance variation cause by residual stresses, the entire structure was stress relieved prior to the machining of critical surfaces. The structure was also painted with a urethane coating material to combat the corrosive environment of abrasivejet cutting.

Carriages - There are three carriages that move upon the main framework corresponding to each of the three axes of movement (See Figure 3). The largest carriage, traversing the 6 ft. cutting dimension, was fabricated from aluminum and rests upon four pillow blocks at each corner. Upon this large carriage the other two carriages ride. To reduce dynamic deflection in the large carriage, two wide-flange I-beams 62" long were used. These aluminum I-beams were spaced 24" apart and bolted along the top and bottom flanges to 1/2" precision aluminum plates. Aluminum was chosen to reduce the momentum associated with accelerating a heavier, steel structure. A large slot was machined in the aluminum plate to allow the vertical carriage to be centered and extended below the aluminum large carriage.

The smaller carriage, traversing the 4 ft. cutting dimension, was constructed from mild carbon steel. This carriage consists of a 16" section of a 4-inch box-beam with a 1/4" wall thickness. This section of box-beam rests on two pillow block assemblies at each end. A mounting plate is attached to this section where a 24-inch ballscrew assembly fastens.

The ballscrew assembly moves the vertical carriage, a 37-inch length of 4" diameter aluminum tubing (originally a box-beam design) with a 1/2" wall thickness. This aluminum carriage has been anodized to

resist corrosion, and enables vertical positioning of the nozzle up to a maximum of 15-inches above the workplane. The nozzle body is firmly attached to a horizontal 5/8" aluminum plate welded to the bottom of this vertical carriage.

Workpiece Supports - Two 54-inch stainless steel "T" shaped sections are used to clamp various size workpieces beneath the nozzle. They slide upon two stainless steel angles that are 81" long. Each of the two supports can easily and independently be adjusted with the use of handcranks located along the machine front. The handcrank shafts are attached to two timing belts that, in turn, attach to both sides of a given "T" (See Figure 4). The use of timing belts to drive the workpiece supports not only reduces the amount of time that an operator would spend loading and unloading parts, but eliminates any binding of the 54-inch workholding "T's".

3.2 Controller Architecture

Computer System - The controller architecture centers around the use of a 486 personal computer rather than a traditional "blackbox" controller (See Figure 5). The 486 computer runs at 25 Mhz and has been equipped with a VGA monitor, 122 megabyte hard-drive, 4 megabytes of RAM, a 1.44 meg/3.5" diskette drive, and an ethernet card for networking to other computers on campus.

A 386 computer with an 80387 math co-processor is directly tied to the 486 server and acts as a dedicated slave to which instructions are downloaded. The 386 machine contains only the Galil 3-axis controller card. This card, therefore, receives the sole attention and computing power of the 386 PC. It is the combination and union of these two computers that allows for the rapid computing of tool paths, the real time control of the water jet robot, and the multitasking availability within the X-Windows interface.

The Galil servoboard, with position feedback, provides control of three axes with simultaneous control of two. Additionally it provides eight inputs and outputs used to sense input signals from emergency stops, limit switches, and home sensors, activate the nozzle, activate the abrasive flow, activate the z-axis braking system, and communicate with a teach-pendant located on the machine.

Software - The Robline™ robotics software package, developed at Brigham Young University, has resulted in a new on-line interface that allows control of either a simulated workcell or the actual robotic equipment (up to 18 axes simultaneously) using the same natural programming language (5). Originally written for workstation use, the code has been configured to run in real time on a 486 personal computer, UNIX operating system, and the X-Windows/Motif interface. This user friendly software provides for the development of a computer model of the water jet cutting machine, including both physical geometries and kinematic characteristics of the machine. Once created, a wireframe of the machine can be displayed and animated during or before tool path motion. The programming control of the simulation or actual movement of the water jet nozzle becomes transparent to the user and the debugging of cutting geometry is greatly simplified.

Robline™ is a software dependent robotics package that eliminates the need for specific controller components as well as M and G encoding. Motion commands are sent to an independent device server, which applies compensation techniques (discussed later) and forwards resulting commands to either the computer simulation, the water jet cutting machine, or other programmable devices. The water jet or additional devices then use a specific software interface that responds to the server commands and directs robot tasks.

An "ideal" task may be programmed off-line and interference checking and calibration techniques may be used to compensate for any performance deviations in the actual machine. This is done by using sensors to map the inaccuracies of the water jet robot and the rigid body positions of workcell objects relative to the robot. The Robline™ server then compares the measured positions of these parts to ideal values in the geometric database, and stores corrective information to be used during cutting processes. This allows inaccuracies to approach the repeatability limits of the machine.

Teach-Pendant & Other Components - A 16 key teach-pendant, located at the cutting machine, is directly tied into the computer (See Figure 6). It provides the ability to adjust cutting speeds, jog in all three axes, activate the nozzle, activate the abrasive flow, and start preprogrammed tool paths. With use of the teach-pendant an operator can turn on either the abrasive or non-abrasive jet and jog the nozzle for "bandsaw" operations as well as position the nozzle accurately upon a workpiece.

3.3 Motion Components

Ballscrews & Slides - The three carriages are supported by Thompson fully supported "superglide" C-section slides and power is transmitted from the motors to the carriages via Thompson precision preloaded ballscrews. Each ballscrew, except for the vertical z-axis assembly, is 1.0 inch in diameter with a pitch of 4-turns per inch. The vertical ballscrew is 1/2" in diameter with a pitch of 5-turns per inch.

Motors & Amplifiers - Three ElectroCraft DC brush servo motors are coupled to each of the three preloaded ballscrews and used to provide motion in each axial direction. The motors are equipped with both ElectroCraft tachometers and Renco 1000 line encoders. The motors are powered by compact, surface mounted PWM servo amplifiers that, in turn, receive controlling signals from the Galil servoboard located in the 386 computer.

3.4 High-Pressure System

Both the high-pressure and abrasive systems were purchased from FLOW Systems International. The high pressure intensifier is FLOW System's 9X Waternife™. The Waternife™ can pressurize water up to 55,000 psi. The nozzle used with BYU's water jet cutter is the PASER™ II abrasivejet. This nozzle body when used with FLOW System's abrasive hopper and metering valve permits cutting of very hard materials such as glass and Kevlar.

3.5 Water Containment Devices

Tank Water Catcher - The tank designed for BYU's cutting machine disposes of the water and energy remaining after the jet passes through the workpiece (See Figure 7). The tank is constructed of an outer carbon steel structure (painted to combat corrosion) that supports a 74" long x 50" wide x 30" deep stainless steel liner. Placed within this stainless liner are 3 protective levels of 4" angle-iron baffles. Attached to the outside of the liner is the tank drainage system. Originally designed to fill with water, the tank has a leveling drain that feeds into a 1-1/2" drainage line slightly above the baffles. Currently the tank is being used "dry" with the lower drainage line left open.

The tank was designed with ease of maintenance in mind. The entire structure rests upon four 6" casters allowing the tank to be wheeled out from underneath the main structure. Without the use of settling tanks, abrasive debris will build up over time requiring cleaning of the tank contents. This is easily done by wheeling the tank to a cleaning area, loosening the 6" plug in the bottom, and rinsing the debris from the tank.

"Roll-Top" Tank Covers - The two "roll-top" tank covers are made from laminated pack-cloth sewn together to construct 40 separate pockets. Inside these pockets 0.25" x 1.375" x 54" wooden stiffeners have been placed. Each assembly rides in tracks mounted along the frame and attaches to a stainless steel workpiece support (See Figure 8). As a workpiece support is positioned along the table the "roll-top" cover follows, covering the unused opening of the tank. When retracted the covers pack into pockets located on both ends. By covering the unused portions of the tank the overspray caused by jet dispersion is greatly reduced, the majority of which is captured beneath the workplane. Additionally, the high decibel noise created by the jet and echoed by most tanks is reduced.

Septum - To eliminate any possibility of abrasive overspray settling on the precision mechanical mechanisms located in the upper portion of the machine, a septum has been used in conjunction with stainless steel panels along other exposed sides. This septum provides a tight seal against the steel framework while still allowing the nozzle to move about the workcell (See Figure 9). It is fabricated from a tightly woven gortex fabric rubberized on the upper side and sown together into a 182" x 148" piece. To contain such a large piece, such that it does not drag on the workpiece and risk being cut, the septum was suspended and gathered upon 8 recoiling tension cords (See Figure 10). These cords lift the septum fabric by passing through "D-rings" sewed along the septum and attaching to the above carriages.

3.5 Site Facilities

The room that houses BYU's water jet cutting machine was designed to isolate the machine from both the operator and the computer controller (See Figure 11). By isolating the operator from the machine the hazards posed by harmful noise levels are reduced. Additional benefits come from isolating the corrosive environment of the abrasive jet from the computer and other machines in the shop.

4.0 CONCLUSION

The machine designed and produced by the senior engineering student team at BYU successfully addresses and exceeds the original wants posed by its customer (BYU). This was accomplished by first qualifying the customer wants with Quality Function Deployment (QFD), then applying engineering knowledge to a thorough design process that included preliminary, detailed, robustness, and process design cycles.

By fabricating a robust structure, assembling stiff carriages, and using precision motion components, the resulting water jet cutting machine is estimated to achieve accuracies better than ±0.010" across the 4' x 6' cutting area. With the use of Robline™ and the 486 personal computer these inaccuracies can be brought down to the estimated ±0.003" repeatability limit. The use of a non-intimidating personal computer to control the machine makes it very user friendly, as well as, allowing for future expansion and customization of the software dependent controller architecture. Additional features that aid in the usefulness of BYU's machine include features such as the easily removed and cleaned catching tank, the adjustable workpiece supports, the teach-pendant at the machine, the "roll-top" covers, and the protective septum device.

This machine will be used for manufacturing development activities associated with BYU's Advanced Composites Manufacturing Engineering Center and its associated Consortium of over thirty companies. The machine will also be used in activities associated with BYU's new undergraduate and graduate programs in Manufacturing Engineering.

REFERENCES

1. Ingersoll Rand. "Ingersoll Rand introduces first high-accuracy, moving gantry waterjet cutting system." WJTA Jet News Apr. 1991: 7.

2. QFD/CAPTURE. Computer Software. International TechneGroup Inc., 1988.

3. Romeo, Frank. Address. SME Conference on Hydro-Abrasive Jet Cutting of Composites. Arlington, Texas, 9 Oct., 1990.

4. Hulsey, Gary. Automation and Robotics Engineer, Univ. of Texas at Arlington. Personal Interviews. Feb. 1991.

5. Red, W. Edward, and Mark G. Dixon. "Robots - Programmed for Success." Manufacturing Engineering May 1990: 43-7.

- **Simultaneous Control of 2 Axes**
- **Accuracy to ±0.005 inches or Better**
- **Repeatability to ±0.003 inches**
- **98% Overspray Containment**
- **85 dB Operator Noise Level**
- **PC Based Controller Interface**
- **$25,000 Budget for Motion Control Table including Controller**
- **April, 1991 Completion Deadline**
- **4 ft. by 6 ft. Cutting Area**
- **15 inches of height adjustment**
- **250 pound workpiece capacity**

Table 1 - Listing of Desired Major Functional Machine Features.

- **Completely Enclosed Overhead Gantry**
- **Simultaneous X-Y Control - Motorized Z Control**
- **Preloaded Thompson Ball-Screws**
- **Fully Supported Thompson C-Section Roller Slides**
- **FLOW Systems Waternife 9X^{tm} Intensifier**
- **FLOW Systems Paser^{tm} II Abrasive Cutting Nozzle**
- **Septum Overspray Containment**
- **Roll-Out Stainless Tank Water Catcher**
- **Adjustable Workpiece Supports with Catcher Covers**
- **Robline^{tm} Robotics Software with Error Compensation**
- **486 PC with Unix Operating System & X-Windows**
- **GALIL Servoboard with Position Feedback**
- **ElectroCraft DC Servo Motors**

Table 2 - Attributes of Final Concept.

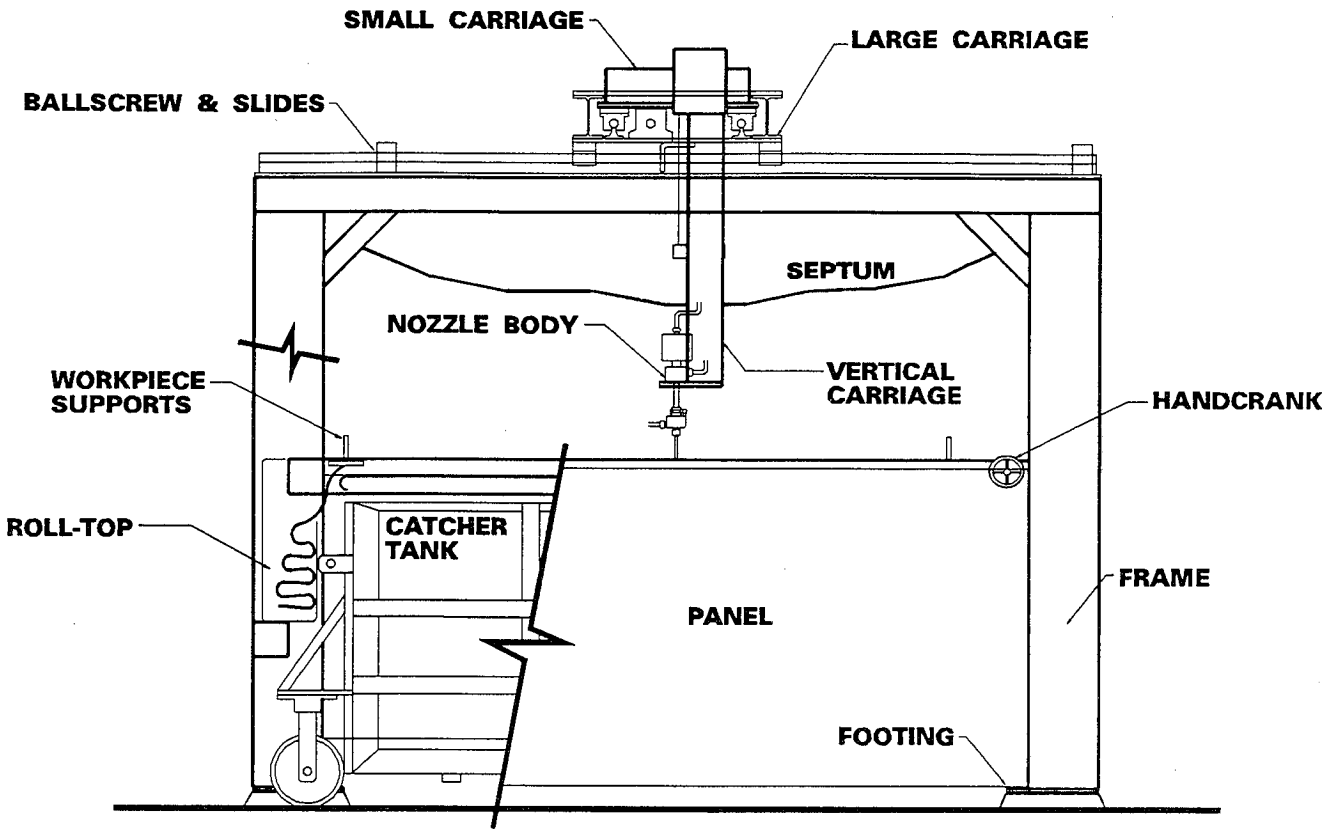

Figure 1 - Water Jet Machine Assembly.

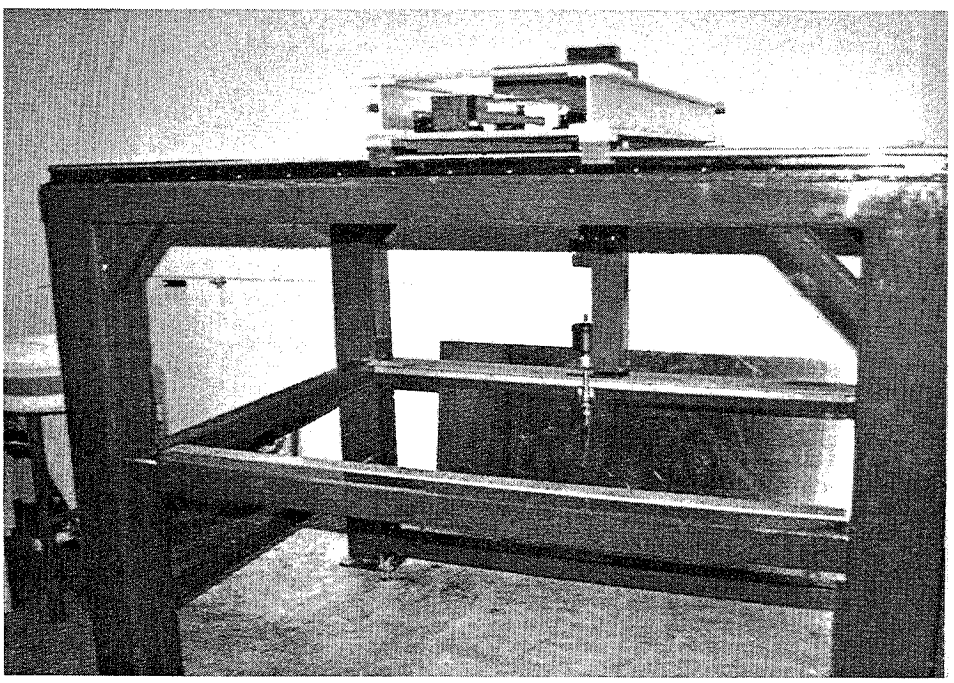

Figure 2 - Main Framework Structure.

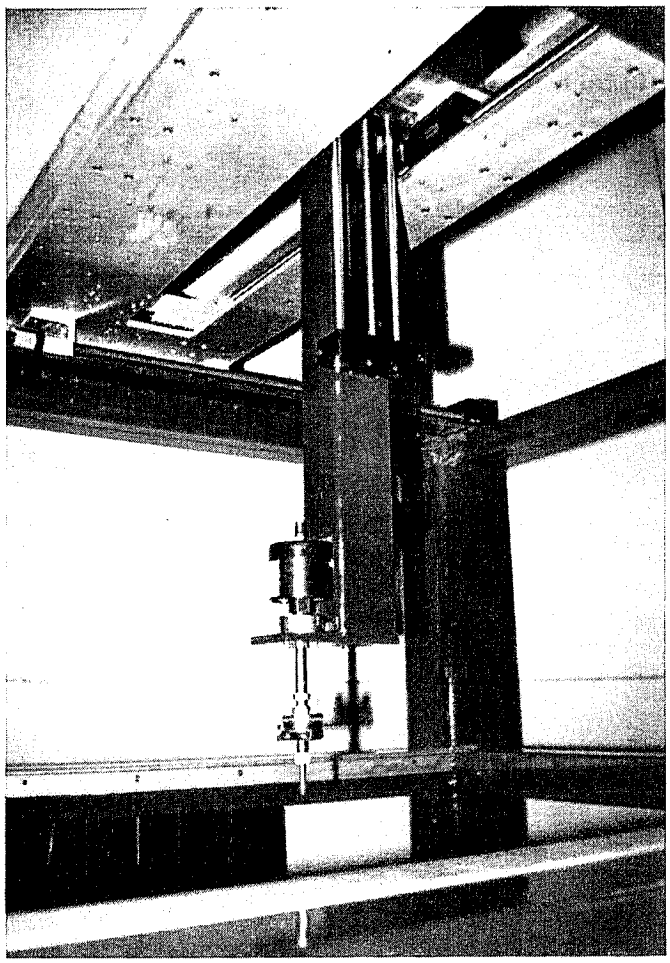

Figure 3 - Carriage Assemblies.

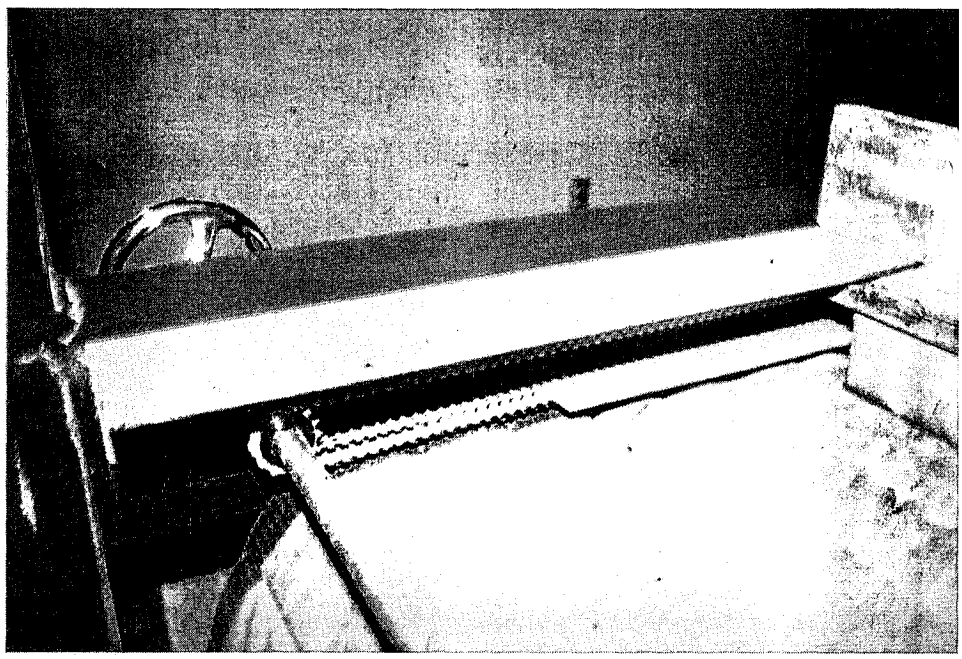

Figure 4 - Workpiece Support with Timing Belt Mechanism.

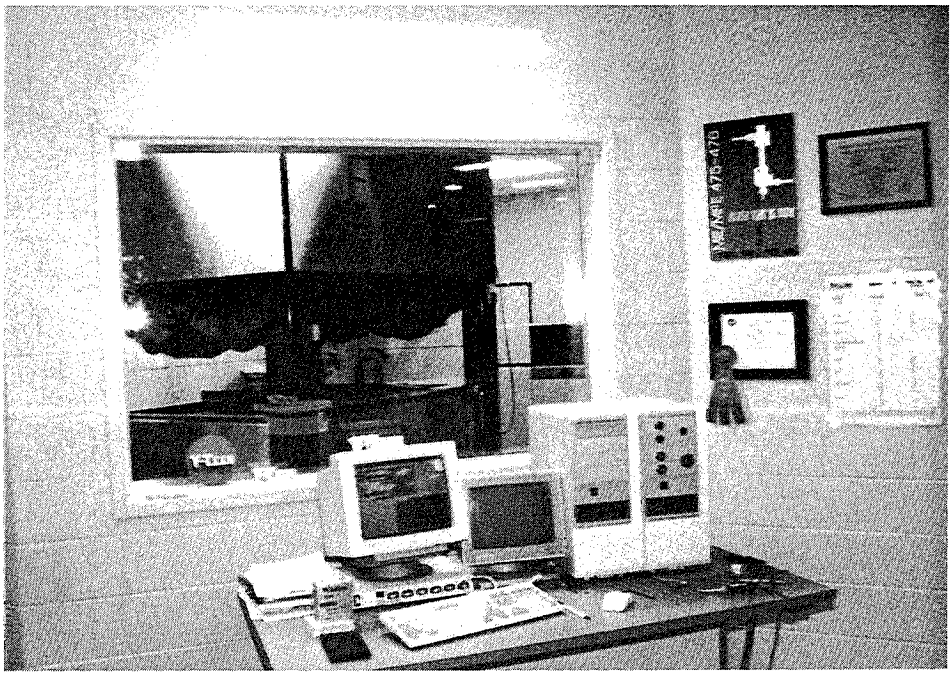

Figure 5 - Computer Controller.

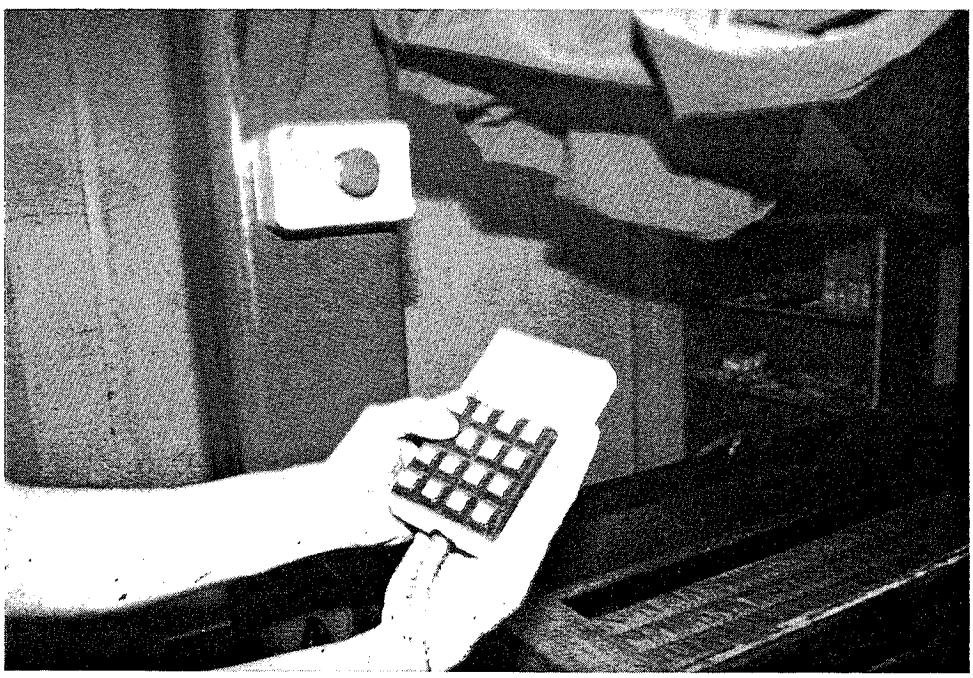

Figure 6 - Teach-Pendant.

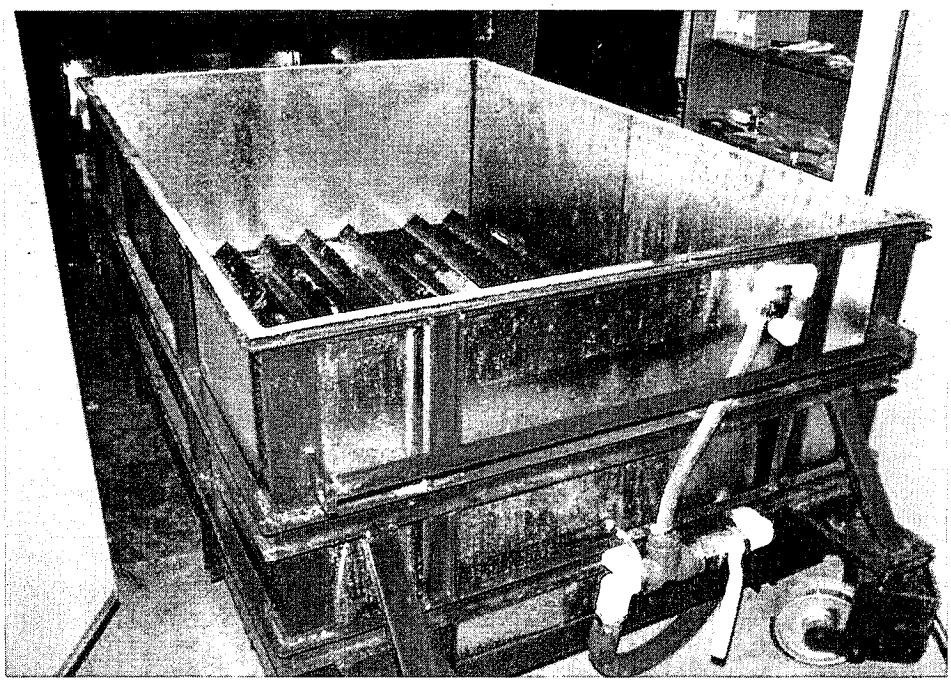

Figure 7 - Water Catcher Tank.

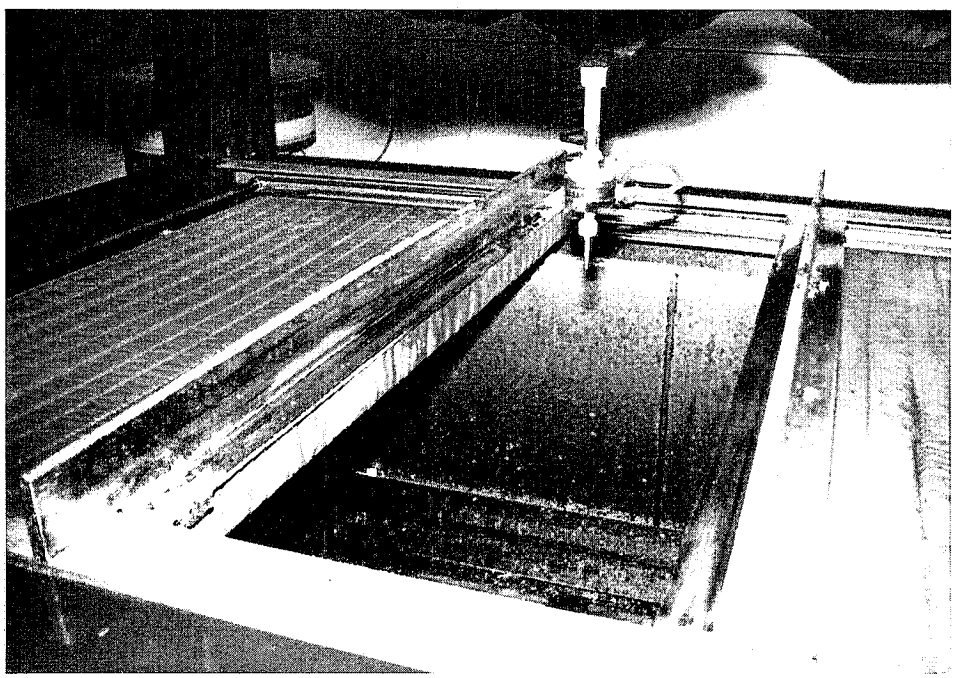

Figure 8 - "Roll-Top" Tank Covers.

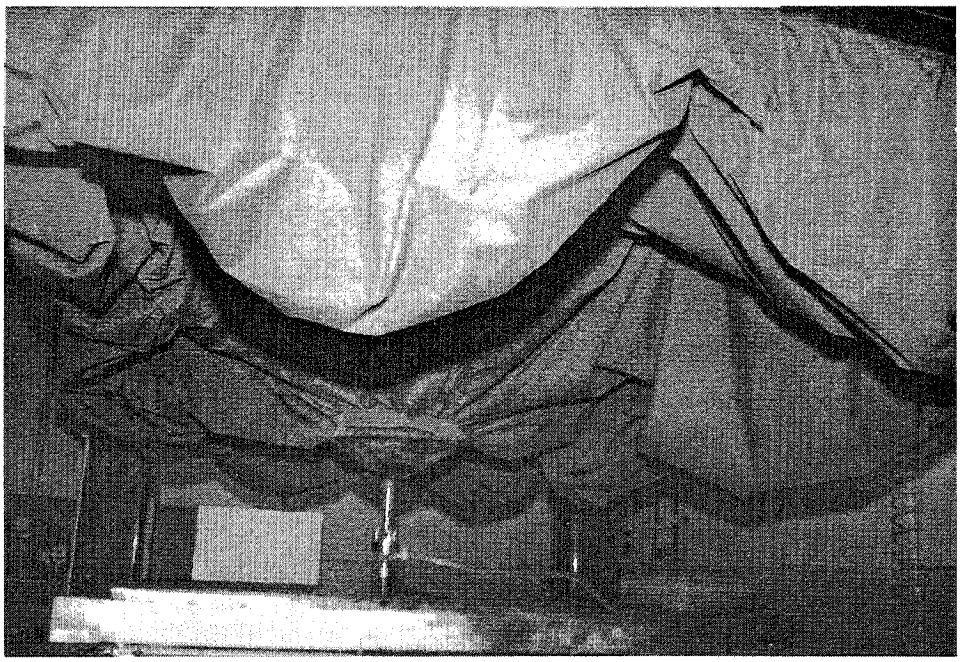

Figure 9 - Septum.

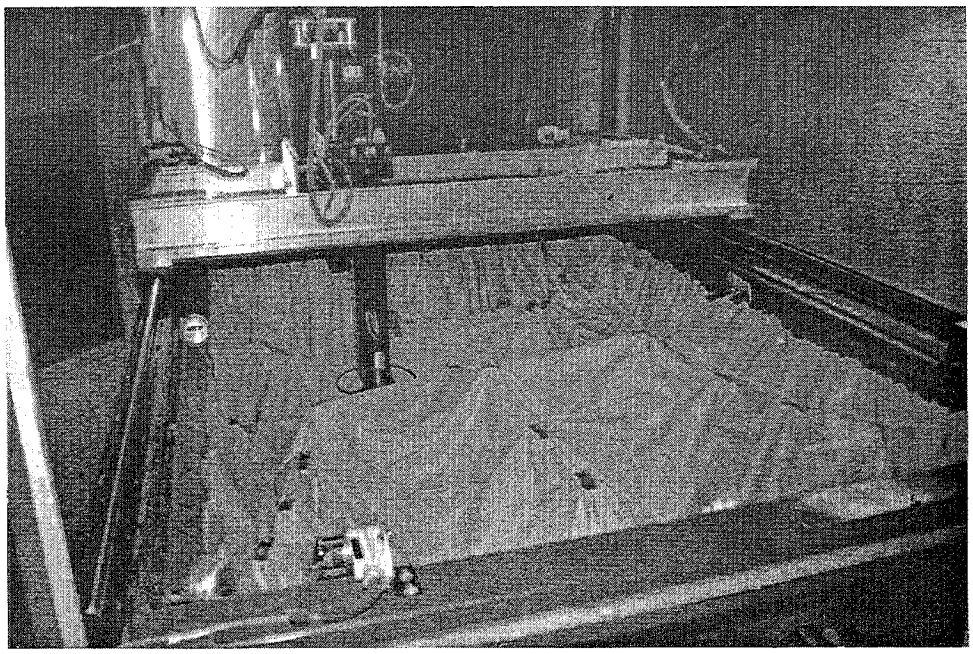

Figure 10 - Inner Septum showing Gathering Mechanism.

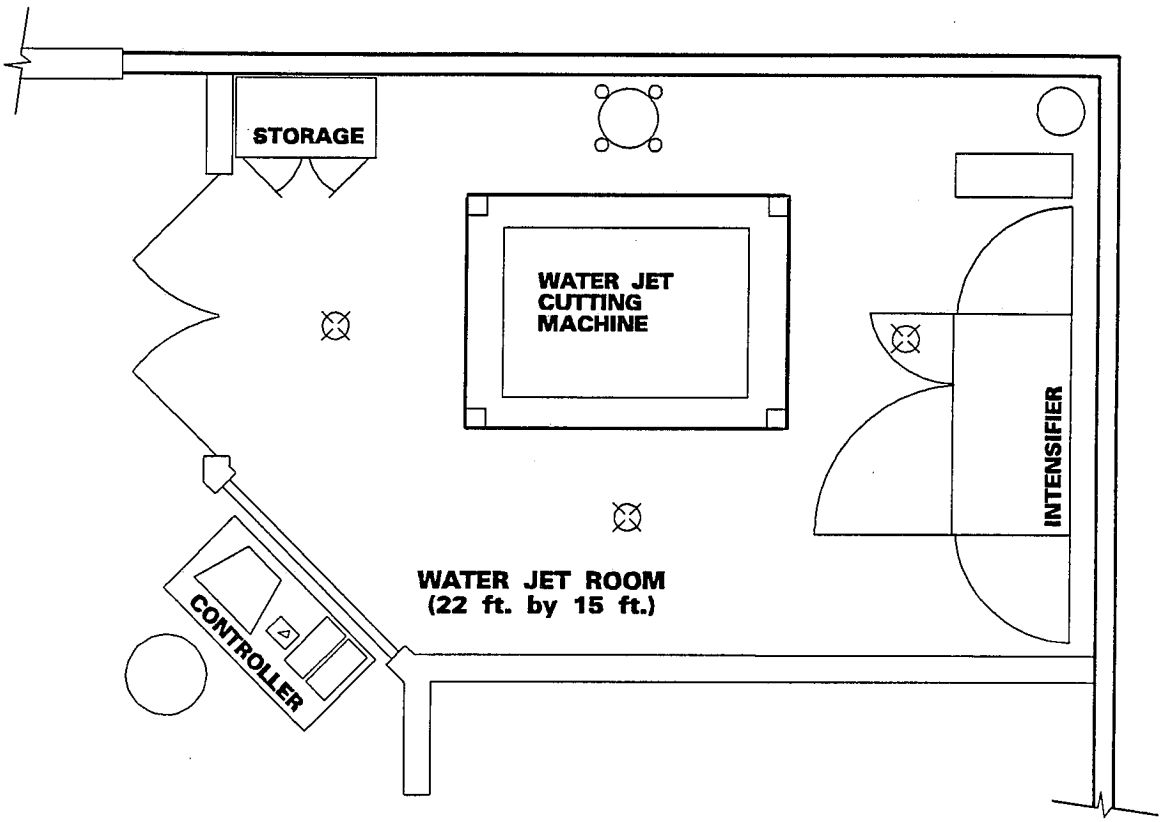

Figure 11 - Water Jet Room.

6th American Water Jet Conference
August 24 - 27, 1991: Houston, Texas

Paper 18

Procedure Optimization and Hardware Improvements in Abrasive Waterjet Cutting Systems

by,
Kathy Zaring, Manager, Shapecutting Systems
Glenn Erichsen, Research Engineer
Charles Burnham, Product Manager, Shapecutting and Abrasivejet

Flow International, Corp.
Kent, Washington
USA

ABSTRACT

Recent research in abrasive waterjet utilization has generated excellent product enhancements and methods for process optimization. Many hardware enhancements address the five axis, fully automated cutting market. Others minimize the operator intervention when piercing at low pressures with an AWJ system. While still others minimize the "ghosting" that can be seen on the surface of materials cut with an AWJ.

How to use the AWJ efficiently has also been addressed. A database consisting of optimum operating parameters and cut speeds is now available to lessen the learning curve for a new user and to help experienced users cut more efficiently and cost effectively.

Organized and Sponsored by the Water Jet Technology Association.

1.0 INTRODUCTION

Abrasive waterjet (AWJ) cutting works by combining a focused jet of ultra-high pressure (up to 379,212 KPa {55 kpsi}) water with granular abrasives to form an extremely powerful means of cutting and piercing virtually all hard materials, from metals and composites, to glass and ceramics.

AWJ technology has matured considerably over the past 2 years to become a widely used, reliable machining process. However, this relatively young process is still developing. Research and development continues to push the technology toward fully automated systems. The goal is to achieve the highest efficiency with no operator guesswork.

AWJ's offer many advantages over other non-traditional machining methods. These advantages include:

- Omnidirectional cutting capability to cut all types of materials.
- No heat affected zones on the cut materials.
- Low cutting forces; usually less than 2.27 kg (5 lbs) vertically.
- Generally fewer process steps.
- Smaller kerf width than plasma or routing.
- Tight tolerance cutting.
- Very simple or sometimes no tooling required.
- Reliable, repeatable part production.

This paper will give an overview of the components of an abrasivejet cutting system (minus the high pressure pumping system) and explain the function of each. It will then detail the options currently available to fully automate a multi-axis cutting cell. Other system enhancing options will also be detailed, including the FLOWpro cutting database and a dehazing device.

2.0 BASIC SYSTEM

The basic system components of an AWJ cutting system include the Abrasive Metering System and the Abrasive Cutting Head (**Figure 1**). Also necessary for an AWJ system is a catcher to confine and dissipate the spent abrasive jet. The components are integrated into any number of motion devices to produce the cut parts required for a variety of applications.

The Abrasive Metering System consists of the abrasive hopper, the abrasive, the abrasive metering valve, and the abrasive delivery line. The reliability and cutting efficiency of AWJ cutting is very dependent on the smooth operation of the metering system. The hopper stores the clean, dry abrasive for use when cutting. High quality, well screened abrasives are needed for consistent AWJ cutting. Wet or poor quality abrasives will have poor flow characteristics. Attached directly to the exit port of the hopper is the abrasive metering valve. Its function is to turn the flow of abrasive on and off, to meter the amount of abrasive used and to purge the abrasive feed line of any transient water when the abrasive waterjet is not in use.

Working in conjunction with the Abrasive Metering System is the Abrasive Cutting System (**Figure 2**). The Abrasive Cutting System consists of the abrasivejet cutting head, including the high pressure valve actuator, valve body, nozzle body extension tube, waterjet orifice, abrasive mixing chamber and mixing tube. The cutting head is pneumatically operated with its operation tied into that of the abrasive metering valve, i.e. when the cutting head is activated to begin the flow of high pressure water, the abrasive metering valve is opened to begin the flow of abrasive.

When the abrasive cutting head is actuated, high pressure water flows through the orifice into the mixing chamber and out through the mixing tube. As the water enters the mixing chamber, it creates an area of partial vacuum, which draws the metered flow of abrasive particles through the abrasive feed line and into the mixing chamber. The abrasive combines with the waterjet to create the high energy abrasivejet cutting stream. This stream exits the cutting head through the mixing tube. The mixing chamber assembly includes alignment screws and a gimballed mount. These alignment screws enable the user to quickly align the waterjet stream to the center of the mixing tube. The alignment is necessary to achieve the most powerful cutting stream and to maintain long mixing tube life.

Improvements in the rate of wear of the consumable materials of the abrasivejet cutting head have enhanced its use for continuous cutting and tight tolerance applications. Previous cutting head technology required the replacement of wear parts, particularly the mixing tube, and realignment of the cutting head generally every one to two hours, depending on the application and the cutting accuracy required. This frequent changing of worn mixing tubes required constant operator attention and necessitated much system downtime.

The greatly extended mixing tube life permits parts which are cut at the end of a shift to be within several thousandths of an inch tolerance to those cut at the start of the shift, without any adjustments to the machine tool for kerf compensation or numerous replacements of mixing tubes, as was previously required. This translates to less downtime per shift higher throughput potential and tighter cut part tolerances.

3.0 CATCHERS

Abrasivejet cutting develops a large amount of energy (up to 67 KW {50 HP}) at the cutting nozzle. As much as 75% of that energy may be retained in the stream after it has passed through a cut. Three basic type of catchers are available to dissipate this energy. They are room catchers, tank catchers and compact catchers. Each catcher dissipates the remaining energy of the abrasivejet stream and collects the spent abrasives and kerf material.

A tank catcher is a large steel container permanently positioned beneath the work surface within the work area of the AWJ motion equipment. Tank catchers are supplied for applications where the work piece is stationary and the end effector is mobile and capable of horizontal or near horizontal cuts such as a 2- or 3-axis gantry robot.

Tank catchers are filled with at least 50.8 cm (20 inches) of water to absorb residual energy. Tank catchers can also be filled with other energy absorbing media in addition to the water. The typical energy absorbing media used for these catchers is steel balls. The combinations of energy absorbing media and water is preferred over only water in installations where quieter operation is required. Tank catchers also have material supports which can be as simple as resting the material directly on the steel balls or as elaborate as dedicated palletized fixturing.

When using a standard tank catcher, the spent abrasives and kerf material will settle out and remain in the tank, while the water drains off. The tank must then be cleaned manually as it fills with solids. This clean-out requires that the system be shut down until cleaning is complete. Frequency of cleaning varies based on system usage.

The largest breakthrough in catcher technology has been in the emergence of the self-cleaning catcher (**Figure 3**). This catcher is used for work envelopes anywhere from 45.72 cm x 45.72 cm (18 inches x 18 inches) to 1.83 m x 3.05 m (6 feet x 10 feet). The system consists of a catcher tank with a properly sloping bottom. This sloped bottom tank is filled with water (and at the discretion of the user, a layer of steel balls). The spent abrasive and kerf materials drain out of the catcher along with the cutting water. These materials then go through a particulate separation device where the abrasive particles settle out and the clean water is drained off. The clean water is pumped back into the catcher to provide a constant supply of flush water, while the solids are dropped into a holding drum. Any excess clean overflow water is directed to drain. When the holding drum becomes full, it is removed and replaced with an empty drum. Drums are changed easily and no system downtime is required.

This catcher technology is very user friendly and useful for all types of cutting applications. It makes the disposal of spent abrasive a much less time consuming and labor intensive job. It also facilitates the disposal of hazardous waste material if what is being cut is considered a hazardous waste.

Compact catchers (**Figure 4**) are small containers filled with energy absorbing media, typically stainless steel balls. These catchers are usually mounted to move with the cutting head via a "C" frame bracket and are used primarily in 3-dimensional machining. After the abrasivejet stream passes through the workpiece, it enters the catcher and strikes the steel balls, sending them into motion. The continuous collision and agitation of the balls effectively absorbs and dissipates residual abrasive waterjet energy. The catcher bodies are not wear items, but the stainless steel balls are. The steel balls are consumed at a predictable rate and are automatically replenished from a small reservoir on the catcher.

The process waste produced by AWJ cutting is a slurry consisting of water and solid sediments, which are minute particles of abrasive grit, kerf material and catcher ball fragments. To prevent the slurry from separating and clogging the outlet drain of compact catchers, a vacuum and waste separation system is supplied to constantly evacuate process waste and transfer it to a waste separation and disposal system.

Compact catcher bodies are designed as small as possible in order to function in tight spaces. Compact catchers are ideally suited for robotic applications where a low profile cutting head is necessary. Following special operating procedures also allows use of compact catchers in non-horizontal cutting applications.

4.0 OPTIONS FOR FULL SYSTEM AUTOMATION

When integrating an AWJ onto a robotic system, care must be taken to assure proper operation of both the abrasive metering system and the abrasive cutting head. A number of system options exist that are well suited for multi-axis cutting installations to make them as automated and trouble free as possible.

Currently available is an Automated Metering Valve. Its function is the same as that of the standard manual valve, that is, to turn off and on the abrasive flow and to meter the amount of abrasive used for cutting. This metering valve, however, makes use of a servo motor to position the opening of the valve to flow the proper amount of abrasive for the cutting application. This automatic positioning can be programmed into the cutting program directly on the controller of the robotic system. The operator need never to touch the valve for adjustment, but will adjust the flow as he would another machine axis.

Also available is the Abrasive Loss of Flow Switch. This switch is tied into the abrasive feed system and indicates when abrasive flow has been interrupted for any reason. This interruption can trigger a system shut-down or sound a warning, before any workpiece damage can occur, whichever the user desires. The indication of loss of abrasive flow is invaluable when cutting laminated or brittle parts.

Another system enhancement available is a Bulk Abrasive Transfer System. This system transports abrasive from a large storage hopper to a smaller metering hopper situated relatively close to the abrasivejet cutting head. A bulk transfer system is especially useful when the size of the cutting system is large and the hopper, in order to be near the cutting head, is inaccessible. The system contains sensors to indicate low abrasive levels in both the metering hopper and the storage hopper. When the metering hopper is low, the abrasive is transported from the storage hopper with the use of compressed air. A batch of abrasive drops into the transporter and is pushed through the system piping to the metering hopper with the use of low pressure compressed air. The low pressure minimizes component wear from the abrasive particles. A hopper close to the cutting head has the advantage of providing consistent abrasive flows for all required cutting parameters.

Finally, the ideal tool for multi-axis cutting systems is the pre-aligned Paser abrasivejet cartridge. This tool has been developed to cut the amount of operator involvement with the cutting system to a minimum and improve part production accuracy. This part is simply attached to the extension tube of the abrasivejet cutting head and cutting can begin. No alignment of jet stream to mixing tube is necessary. The tool center point (TCP) remains consistent from one Paser abrasivejet cartridge to another, thus making it indispensable for 3-dimensional cutting.

5.0 PART QUALITY IMPROVEMENTS

For those applications where the surface frosting created during AWJ machining is unacceptable, a new device is now available. It is called the Paser Dehazer. The Dehazer easily attaches to the cutting head and works by surrounding the cutting stream with low pressure water. This minimizes the surface frosting by stripping away the low powered shroud that surrounds the high velocity abrasivejet stream. The Dehazer also has the added benefit of minimizing noise and airborne abrasive grit. The Dehazer is especially useful when cutting glass, brass, marble or any material with a shiny surface.

6.0 DATABASE DEVELOPMENT

A large emphasis has been placed on improving the components of the abrasive waterjet system. Equally important is the need to understand the proper way to operate an abrasive waterjet effectively for each application.

There are many variables that affect the performance of an AWJ cutting system. Among the most important are water pressure, abrasive flow rate, abrasive type, waterjet orifice (jewel) size, mixing tube geometry, the type of material being cut and the material thickness. Because these variables may be adjusted over a wide range of values, it is possible to operate an AWJ in a very inefficient manner.

To assist AWJ users in running their system effectively, a computer software tool called FLOWpro has been developed. The FLOWpro software offers AWJ users a simple yet powerful means of determining how to adjust an abrasive-waterjet cutting system for superior performance. The software accomplishes this with four main features:

1. Recommended AWJ cutting data for commonly cut materials. The cutting parameters as listed in FLOWpro are a list of process parameter settings, resulting cut speed and surface quality for a variety of common materials. If a user is going to cut 2.54 cm (1 inch) thick stainless steel, they just look up the data in FLOWpro and it tells them exactly how to cut it.

   The data is given for:

   - Material thickness ranging from 0.154 cm to 5.08 cm (.060 inches to 2 inches)
   - Water pressure in both 275,862 KPa (40 kpsi) and 344,828 KPa (50 kpsi)
   - Cut speed of quality cut and separation cut
   - Three standard jewel/mixing tube combinations

2. FLOWpro allows a user to add their own materials and settings. The user data is then merged with the Flow supplied data, ready to be referenced again at any time in the future.

3. A dual bar-graph compares costs per inch of cut to cut speed. Here, the user can very quickly see how much it costs per inch to cut his material with the Paser II abrasive waterjet system. The costs are accurate because users input their own labor, power, water, pump and abrasive costs.

4. FLOWpro also includes a method for storing client and part information. This allows the users to list all their customers, the jobs performed and the parameters previously used to cut the materials for those jobs. Everything needed to run a repeat job is at their fingertips.

Because the number of process variables and their possible ranges are so great in an AWJ system, it is important to find a way to optimize the cutting process. Through experience from theoretical insight and empirical testing, the range of the variables has been dramatically reduced to allow a user to begin cutting in a practical and efficient manner. The settings listed in FLOWpro were selected to give an optimum cutting speed in a cost effective manner. These settings were arrived at through months of testing and empirical analysis of the AWJ cutting process.

For example, the size relationship between the jewel and mixing tube is very important. A mixing tube that is too large coupled with a jewel that is too small will not allow the abrasive to be accelerated properly. The inverse condition of a mixing tube that is too small coupled with a jewel that is too large will create frictional drag losses and poor abrasive entrainment. The jewel/mixing tube combinations listed in FLOWpro have been chosen to balance these two effects.

Most importantly, the abrasive flow rate, water pressure, orifice size and material thickness have been matched to give the highest cutting speed at the lowest cost.

The experience and knowledge incorporated into FLOWpro can dramatically reduce the time it takes to get an AWJ system operating efficiently. Combined with recent hardware improvements, FLOWpro will help in the continuing advancement of AWJ technology.

7.0 CONCLUSION

Abrasive waterjet cutting continues to grow and is coming into its own as an alternate machining method. With recent improvements, we are one step closer to the reality of full automation with abrasive waterjets. Future research and product development will continue to address the issues of user friendliness and full automation. This powerful process will continue to grow and mature in the coming years.

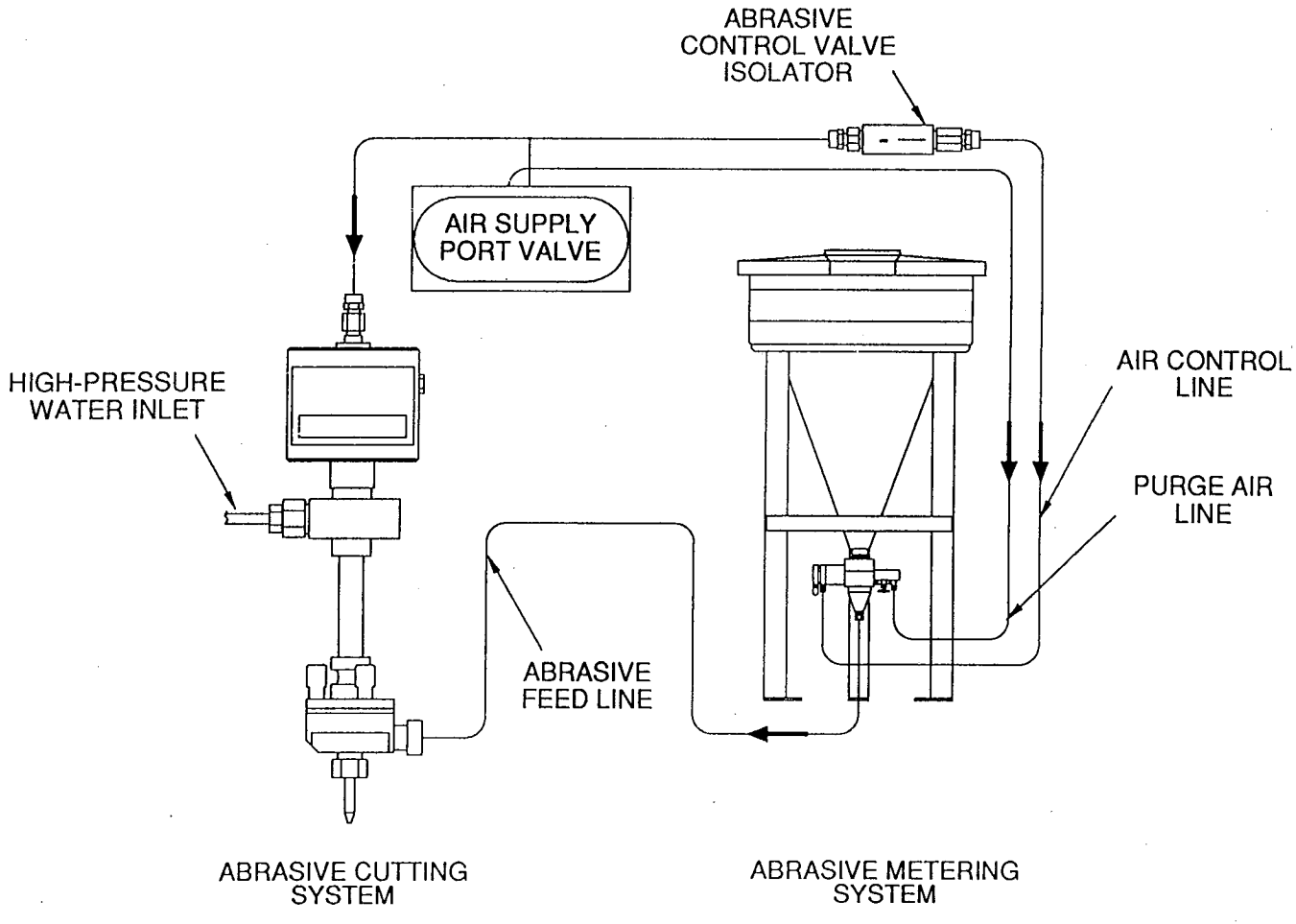

Figure 1 System Package Abrasive Waterjet

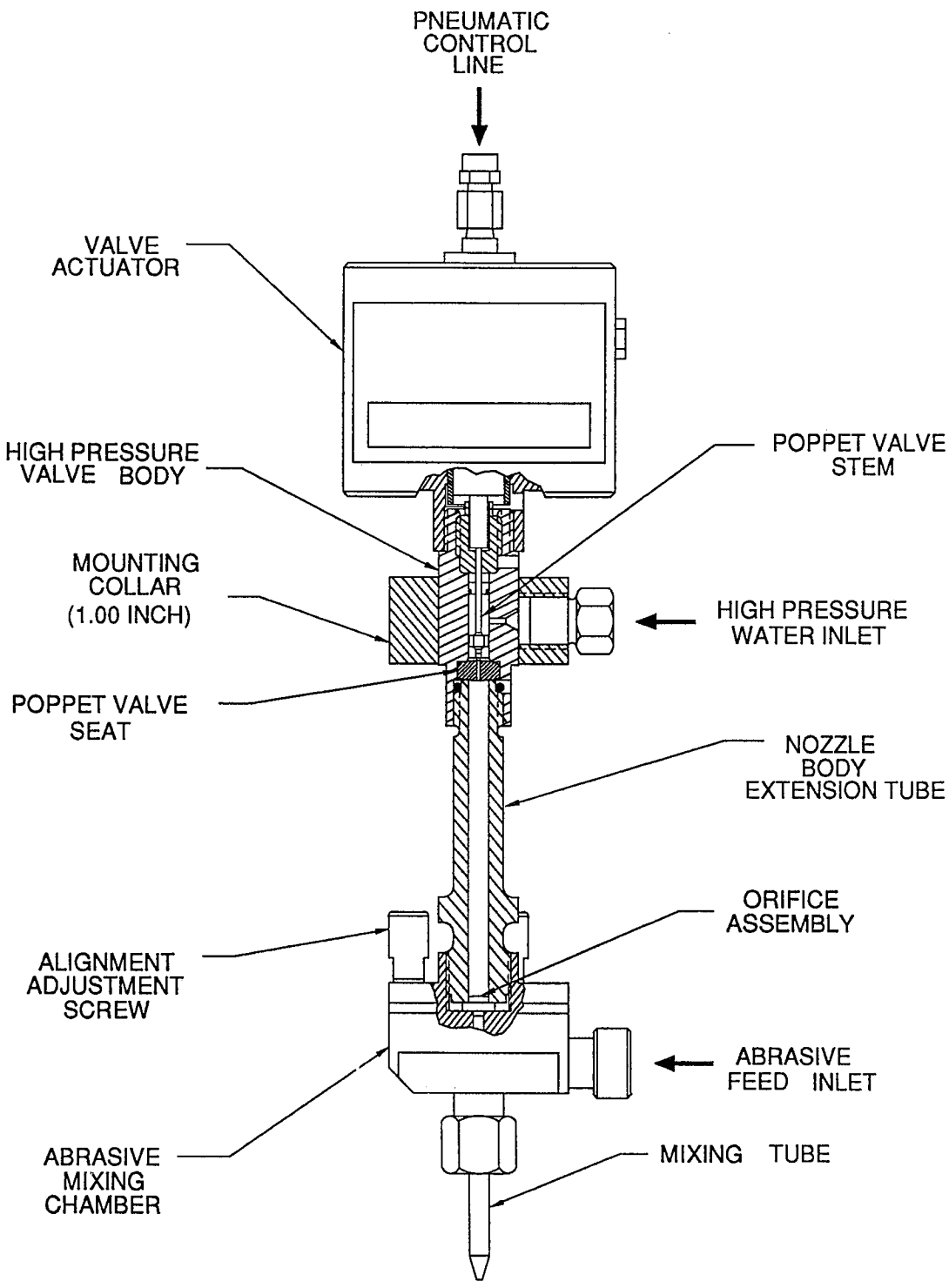

Figure 2 Abrasivejet Cutting Head

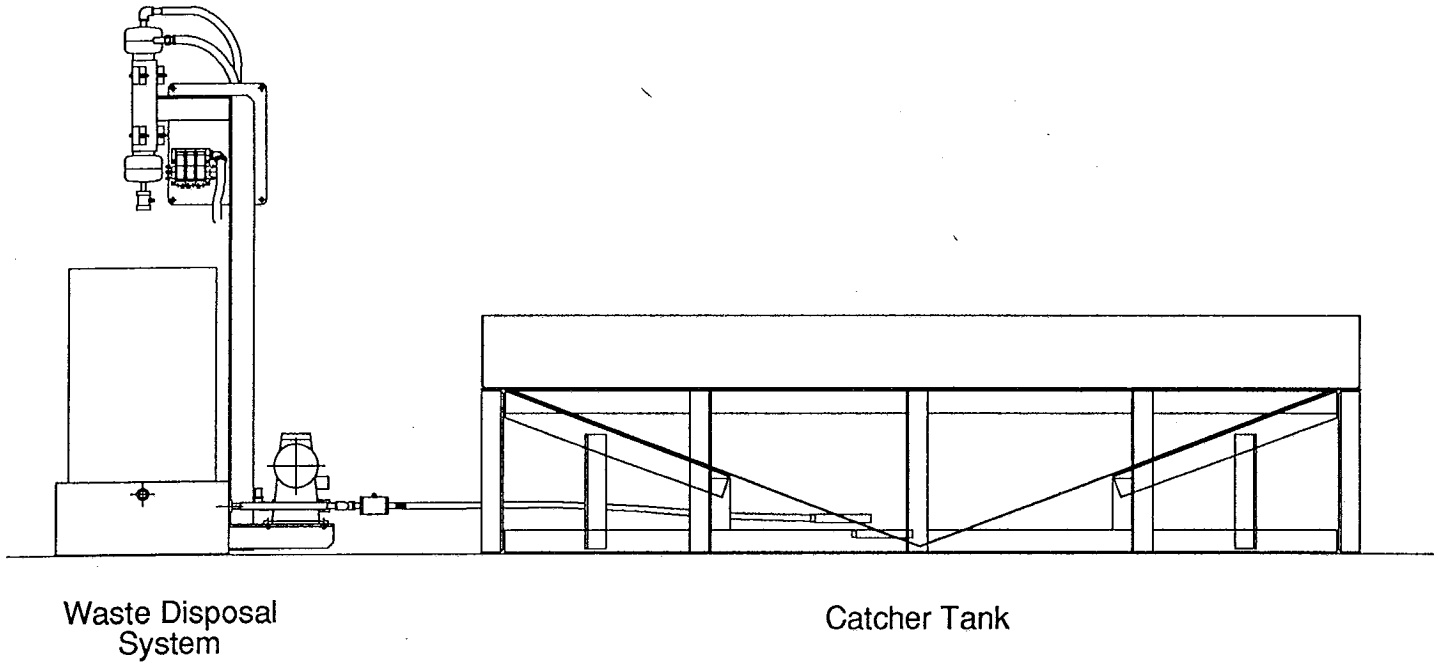

Figure 3 Self-Cleaning Catcher System

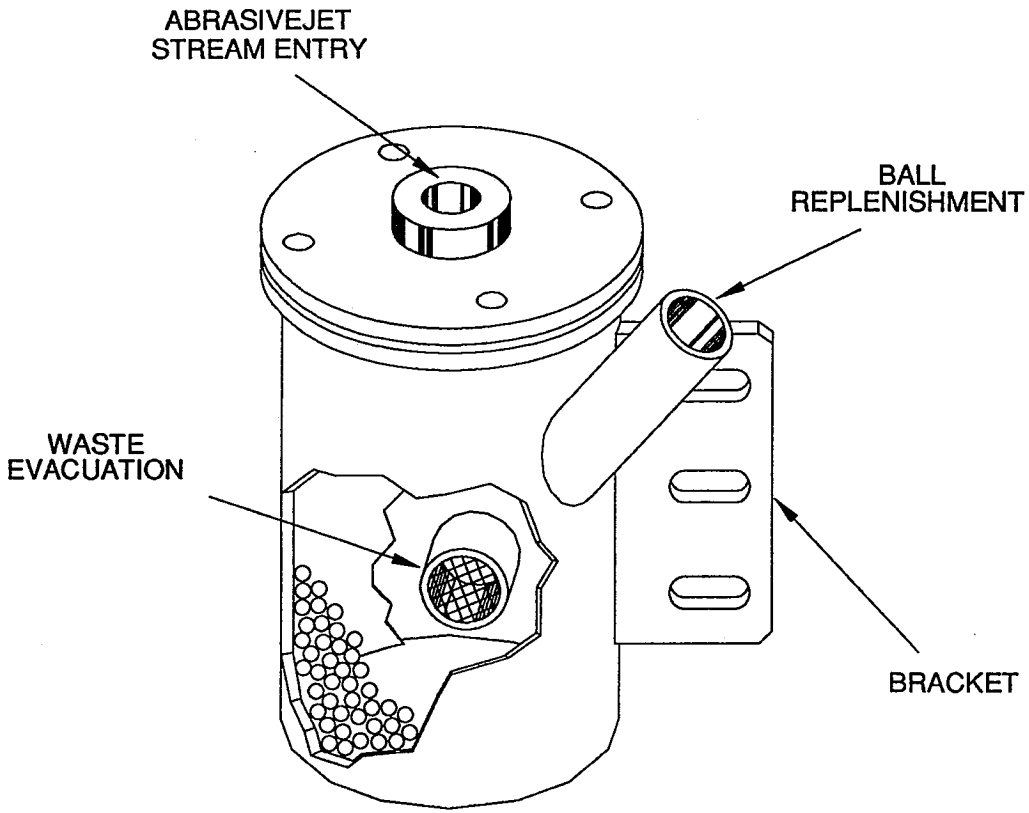

Figure 4 Compact Catcher

6th American Water Jet Conference
August 24 - 27, 1991: Houston, Texas

Paper 19

Water Treatment Process for Waterjet Cutting

Robert Mc Faul
Culligan International Company, USA

ABSTRACT

Because water is exiting the orifice at about three times the speed of sound, the quickest way to destroy an orifice is to have any type of suspended solids flow through it. While OEM's provide a 10-5-1 micron filter piped in series to combat this, other treatment of the raw water is required. Therefore, this paper will focus on the three major processes that are being used for this application - Softening - Reverse Osmosis and Deionization.

Water is such an important element in waterjet cutting that one would think that the industry would have established standards on water quality. If this were the case, water treatment systems in use throughout the industry would produce water that meets said standards. Unfortunately, such is not the case. An industry observer soon learns that there are variations of water treatment systems in use, with many of them not providing the level of water quality needed to keep systems operating efficiently. These inefficient systems can and do cause waterjet orifice clogging that results in high orifice replacement costs, intensifier pump replacements, check valve problems, reduced pump seal life, and production line downtime that can run costs -- as high as $20,000 to $30,000 per day!

It seems a fairly simple problem to solve, and it is. Right now, what the industry needs more than anything else is education on the types of equipment needed to produce the water it requires. While the waterjet cutting industry is relatively in its infancy, water treatment is a mature business. Sizing and specifying the right system is a fairly easy job for water treatment manufacturers. They know the treatment processes to be used, and can design a system to meet any waterjet cutting need.

First of all, all water is not alike. It may look the same and feel the same, and unless there is something drastically wrong with it, it usually tastes the same.
But similarities end there. In the laboratory, under analysis, we can find more differences in water supplies than most of us ever imagined. It is a routine procedure to identify the impurities and contaminants in water that cause problems in waterjet cutting.

Every water supply has something in it besides two parts hydrogen and one part oxygen -- H-2-O. Water may contain suspended particulate matter; dissolved minerals such as sodium, calcium and magnesium; iron; chlorides and nitrates, plus a variety of toxic substances too numerous to mention.

The two major types of contaminants that cause problems for waterjet cutting are particulate matter (sediment) and the total dissolved solids, primarily calcium and magnesium. In the water treatment industry, total dissolved solids are referred to as TDS. Particulate matter causes rapid orifice wear. Dissolved solids clog orifices and render them inefficient. The orifices themselve cost money, but much less than the cost of high rejects, and nothing compared to the high costs of production line downtime, a cost that no plant can afford.

It is well recognized that clogged orifices are a problem. Perhaps not so well known is how fast this problem can occur, and how much damage it can cause. Figure 1 is therefore very enlightening.

This is an orifice that has operated for 34 hours on untreated water drawn from a tap in a municipal water system, in other words hard water. More specifically, the water hardness in

this case was 8 grains per gallon (GPG). As you can see, the orifice is almost completely clogged.

Figure 2 shows an orifice that has operated for 78 hours on softened water. One might think that softening the water would solve the problem of nozzle clogging. Not so. This orifice will cause rejects.

A third example is in Figure 3.

This orifice has operated for more than 200 hours using deionized water. It is still clean and open, and can provide full water flow for precise, efficient cutting.

The difference in the three nozzles reflects the difference in water quality -- essentially the difference in the total dissolved solids, or TDS of the water. Premised upon customer history, when high total dissolved solids are present, there is little difference in orifice life whether the orifice is a man made sapphire or diamond.

All water contains a certain amount of TDS. Municipal treatment systems filter and chlorinate the water, but they do not reduce TDS.

High water pressures and small waterjet cutting orifices used in this industry create a need for water with low particulate matter - sediment - and low TDS. To remove particulate matter, waterjet cutting systems manufacturers typically provide cartridge filters, usually a set of 10, 5 and 0.5-micron prefilters connected in series.

Filtering the water removes particulate matter only. And as shown in Figure 2, softening the water does not solve the problem either. The orifice in Figure 2 was almost completely clogged after 78 hours of operation.

Why doesn't filtering and softening do the job?

Neither softening nor filtration reduce the dissolved solids content of water. Water softening is done by a process called ion exchange, in which hard dissolved minerals such as calcium and magnesium ions are exchanged for the soft dissolved mineral sodium. And since this exchange takes place on a one-for-one basis -- one soft ion for one hard ion - the <u>total</u> dissolved solids content of the water does not change.

The orifice in Figure 1 operating on untreated water was clogged because minerals in the water build up scale in the orifice. This happens because dissolved minerals precipitate out of water and become firmly attached to the surfaces of anything they contact. The orifice operating on softened water lasted longer but was well on the way to clogging after 78 hours. Soft minerals won't build up as fast, but eventually they do cause problems.

The orifice in Figure 3 did not clog because there were virtually no dissolved minerals in the water to precipitate out and build up mineral scale. The water was deionized, a process that removes both the hard and soft dissolved minerals from water. Like softening, it is an ion exchange process, but through the use of different kinds of water treatment resins, deionization provides a solids-free water.

Another water treatment process that produces solids-free water is reverse osmosis. Like deionization, it can keep the orifice cutting sharply and cleanly, make them last longer and provide the benefits of high quality water. One supplier states as a rule of thumb that an orifice life is extended 10 times when quality water is used.

That brings us to the bottom line -- if users of waterjet cutting systems are to get the maximum benefit from their systems, reduce orifice replacement cost, lower pump seal cost and keep rejects low and production high, proper water treatment is mandatory.

Especially for applications like waterjet, there is a definite correlation between water quality and overall profit.

There are four basic water treatment process that the waterjet user should consider: filtration, softening, deionization and reverse osmosis.

FILTRATION The filter elements supplied to O.E.M.'s that were previously mentioned do an effective job of removing particulate matter that can damage waterjet orifices. However, if the supply water has large amounts of suspended matter (turbidity), a larger filter should be considered.

Most commercial/industrial filters use the multi-media principle called depth filtration, in which several layers of different types of media are contained in the same filter tank as shown in Figure 4.

Typically, a depth filter will use four such layers, and starting from the top down, each layer is finer and heavier and has a higher specific gravity. A light top layer of coarse material traps large particles. The second layer traps smaller particles and the third and fourth successfully trap smaller particles. Therefore, the entire filter bed is being utilized.

Depth filters can trap particles as small as 10 microns. Using filter aids such as coagulants, they can trap particles as small as one micron.

When a depth filter is saturated it is regenerated, usually on a time basis or pressure differential basis. Backwashing flushes particulate matter from the tank and makes the filter ready for use again. Since the various media layers are of different weight and specific gravity, they automatically restratify themselves after the backwash cycle. The filter is then put back on line.

Depth filters come in various tank sizes from 7 to over 100 inches in diameter. The size to be used depends on the gallonage requirements of the waterjet cutting system. Figure 5 summarizes the characteristics of depth filtration.

Due to extreme water conditions, two other types of filtration should be mentioned. The first is carbon filtration, (shown in Figure 6), which is primarily used for removal of tastes and odors from water. These associated problems are typically caused by organic material in the raw water. The second is green-sand filtration which is used when iron and manganese are present. The result to the end user is staining, even though the water may appear to be clear.

SOFTENING As mentioned, softening is not recommended as the sole water treatment process for the waterjet cutting industry.

However, it is often recommended as a pre-treatment step for deionization or reverse osmosis systems.

In terms of defining when is water hard, the following classifies water hardness, compliments of the U.S. Department of Interior. Their breakdown in grains per gallon are as follows:

Less than 1 - Soft
1 - 3.5 - Moderately hard
3.5 - 7.0 - Hard
7.0 - 10.5 - Very hard
10.5 & Above - Extremely hard

A discussion of the fundamentals is therefore in order. A softener's function is to remove the hardness from water.

Hard water is defined as water that contains dissolved calcium and magnesium, minerals that are found in the earth and that dissolve into the water supply. Well water usually has a higher hardness than surface water from rivers and lakes, but most water supplies contain some hardness.

Hardness can be measured as grains per gallon, milligrams, per liter or parts per million. One grain per gallon is roughly equivalent in weight to a grain of wheat, hence the term. One milligram per liter and one part per million are roughly equivalent to each other, and the terms are used interchangeably in the water treatment industry. One grain is also equal to 17.1 parts per million or 17.1 milligrams per liter. More precise measurements of waterborne contaminants, such as iron or sulfur, are stated in parts per million. Modern analytical instruments also routinely measure in the parts per billion range, for water that must be ultrapure for use in pharmaceuticals, kidney machines, electronics, and so on.

Ion exchange softeners consist of a resin tank to hold the ion exchange resin, a brine tank that contains salt for softener regeneration and a control valve.

In operation, water flows down through the resin bed, an artificial plastic material made of millions of tiny beads. As the water passes across the beads, the calcium and magnesium, which have positive charges, are attracted and held by negatively charged exchange sites on the porous resin beads. In turn, the sodium ions on the beads are released and pass into the water supply, which is why softened water contains sodium. The amount of sodium released is equal to the amount of combined calcium and magnesium, since the ion exchange process takes place on a one-for-one basis.

The time will come when the beads have no more sodium ions and cannot absorb any more calcium or magnesium ions.

At this point, the resin bed is exhausted and must be regenerated. Regeneration is done with a brine solution, prepared in the brine or salt tank. Since salt is sodium chloride, during regeneration the sodium ions replace the calcium and magnesium ions on the beads, and the resin bed is once again ready for service.

The regeneration process in most softeners is performed by automatic controls and valves, but can be overridden manually. Most controls operate on a time basis and also are available to regenerate on a volume basis. In addition, sensors are employed in more sophisticated softeners which compensate for variations in water usage or water hardness.

Softening is sometimes used to provide softened water to the deionizer. This increases the service cycle life of the deionizer, thereby fewer deionizer regenerations. This practice saves money; it is less expensive to regenerate a softener with salt than a deionizer with chemicals. Softening can also be used as pre-treatment for a reverse osmosis unit. Hardness minerals in unsoftened water can scale up reverse osmosis membranes, causing premature membrane replacement, which increases RO system operating costs.

Another consideration is if the waterjet cutting machine is on an application that operates 24 hours per day, a duplex softener should be installed. The reason for this is that when a softener is in its regeneration cycle - approximately 70 minutes - the raw water is sent to service. Therefore, the only way you can be insured of a constant supply of soft water, is to have a duplex system. Duplex systems are inter-wired so that only one softener can be regenerated at a time.

Ion exchange softeners remove more than hardness minerals from water.

They also remove small quantities of iron, barium, manganese, naturally occurring radium 226 and 228, cadmium, lead and silver.

In terms of performance, most ion exchange softeners reduce hardness to less than one grain per gallon, a level that is relatively harmless in most industrial equipment.

DEIONIZATION Deionizers also use the ion exchange process, but are more sophisticated than softeners. Whereas a softener uses one resin only, a cation resin, a deionizer uses both a cation and an anion resin.

A two-tank deionizer (Figure 7) contains cation resin in the first tank and the anion resin in the second tank. As water passes through the cation resin, which is in hydrogen form rather than the sodium form used in softeners, the various cations such as calcium, magnesium, iron, etc., are removed and replaced by free mineral acidity, or FMA. The water then passes through the anion unit, where anions such as chloride and sulfate are removed and replaced by hydroxide. FMA and hydroxide combine to form water, now free of all ionic impurities.

There are other deionizer arrangements, such as a two-bed strong base anion resin, a two-bed weak base, and mixed bed. Strong base and weak base resins have different chemical formulations, to do different jobs.

A weak base anion resin does not remove silica or carbon dioxide from the water. It produces water with a qualilty of about 50,000 ohms specific resistivity, and a pH slightly below 7.

A strong base resin removes both silica and carbon dioxide, produces a water with a quality of up to 200,000 ohms specific resistivity, and a pH of 7.5 to 9.5.

Obviously the choice of which resin to use, strong or weak base, depends on the chemistry of the incoming water and the desired quality of the product water. Weak base resins cost less, so there is no need to use strong base resins if silica or carbon dioxide are not present in the water supply.

In a mixed-bed deionizer, both the cation and anion resins are mixed in the same tank. Instead of one contact with the cation and anion resins, there are literally millions of contacts with both types of resin, with the ion exchange process taking place with each contact. In effect, it is like passing the water through a multitude of two-tank deionizers. Predictably, mixed-bed deionizers produce water of much higher quality than two-bed deionizers, from one million to 18 megohms specific resistivity.

Water quality can also be measured in parts per million of dissolved solids. Deionizers can be equipped with a TDS monitor that provides a continual readout of this measurement. It should be mentioned about the piping system materials. Pure water applications such as deionizers, are very sensitive to piping materials. Without proper piping selection the end user could be adding back impurities into the treated water supply. Basically, the downstream service piping for the deionized water must be corrosion resistant material. This may consist of PVC, stainless steel or other corrosion resistant piping.

REVERSE OSMOSIS Reverse osmosis is an amazingly simple process of producing high quality water. Water is forced under high pressure through a semi-permeable membrane, which traps particulate and dissolved matter and washes them away to drain, while separating the purified water for use.

In the natural osmosis that occurs in nature, osmosis is the passage of a liquid through a membrane from a state of low concentration of solids to a state of high concentration. A tree leaf, cells in the human body, the liver, all use natural osmosis.

But to purify water, it is necessary to change the water from a state of high concentration to low. The osmotic process must be reversed.

That is what happens in an RO unit as shown in Figure 8.

Feed water is forced under high pressure through a membrane, usually a film wound on a perforated plastic tube. Product water for use, called permeate, enters the tube and is piped to service. Water that contains the rejected impurities, called concentrate, is piped to drain.

Reverse osmosis achieves about 97 to 98 percent rejection of solids from the incoming water supply. A reputable manufacturer of reverse osmosis systems will guarantee a rejection of over 95%, and in practice, rejection levels are above that. A reverse osmosis system is also very effective in removing virtually all suspended matter plus various bacteria and other micro-organisms. The amount of solids left in water after reverse osmosis treatment depends on the amount of solids in the incoming water, a fact revealed by the water analysis.

For example, much of Southern California receives their water from the Colorado River supply which has a TDS that typically runs about 500 part per million (PPM). The product water supply from a reverse osmosis system will have a TDS of under 10 PPM, or less than one half a grain per gallon.

Thus, either deionization or reverse osmosis can produce water of sufficient quality for the waterjet cutting industry. If the ultimate in water quality is required, a water treatment system may incorporate depth filtration, softening, reverse osmosis, deionization and even sub-micron filtration. The systems approach can be costly, and should be used only if engineering studies indicate a strong need for it.

It is obvious that because of the choices involved, users should deal with suppliers that provide all types of water treatment systems and use all known processes, so that objective recommendations can be made. For example, a supplier that offers deionizers only will recommend deionization, not because that is what is needed, but because that is what the supplier provides.

It is just as important to select a supplier who can provide service locally. Irrespective of the manufacturer, water treatment systems do require maintenance from time to time, and it is vital that their operation be continuous. Water treatment system downtime translates to production line downtime.

Just as obvious, some engineering evaluations are required in order to determine the answers to the question of which type and how much water treatment is required. Such evaluations must consider:

1) water chemistry
2) the water treatment process or combination of processes to be used
3) the economics of water treatment

To determine water chemistry, a water analysis is needed. This is absolutely a must, because without it no feasible determination can be made as to if a water treatment system is needed, and if so, what type of system best suits the analysis. Most manufacturers of water treatment systems provide analytical laboratory services, and most are reliable. If in doubt, the prospective buyer can always have water analyzed by an independent laboratory. It is recommended that the laboratory chosen be certified by the state Environmental Protection Agency.

Water analysis should be studied for validity. Some checks to make include:

1) total hardness must equal total calcium and magnesium, usually expressed as MG/L or GPG.
2) total cations and total anions must be within 10 percent of each other.
3) the analysis should include deionizer calculations.

Another factor to look for in water analysis includes the amount of turbidity, which is an indication of the suspended particulate matter.

The analysis should show the pH of the water. The pH scale runs from 0 to 14, with 7.0 being the numerical neutral point. Low pH waters are acidic and corrosive; high pH waters are alkaline and tend to build up scale faster. Hopefully, any variation from neutral should be slightly toward the alkaline side because scale is easier to tolerate and correct than corrosion. Chemical feeders or neutralizer filters that maintain pH at acceptable levels may be required in certain situations.

It is recommended that free chlorine be tested on site, since chlorine escapes from water samples sent to laboratories. High amounts of chlorine typically require the use of an activated carbon filter.

In an RO system, from one third to two thirds of the water passing through the system is sent to drain, depending on the recovery rate of the RO system. That water cost must be figured as part of the operating costs. Some users are able to recycle that water for other uses, and in such cases it should also be part of the calculation.

Reverse osmosis modules must eventually be replaced and this cost must be factored into the equation. As a general rule of thumb, the higher the TDS of the incoming water, the more economical it is to use reverse osmosis to produce high quality water. The reason is that the cost of regenerant tank exchanges or the cost of operating an on-site deionizer becomes high enough at a certain point to warrant buying a reverse osmosis system. One recent trade publication documented that based on per 1000 gallons, RO costs less per gallon than DI whenever the TDS is 200 PPM or above.

Since both deionization and reverse osmosis provide the water quality necessary in waterjet cutting, the following are the major benefits of the two systems.

DEIONIZATION

- 100% removal of Total Dissolved Solids
- Produces gallon of good water for every gallon used
- Mineral bed life longer than membrane life
- Requires less space than reverse osmosis

REVERSE OSMOSIS

- Lower operating cost
- Effective in organic and micro-organism removal
- Less aggressive than deionized water
- More stable pH and consistent quality
- Does not require handling hazardous chemicals (vs automatic deionization)

The waterjet cutting industry is in need of water quality standards, similar to those used by the American Society for Testing Materials, the U.S. Pharmacopoeia, plus other associations in the the electronic and medical communities. As more is learned about the effects of water on the industry, that knowledge should be gathered by an industry committee for the purpose of creating and promulgating a water quality standard. Representatives from the water treatment industry should be members of such a committee.

The benefits of an industry standard would be to simplify the design and selection of water treatment systems, and to provide members of the waterjet cutting industry a guideline on desired levels of water quality. It is hoped that this paper will serve as a base of knowledge from which a Waterjet Water Quality Standard can be created for all to use, and from which all can benefit.

The water analysis provides instant clues as to whether some water treatment processes should be employed in the system - depth filters, activated carbon units or pH control equipment.

In any case, the major decision is whether to use deionization or reverse osmosis as the principal treatment process. Both produce high quality water with TDS approaching zero, and both provide water that is free of other contaminants harmful to waterjet cutting systems. If the decision is made to use deionization, another decision must be made, either an automatic on-site deionizer, or exchange service deionizer tanks.

The principal costs of an on-site deionizer are the initial purchase price, cost of regenerant chemicals, cost of water used in the backwash/regeneration cycle, neutralization and labor. Deionized water can also be provided by exchange service deionizer tanks known as portable exchange or PE tanks. These are usually 9, 12 or 14-inch cylinders that measure about 44 inches high, and are supplied by a local water treatment dealer in quantities sufficient to meet the volume demands of the user. The dealer periodically picks up tanks from the user, leaves freshly regenerated tanks in their place, and takes the exhausted tanks back to his plant for regeneration.

The user pays for such services according to the number of tanks used, the number of regenerations required, the volume of water used on a cost-per-gallon basis, or a combination of these factors. Probably the biggest advantage of using exchange service tanks is that the user does not have to handle regenerant chemicals and thereby, there is no possible disposal problem. Also, there is no cost for chemicals or labor. These costs are all built into the water treatment dealer's charges, but the use of exchange tanks greatly simplifies both the mechanics and accounting of obtaining high quality water. The cost of using exchange service tanks includes:

1) monthly rental per tank
2) regeneration charges
   --or--
3) cost per gallon of water used

If water is paid for by the gallon, that cost can range from 3 cents to 40 cents per gallon, depending again on local factors and water chemistry.

The costs of using reverse osmosis includes:

1) acquisition cost of the RO unit
2) electrical operating cost
3) water cost
4) eventual module replacement cost

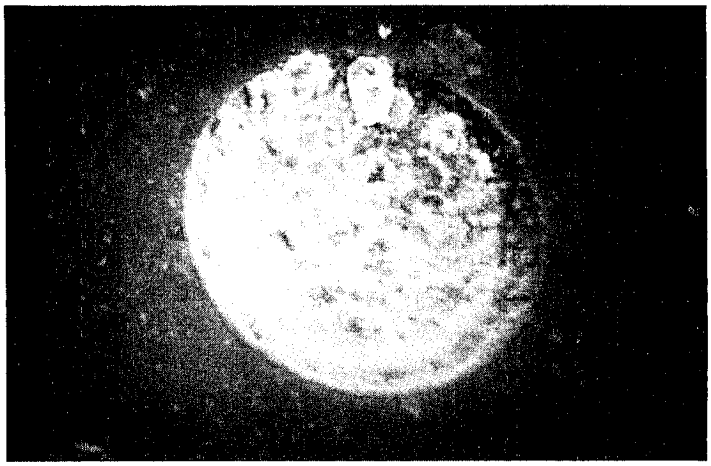

Figure 1. Orifice operating on untreated water after 34 hours.

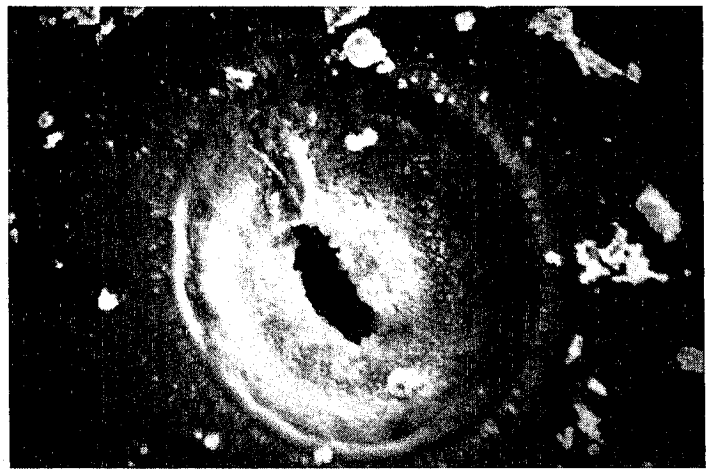

Figure 2. Orifice operating on soft water after 78 hours.

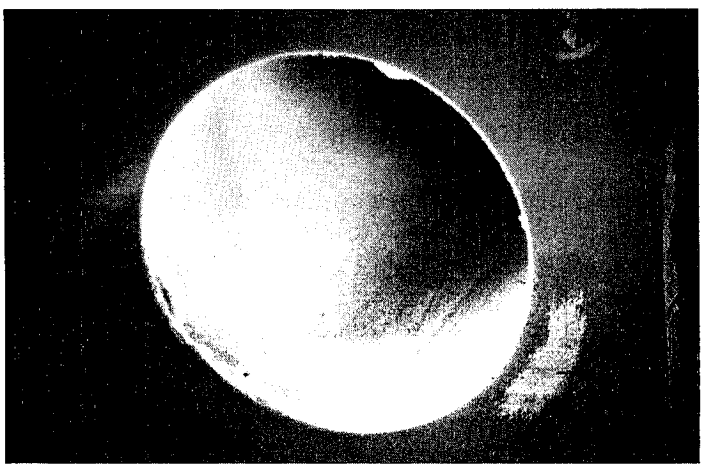

Figure 3. Orifice operating on deionized water after 200+ hours.

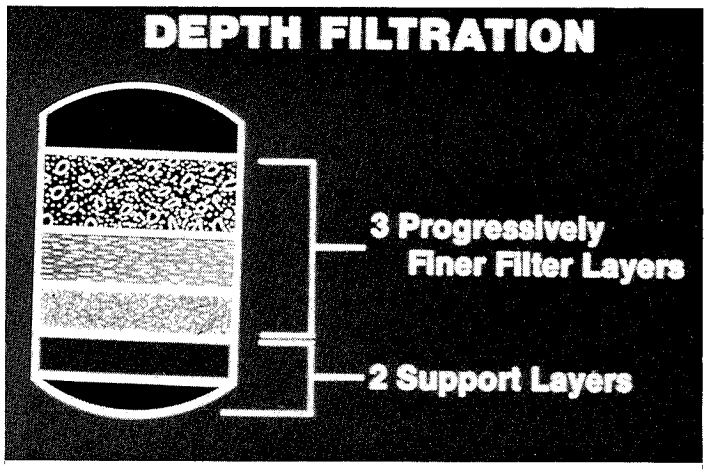

Figure 4. Depth Filtration.

Figure 5. Depth Filtration Specifications.

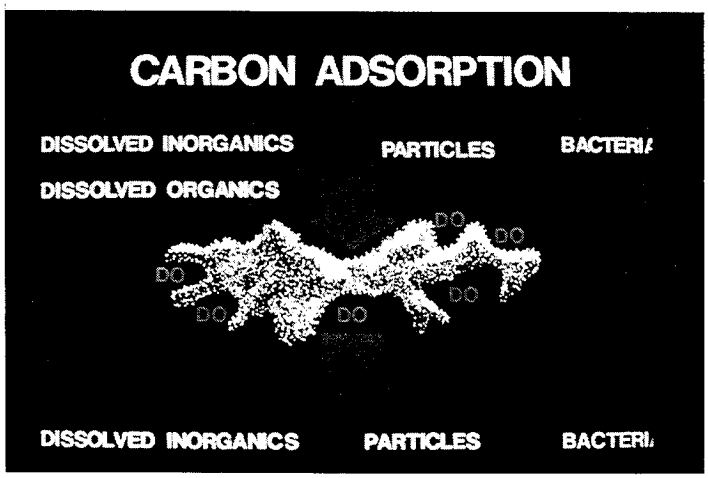

Figure 6. Carbon Absorption Filtration.

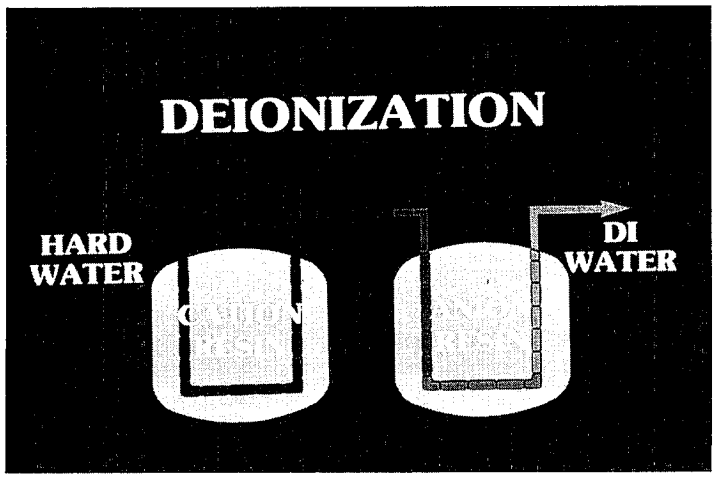

Figure 7. Two-Tank Deionization.

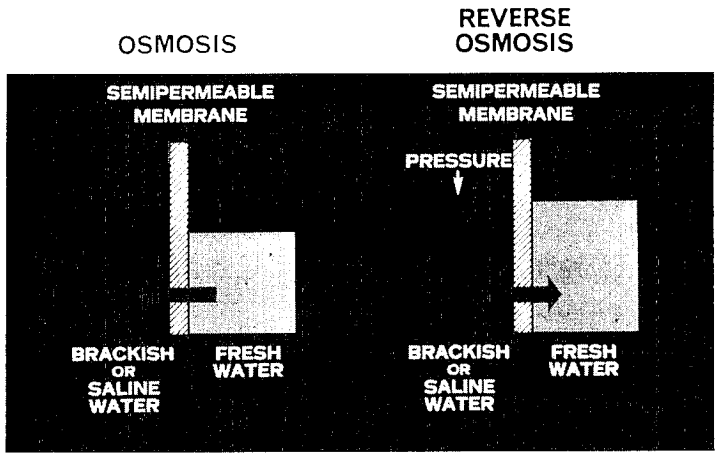

Figure 8a. Principle of Reverse Osmosis Water Treatment.

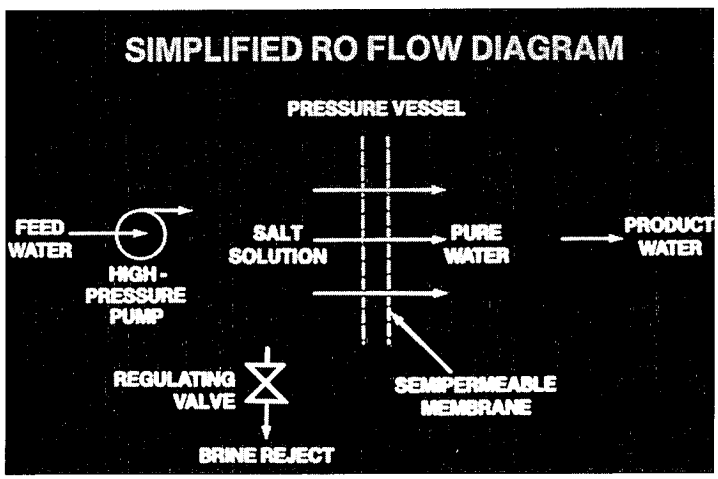

Figure 8b. Reverse Osmosis Flow Diagram.

6th American Water Jet Conference
August 24 - 27, 1991: Houston, Texas Paper 20

Integration of Ultra-High Water Pressure Jet Cutting with Multi Axis Control Devices.

Spencer T. Johnson
Jet Edge, Inc.-Minneapolis, MN

ABSTRACT

As the acceptance and application of ultra pressure waterjets rapidly grows so does the need to accurately maneuver and control these waterjets. This paper provides an overview of several successful applications of up to 6 axis robotic integrations along with the engineering and design considerations unique to ultra-high pressure water plumbing systems. This includes a description of swivels, valves, rigid and flexible tubing or hose and other typical hardware. Also included is a review of equipment protection for existing motion control devices.

Organized and Sponsored by the Water Jet Technology Association.

1.0 INTRODUCTION

In the last few years ultra-high pressure waterjet technology has increasingly been moving from "high tech" proprietary product manufacturing into the general machine shop mainstream. When waterjet equipment first entered the market place the high initial cost of these sometimes temperamental machines tended to limit their application to exotic material fabrication.

With many of these uses being defense or aerospace related there was an almost "cost is no object" attitude toward equipment acquisition. As a result, waterjet manufacturers and their customers were able to build very specialized systems incorporating very accurate multi axis motion controls plus excellent environmental protection of the machine tool. This trend in waterjet technology continues for the larger inhouse fabrication facilities and a few major job shop users.

The proliferation of lower cost motion control alternatives to these custom systems combined with the increasingly user friendly nature of waterjet equipment now allows many traditional manufacturers to adopt waterjet technology.

The development of waterjet technology has been echoed in the advances made in motion control systems. The concurrent maturing of these two industries has given manufacturing operations new opportunities and applications for waterjet cutting.

There are several development trends in both robotic and waterjet equipment that are responsible for the increased usage of these technologies. For the waterjet equipment some of the factors that are most influential are:

* Higher water pressure 413 MPA (60,000 psi)
* Lower water volume .5 LPM (.15 gpm)(As a factor of reaction force.) $F_R(lbs)=.052\sqrt{psi} \times gpm$
* Component reliability
* Reduced component size and weight
* Ancillary component development ie: swivels, valves, tubing, hose

Areas contributing to the successful application of robotics are:

* Improved path accuracy
* Lower cost
* Ease of programming
* High speeds
* Payload capacity
* Flexibility of location
* Reliability

When evaluating these trends it is necessary to consider the overall objectives in the manufacturing environment and how these factors affect the successful implementation of robotic waterjet cutting systems.

The applications reviewed in this paper center around manufacturers of automotive headliners. A variety of factors has made this application one of the largest users of waterjet equipment in the United States.

Headliners are typically a multi layer thermo formed lamination consisting of compressed glass fiber 3-6 mm. thick, polyurethane foam 2-4 mm. thick and synthetic decorative fabric 1-2 mm.(Fig 1) All three materials can be cut using conventional manual methods however the high volume of parts produced and the irritating nature of glass fiber particles is detrimental to the health and safety of workers. Also the handling of these parts manually presented an opportunity for the fabric to be damaged or discolored.

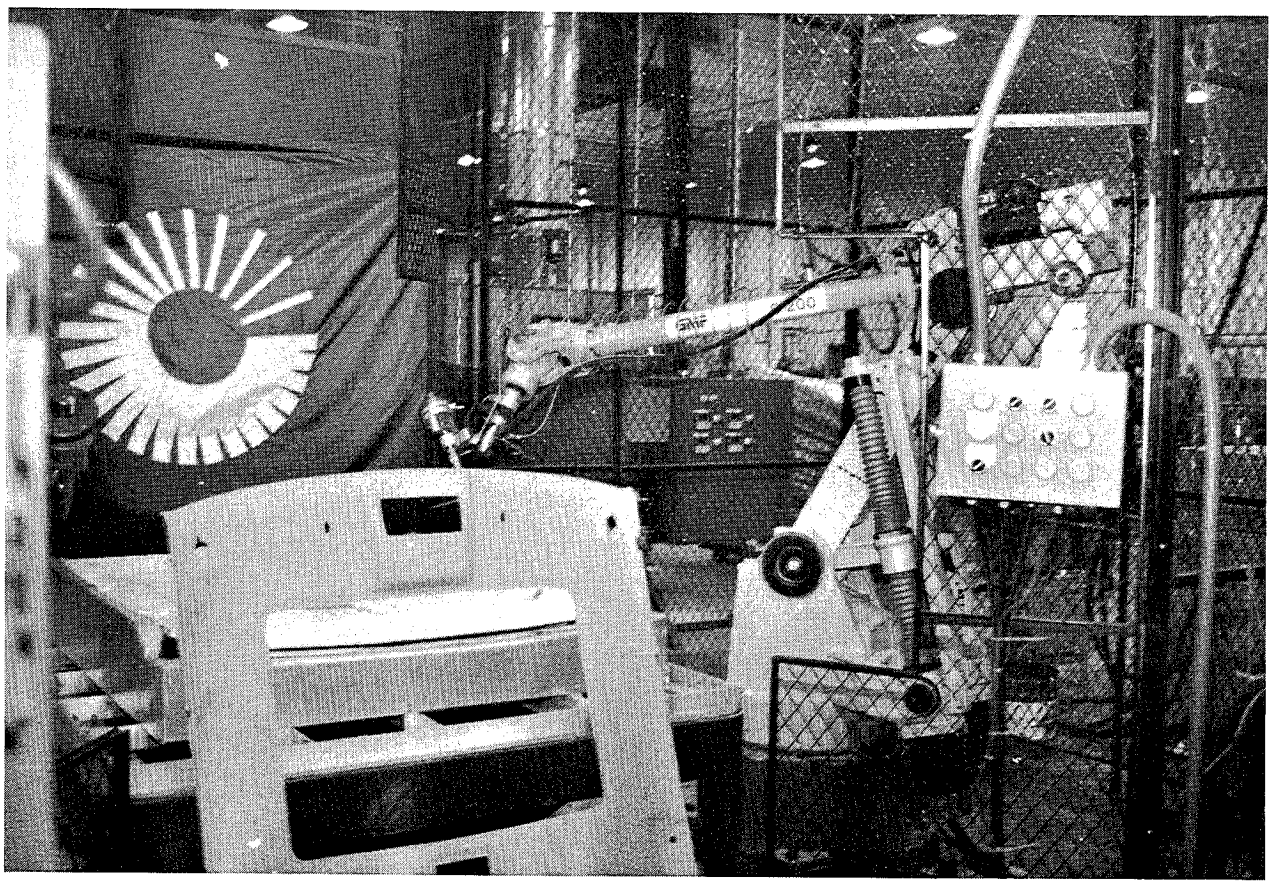

Fig 1 Completed automobile headliner.

With the development of reliable, accurate ultra-high water pressure jet cutting equipment came the capability to cut this strong yet delicate material cleanly and quickly. Water pressures in excess of 309 MPA (45,000 psi) are required to reliably cut this material when maintaining production rates of over 100 pieces per hour using waterjet orifices less than .254 mm (.010 inches).

By utilizing these low water volumes, less than 1.74 LPM (.46 gpm) at ultra-high water pressures, reaction force remains at a low enough level 22.2N (5LBF) to remain within the payload capacity of most smaller high accuracy pedestal robots. The typical capacity at the wrist for the units described is 10kg (22 Lbs.) which dictates an end of arm device under this total weight including reaction force. (Fig 2)

This weight requirement is satisfied through the use of the compact low mass on-off devices available today for ultra-high water pressure systems. On-off valve weights of less than 5kg (11 lbs.) are available. Exceeding this parameter will over load the robot arm and adversely affect accuracy of cut, typically better that .20 mm (.008").

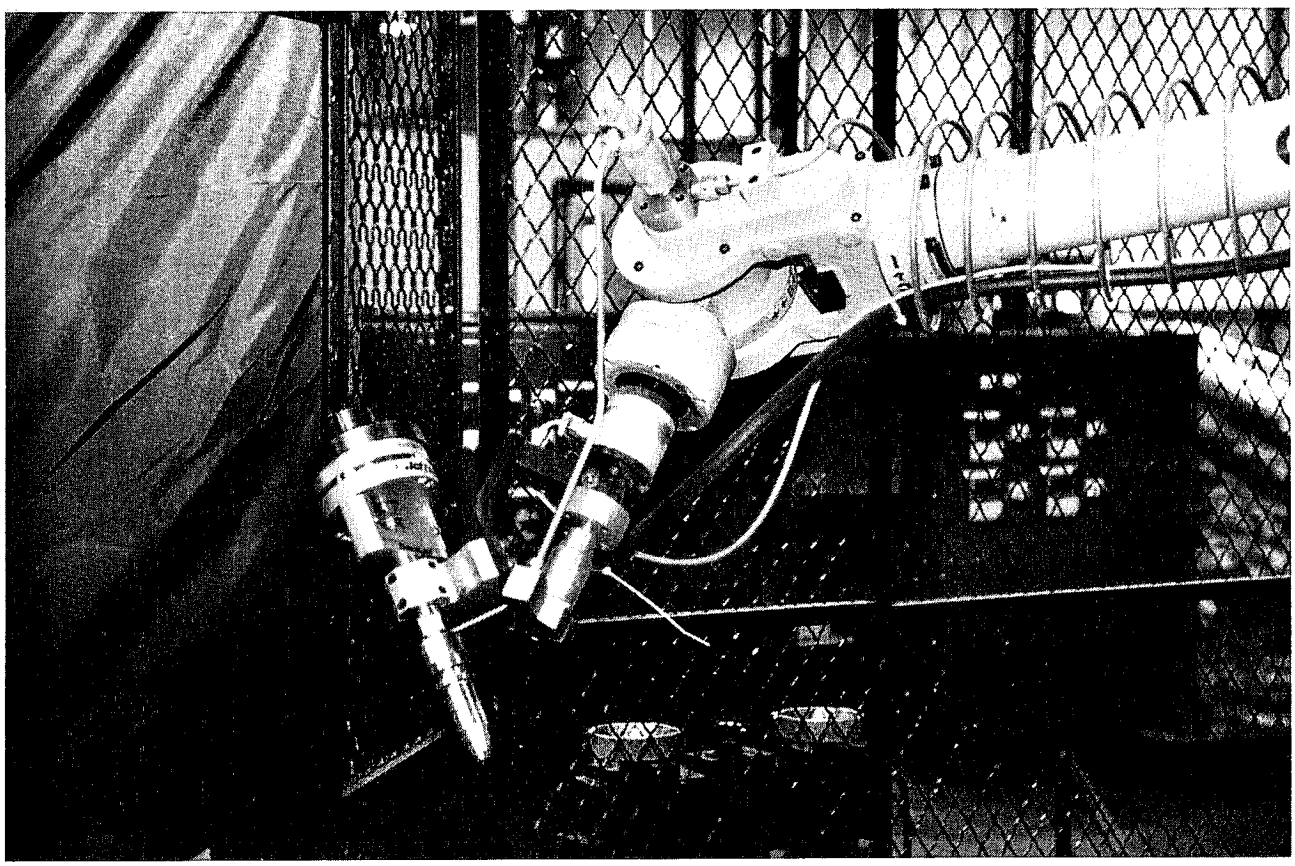

Fig 2 End-of-arm waterjet on-off device.

2.0 APPLICATION REVIEW

The first system presented utilizes two pedestal type robots in a standard floor mounted configuration (Fig 3). The particular model of robot selected was dependent on the customer criteria that either motion device be capable of performing all cutting of the piece part thus allowing for on line maintenance or repair without interruption of the production line.

With this criteria established the first step in designing the work cell was evaluation of the piece part and the available work envelope of the robot (Fig 4). This step required the analysis of the intended cut paths and their orientation. The part is generally flat requiring a perimeter cut all around plus one central sunroof opening. The finished part did not require any cut to be made at an orientation greater than 90° from vertical. Given the overall outside dimensions coupled with the dimensions of the end of arm mounted jet cutting head (Fig 5), a further study of the work envelope was made. This study yielded an end of arm tool design that offered maximum use of the various axis of motion within the work envelope.

By starting with the piece part and working backwards toward the ultra-high water pressure intensifier pump a logical, simple plumbing system can be developed for most motion systems. The next area of consideration after the end of arm device is therefore the accommodation of the various jointed movements of the individual axis.

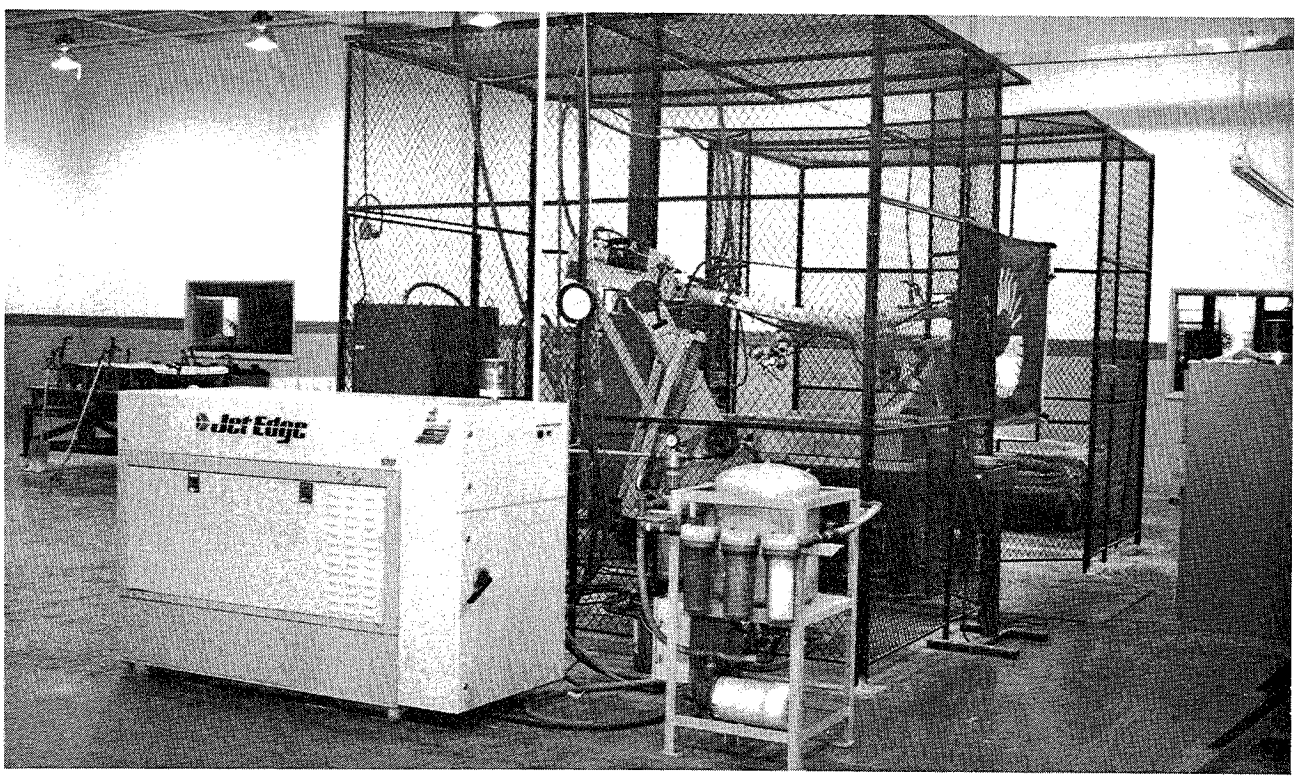

Fig 3 Floor mounted pedestal robot and ultra-high water pressure intensifier pump.

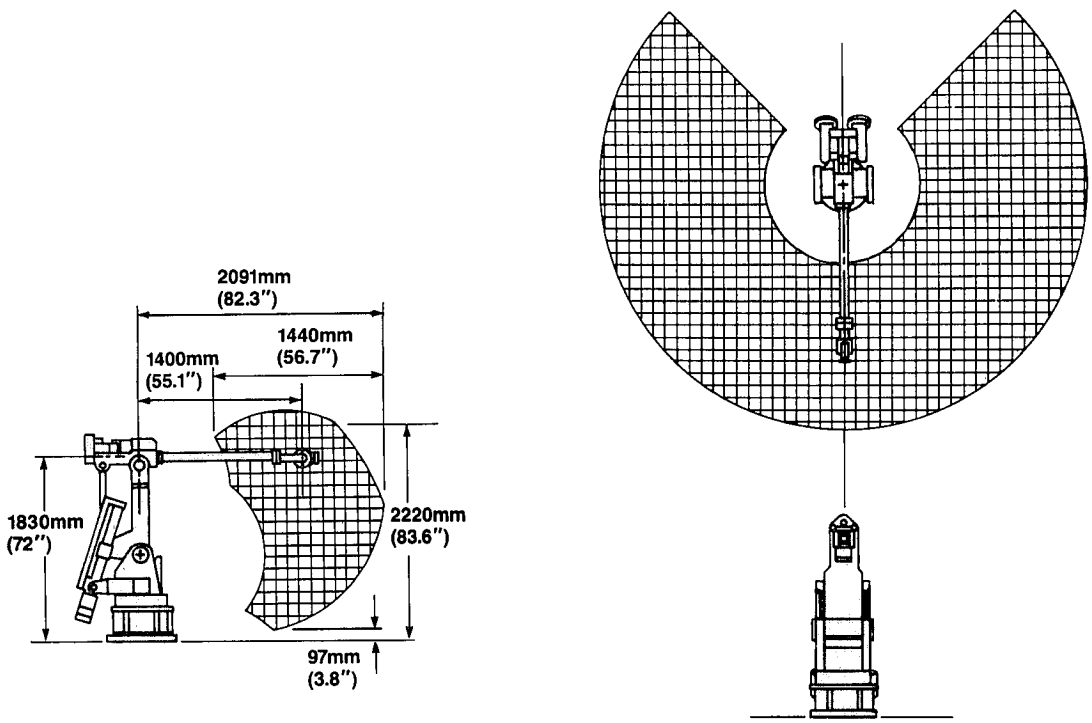

Fig 4 Work envelope of GMF S-200 robot.

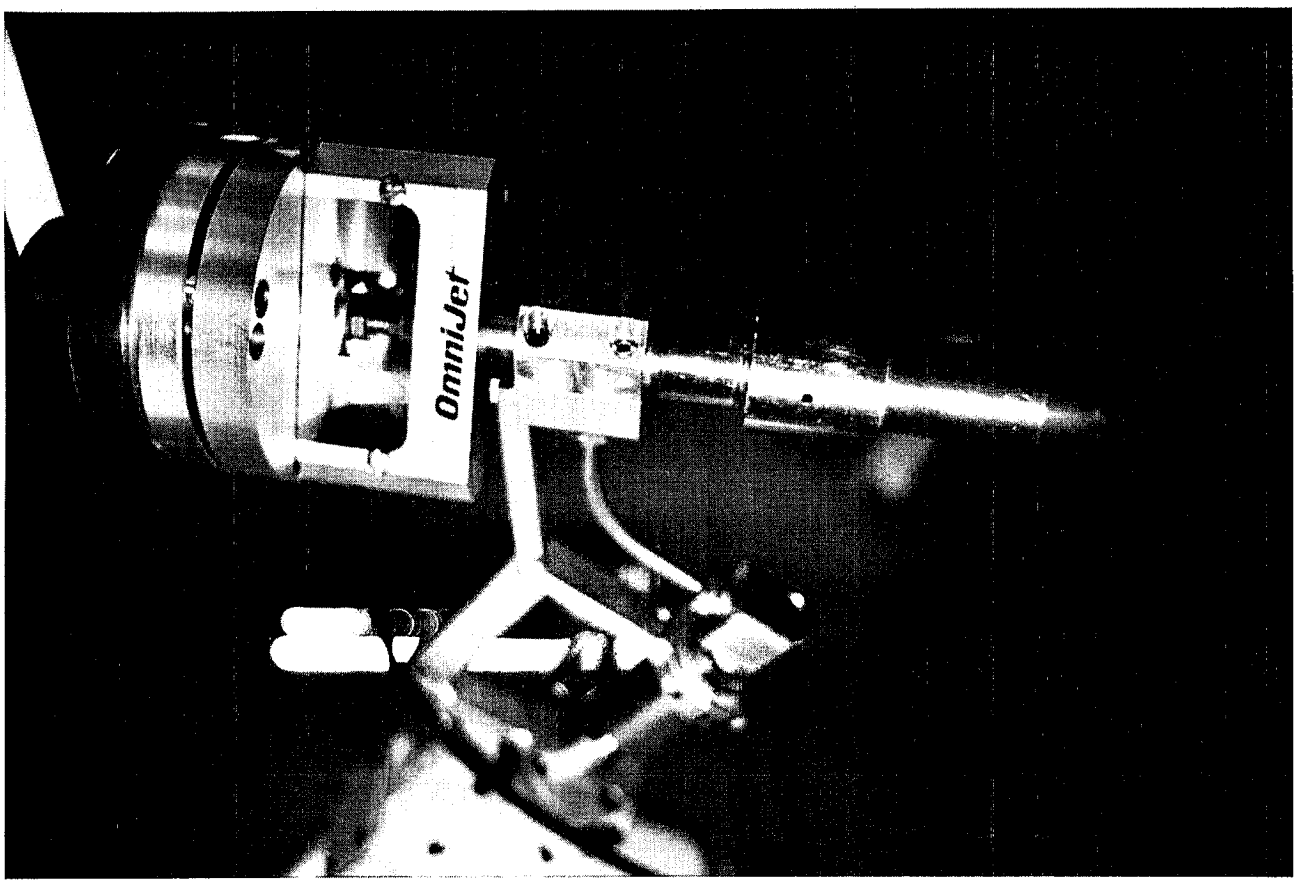

Fig 5 Typical waterjet cutting head.

The current generation of pedestal robots generally do not provide internal passageways concentric to axis motion. It is necessary then to route the plumbing external to the robot, again without interfering with the motion of the robot.

At this time a decision as to the water pressures utilized and the type of tubing or hose must be made. For water pressures over (248 MPA) 36,000 psi stainless steel tubing having 3 to 1 O.D. to I.D. ratio is most often selected. The limited availability and lack of flexibility of hose having adequate safety ratings has for most applications been limited to under (248 MPA) uses.

The application being described here required continuous working pressures over 300 MPA therefore is was decided to use stainless steel tubing combined with 413 MPA rated swivel joints (Fig 6). Starting at the wrist (joint #6) a swivel was integrated into the end of arm tool to ensure support and location for the swivel and the ultra water pressure tubing attached. The ultra pressure tubing was then routed as closely to the robot arm as possible to the next swivel located concentric to joint #5. The external path of the tubing dictated by the robot design results in an approximately 10° reduction of the original 370° range of motion at the 6th axis. This dead zone was positioned in such a manner as to leave the working range of the robot unaffected.

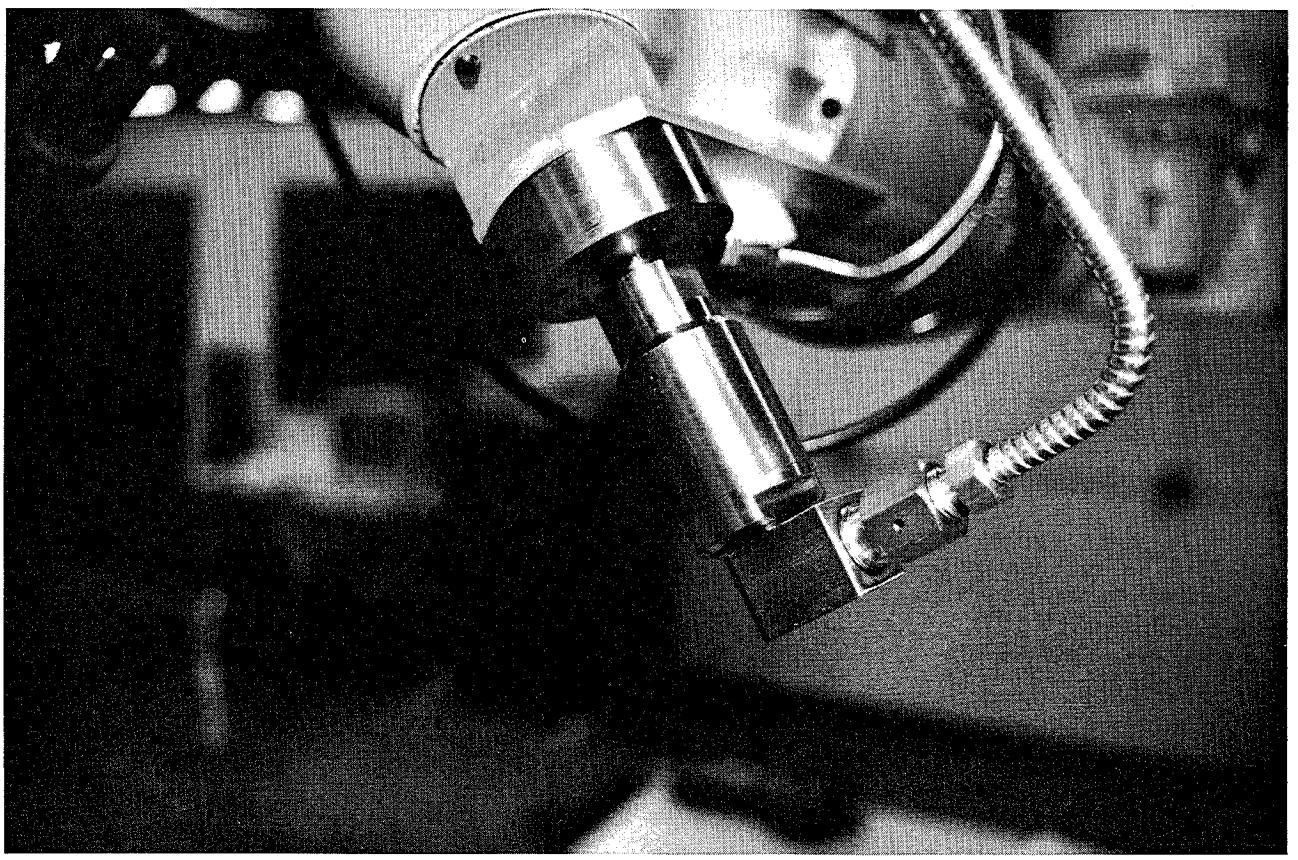

Fig 6 Ultra-high pressure rated 360° swivel.

Following joint #5 a coil consisting of 11 turns of 6.35 mm tubing was used to allow unrestricted 370° rotation of the 4th axis while maintaining a low profile. The coil terminates at the third swivel located on the stationary portion of the 4th axis housing. A strain relief and anti rotation clamping block was provided at each end of the coil.

Due to the limited X-Y-Z movement of the third swivel the remaining motion compliance could be performed by the use of a whip of 6.35 mm tubing. A whip is essentially a long length of tubing that provides freedom of motion through the use of the relative flexibility of this small diameter tube.

This system is currently in use entering its second year of full production for a tier one automotive supplier.

The second system reviewed shares the dual robot design with some interesting variations. In this application the finished part size was smaller which allowed the use of a robot with a smaller work envelope enhanced by unique end of arm devices. Another deviation from the previous system is the "wall" mounting of the two units giving an extremely open work zone. (Fig 7)

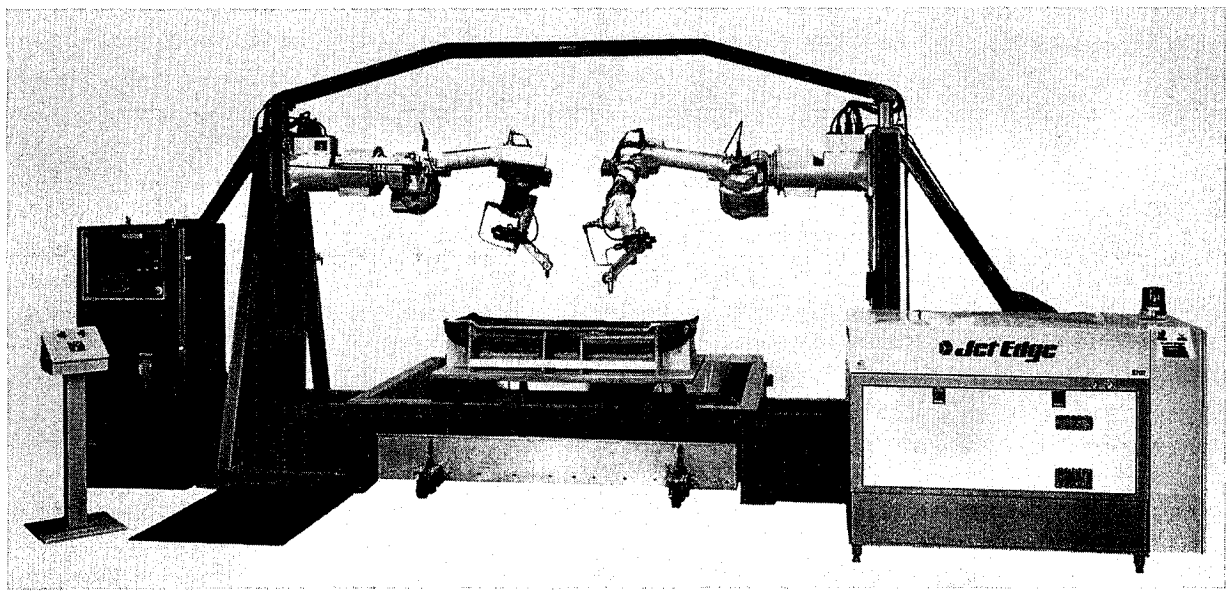

WATER JET CUTTING SYSTEM

Fig 7 Typical wall mounted robotic waterjet cutting cell.

The first step as before was a review of the piece part geometry and intended position of the cuts. This process revealed the need for cuts in excess of 90° from vertical along with some tight clearance areas. To accommodate these concerns an extended reach, low profile end of arm tool was fabricated. The tool incorporated a remote on-off valve configuration isolating the cutting tip from the valve via ultra water pressure rated tubing.

In this situation the particular robot design (Fig 8) was well suited to an all swivel plumbing scheme. On axis 6,5,3,2, and 1 swivels were used in rigid mounted locations. The fourth axis utilized a coil formed from 6.35 mm tubing again for rotational freedom. The mounting of swivels, valves and tubing was done using as many of the robot's standard attachment points as possible.

This system is currently in operation producing a finished part once every 28 seconds.

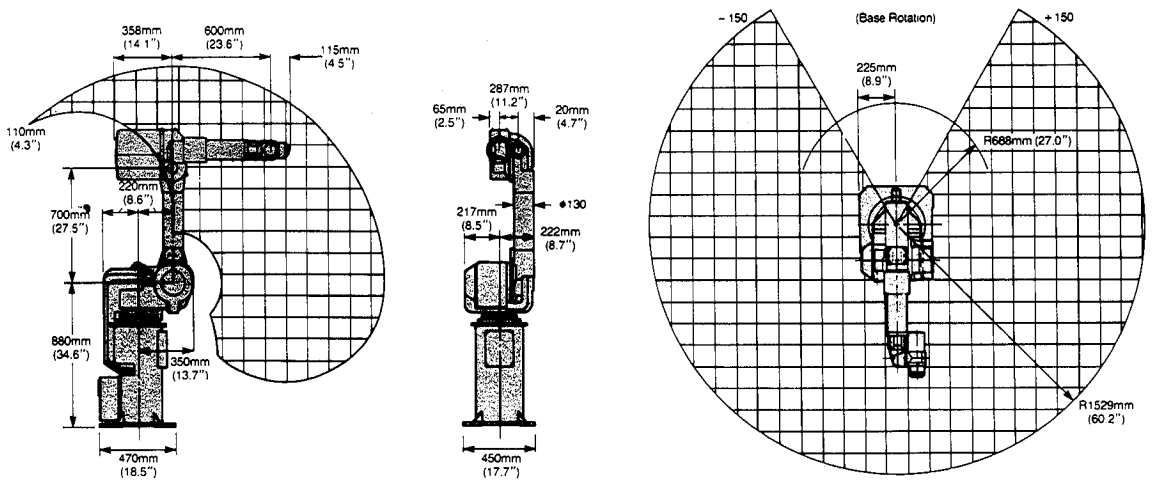

Fig 8 Work envelope of GMF S-10 robot.

3.0 SAFETY CONSIDERATIONS

When implementing automated systems into the manufacturing environment the safety of personnel and protection of these expensive components must be considered. A series of protection systems were incorporated in both of the previous application reviews.

System one used a combination of pressure sensitive mats, dual palm buttons and a steel wire cage to protect the operators (Fig 9). The pressure mats were located at either side of the load-unload area extending across this access area to meet with the wire cage extensions. Any pressure on these mats prohibited the robots or the waterjets from being acctuated through operator or control actions. In the event a person entering this area steps on the mats during the production cycle the waterjet and robot shut down immediately. The design of certain ultra water pressure on-off valves including the Omni-Jet shown are of the fail safe type. Any interruption of the electronic or pneumatic circuit will cause these waterjets to close as they do not require outside forces to perform the shut off function.

Additional operator safety is provided through the use of dual palm button type control stations. These stations require the two load-unload personnel to step away from the work area and simultaneously depress two buttons, one with each hand. The palm button enclosure design precludes tampering or single hand actuation.

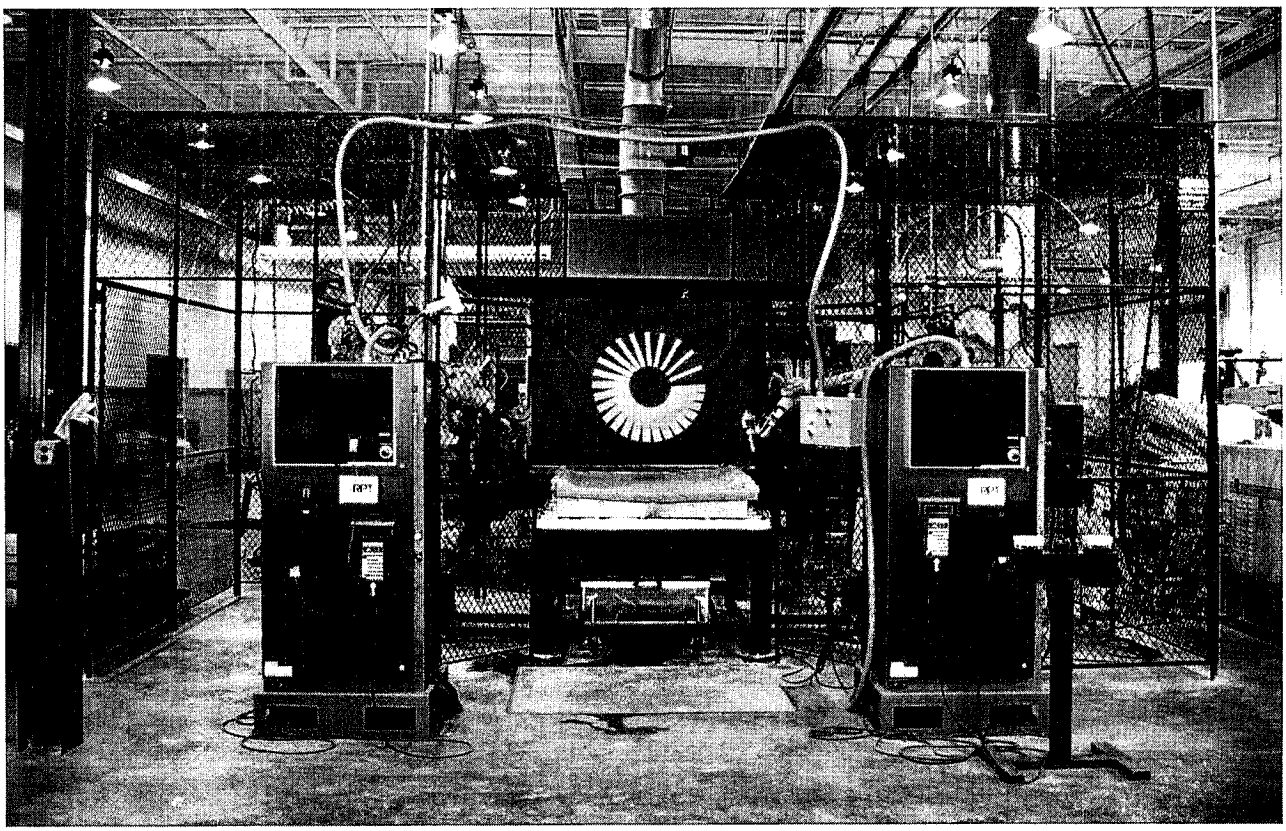

Fig 9 Enclosed work cell with protection devices.

In order to prevent access to the actual operating area of the robot the wire cage extends 3.05 m (10 ft.) from the floor to a totally enclosed wire screen "ceiling" (Fig 9). Each robot may be accessed for maintenance through interlocked doorways. Switches located on the door latches will cause system shutdown in the event of access. The doors are also provided with key type locks to prevent unauthorized entry.

The second issue to be addressed is the protection of the equipment against damage through abuse or neglect. With this installation the robot logic controllers took overall control of all safety functions. Equipment protection began with overload devices located at the wrist #6 joint to halt the robot movement in the event of the waterjet nozzle striking an obstruction. This shutdown circuit stops all motion and shuts off the waterjet.

For other fault conditions the robot performs continuous on line diagnostics and reacts to outside inputs from various sources. The intensifier pump used in each system is a 40hp microprocessor controlled unit. The microprocessor built into the pump unit monitors incoming water pressure, hydraulic oil temperature, hydraulic fluid level, intensifier stroke rate and seal condition indicators. Depending on the signal sent from the intensifier microprocessor the robot controller will respond with either an audible alarm or a complete system shut down. An additional option feature in each system is the inclusion of an auto pressure bleeddown valve. These devices relieve all system water pressure anytime the intensifier pump is shut down via emergency stop.

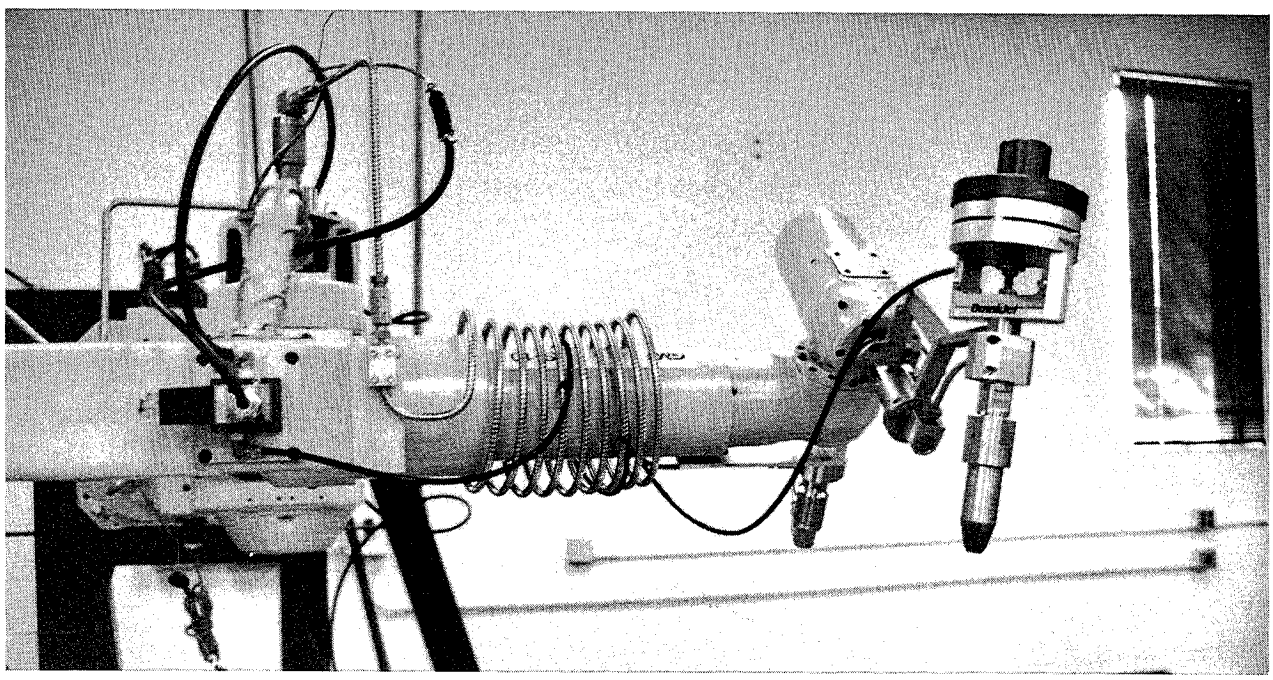

Fig 10 Coil protected by spiral wrap shielding.

The second robotic system described was very similar to the protection systems used. The significant deviation from the first system is the use of a total enclosure around a mechanically driven production line. Here a room was built using water resistant materials with automatic access doors for the moving line. The operators were isolated from the robots through the use of plexiglass windows and again interlocked doors.

A feature typically found in any ultra-high water pressure jet cutting system is the use of a secondary spiral wrapped jacket covering the stainless steel lines (Fig 10). When operators are anticipated to be within 1 meter of a high pressure line it is advisable to incorporate this feature. In some instances this jacket is not illustrated for clarity.

4.0 CONCLUSIONS

The merging of pedestal robots and ultra-high water pressure technology, two young technologies has resulted in these systems being accepted proven techniques for handling a variety of complex manufacturing processes. The robotic waterjet systems presented illustrate that with proper analysis of the desired end result an integrated system can be developed using standard components to deliver outstanding performance capabilities at an acceptable cost.

The future for robotic waterjet cutting appears excellent as the trends described earlier accelerate allowing more potential users to adopt these processes. As accuracies continue to improve in robots concurrent with further advances in ultra-high waterjet technology these systems will begin transitioning into many areas once considered to demand traditional machine tool processes.

6th American Water Jet Conference
August 24 - 27, 1991: Houston, Texas Paper 21

COMPUTERIZED WATERJET AND ABRASIVEJET CUTTING *

DUANE E. SNIDER, CMfgT

WATER JET SPECIALTIES

Burlington, Ontario, Canada

Organized and Sponsored by the Water Jet Technology Association.

ABSTRACT

Waterjet and abrasive jet cutting methods offer the unique ability to machine very soft and very hard materials with a cool beam-like jet of water. This process is employed by a variety of industries in a vast spectrum of applications worldwide.

No longer a curiosity, 24 hour production lines have proven the process and hardware as very reliable and offers many technical and economic advantages over existing traditional methods

This omnidirectional cutting tool is ideally suited for automation and complementary robotic workcell integrations.

1.0 INTRODUCTION

New materials, higher production quotas, intricate profiling manipulation are only a few overwhelming challenges posing considerable problems to conventional methods of cutting.

Integrating two technologies such as a robot to a high pressure intensifier system generally requires a basic theory of simple machine dynamics

2.0 WATERJET CONSIDERATIONS

Concentrating and sustaining a needle-like jet travelling supersonic (Mach 3) and powered hydraulically from 18 Kw to 75 Kw (25 to 100 horsepower)motor(typically) generates a laminar flow of water focused through a sapphire or diamond orifice resulting in a powerful compressive-shear cutting action at close range.

3.0 INTENSIFIER

The intensifier is a double acting reciprocating pump with a typical 20:1 intensification ratio.

(See Figure 1)

The hydraulic power is supplied from an electrically powered radial piston pump of variable displacement. As the pressure is increased, the intensifier shifts back and forth while the system maintains the pressure until an outlet is opened, such as the cutting nozzle being actuated. At this point the intensifier will cycle at a rate proportional to the output flow rating of the outlet orifice, or nozzle. At full pressure, 378,950 kPa (55,000 psi), the water is compressed approximately 12% and is relieved of pressure spikes as it travels through an attenuator ensuring consistent nozzle pressure and suppressing any potential fatigue failure of the equipment.

4.0 WATER

The incoming water to the intensifier is a site-specific issue that depends on the quality of the source water. The inlet water should have the suspended particulate matter removed (filtered) to 0.5 micron absolute. Other methods such as Reverse Osmosis or Mixed Bed Deionization Systems can improve the orifice life at least ten times, whereas the initial capital cost may offset some interested users. A local water analysis is recommended if you seem to have orifice problems.

5.0 PLUMBING

High pressure stainless steel tubing should be rated to 413,400 kPa (60,000 psi) and is available in 6.35mm (1/4"), 9.525mm (3/8") and 14.300mm (9.16") sizes, with a 3:1 wall thickness ratio typical.

The 6.35 mm (1/4") tubing is usually used at or near the robot cutting head and is usually plumbed in the least restrictive way, depending on the required movement of the robot. The whip and coil exploit the flexibility of the tubing allowing movement of the robot, but usually take up a large air space and need external recoil supports. Swivel joints are commonly used and are usually mounted on the robot arm in line with the joint rotation. It is critical to align the swivel shaft rotation centerline with the robot movement, since sideloads cannot be tolerated to a great extent if improperly installed. The distance from the intensifier pump to the nozzle should not exceed 137m (450 ft).

6.0 CUTTING PARAMETERS

Establishing cutting parameters will lay the groundwork for the type and style of system required for the application. Although the process can cut through both hard and soft materials, the material structure, such as large air gaps in honeycombs will render a coherent jet into an inefficient spray.

The decision to use waterjet or abrasivejet rests with the costs, material hardness, desired surface finish, production rates etc. The operating costs using a compressive shear waterjet is typically $2.00 per hour. The additional costs for consumables with an abrasivejet start at $10.00 per hour and can sharply escalate with more abrasive use.

The abrasivejet is essentially all the standard waterjet hardware from the pump to the sapphire or diamond orifice, but has an abrasive mixing chamber attached and a wear resistant mixing tube. (See Figure 2).

The speed of the waterjet accelerates the abrasive particle (garnet) having sufficient mass and weight, travelling down through the mixing tube and into the target material.

The process identity has now transformed to "erosive shear". The abrasives strike the workpiece at a rate over 100,000 times per second and simulates a micro-machining process. The water is now merely the vehicle and coolant. The abrasivejet is a very powerful tool for linear cutting, turning, and recently milling and drilling. The abrasivejet will leave a polished or sand-blasted edge quality typically having 65 - 110 microns finish.

The required horsepower for a system depends upon the number of nozzles employed and the amount of water needed to satisfy the established orifice size. Orifice sizes range from .07mm (.003") and upwards in increments of .025mm (.001").

Process parameters are best noted to reduce any inefficiencies when cutting. An intensifier pump should not be operated at its maximum limit for too long a period of time if the same results can be obtained by reducing the pressure of the pump, or the speed of the robot (joint fatigue) or the abrasive (if used). These changes can translate into noticeable cost savings over the course of a year. Typically, the garnet abrasive demands 70 - 80% of the consumable operating costs.

Cutting specifications should note the following:

* Waterjet pressure
* Waterjet orifice size
* Stand off distance
* Abrasive Size & Type
* Mixing tube length and diameter
* Jet angle - entry & exit
* Kerf angle
* Surface finish
* Speeds
* Tolerances
* Costs

The outstanding benefits of fluid jet cutting are:

* No thermal effects or heat affected zones
* No chipping or cracking of brittle materials
* Low tooling costs
* Low material loss
* Eliminates most deburring
* Single pass cutting
* Minimal airborne dust
* Omnidirectional shape, contour cutting
* Environmentally friendly

7.0 CHARACTERISTICS

Some general process disadvantages include an inability for critical tolerance cutting unless intensive process monitoring is available.

Some cuts may have a kerf angle, or vee-shape, controlled by nozzle traverse speed, especially when cornering.

Garnet embedment may occur with some materials, and can be removed with vibratory, polishing, or wash processes.

Improperly pierced holes may leave a gouge mark.

Some very slight work hardening may occur in a few types of materials only.

Overall, the abrasive waterjet is an excellent tool for hard to machine alloys and composites.

8.0 ROBOTIC CONSIDERATIONS

The typical waterjet nozzle weighs approximately 3.5 kg (8 lbs) and considering on/off back pressure reaction and end effector weight, a robot with at least 10 kg (22 lb) payload is recommended. An integrated catcher could also add another 22 kg (50 lbs). Pedestal Robots with welding background or sealant dispensing are complementary to the continuous process of the waterjet. Gantry robots are exceptional for their rigidity and are usually closer to machine tool specifications concerning accuracy and repeatability. The recommended programming method is to download a CAD defined tool path. The point to point teach method suffers from the recovery time if the program is lost or an engineering modification occurs.

Memory capacity is an issue if you have many programs or large programs requiring large local memory or requiring an interactive storage device. Also, consider if the control can accept a program while executing another.

The control processor should also be fast enough to insure the cutting head is tracking the path at the correct speed at all times.

CAD downloaded programs have a certain spacing of point definitions. This may conflict with the robots processing speed compared to the programmed cutting speed resulting in motor drive oscillations, and a rough striated cut. Do not confuse this with what could be incorrect cutting pressures, speeds, abrasive flow, etc. The waterjet or abrasivejet will reflect any mechanical vibrations or backlash and this will show up on the cut edge.

Pedestal robots may have more difficulty on sharp corners or circular interpolation moves. Waterjet and Abrasivejet machines should not have any uncovered bearings or ways whatsoever. Way covers are essential and some positive air pressure internally will greatly help prevent contamination. The controller should be well protected and ventilated. The whole workcell is better off in an enclosed area for cleanliness and noise suppression. The floor foundation should be of machine tool quality to insure the robot and

fixtures maintain their relationship. The floor grating can act as a catcher tank or the catcher can be under the gantry **(See Figure 3)**. The weir tank will allow sufficient drainage and dredging is required periodically.

The fixtures do not entirely need to be ruggedly strong since the waterjet creates minimal vertical or lateral forces. Fixture supports can be built with disposable sections and can use any cost effective material suitable for deflecting a jet (tool steel, ball bearings, wood). The final cut accuracy results from the repeatability of the robot AND the fixture too.

Emergency stop buttons, light curtains and software limits to robot joints should be used liberally as safety is the number one priority for turn-key systems.

9.0 CONCLUSION

Waterjet cutting has a definite unique niche as an industrial production tool. Feasibility of the process is initially established through parametric cutting of the part and material. Optimization of the process depends upon the hardware demands created by the proper orifice sizing, pressure requirements, mechanical fatigue (RE: High speed applications and/or pressures,), etc. The human factor is above all and will remain to be, the most important factor of a successful production system. All key personnel must have a thorough understanding of the theory and mechanics of the system. Respect of the process from a safety point of view, as well as, a production uptime stance depends upon proper training instructions and understanding simple machine dynamics.

10.0 BIBLIOGRAPHY

* D.E. Snider, "Waterjet Cutting in a Production Environment", Water Jet Specialties, Proceedings of the 5th American Waterjet Conference, 1989.

* Mohamed Hashish, "Advanced Machining with Waterjet Cutting Applications", Quest Integrated, Automated Waterjet Cutting Processes - SME 1990.

* Gary Ayers, "Principles of Waterjet Cutting", Flow International, Tappi Journal, September 1987.

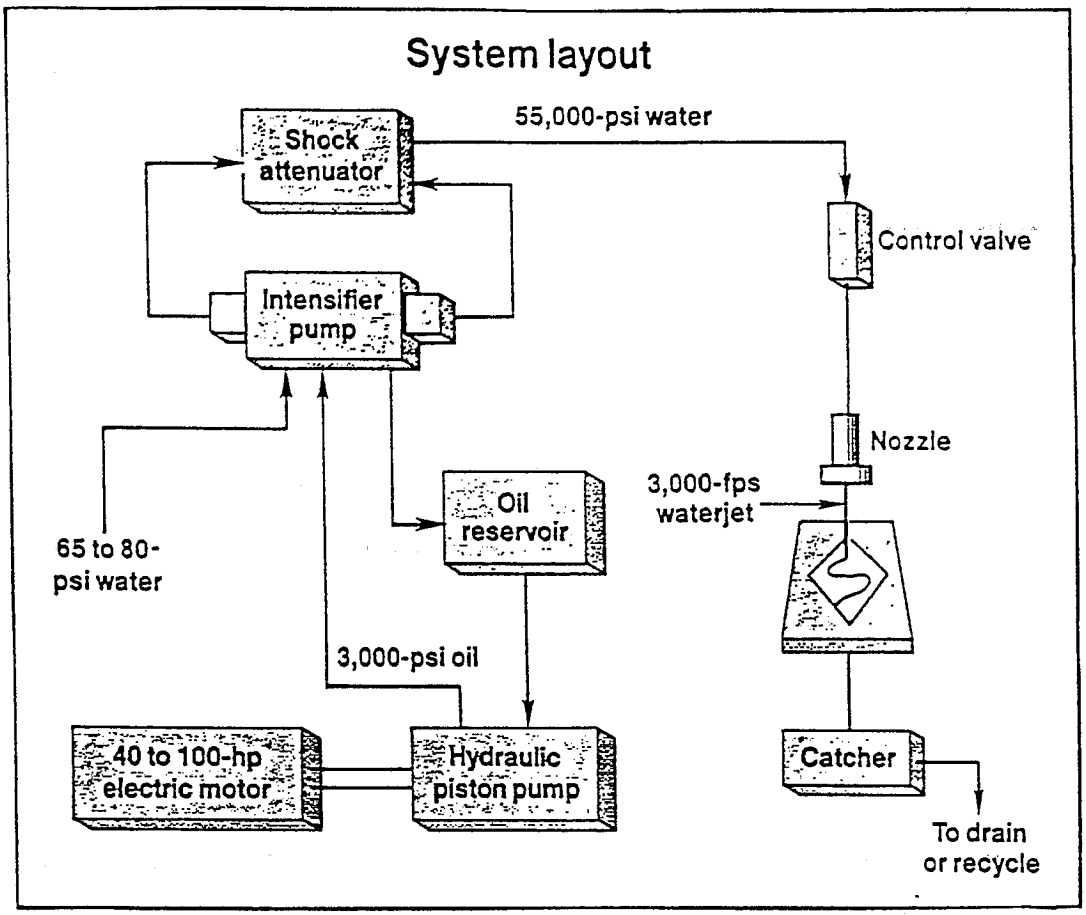

FIGURE 1 SCHEMATIC OF A HIGH PRESSURE INTENSIFIER SYSTEM

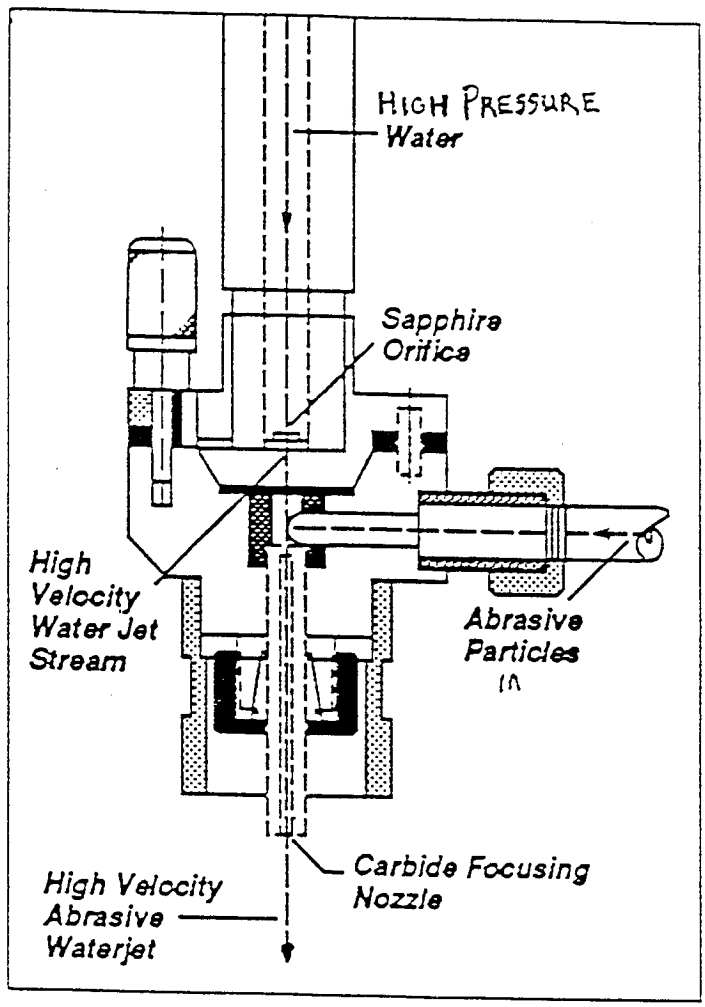

FIGURE 2 ABRASIVE WATERJET NOZZLE

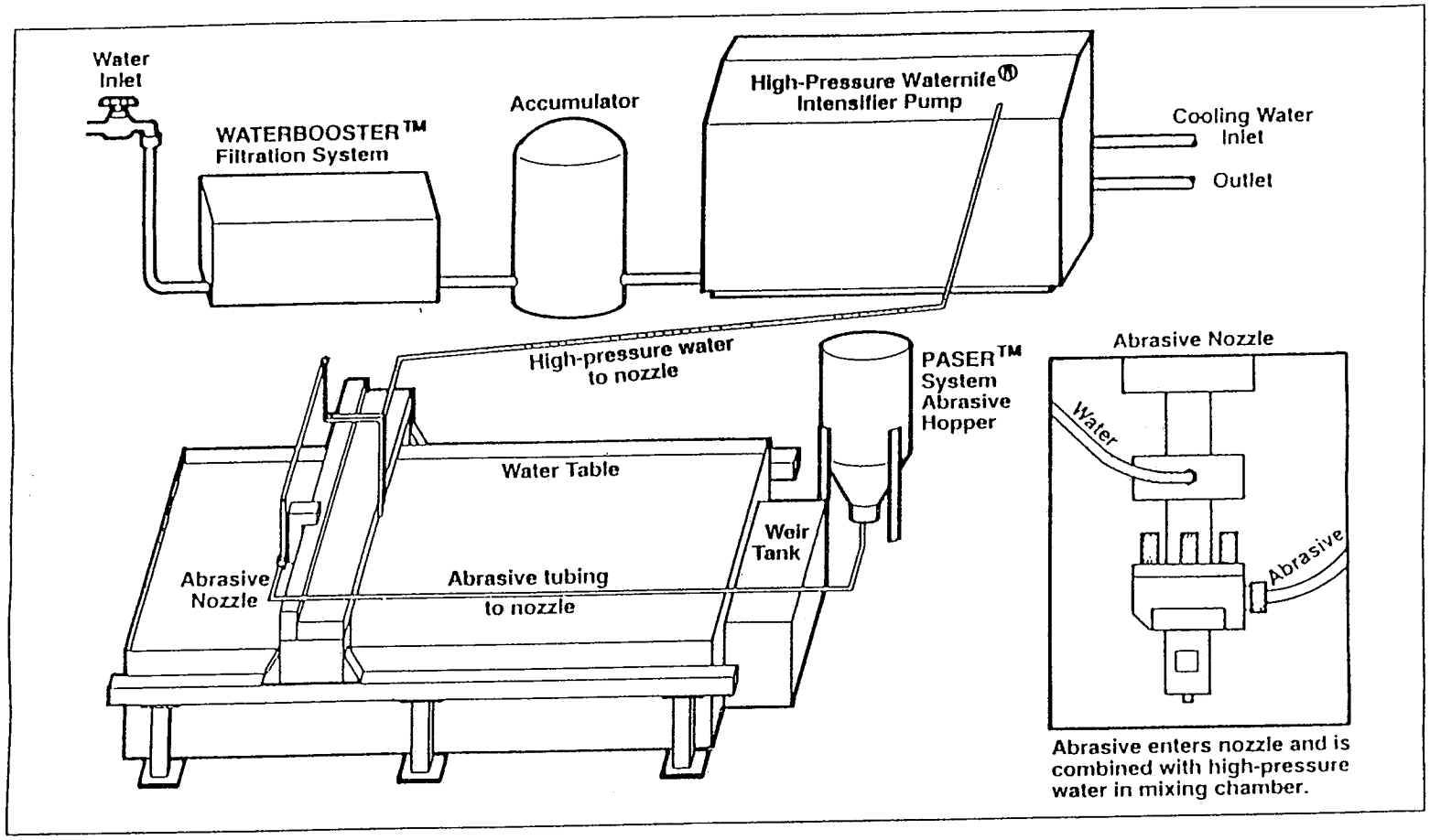

FIGURE 3 TYPICAL X-Y GANTRY ABRASIVEJET LAYOUT

6th American Water Jet Conference
August 24 - 27, 1991: Houston, Texas Paper 22

MEASUREMENT OF PARTICLE VELOCITIES IN AN ABRASIVE JET CUTTING SYSTEM

Arthur L. Miller and John H. Archibald

Bureau of Mines, U.S. Department of the Interior
Minneapolis, Minnesota 55417-3099, USA

ABSTRACT

An electronic velocimeter was designed and built at the Bureau of Mines to measure quasi-instantaneous abrasive particle velocities in a three-phase abrasive jet cutting system. The jetting system consists of a 2-mm-diameter nozzle delivering 1.1 L/s (20 gpm) of water at 69 MPa (10,000 psi), directed into a 14-mm I.D. "collimating" pipe of variable length. The disintegrating water jet entrains abrasives and air via an entrainment port 10 cm downstream of the nozzle exit. The resulting three-phase slurry mixes in the collimating pipe. The high velocity droplets and vapor of the disintegrating water jet transfer momentum to the slower incoming abrasives in the collimating pipe. Measurements with the electronic velocimeter were used to estimate velocity profiles for the particles and thereby determine the rate of momentum transfer.

Measured data were used to construct a velocity profile for the abrasive particles. This profile was compared to theoretical profiles generated using a viscous drag model for particle acceleration. Momentum transfer in the system was analyzed by comparing local measured particle velocities with: 1) maximum theoretical values; 2) previous measurements of average velocity for the three-phase mixture. It was found that particle velocities did not reach the maximum theoretical values, but continued to asymptotically approach the average mixture velocity up to 3 meters away from the nozzle.

Organized and Sponsored by the Water Jet Technology Association.

1.0 INTRODUCTION

In analyzing the cutting capabilities of abrasive jet systems, the velocity of individual abrasive particles is often overlooked as a dependent variable. This variable is usually ignored due to difficulty in measuring particle velocity. At the Bureau of Mines, a scheme has been developed which gives an indication of abrasive particle velocity. This scheme was devised with the following goals in mind: 1) estimate velocity profiles of individual abrasive particles in the system, 2) determine momentum transfer rate between the jet and the particles.

2.0 VELOCITY MEASUREMENTS

The jetting system consists of a 2-mm-diameter nozzle operating at 69 MPa (10,000 psi) exiting into a coaxial "collimating" pipe which is 14-mm I.D. and variable in length (fig. 1). The flow rate through this nozzle is 1.1 L/s (20 gpm) and the average velocity of the water exiting the nozzle is approximately 350 m/s (1150 ft/s). As the jet disintegrates in the pipe, it loses energy to evaporation, surface area creation, and temperature rise (ref. 6). The expected loss, as cited in reference 6, results in an estimated two-phase average velocity of 310 m/s (1020 ft/s) in the collimating pipe. At a point 10 cm from the nozzle exit, an entrainment port allows the addition of abrasives (typically 1-mm silica) and air into this high-speed flow. In order to determine how the abrasive particles behave as they mix with the jet, quasi-instantaneous velocity measurements were made using an electronic velocimeter at points from 10 cm (entrainment point) to 3 m downstream from the nozzle. Several measurements were made at each point in order to get an average velocity for a particle at that location. It would be expected that particles would have varying velocities depending upon how they interacted with the jet. Using the averaged data, the acceleration behavior of a "typical" particle was estimated.

2.1 ELECTRONIC VELOCIMETER

A small portable electronic velocimeter was designed and built at the Bureau of Mines in order to elucidate particle behavior in collimating pipes. The device fits over the outside of a 20-mm O.D. collimating pipe and slides easily to any axial position along the pipe. The velocimeter (fig. 1) consists of two energized electromagnetic coils placed a known distance apart (4.2 cm), each wrapped with a secondary coil. The primary coils carry approximately 3/4 amp at 2 volts. Any object which has magnetic permeability will cause a transient disturbance of the magnetic flux lines as it moves through either of these primary coils. Such a disturbance induces a small transient voltage in the respective secondary coil. For a secondary coil of given size and number of windings, the transient voltage measured across it is proportional to the size, speed and magnetic permeability of the object passing through the primary coil.

The approximate linear velocity of a magnetically permeable particle was determined by: 1) directing the particle through a nonmagnetic pipe on which the two coils were mounted (fig. 1); 2) using a storage oscilloscope, capturing the induced transient voltage signals from each of the secondary coils on a separate channel; 3) measuring the time increment between the two signals; 4) calculating the quasi-instantaneous velocity

of the particle using this time increment and the known distance between the coils.

2.2 TRACER PARTICLES

In order to use the velocimeter to measure particle velocities in the collimated jet, a tracer particle was needed which had the size, shape, and density of the abrasive particles, but whose magnetic permeability would be sufficient to produce detectable signals as it passed through the coils. After numerous trials, it was found that "plastiform" magnet material, cut into cubes as small as 3.26 mm, would give adequate signals. "Plastiform" magnets are a rubber base containing barium ferrite, and have a specific gravity of 3.56, which is much closer to that of silica abrasives (2.65) than any other magnetically permeable material we investigated. Since the specific gravity of "Plastiform" particles are similar to that of silica abrasives and the particles are cut quite small, it was estimated that a single tracer seeded into the silica abrasive supply would give a reasonable indication of abrasive particle velocity. The effect of tracer particle density on experimental results is discussed in the next section.

2.3 EXPERIMENTAL DATA

As a single tracer particle passed through the coils of the velocimeter as part of a flux of silica particles, the transient voltage produced by the upstream secondary coil set off an electronic trigger, and a storage oscilloscope began recording a pair of signals as shown in figure 2. The time between the peaks of the signals corresponds to the transit time of a tracer particle from coil 1 to coil 2. From this transit time and the distance between the coils, the particle velocity is calculated. Approximately 10 velocity values were obtained at several axial positions by this method (fig. 3). The velocity values at each position varied by as much as 10 m/s for velocities in the range of 35-240 m/s, which may be due to nonuniform interaction of the jet with individual particles. The velocity values were, therefore, averaged at each position. These velocity versus distance curves provide an indication of the effect of momentum transfer on the behavior of a "typical" particle.

The four lower curves of figure 3 represent four different types of tracer particles: 1) 3.26-mm steel shot, 2) 3.26-mm magnet particles, 3) 4.34-mm steel shot, and 4) 4.34-mm magnet particles. Note that the steel particles have a specific gravity of 7.84, while the magnets are the rubberized type with a specific gravity of 3.56. This is important, as the lighter magnets will behave more like silica abrasive particles which have a specific gravity of 2.65. In order to determine the effect of specific gravity on the velocity profiles, the data were extrapolated to provide a 5th curve which is an estimate of the behavior of silica particles.

This was done as follows:

1. At a given location the measured average velocities of two similar-sized particles of different specific gravity were compared.

2. The velocity difference was divided by the difference in specific gravity to get a linear relation for the effect of specific gravity on velocity.

3. The velocity of a third particle of known specific gravity was estimated by extrapolating using this linear relation.

4. The process was repeated using particles of similar specific gravity, but different size in order to provide an extrapolation for the effect of particle size on velocity. For this experiment, difference in shape factor was not considered.

Although this two-point linear extrapolation process is limited, the upper most curve should give a reasonable indication of particle acceleration for silica abrasives.

3.0 VELOCITY PROFILES IN THE PIPE

The data of figure 3 demonstrate the following: 1) entrainment velocities (of incoming airborne particles) are relatively low (10-20 m/s); 2) particle acceleration is very high in the first 25-40 cm after the nozzle, and is significant for the entire 3-meter pipe, especially in the case of steel particles; 3) particle acceleration is strongly dependent on particle density, which is seen by the sizable separation between the lower two curves, (steel-specific gravity of 7.84) and the two curves above them (magnets-specific gravity of 3.56); 4) particle acceleration is weakly dependent on particle size (the lower two curves are close together although they represent a 33 percent increase in particle diameter); 5) the uppermost curve, extrapolated from the measured data, is an estimated velocity profile of 1-mm silica abrasive particles; and 6) the "plastiform" particle velocities are less consistent than the velocities for the steel particles. This may be due to inconsistencies in the shape and size of the hand-cut magnetic particles.

The data of figure 3 suggest that a particle with specific gravity of 2.65 would accelerate to a velocity of approximately 260 m/s within 50 cm from the jet nozzle, and would reach 75 percent of that value in the first 25 cm of its displacement.

3.0.1 EFFECT OF ABRASIVE FEED RATE

The effect of increasing the feed rate of abrasives is shown in figure 4. This data represents the measured velocity of 3.26-mm steel shot seeded into the abrasive supply for three different abrasive feed rates. The measured average particle velocity at a given distance from the nozzle decreases incrementally as the mass flow rate of abrasive is increased from approximately 0.1 to 0.4 kg/s. The fact that the lower two curves have a flatter profile suggests the following: 1) higher initial momentum transfer to the larger amount of abrasive lowers the average velocity, 2) with the average velocity of the jet lowered, there is smaller velocity differential available for momentum transfer, 3) these effects are evident in the lower two curves which are very flat indicating that the three phases are approaching an equilibrium velocity. Momentum transfer is discussed more in section 4.0.

3.1 THEORETICAL MODEL FOR ACCELERATION

A model was developed to estimate acceleration of abrasive particles. The model assumes the particles are accelerated by fluid drag forces alone. A BASIC program was written to solve the equation $F_{drag} = m\ dv/dt$ for fluid acting on a single spherical particle. The program incorporates an Eulerian time-step solution method (ref. 1). Acceleration is determined based on separate initial velocities for the fluid and particle, while drag coefficients are calculated using the Stokes-Oseen curves for drag on spheres (ref. 2). An equation was developed which approximates the Stokes curve for Reynold's numbers applicable to the conditions of the present problem. This equation is incorporated in the program so that a new particle Reynold's number and subsequent drag coefficient may be calculated for each time-step iteration.

The model was first used to estimate particle acceleration in a high-speed air flow. Assuming a 320 m/s flow of air at 69 Kpa (100 psi) in our 3-m collimating pipe, with an inlet abrasive velocity of 15-m/s the model predicts a velocity profile as shown in fig. 5. Figure 5 predicts that 1.51-mm silica particles would reach over 240 m/s (790 f/s) under these flow conditions. This suggests that air could accelerate abrasives enough to cut rock, given a long enough collimating pipe. (Perhaps with the addition of some entrained water to reduce dust and enhance cutting.)

This preliminary model yields reasonable predictions of particle acceleration. Further development would be to amend the model to incorporate water particles, to account for the effect of particle shape factor, to allow for momentum transfer between the constituents, and to account for frictional losses. As a step in this direction, the model was adjusted to incorporate the effect of a two-phase fluid. Based on the data of reference 5, the fluid in the collimating pipe may be approximated as a fairly homogeneous mixture of water vapor and fine droplets. It was hypothesized that if the density and effective viscosity of this homogeneous fluid could be estimated, then the above drag model might be applicable, since fluid density and viscosity determine the drag force on a particle with a given velocity via the $v = \mu/\rho$ term in the Reynold's number.

v = kinematic viscosity
μ = dynamic (absolute) viscosity
ρ = density

Much research has been devoted to the topic of two-phase correction factors (refs. 3,4,10). Mixture density is normally calculated as a weighted average. For a gas-liquid mixture, this is

$$\rho_m = \alpha(\rho_g) + (1-\alpha)\ \rho_l \qquad (1)$$

Where the subscripts m,g,l stand for mixture, gas, and liquid respectively, and α is the void fraction (volume fraction of gas).

Determining the effective dynamic (absolute) viscosity of a two-phase fluid is less straightforward. The effective viscosity is highly dependent upon the mass and/or volume ratio of the constituents as well as on their individual viscosities (ref. 10). Two typical methods for estimating the effective viscosity are presented below.

3.1.1. DENSITY AND VISCOSITY ESTIMATES

Mass fraction approach - Mc Adams (ref. 4) presented an expression:

$$\frac{1}{\mu_m} = \frac{X}{\mu_g} + \frac{1-X}{\mu_l} \qquad (2)$$

Where X is the mass fraction of gas in a gas-liquid flow.

Volume fraction approach - Dukler (ref. 3) presented a form of the equation

$$\mu_m = \alpha_g(\mu_g) + (1-\alpha_g)\mu_l \qquad (3)$$

Where α_g = void fraction.

The values X = 0.0008 and α = 0.979 were calculated for two-phase liquid/vapor flow in the collimating pipe using the densities for water and its vapor, along with the area ratio between the exiting jet stream and the pipe I.D. Equation 1 then gives an average mixture density:

$$\rho_m = 20.97\ Kg/m^3$$

Equations 2 and 3 were used to estimate the effective dynamic viscosity of the two-phase collimated fluid. Assuming a temperature of 60° F, the values μ_l = 1.21 cp and μ_g = 0.013 cp (ref. 2) were used along with the above X and α values to yield two values for mixture viscosity.

Equation 2 (mass weighted) --- μ_m = 1.13 cp
Equation 3 (volume weighted) --- μ_m = 0.038 cp

The considerable difference in the two values results because the two-phased collimated flow is over 97 percent gas by volume, but over 99 percent liquid by mass. Now the effective kinematic viscosity of the mixture

$$\nu_m = \mu_m/\rho_m$$

can be calculated for use in the viscous drag model. This term will effect the applied Reynold's number, changing the calculated drag coefficient and, thus the simulated acceleration force on the particle.

3.2 PREDICTING PARTICLE BEHAVIOR

The ability of the two-phase adjusted drag model to predict the acceleration of a "plastiform" particle can be seen in figure 6. In this figure, the measured velocity values were not averaged, and the spread in the data can be readily seen. It was found that the effective dynamic mixture viscosity calculated using equation 2 (mass-weighted approach), gave the best match to the measured data. This behavior is not necessarily expected, since the viscosity of a fluid is a term which depends on the continuum assumption of a fluid. Normally one would expect the effective viscosity of a two-phase fluid to be more like that of the continuous phase (gas in this case) than the suspended phase. It is apparent that neither of the values for mixture viscosity adequately predict the abrupt acceleration near the nozzle. This underestimation of the particle acceleration might be amended by including interaction

between water droplets and abrasive particles, particularly in the first 20-30 cm after the nozzle. It was also found that the average density "ρ_m" which appears in the drag force term had a significant effect on the accuracy of the model. Both this term and μ_m depend upon the void fraction (equations 1-3), which means that the model is sensitive to estimation of void fraction in the system. This, unfortunately, makes the model difficult to apply in situations where α is not accurately known.

This simple model assumed a constant two-phase fluid velocity in the pipe. The velocity value used in the model was approximately 310 m/s as suggested in reference 6 for the two-phase flow. Note that the predicted curves of figure 6 do not flatten out as the data do. A refinement of the model which incorporates velocity degradation in the pipe would likely amend this discrepancy.

4.0 MOMENTUM TRANSFER

A simple momentum balance was used to calculate the maximum average velocity of the multi-phased collimated fluid. The main assumptions were that the collimated fluid velocity was 310 m/s, and that complete momentum transfer had occurred between the abrasive particles and the collimated fluid. Figure 7 indicates a multi-phase velocity of about 275-m/s for an abrasive flow rate of 0.15-kg/s. This is slightly higher than the average velocity of the collimated mixture measured earlier by D. Swanson (ref. 8) in a similar experimental apparatus. This is likely due to flow losses in the collimating pipe as cited in reference 6. This theoretical curve will be used as a basis for comparison of particle velocity measurements.

Using figure 7, the data of figure 4 were normalized as follows: 1) for each abrasive feed rate in turn, a maximum theoretical velocity was taken from figure 7 (which assumes complete momentum transfer), 2) all velocity values on a given curve (of fig. 4) were divided through by this maximum value, giving relative percentages of momentum transfer completed.

The normalized data are plotted in figure 8. There is an apparent difference in the momentum transfer rate. For the heavier abrasive loading (0.423 kg/s), only about 55 percent of available momentum was transferred in this particular (3-m) collimating pipe, while for the lighter particle loadings nearly 65 percent of momentum transfer was completed. This suggests that the increased number of abrasive particles actually hinders the momentum transfer process slightly. This was not expected, since one would think that the more numerous particles would effectively reduce the flow area and create a higher drag coefficient (ref. 7). This might be explained by the reasoning that the heavier particle loading lowers the mixture velocity such that the resulting smaller velocity differential decreases momentum transfer. Another possible explanation is that the numerous incoming solid particles aid disintegration of the jet near the entrainment region, thereby changing the dynamics of the momentum transfer process. The relation between particle loading and momentum transfer rate requires further investigation.

5.0 CONCLUSION

The electronic velocimeter in conjunction with seeded "plastiform" magnetic particles gave an indication of abrasive particle behavior. Measured velocities were used to estimate the velocity profiles of silica abrasive particles. Velocity profiles generated from the data showed that particle acceleration is strongly dependent upon particle specific gravity and weakly dependent on particle size. A viscous drag model with two-phase correction for kinematic viscosity and mixture density, though somewhat sensitive to void fraction estimation, was able to predict approximate particle velocity profiles.

Momentum transfer to the abrasives is high in the first 25 cm of the collimating pipe, where particles reach approximately 75 percent of their final velocity. Momentum transfer rate decreases asymptotically as might be expected, but in no instance did the particle velocity decline in the pipe. This included pipes up to 3 m in length and abrasive flow rates as high as 0.423 kg/s. The results from Table 12 (ref. 8) indicate that with an abrasive flow rate of 0.15 kg/s, the three-phase fluid decelerates as shown in figure 9. The measured velocity data of figure 4 for abrasive flow rates of 0.104 and 0.232 kg/s are plotted in figure 9 as well. Extrapolation of these data, as suggested by the dotted lines, suggests that for an abrasive feed rate of about 0.15 kg/s, momentum transfer from the fluid to the seeded steel shot would continue up to about 5 m from the nozzle. The lighter abrasive particles would reach momentum equilibrium sooner, but the data of figure 3 suggest that this would not take place until at least 3 m from the nozzle. This indicates that the use of long mixing tubes in abrasive jetting systems will enhance momentum transfer to the abrasive particles, and thus provide more efficient cutting.

REFERENCES

1. Chapra, S. L., and R. P. Canale, "Numerical Methods for Engineers," 2nd Ed., McGraw-Hill, Inc., 1988, pp. 577.

2. Daily, J. W., and D. R. F. Harleman, "Fluid Dynamics," Addison-Wesley, Inc., 1966, pp. 9, 176.

3. Dukler, A. E., "Pressure Drop and Hold-Up in Two-Phase Flow," A.I., ch. E.J., Vol. 10, No. 1, 1964, pp. 38-51.

4. Mc Adams, W. H., "Vaporization Inside Horizontal Tubes II," Benzene-Oil Mixtures, Trans. ASME, Vol. 64, 1942, pp. 193.

5. Miller, A. L., R. W. Kugel, and G. A. Savanick, "The Dynamics of Multi-Phase Flow in Collimated Jets," Proc. 5th American Water Jet Technology Assoc. and National Research Council of Canada Meeting, Toronto, Ontario, Canada, Aug. 29-31, 1989, pp. 179-189.

6. Miller, A. L., "Disintegration of a Confined High-Speed Water Jet," M.S. Thesis, University of MN, Minneapolis, MN, Jan. 1990, pp. 46.

7. Olson, R. M., "Essentials of Engineering Fluid Mechanics," Intext Press, 1973, pp. 423.

8. Swanson, D. E., "Collimated Abrasive Water-Jet Behavior," U.S. Bureau of Mines, RI 9271, 1989, pp. 36-39.

9. Swanson, R. K., M. Kilman, S. Cerwin, and W. Tarver, "Study of Particle Velocities in Water Driven Abrasive Jet Cutting," Proc. 4th U.S. Water Jet Conf., Univ. of California, Berkeley, CA, Aug. 26-28, 1987, pp. 103-108.

10. Wallis, G. B., "One-Dimensional Two-Phase Flow," McGraw-Hill, Inc. 1969, pp. 27-29, pp. 222-227.

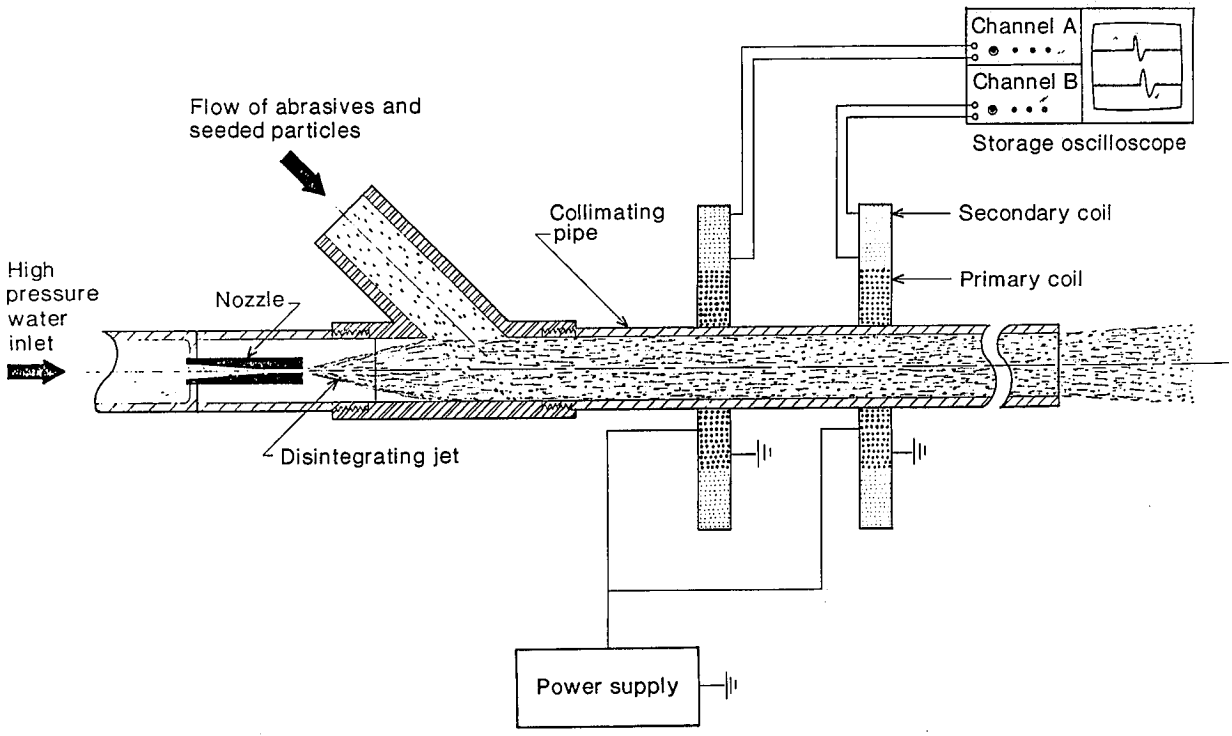

Figure 1. - Jetting and Electronic Velocimeter Hardware.

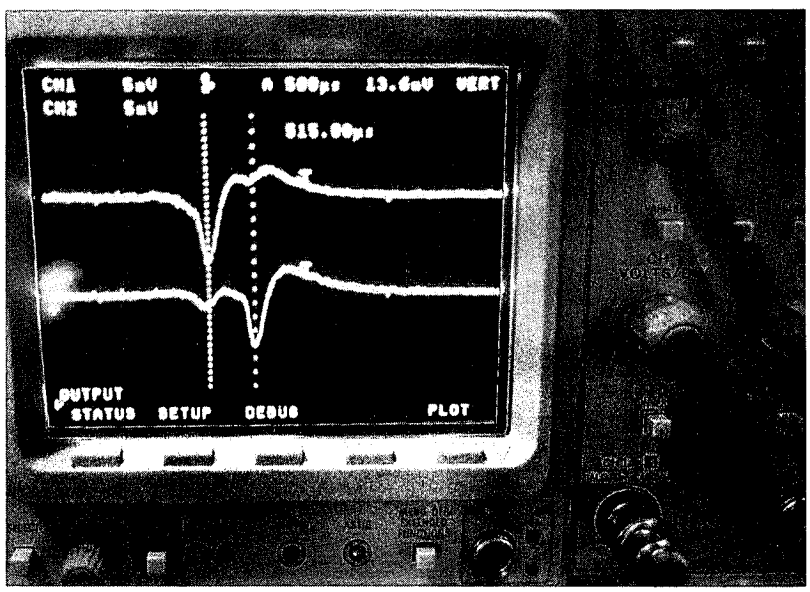

Figure 2. - A Pair of Signals From a Tracer Particle.

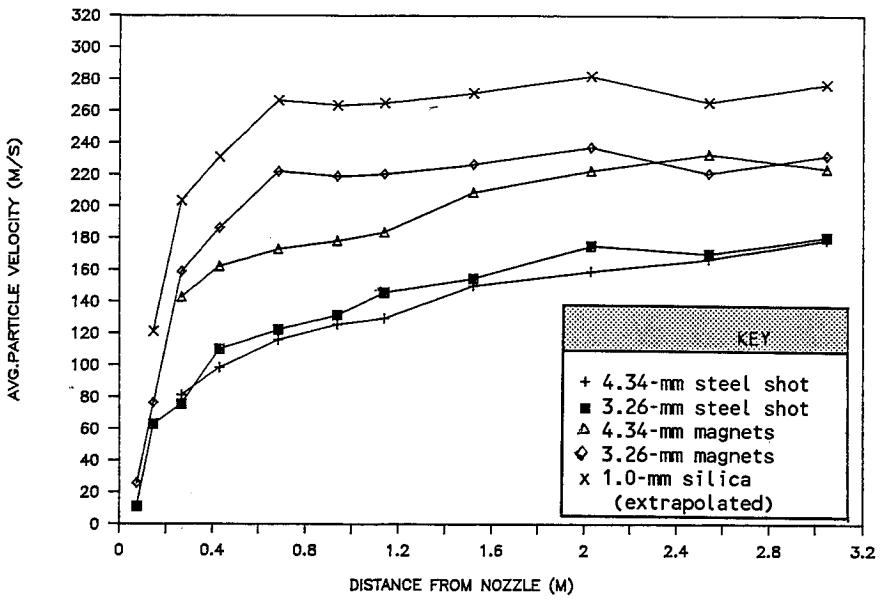

Figure 3. - The Effect of Specific Gravity and Particle Size on Velocity Profiles. Four Lower Curves - Average Velocities Measured With Electronic Velocimeter. Upper Curve - Abrasive Velocity Estimated by Extrapolating Measured Data.

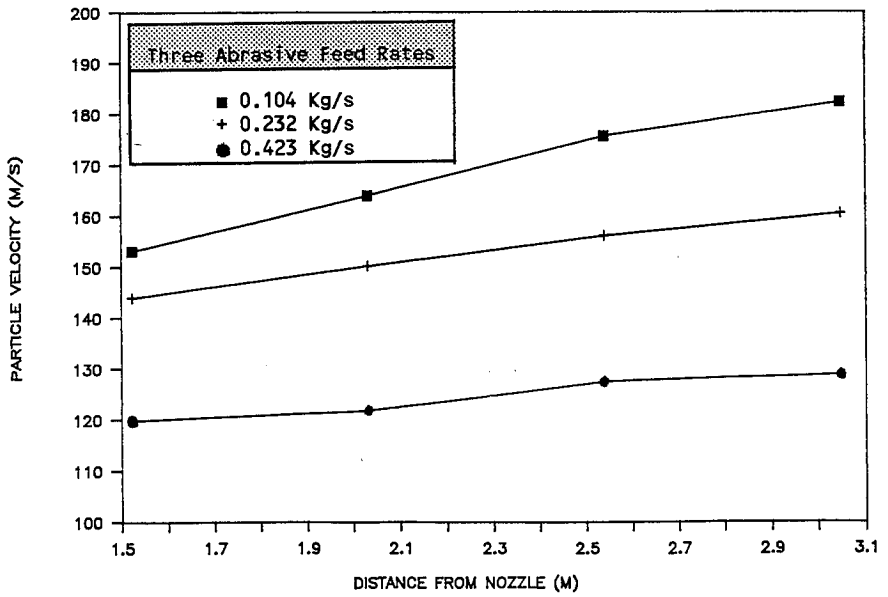

Figure 4.- The Effect of Increasing Abrasive Mass Flow Rate on Particle Velocity (69 MPa, 1.1 L/s Jet, Abrasive Supply Seeded With 3.26-mm Steel Shot).

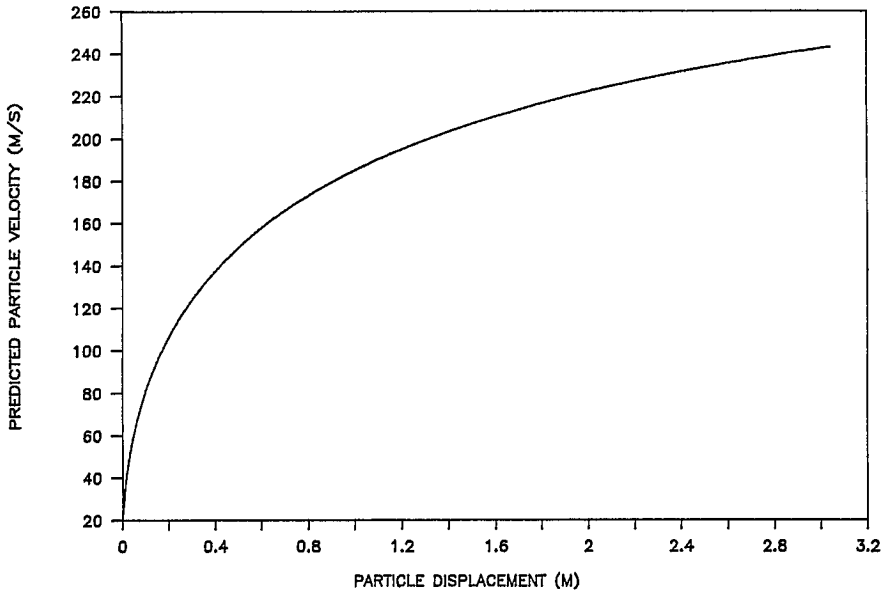

Figure 5. - Predicted Velocity Profile for 1.51-mm Silica Particles Using Single-Phase Viscous Drag Model (Assumes Air at 320 m/s and 100 psig).

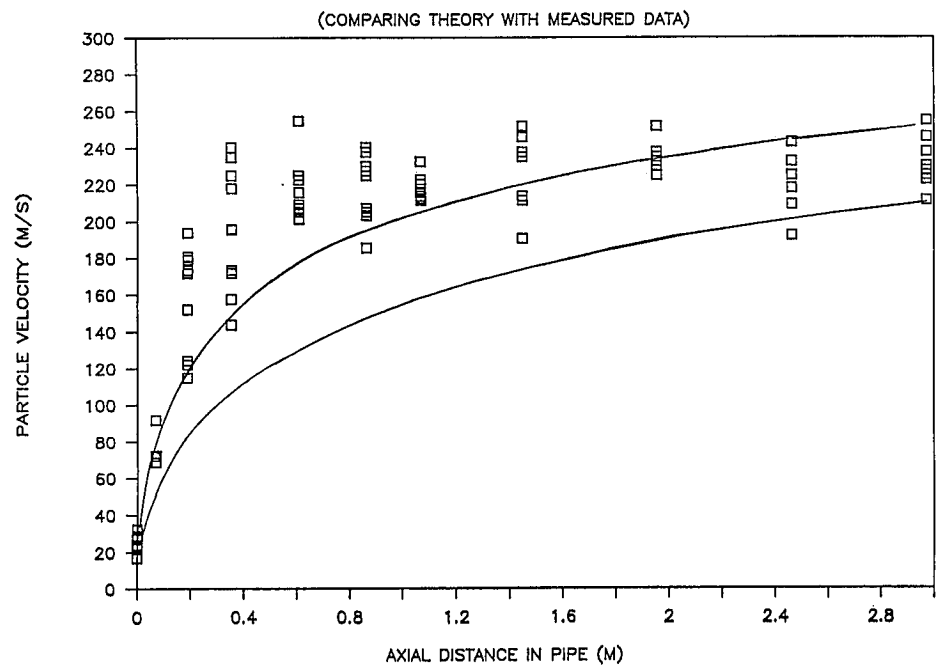

Figure 6. - Data - Measured Velocities of 3.26-mm "Plastiform" Particles. Superimposed Curves - Predicted Velocity Profiles of "Plastiform" Particles Using Mass-Weighted (Upper Curve) and Volume-Weighted Viscosity (Lower Curve). Two-Phase Adjusted Viscous Drag Model Was Used With Fluid Velocity of 310 m/s.

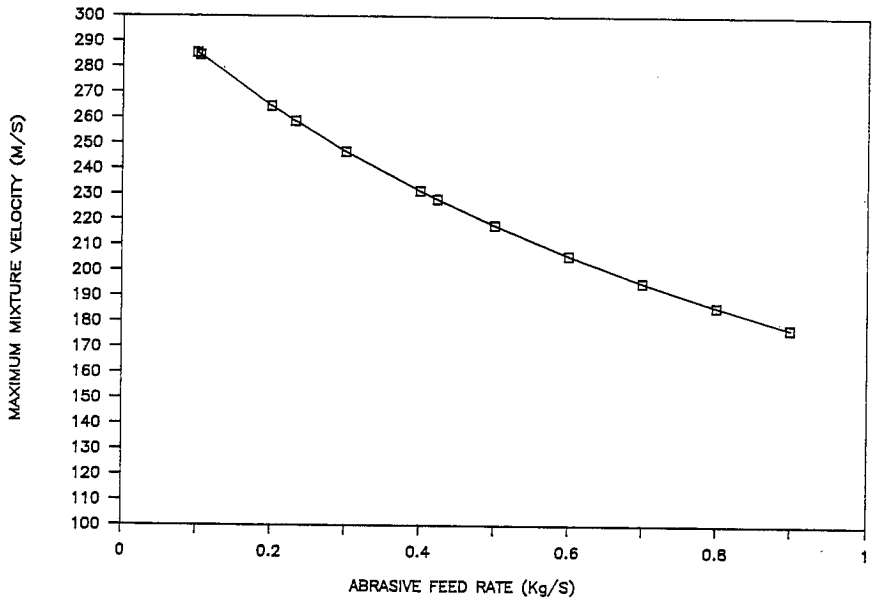

Figure 7. - Maximum Theoretical Velocity of Three-Phase Mixture (Assumed 1.1-L/s Fluid Flow at 310 m/s and Abrasive Feed at 15 m/s).

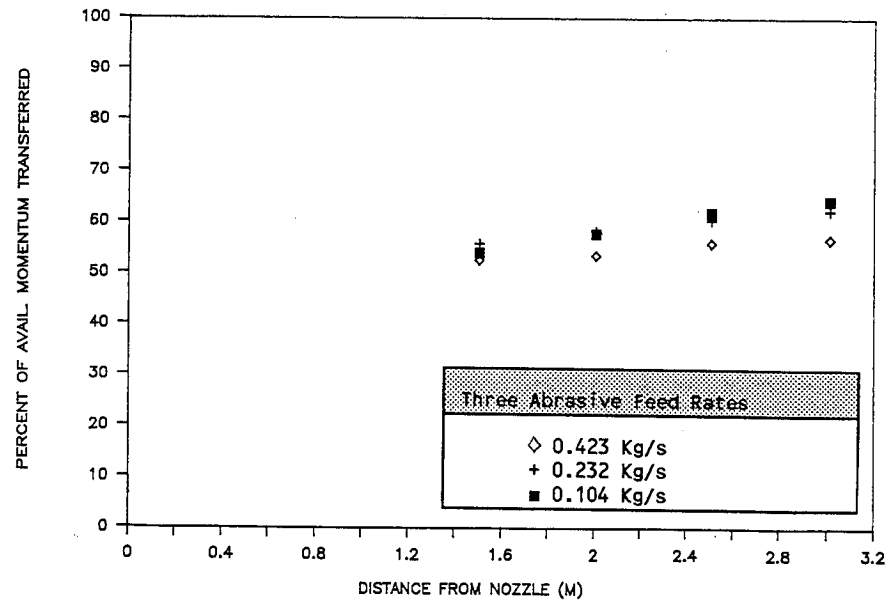

Figure 8. - Percent of Total Available Momentum Transferred to Particles for Three Abrasive Flow Rates. (69 MPa, 1.1 L/s Jet, Abrasive Supply Seeded With 3.26-mm Steel Shot.)

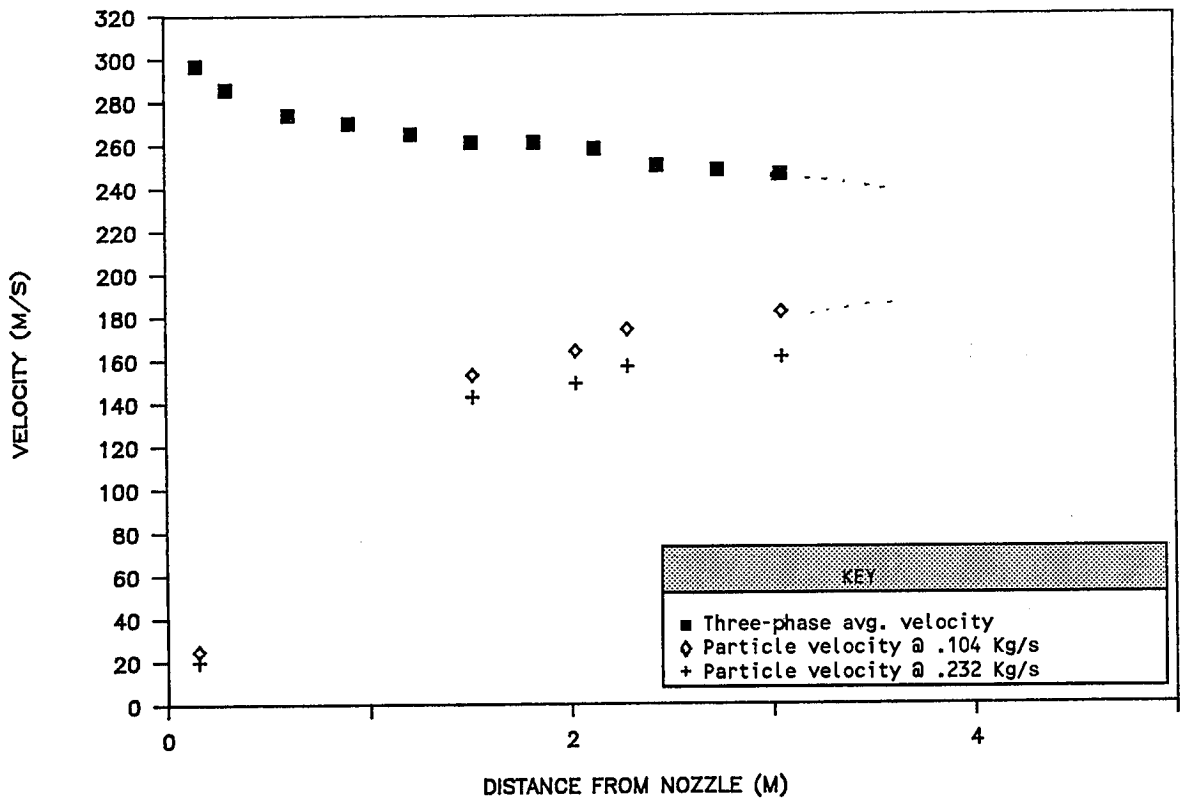

Figure 9. - Comparison of Three-Phase Mixture Velocity With Individual Particle Velocity. Upper Data - Three-Phase Average Velocities from Reference 8 (0.15-Kg/s Abrasive Feed). Lower Data - Measured Velocities of 3.26-mm Steel Shot Seeded Into Abrasives at Feed Rates of 0.104 and 0.232 Kg/s.

6th American Water Jet Conference
August 24 - 27, 1991: Houston, Texas Paper 23

Correlation Between Particle Velocity And Conditions Of Abrasive Waterjet Formation

Wei-Long Chen
Waterjet System Division, Ingersoll-Rand Company, U.S.A.

E.S.Geskin
New Jersey Institute of Technology, U.S.A.

ABSTRACT

Water and abrasive particle velocities in an abrasive waterjet (AWJ) were measured by the use of a Laser Transit Anemometer (LTA). The measurements were performed at different diameters of water orifice and focusing tube, abrasive mass flow rates and particle sizes. An empirical equation for the prediction of mean value of the particle velocity for a certain given conditions was constructed. The coefficient of correlation between experimental and computed results is equal to 0.93. The obtained equation has shown the correlation between the kinematic characteristics of AWJ and its formation. The weight of each parameter employed in this study can also be evaluated from this equation. The obtained information can be used to improve the energy transfer efficiency from water flow to the entrained abrasive particles.

1.0 INTRODUCTION

An abrasive waterjet (or AWJ for short) is formed when a high-velocity waterjet is mixed with abrasive particles and expelled through a focusing tube. The high-velocity waterjet is generated by the highly pressurized water passing through the sapphire orifice, which is called sapphire waterjet in this study for distinction. The cutting of material is a process in which material removal takes place due to the erosion action of such abrasive particles striking upon the work surface [1]. The determination of particle velocities at different conditions of AWJ formation is essential to the understanding of the erosion mechanism involved in AWJ cutting process and to the establishment of the prediction model of cutting results.

The velocities of particles in a stream of gas or liquid can be determined theoretically by solving the particle motion equations based on the given initial and boundary conditions. For an AWJ, which is our area of interest, theoretical determination is not possible due to an insufficient knowledge of particle acceleration mechanism. Also the entry of air inside the mixture at the time of particle injection poses increasing difficulties to find a theoretical solution.

The purpose of this study is to construct an empirical equation for the prediction of mean value of particle velocity at a certain given condition. The measurement of particle velocity was conducted at different diameters of water orifice and focusing tube, different abrasive mass flow rates and different grade sizes of particles. Other operational parameters were left unchanged from those normally used in AWJ cutting practice, i.e., water pressure maintained at 325 MPa., garnet sand was the abrasive used and the length of focusing tube was kept at 51 mm. A Laser Transit Anemometer from Dentec Electronic Co. was used to measure particle velocities. The abrasive waterjet cutting system, including intensifier, CNC controlled motion station and abrasive nozzle assembly, was designed and manufactured by Ingersoll-Rand Company.

2.0 DESCRIPTION OF EQUATION DERIVATION

The operational principle of LTA has been presented in [2]. The feasibility of LTA in measuring the velocities of waterjet and its entrained particles has also been proven in the same report by comparing the results of LTA measurements with the data obtained by the well established techniques, such as force measurements and Schilieren photography.

The experimental matrix used in this study is shown in Figure 1. A factorial approach to the experimental design was adopted for this study. The experiments were conducted in two suites. The first suite was an investigation covering all the combination of the diameters of water orifice and focusing tube, which were available and commonly used in industry, at a constant mass flow rate value of 68 g/min. The second suite was to study the effects of other parameters on the particle velocity under certain sizes of water orifice and focusing tube. The selection of the values of abrasive mass flow rates used in all diameter combinations is based on the consideration of the wear within the focusing tube. This approach not only ensures that the data taken was sufficient for a sound statistical analysis to derive an empirical equation, but also enables us to understand the relative importance of the various parameters investigated.

Four different regression models such as linear, power, exponential, and natural logarithm were used to construct the empirical equation. The selection of a desired regression model was based on the comparison of the value of correlation coefficients associated with each regression model. TempleGraph, developed by Mihalisin Associates, is a software package used in this study to analyze experimental data via regression operation and represent the obtained results graphically.

3.0 RESULTING EQUATION AND DISCUSSIONS

3.1 RESULTING EQUATION

The regression analysis of the values of the parameters such as $V_{s.w.}$, $V_{c.w.}$, V_a, d_n, d_c and m_a was carried out. The results with higher correlation coefficients are shown in Figures 2-4. It was observed that the following equation has the highest value correlation coefficient:

$$Y = a * X^b$$

where

$$Y = (V_{c.w.} - V_a)/V_{s.w.}$$

$$X = (Q_a/Q_w)^D;\ D = (d_n/d_c)^2$$

$$a = 0.627$$

$$b = 2.557$$

$V_{s.w.}$: the velocity of sapphire waterjet

$V_{c.w.}$: the velocity of waterjet passed through the focusing tube while the abrasive inlet valve is kept closed. (Such waterjet is called carbide waterjet for distinction with sapphire waterjet in this study)

V_a : velocity of abrasive particles

Q_a : volume flow rate of abrasives

Q_w : volume flow rate of water

The above equation is derived using the volume flow rate instead of mass flow rate. The main reason behind this is the availability of this equation for potential application where different types of fluid media are used.

3.2 APPLICATION OF RESULTING EQUATION

The obtained resulting equation enables us to predict the mean value of the velocities of particles entrained in an AWJ. The procedure for the computation is illustrated as follows:

1). The value of $(V_{c.w.}-V_a)/V_{s.w}$ is obtained from given values of d_n, d_c and Q_a.

2). The value of $V_{s.w}$ is determined by the product of a coeffi-

cient and the velocity computed from Bernoulli's equation. This coefficient is used to take into account the pressure drop that occurred within the sapphire orifice. The value of this coefficient is chosen as 0.85 which is determined from the ratio of measured and computed velocities as presented in [2] and as shown in Figure 5.

3). As mentioned in the preceding section, the ratio of $V_{c.w.}/V_{s.w}$ depends on the superiority of the alignment between the sapphire orifice and focusing tube. As of today, there is no available data which can provide us such information to determine this ratio. Ideally, this ratio is expected to be equal to 1 and this value is used in our computation.

The computed velocities according to the above procedure and the corresponding measured particle velocities are shown in Figure 6. The difference between the two values does not exceed +/- 100 m/sec.

3.3 DISCUSSIONS

The acceleration of the particles entrained in an AWJ occurs within the focusing tube and results from momentum transfer with sapphire waterjet [3]. Therefore, the velocities of those particles not only depend on the sapphire waterjet but are also affected by the alignment between the water orifice and focusing tube used. The superiority of such alignment can be determined from the magnitude of the velocity of waterjet passing through the focusing tube while the the abrasive inlet valve is kept closed. The procedure for alignment and its influence on the entrained particles was reported in [2]. The velocity difference between carbide waterjet and entrained abrasives, (Vc.w.- Va), is a measure of momentum transfer between the waterjet and entrained abrasives. The higher its value, the lower the abrasive velocity Va and therefore, lower mixing efficiency.

The characteristics of an AWJ formed in the certain range of diameter ratio of sapphire orifice and focusing tube is expected to be different with an AWJ formed in some other ranges of such diameter ratio. For example, an AWJ formed with very small ratio of d_n/d_c has the same characteristics as a free jet (jet submerged in the air) whereas the AWJ with d_n/d_c equal to 1 is essentially considered as the flow in a straight pipe. Therefore, the use of the obtained equation is limited to the diameter ratio in the range used in this study, which ranges from 0.11 to 0.41. For the diameter ratio outside this range, further study is required.

As shown in the resulting equation, the effect of the particle size has not been taken into consideration. It is based on the fact that the velocities of entrained particles are practically

independent of the size of added particles, which was reported in [2]. The reason of similarity of velocity at different sizes of particle is the disintegration of the added particles during the acceleration process [4].

As mentioned in preceding section, the parameters investigated in this study are the diameters of sapphire orifice and focusing tube, the size of added particles and its mass flow rate. For other parameters such as the length of focusing tube and water pressure are kept constant. Therefore, the obtained equation is only applicable to calculate the velocities of particles in an AWJ under considered conditions. However, it may be expected that the kinematic variable $(V_{c.w.}-V_a)/V_{s.w.}$ can be also used in the construction of the equation for a wider range of experimental processes.

4.0 CONCLUSIONS

An optical instrument(LTA) was used to measure the velocities of the particles entrained in an AWJ at different diameters of sapphire orifice and focusing tube, different abrasive mass flow rates and sizes of particles. An empirical equation for predicting the mean value of the particle velocity under considered conditions was constructed based on the obtained experimental results. The correlation coefficient between experimental and computed results is equal to 0.93. The resulting equation has provided the following information:

1). The velocities of particles entrained in an AWJ are strongly correlated to the alignment between the sapphire orifice and focusing tube. The alignment technique used in this study does not allow us to generate the particle velocity distribution at same values of operational parameters.

2). The kinematics of an AWJ is determined by the dimensionless group $(V_{c.w.}-V_a)/V_{s.w.}$.

3). As depicted in the derived equation, the velocity of sapphire waterjet has the highest influence on particle velocities, which is determined by the water discharge pressure and the nozzle coefficient.

4). In addition to predicting the particle velocity, the obtained equation enables us to estimate the weight of each parameter employed in this study as well.

5.0 ACKNOWLEDGMENT

The authors gratefully acknowledge NSF support under grant no. DMC8810639 "Fundamental Study of Abrasive Waterjet".

REFERENCES

1. Hashish, M., "On the Modeling of Abrasive-Waterjet Cutting", Proceedings of 7th International Symposium on Jet Cutting Technology, Ottawa, Canada, 1984
2. Chen, W.L. and Geskin, E.S., "Measurement of the Velocity of Abrasive Waterjet by the Use of Laser Transit Anemometer", Proceedings of 10th International Symposium on Jet Cutting Technology, Amsterdam, 1990
3. Isobe, T., Yoshida, H. and Nishi, K.,"Distribution of Abrasive Particles in Abrasive Water Jet and Acceleration Mechanism", Proceedings of 9th International Symposium on Jet Cutting Technology, 1988
4. Galecki, G. and Mazurkiewicz, M., "Hydroabrasive Cutting Head-Energy Transfer Efficiency", Proceedings of 4th U.S. Water Jet Conference. 1987

Dn / Dc	0.3556 (mm)	0.3048 (mm)	0.254 (mm)	0.1778 (mm)
	Ma(g/min)			
0.863 (mm)	13, 68	13, 68	13, 68 ,30* 144*, 343*	13, 68
1.09 (mm)	13, 68	68	13, 68, 68*	13, 68, 145
1.6 (mm)	68, 145 300, 477 240, 500	68	68, 68*, 68'	68, 68* 68', 68x

Footnotes:
No Symbol: 0220
* : 890
' : 0120
x : 850

Figure 1: Experimental Matrix

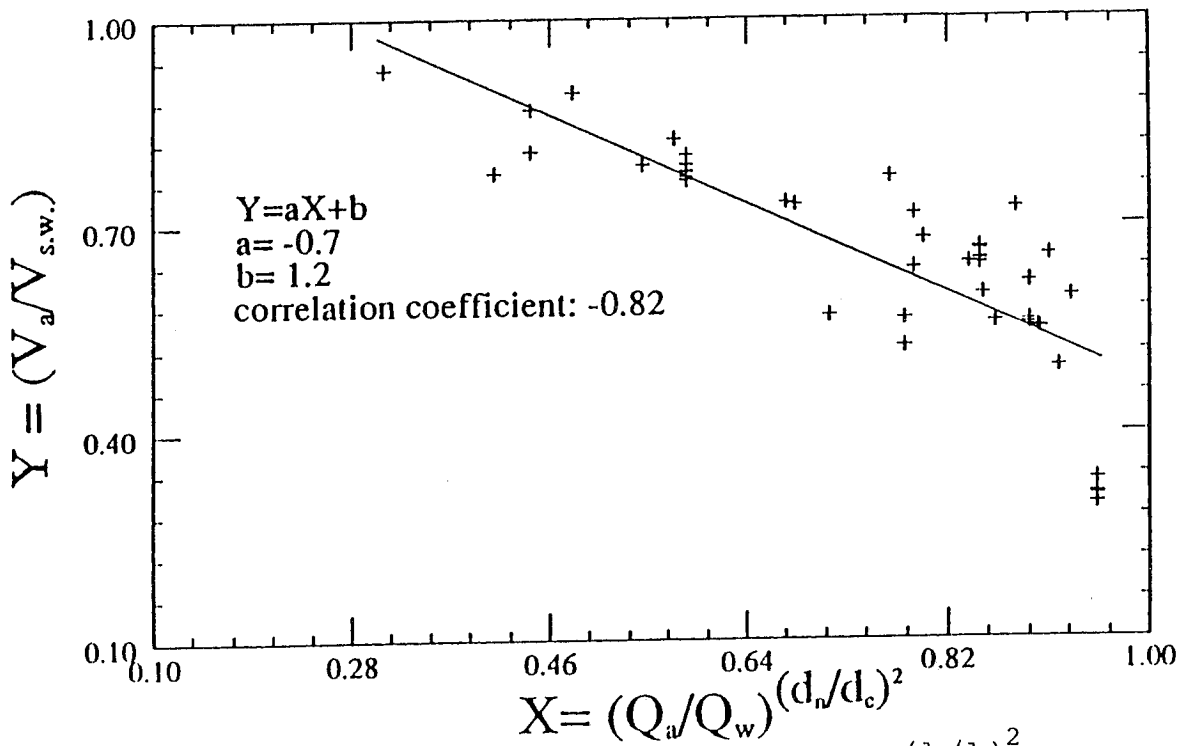

Figure 2: Correlation between (Va/$V_{s.w}$) and (Qa/Qw) $(d_n/d_c)^2$

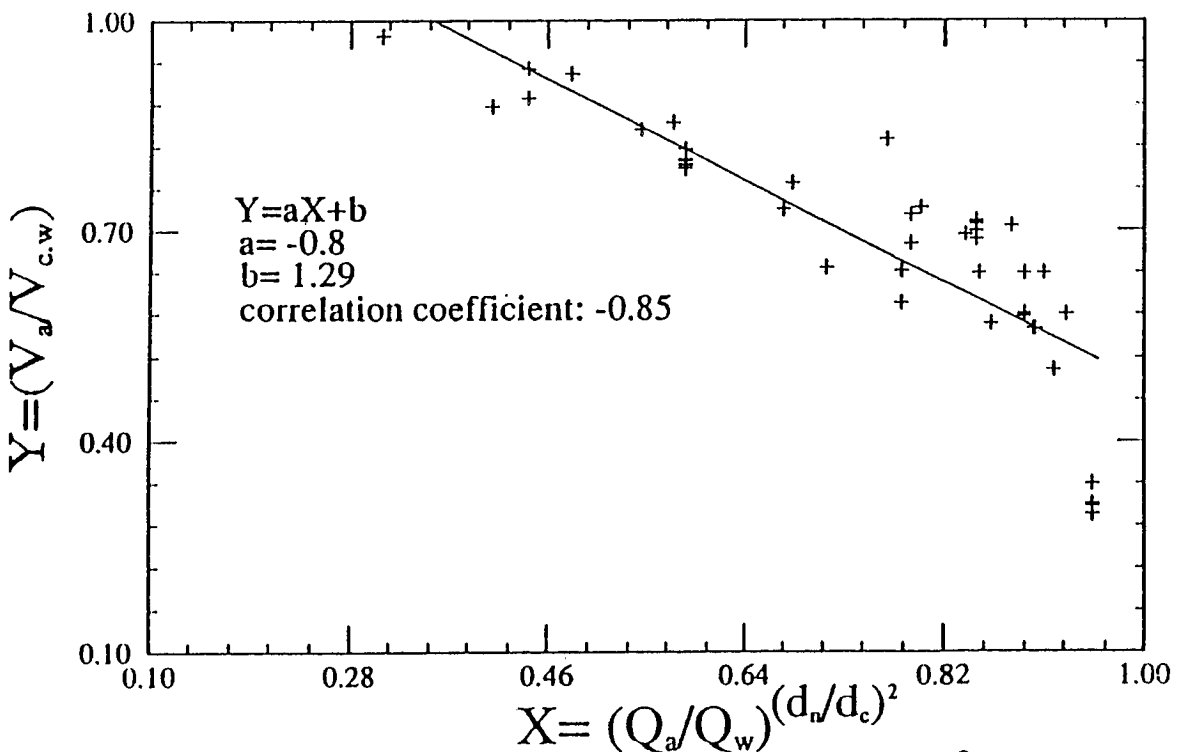

Figure 3: Correlation between (Va/Vc.w) and Qa/Qw $(d_n d_c)^2$

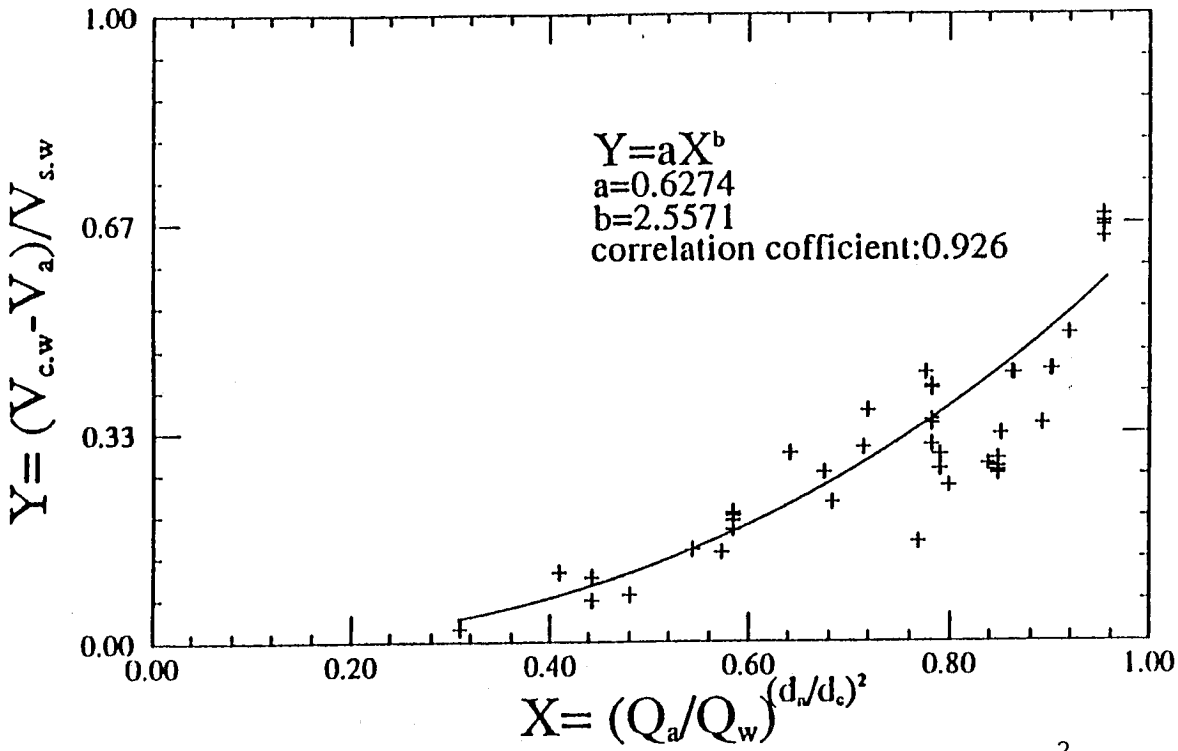

Figure 4: Correlation between $(Vc.w-Va)/V_{s.w}$ and $(Qa/Qw)^{(d_n d_c)^2}$

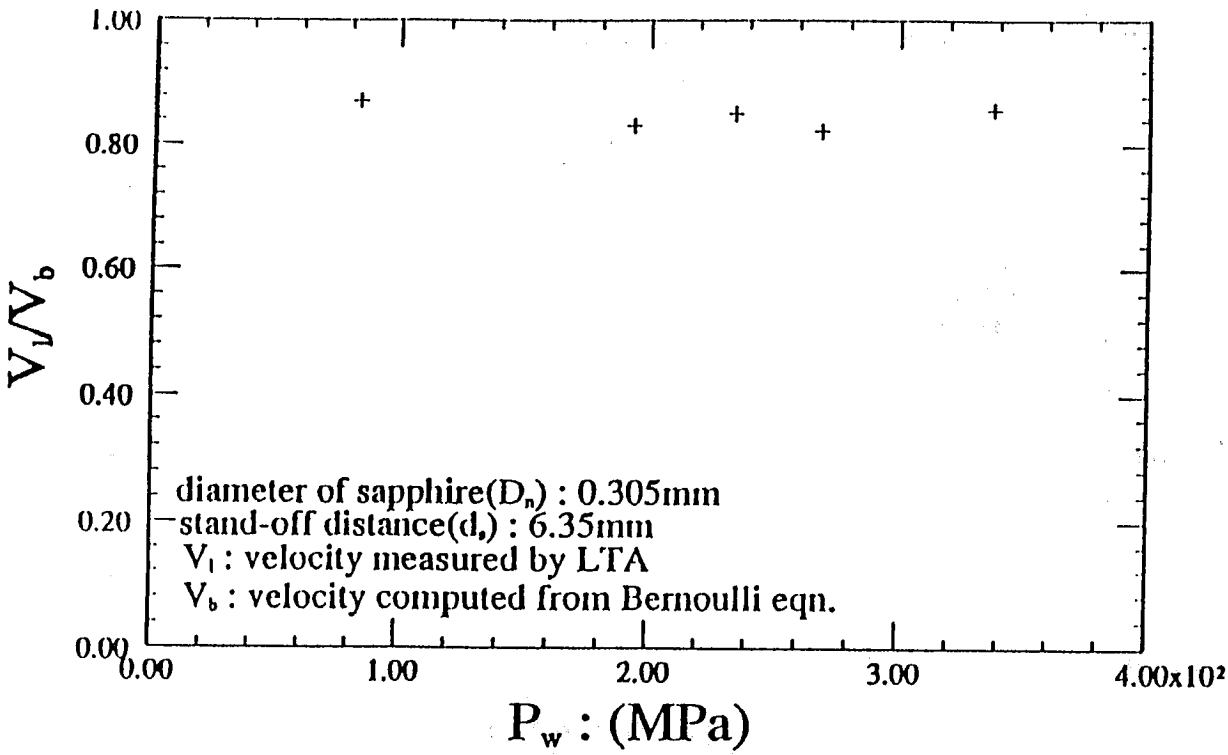

Figure 5: Comparison between LTA Measurements and Bernoull: Equation Computation

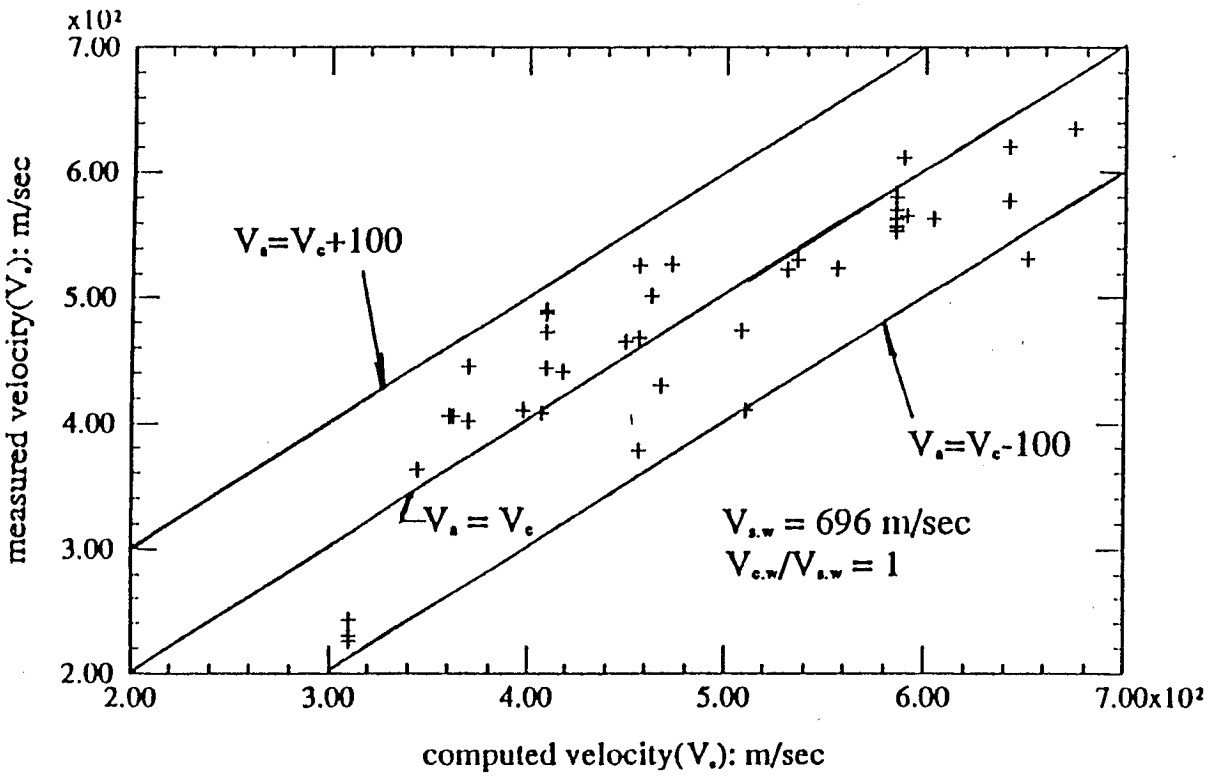

Figure 6: Comparison between computed and measured velocities.

6th American Water Jet Conference
August 24 - 27, 1991: Houston, Texas Paper 24

Long Life Abrasive Water Jet Nozzles and Their Effect on AWJ Cutting

Greg A. Mort
Boride Products, Inc.
Traverse City, MI, USA

ABSTRACT

An investigation of wear materials for abrasive water jet (AWJ) cutting nozzles (mixing tube, focusing tube) was conducted, aimed at increasing nozzle predictability, consistency, and life. Material wear characteristics were investigated using ASTM abrasion and erosion tests. Materials which performed well under ASTM test conditions were selected for further laboratory and field tests. The additional tests performed, investigated performance by varying the nozzle bore, length, materials, and changing the abrasive feed rates and types. Dow XUS35516 Developmental Composite Carbide (Composite Carbide) nozzles demonstrated more than 20 times the life of tungsten carbide/cobalt, extending nozzle life to an average of 70 hours. The wear rates demonstrated a high degree of predictability and consistency.

Organized and Sponsored by the Water Jet Technology Association.

1.0 INTRODUCTION

The introduction of long-life abrasive water jet nozzles has significantly broadened the potential for AWJ cutting technology & applications. Near net shape cutting and consistent long uninterrupted cuts can now be accomplished.

This paper will discuss the wear properties of several nozzle materials. A variety of ceramics and cermets will be investigated under various laboratory and field conditions. Data will be shown comparing the above materials to the standard tungsten carbide/cobalt nozzles.

2.0 WEAR PROPERTIES OF HARD MATERIALS

To qualify materials, three ASTM laboratory procedures were conducted for screening purposes; ASTM G-65, ASTM G-76, and ASTM B-611. These test procedures are contained in Appendix A.

A compilation of results for ceramic and cemented carbide compositions commonly used for nozzles is shown in Table 1 and Figures 1, 2, and 3.

All of the results reported in Table 1 were obtained using our laboratory test devices under identical conditions.

When we compare the dry abrasion test results (G65), the Composite Carbide is clearly the most wear resistant at 693 $1/cm^3$; the tungsten carbide/cobalt system was the next highest, in the range of 275-440 $1/cm^3$; and the ceramic materials the least resistant, ranging from 129-150 $1/cm^3$. There is no clear indication that high hardness automatically implies high abrasion resistance.

In comparing the erosion resistance (G76), Composite Carbide is in the range of .05-.090 mm^3/gm x 1000, followed by boron carbide .26-.42 mm^3/gm x 1000, tungsten carbide/cobalt materials 4.8-21.4 mm^3/gm x 1000, and finally, the general group of ceramic materials 15-40 mm^3/gm x 1000. In this type of test, the higher hardness materials display better wear resistance.

The slurry abrasive test B-611 is a very severe test. Under these conditions none of the hard materials tested can compare with the slurry abrasion resistance of the Composite Carbide (904 $1/cm^3$ compared to .8-48 $1/cm^3$ for all other materials tested). Composite Carbide was two orders of magnitude more wear resistance than its closest rival Tungsten Carbide/Cobalt.

3.0 UNIVERSITY OF RHODE ISLAND (URI) SCREENING EXPERIMENTS

A project was initiated at URI to conduct actual AWJ experiments using several materials which showed the high abrasion and erosion properties under ASTM procedures. The study was designed to compare nozzle materials under identical conditions with three different abrasives; garnet, aluminum oxide and silicon carbide. Also three different suppliers and four different grits of garnet were evaluated using the standard tungsten carbide and Composite Carbide nozzles.

The abrasive cutting was performed with a Flow System model 11 x pump water jet cutting system. The water jet stream was controlled at 241 MPa (35,000 psi). The jewel ranged from .228-.457mm (.009-.018 inch) bore and nozzles used ranged from .812-1.574mm (.032-.062 inch) bores. The abrasives were gravity fed to the nozzles at various rates of .20-.68 kg/min (.45-1.50 lbs/minute). The jewel/bore combinations used were as follows: .227/.813mm (.009/.032), .330/1.118mm (.013/.044), and .457/1.524mm (.018/.060). A AWJ cutting head system is shown schematically in Figure 4.

Abrasives - Most of the nozzles were tested with three different abrasives; 80-mesh garnet [$Fe_3Al_2(SiO_4)_3$], aluminum oxide (Al_2O_3), and silicon carbide (SiC). Presently, garnet is the principal abrasive used by the AWJ industry. Alumina and Silicon Carbide are used for very special applications, however, nozzle wear is so rapid it is not economically practical for most applications.

Material performance data with garnet abrasive is shown in Figure 5, aluminum oxide abrasive is shown in Figure 6, and silicon carbide abrasive in figure 7. An in-depth study of nozzles with silicon carbide abrasive was not conducted because the results in (Figure 7) would indicate that the 1-5 minute life time would prohibit its use with any of the nozzle materials tested.

Garnet is the most widely used abrasive in the AWJ industry, which prompted an in-depth study of this abrasive using three brands and four grits which were commercially available. Nozzles made from standard tungsten carbide and Composite Carbide (because of superior wear properties) were chosen for this experiment.

The useful life of a nozzle is assumed to be terminated when the exit bore has increased in diameter by 20 mm. Actual wear life is determined in the work place where it is measured by such factors as quality of cut, maintenance of cutting speeds, width of cut, etc.

For the Aluminum Oxide abrasive system (Figure 6), Boron Carbide appeared to have the best wear life (45-80 min) and may be economically justified for certain difficult cutting jobs. It would appear that the use of commercial Tungsten Carbide nozzles (2.8 min) would be impractical with this abrasive. The Composite Carbide nozzle appears to be equivalent to Boron Carbide. The two experimental grades of Boron Carbide did not show a significant improvement in wear resistance over commercial hot pressed B_4C materials.

The garnet abrasive testing (Figure 5) gave very unusual results, in that the B_4C-based systems were only 1.5-2.0 times over that of the commercial tungsten carbide product, consequently, the B_4C Systems would not be economically competitive. However, the Composite Carbide nozzle showed an outstanding improvement in wear life exceeding 15 times longer than the commercial tungsten carbide.

4.0 ABRASIVE WATER JET CUTTING FIELD TESTS

The exceptional wear resistance observed for the Composite Carbide nozzles with garnet abrasives led us to concentrate on this material as being the best candidate for further AWJ cutting field testing. The previous studies indicated that the Composite Carbide wear

resistance was at least 15 times greater than that observed for the standard tungsten carbide used for this application.

As a consequence, several field tests were performed at various abrasive water jet cutting shops.

1. ANC Machining, Worcester, MA (Job Shop #1)

   This was the first field test that clearly established the superior wear resistance of the new Composite Carbide material over commercial grade tungsten carbide in actual operating conditions. This shop does a variety of jobs requiring different abrasive mesh sizes, cutting speeds, and cutting times. Consequently, the cutting conditions varied significantly during the life of the Composite Carbide nozzles which is typical of many of job shops currently involved in water jet cutting. Wear rates were determined to be an average of 6.9×10^{-3} mm/hr for the Composite Carbide material vs. 127×10^{-3} mm/hr for the commercial tungsten carbide nozzles; two orders of magnitude improvement in wear life. These results are indicated in Figure 9.

Some of the benefits that ANC attached to the long life Composite Carbide nozzles were:

- Less operator attention required.
- It offered us more capability so we could expand our customer base; i.e. jobs involved long cutting times >3 hours. The current nozzle life of approximately 4 hours makes it difficult to accomplish a consistent, high quality, finished cut on materials (jobs) requiring several hours of cutting time.
- Lower operating costs (less nozzle cost per hour of running time).
- Higher quality of cut.

2. Trade-A-Blade, Indianapolis, IN (Job Shop #2)

   This shop does routine cutting of worn steel saw blades which are refinished and resold. They basically cut the same material on a continuous basis. Consequently, the cutting conditions are normally constant and controlled. This shop's results gave us the most consistent wear rate comparison between the Composite Carbide material ($.36 \times 10^{-2}$ mm/hr) and tungsten carbide (15×10^{-2} mm/hr); Figure 10. In this case the Composite Carbide nozzle was found to be 41 times more wear resistant.

   The lower wear rates observed are believed to be due to the fact that this shop uses an abrasive feed rate of .23 kg/min (0.5 lb/min) while most shops use feed rates between .45-.68 kg/min (1-1.5 lb/min).

   The major advantage they saw in the long life Composite Carbide nozzles was that it required significantly less operator attention to maintain a cut within their required tolerances;

they currently must continuously reduce feed rates, over the 3-4 hour life of their present nozzle, in order to maintain an acceptable edge finish.

3. Hydro-Abrasive Machining, Inc., Los Angeles, CA (Job Shop #3)

Hydro-Abrasive Machining, Inc. is a large job shop with major aerospace customers. The results from this test are shown in Figure 11.

The typical abrasive feed rate for this shop is .45 kg/min (1.0 lb/min). Observed wear rates were 76.2 x 10^{-3} mm/hr for the Tungsten Carbide material and 7.6 x 10^{-3} mm/hr for the Composite Carbide.

A significant attribute of Composite Carbide to this firm was the fact that a superior edge finish could be obtained. They reported that cutting was normally out of tolerance in 1.5 hours using their current commercial Tungsten Carbide nozzle material. As a result of the improved edge finish, the customer tightened the tolerances such that it cannot be met without using the Composite Carbide nozzle.

4. Remcon INC., Bath, OH (Job Shop #4)

Remcon is a contract distributor and has in-house job shop facilities. Remcon collected data from nozzles that were tested at several undisclosed water jet cutting shops. Actual production was run using garnet and mineral aggregate abrasives. The results are shown in Figures 12 & 13.

5. Flow International, Corp., Kent, WA

Flow International carried out laboratory and field tests using a local job shop and in-house test facilities.

The Composite Carbide nozzles were evaluated versus their commercial tungsten carbide nozzles using garnet abrasive. In addition, they were also evaluated against a Boride Products' hot pressed Boron Carbide nozzle using alumina abrasive.

The laboratory testing confirmed our previous data giving a relative average wear resistance for the Composite Carbide nozzle of .84 x 10^{-2} mm/hr and 35.6 x 10^{-2} mm/hr for the Tungsten Carbide nozzle; 42.5 times more resistant (Figure 14). These wear rates for both nozzle materials are higher than most of those reported above because the abrasive feed rate used in these tests were much higher .68 kg/min (1.5 lbs/min). Identical results were obtained at Hydro-Sabre Technologies, a local job shop, in a twenty-five hour test. Figure 15 shows test results using alumina abrasive.

In addition to the standard wear rate measurements, Flow International measured wear eccentricity as a function of time. These results are compared with their commercial tungsten carbide nozzle in Figure 16. The Composite Carbide nozzle wore evenly throughout the twenty-five hour test whereas the tungsten carbide

nozzle began to wear eccentrically in two or three hours. Flow indicates that an eccentric wear pattern, greater than 26 mm (1.03), significantly affects cutting quality.

6. Ingersoll-Rand, Baxter Springs, KS

Ingersoll-Rand tested several Composite Carbide nozzles and measured bore growth at 40-65 hour intervals. Data is shown in Figure 17. Again the laboratory confirmed our previous findings that Composite Carbide has greater than 15 times the wear life over Tungsten Carbide.

7. Jet Edge, Inc., Minneapolis, MN

Jet Edge conducted a 49 hour laboratory test measuring the bore approximately every 1-2 hours. The wear showed very consistent results over time. The data is shown in Figure 18. This data shows the nozzle to be extremely predictable.

8. Sugino Corp. Schaumburg, IL

Sugino conducted tests comparing two Composite Carbide nozzles to Tungsten Carbide. The results are consistent as seen with other equipment manufacturers. The results are shown in Figure 19.

An overall summary of the wear rate in mm/hour is shown in Figure 20. This data compares the exit bore rate in mm/hour of Composite Carbide, Boron Carbide and Tungsten Carbide nozzles using garnet, aluminum oxide and silicon carbide abrasives. The data was calculated from Figures 9-19.

5.0 BENEFITS OF A LONG LIFE COMPOSITE CARBIDE NOZZLE

Several benefits can be attributed to a long life Composite Carbide nozzle, offering the end-user many advantages and opportunities for AWJ equipment.

Some advantages we observed during our laboratory and field testing along with feedback supplied by users is listed below:

- It expands the capability and technology for users; jobs involving long cutting times >3 hours.
- Less operator attention required.
- Lower operating costs (less cost per hour of running time).
- Higher quality of cut, better edge finish.
- More accurate efficient stream due to a better eccentric wear pattern.
- Allows for greater repeatability.
- Offers a more consistent accurate cut.

- Enabling technology; the ability to broaden markets and closer to near net machining.

- Reduction in abrasive consumption.

- Ability to hold close tolerances.

- Reduced down time of AWJ equipment.

6.0 CONCLUSIONS

One of the major historical drawbacks of AWJ cutting was nozzle wear and dependability, causing more operator involvement, increased costs due to down time and exclusion from certain materials and markets.

We have demonstrated the advantages and benefits of increased productivity and quality by using a long life Composite Carbide nozzle. The data concludes that Composite Carbide nozzles offer an average extended life on the order of 70 hours while maintaining accuracy and consistency and dependable wear. This consistent wear enables the user to control his AWJ system more accurately while opening up new potential markets where long continuous cutting of greater than 3 hours is of importance.

The ASTM data, URI laboratory and field testing have all shown consistent results and considerable increase in performance with Composite Carbide nozzles. Some of the major benefits of using a long life Composite Carbide nozzle include higher quality cuts, consistent wear than can be monitored, improved edge finishes, more efficient stream through better concentricity, greater repeatability and the ability to hold closer tolerances and more AWJ cutting toward near net shape cutting.

The long life Composite Carbide nozzle is available from all leading AWJ equipment manufacturers.

APPENDIX A

The ASTM G-65 procedure involves the abrading of a standard test specimen with 50-90 mesh silica sand. The sand is introduced between the test specimen and a rotating rubber lined wheel. The test specimen is pressed against the rotating wheel which is rotating in the direction of sand flow. The specimens are weighed before and after the test and the loss in mass is recorded. The test apparatus is qualified by standardizing against D-2 tool steel. Abrasion is reported as a wear number, i.e. [1/volume $(mm)^3$ loss]. The value of the test method lies in predicting the relative ranking of various materials in the same scratching abrasive environment.

The ASTM G-76-83 procedure involves a small nozzle delivering a stream of gas containing abrasive particles which impacts the surface of the test specimen. The specific equipment used was a S.S. White Model H Air abrasive unit to control the abrasive flux and velocity. A nitrogen gas stream with entrained abrasive is directed at the test specimen through a 50 mm long by 1.5 mm I.D. tungsten carbide nozzle. Particle velocity is measured using a rotating double disk. The abrasive material used was 50 μm aluminum oxide particles. Tests were performed at both a 90° and 30° impact angle. A dimple-like wear scar is produced by this test and a weight loss is measured. The test results are reported as volume (mm^3) lost per gram of abrasive used. The smaller the number, the more erosion resistant the material. Again, the importance of this test is a ranking of materials under a specific test condition.

The ASTM B-611 procedure measures the wear rate of a test specimen pressed against the periphery of a steel wheel rotating through an aluminum oxide slurry. The specimen is held against the rotation wheel with a specific force, i.e. 20 Kg, applied, by a 10 Kg weight attached to a lever arm. The abrasive slurry was prepared by mixing 30 mesh aluminum oxide grit (57 Alundum - Norton Co.) with water in the proportion of one cubic centimeter per four grams of grit. The wheel was rotated for 1000 revolutions at a rate of 100 rpm. The direction of rotation was from the slurry to the specimen. Abrasive resistance is determined by weighing the specimen and is reported as cubic centimeters of material lost per revolution. The wear number (W) is reported in reciprocal cubic centimeters. This wear test is primarily a screening test to determine the relative abrasive wear resistance of different materials under identical high stress abrasive conditions.

Acknowledgements

Boride would like to thank the following individuals and companies for their contributions to obtain the data shown in this report.

. Chris Lalos - ANC Tool & Manufacturing, Inc.
. Angelo Bougiouris - ANC Tool & Manufacturing, Inc.
. Ken Groves - The Dow Chemical Company
. Kathy Zaring - Flow International, Corp.
. Chip Burnham - Flow International, Corp.
. Richard Woolman - Hydro-Abrasive Machining, Inc.
. Martin Taylor - Hydro-Abrasive Machining, Inc.
. Jose Munoz - Ingersoll-Rand
. Eric Chalmers - Jet Edge, Inc.
. Bob Kiehl - Remcon, Inc.
. Jeff Yunker - Sugino Corporation
. Randy Bingham - Trade-A-Blade Co.
. Dr. Thomas Kim - University of Rhode Island

References

1. "Summary of Abrasive Water Jet Nozzle Laboratory and Field Experiments", Ken Groves, The Dow Chemical Co., Midland, MI, March 13, 1989.

2. "A New Class of Wear Materials from the ROC Process", P. A. Doty and Ken Groves, The Dow Chemical Company, and G. A. Mort, Boride Products, Inc.

WEAR PROPERTIES OF HARD MATERIALS

Material	Typical Vickers Hardness kg/mm^2	WEAR TEST DATA Dry Abrasion $1/cm^3$	Erosion 30° mm3/gm.1000	Erosion 90° mm3/gm.1000	Wet Abrasion $1/cm^3$
Composite Carbide	2650	693	0.09	0.05	904
K68 [6% Cobalt]	1800	440	21.4	8.7	48
K602 [1.5% Cobalt]	---	275	5.8	4.8	---
Al_2O_3	2000	---	30.4	39.5	0.8
Si_3N_4	1550	---	15.0	25.5	4.1
SiC	2800	150	---	18.0	7.8
B_4C	3100	139	0.42	0.26	11
TiB_2	---	129	---	---	2.65

Dry Abrasion [ASTM G65]: Dry sand rubber wheel test. Wear number is 1/volume loss.

Erosion [ASTM G76]: Wear data reported as volume loss per gram of abrasive.

Wet Abrasion [ASTM B611]: Steel wheel, Al_2O_3 slurry test. Wear number is 1/volume loss.

TABLE 1

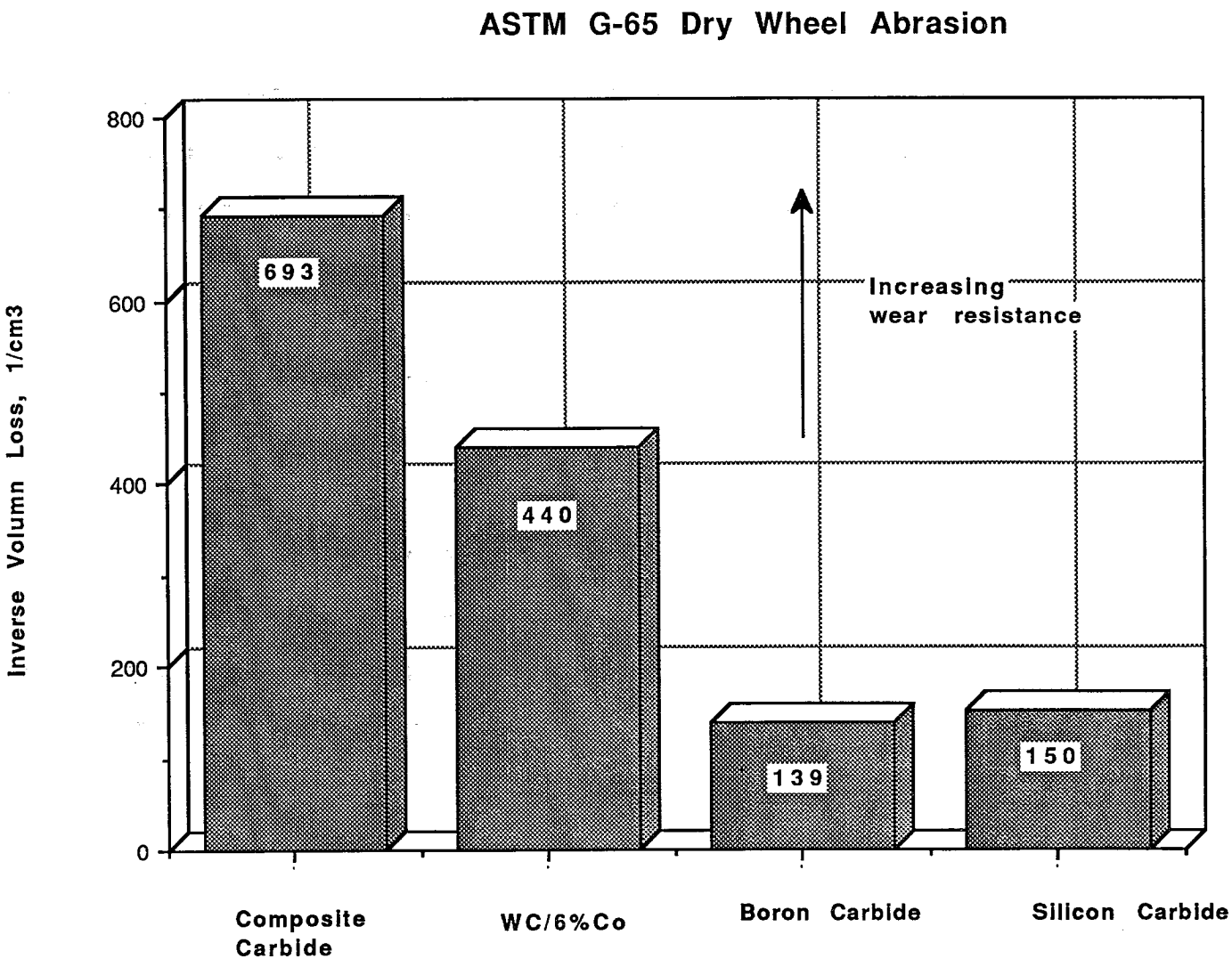
ASTM G-65 Dry Wheel Abrasion
Inverse Volumn Loss, 1/cm3
800
600
400
200
0
693
440
139
150
Increasing
wear resistance
Composite
Carbide
WC/6%Co
Boron Carbide
Silicon Carbide

FIGURE 1

ASTM G-76 Erosion Test

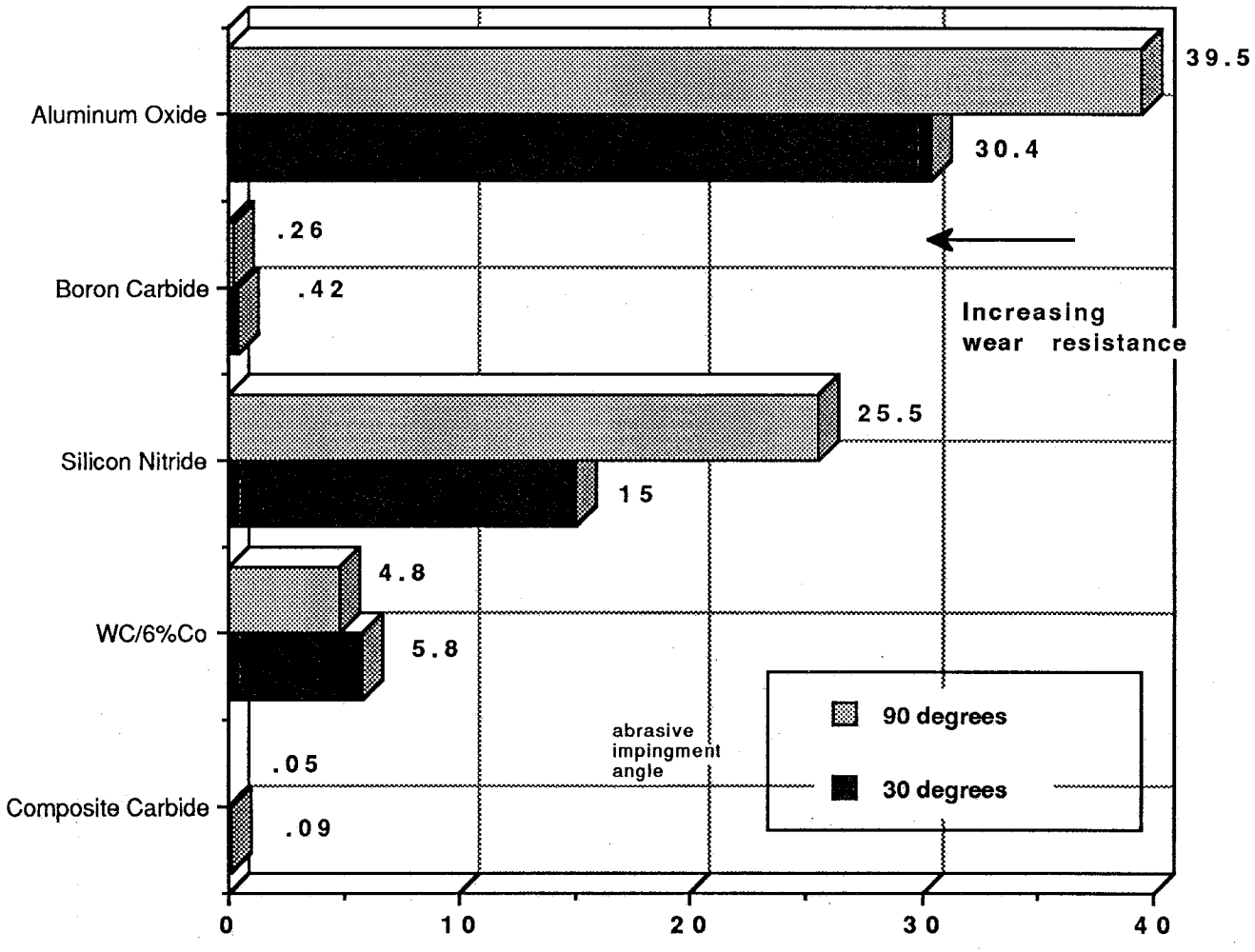

Volumn Loss, mm3/gm x 1000

Figure 2

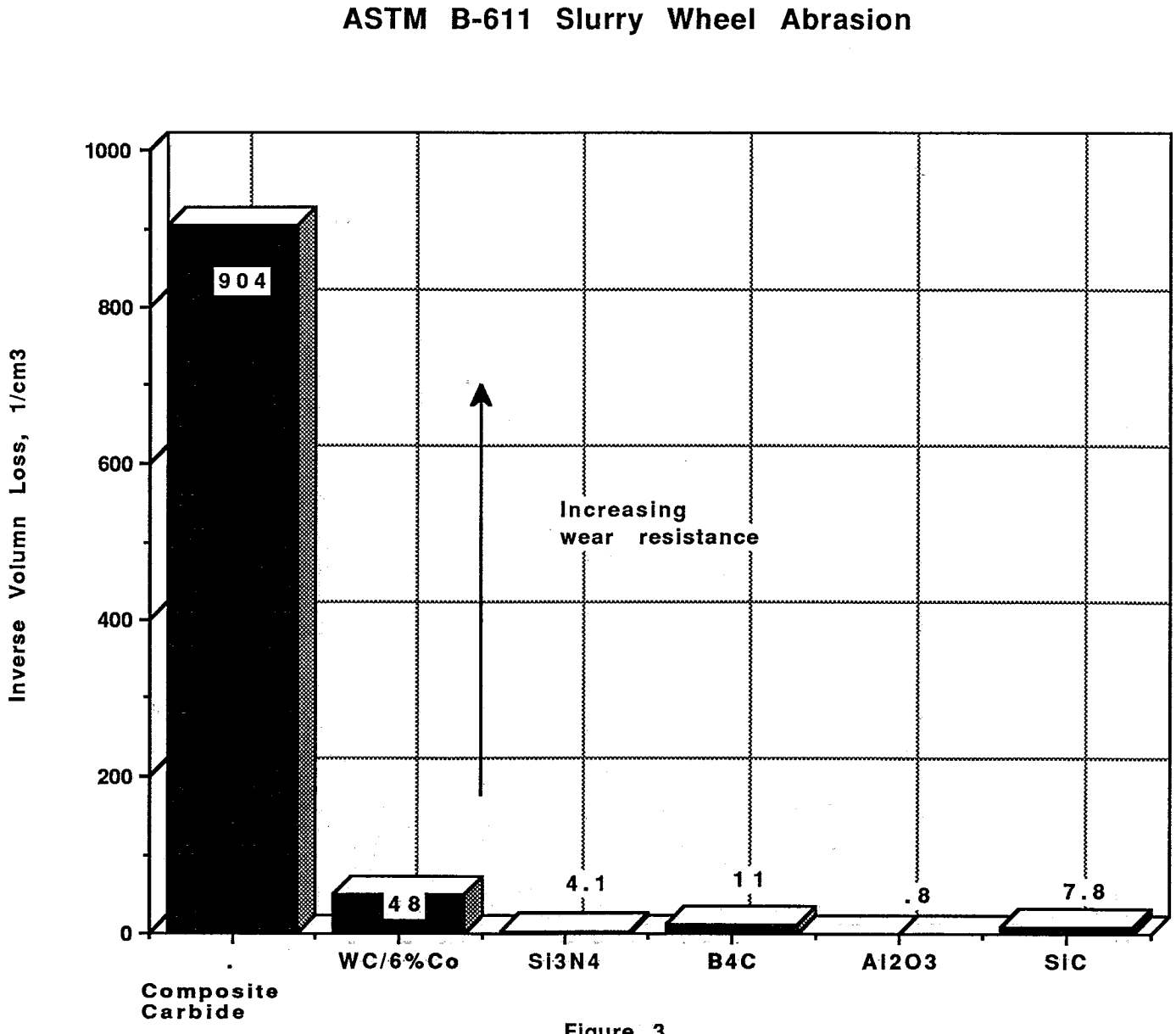
ASTM B-611 Slurry Wheel Abrasion
Inverse Volumn Loss, 1/cm3
1000
800
600
400
200
0
904
48
4.1
11
.8
7.8
Increasing
wear resistance
.
Composite
Carbide
WC/6%Co
Si3N4
B4C
Al2O3
SiC

Figure 3

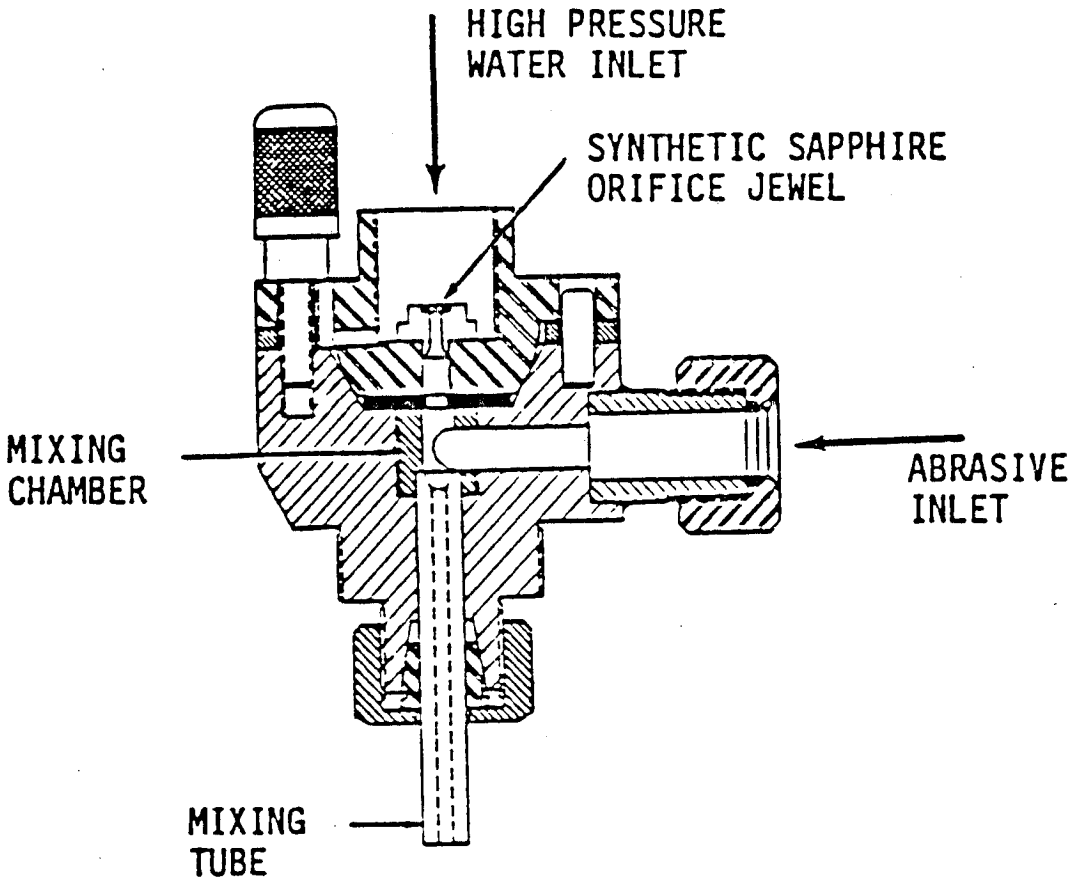

Schematic of abrasive nozzle assembly.

FIGURE 4

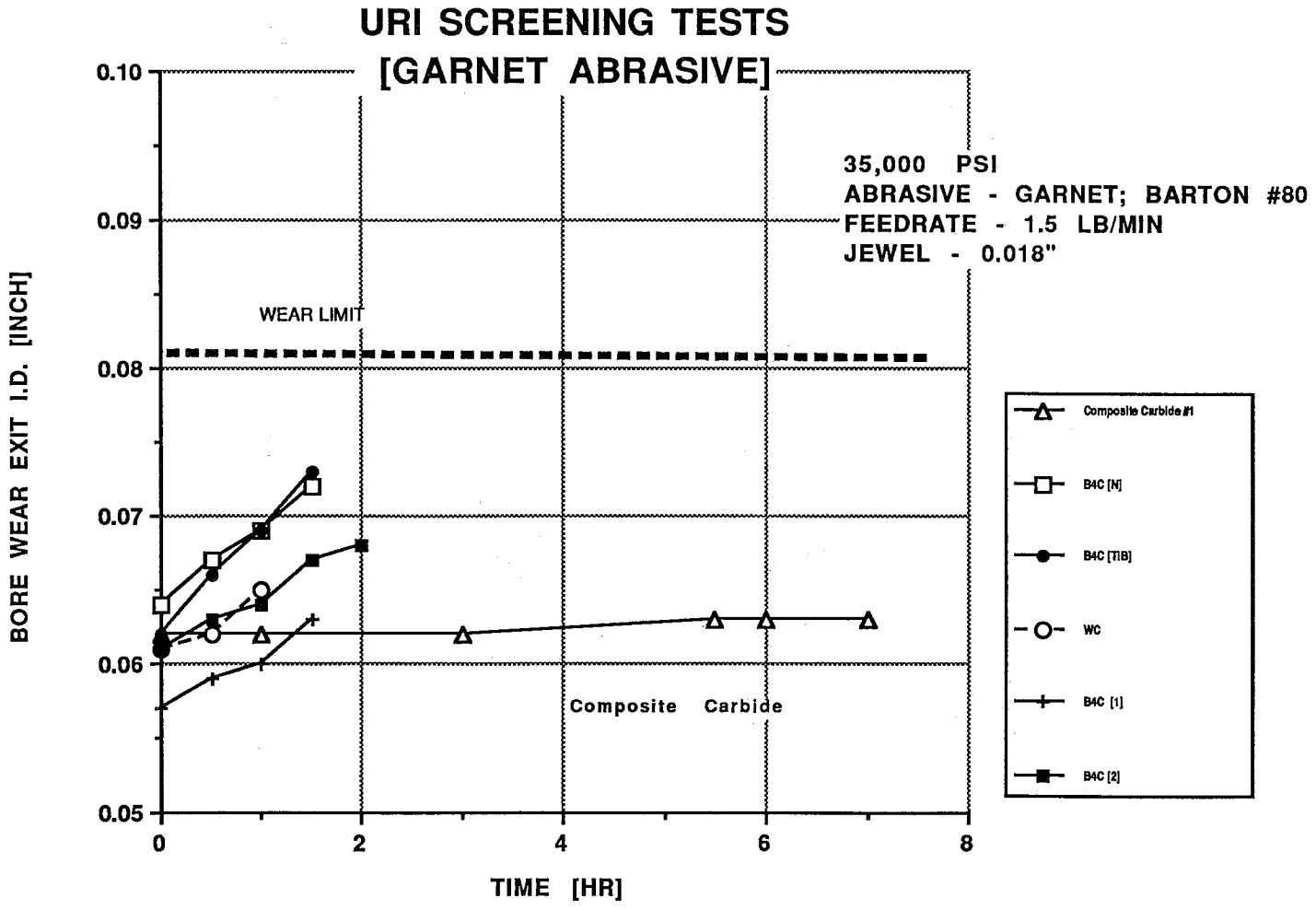
URI SCREENING TESTS
[GARNET ABRASIVE]
35,000 PSI
ABRASIVE - GARNET; BARTON #80
FEEDRATE - 1.5 LB/MIN
JEWEL - 0.018"
WEAR LIMIT
Composite Carbide
BORE WEAR EXIT I.D. [INCH]
TIME [HR]
0.10
0.09
0.08
0.07
0.06
0.05
0
2
4
6
8
Composite Carbide #1
B4C [N]
B4C [TiB]
WC
B4C [1]
B4C [2]

FIGURE 5

URI SCREENING TESTS
[ALUMINUM OXIDE ABRASIVE]

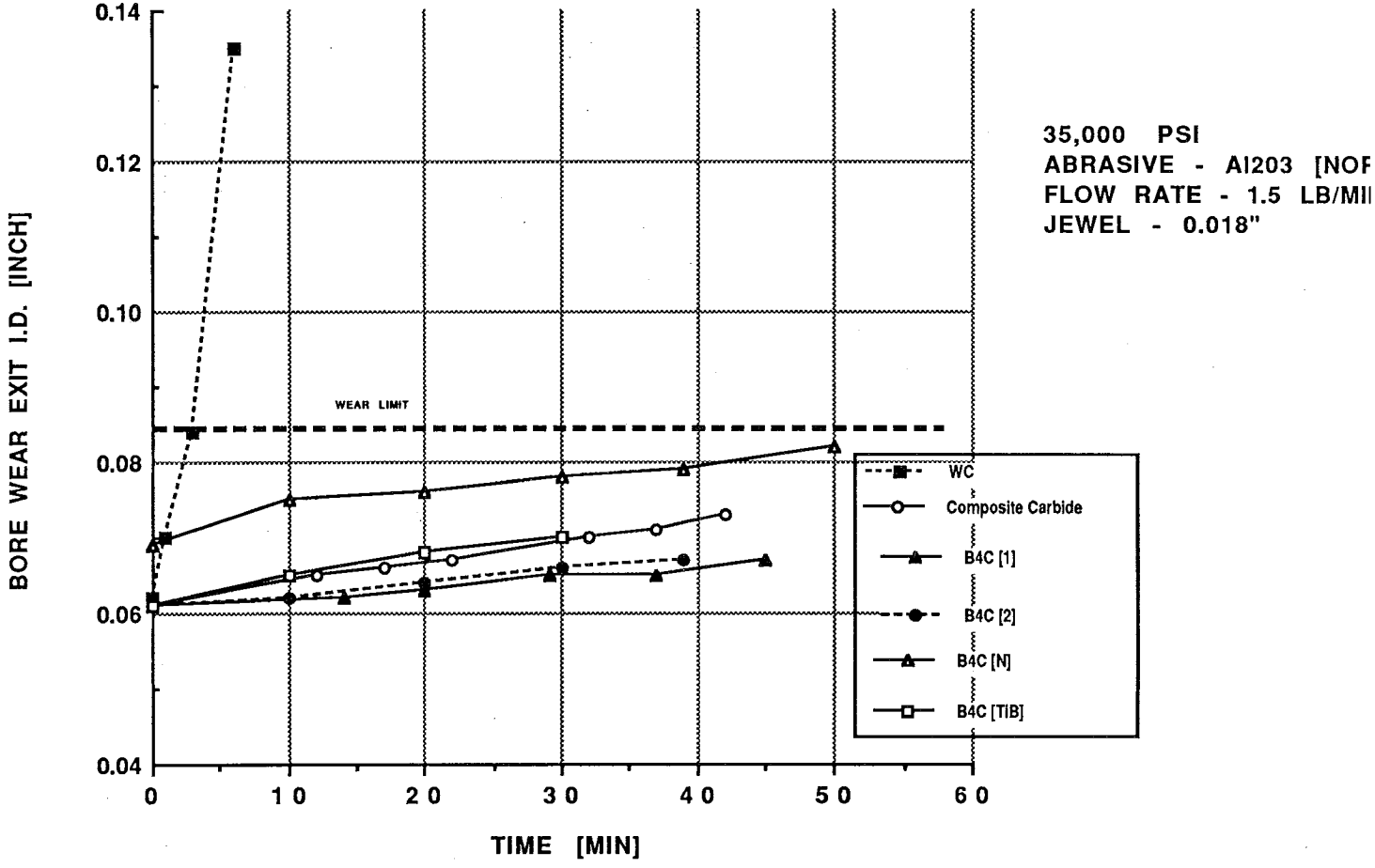

FIGURE 6

URI SCREENING TESTS
[SILICON CARBIDE ABRASIVE]

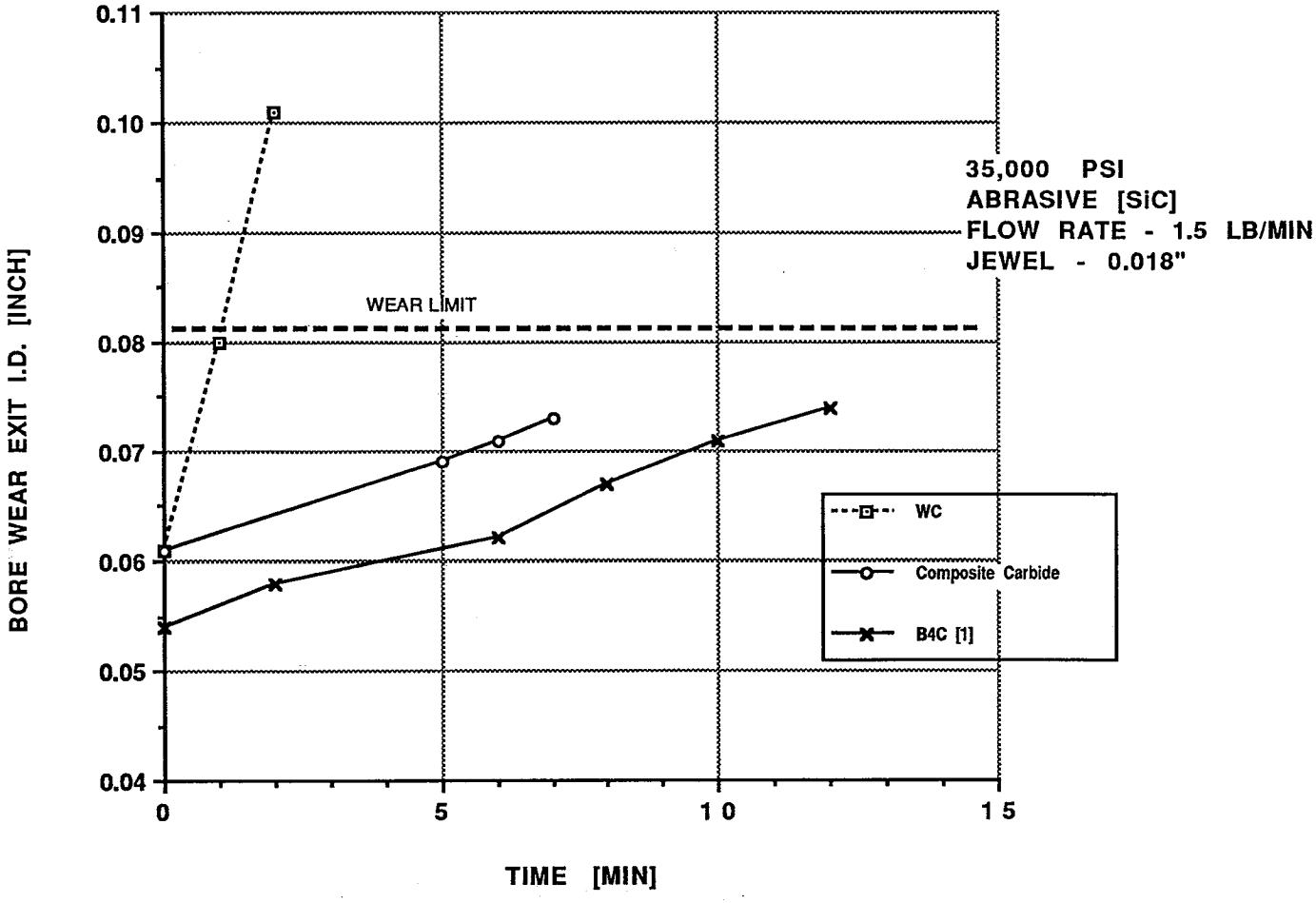

FIGURE # 7

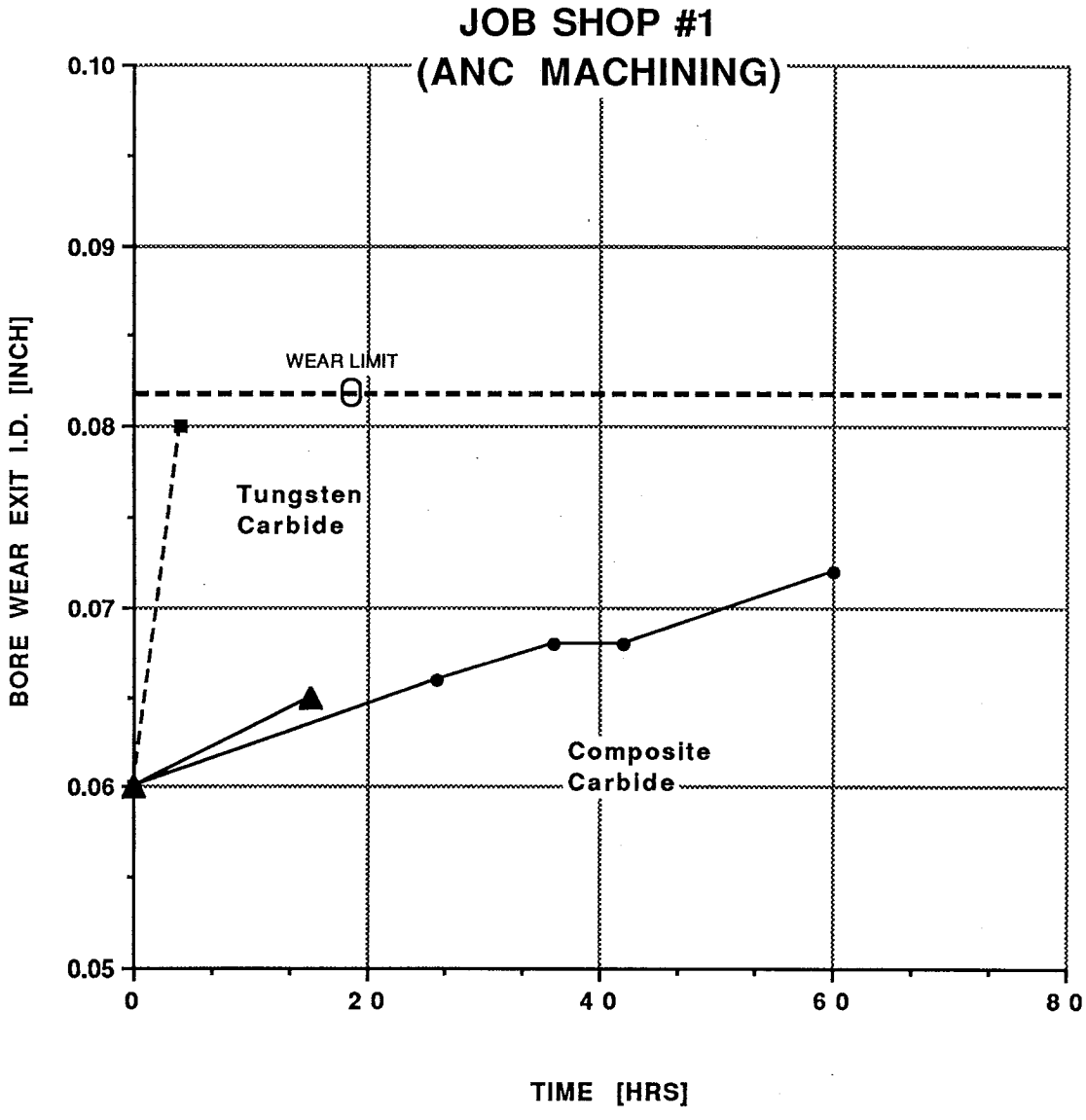

35,000 PSI
ABRASIVE - GARNET; IGE 60
FEEDRATE - 1.5 LB/HR
JEWEL 0.018"

FIGURE 9

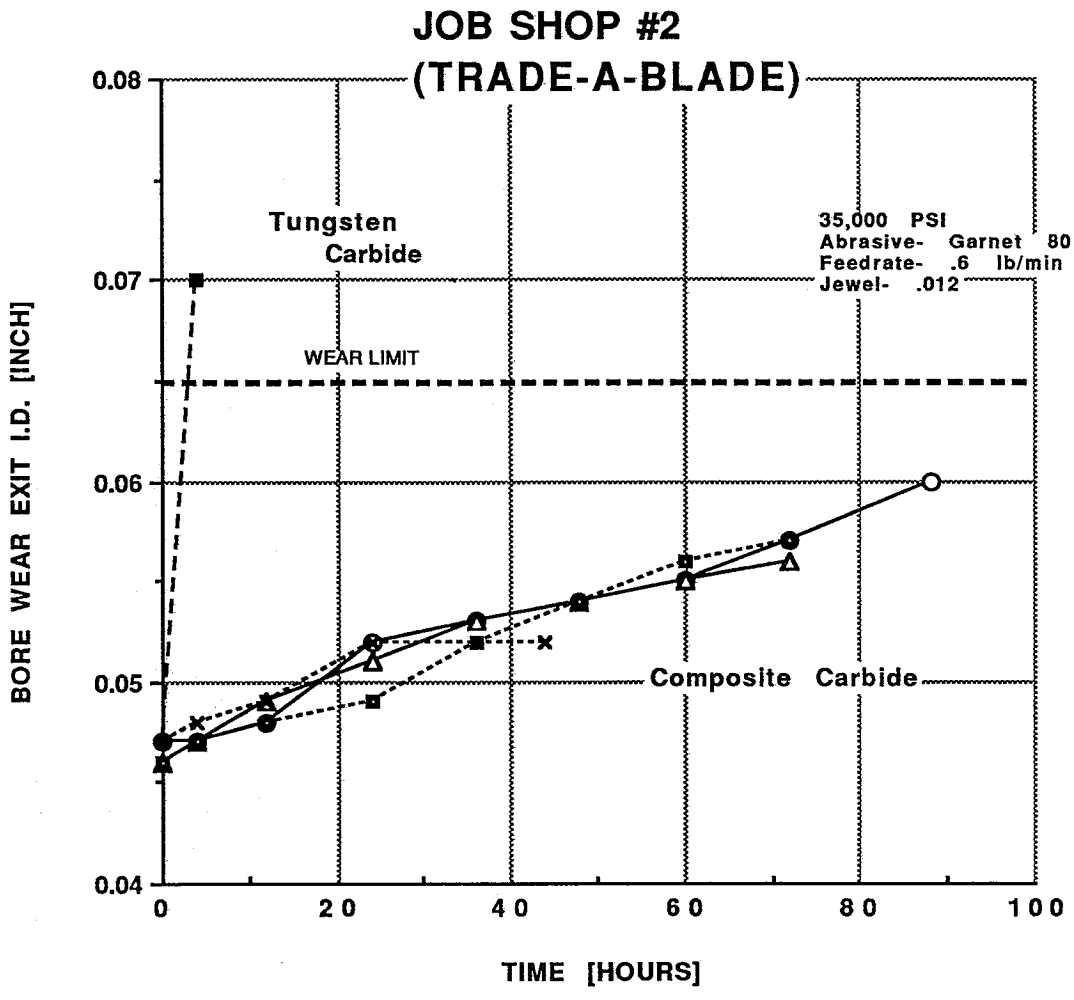
JOB SHOP #2
(TRADE-A-BLADE)
0.08
0.07
0.06
0.05
0.04
Tungsten
Carbide
35,000 PSI
Abrasive- Garnet 80
Feedrate- .6 lb/min
Jewel- .012
WEAR LIMIT
Composite Carbide
BORE WEAR EXIT I.D. [INCH]
0
20
40
60
80
100
TIME [HOURS]

FIGURE 10

JOB SHOP #3

(HYDRO-ABRASIVE MACHINING, INC.)

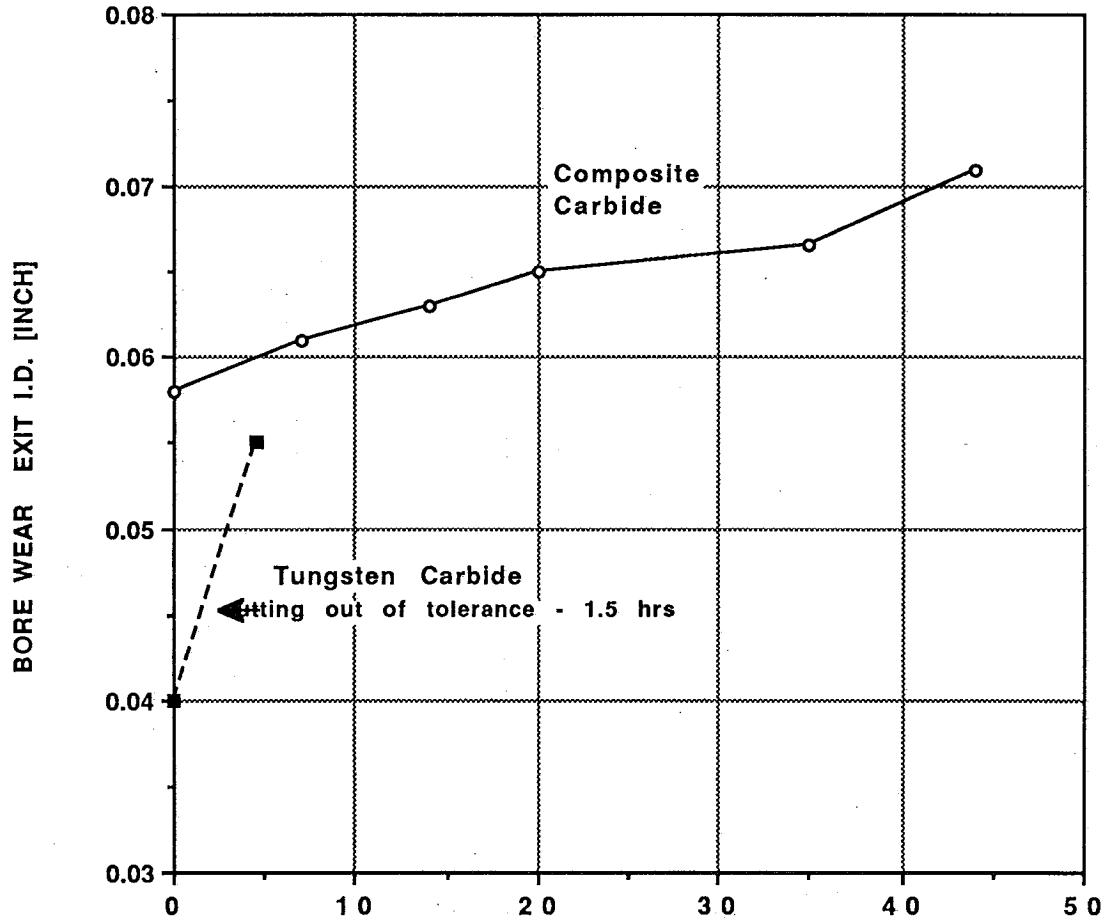

45,000 PSI
ABRASIVE - GARNET: I.G. #8
FEED RATE - 1.0 lb / min
JEWEL - 0.015"

FIGURE 11

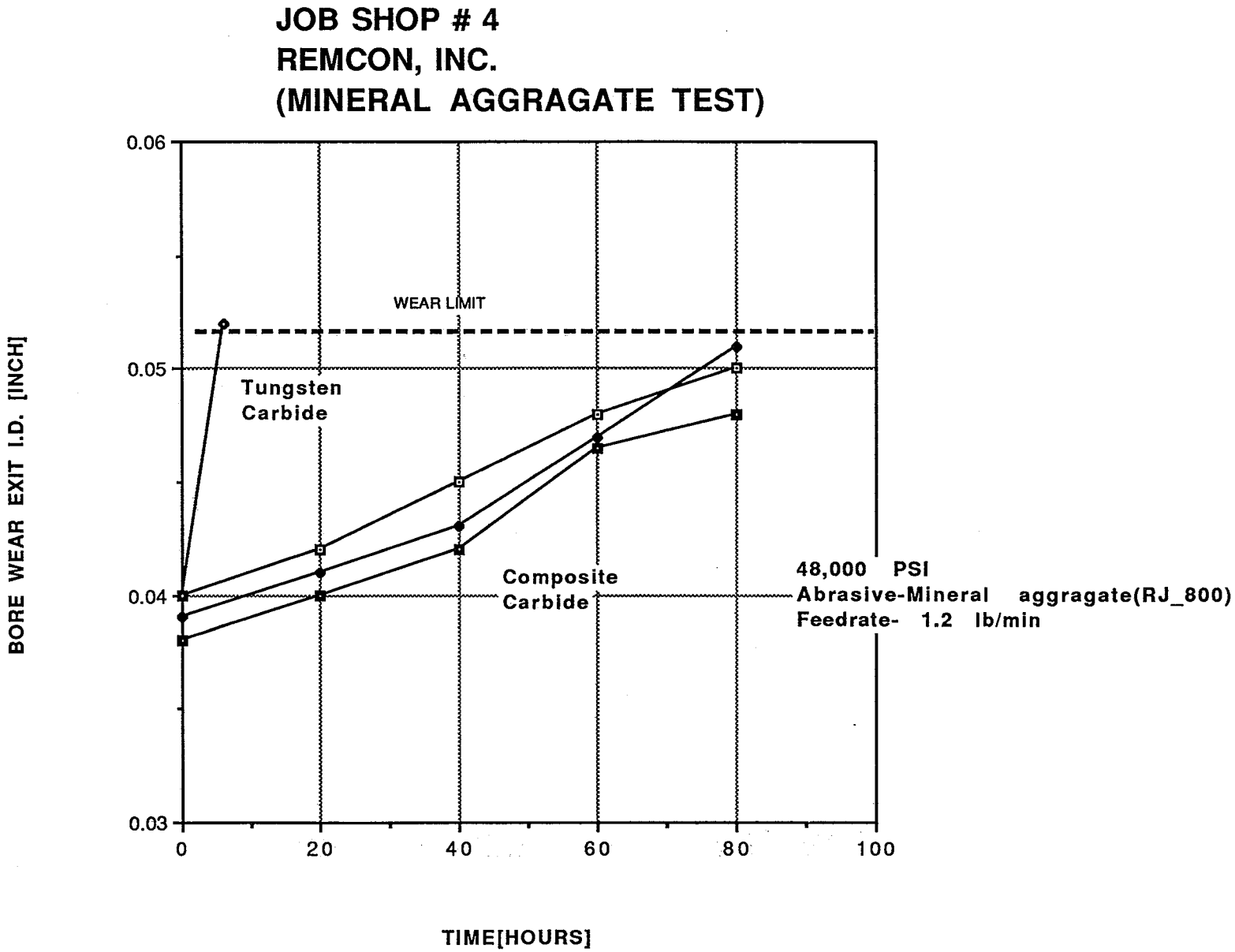
JOB SHOP # 4
REMCON, INC.
(MINERAL AGGRAGATE TEST)
BORE WEAR EXIT I.D. [INCH]
0.06
0.05
0.04
0.03
WEAR LIMIT
Tungsten Carbide
Composite Carbide
48,000 PSI
Abrasive-Mineral aggragate(RJ_800)
Feedrate- 1.2 lb/min
0
20
40
60
80
100
TIME[HOURS]

FIGURE 12

JOB SHOP #4
(REMCON, INC.)

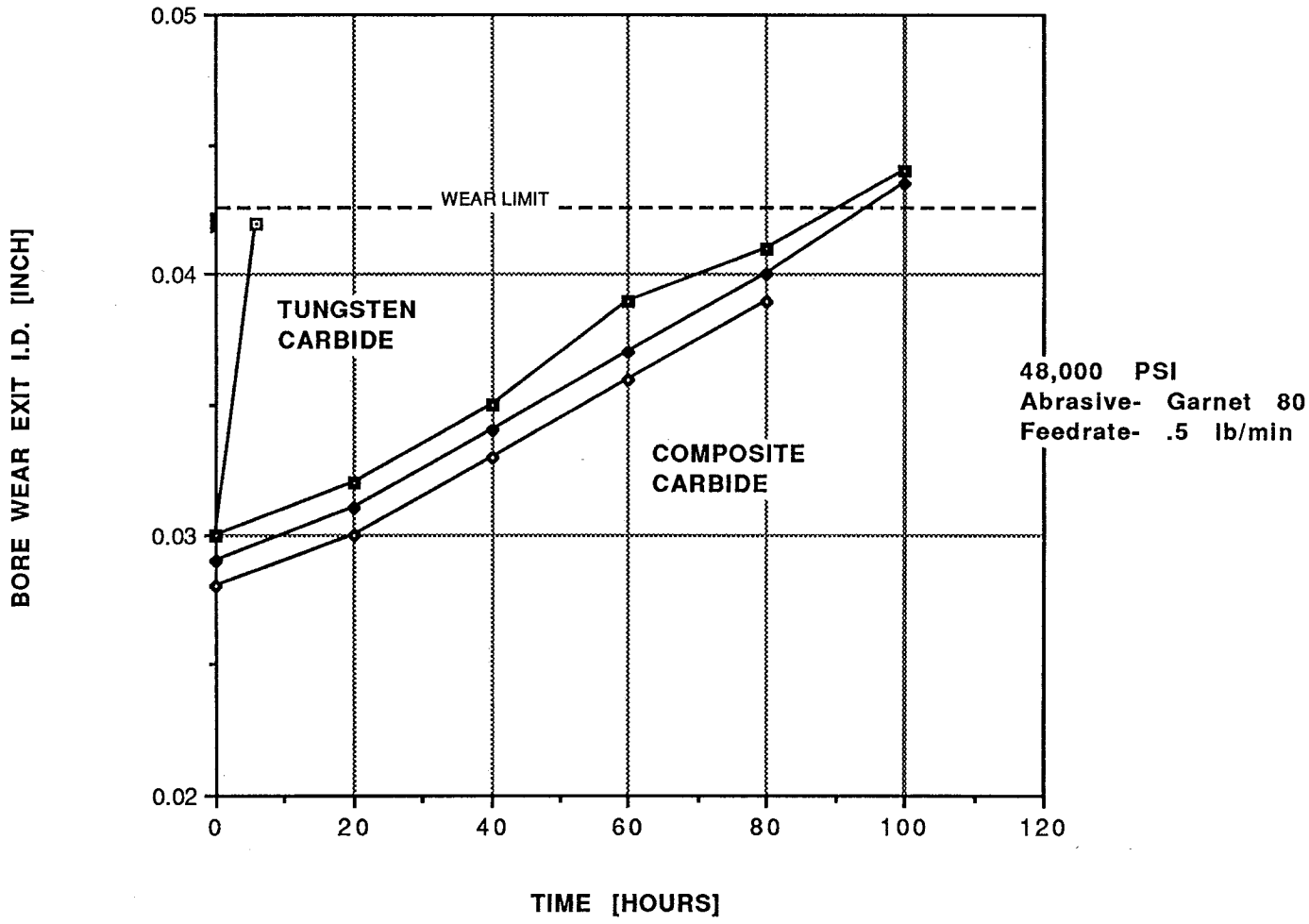

FIGURE 13

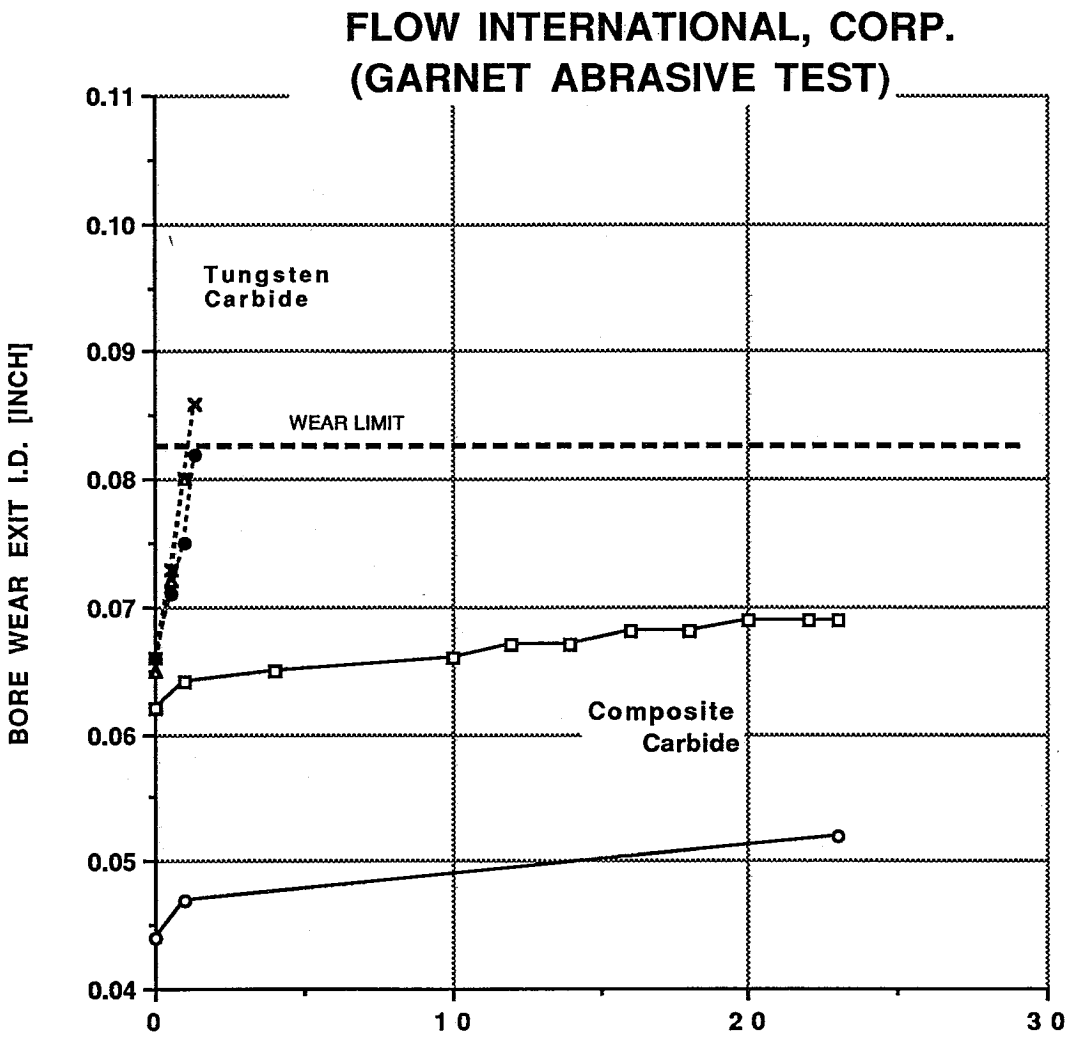

35 KSI
ABRASIVE - GARNE
FEEDRATE - 1.5 LB
JEWEL - 0.018"

FIGURE 14

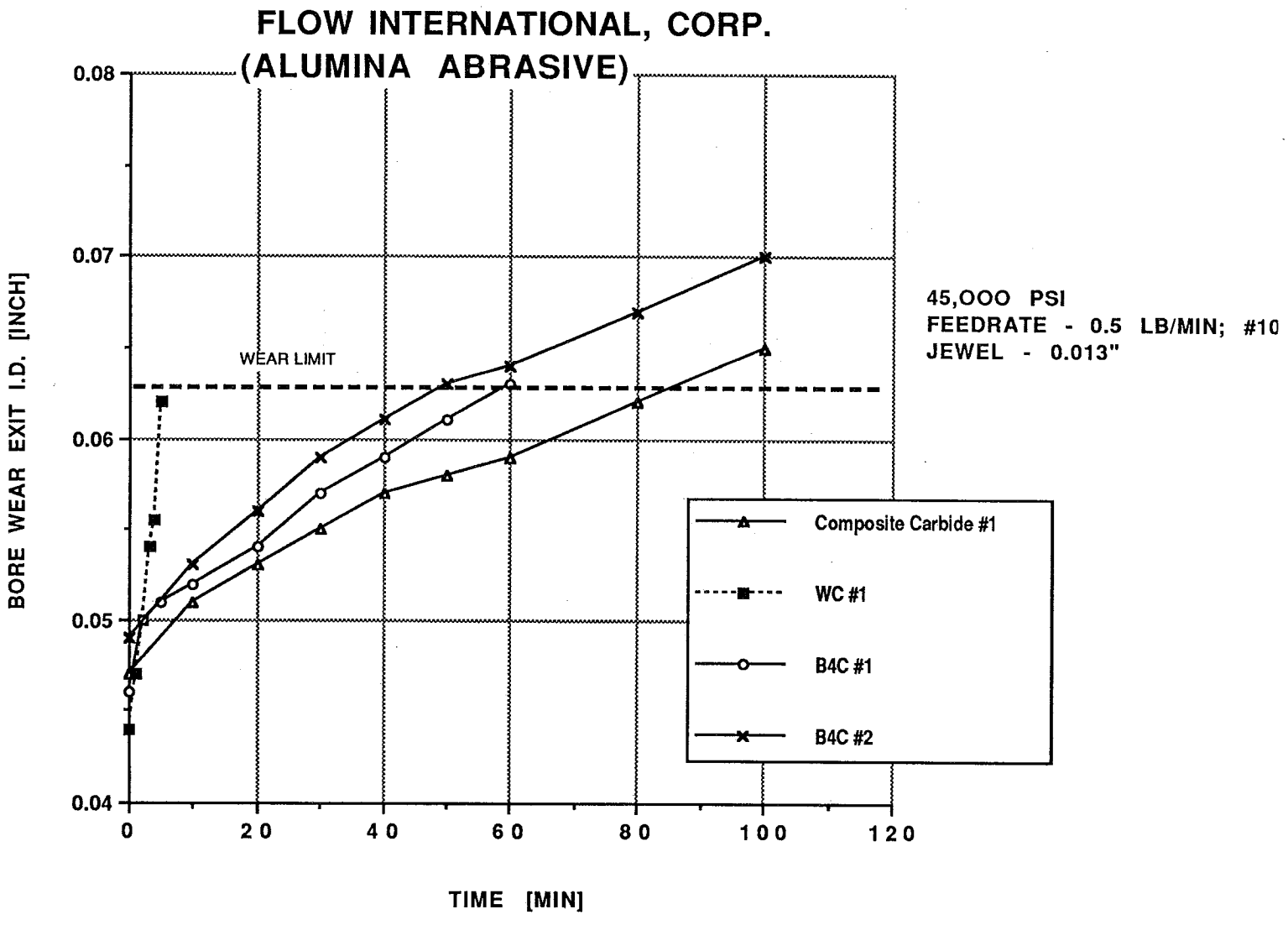
FLOW INTERNATIONAL, CORP.
(ALUMINA ABRASIVE)
BORE WEAR EXIT I.D. [INCH]
0.08
0.07
0.06
0.05
0.04
WEAR LIMIT
0
20
40
60
80
100
120
TIME [MIN]
45,000 PSI
FEEDRATE - 0.5 LB/MIN; #10
JEWEL - 0.013"
Composite Carbide #1
WC #1
B4C #1
B4C #2

FIGURE 15

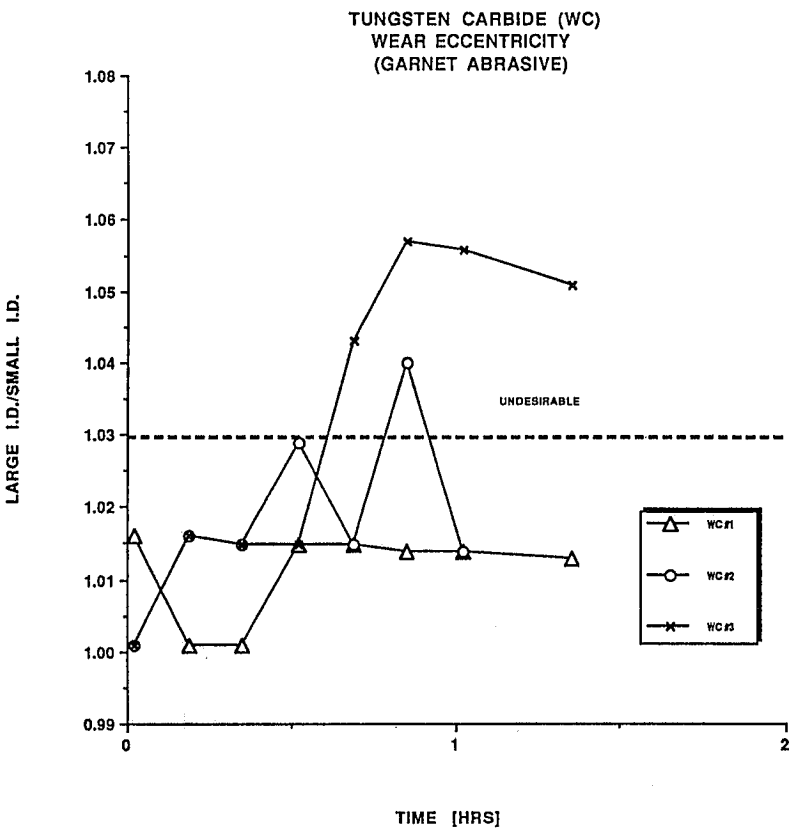
TUNGSTEN CARBIDE (WC)
WEAR ECCENTRICITY
(GARNET ABRASIVE)
LARGE I.D./SMALL I.D.
1.08
1.07
1.06
1.05
1.04
1.03
1.02
1.01
1.00
0.99
UNDESIRABLE
WC#1
WC#2
WC#3
0
1
2
TIME [HRS]

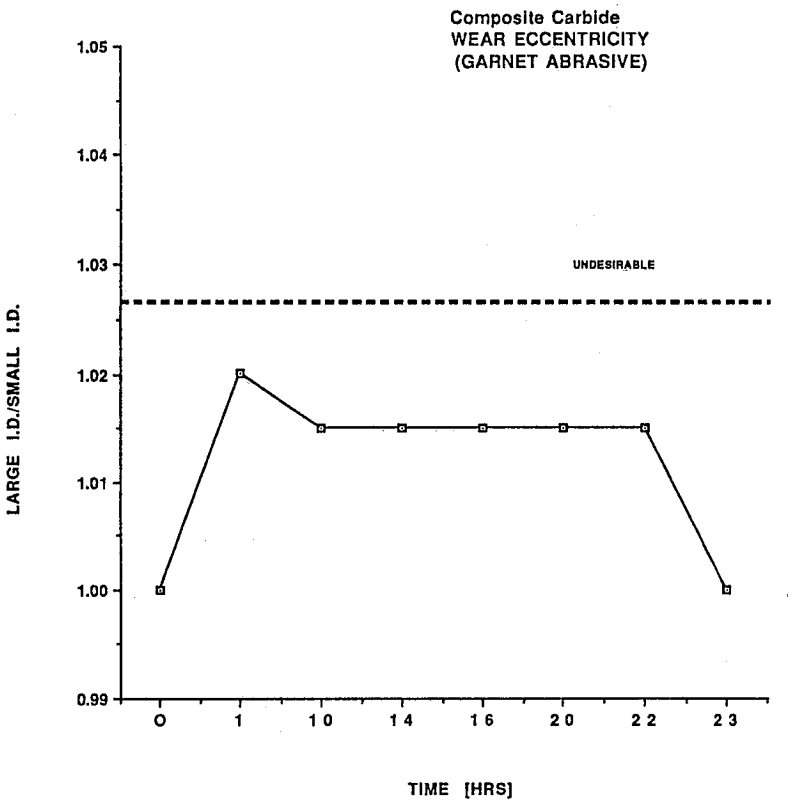
Composite Carbide
WEAR ECCENTRICITY
(GARNET ABRASIVE)
LARGE I.D./SMALL I.D.
1.05
1.04
1.03
1.02
1.01
1.00
0.99
UNDESIRABLE
0
1
10
14
16
20
22
23
TIME [HRS]

FIGURE 16

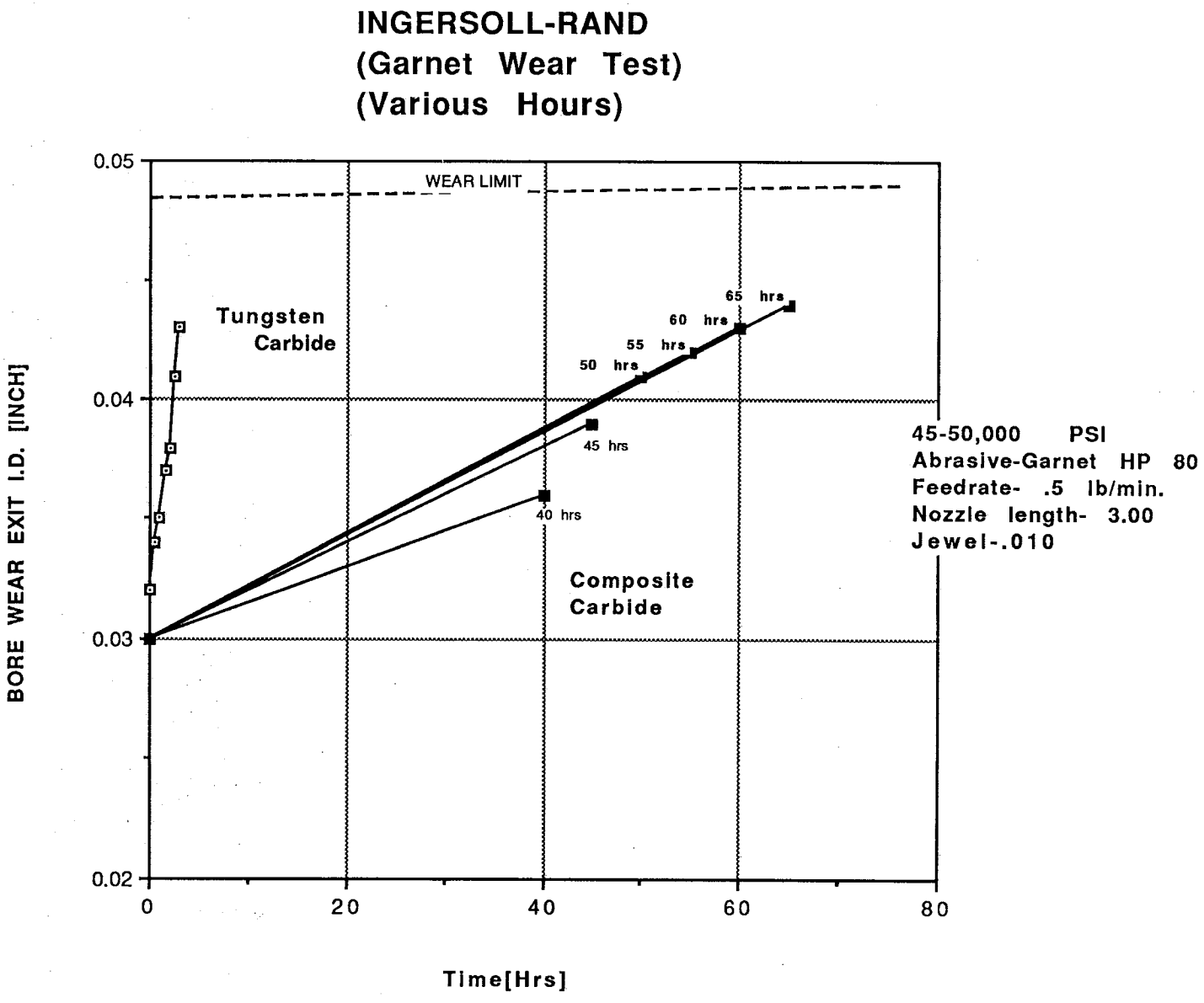
INGERSOLL-RAND
(Garnet Wear Test)
(Various Hours)
0.05
0.04
0.03
0.02
WEAR LIMIT
Tungsten Carbide
65 hrs
60 hrs
55 hrs
50 hrs
45 hrs
40 hrs
Composite Carbide
45-50,000 PSI
Abrasive-Garnet HP 80
Feedrate- .5 lb/min.
Nozzle length- 3.00
Jewel-.010
BORE WEAR EXIT I.D. [INCH]
0
20
40
60
80
Time[Hrs]

FIGURE 17

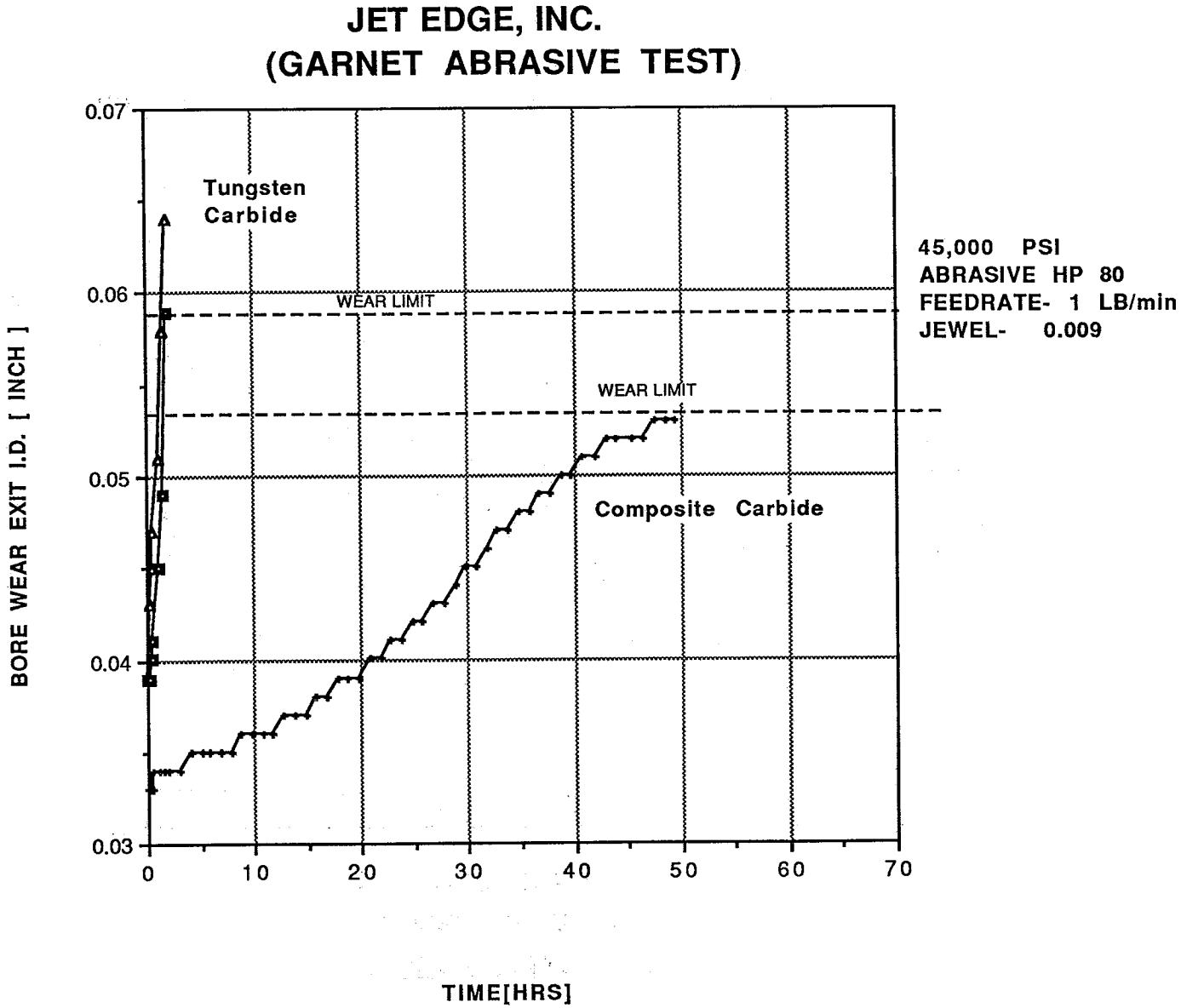
JET EDGE, INC.
(GARNET ABRASIVE TEST)
0.07
0.06
0.05
0.04
0.03
Tungsten Carbide
WEAR LIMIT
WEAR LIMIT
Composite Carbide
45,000 PSI
ABRASIVE HP 80
FEEDRATE- 1 LB/min
JEWEL- 0.009
BORE WEAR EXIT I.D. [INCH]
0
10
20
30
40
50
60
70
TIME[HRS]

FIGURE 18

SUGINO CORP.
(GARNET ABRASIVE TEST)

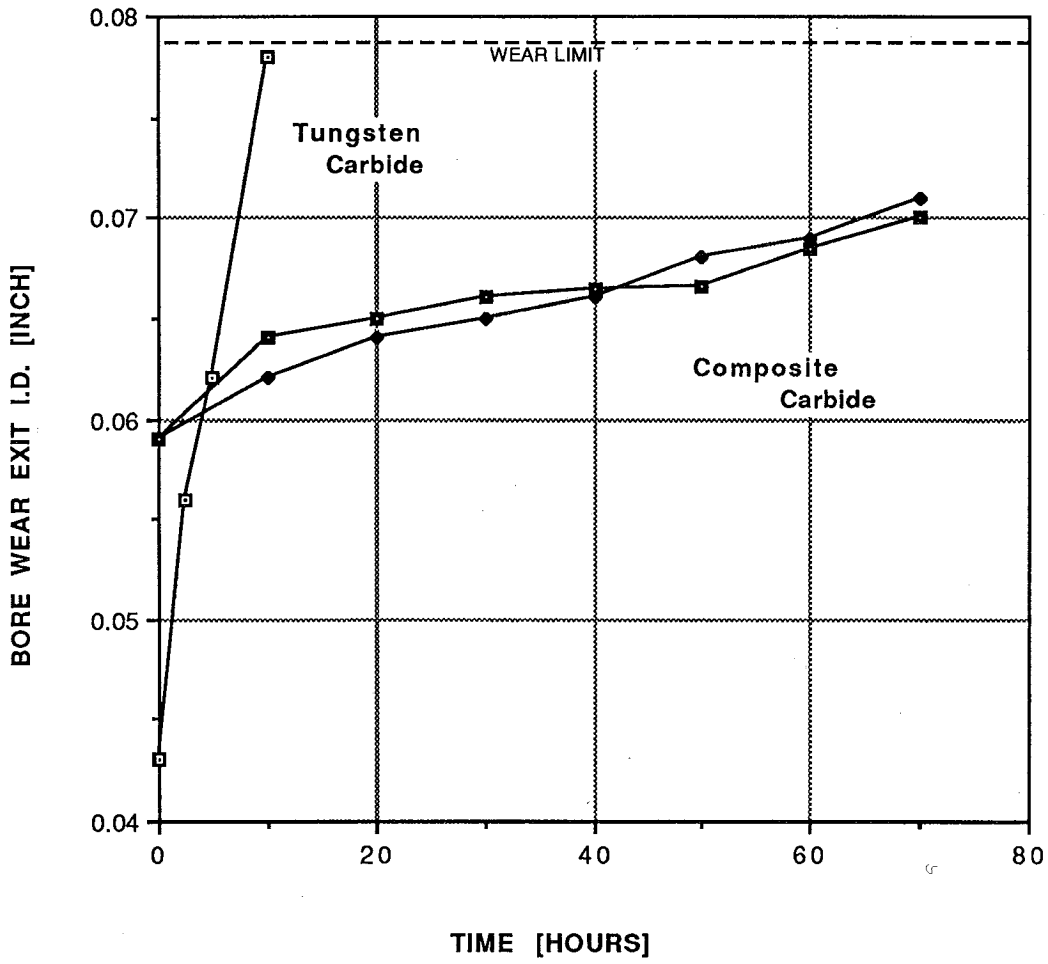

44,000 PSI
Abrasive- Garnet 80
Feedrate- 3/4-1 1/4 lb/min
Jewel- .014

FIGURE 19

ALTERNATIVE ABRASIVE FEED
SCREENING STUDY

Bore Exit Wear Rate
(mm/hour)

Nozzle Material	Garnet	Alumina	Silicon Carbide
Composite Carbide	$.48 \times 10^{-2}$	4.3×10^{-1}	2.5
Boron Carbide	30.5×10^{-2}	2.4×10^{-1}	3.0
Tungsten Carbide	13.2×10^{-2}	185×10^{-1}	34

Figure 20

6th American Water Jet Conference
August 24 - 27, 1991: Houston, Texas

Paper 25

Effect of Parameter Selection on Abrasive Waterjet Performance

E.J. Chalmers
Jet Edge, Inc.
Minneapolis, USA

ABSTRACT

A practical evaluation of the effects of orifice size, abrasive nozzle size, pressure and abrasive mass flow rate on depth of cut was performed. Three different nozzle sizes: .76 mm I.D., 1.14 mm I.D. and 1.65 mm I.D. were tested. A range of orifice sizes were tested with each nozzle. Pressure and abrasive flow rate were then varied with each set-up to create an encompassing range of variable combinations. Depth of cut is used as the means of comparing the performance of each combination of variables. The results show that maximum depth of cut occurs with a 3:1 nozzle to orifice diameter ratio without jet spreading. The optimum abrasive to water mass flow ratio for efficient cutting ranges from 0.17 for the 0.79 mm nozzle to 0.10 for the 1.65 mm nozzle.

Organized and Sponsored by the Water Jet Technology Association.

1.0 INTRODUCTION

Abrasive waterjet cutting rates are largely a function of operator controlled parameters, or variables. The interaction of these parameters is a complex problem. To optimize cutting rate performance it is necessary to understand this interaction so that the best parameter selection is made for the application.

The operator normally has control over the following parameters:
- Abrasive type, size and mass flow rate
- Operating pressure
- Orifice size
- Abrasive nozzle size

The quantity of active variables (4) makes the process of defining the interdependent relationships difficult.

This paper explores the effect of varying these parameters on the depth of cut. Feed rate, material cut, abrasive type and abrasive particle size are held constant. The resulting depth of cut is used to compare the relative effectiveness of each set-up.

2.0 TEST CUT METHOD

Test cuts were performed using a Jet Edge Permalign Abrasive Head (FIG. 1) and hopper with slide gate abrasive flow regulator (FIG. 2).

Three different abrasive nozzle sizes were used: .76 mm I.D. x 51 mm length, 1.14 mm I.D. x 76 mm and 1.65 mm I.D. x 76 mm.

Orifices were used with a diameter ratio; d_A/d_W, ranging between 4.3:1 to 2.1:1. Four ratios were tested with each nozzle.

Test cuts were made at pressures from 207 MPa to 379 MPa in increments of 34 MPa.

Abrasive mass flow rates were increased until the depth of cut reached a maximum.

Only 80 mesh garnet was used since this is a commonly used abrasive.

All test cuts were performed on 1018 mild steel. The results are intended to serve as a means of comparing the relative cutting power of different set-ups on ductile materials.

The cutting speed was held constant at 2.5 mm/sec. for all cuts.

3.0 EFFECT OF INCREASING ABRASIVE

Test cuts were performed with a given size orifice, abrasive nozzle and at a given pressure. Figures 3-8 show depth of cut h as a function of abrasive mass flow rate m_A. The curves show a common trend. As m_A increases the slope decreases until the maximum h is achieved. Thereafter, depth of cut decreases. Excess abrasive reduces the mixing efficiency in the nozzle resulting in reduced depth of cut.

4.0 RELATIONSHIP BETWEEN THE ORIFICE SIZE AND THE ABRASIVE NOZZLE SIZE

Figures 3, 4 and 5 show h as a function of m_A for nozzle to orifice diameter ratios between 2.14 and 4.34. Values are shown at 310 MPa since this is a commonly used pressure. These curves are representative of those at other pressures with the exception that h is proportional to pressure.

Figure 3 shows curves for nozzle size .76 mm I.D. x 51 mm long. Increasing orifice size increases maximum depth of cut at a given pressure. Increasing orifice size also increases m_A corresponding with h_{max}. Using depth of cut as the criteria the best performance is with d_W = 0.35. The two larger orifices created a stream that expanded as it exited the nozzle. Kerf width of the cut was the same for all orifices but the stream expansion was visually unacceptable. Based on FIG. 3 and observation, d_A/d_W of 3 was the most effective with a d_A of .76.

FIG. 4 shows h as a function of m_A using a 1.14 mm I.D. nozzle. The spread between curves is less than that shown in FIG. 3. The .46 mm diameter orifice had an expanding stream. The best performing combination was the .38 mm orifice (d_A/d_W = 3.0).

FIG 5. gives similar curves for d_A = 1.65 mm. These curves show that there is much less sensitivity to orifice size with a d_A/d_W less than 3.6. The .61 mm orifice caused an expanding stream. The optimal ratio for this size nozzle is between 3 and 3.5.

5.0 OPTIMIZING DEPTH OF CUT AT VARIOUS PRESSURES

FIGS. 6, 7 and 8 show depth of cut at various pressures and abrasive flow rates using d_A/d_W = 3. The graph for the .76 mm nozzle has a pronounced peak whereas the shape of the curves for the 1.14 mm and 1.65 mm graphs is much flatter. These two larger combinations sustain a given maximum depth of cut (h_{max}) over a greater amount of m_A.

Increasing pressure also increase h_{max} with a corresponding increase in m_A. FIGS. 6, 7 and 8 show a line drawn through h_{max} of each of the six pressure curves. This line corresponds to a specific value of m_A/m_W. The plots show that near h_{max} increasing amounts of abrasive are required for decreasing

improvements in depth of cut. To avoid excessive use of abrasive the optimum depth of cut is defined as occurring at .85 h_{max}. A second line is drawn on each graph for .85 h_{max}. This line also has a corresponding value of m_A/m_W for optimal cutting rate.

Orifice/Nozzle Combination	m_A/m_W @ h_{max}	m_A/m_W @ .85 h_{max}
.25 mm/.76 mm	.3	.17
.38 mm/1.14 mm	.19	.12
.53 mm/1.65 mm	.19	.10

Operating at a performance level equal to .85 h_{max} requires an average of 53% of the amount of abrasive necessary for h_{max}. A relatively small loss in depth of cut provides for a significant reduction in abrasive usage.

6.0 EFFECT OF PRESSURE ON DEPTH OF CUT

Previous findings by others have found that depth of cut is directly proportional to pressure. The results of these test cuts confirm this. FIG. 9 shows plots for the three primary orifice/nozzle combinations with a 3:1 diameter ratio. The plots show that h is proportional to P with m_A held constant.

7.0 CONCLUSIONS

The results of depth of cut testing with abrasive nozzles sizes; .76 mm I.D. x 51 long, 1.14 mm I.D. x 76, 1.65 I.D. x 76 mm are:

1. A nozzle to orifice size ratio of three provides for maximum depth of cut at a give abrasive flow rate without stream expansion at the nozzle exit.

2. Increasing the amount of abrasive increases the depth of cut at a diminishing rate. A maximum value is reached, then the depth decreases due to inefficient mixing.

3. Using a 3:1 nozzle to orifice diameter ratio the maximum depth of cut occurs at a specific value of m_A/m_W for a given size nozzle. Higher pressure creates greater mass flow rate which can efficiently accelerate a proportionally higher amount of abrasive.

4. Performing cuts with abrasive flow rates that provide maximum depth of cut is inefficient. This is due to the fact that depth of cut diminishes with increasing abrasive. Operating at 85 percent of the maximum depth requires approximately 47 percent less abrasive (m_A/m_W at .85 h_{max} is .17 for the .76 mm nozzle, .12 for the 1.14 mm nozzle and .10 for the 1.65 mm nozzle).

ACKNOWLEDGMENTS

Test cut work was performed by Dean Carlson. Support for this program was provided by Jet Edge, Inc.

NOMENCLATURE

d_A = Orifice diameter (mm)
d_W = Abrasive nozzle diameter (mm)
m_A = Abrasive mass flow rate (g/s)
m_W = Water mass flow rate (g/s)
V = Traverse rate (mm/sec)
h = Depth of cut (mm)
h_{max} = Maximum depth of cut achieved with a set of fixed parameters (mm)

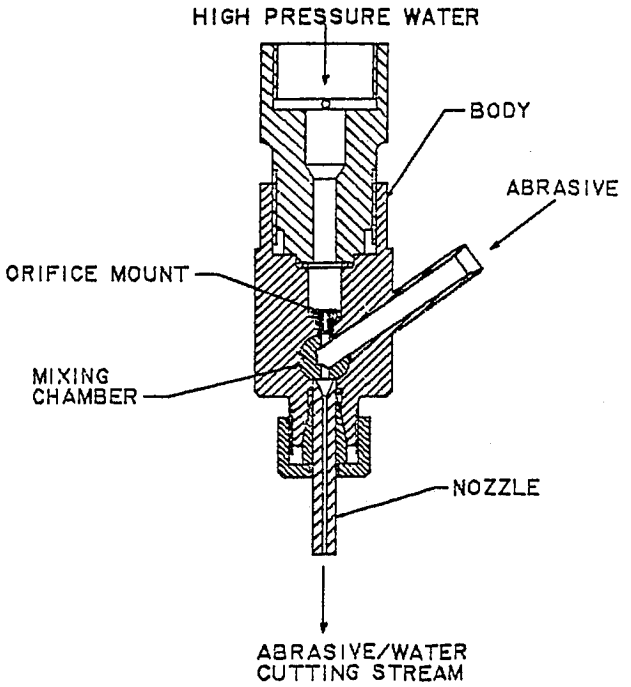

ABRASIVE HEAD ASSEMBLY

FIG. 1

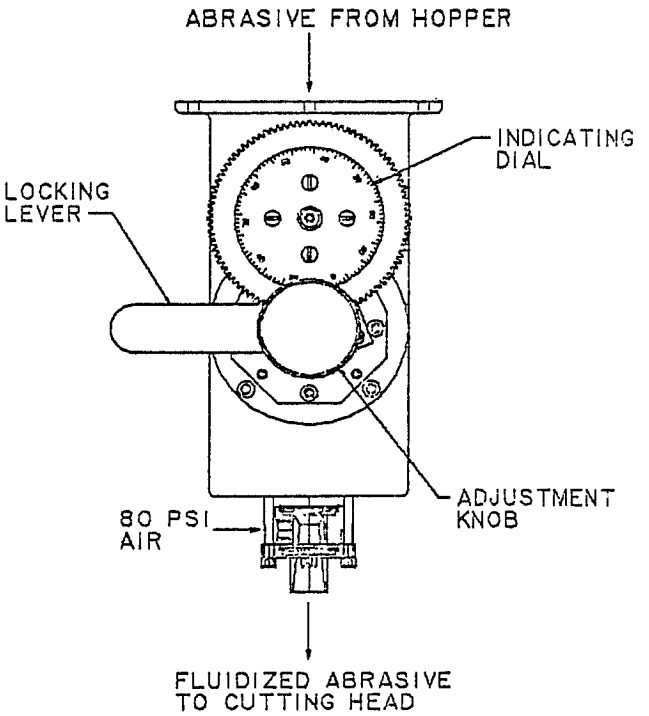

ABRASIVE DELIVERY REGULATOR ASSEMBLY

FIG. 2

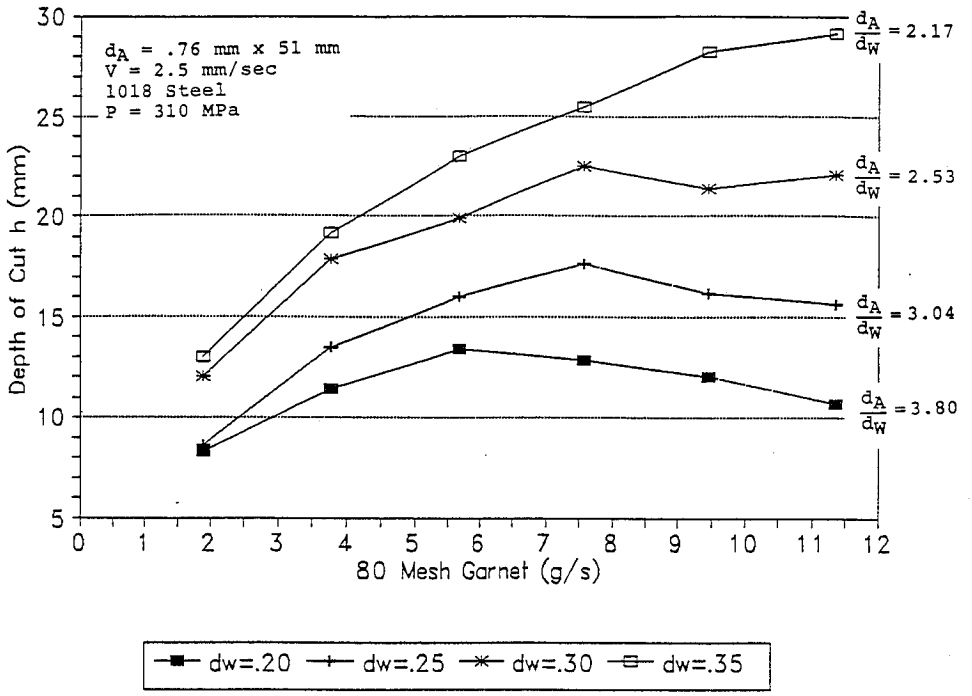

FIG. 3 Depth of cut with varying abrasive rate using a .76 mm nozzle with different orifices at 310 MPa.

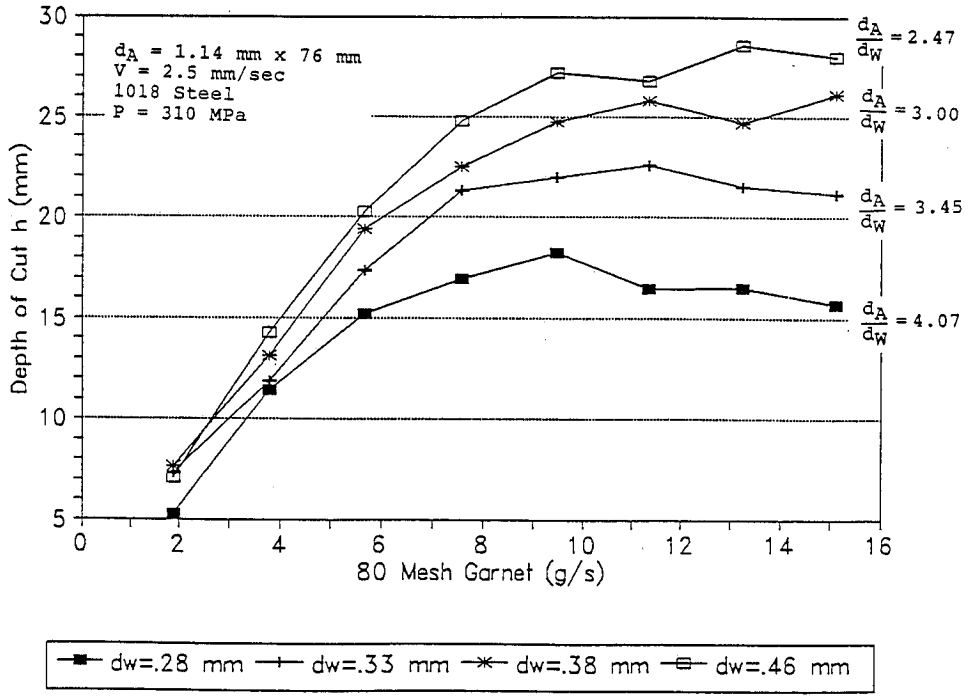

FIG. 4 Depth of cut with varying abrasive using a 1.14 mm nozzle with different orifices at 310 MPa.

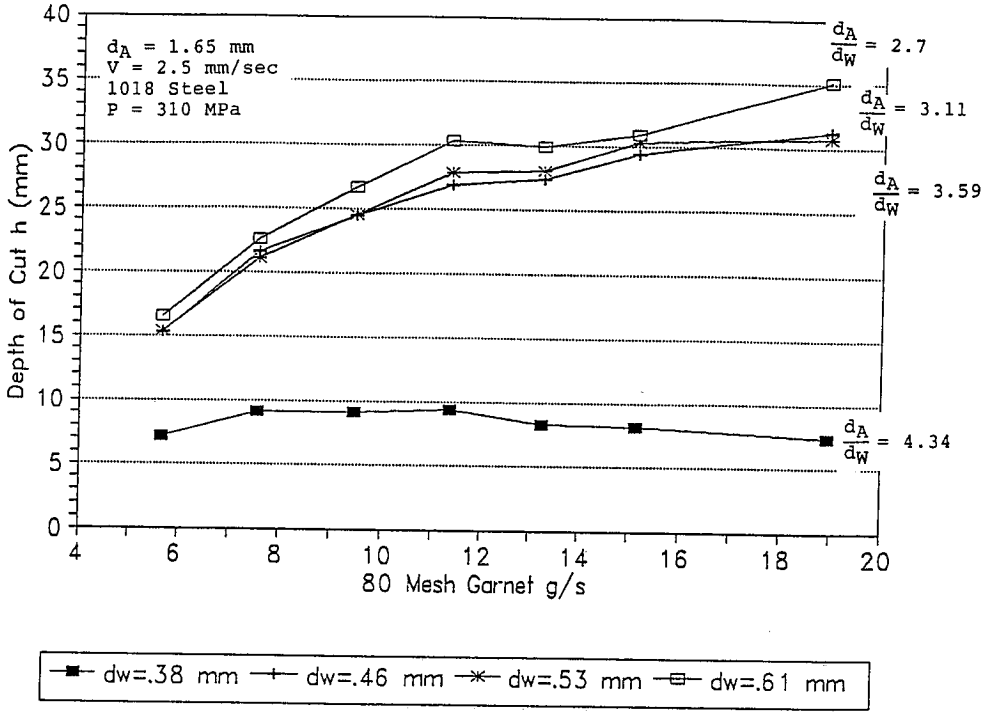

FIG. 5 Depth of cut with varying abrasive rate using a 1.65 mm x 76 mm nozzle with different orifices at 310 MPa.

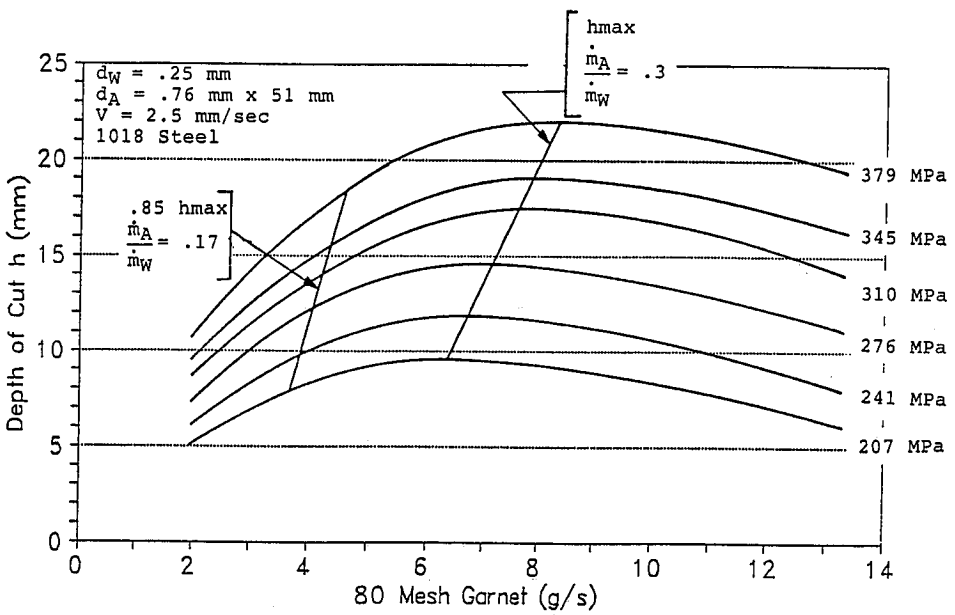

FIG. 6 Depth of cut with varying abrasive for .25 diameter orifice and .76 I.D. x 51 long nozzle.

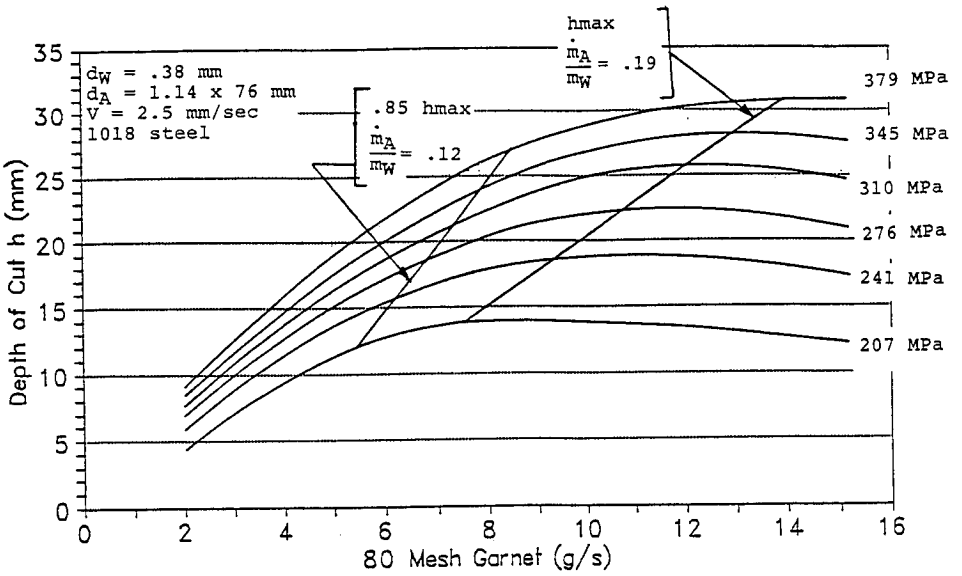

FIG. 7 Depth of cut with varying abrasive for .38 diameter orifice and 1.14 I.D. x 76 long nozzle.

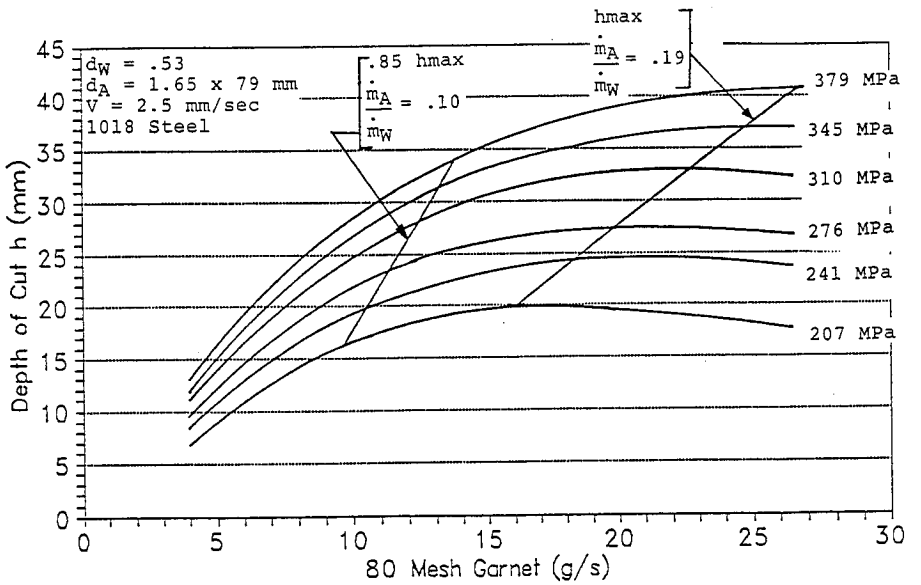

FIG. 8 Depth of cut with varying abrasive for .53 diameter orifice and 1.65 I.D. x 76 long nozzle.

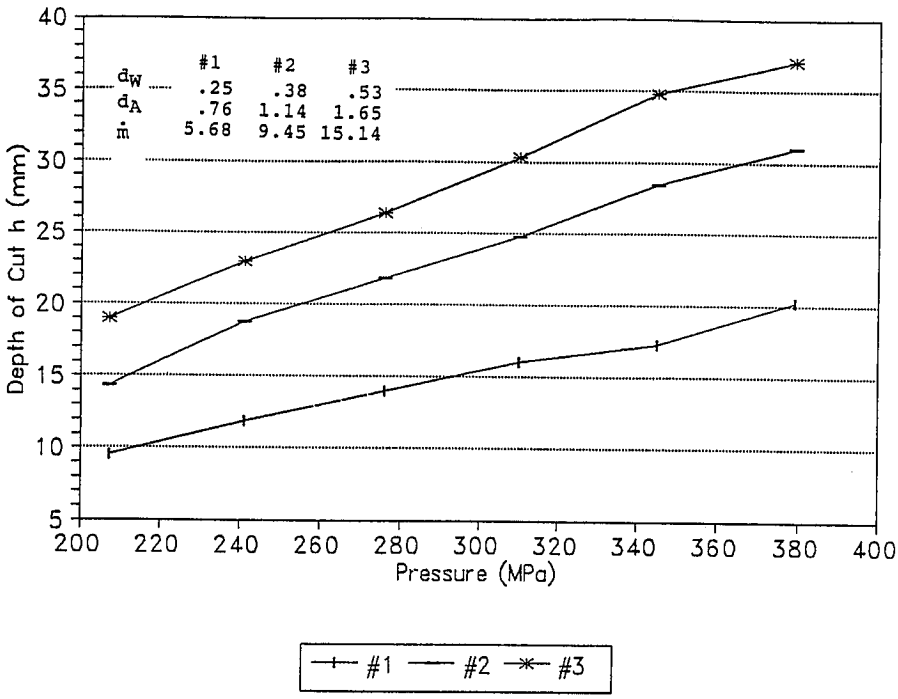

FIG. 9 Effect of pressure on depth of cut with constant abrasive rate.

6th American Water Jet Conference
August 24 - 27, 1991: Houston, Texas

Paper **26**

Laser-Velocimetry Investigations of the Flow in Abrasive Water Jets with Varying Cutting Head Geometry

Dipl.-Ing. U. Himmelreich
Prof. Dipl.-Ing. W. Riess
Institute for Turbomachines
University of Hannover
Germany

ABSTRACT

Hydodynamically an Abrasive Water Jet (AWJ) is described by the phase velocity profiles, the turbulence distribution and the mass distribution of the phases. To yield knowledge about AWJ formation a measurement of these quantities is required. The present work deals with velocity and turbulence measurements in the flowfield of an AWJ, performed by Laser-Two-Focus (L-2-F) velocimetry. The jet is discharged from an injector type cutting head with variing mixing tube (focus) geometry.

A description of the L-2-F method and the statistical evaluation of measurement data is presented. The effect of discharge pressure, abrasive mass flow rate and geometry parameters is deduced from the measurement results. Velocity and turbulence profiles of AWJs and pure water jets at the focus outlet are investigated. The results of centerline velocity measurements in effect of the AWJ setup parameters are discussed comparing to the data of other authors and theoretical calculations.

1.0 INTRODUCTION

The efficiency of Abrasive Water Jet (AWJ) cutting and cleaning is mainly governed by the velocity and the distribution of the abrasive particles in the multiphase jet. For the generation of AWJs two methods have been established:

1.) By the Diajet-technique /4/, where a suspension is premixed in a tank and ejected through a two phase nozzle with relatively low pressure in the system. The pressure is limited to about 350 bars by nozzle wear.

2.) By an injector-type cutting head /1,3/, where the abrasives are fed separately to a mixing tube, called focusing nozzle, downstream the waterjet nozzle. Commonly used with this technique are water pressures in the range from 700 up to 4000 bars.

In the case of an injector type cutting head, the abrasives can be fed as a water suspension or more commonly by air, resulting in a three-phase flow inside the cutting head. Downstream the cutting head develops a regime of droplet and particle flow with an increasing rate of air entrainment in the free jet.

Though jet cutting has won an important practical meaning, there has been only little understanding of the mechanisms governing the mixing process and the spreading of AWJs until now. Also low efficiency of commercially processed cutting heads has been mentioned /6/. Hydrodynamically an AWJ is described by the phase velocity profiles, the turbulence distribution and the mass distribution of the phases. A measurement of these quantities is only possible by nonintrusive means, because of the rough conditions inside an abrasive waterjet.

For that reason at the Institute of Turbomachines the Laser-2-Focus (L-2-F) method was chosen for the measurement of phase velocities and turbulence and a Laser-Light-Sheet (LLS) technique for the investigation of mass distribution and additional abrasive particle velocity measurements. The present work deals with L-2-F measurements taken from an injector-type cutting head driven with variing process parameters and focusing nozzle dimensions. The results and special features of the L-2-F velocimetry will be described. The influence of AWJ setup parameters on velocity and turbulence in the jet will be discussed in comparison with the data of other authors and theoretical equations.

2.0 PRINCIPLES OF THE LASER-2-FOCUS VELOCIMETRY

A detailed description of the main components and the beam tracing of the Laser- 2-Focus velocimeter used in our tests is given in a previous paper (/7/) and the work of Schodl (/9/).

The L-2-F measuring volume (Fig.1) is made up by the two focal spots of the upstream, so called startbeam, and the downstream, so called stopbeam, emitted from the optical head.

Its characteristic dimensions are a beam waist diameter d of 12 microns, a beam spacing s of 278 microns and an active length l' about 1000 microns. Active length means the area of sufficient high light intensity, from where backscattered lightpulses can be received by the optical head. In the AWJ two kinds of scattering particles exist :
the solid abrasive particles (big spheres) and nonuniform waterdroplets in an ambient airstream .

As a particle passes through both focal spots, it emits two scattered lightpulses with a characteristic timeshift. This timeshift will be measured and is called Time of Flight (TOF). At each measuring point a sample of TOF measurements is recorded and evaluated statistically. A rotation of the measuring volume has not been performed in the cases discussed here, because the flow is assumed to be directed vertically downwards.

The statistical evaluation is declared with aid of Fig.2. A sample of TOF measurements is digitized and stored in a multichannel analyzer (MCA) with a resolution of 256 channels. The channel numbers are given on the abscissa, the last channel is preset to a maximal TOF value. Each channel is assigned to a narrow TOF interval. On the ordinate is given the number of counts in each channel.

In the diagram is shown a recorded TOF distribution with a significant maximum, given by the little squares. The dotted line represents the average value of random measurements (start and stop pulse released by different particles) and is assigned to the noiselevel. The counts in each channel, lowered by the noiselevel, are fitted together by a smoothing function, given by the solid curve.

From this processed TOF distribution is evaluated the mean value $\bar{t}$ statistically, from which is calculated the mean velocity $\bar{w}$. The broadening of the curve is a measure for the degree of turbulence.

The mathematical evaluation results from the following equations :
The mean value of Time of Flight is calculated from

$$\bar{t} \approx \frac{\sum_j \sum_i t_i \cdot N_{i,j}}{\sum_j \sum_i N_{i,j}} \qquad (1),$$

which is an approach for the probability density function. "i" is the channel number and "j" the angular position of the L-2-F stopbeam. $N_{i,j}$ represents the number of counts for each "i" and "j". For a constant angle is j = 1.

The mean velocity is calculated from

$$\bar{w} = s \; / \; \bar{t} \qquad (2),$$

dividing the spot separation s through eq.(1).

The standard deviation is given by

$$\sigma_w = \sqrt{\frac{\sum_i (w_i - \bar{w})^2 \cdot N_i}{\sum_i N_i - 1}} \quad (3),$$

with $w_i = s / t_i$,calculated from the TOF distribution.

The parallel turbulence (velocity fluctuations) approximates from

$$Tu \approx \sigma_w / \bar{w} \quad (4).$$

If two kinds of particles with a significant velocity difference occur in the same flow, a dual peak in the TOF distribution develops. In that case, the statistical evaluation has to be performed two times over confined regions of the TOF distribution. To establish regions of interest, which contribute to a singular peak, the minima and maxima in the TOF distribution have to be investigated. The minimum between the peaks serves as the borderline for the integration of the probability density functions. Another method to establish two regions of interest is the definition of an empirical function to contribute the TOF events between the maxima corresponding to a sort of particle. This method is preferred if the maxima are disposed close together, because the prediction of the mean values will be errouneus with the first method. To determine the jet turbulence the standard deviation over the whole TOF distribution is calculated, because the classical definition for turbulence is not readily applicable to to a single phase of multiphase flow.

The main advantages of L-2-F velocimetry compared to LDA-technique are the capability of processing high data rates, particles of different size and a velocity range from less than 1 up to 1000 m/s without changing of the optical arrangement. Further the small dimensions of the probe volume are advantegeous in narrow flow patterns. With this features the L-2-F velocimetry appears as the most feasible method for measurements in high speed waterjets. A disadvantage is the increasing noise rate with increasing turbulence intensities and the limitation to turbulence rates of about 30 %.

3.0 EXPERIMENTAL SETUP

In Fig.3 is shown the injector type abrasive cutting head, used in our tests. The geometry parameters (D,L) of foci investigated are given in the table. The waterjet nozzle diameter is 0.4 mm, the distance between the nozzle and the focus inlet is held constant. The

discharge pressure has been varied between 500 and 3000 bars, the abrasive mass flow up to 11.25 g/s. The abrasive particles were glass spheres of 0.28 mm bulk mean diameter and a density of $2.4 g/cm^3$. Furthermore, the effect of the focus alignment on the jet formation cannot be quantified.

In all our tests the cutting head was processed in atmospheric air and the abrasives were fed by sucked-in air. The measuring position was about 5 mm downstream the focus outlet in the standard setup.

A view of the test rig is shown on Fig.4. The jet cutting tool is assembled into a glass basin to sample water and abrasives, which can be seen in front of the fotograph.
For positioning and traversing purposes the cutting head is mounted to a 2-axis traverse table (horizontally) and a 200 mm up and down adjustment device. The high pressure waterjet is supplied from an intensifier pump with a maximum pressure of 4000 bars, a maximum flowrate of 4 l/min and an electrical power about 40 kW. The operating pressure can be adjusted from a remote steering device. The abrasives are fed into the injector by a frequency controlled vibration feeder (left hand).
The L-2-F optical head is positioned behind the testbasin, so that the Laser beam waists are focused on the axis of the jet with the optical axis normal to the frontscreen. The angular position is adjusted with a mirror. The focusing of the measuring volume to a certain position is realized by traversing the optical head in the beam direction. The L-2-F electronic cabinet, the AT computer for data processing and the NC processor of the traverse table are shown in the background.

4.0 TYPICAL RESULTS OF L-2-F MEASUREMENTS

On Figs. 5a - d are shown some TOF distributions, measured with the L-2-F velocimeter. Some typical effects of AWJ setup parameters and correlations between the jet formation and the recorded measurements will be explained with the aid of these diagrams. The measuring position was on the centerline of the jet 5 mm beyond the focus outlet.

5a) TOF distribution of a pure waterjet at the exit of a focus with 1.6 mm diameter and 40 mm length, discharged with a pressure of 1000 bars. The maximum appears at 0.67 microsec, the calculated mean velocity is about 411 m/s. The diagram shows a clear narrow peak due to a low jet turbulence about 3.8%.

5b) In this diagram occurs a dual peak in the TOF distribution of an AWJ with 1 g/s abrasive load rate (or 18% of $\dot{m}_W$), caused by significant phase velocity differences after an insufficient mixing process. The jet was discharged with a pressure of 1000 bars through a focus of 1.6 mm diam. and 30 mm length. The left peak, contributed to the water phase, has it's maximum at 0.67 microsc. (mean velocity $v_W = 413.2 \quad m/s$), the right peak, contributed to the abrasives, at 0.99 microsec. (mean velocity $v_p = 257,25 \quad m/s$). The average jet velocity v_j amounts to 267.76

m/s, the turbulence to 21.1%. Some TOF distributions gained with the 2.0 x 40 mm (D x L) focus, $p_0 = 1000$ *bars*, look similar to Fig. 5b, but also for higher abrasive mass flow.

5c) In this diagram the TOF distribution of the same AWJ as in 5b is shown, discharged through a focus of 1.6 mm diam. but a length of 40 mm. The two peaks have moved closer together, due to an enhanced mixing process. The separate water peak has nearly vanished and it is assumed, that the data of the droplet and abrasive phase are covered by one widely broadened peak. The common maximum occurs at 0.89 microsec, the jet velocity v_j amounts to 284.2 m/s and the turbulence has decreased to 14.3%.

5d) TOF distribution of an AWJ with an abrasive load rate of 4.5 g/s 5.7% of $\dot{m}_w$), discharged with a pressure of 2000 bars through a focus of 1.6 x 40 mm (D x L). The maximum occurs at 0.67 microsec., the jet velocity v_j is calculatid to 388 m/s and the turbulence to 10.5%. A quite good AWJ formation can be deducted, the phase velocities are close together.

The following deductions can be made from Fig. 5:
If a dual peak occurs in the TOF distribution (5b), two fractions with significant velocity differences exist in the jet. One fraction is formed by water remaining unaffected by the mixing process, assigned to the left peak, whereas the second is formed by abrasives and water droplets after contact, assigned to the right peak.

The main reasons for an uneffective mixing process are a too short focus (5b,c), or in other terms a low length to diameter ratio (L/D $\leq$ 20) of the focus combined with relatively low discharge pressures. Furthermore the momentum exchange between the phases will be improved by small focus diameters and higher abrasive load rates. However, momentum losses due to impacts will also increase. An increased effectivity of the mixing process is accompanied by a reduced broadening of the TOF distribution (5c,d). Higher discharge pressure, proper focus geometry and abrasive load rates of 5 - 10% of m_w result in a turbulence rate of 8 - 12 % for centerline measurements (5d).

5.0 RESULTS OF PARAMETER VARIATION

5.1 VELOCITY AND TURBULENCE PROFILES

To demonstrate the effect of the focus on a pure waterjet, in Fig. 6 are plotted the velocity profiles beyond a sole sapphire nozzle and foci of variing diameter. The discharge pressure is 1000 bars, the measuring position is 65 mm downstream the waterjet nozzle in each case. Without a focus (solid line), the velocity in the borderzone of the jet is significantly higher and equals nearly the centerline velocity, because the momentum exchange with the ambient air is weak. The diameter has expanded to more than 2 mm.

The asymmetry of the velocity profile may occur from sapphire nozzle anisotropy, leading to a locally increased turbulence.

Using a cutting head with a smaller focus diameter results in a reduction of the jet diameter. The radial slope of velocity increases at the border due to the influence of wall friction in the focus. For the D = 2.0 mm (dotted line) and 1.6 mm (dashed line) focus the centerline velocity only slightly decreases compared to the sapphire nozzle, whereas it dereases about 20% for the 1.1 mm focus (dashed dot line). The velocity profile developing in a narrow focus shows a pipe flow like contour.
The symmetry of the 1.6 mm focus profile confirms a quite good focus alignment. The elevation on the right side of the 2.0 mm focus profile may be influenced by the suction stub. The profile asymmetry for the 1.1 mm focus is a consequence of misalignment, to which narrow foci are more sensitive.

The curves in Fig.7 have been recorded for an AWJ of 2.25 g/s abrasive load rate and the same conditions as mentioned above. Three effects caused by the solid particles can be observed : 1.) the jet diameter increases, 2.) the jet velocity v_J decreases significantly, especially on the centerline, 3.) for the 2.0 and the 1.6 mm focus the velocity in the borderzone exceeds the centerline value.

A very significant raise of v_J to the outer radii occurs with the 2.0 mm focus, combined with a low abrasives/droplet concentration in the center region, where a measurement was impossible. From this profile a severe disintegration of the jet beyond the focus is concluded. A focus diameter of $5d_0$ or more shows to be not suitable for an efficient AWJ mixing process. The raise of borderzone velocity for the 1.6 mm focus is contributed to single abrasive particles and droplets. In the center region the mixing process between the phases continues, resulting in a slightly lower velocity due to turbulent momentum losses, but a disintegration of the jet is avoided. Right to the edge of the jet L-2-F measurements are not possible, because there exists a zone of turbulent vortices, separating from the jet. However, there must occur a steep decrease of the radial velocity profile to the surrounding. At least, the 1.1 mm focus still shows a pipe flow profile, indicating, that the effects of wall friction and impact control the turbulent mixing losses.

The propagation of the turbulent mixing process in the center region of an AWJ downstream the focus outlet is affirmated by Fig.8. In this diagram the velocity and turbulence profile of an AWJ is compared to a pure water jet. The discharge pressure is 2000 bars, the focus geometry 1.6 x 40 mm (D x L). A severe increase of the turbulence inside the AWJ is observed, whereas in the pure water jet the turbulence increases with the radius due to boundary effects. Furthermore the smooth and symmetric velocity profile of the AWJ results from proper setup of the cutting head and the process parameters. The pure water jet velocity is reduced by increasing wall friction compared to the ideal value after Bernoulli's equation (632 m/s).

5.2 CENTERLINE VELOCITY

The centerline velocity (focus 2.0 x 40: 1 mm out of axis, ref. Fig.7) of an AWJ with 2.25 g/s abrasive mass flow is depicted in Fig.9 versus the discharge pressure. Parameter is the focus geometry, the solid line represents the ideal values after Bernoulli's equation and the law of momentum conservation. The differences between the foci are considerably low. With increasing discharge pressure increases the deviation to the calculated velocity due to momentum losses by wall friction, wall impact of particles and droplet deformation or breakup from phase interaction.

On Fig.10 is shown the centerline velocity of a 2000 bar AWJ versus the abrasive mass flow for diverse foci compared to calculated values, given by the solid line. The range covered by the measurements reaches up to 11.25 g/s respectively 14.2% of $\dot{m}_w$ abrasive mass flow rate. Feeding of low abrasive mass flows causes a severe decrease of v_J with all foci by turbulent mixing losses (impacts and droplet deformation), due to the presence of the solid phase. For feedrates exceeding about 3 g/s the slope of the curve becomes degressive with 2.0 and 1.6 mm focus diameter. The mixing losses do not increase linearly with abrasive mass flow. For the 1.1 mm focus occurs a more steadey decrease of v_J with the feed rate, indicating, that wall effects prevail the effects of phase interaction.

The validity of our measurement results is demonstrated by their comparison with the data of other authors. /2/. There is quite good agreement with the phase velocity data of Hashish /5/ in the range between 1400 and 2800 bars discharge pressure. He had used a pair of magnetic coils surrounding the focus to measure the 'time of flight' of steel particles and a Laser technique for the water velocity in time. Isobe et al /8/ have measured AWJ velocities from 50% up to 70% of the calculated ideal velocities, performed with a discharge pressure of 1960 bars and focus diameters of $3.1-4.0d_0$. They have determined the particle velocity by counting impact craters of abrasives, which have hit an aluminium plate in a certain time interval. Chen and Geskin /2/, having used Laser Transit Anemometry for AWJ velocity measurements as the authors, found a similar correlation between jet velocity and abrasive mass flow. Furthermore they observed also a decreasing pure water jet velocity with decreasing focus diameter, but an increasing abrasive velocity. This deviation may be caused by different stand off distances or focus misalignment in our tests.

6.0 CONCLUSIONS

The Laser-2-Focus velocity and turbulence measurements on an AWJ discharged from an injector type cutting head have yielded the following results :

if the mixing process is uneffective, the measured TOF distribution shows a dual peak due to a significant phase velocity separation;

- discharge pressures beyond 1000 bars, low abrasive load rates and a low length/diameter ratio of the focus (≤ 20) support uneffective mixing;
- a focus diameter $\geq 5d_0$ causes AWJ disintegration beyond the outlet;
- proper AWJ formation is yielded by discharge pressures exceeding 1500 bars, abrasive load rates of 5 - 10% ,a focus diameter of 3 - $4d_0$ and a focus length about 25 diameters D;
- for pure water jets and AWJs a narrow foci develops a pipe flow like velocity and turbulence profile beyond the focus, for AWJs in foci of larger diameter increases the velocity to the outer radii and the turbulence in the center region;
- momentum losses reducing the jet velocity signifcantly during jet formation are caused by turbulent phase interaction, abrasive wall impacts and wall friction.

REFERENCES

/1/ Blickwedel,H.: Erzeugung und Wirkung von Hochdruck Abrasivstrahlen. Fortschritt-Berichte VDI Reihe 2: Fertigungstechnik Nr. 206, 1990 (in german).

/2/ Chen,W.-L.; E.S.Geskin: Measurement of the Velocity of Abrasive Waterjet by the Use of Laser Transit Anemometer. 10th Int. Symp. on Jet Cutting Techn., STI, Paper B4, 31. Oct. - 2. Nov. 1990, Amsterdam, Netherlands.

/3/ Ehlbeck,U.; H.Blickwedel; H.Oweinah; M.Lierheimer; M.Schmelzer: Der Wasserstrahl als Werkzeug. METAV 88, VDI-Fachtagung, 8./9. Jun. 1988, Duesseldorf, Germany (in german).

/4/ Fairhurst,R.M.; R.A.Heron; D.H.Saunders: DIAJET – a new Abrasive Water Jet Cutting Technique. Proc. of the 8th Int. Symp. on Jet Cutting Techn., BHRA, 9. - 11. Sept. 1986, Durham, UK.

/5/ Hashish,M.: Measurement of Abrasive-Waterjet Particle Velocities. Flow Technical Report No. 320, Mar. 1985.

/6/ Hashish,M.: Abrasive-Fluidjet Machining Systems: Entrainment versus direct Pumping. Proc. of the 10th Int. Symp. on Jet Cutting Techn., STI, Paper F4, 31. Oct - 2. Nov. 1990, Amsterdam, Netherlands.

/7/ Himmelreich,U.; W.Riess: Hydrodynamic Investigations on Abrasive Water Jet Cutting Tools. Proc. of the 10th Int. Symp. on Jet Cutting Techn., STI, Paper F1, 31. Oct - 2. Nov. 1990, Amsterdam, Netherlands. Water Jet Cutting Tools.

/8/ Isobe,T.; K.Nishi; H.Yoshida: Distribution of Abrasive Particles in Abrasive Waterjet and Acceleration Mechnism. Proc. of the 9th Int. Symp. on Jet Cutting Techn., Paper E2, pp. 217 - 238, 4. - 6. Oct. 1988, Sendai, Japan.

/9/ Schodl,R.: Entwicklung des Laser-2-Fokus Verfahrens fuer die beruehrungslose Messung der Stroemungsvektoren, insbesondere in Turbomaschinen. Deutsche Luft- und Raumfahrt, Report No. DLR-FB 77-65, 1977, Koeln, Germany (in german).

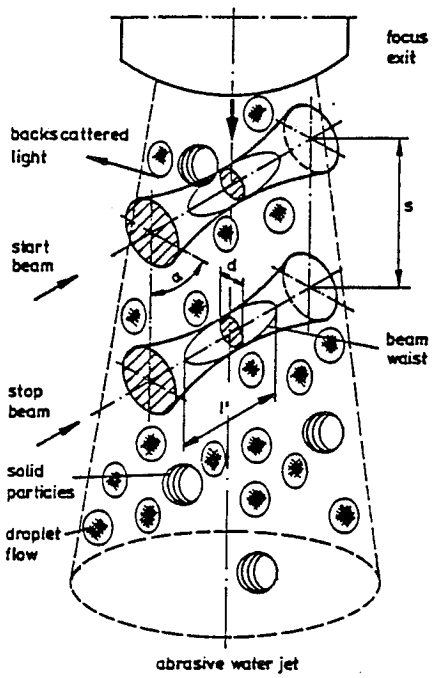

Fig.1 L – 2 – F Measuring Volume

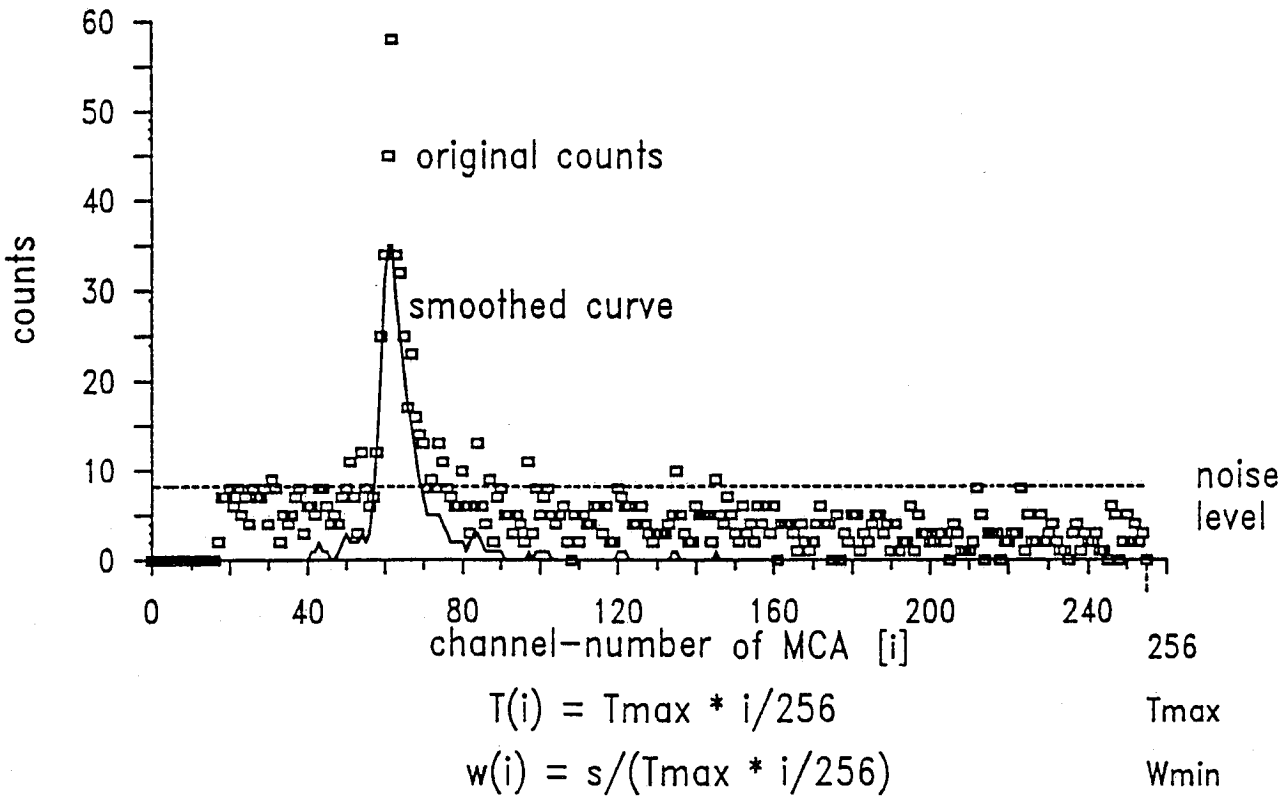

Fig.2 Evaluation of L – 2 – F 'Time of Flight' Distribution

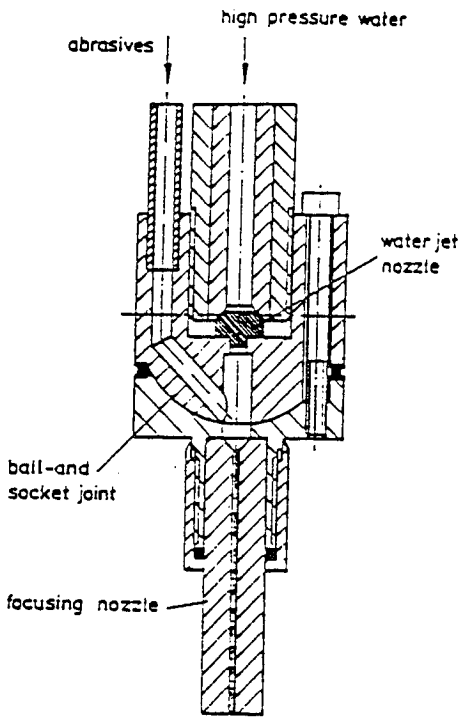

focus geometries	
D	L
1.1	40
1.6	30
1.6	40
2.0	40

Fig.3 Abrasive Cutting Head

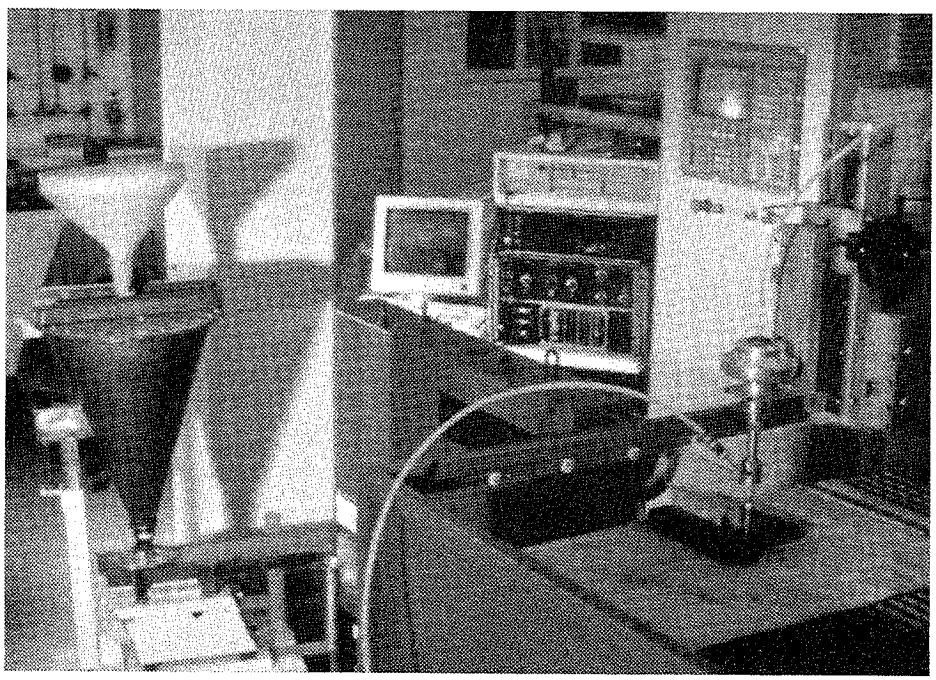

Fig.4 View of the Test Rig

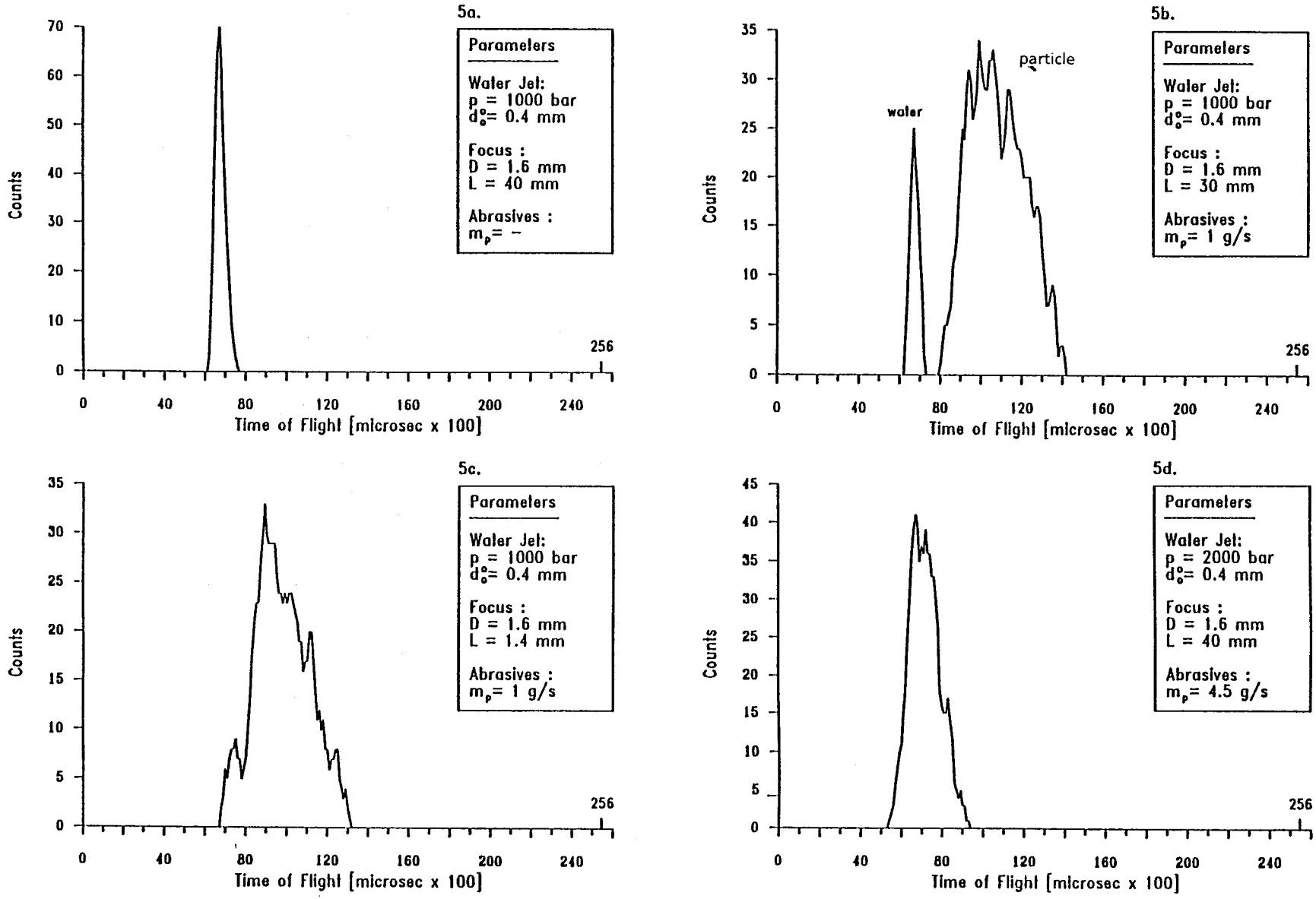

Fig.5 Characteristic L – 2 – F Time of Flight distribution

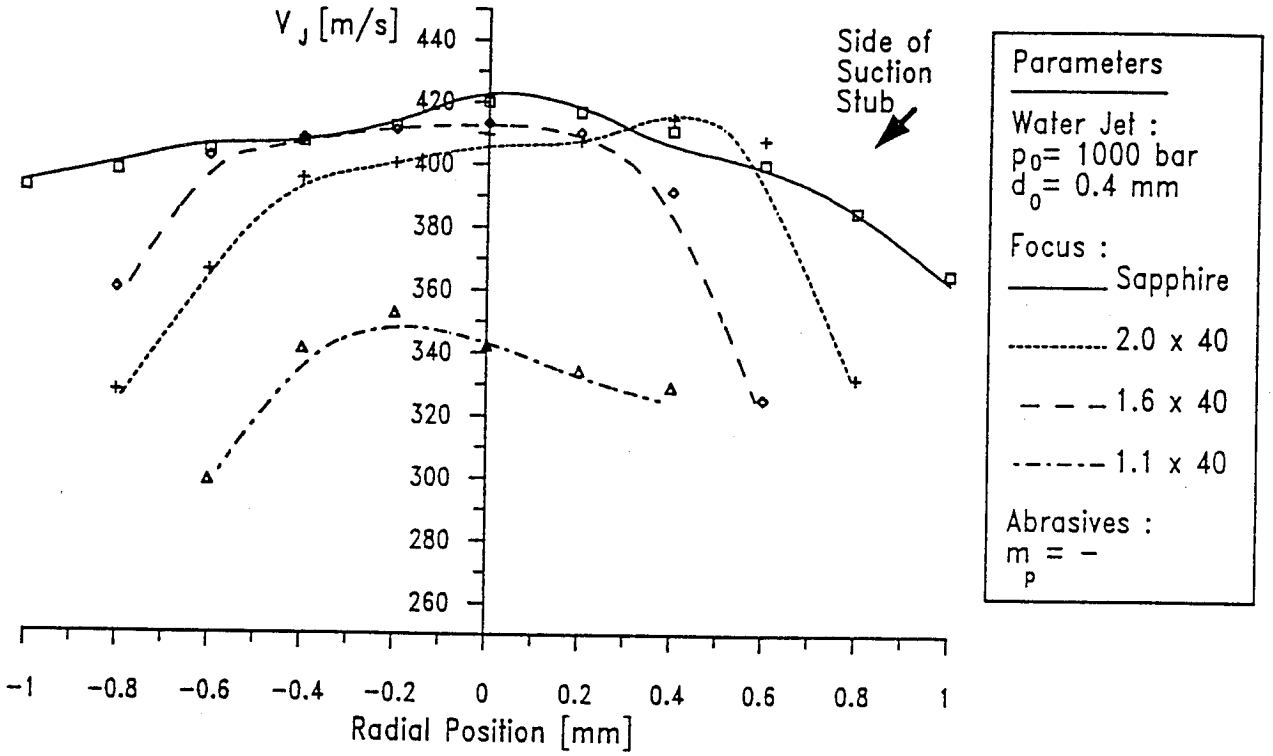

Fig.6 Velocity profiles of a pure waterjet

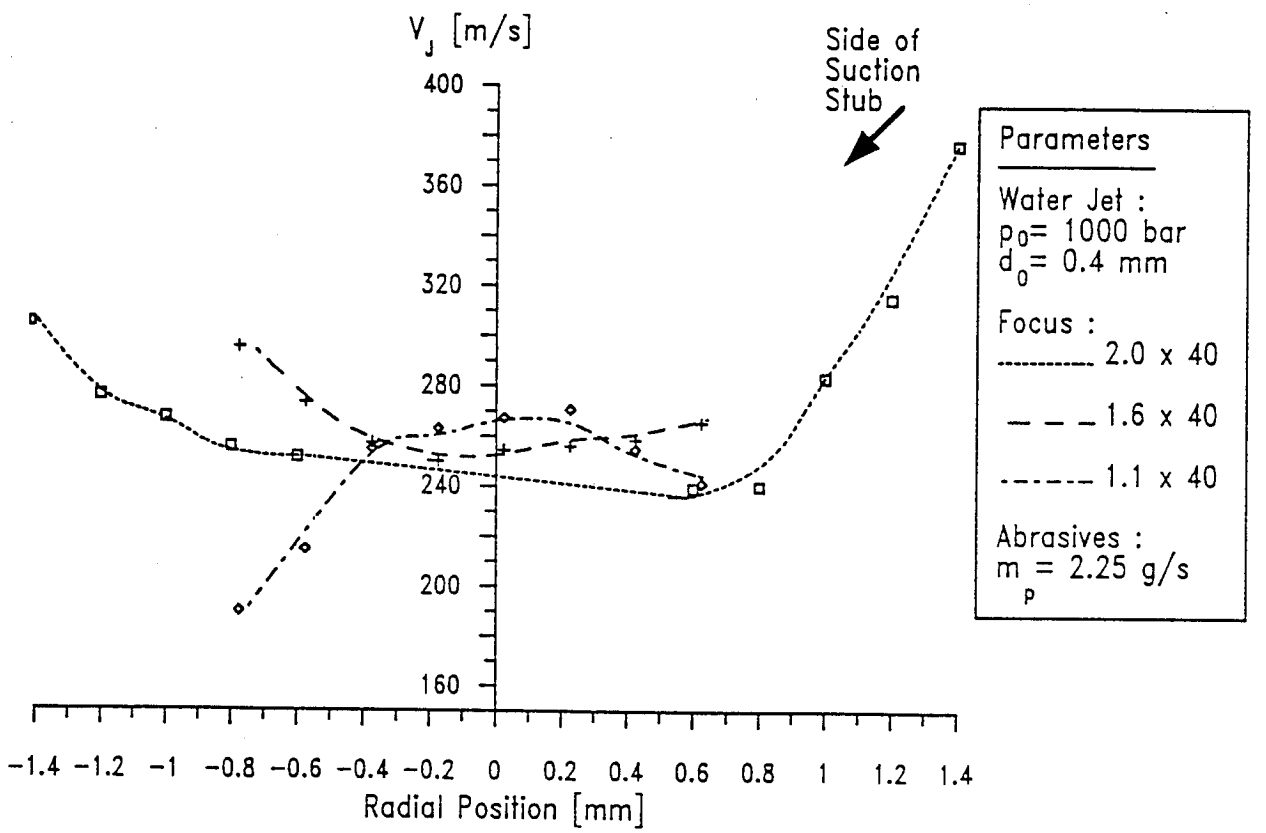

Fig. 7 Velocity Profiles of an Abracive Water Jet with diverse Foci

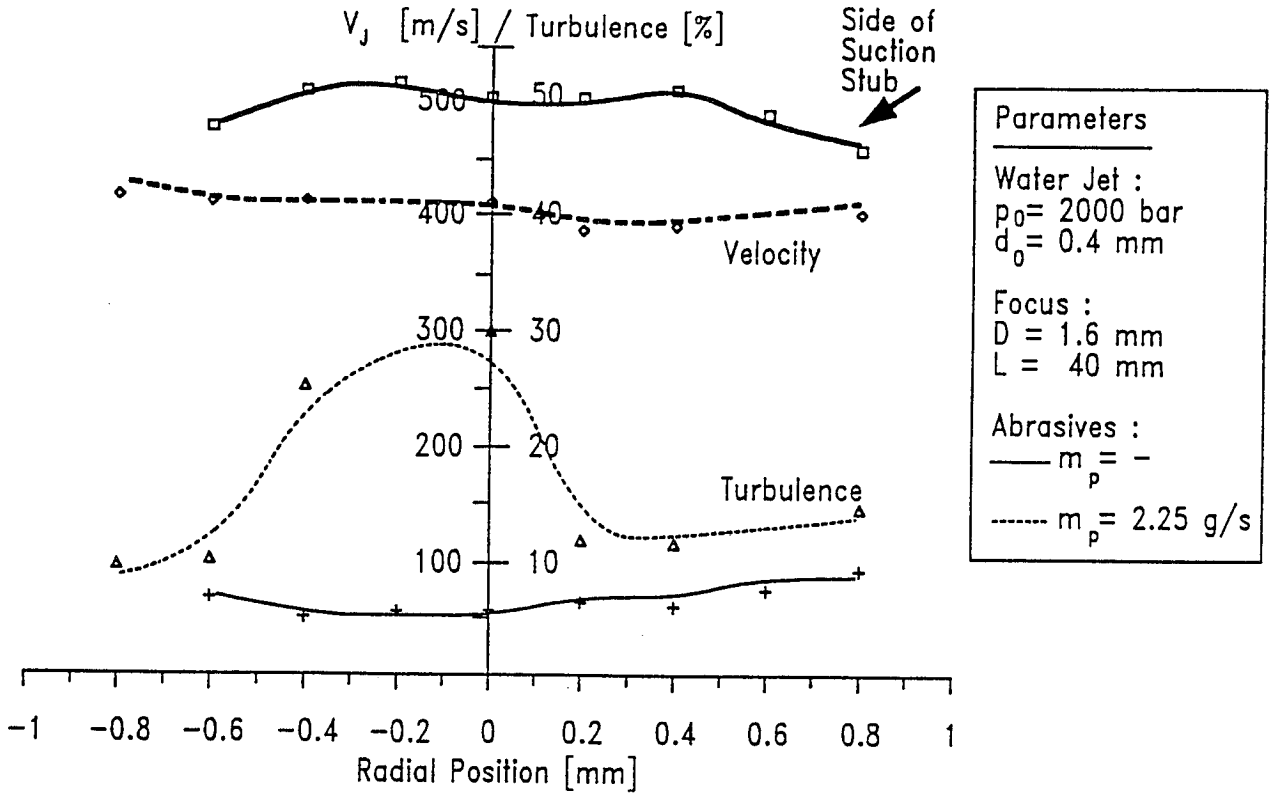

Fig.8 Velocity and Turbolence Profiles of an AWJ and pure water jet

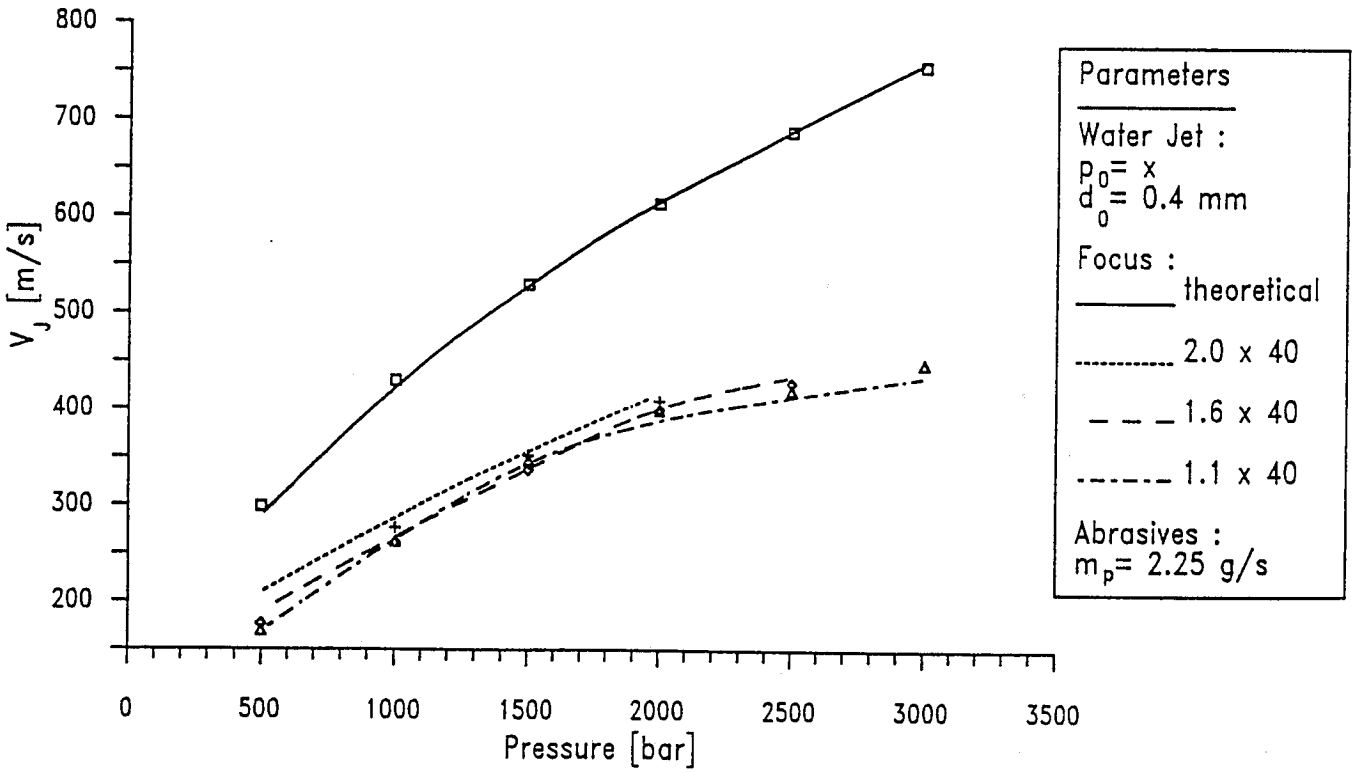

Fig. 9 Velocity in Effect of the Discharge Pressure

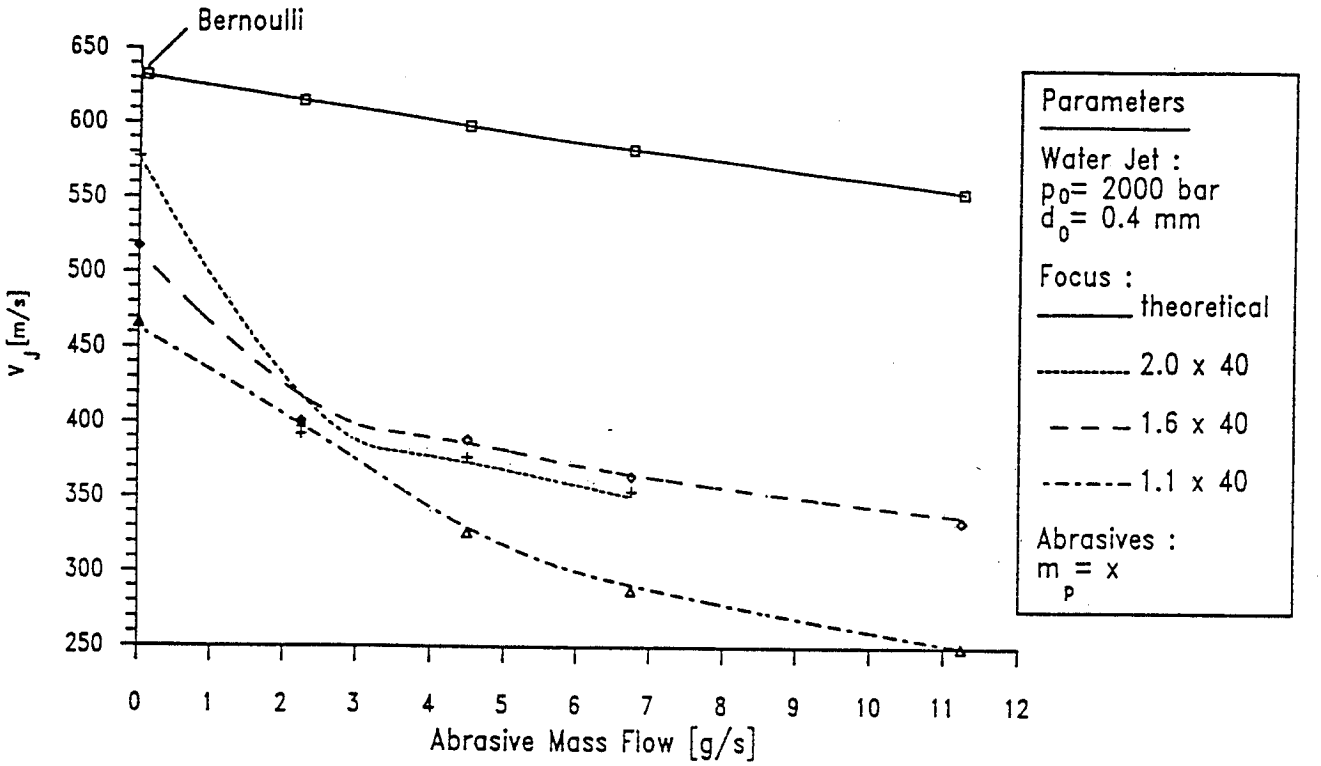

Fig.10 AWJ Velocity in Effect of the Abrasive Mass Flow

NOMENCLATURE

d_0 =	water jet nozzle diameter	[mm]
D =	focus diameter	[mm]
L =	focus length	[mm]
$\dot{m}_p$ =	abrasive mass flow	[g/s]
$\dot{m}_w$ =	water mass flow	[g/s]
N =	number of counts	[-]
p_0 =	water discharge pressure	[bar]
s =	spot separation of L-2-F	[μm]
t_i =	TOF interval	[μs]
$\bar{t}$ =	TOF mean value	[μs]
T_{max} =	last MCA channel preset	[μs]
Tu =	parallel turbulence	[%]
v_J =	phase average velocity of jet	[m/s]
v_p =	abrasive phase velocity	[m/s]
v_w =	water/droplet velocity	[m/s]
w_i =	velocity assigned to t_i	[m/s]
$\bar{w}$ =	mean velocity from TOF distribution	[m/s]
σ_w =	standard deviation of TOF distribution	[-]

6th American Water Jet Conference
August 24 - 27, 1991: Houston, Texas Paper 27

INVESTIGATION ON WATER–JET CUTTING OF CONCRETE IN WATER SURROUNDINGS

A. Klich and A. Kalukiewicz
Institute of Mining and Dressing Machines and Automation
University of Mining and Matallurgy
30–095 Cracow, POLAND

ABSTRACT

The research stand for examining water–jet cutting effectiveness under the surface of water is described in the paper. It is possible to move concrete bloos in the water container under the rotating nozzle. The diameter of the nozzle could be either 0.8 mm and 1.0 mm while the pressure of jet is up to 200 MPa. The pressure of water in the container is 1 MPa. The traverse speed of the nozzle against the concrete specimen could vary up to 3.6 m/s. The results of the experiment are presented in the paper, especially cutting capacity as dependent on jet parameters, water pressure in the container and concrete strength.

Organized and Sponsored by the Water Jet Technology Association.

1.0 INTRODUCTION

For a dozen or so years techniques of mining rock with high–pressure water jets as a cutting tool have been developed in Poland. Relevant investigations have been also carried out at the University of Mining and Metallurgy in Cracow, Poland since 1974. Some results of this research were presented, among others, during the 5th American Water Jet Conference in Toronto [5].

Investigations made so far and applied in practice concerned the action of water jet as an independent cutting tool or as an agent aiding conventional mining. In the works presented, water jet is forced out of the nozzle to the atmosphere and according to the jet parameters and its kinematics, and to the properties of rock under cutting it can wear away its structure. Effects of mining through "cutting in the air" dependent on the pressure applied, nozzle diameter, speed of the nozzle motion and the rock strength, have been already fairly well recognized and results of these investigations have found practical application also in other industries. Water jet forced out of the nozzle into the atmosphere is dispersed depending on the nozzle geometrical parameters and on the hydraulic ones. When speaking about water jets used for cutting rock, the term "cutting in the air" does not seem to be very accurate, since the jet passes through a gas medium only between the nozzle outlet and the rock surface. Having penetrated the rock, the jet operates in a hole or fissure partly filled with water.

In recent years a new design of a full-face machine for driving mine shafts has been worked out at the Institute of Mining and Dressing Machines and Automation at the University Mining ond Metallurgy in Cracow (Fig.1.). One of the versions is meant to transport the excavated material from the bottom of the shaft under driving. Thus the ripping head will operate immersed in water. Since disc tools are to be aided with continous high–pressure water jets to 250 MPa and the nozzle diameters of 0.3 to 0.8 mm, it is necessary to determine the effectiveness of jet action under water. The same applies to water jet aiding drilling operations of drilling equipment in which flushing is used. Here, the effectiveness of the jet forced out into an aqueous medium must be tested.

2.0 TEST STAND AND LABORATORY TESTS OF ROCK CUTTING

A special test stand has been built (Fig. 2 and 3). It consists of:
- a high–presuure (to 200 MPa) system,
- a container wit the capacity of 0.785 m^3 and pressure regulation system,
- a pressure transmission system from the hydromonitor to the container (Fig.4),

- a samples guiding and shifting system in the container(Fig. 5 and 6),
- a recording–measurement system.

A device designed by the authors, makes it possible to produce pressure to 320 MPa in three (placed in parallel) intensifiers with the transmission ratio 1:10. Maximum flow rate oil equals 236 l/min and of water 23.6 l/min. The power of the supply station equals 90 kW.

The water container is made of steel. Its internal dimensions are:
- height – 1000 mm,
- diameter – 1000 mm,
- capacity – 0.785 m^3.

It is a cylinder with a bottom part welded on, placed on a supporting structure. An elastic joint is provided on the side wall for a high–pressure conduit leding from the hydromonitor to the nozzle in the container. The conduit rotates together with the hydromonitor. The rated pressure for this container is 1 MPa. The container is covered from above by a sealed steel plate in which a water pressure regulation and stabilization system is fixed. The container is furnished with an overflow valve and pressure sensors.

Samples of a material under testing, e.g. concrete slabs with the dimensions of 45x45x12 cm are placed inside the container. It is possible to shift these samples in three directions in realtion to the rotating nozzle. Thus, it is possible to change e.g. the distance of the nozzle from the sample, the rest of the hydraulic and mechanical parameters being stable. In consequence it makes possible to determine the dependence of the effect of sample incision on the distance of the nozzle from the sample surface.

Comparative incisions were made by "cutting in the air", i.e. when the container was empty of water, when it was filled ("under water"), and when outer pressure to 1 MPa was produced ("under water and pressure"), to determine the influence an aqueous medium and its pressure on the effect of sample incision. Photographs of exemplary samples are shown in Fig. 7. Diagrams in Fig. 8. present cummulative results of the investigations.

3.0 CONCLUSIONS

1. A high–pressure water jet forced out into the aqueous medium maintains its coherence, which makes it possible to make incision depths comparable with that obtained through "cutting in the air".
2. With certain parameters ranges (see Fig. 8.) an increase of the effects of

cutting under water and under outer pressure is observed in comparison with those of "cutting in the air".

3. Increase in the effectiveness of cutting under water and under pressure to 1 MPa may be explained by the formation of a layer of water vapour on the border line between the jet water and the surrounding water – kind of vapour pipe guiding the jet, or by the growth of the jet mass brought about by the improved conditions of water flow from the surrounding to the jet.
4. Increase in the effectiveness of cutting under water and under outer pressure may be also explained by the concentration of cavitation effects in the region near the jet axis, with the radius smaller than in the case of cutting without the outer pressure.
5. Precise explanation of the mechanism of the growth of incision depth through cutting under water at the increase of the pressure of water in which the jet operates requires further research.

4.0 REFERENCES

1. F. Erdmann-Jesnitzer, A. M. Hassan, H. Louis, "A Study of the Effect of Nozzle Configuration on the Performance of Submerged Water Jets, *4th International Symposium on Jet Cutting Technology*, April 12th-14th, Badford, England.
2. A. Kalukiewicz, "Study of Mining Coal with Water Jet" (doctoral dissertation), in Polish, Kraków, 1984, Poland.
3. Z. Kawecki, J. Puchała, "The Method of Mining Rock with Continous Water Jet and the Device to Meet This Purpose", Polish Patent No 98322/30, 1981.
4. Z. Kawecki, J. Puchała, "Study of Technique of Mining Rock with High–Pressure Pulsating Jet", *A Report for Mining Mechanization Centre KOMAG*, 1974 Gliwice, Poland
5. A. Klich, A. Kalukiewicz, "High-Pressure Water-Jet as a Cutting tool", *5th American Water Jet Conference*, 1989, Toronto, Canada.

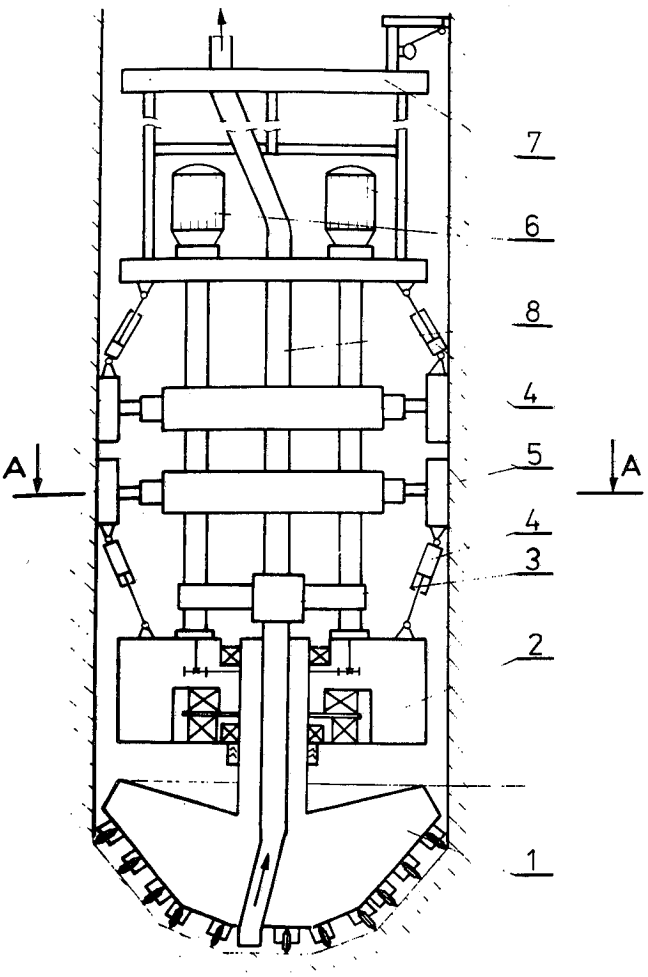

Figure 1: Diagram of the full-face machine for driving mine shafts with a hydraulic transport of excavated material.

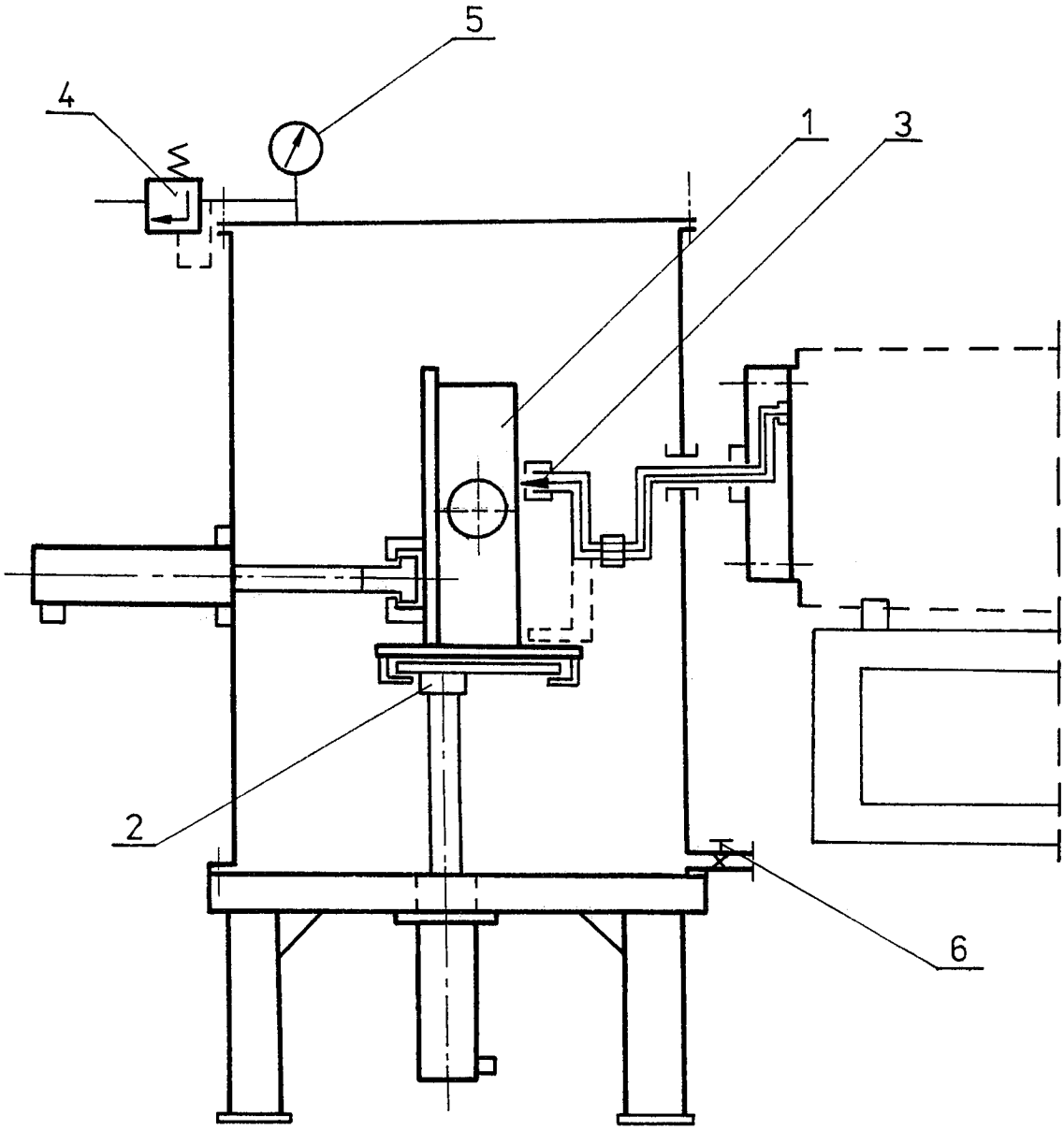

Figure 2: Diagram of the water container with the sample shifting system:
1 - rock sample
2 - sample shifting system
3 - nozzle
4 - overflow valve
5 - manometer
6 - cut-off valve.

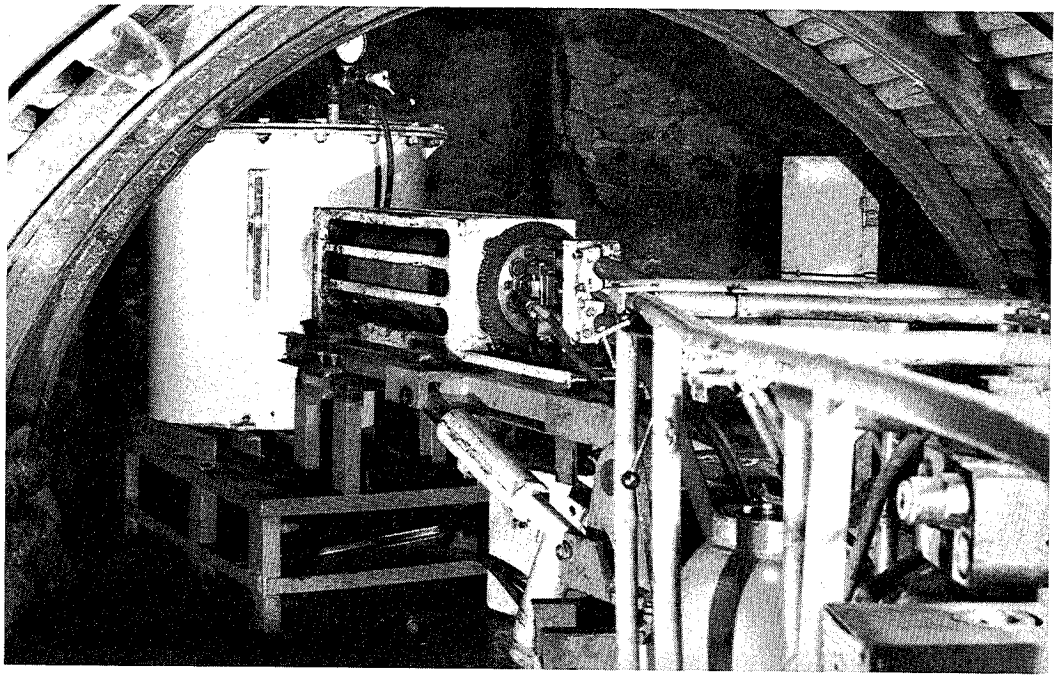

Figure 3: Stand for testing high-pressure jets under water.

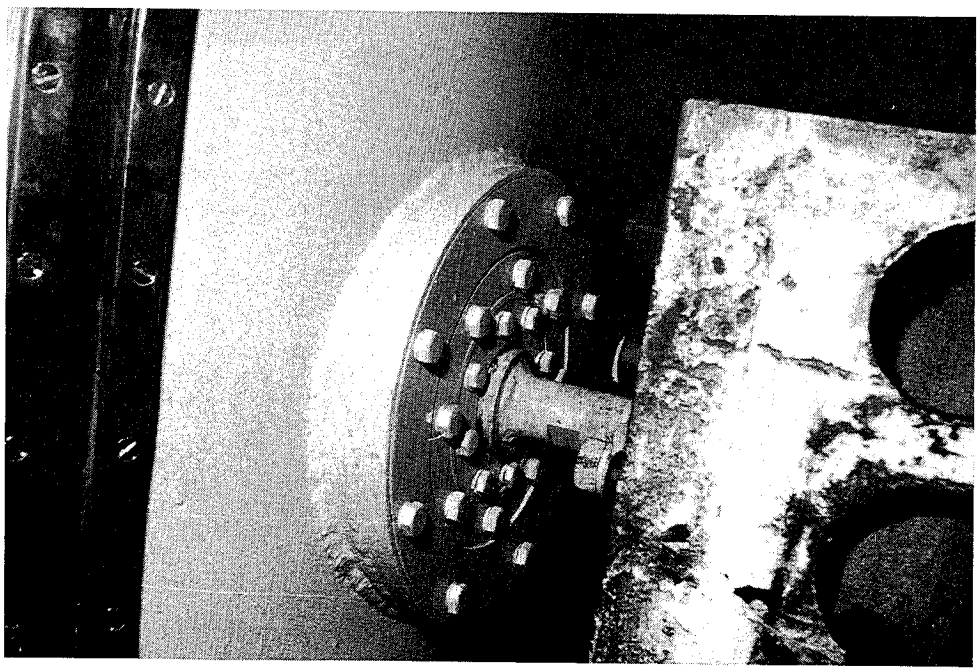

Figure 4: View of the hydromonitor joint with the container.

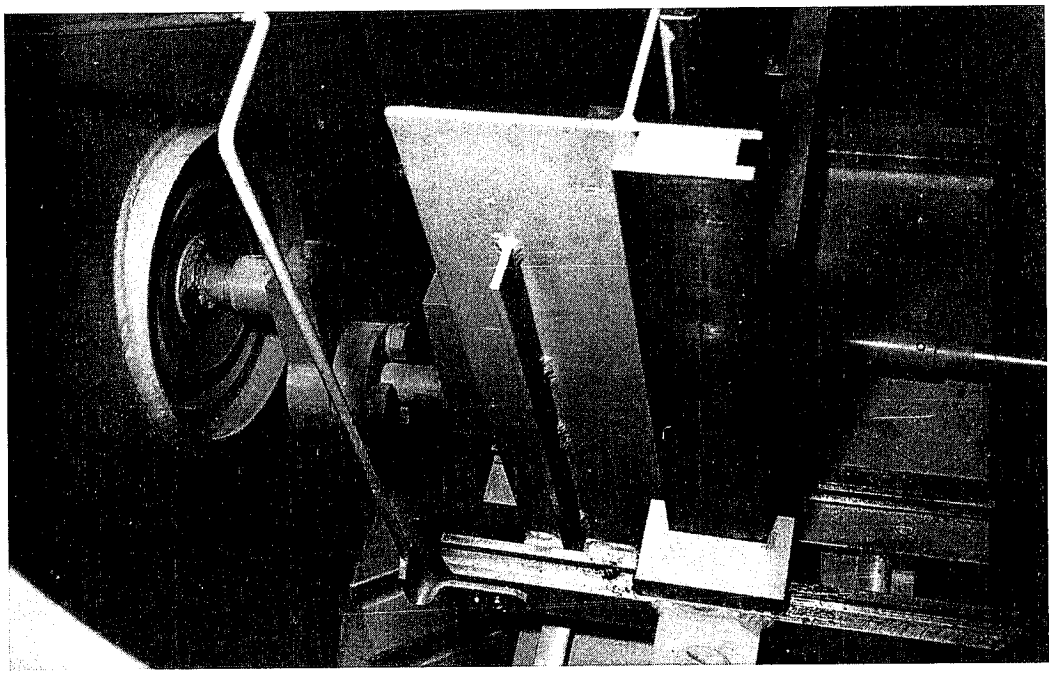

Figure 5: View of the container inside; on the left - conduit from the hydromonitor, on the right - fixing and shifting system of rock samples.

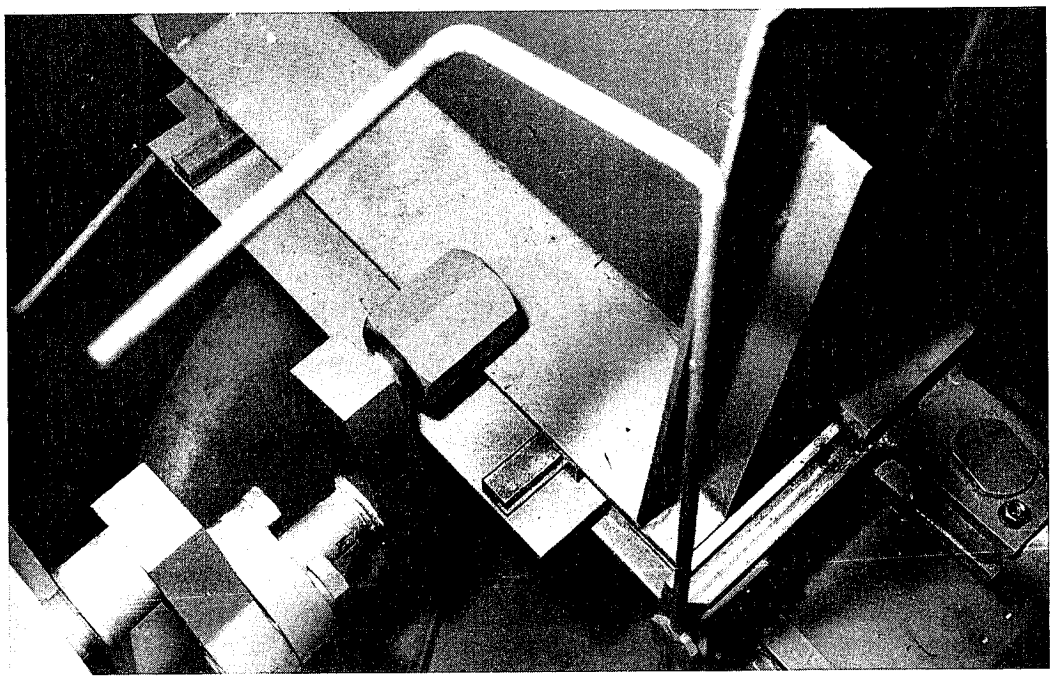

Figure 6: View of the high–pressure articulated conduit with a nut damping the nozzle insert.

on the left – in the air on the right – under water

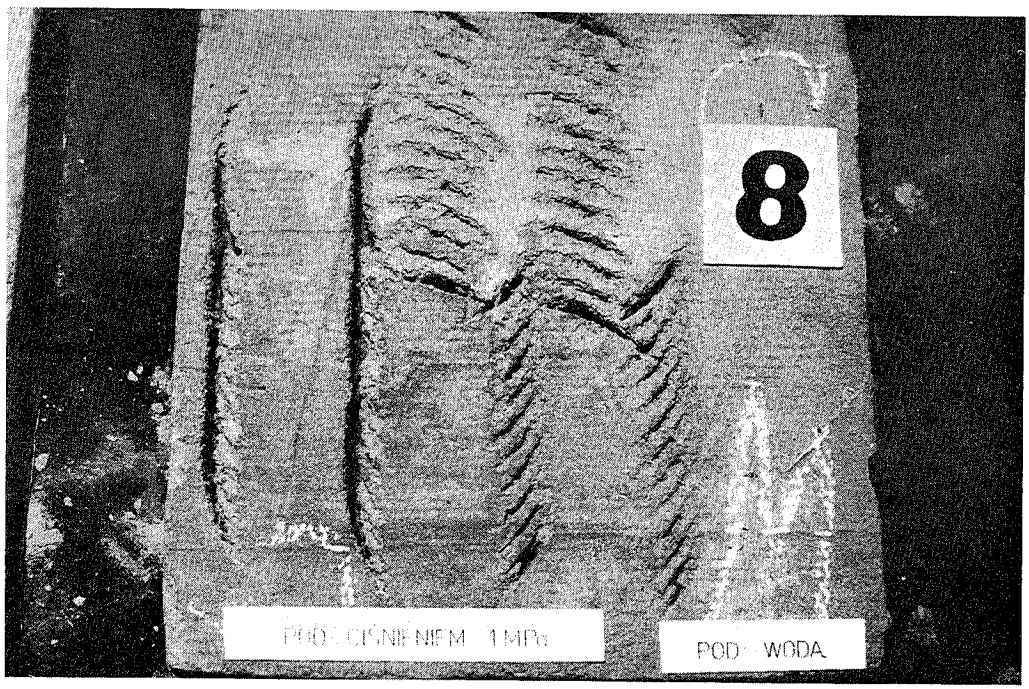

on the left – under water and under outer pressure 1 MPa on the right – under water

Figure 7: Exemplary samples with incisions made by a high-pressure jet.

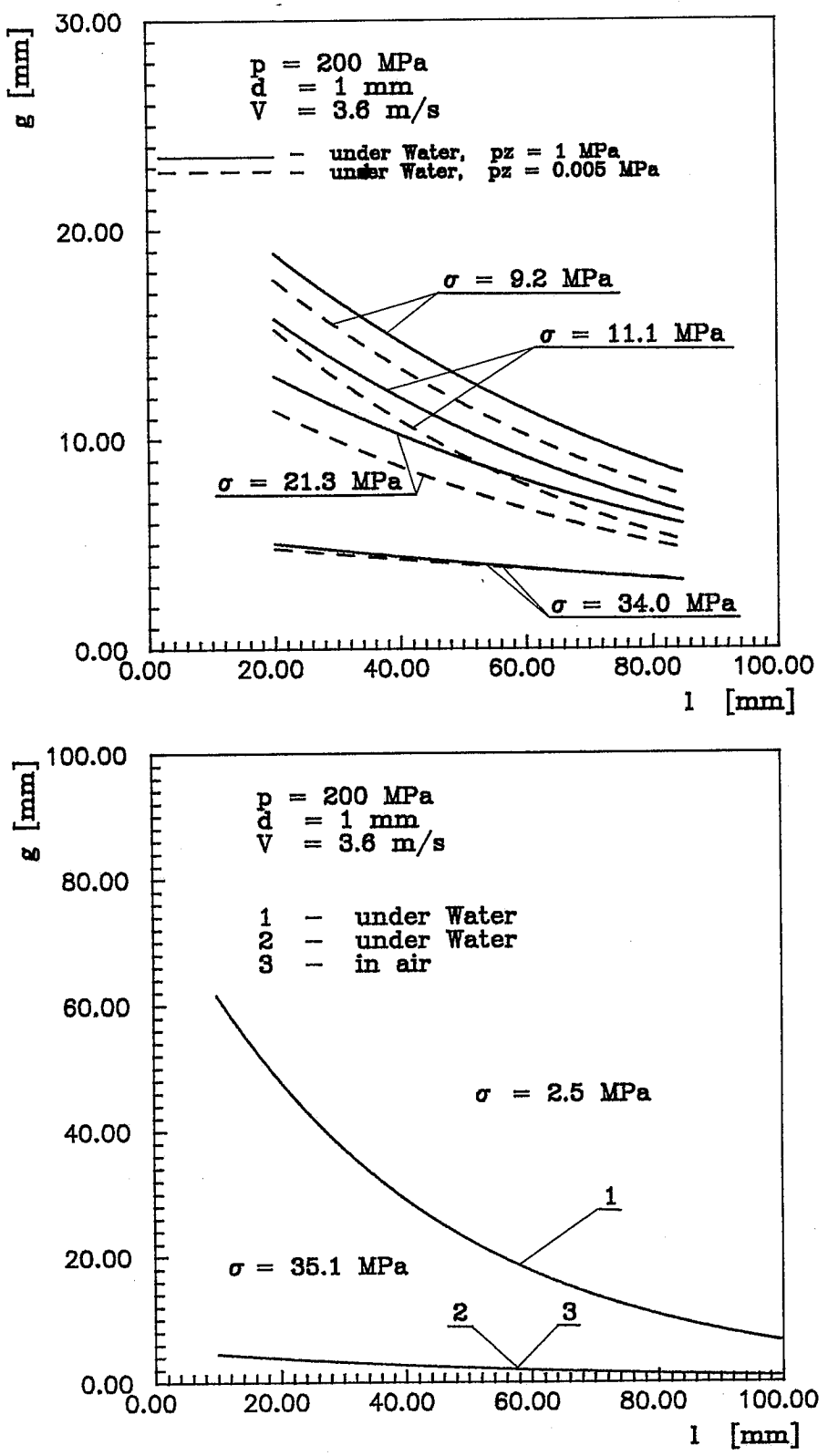

Fig. 8. Dependences of the cutting depth on pressure for varying compressive strength of rock

6th American Water Jet Conference
August 24 - 27, 1991: Houston, Texas Paper 28

Effect of Nozzle Traverse Rate and Number of Passes on Soft Ground Cutting by Water Jet

Hiroshi Yoshida and Risaburo Asano
Kajima Institute of Construction Technology
Tokyo, Japan

Hiroaki Kubo, Shunji Jinbo and Susumu Uesawa
Chemical Grouting Co., Ltd.
Tokyo, Japan

ABSTRACT

This report describes experiments by which the relations between water jet cutting efficiency and two factors--nozzle traverse rate and number of passes--were investigated. The procedure basically consisted of measuring the time required for a jet to arrive at various measuring points located in a plot of soft model soil. These experiments, the second in series, were performed in order to determine work execution specifications for utilizing the water jet, on a greater volume of soil during a given time. With the results of these experiments, we were able to comprehend the relationships these two factors have with soil cutting distance. We could also clarify limits for each important variable of water jet ground cutting within which good cutting efficiency is attainable.

Organized and Sponsored by the Water Jet Technology Association.

1.0 INTRODUCTION

The jet grout technique was commercialized in 1971 as a means of soil improvement which utilizes the water jet, and is now in use around the world. Recently, however, growing demands for wider coverage and lower costs have emerged. Because meeting this demand with current work execution specifications has been impossible, we have performed these basic experiments to understand the characteristics of the factors involved in ground cutting by water jet.

The soil improvement technique which utilizes the water jet consolidates cylindrical regions of soil using a device which injects a consolidating agent into the space momentarily opened by a water jet. The operation begins with the jet being inserted into the soil at a given depth, and the jet's nozzle is then rotated while emitting a high speed jet perpendicular to its axis of rotation while being withdrawn incrementally.

In the application of this technique, an increase in the distance the water jet cuts results in the enlargement of the quantity of improved soil. When loose sandy soil is cut by water jet, the jet's pressure, flow rate, nozzle traverse rate, and number of passes, along with the properties of soil being cut, are considered to be the most important variables affecting cutting efficiency. In a previous report, we reviewed water jet pressure and flow rate, which are the most important among the above factors. Here, we report on nozzle traverse rate and number of passes, which are second to the above two factors in terms of relative importance regarding cutting efficiency.

2.0 METHODS OF EXPERIMENT AND EQUIPMENT

We first investigated the relationships between cutting distance and nozzle rotation rate (which is linked to nozzle traverse rate) and the number of passes made in a particular plane. Water jet pressure was fixed at 30 MPa and flow rate at 300 l/min, on the basis of the results of previous experiments. We also conducted experiments on the effect of rotation rate and number of passes on soil consolidation, applying the results of the above exploratory experiments.

2.1 Model soil

Model soil was placed in an octagonal well as shown in Fig. 1. The well was 5 m wide and 5 m deep, and was filled with sand having the grain characteristics listed in Table 1 which was then compacted with water. The physical properties of the model soil are listed in Table 2.

2.2 Exploratory experiments

2.2.1 Values of variables

The values of each variable were set as follows on the basis of the

results of preliminary calculations:

(a) Rotation rate: Starting from 1.25 rpm, rotation speed was doubled repeatedly and tested up to about 320 rpm because these speeds were easily measurable.

(b) Number of passes: The number of passes tested was from 1 to 20. With twenty passes, double cutting distance might be achieved.

The combinations of rotation speeds and numbers of passes are shown in Table 3. Each combination was tested twice.

2.2.2 Procedures

The water jet's cutting speeds and cutting distances were obtained by measuring the times required for the water jet to reach each of the measuring points, with the high speed jet nozzle rotating at a given depth in the model ground.

(a) Measuring equipment: As shown in Figure 1, nine measuring points were prepared. Measuring rods, each having at its tip a vibration sensor capable of detecting the striking of the rod by the water jet, were firmly fixed at their upper and lower ends. The measuring points were arranged in a spiral in increments of 50 cm from 0.5 to 4.5 m from the nozzle and at angles of 10 degrees between each other and the nozzle.

(b) Jetting equipment: A nozzle 5.5 mm in diameter was fixed to a duplex tube 140 mm in diameter. To produce the desired water jet, four pumps, Achemat, TX-75 and 150, and PG-75 made by Isuzu, Union, and Kokenkogyo respectively, were connected in tandem. A diagram of the jetting apparatus appears in Figure 2.

(c) Method of measurement: A sensor was attached to the the outer portion of the duplex tube, and the time that lapsed from the moment the sensor detected the production of a water jet to the jet's arrival at a measuring point (sensed by a vibration sensor) was recorded by a data recorder. Elapsed time was read from the recording paper. A flow chart describing the measurements is shown in Fig. 3.

2.3 Consolidation experiments

2.3.1 Values of variables

The consolidation experiments were performed as an integrated application of the results of the exploratory experiments, to examine the relationship between the ground cutting speed of the water jet as measured in the exploratory experiments and the extent of consolidation for soil improvement.

For this purpose, the values of variables selected were limited to those which were within the range in which cutting efficiency had been determined to be satisfactory by the exploratory experiment. The rotation speeds and numbers of passes shown in Table 4 were used.

2.3.2 Method

The consolidation experiments, as the exploratory experiments, were

performed on model soil placed within a well. A high-speed jet nozzle was rotated and withdrawn as a 100% W/C consolidation agent was directly injected by a Halliburton HT-400 pump to produce a consolidated body of soil. A simplified diagram of the injection apparatus appears in Figure 4, and Table 5 specifies the consolidation agent used.

The length of the body of consolidated soil to be produced was limited to 1 m by the size of the well used for the experiment, and after the consolidation work the properties of the consolidated body were examined. The diameter and the strength of the consolidated body were measured as follows:

(a) Diameter: After the consolidation work, the sand in the well was removed and the distance from the center to the edge of the consolidated body was measured.

(b) Strength: After breaking the consolidated body, block samples were taken from three locations within it. Later, three pieces were extracted from them and uniaxial compression tests were performed on the test pieces.

3.0 RESULTS OF EXPERIMENTS AND SUMMARY OF RESULTS

3.1 Exploratory experiment

A sample data sheet, with records of jet arrival times measured by means of vibration sensors, is shown in Figure 5. The length of time from the moment the nozzle was directed at a measuring point to the time the measuring equipment senses the striking of the jet, as read from the data sheet, was considered to be the arrival time of the jet. An example of raw data taken from a data sheet is shown in Figure 6.

The relationships between the arrival time obtained from a data sheet and the rotation rate and number of passes was clarified, and an empirical formula was established by translating these relationships into individual indices because these factors are essentially independent of each other. Calculated arrival times are shown in Figure 7.

3.2 Consolidation experiment

The results of examinations of the consolidated bodies produced in each experiment are shown in Table 6. By substituting the diameter of the consolidated bodies at each level of factors into the empirical formula, figures for cutting speeds were obtained. Fig. 9 shows the relationship between cutting distance and the factors, which were freshly calculated using the empirical formula, applying the averaged value of the cutting speeds as the model ground cutting constant. Also, actual cutting distances are plotted in the figure.

3.3 Summary of results

The results of the experiments can be summarized as follows:

3.3.1 Relationship between rotation rate and cutting distance (see Figure 9)

Cutting distance decreases as rotation rate increases. While vibrations in cutting distance are considerable up to 10 rpm, rotation rates beyond this produce nearly identical cutting distances. Therefore, the range of rotation rates within which cutting is efficient is considered to be from 1.25 to 5 rpm.

3.3.2 Relationship between number of passes and cutting distance (see Figure 10)

Cutting distance gradually increases up to the 10 passes, but, beyond this it stops increasing. Thus, the number of passes for efficient cutting might be from 1 to 10.

3.3.3 Properties of consolidated bodies produced by direct injection of consolidation agent

The following were determined from the results of consolidation experiments:

i) The largest diameter was 3.4 m (rotation speed=2.5 rpm, number of passes=5; see Figure 8).

ii) An improved soil body 2 m in diameter was produced with a withdrawal speed of 2 min/m (rotation speed=5 rpm, number of passes=5, set-up distance=10 cm; see Figure 8).

iii) Consolidation agent was entrained within an area 20 cm wide (rotation speed=1.25 rpm, number of passes=6).

iv) The injection rate (amount of consolidation agent Q/volume of improved soil V correlates with the strength of the improved soil body (see Figure 11).

4.0 REVIEW

On the basis of the results obtained from experiments performed previously, optimum specifications for the main factors of jet pressure and flow rate were determined to be as follows:

Jet pressure: 30 MPa
Jet flow rate: 300 l/min

The experiments described in this report, however, did not lead to precise specifications for rotation rate or number of passes. However, it is proposed that these factors remain within the following ranges:

Rotation rate: 1.25 - 5 rpm
Number of passes: 1 - 10

The reason for the lack of precise recommendations is that there are many problems to be solved before a soil improvement technique able to produce larger volumes is put to practical use. The specifications for the use of such a technique must incorporate solutions to these problems. The main problems to be addressed are the economy of the technique, the uniformity of the quality of the improved soil, and the properties of the soil to be improved. These are the remaining major factors concerning soil cutting by water jet

to be dealt with.

The economy of technique depends on the improved efficiency of work execution, and as this efficiency depends significantly on the time used in withdrawing the nozzle, rotation rate and number of passes must be set with the rate of withdrawal taken into consideration. Withdrawal rate is a function of rotation rate, number of passes, and set-up distance, and this relation can be expressed by the formula below.

$$T_m = \frac{100 \cdot N}{Rn \cdot Pt}$$

Where T_m = withdrawal rate (min/m)
N = Number of passes
Rn = rotation rate (rpm)
Pt = set-up distance (cm)

This means that, at a given increment, the higher the rotation speed and the fewer the number of passes, the shorter the withdrawal time.

The problem regarding the uniformity of the quality of improved soil is how to make its quality more consistent. To solve this, it seems, a moderately high number of passes must be considered necessary.

As for the cutting characteristics of the soil concerned, a soil improvement technique must be applicable both to sandy soils with differing N values and to cohesive soils with grain sizes other than those used in the experiments. In the exploratory experiments, cutting characteristics were investigated only for the occasion of $N \fallingdotseq 5$. In the future, we intend to perform field experiments on a large coverage soil improvement technique in various type of soils and, on the basis of the results, determine better execution specifications for soil improvement work.

Accordingly empirical formulas are not presented in this report because it is expected that they will be subject to a number of corrections and modifications before being finalized.

Unexpected results produced by these experiments were that the cutting distances measured in the exploratory experiments were much smaller than those measured in previous experiments. Also, the diameters of consolidated bodies were smaller by half than expected. The reason for these phenomena seems to be that the turbulence caused by the cutting liquid being forced to change its course of movement 90° at the tip of the nozzle went beyond the limits within which it is negligible, as is the case for the conventional technique, because of the high flow rate and because liquid contained particles.

With regard to the consolidation experiments, it was planned that data filling a matrix of three rotation rates and three numbers of passes without repetition be acquired. Actually, successive

failures and breakdowns of the jet generator necessitated that much time be spent on repairs. One cause of these failures was equipment attrition caused by the very large amount of friction generated by directly injecting the consolidation agent with a high-speed jet. Therefore, antifriction materials must be considered putting a large coverage soil improving technique into practical use.

5.0 AFTERWORD

These experiments on nozzle traverse rate and number of passes were conducted in model ground of N≒5. In the future, we plan to examine the path of liquid within the nozzle and the nozzle material, and clarify the relationships between these factors and cutting distance by field experiments simulating actual working conditions.

REFERENCES

1. Yahiro, T., Yoshida, H. and Nishi, K.,"Construction Technique Easy to Understand, Underground Construction Utilizing Water Jet"

2. "Effect of Pressure and Flow Rate in Soil Excavation by Water Jet," the 5th American Water Jet Conference

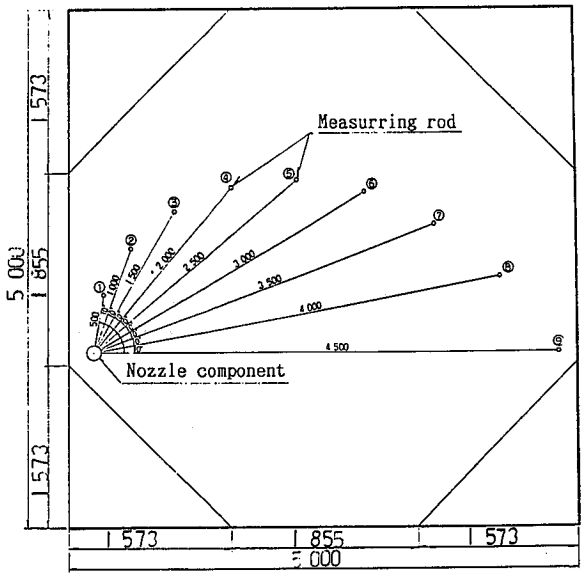

Fig. 1 Plan View of Octagonal Soil Well with Measuring Point

Table 1 Grain Caracteristics of Model Soil

Gravel (2 mm or more)	%	6
Sand (2 mm～74 μm)	%	90
Silt (74～5 μm)	%	4
Clay (5 μm or less)	%	
Maximum grain size	mm	19.1
Uniformity coefficient	U	2.4
Coefficient of curvature	U_c	1.0
Specific gravity of soil particle	G_s	2.3

Table 2 Soil Properties after Compaction by Watering

Natural moisture content		%	22.6
Compaction characteristic	Optimum moisture content	%	23.1
	Maximum dry density	t/m³	1.43
N-value, S P T blow count			3～6

Table 3 Combination of Variable in Exploratory Experiment

		Rotation rate(rpm)								
		1.25	2.5	5	10	20	40	80	160	320
Number of passes	1～20	○	○	◎	○	○	○	○	○	○

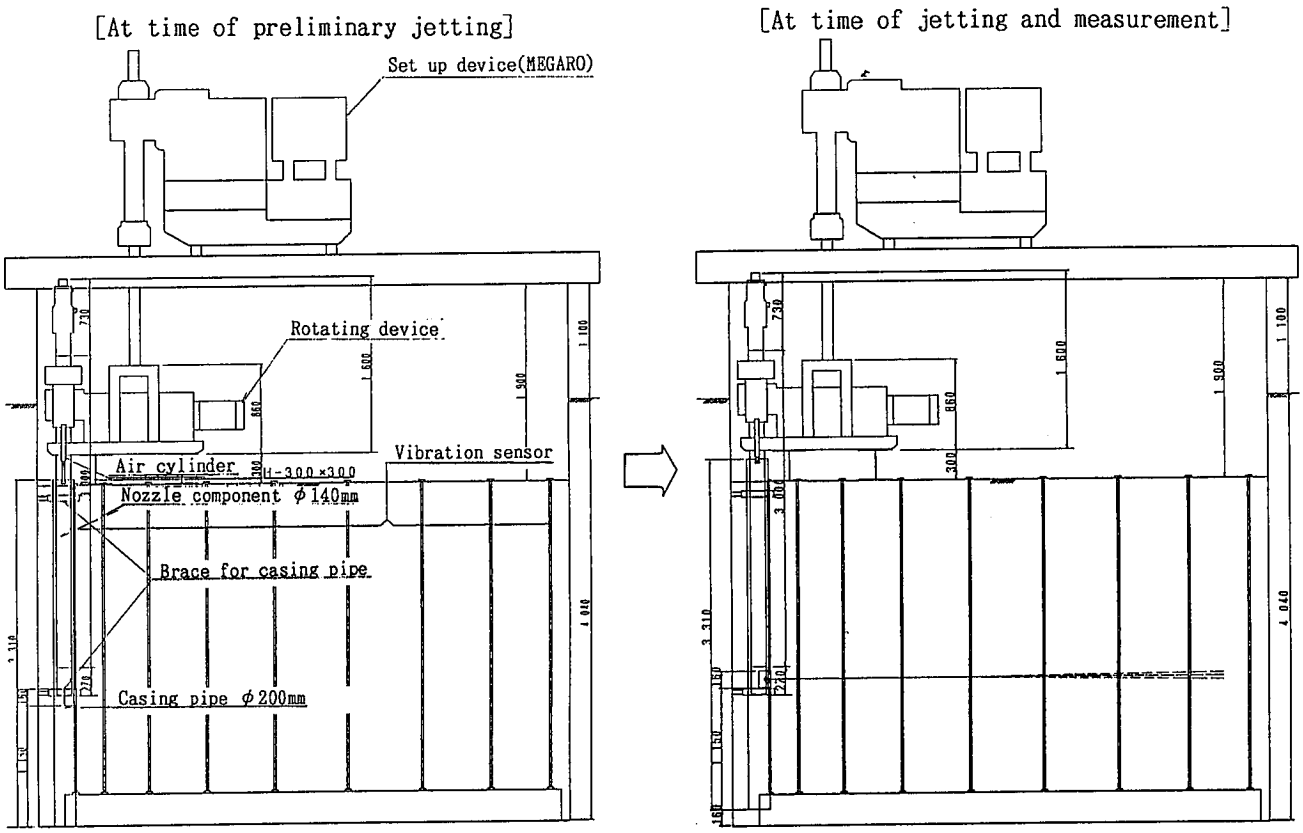

Fig. 2 Jetting Apparatus

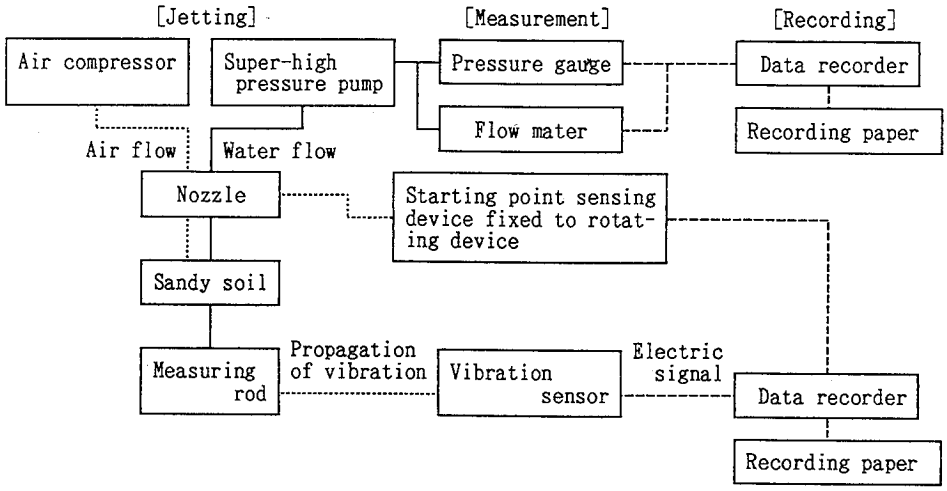

Fig. 3 Measurement Flow Chart

Table 4 Combination of Variable in Consolidation Experiments

Set up distance (cm)		5			10
Rotation rate (rpm)		1.25	2.5	5	
Pass number	1	—	③	④	⑦
	5	⑥	②	—	—
	10	—	—	①	—

Notes:
1) Circled number in the table represent exeriment numbers.
2) No.5 level ground experiment (Rs=1.25 rpm, N=6) and No.8 experiment (conventional C-JG technique) were also performed.

Table 5 Consolidation Agent

Cement	760 kg/m³
Dispersant	9 kg/m³
Water	760 kg/m³

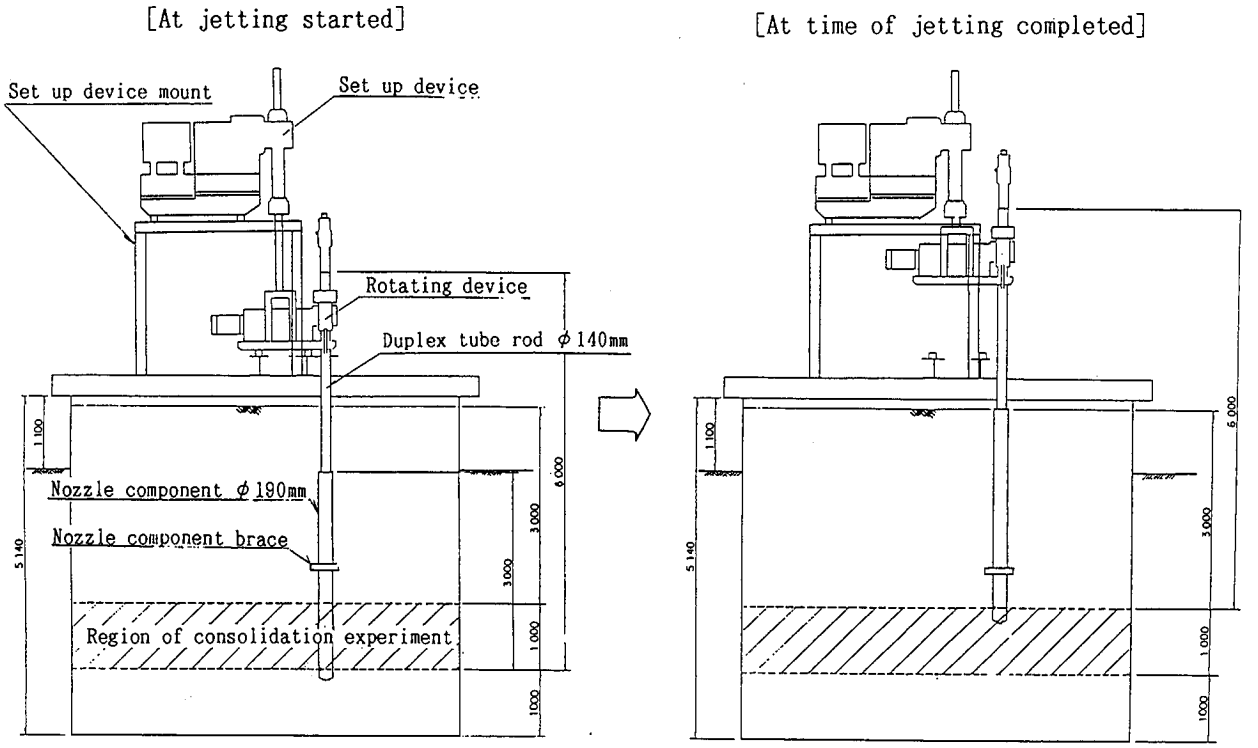

Fig. 4 Simplified Diagram of Jetting Apparatus for Consolidation Experiment

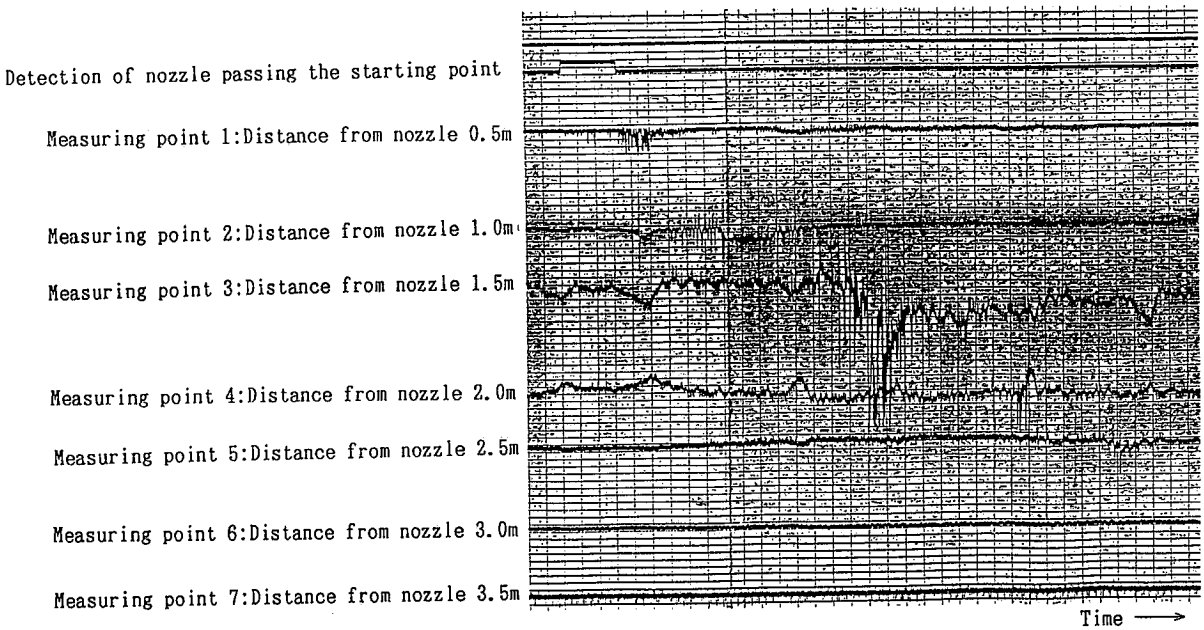

Fig. 5 Sample Data Sheet with Records of Arrival Time

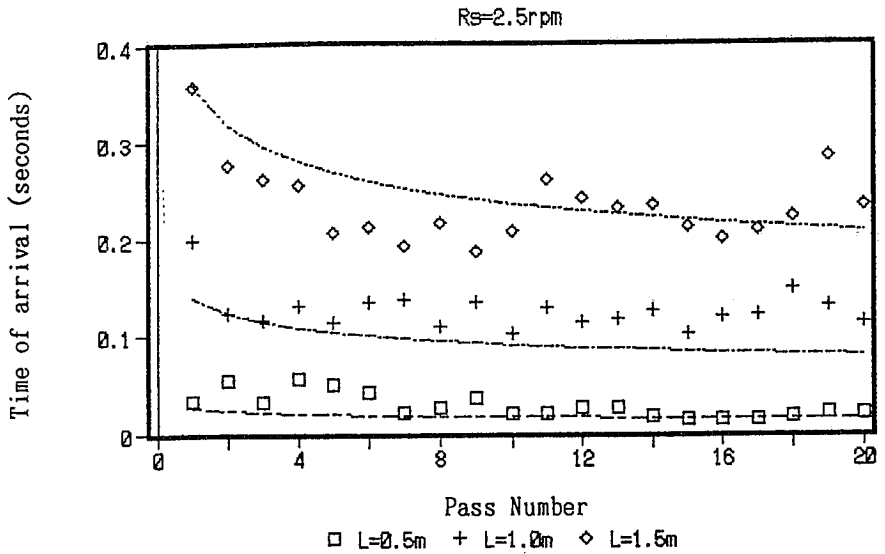

Fig. 6 Example of Raw Data

Table 6 Results of Consolidated Body Examinations

Set up distance (cm)		5			10
Rotation rate (rpm)		1.25	2.5	5	
Number of passes	Diametet	—	2.30m	2.18m	2.44m
	Strength		14.4MPa	16.0MPa	13.9MPa
	Diametet	3.16m	3.38m	—	—
	Strength	30.1MPa	17.8MPa		
	Diametet	—	—	2.76m	—
	Strength			21.9MPa	

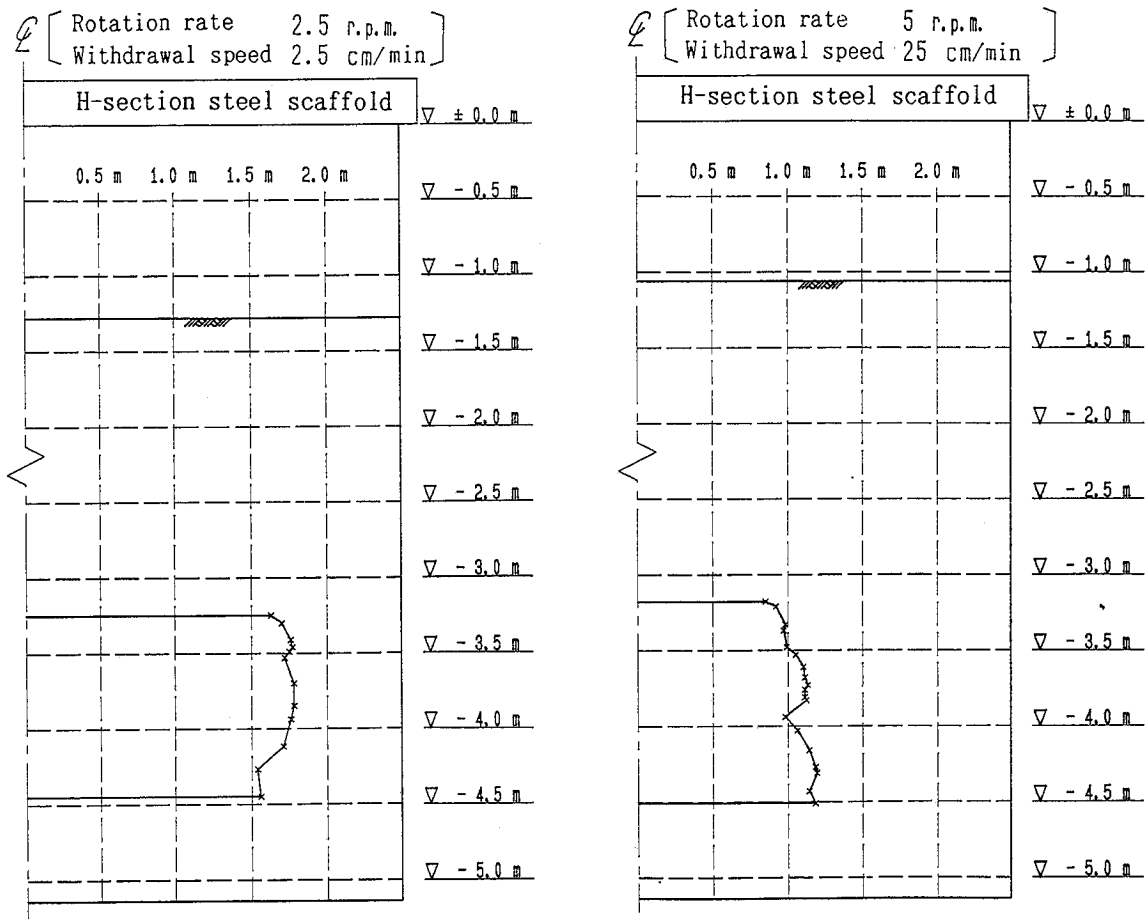

Fig. 8 Examples of Consolidated Body Cross-Section

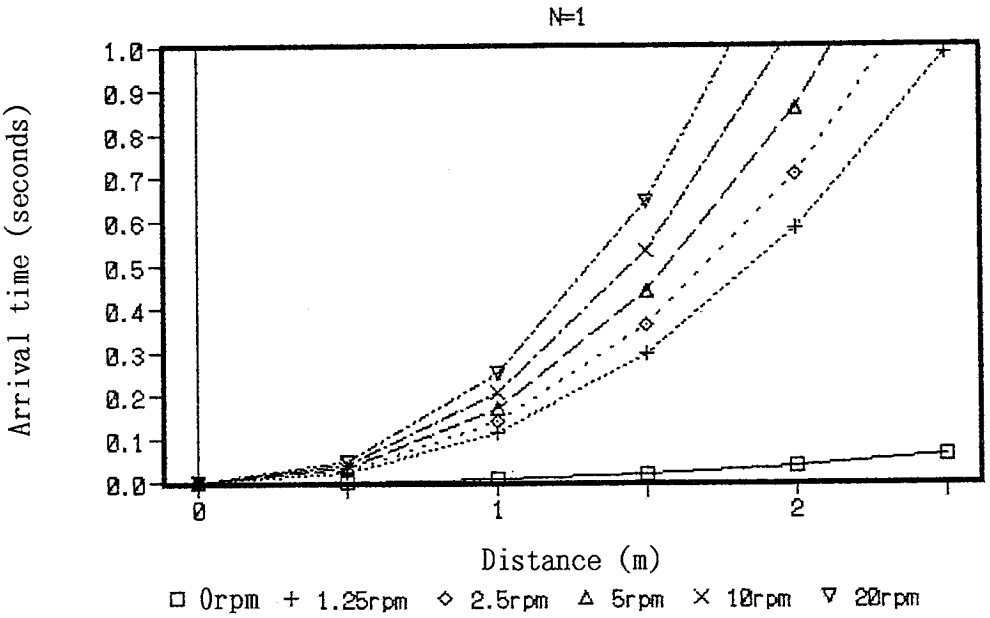

Fig. 7 Calculated Arrival Times

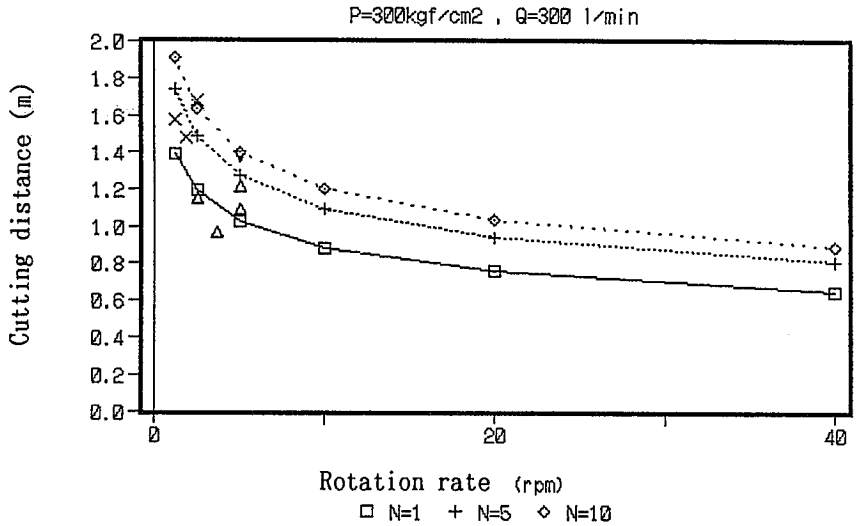

Fig. 9 Relationship between Cutting Distance and Nozzle Traverse Rate

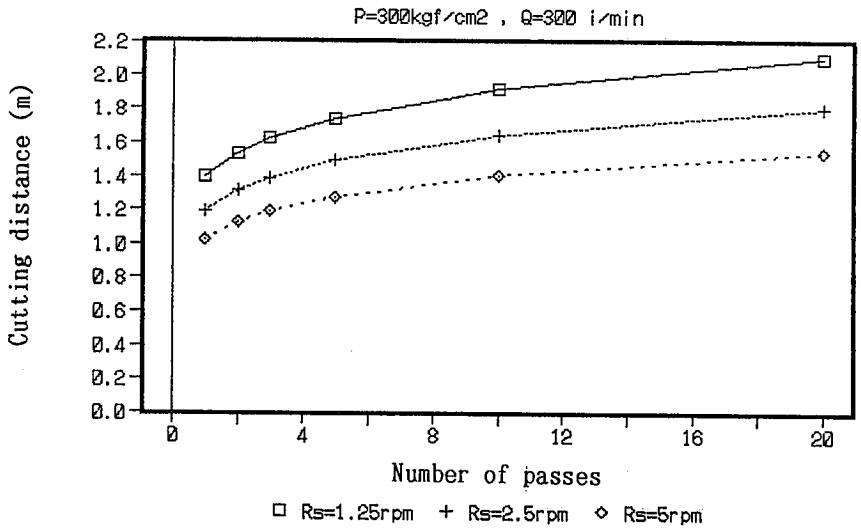

Fig.10 Relationship between Cutting Distance and Number of Passes

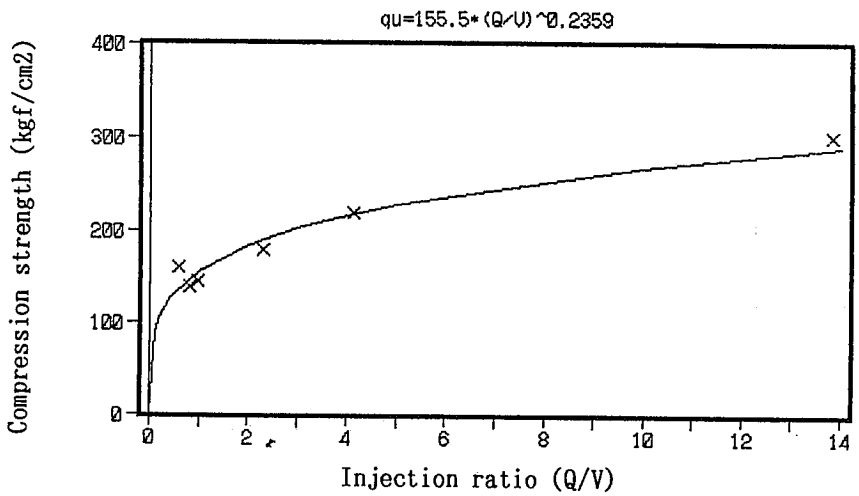

Fig.11 Relationship between Consolidation Agent Injection Ratio and Strength of Improved Body

6th American Water Jet Conference
August 24 - 27, 1991: Houston, Texas

Paper 29

ONE OF THE WORLD'S BIGGEST HYDRO-ABRASIVE CUTTERS

Michel Pilon
Aquacoupe Technologie Inc.
Ste-Therese, Quebec, Canada

ABSTRACT

General Electric of Canada, located in Montreal, operates a reconditioning department for locomotives. One of the tasks of the department involves stripping the locomotive's bodywork off of its chassis. The operation is very hazardous because of the infiltration of diesel oil in the body of old locomotives.

In collaboration with Aquacoupe Technologie, General Electric has developed a 5 axis hydro-abrasive cutter to enable the separation of the bodywork while eliminating any possibility of fire.

Organized and Sponsored by the Water Jet Technology Association.

6th American Water Jet Conference
August 24 - 27, 1991: Houston, Texas

Paper 30

WATER JET CUTTING OF CONCRETE

A. W. Momber

Leipzig University of Technology, Germany

ABSTRACT

Pressure water jetting plays an important role as a tool for concrete sanitation, concrete decontamination and cutting and trenching of concrete. The present paper attempts to mediate principles of application of unmodified pressure jets. In detail the effect of some selected process parameters (pressure, nozzle diameter, standoff distance, traverse rate, multipass cutting) is elaborated. The result is that for all process parameters optimum and critical values exist.

Organized and Sponsored by the Water Jet Technology Association.

1.0 INTRODUCTION

High-speed water jet techniques are universally used for concrete processing. The field of application ranges from cleaning and roughening to cutting the material (Fig. 1).
For optimizing these processes it is necessary to know the relations between jet and process parameters and target parameters. Traditionally the cut depth h is used to estimate the efficiency of water jet processing.
The aim of the present paper is to contribute to the completion of the concept of material- and problem-determined parameter variation.

The relevant variation parameters can be subdivided into two groups (Fig. 2).

The first group includes parameters which are connected with the jet generation (determined by the tool used):

- jet pressure (p),
- nozzle diameter (d),
- nozzle design.

The second group includes parameters which are connected with the cutting process (process oriented):

- standoff distance (x),
- traverse rate (u) and loading time (t), respectively,
- pass width (s),
- angle of attack (φ),
- number of passes (n).

2.0 EFFECT OF WATER JET PRESSURE

The effect of the jet pressure on the cutting process is shown in Fig. 3. From measurements carried out by several authors (Hamada, Puchala, Reichman, Werner) a linear progress of function can be deduced.

$$h(p) = C_1 * (p - p_C) \qquad p \geq p_C \qquad (1)$$

$$C_1 = dh / dp ,$$

where p_c is a critical (threshold) pressure describing a critical jet velocity.
The comparison between this value and primary material properties is yet vague. But it seems sure that there is no connection with the compressive strength of concrete (Fig.4).
With regard to the permeability and brittleness of concrete two conceptions can be applied (Rehbinder, Wiedemeier).
According to Wiedemeier the threshold pressure of brittle materials is a function of its fracture toughness. It is possible to treat concrete as a brittle material. One of the main conditions of crack-determined failure processes - the existence of microcracks - is given in every concrete structure (approximately 1 - 10 cracks / cm^2).
Rehbinder's erosion conception about the destruction of materials due to water jets is based on the permeability. Cement matrix as well as concrete are permeable owing to a continuous capillary pore system. Consequently, the threshold pressure may be a function of cohesion forces between different parts of the concrete structure. One of the possibilities to handle this problem is shown in Fig. 5. But one can also understand that erosion takes place primarily in the zone between cement matrix and aggregates, which is is characterized by a high porosity.

The threshold problem may be interpreted as follow:
The threshold values are most probably functions of the traverse rate (Momber/1989a).

- At low traverse rates an "erosion" threshold pressure (p_e) exists, which is a function of the erosion resistance (cohesion forces F) of the cement matrix only ($p_e \sim F$);

- At high traverse rates a "fracture" threshold pressure (p_f) can be noticed. It is a function of the fracture toughness of the concrete ($p_f \sim K_{Ic}$).

Probably a third "aggregate" threshold pressure p_a can be defined, which is a function of aggregate properties.

Using equation (1) and $E = K * p^{1.5}$, the optimum working pressure p_O is:

$$p_O = 3 * p_C \qquad (2)$$

3.0 EFFECT OF NOZZLE DIAMETER

Contrary to abrasive water jets in plain water jet cutting the nozzle diameter does not influence the velocity of the jet mainly.

The tendency shown in Fig. 6a strongly (Hamada, Momber/1989, Puchala, Reichman, Werner, Yoshida) can be described by equation (3).

$$h(d) = C_2 * d \qquad (3)$$

$$C_2 = dh / dd$$

If one expands function (3) linearly, e.g., according to Yoshida, a critical nozzle diameter d_C can be obtained, which represents a critical volume stream and thus a critical jet energy (Fig. 6b). Medeot defines such a critical jet energy as the prerequisite for the destruction of concrete. He obtaines this energy from the strain-stress curve. Indeed, from Hassan it is well known, that it is not only the loading intensity that determines the threshold pressure of a material but also the loading regime. Using droplet jets or non-stationary jets it is possible to reduce the threshold pressures of given materials in comparison with continuous jets at the same energetical level. A comparative calculation of some results obtained by Hamada is in contradiction with the energetical "threshold" conception too.
According to Rehbinder a critical fluid stream and thus a critical nozzle diameter d_C must exist so that erosion can occur. This critical value depends on the permeability of the material and can be described by equation (4).

$$d_C >> \frac{2 * k * \sqrt{p / \rho}}{\vartheta} \qquad (4)$$

This leads to a second critical diameter (d_m) beyond which no increase in cut depth occurs. It is possible that part of the water stream radially crosses the concrete surface and does not penetrate into the pore structure. Labus and Schmid estimated such a decrease in rise of the diameter-cut depth curve (Fig. 6b).

Another way to enlarge the range of function (3) is to breake it. So it is possible to lead it to the zero point (Fig. 6c). Probably the reason for such a breaking is a critical ratio R of the jet diameter to a mean aggregate grain diameter d_A.

$$R = d / d_A \qquad (5)$$

4.0 EFFECT OF STANDOFF DISTANCE

Fig. 7 shows the tendency of the results obtained by several authors (Hamada, Labus, Momber/1989, Reichman, Werner). It is possible to discern two types of curves; but both types follow equation (6).

$$h(x) = C_3 * x^{C_4} * \exp(C_5 * x) \; ; \; C_5 < 0 \qquad (6)$$

It is evident that the actual shape of the curve depends on the pressure range. For relatively low pressures ($p \approx p_C$)

$$0 < C_4 < 1,$$

whereas high pressures ($p >> p_C$) lead to

$$C_4 < 0$$

Consequently, equation (7) can be formulated.

$$C_4 = f(p/p_C) \; , \qquad (7)$$

i.e., a low loading intensity can be partly compensated by a loading regime adapted. At low pressures the dynamic component of loading plays an important role for brittle materials which will be confined with rising pressure. This fact is in contrast with the idea of a critical destruction energy.
According to Werner the actual shape of the h(x)-curve is a function of the nozzle diameter.

It is interesting to note that Hashish's theory, based on the Bingham behaviour of materials, leads to similar results (Hashish/1978).

5.0 EFFECT OF TRAVERSE RATE

Fig.8 shows that an increase of the traverse rate generally reduces the depth of cut (Hamada, Labus, Norsworthy, Puchala, Werner, Yoshida). To describe this relation equation (8) can be used (Hashish/1978).

$$h(u) = h_0 * \{ 1 - \exp[-C_6 / (u-u_C)] \} \qquad (8)$$

$$u \geq u_C \; ,$$

where u_c is the traverse rate below which no increase in depth of cut occurs; h_0 is the maximum possible depth of cut achieved if $u = u_c$. The reasons are losses of jet energy due to damping (cut bottom) and friction (cut wall).
A second critical traverse rate u_m which is theoretically derived from Hashish and Rehbinder was not found experimentally. If this critial rate is exceeded, the jet is not able to destroy the material (see Table 1).
But such a critical value results from an analogical analysis of loading time. Fig. 8 shows a critical incubation time t_c below which no cutting occurs. This incubation phase contains the jet impact and the related compressive waves which are necessary to produce a sufficient number of microcracks and to cause part of the existing microcracks to propagate.

6.0 EFFECT OF NUMBER OF PASSES

The effect of multipass concrete cutting has first been investigated by Norsworthy and Olsen. Further results can be found in Labus, Reichman and Yoshida . Multipass cutting reduces damping and friction effects. During the first pass the pores in the cement gel matrix will be filled with water; so the following "erosive" attacks can be harder.
From Fig. 9 one can deduce a critical number of passes n_c for which the rate of increase in cut depth is inefficient. At a certain value of cut depth energy losses due to damping exceed the losses due to friction. This critical depth is the limit for an effective fast multipass cutting process.
An optimal number of cutting passes can be graphically determined by a method of Hashish.

The optimization procedure of multipass cutting is comparable to the optimisation of discontinuous jet cutting. The following statements can be made:

- number of passes (n) $\hat{=}$ frequency of jet pulses (f),
- traverse rate (u) $\hat{=}$ length of a single pulse (l).

7.0 EFFECT OF PASS WIDTH

One possibility of producing very deep cuts in concrete is the use of a multijet cutting system (Reichman). An example is shown in Fig. 10. The distance between the centres of the nozzles can be defined as pass width s. This parameter influences the energy consumption of the cutting tool.
Fig. 10 shows that there is an optimal value s_0 . Table 2 shows some values depending on the jet diameter.

8.0 EFFECT OF ANGLE OF ATTACK

The angle of impingement influences the mechanism of loading. Fig. 11 shows tendencies of angle variation during concrete cutting (Momber/1989b).
A clear peak at an angle of 45 degrees can be seen. Probably, this relation is valid only for low pressure ranges (Momber). In this case a horizontal component of the jet force is necessary to wash out and remove the aggregate grains nondestroyed. The influence of the cutting process due to angle variation rises with the diameter of the jet nozzles (Werner).

9.0 CONCLUSIONS

The trends of the effect of the jet cutting parameters investigated on the depth of cut obtained in concrete can be summarized as follows:

parameter	trends of cut depth data
pressure	- approximately linear for high traverse rates - minimum critical pressure exists
nozzle diameter	- initially linear - minimum critical diameters exist probably - optimum diameters exist probably
standoff distance	- optimum standoff distances exist at low pressures and small nozzle diameters - large standoff distances generally reduce depth of cut at high pressures
traverse rate	- complex function - minimum critical rates exist - maximum critical rates exist probably
number of passes	- sometimes multipass cutting is more efficient than single pass cutting
pass width	- optimum pass widths exist
angle of attack	- optimum values as functions of the pressure rates exist

All tendencies can be better interpreted if one succeeds in describing the destruction process and the behaviour of concrete under water jet loading more exactly.
Further contributions to this subject can be found in publications of the Leipzig University (Momber).

REFERENCES

1. Hamada, H., Fukuda, T., Sijoh, A., Basic study of concrete cutting by high pressure continuous water jets, 2nd International Symposium on Jet Cutting Technology (ISJCT), Paper G 2, Cambridge, 1974
2. Hashish, M., du Plessis, M., The application of a generalized jet cutting equation, 4th ISJCT, Paper F 1, Canterbury 1978
3. Hashish, M., Reichman, J., Analysis of water jet cutting at high traverse rates, 5th ISJCT, Paper B 2, Hannover 1980
4. Hassan, A., Beitrag zur technischen Anwendung von Hochgeschwindigkeitsstrahlen unter Wasser, Dissertation, Universität Hannover, 1978
5. Labus, T., Hilaris, J., Highway maintenance application of jet cutting technology, 4th ISJCT, Paper G 1, Canterbury, 1978
6. Medeot, R., History, theory and practice of hydrodemolition, 5th American Water Jet Conference (AWJC), Paper 10, Toronto, 1989
7. Momber (Bauda), A., Untersuchungen zur Anwendung des HDW-Verfahrens zur Bearbeitung von Beton, Dissertation, TH Leipzig, 1989
8. Momber, A., The processing of artificial rocks with water jets, Conference Mining Geomechanics '89, Hradec n.M., 1989a, proceedings, p 409
9. Momber, A., Belastungsarten und Widerstandskennwerte bei der Bearbeitung von Beton mit Hochruckwasserstrahlen, betontechnik, Nr. 2, 1990, Berlin, S. 56
10. Momber, A., Werner, M., Betonabtrag mit Hochruckwasserstrahlen, erscheint in: betontechnik 1991
11. Norsworthy, A., Mohaupt, U., Burns, D., Concrete cutting with water jets at pressures up to 485 MPa, 2nd ISJCT, Paper G 3, Cambridge, 1974
12. Olsen, J., Jet slotting of concrete, 2nd ISJCT, Paper G 1 Cambridge, 1974
13. Puchala, R., Lechem, A., Hawrylewicz, B., Mass concrete removal by high pressure water jet, 8th ISJCT, Paper 22, Durham, 1988
14. Rehbinder, G., The drag force on the grains in a permeable medium subjected to a water jet, Journal of Applied Mathematics and Physics, Vol. 28, 1977, p 1005
15. Rehbinder, G., A theory about cutting rock with a water jet, Rock Mechanics, Vol. 12, 1978, p 247
16. Reichman, J., Kirby, M., The development of a water jet cutting system for trenching in concrete. 5th ISJCT, Paper D1, Hannover, 1980
17. Schmid, R., High pressure hydro milling of concrete surfaces, 5th AWJC, Paper 15, Toronto, 1989
18. Werner, M., Untersuchungen strahlseitiger und materialspezifischer Einflußgrößen bei der Untergrundvorbehandlung von Beton mit Hochdruckwasserstrahlen, Intern. Kolloquium Industriefußböden '91, Esslingen, 1991, proceedings, p 439

19. Wiedemeier, J., Flüssigkeitsstrahlen hoher Relativgeschwindigkeit und Bruchkinetik spröder Wrekstoffe, Dissertation, Univ. Hannover, 1981
20. Yoshida, H., Nishi, K., Isobe, T., Concrete cutting using rotating water jets, 5th AWJC, Paper 12, Toronto 1989

NOMENCLATURE

Ci	-	Constants
d	-	Jet nozzle diameter (mm)
da	-	Aggregate grain diameter (mm)
dc	-	Critical nozzle diameter (mm)
dm	-	Critical nozzle diameter (mm)
E	-	Jet energy (Nm)
F	-	Cohesion force (N)
f	-	Jet pulse frequency (Hz)
h	-	Cut depth (mm)
ho	-	maximum cut depth (mm)
K	-	Constant
k	-	Permeability (m*m)
KIc	-	Critical stress intensity factor (MPa*mm$^{1/2}$)
l	-	Pulse length (s)
n	-	Number of passes
nc	-	Critical number of passes
p	-	Jet pressure (Pa)
pc	-	Threshold pressure (Pa)
pe	-	Erosion threshold pressure (Pa)
pf	-	Fracture threshold pressure (Pa)
po	-	Optimum jet pressure (Pa)
R	-	Ratio d/da
s	-	Pass width (mm)
so	-	Optimum pass width (mm)
t	-	Loading time (s)
tc	-	Incubation time (s)
u	-	Traverse rate (m/s)
uc	-	Critical traverse rate (m/s)
um	-	Critical traverse rate (m/s)
x	-	Standoff distance (mm)
φ	-	Angle of attack (degree)
ρ	-	Density of jet fluid (kg/m)
ν	-	Dynamic viscosity of jet fluid (Pa*s)

Material	Critical maximum traverse rate
	cm/s
Coal	477
Concrete	37
Wilkenson Sandstone	31,4
Limestone	101

Table 1 Approximate values of critical maximum traverse rate for different materials (Hashish/1978)

so / d	Author
7	Norsworthy
10,7	Momber (1989)
10,8	Hamada

Table 2 Relationship between nozzle diameter and optimum distance between parallel cuts (Momber/1989)

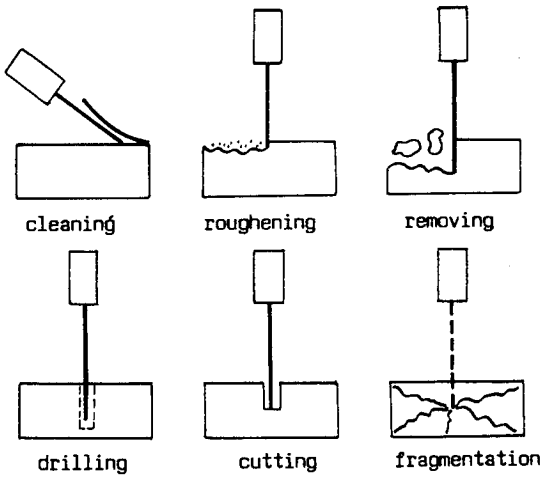

Fig. 1 Cases of Application of Water Jets for Concrete Processing

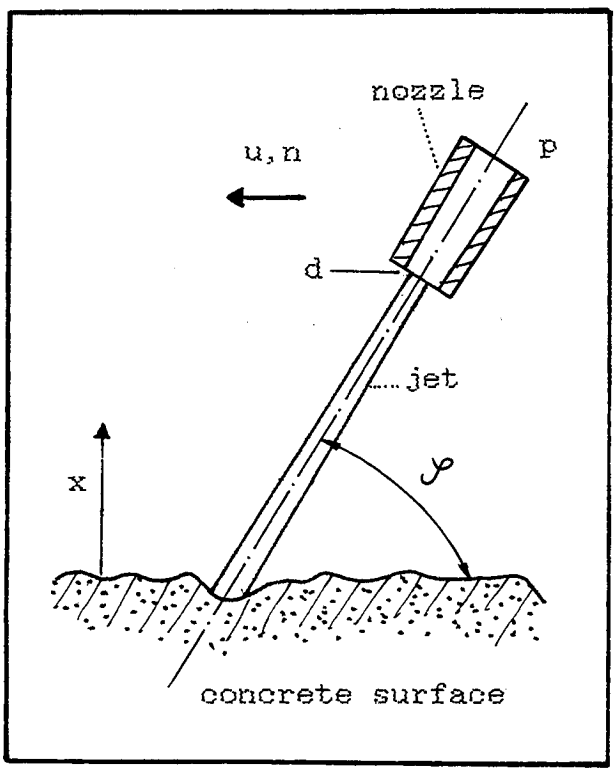

Fig. 2 Parameters Influencing Cutting Performance

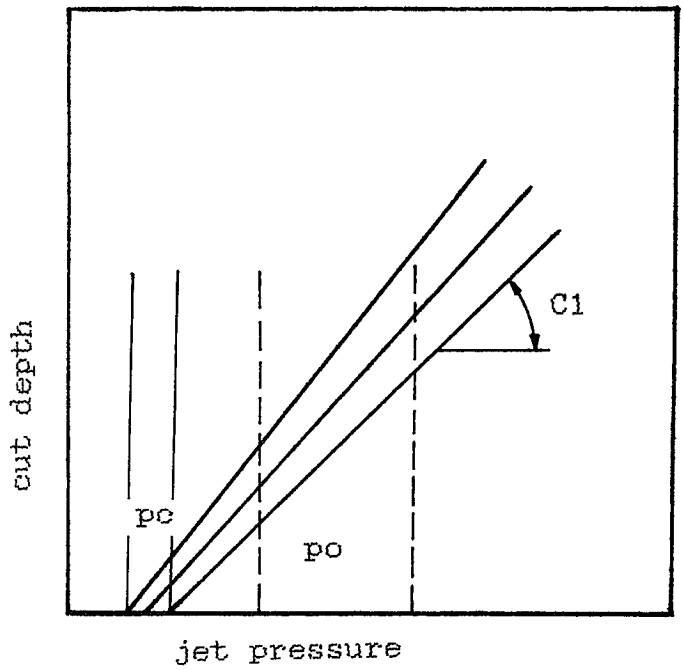

Fig. 3 Pressure Effect on Cut Depth in Concrete

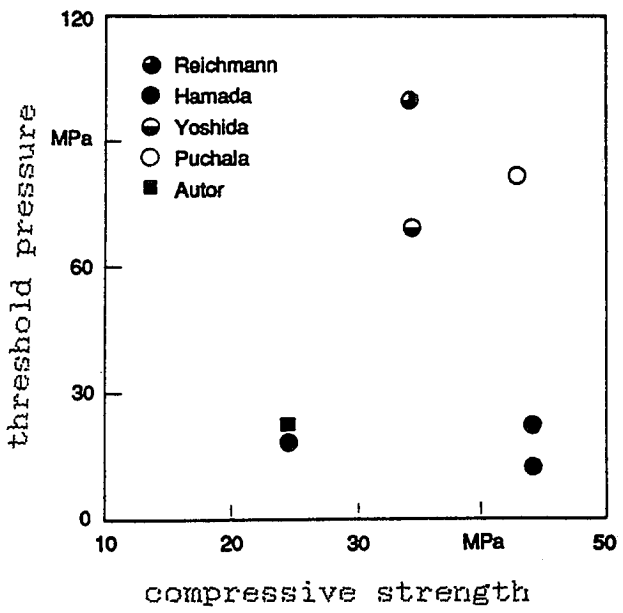

Fig. 4 Connection between Compressive Strength and Threshold Pressure of Concrete

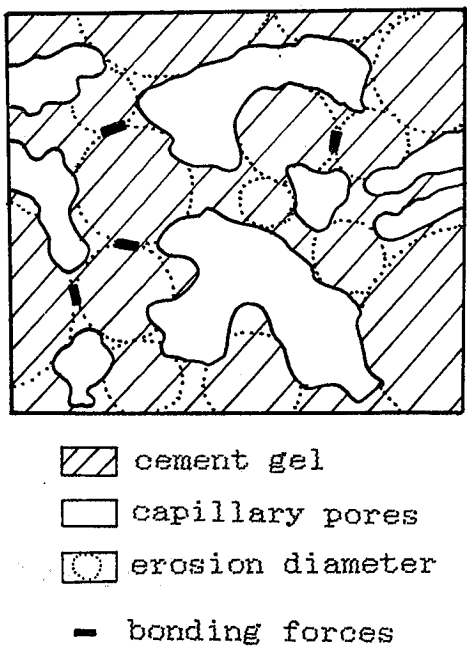

Fig. 5 Erosion Modell for Concrete

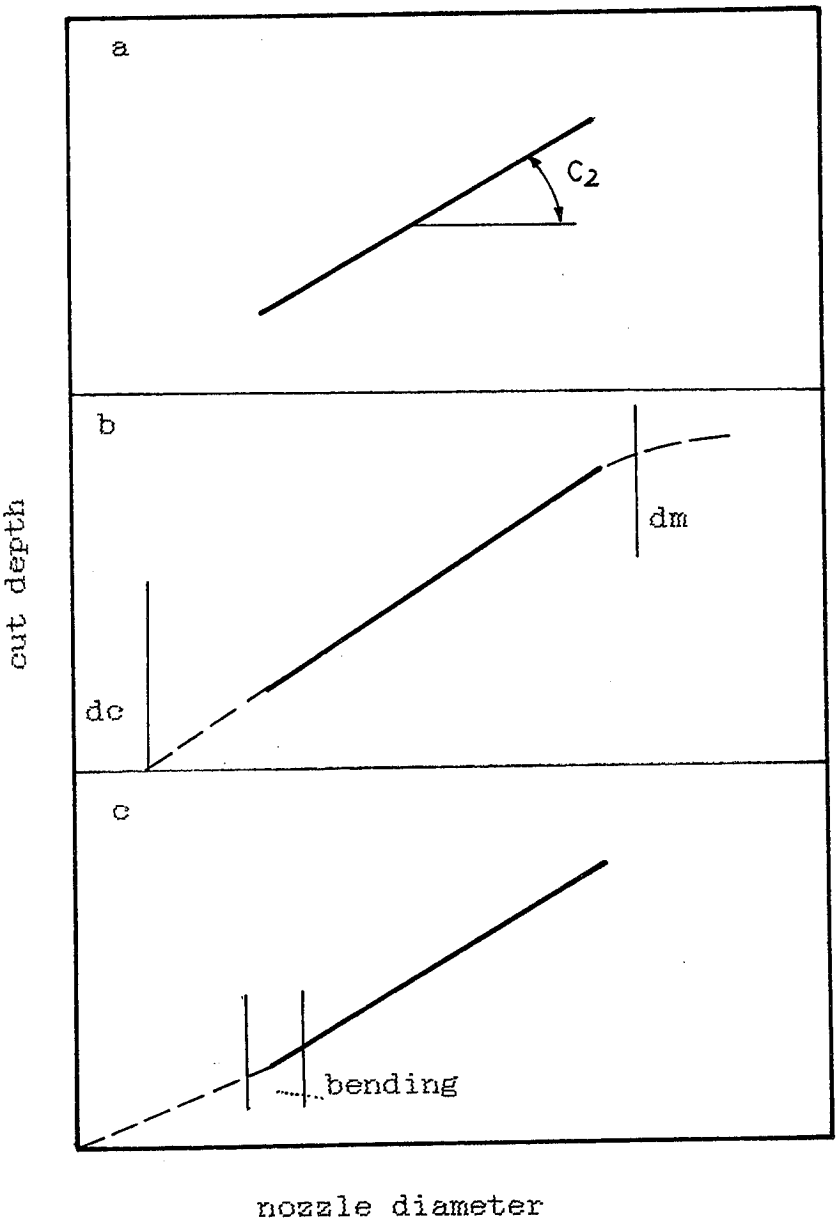

Fig. 6 Nozzle Diameter Effect on Cut Depth in Concrete

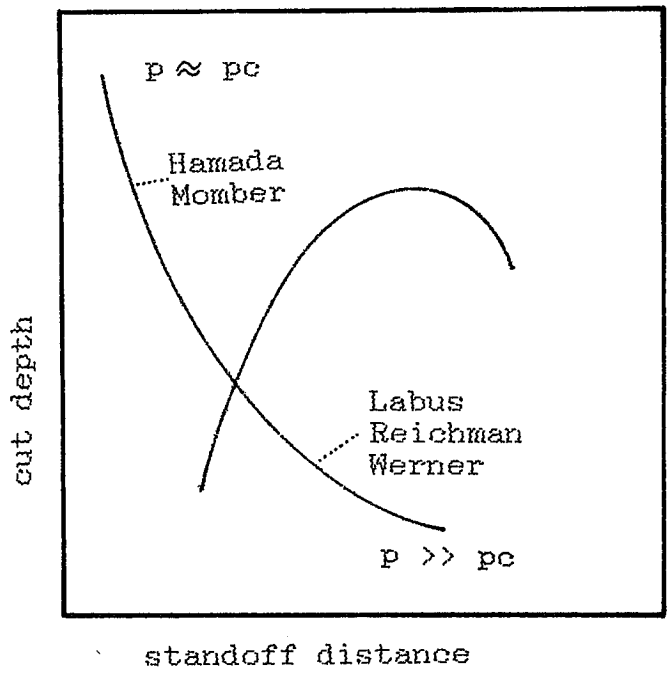

Fig. 7 Standoff Distance Effect on Cut Depth in Concrete

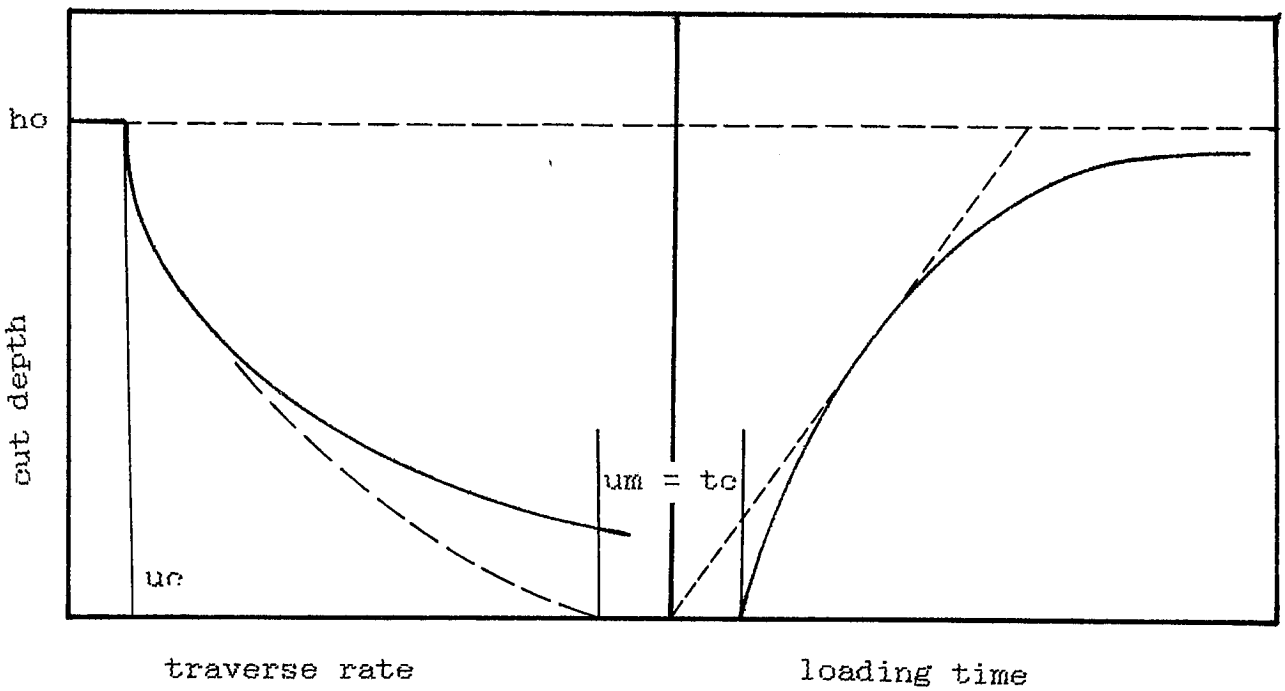

Fig. 8 Traverse Rate Effect on Cut Depth in Concrete

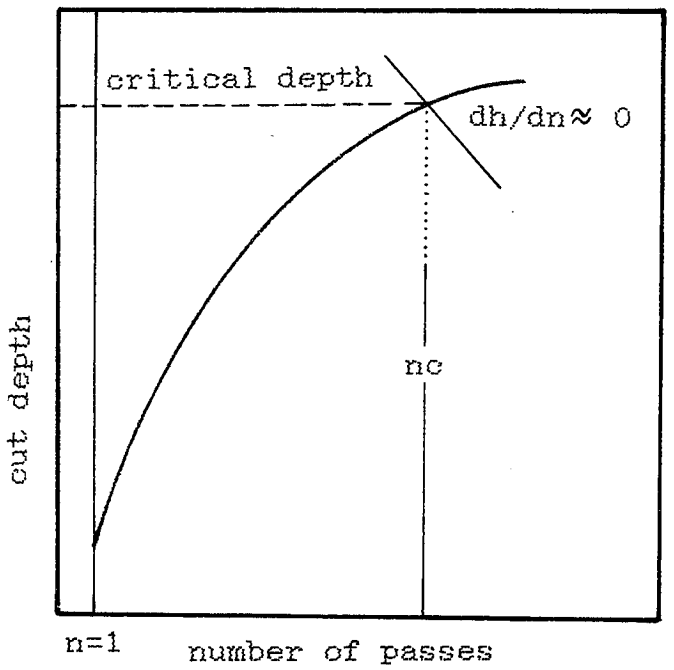

Fig. 9 Multipass Cutting Effect on Concrete

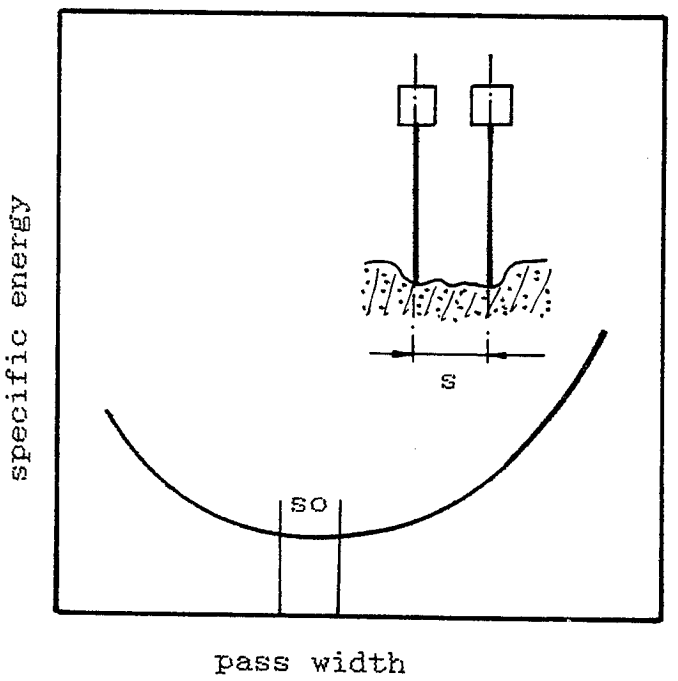

Fig. 10 Pass Width Effect on Specific Energy During Deep Concrete Cutting

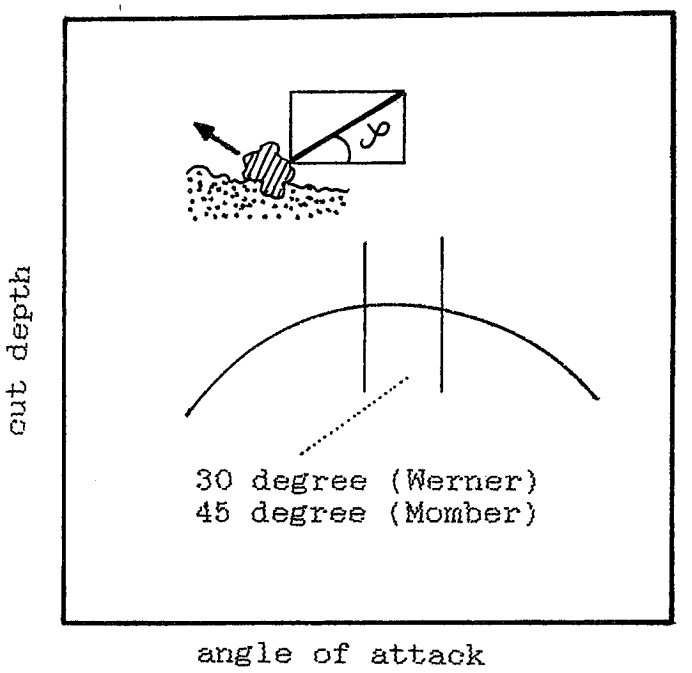

Fig. 11 Angle of Attack Effect on Cut Depth in Concrete

6th American Water Jet Conference
August 24 - 27, 1991: Houston, Texas Paper 31

Computational Fluid Dynamics Analysis of Submerged Cavitating Water Jets

M.K.Y. Lai, M.M. Vijay and C. Zou*
Combustion and Fluids Engineering Laboratory
Institute of Mechanical Engineering
National Research Council of Canada
Ottawa, Ontario, Canada, K1A 0R6

* Visiting Scholar, China University of Mining & Technology
Xuzhou, Jiangsu, China (P.R.C)

ABSTRACT

A Computational Fluid Dynamics (CFD) analysis for the prediction of turbulent, submerged water jets, produced by three different types of nozzles is presented. The analysis is based on the numerical solution of the conservation equations of continuity, momentum, and the standard k-ϵ turbulence model. The ability of the analysis to predict the flow characteristics (velocity, pressure, and turbulence kinetic energy) within the nozzles and the free unconfined region immediately downstream of the nozzle exit is demonstrated. An attempt is made to compare the results predicted from the analysis with the characteristics of the jets observed in the flow visualization tests.

Organized and Sponsored by the Water Jet Technology Association.

1.0 INTRODUCTION

There has been a great deal of interest in exploiting the destructive power of cavitation bubbles to enhance the cutting or fragmentation ability of high speed plain water jets (refer to the references listed in the publications by Puchala, 1984 and Vijay, 1990). Although natural cavitating jets have the potential of enhancing the cutting ability of plain water jets, their effectiveness as shown in Fig. 1, appears to be limited to very short standoff distances. The term 'natural cavitation' is used here to imply the absence of external excitement of the jet (Shimizu, 1986). Furthermore, while cavitation is desired in the jet, it is crucial to avoid the collapse of the bubbles within the nozzle, or else as shown in Fig. 2, the ensuing erosion of the nozzle walls, within a short period of time, will completely destroy the quality of the jet and hence its cutting ability. In order to encourage wide spread practical applications akin, for example, to abrasive-entrained water jets, it is very important to eliminate such drawbacks. These considerations require a thorough understanding of the characteristics of the flow both inside and outside of the nozzles. However, a cursory study of the literature (Arndt, 1981; Chahine, 1984; Duncan, 1989; Knapp, 1970; Lesser, 1987; Plesset, 1977; Shimizu, 1986, 1988, Vijay, 1990 and Webster 1963) shows that cavitation is a highly complex phenomenon and is not readily amenable to theoretical treatment.

The process of cavitation involves the initiation, growth, transport and collapse of vapor bubbles (not air) on the target material. The complexity of the problem can be appreciated by the fact that the flows in the most general case involve multi-phases, high intensity turbulence, and high speed flows in small passages. Such problems can best be addressed through Computational Fluid Dynamics (CFD) analysis because comprehensive empirical correlations of experimental data will be difficult, costly and time-consuming. The CFD analysis of the flow will quickly assist in interpreting the experimental results obtained with the existing nozzles or provide guidelines for improving their performance.

The study reported in this paper addresses the CFD analysis of the complex flows through nozzle passages as well as the free unconfined region immediately downstream of the nozzle exit plane. Submerged pure water jets produced by three different types of nozzle configurations are examined. The predicted distributions of velocity, turbulence kinetic energy and local cavitation number are presented. An attempt is made to explain the main features of the photographic observations of the jets (Vijay,1990) from these predictions. As pointed out above, the process of cavitation encompasses the growth and collapse of the bubbles. This paper is not concerned with the collapse mechanisms (see Duncan, 1989 and Lesser, 1987). Moreover, the CFD approach presented here is quite different from that of Chahine (1984) and Shimizu (1986 and 1988) as these authors did not include turbulence parameters in their numerical studies.

2.0 STATEMENT OF THE PROBLEM

The nozzles considered for the CFD study are shown in Fig. 3 and their specifications are listed in Table 1. These nozzles were chosen because ample visualization and erosion results were available (Vijay, 1990) for possible comparison with the CFD predictions. Nozzle #1 is a simple conical entry nozzle. Nozzle #2 incorporated a centre-body insert and was designed by assuming that the insert would not only enhance cavitation activity, but also produce cavitation bubbles confined within the central area of the jet due to separation of the flow within the nozzle. Nozzle #3 consisted of a cylindrical pin located in the parallel section of the conical entry nozzle. The pin is a blunt body and, therefore, should trigger cavitation due to the low pressure

in its wake. In the CFD analysis, the pin in the transverse direction was modeled as a cylindrical pin in the axial direction (Fig. 4.), with an effective diameter equal to $\sqrt{(4DD''/\pi)}$. Although this configuration is not geometrically similar to the former, the approximation was worthwhile from the standpoint of simplicity in the grid generation for the CFD analysis.

The operating conditions considered were: ambient pressure, P_a = 0.1 MPa and the mass flow rate of water, m = 0.6 kg/s. At these operating conditions, all the three nozzles have approximately equal global cavitation numbers [defined in Eq. (9) with $P = P_a$].

3.0 CFD ANALYSIS

Of the available CFD analyses, an ensemble-averaged Navier-Stokes approach was selected for the present study. The computer code, termed here as WATERJET, is a version of the NRC TURCOM code (Lai, 1987) developed for three-dimensional, viscous fluid dynamics applications. Its methodology is derived from the well-known TEACH-2E code of Gosman (1976). WATERJET is based on the numerical solution of the governing equations of mass and momentum in a cylindrical coordinate system. The k-ϵ turbulence submodel (Launder, 1974) is employed to calculate parameters of the turbulent field, from which the Reynolds stresses are extracted. The current version of the WATERJET code is only set up to solve single-phase flow problems. In other words, the occurrence of cavitation can only be inferred from the velocity and pressure fields obtained from the model.

3.1 Governing Equations

The complete set of ensemble-averaged conservation equations of mass and momentum is expressed, in vector notation, as:

$$\nabla\cdot(\rho\underset{\sim}{U}) = 0 \tag{1}$$

$$\nabla\cdot(\rho\underset{\sim}{U}\underset{\sim}{U} + \rho\overline{\underset{\sim}{u}\underset{\sim}{u}} + P\underset{\approx}{I}) = \nabla\cdot\underset{\approx}{\tau} \tag{2}$$

where

$$\underset{\approx}{\tau} = \mu[(\nabla\underset{\sim}{U}) + (\nabla\underset{\sim}{U})^T] - \frac{2}{3}\mu\nabla\cdot\underset{\sim}{U}\underset{\approx}{I}. \tag{3}$$

The Boussinesq eddy viscosity hypothesis is used to express the Reynolds stresses as:

$$-\rho\overline{\underset{\sim}{u}\underset{\sim}{u}} = \mu_t[(\nabla\underset{\sim}{U}) + (\nabla\underset{\sim}{U})^T] - \frac{2}{3}(\rho k + \mu_t\nabla\cdot\underset{\sim}{U})\underset{\approx}{I}. \tag{4}$$

The turbulent viscosity μ_t is determined by dimensional arguments from the Prandtl-Kolmogorov definition:

$$\mu_t = C_\mu\rho k^2/\epsilon \tag{5}$$

with k and ϵ derived from their own transport equations:

$$\nabla\cdot[\rho\underset{\sim}{U}k - (\mu+\mu_t)/\sigma_k\nabla k] = G - \rho\epsilon \tag{6}$$

$$\nabla\cdot[\rho\underset{\sim}{U}\epsilon - (\mu+\mu_t)/\sigma_\epsilon\nabla\epsilon] = (C_1 G - C_2\rho\epsilon)\epsilon/k \tag{7}$$

where
$$G = \{\mu_t[(\nabla\underset{\sim}{U}) + (\nabla\underset{\sim}{U})^T] - \frac{2}{3}(\mu_t\nabla\cdot\underset{\sim}{U} + \rho k)\underset{\approx}{I}\}:\nabla\underset{\sim}{U}. \tag{8}$$

The turbulence model constants (C_μ, C_1, C_2, σ_k, σ_ϵ) are given by Launder (1974).

The local cavitation number σ is defined as:

$$\sigma = 2(P - P_v)/(\rho V^2) \tag{9}$$

where V is calculated using the given mass flow rate and the orifice diameter:

$$V = 4m/(\pi\rho D^2) \tag{10}$$

In practice, this implies that due to differences in the discharge coefficients of the nozzles, the pressure at the inlet of the nozzles should be different to obtain the same mass flow rates. The local cavitation number (σ) is an important parameter to understand the process of cavitation. For inception, where the bubbles just start to appear, the value of σ is slightly positive or close to zero. The probability or degree of cavitation (that is, the population of cavitation bubbles) is indicated by the magnitudes of the negative values of σ. This information cannot be obtained from the most frequently reported global value of σ, which is calculated simply by using $P = P_a$, in Eq. (9). Equations (2) and (3) show that, for high Reynolds number flows (i.e., $\mu \approx 0$), the origin for the negative values of σ is due to two factors: (i) an increase in dynamic velocity head, and (ii) the effect of Reynolds stresses. The first is a result of the geometry of nozzle passages. The second is caused by the shear layer between the slow moving ambient water and the high speed water jet emerging from the nozzles, and also by the turbulent mixing in the wake behind the insert or the pin.

3.2 Boundary Conditions

As indicated in Fig. 4, there are five types of boundaries associated with the solution domain. The corresponding boundary conditions are as follows:

Inlet Plane

No detailed measurements of the velocity or the turbulence fields are available except the total water flow rate through the nozzle. Thus, the inlet velocity distribution was assumed to be uniform in the nozzle passages. The angle of velocity vector is given by the passage angle. Boundary conditions for k were calculated by using a turbulence intensity of 10% of the inlet velocity through a passage and by prescribing 3% of the typical dimension of flow passage for the length scale of ϵ.

Outlet Plane

The normal velocity distribution was uniformly modified to conserve net water flow rate entering the solution domain through the inlet as well as the entrainment boundary. Zero normal gradient was imposed for other variables.

Axis of symmetry

Zero normal gradient conditions were imposed for all variables, except the radial

velocity which was assumed to be zero.

Solid wall

At the nozzle and insert walls, no-slip and impermeable boundary conditions were imposed. Velocities were set to zero. The wall shear stresses and the values of k and ϵ close to the walls were modeled by the wall function method (Launder, 1974), which was based on the assumptions of local equilibrium and logarithmic law.

Entrainment boundary

The ambient water is entrained through the entrainment boundary. As a result of this entrainment, the jet flow rate continuously increases downstream along the jet axis. Zero normal gradients were assumed for all variables. This condition was implemented as an integral part of the solution.

3.3 Solution Procedure

WATERJET solves the finite volume approximations to the governing equations in primitive variables. Hybrid upwind/central differencing was used to discretize the equations on a staggered grid. The SIMPLE algorithm (Patankar, 1972) was employed to obtain the velocity and pressure fields. Each discretized equation was solved sequentially in an iterative fashion using a line-by-line method.

All the results were obtained by using 76x35 (nozzles #1, #2) and 47x31 (nozzle #3) grid points in the axial and radial directions respectively. Under-relaxation factors of 0.2 for the velocities and 0.75 for the other dependent variables were used. Two sweeps for the governing equations were employed. The solution was assumed to have converged when the sum of the normalized absolute residuals had fallen below 10^{-3}. To achieve this convergence, the number of iterations required was about 600. The CPU time on the IBM 3090 computer was approximately 0.2 s per iteration.

4.0 PRESENTATION OF RESULTS

4.1 Nozzle Characteristics

The design and predicted values of the total kinetic energies at the exit plane of the nozzle are defined, respectively, as:

$$KE_d = 0.5\rho V^3 \int dA \tag{11}$$

and

$$KE_p = 0.5\rho \int (\underset{\sim}{U}\cdot\underset{\sim}{U})(\underset{\sim}{U}\cdot\underset{\sim}{n})\,dA. \tag{12}$$

These values, given in Table 2 for the nozzles considered, are important parameters to determine the characteristics of the nozzles as they are related to the hydraulic power available in the jet at the target for erosion.

Under the conditions simulated, the design values were different from the predicted ones, owing to the non-uniform distributions of velocities (see next sub-section). Also, the output power (KE_p) was greater for nozzle #3 than for #1 and #2 by approximately three times. Although KE_p for #2 was practically the same as #1, the cavitation activity might persist to larger standoff distances, aided by the centre body. Thus, from the standpoint of KE_p, nozzle #3 appears to be the best. However,

since performance of the nozzle depends on other considerations such as, for instance, turbulence kinetic energy, transport of cavitation bubbles, etc., the above findings need to be validated by experiments.

4.2 Velocity and Scalar Fields

The predicted results of velocity fields, distributions of the turbulence kinetic energy (k) and the local cavitation numbers (σ) for the three nozzles are depicted in Figs. 5 to 8. All the k values are normalized by the velocity head based on V. For the sake of clarity, the velocities are indicated separately in Figs. 5 and 6. In Fig. 5, the vectors represent only the directions of the local velocities and in Fig. 6, both the magnitude and directions are indicated (the magnitude is indicated not only by the length of the vector, but also by the size of the arrow head). The contour lines in Figs. 7 and 8 represent loci of iso-values of k and σ.

For nozzle #1 (Figs. 5A & 6A), the flow is accelerated towards the throat of the nozzle and turns around the corner. The flow quickly develops within the parallel section and becomes fairly uniform at the nozzle exit. The diameter of the jet outside the nozzle is roughly equal to the orifice diameter, consistent with the flow visualization results depicted in Fig. 9A. Entrainment of the ambient fluid starts immediately downstream of the nozzle.

Within the nozzle, both turbulence kinetic energy and pressure [inferred from cavitation number Eq. (9)] are quite uniform in most regions (Figs. 7A & 8A; contours of high cavitation numbers are not shown). However, towards the parallel section, k increases rapidly as the pressure decreases. At the corner, the cavitation number appears to become negative. This could be real due to the curvature at the corner or could be due to the numerical errors introduced by the algorithms or the coarseness of the grids. If the bubbles do form at this point, they will most likely collapse within the parallel section, depending upon its length, as the pressure recovers in this region. This can cause erosion of the nozzle walls, as shown in Fig. 2. For this nozzle, negative cavitation numbers (and high turbulence kinetic energies) occur mostly in the boundary layer inside the jet development region. This indicates that cavitation takes place in these areas, confirmed indeed by the flow visualization of the jet shown in Fig. 9A. The enlargement of the low pressure region in the turbulent boundary layer is due to large Reynolds (shear) stresses generated, as large k values are found along the boundary layer. Values of k and hence pressure are quite uniform inside the parallel section, and along the centerline of the free jet. Furthermore, k values in the parallel section are much greater than the ones inside the nozzle. This implies that shear effects are important in the parallel section.

For nozzle #2 (Figs. 5B & 6B), a small recirculation zone occurs behind the insert. The size of the wake obviously depends on the size of the insert, the annular gap and the entry angle (α) at the outlet of insert face. Slight increase of k, as compared to nozzle #1, is generated inside the nozzle. However, this seems to be highly localized and does not enhance the turbulence intensity in the parallel section or at the nozzle exit (compare with nozzle #3). Therefore, flow fields and the distributions of k and the pressure are practically the same in the jet development region as for nozzle #1. Cavitation occurs in the jet development region, once again confirmed by the flow visualization results shown in Fig. 9B

For nozzle #3, an elongated and large wake with high pressure depression region forms behind the pin and within the parallel section (Figs. 5C, 6C & 8C). The wake behaves like an irrotational vortex with constant and significant k (Fig. 7C). Near the nozzle exit, the boundary layer of the wake diffuses into the jet centerline and

reduces the maximum velocity (see Fig. 5C). High values of k (Fig. 7C) and quite low values of the local cavitation numbers (Fig. 8C) exist in this zone. In the jet development region, the spread of the jet is wider than the ones observed for nozzles #1 and #2 (Fig. 8). This nozzle seems to produce travelling cavitation right from inside and to extend the cavitation zone over a large area outside of the exit. Agreement between this prediction and the experimental observation of the jet shown in Fig. 9C is truly remarkable.

In terms of the overall comparisons of the numerical nozzle flow predictions with the flow visualization results, it should be pointed out that the global cavitation numbers were not identical. However, the predicted results are very encouraging, which suggests that the WATERJET code is a valuable tool for analyzing the complex flows of high speed submerged water jets. Deficiencies in the WATERJET do exist and may be attributed to a number of factors, the most important one being the lack of detailed information at the inlet plane of the computational domain. The others are the assumptions made in the use of the k-ϵ turbulence model (for example, the specification of the empirical constants), the numerical errors in the numerical procedure, and not accounting for two-phase effects.

5.0 CONCLUSIONS

* The WATERJET code is capable to predict complex flows both within and outside of the nozzles under submerged conditions. With the known limitations of the mathematical model used, the code is adequate for design/analysis of various nozzles.

* Further improvements in the existing mathematical model of the WATERJET are possible with input from the experimental data. An extension of the WATERJET to handle two-phase cavitation phenomenon should be carried out.

* The incorporation of a pin or to a certain extent a centre-body insert into a conical nozzle has been shown numerically to enhance cavitation. However, the overall performance of the nozzles needs to have experimental verifications.

6.0 REFERENCES

1. Arndt, R.E.A., Recent Advances in Cavitation Research, In: Advances in Hydroscience , Ed: Ven Te Chow, Vol. 12, pp. 1-78, 1981

2. Chahine, G.L., Ph. F. Genoux and H.L. Liu, Flow Visualization and Numerical Simulation of Cavitating Self Oscillating Jets, Paper A2, Proc. 7th Int. Symp. on Jet Cutting Technology, Ed: G.A. Watts and J.E.A. Stanbury, BHRA, England, pp. 13-32, 1984.

3. Duncan, J.H., Calculations of the Collapse of a Cavity in the Vicinity of a Compliant Wall, Proc. Int. Symp. on Cavitation Noise and Erosion in Fluid Systems, Ed: R.E.A. Arndt, M.L. Billet and W.K. Blake, The ASME, New York, U.S.A., pp. 127-133, 1989.

4. Gosman, A.D., and F.D.K. Ideriah, TEACH-2E: A General Computer Programme for Two-Dimensional Turbulent Recirculating Flows, Internal Report, Department of Mechanical Engineering, Imperial College, London, England, 1976.

5. Knapp, R.T., J.W. Daily and F.G. Hammitt, Cavitation, McGraw-Hill Book Company, New York, U.S.A., 1970.

6. Lai, K.Y.M., TURCOM: A Computer Code for the Calculation of Transient, Multi-Dimensional, Turbulent, Multi-Component Chemically Reactive Fluid Flows. Part 1: Turbulent, Isothermal and Incompressible Flow, Technical Report TR-GD-011 (NRC No. 27632), National Research Council Canada, Ottawa, Ontario, Canada, 1987.

7. Launder, B.E., and D.B. Spalding, The Numerical Computation of Turbulent Flows, Computer Methods in Applied Mechanics and Engineering, Vol. 3, pp. 269-289, 1974.

8. Lesser, M., and M. Finnstrom, On the Mechanics of a Gas-Filled Collapsing Cavity in a Liquid, Paper 23, Proc. 7th Int. Conf. on Erosion by Liquid and Solid Impact, Ed: J.E. Field and J.P. Dear, pp. 1-7, Cambridge, England, September 1987.

9. Patankar, S.V., and D.B. Spalding, A Calculation Procedure for Heat, Mass and Momentum Transfer in Three-Dimensional Parabolic Flows, International Journal of Heat and Mass Transfer, Vol. 15, pp. 1787-1806, 1972.

10. Plesset, M., and A. Prosperetti, Bubble Dynamics and Cavitation, Annual Review of Fluid Mechanics, Vol. 9, pp. 145-185, 1977.

11. Puchala, R.J., and M.M. Vijay, Study of an Ultrasonically Generated Cavitating or Interrupted Jet: Aspects of Design, Paper B2, Proc. 7th Int. Symp. on Jet Cutting Technology, Ed: G.A. Watts and J.E.A. Stanbury, BHRA, England, pp. 69-82, 1984.

12. Shimizu, S., Discrete-Vortex Simulation of a Two-Dimensional Turbulent Jet, Bull. JSME, Vol. 29, No.254, pp. 2440-2446, 1986.

13. Shimizu, S., and A. Yamaguchi, Discrete-Vortex Simulation of Two-Dimensional Turbulent Impinging Jets with and without Excitation, Paper 13, Proc. 8th Int. Symp. on Jet Cutting Technology, Ed: D. Saunders, BHRA, England, pp. 137-145, 1986.

14. Shimizu, S., and A. Yamaguchi, Structure of Cavitating Jets and its Effects on Erosion, Paper A1, Proc. 9th Int. Symp. on Jet Cutting Technology, Ed: P.A. Wood, BHRA, England, pp. 1-12, 1988.

15. Vijay, M.M., C. Zou, and S. Tavoularis, Study of the Characteristics of Cavitating Water Jets by Photography and Erosion, Paper F2, Proc. 10th Int. Symp. on Jet Cutting Technology, BHR Group Ltd., England, 1990.

16. Webster, E., Cavitation, Ultrasonics, pp. 39-47, 1963.

7.0 NOMENCLATURE

A	cross-sectional area normal to the exit plane of the nozzle
C_1, C_2	empirical constants in the ϵ-equation, Eq. (7)
C_μ	empirical constant in the turbulent viscosity expression, Eq. (5)
D	orifice diameter, Fig. 3
D'	diameter of the centre body, Fig. 3
D"	diameter of the pin, Fig. 3
G	generation term of turbulence kinetic energy, Eq. (6)
I	unit tensor
KE_d	design value of the total kinetic energy at the exit plane of the nozzle, Eq. (11)
KE_p	predicted value of the total kinetic energy at the exit plane of the nozzle, Eq. (12)
k	turbulence kinetic energy

L	length of parallel section of nozzle, Fig. 3
L′	distance between the centre body and the nozzle exit, Fig. 3
L"	distance between the pin and the nozzle exit, Fig. 3
m	mass flow rate of water
n	unit vector normal to the exit plane of the nozzle
P	local pressure
P_a	ambient pressure
P_v	vapour pressure
U	ensemble-averaged velocity vector
u	fluctuating velocity vector
V	average velocity of the jet at the nozzle exit

Greek Symbols

α	nozzle entry angle
ϵ	turbulence energy dissipation rate
μ	molecular viscosity
μ_t	turbulent viscosity
ρ	density
σ	local cavitation number, Eq. (9)
σ_k	Schmidt number in the k-equation, Eq. (6)
σ_ϵ	Schmidt number in the ϵ-equation, Eq. (7)
τ	viscous stress tensor

Superscripts

T	transport of tensor
-	(overbar) ensemble-averaged

Table 1: Geometrical Data of Nozzles Used

Nozzle #	1	2	3
D (mm)	3.18	3.18	3.05
D′ (mm)	-	7.88	-
D" (mm)	-	-	1.59
L (mm)	6.36	6.36	6.10
L′ (mm)	-	21.00	-
L" (mm)	-	-	3.35
α (deg)	20.00	20.00	20.00

Table 2: Flow characteristics of Nozzles

Nozzle #	1	2	3
KE_d (kJ)	1.71	1.71	2.02
KE_p (kJ)	1.77	1.77	5.76

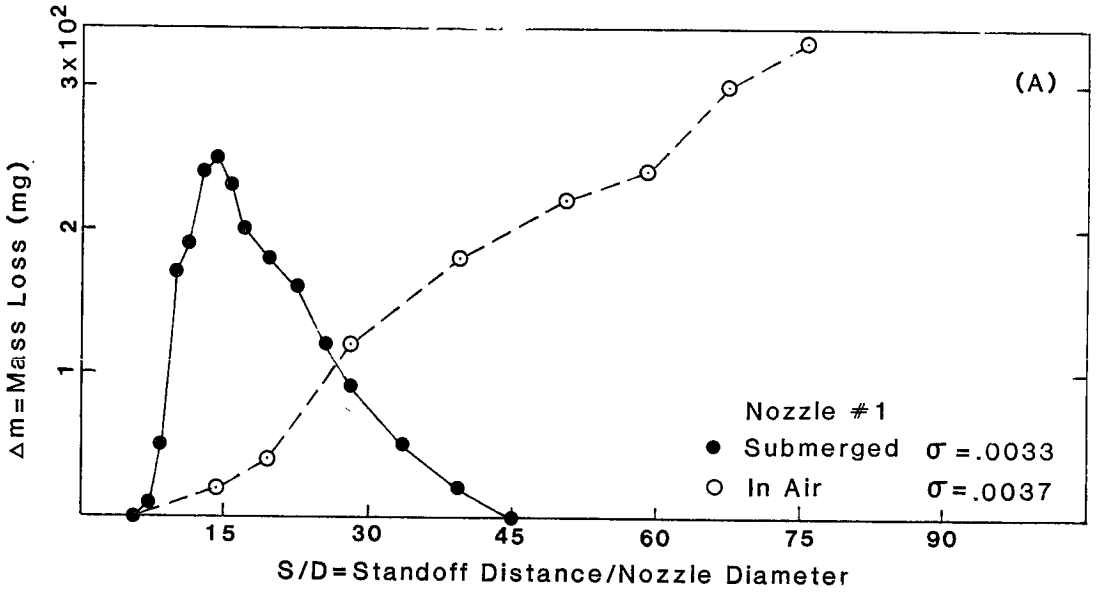

Fig. 1 Plot of mass loss of aluminum samples exposed to jets emerging from nozzle #1 (Vijay, 1990)

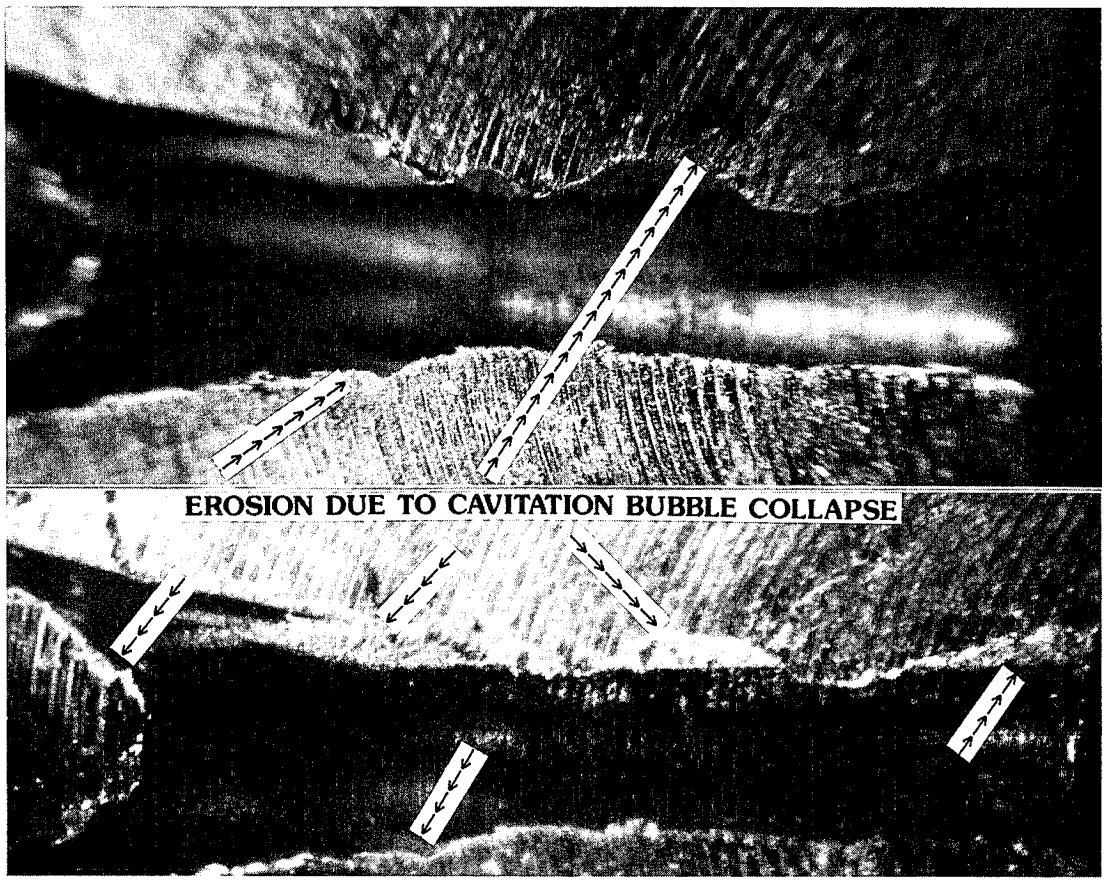

Fig. 2 Erosion of the internal profiles of a nozzle with the pin (similar to #3) due to collapse of cavitation bubbles

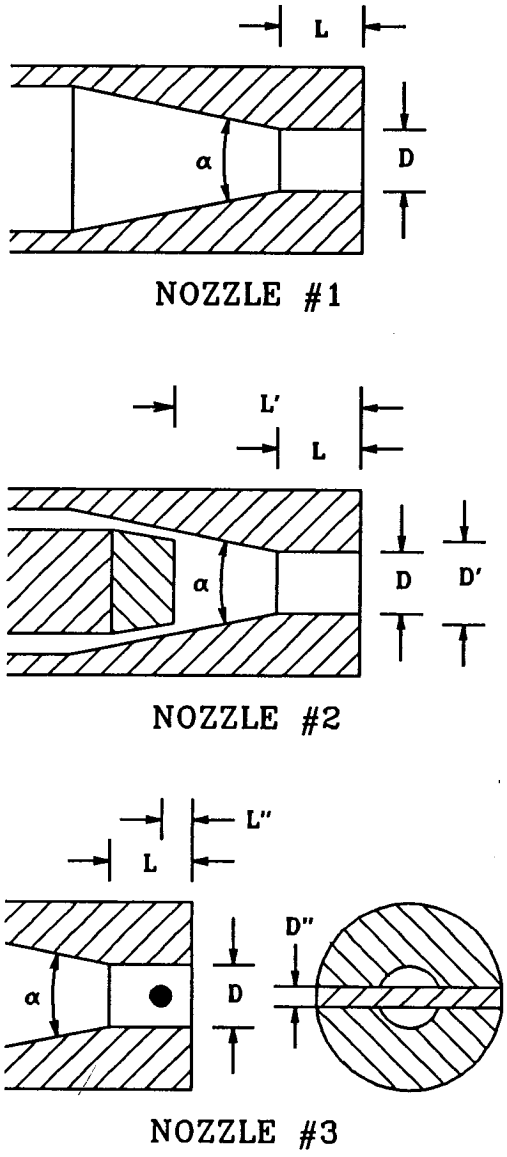

Fig. 3 Schematics of the nozzles used in the analysis

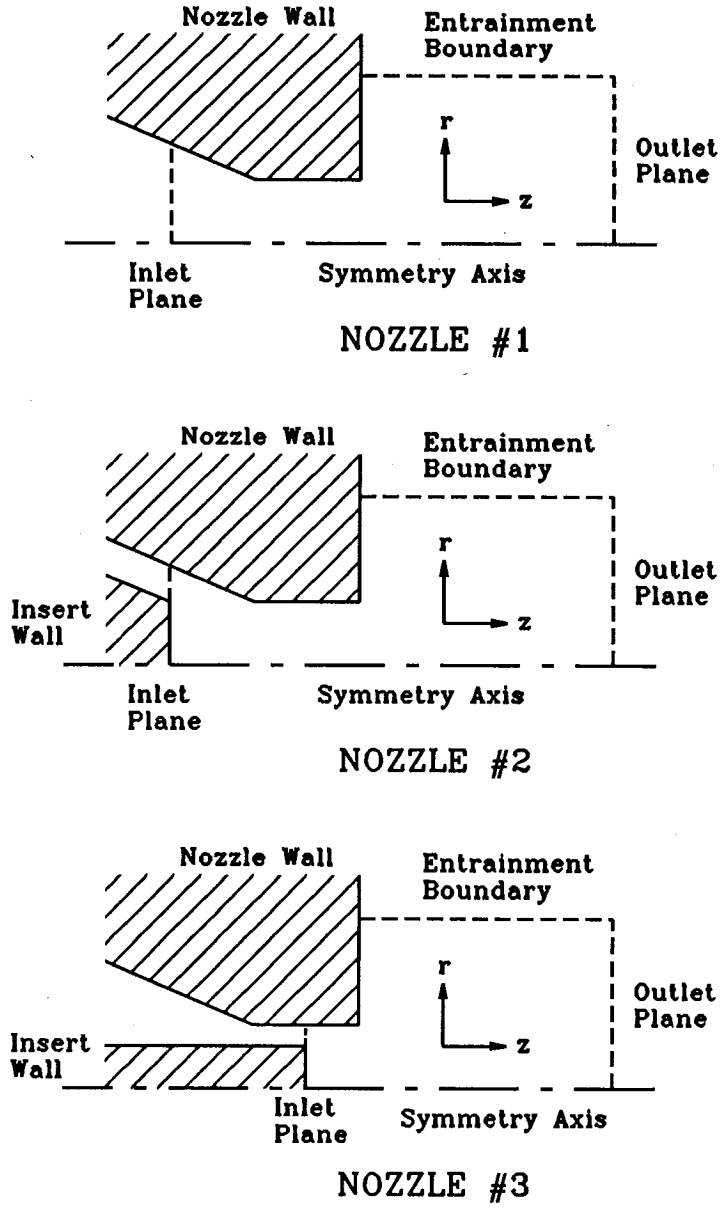

Fig. 4 Solution domain for the nozzles

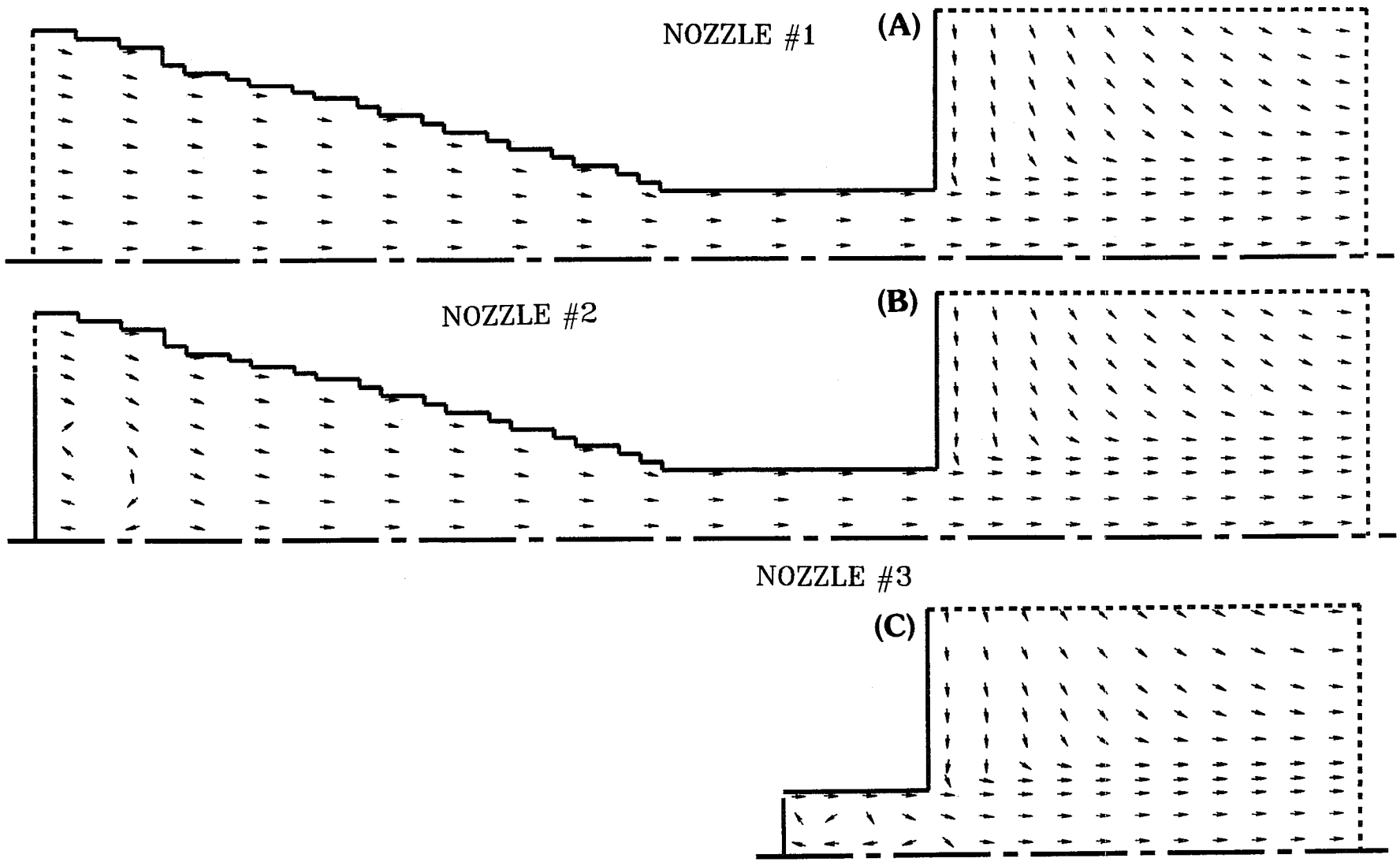

Fig. 5 Distribution of velocity showing only the directions

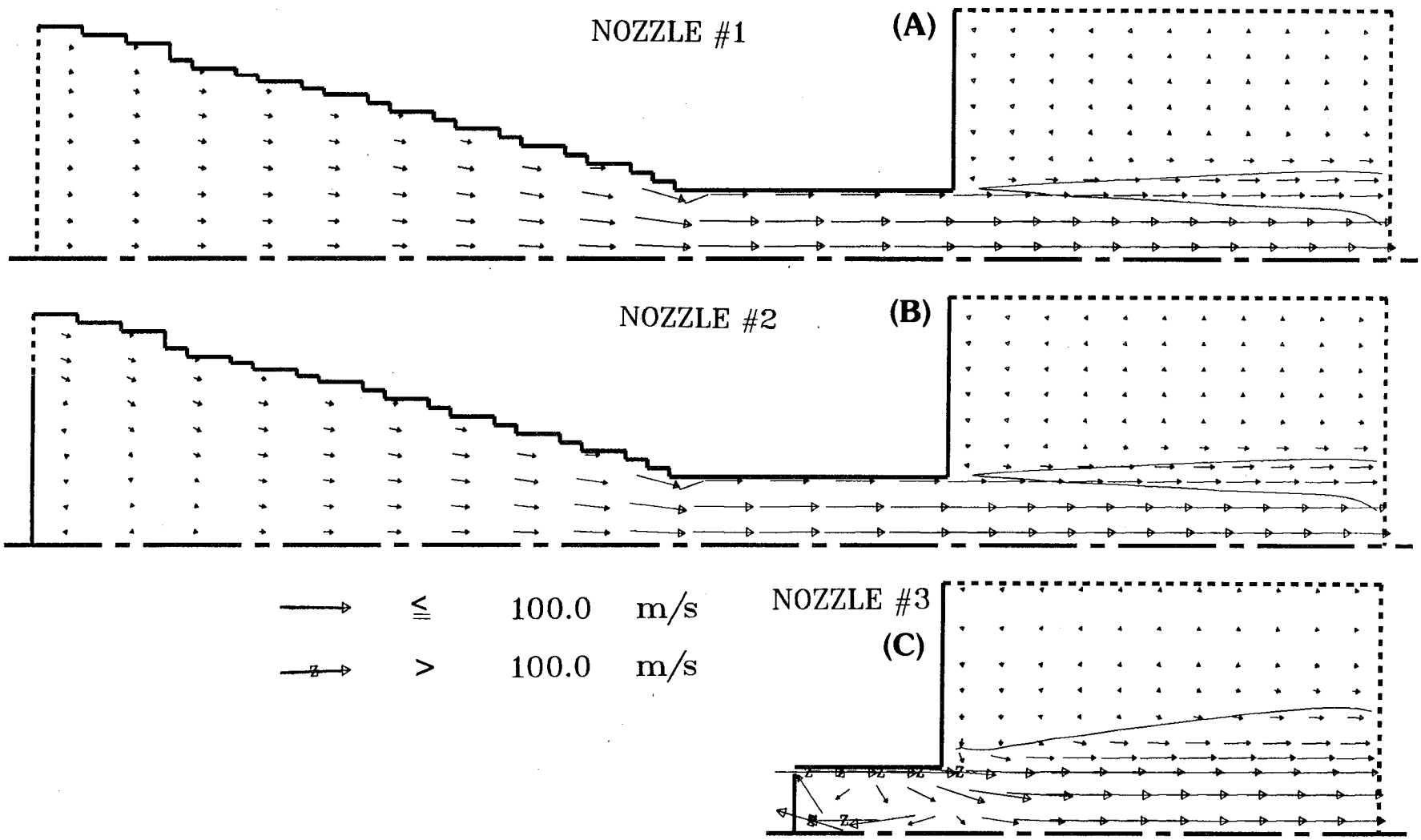

Fig. 6 Distribution of velocity predicted by the analysis

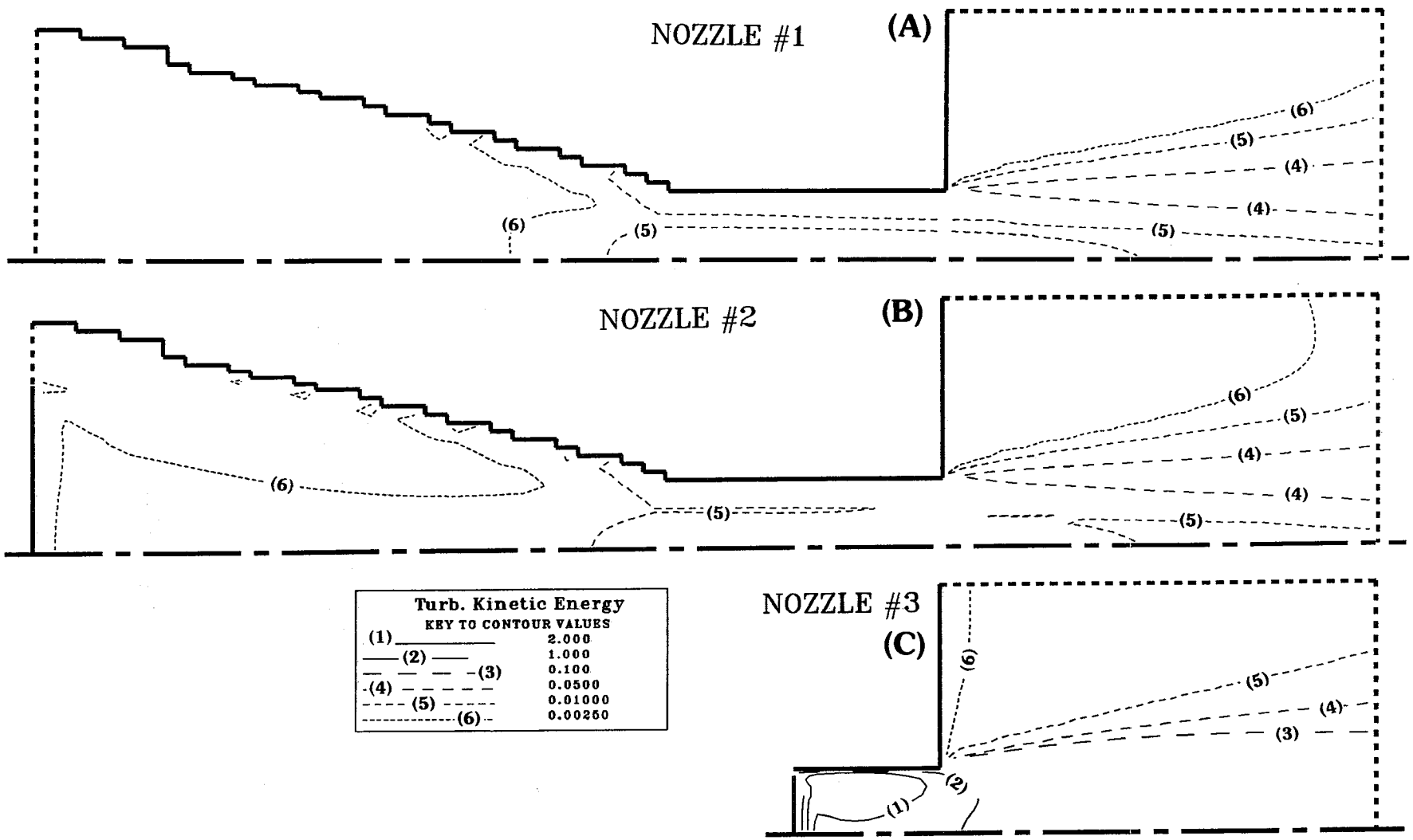

Fig. 7 Distribution of turbulence kinetic energy (k) predicted by the analysis

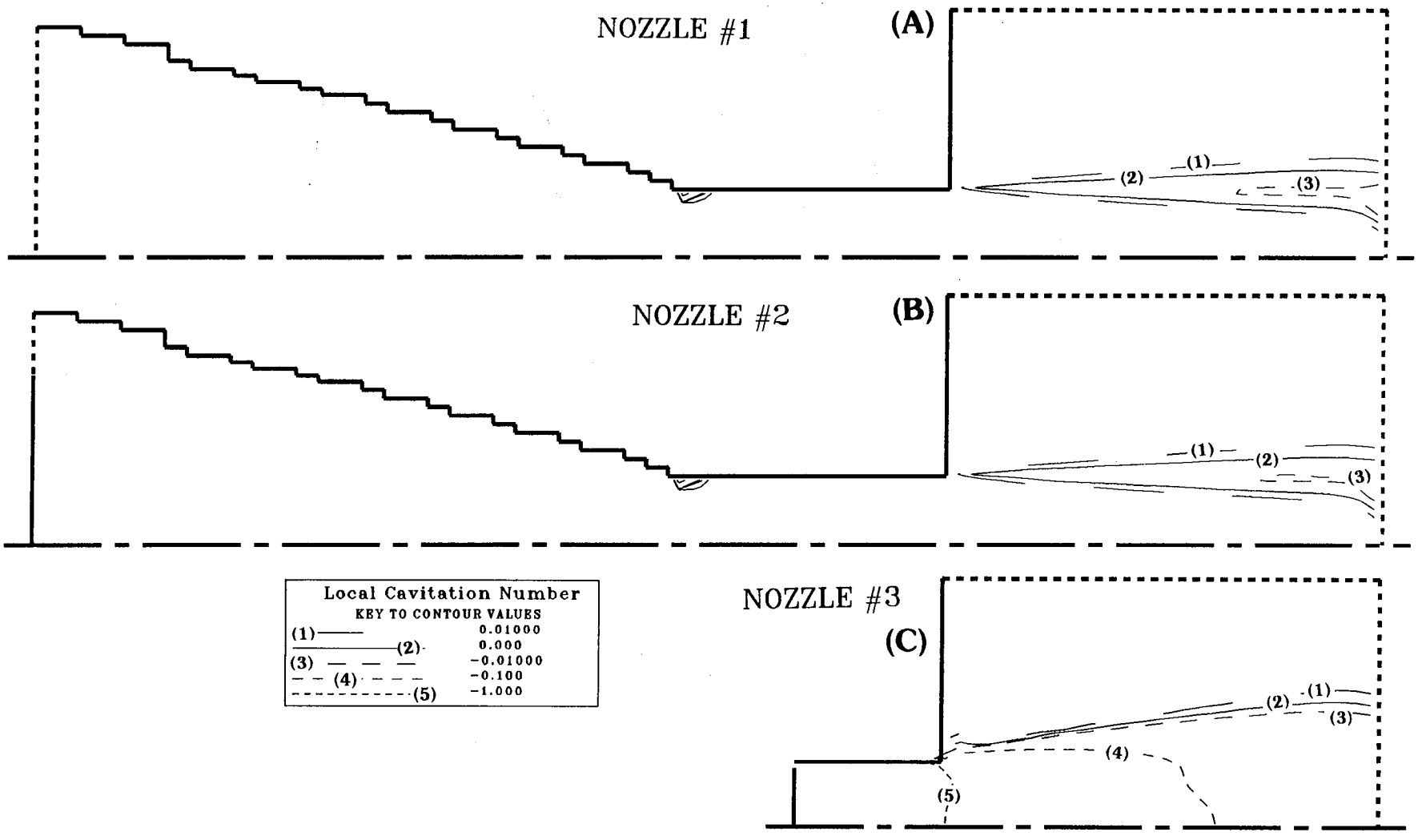

Fig. 8 Distribution of local cavitation number (σ) predicted by the analysis

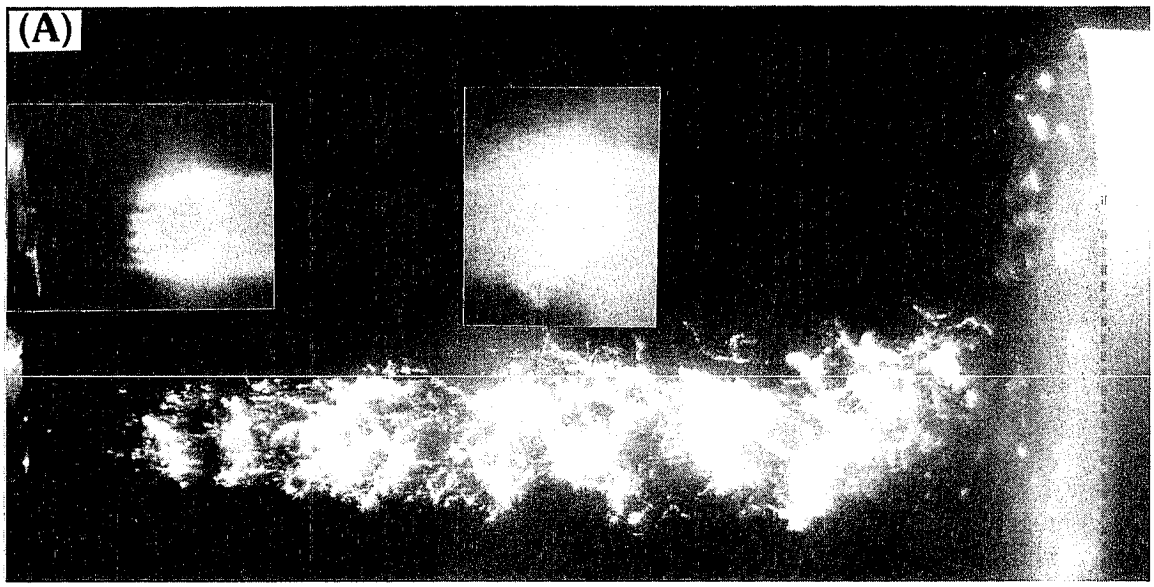

Jet emerging from nozzle #1. Magnification = 2.8
Global cavitation number ≈ 0.0256

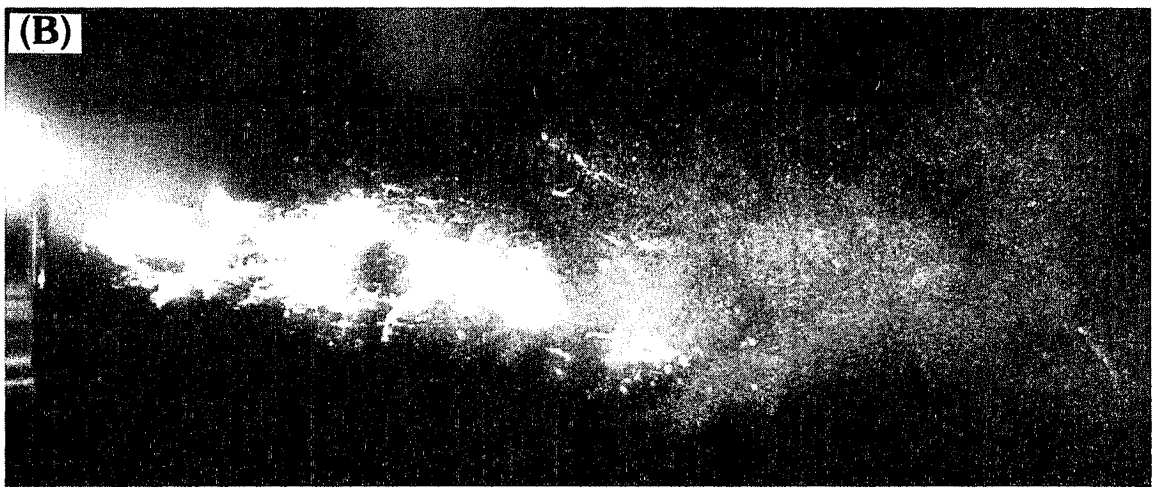

Jet emerging from nozzle #2. Magnification = 2.8
Global cavitation number ≈ 0.0256

Jet emerging from nozzle #3. Magnification = 7.9
Global cavitation number ≈ 0.017

Fig. 9 Patterns of the jets issuing from the nozzles under submerged conditions

6th American Water Jet Conference
August 24 - 27, 1991: Houston, Texas Paper 32

Methods of Process Control for Abrasive Water Jets

Louis, H. and G. Meier
Institute of Material Science
University of Hanover, Germany

ABSTRACT

For the remote-controlled application of abrasive water jets in inaccessible environment like deep-sea it is necessary to develop sensor systems to supervise both the state of the cutting tool and the cutting result.

Regarding the control of the tool measuring the emitted sound is a method to detect the state of the abrasive transport hose.
On the other hand measuring the sucked-in flow rates gives this information, too, and it is also a sensor technique to detect the state of the focusing tube (correlation of flow rate and diameter).
Instead of measuring the flow rate also the pressure loss in a specific length of the transport hose can be measured and correlated with the air flow rate. So the pressure loss can indicate the focus diameter, too.

The supervision of the cutting result was tried to realise by sound pressure measurement and frequency analysis. There are sometimes characteristic frequencies for cutting through which cannot be seen in case of kerfing. But the results of sound frequency analysis as well as the comparison of the sound intensity up to now are not reliable for controlling the cutting result.

Organized and Sponsored by the Water Jet Technology Association.

1.0 Introduction

Abrasive water jets become more and more a useful tool for cutting operations in dangerous and inaccessible environment.
For example an increasing number of offshore structures are reaching the end of their life and must be removed from sea bed or require maintenance and repair work to extend the period of efficient operation.
Additionally abrasive water jets are applicable for cutting dangerous materials like explosives or other health-dangerous materials. Also cutting jobs for dismantling nuclear installations are in discussion.
Most of these jobs have to take place under water to reduce the risk of setting free dangerous materials or radiation. For applications in air the jobs have to be done remote controlled in closed cutting boxes.

The handling techniques for these applications are available but until now the under water application of abrasive water jet technique mostly requires a diver`s presence to monitor the cutting process /1/. Also cutting in closed boxes needs periodical inspection of the tool by men.
To avoid any risk for the operating team and to make the abrasive cutting technique more efficient all the control work has to be done remote controlled, too.
So automatic sensor systems are necessary to control the state of the tool as well as the cutting result.

Controlling the state of the tool means supervising the process of wear inside the cutting head and monitoring the conditions of the abrasive transport (broken or clogged transport hose).
Controlling the cutting result means on the one hand the detection if cutting through or kerfing only.
In addition the online supervision of the quality of the cut surface would be of great importance /2/.

2.0 Experimental setup

To develop useful sensor systems tests were carried out in a water basin.

An intensifier pump was used for the cutting tests, the maximum pressure is 400 MPa with a maximum flow rate of water of 4 l/min. For all the tests a self-designed abrasive mixing head /3, 4/ was used.

For controlling the tool different measuring devices were installed (fig. 1).
For the supervision of the state of the cutting head a system to measure the sucked-in air flow rate was adapted /5/.
Additionally it was tried to detect the pressure loss in a special part of the transport hose (hose length L_h) and to correlate this with the air flow rate.
For both measuring methods it was tried to correlate the measuring results with the diameter of the focusing nozzle.

To supervise the conditions of the abrasive transport tests were carried out using sound analysis. For this purpose a hydrophone (bruel & kjaer 8103) was installed near the cutting head.

This hydrophone was used also for the detection of the cutting result. The frequencies of the sound pressure were analysed by Fourier-Transformation. Sound frequencies were measured for cutting through and kerfing a standard workpiece (austenitic steel).

3.0 Experimental results

3.1 Supervision of the cutting tool

The reliability of the cutting tool depends mostly on the conditions of the abrasive feed and the state of the water jet nozzle and the focus. One possibility to supervise the conditions of the abrasive transport is measuring the sound pressure produced by the cutting head. Fig. 2 shows the results of the sound measurements.

For normal conditions (air sucked in) the sound pressure is very low. In case of sucked-in water (broken transport hose) the sound level increases rapidly. Also when the transport hose is clogged (in that case the cutting head produces a vacuum) the sound level is very high because of cavitation effects.

The diameter of the focusing nozzle can be controlled by measuring the flow rate of the sucked-in air. Fig. 3 shows the flow rate versus the diameter of the focusing nozzle for different pressures. The flow rate can be measured during cutting directly by flow meter. Unfortunately in that case also abrasives have to pass the instrument and can destroy it.

So it seems to be more useful to control the diameter of the focus by measuring the pressure loss in a specific length of the transport hose. Fig. 4 gives the results of tests. The curves are very similar to fig. 3, but the pressure loss is measured in a bypass without any abrasive load of the measurement equipment (see fig. 1). The pressure loss is proportional to the sucked-in air flow rate and so it can be correlated with the focus diameter. In addition also rapid changes of the pressure loss indicate a change of the conditions of the abrasive transport (broken or clogged transport hose).

The air flow rate and so the pressure loss is nearly linear with the pressure (fig. 5). Doubling the length of the hose where the loss is measured causes an increasing of the pressure loss by a factor of 2.

3.2 Supervision of the cutting result

For remote controlled operation of the abrasive cutting process a method is necessary to detect the cutting result. In case of using abrasive water jets optical and mechanical sensor systems are difficult to apply. Because of the suspended particles the optical conditions in the water are very bad, additionally mechanical systems can be destroyed by reflected abrasives. The produced kerf is very small so there is no possibility to bring sensor systems in.
In addition when cutting irregular structures (offshore structures with marine growth) all contacting sensor systems are not applicable because of the risk of sticking. So the measurement of the sound pressure seemed to be useful method to detect the cutting result, because it is a non-contacting system which also is not sensitive against the particle load. To distinguish between cutting through and kerfing sound frequencies were analysed.

Fig. 6 gives the typical analysis of cutting through. The upper part of the figure gives the sound intensity, the lower part the frequency analysis.
This analysis shows a significant maximum between 400 and 500 Hz.

Fig. 7 gives the results for the kerfing tests. The magnification of the sound intensity signal (upper part of the figure) is the same as in fig. 6.
The measured value for the sound pressure in case of kerfing is not constant. So, also the frequency analysis are different at different times.

All the tests were carried out on standard samples (size, material) under similar conditions (cutting parameters, position in the water basin). So, there is no influence of these parameters on the results.
But, unfortunately, up to now the **frequency** analysis does not seem to be a reliable method to detect the cutting result, because besides the results of fig. 6 and 7 different analysis are occuring often, too. Up to now there isn't any reason for this scattering of the occurring frequencies.

Also differences in the sound **intensity** have not been reproducable. So they can't be used for the detection of the cutting result, too.

Finally, there are differences in the sound pressure signal for kerfing and cutting through (Cutting through: constant intensity - kerfing: changing intensity like in fig. 7) but to use these differences for controlling the cutting result during cutting very sophisticated equipment is necessary.

In case of kerfing tests it was tried to correlate the sound signal (changing intensity during cutting - see also fig. 7) with the geometry of the shoulder of the cut.
Fig. 8 gives a comparison of the sound signal and the shoulder of the cut.
For the kerfing tests carried out there was no noticeable correlation between sound intensity and geometry of the bottom of the kerf.

Summing up it may be said that only an analysis of the changes of sound intensity during cutting maybe seems to be a method to control the cutting result. Measuring the present intensity of the sound only or analysing the frequency of the sound signal are not sufficient methods for supervising the cutting process.

Fig. 9 gives another method to detect the case of kerfing. Instead of a hydrophone an accelerometer is fixed on a plate very close to the focusing nozzle. In case of kerfing reflected particles will hit this plate. The sensor is able to detect this signal.
This measuring method is also non-contacting and easy to apply. So further tests will be carried out to qualify this technique for controlling the cutting result.

4.0 Conclusions

Following conclusions are relevant:

- The supervision of the conditions of the abrasive transport can be realised by sound intensity measurement. Normal conditions cause the lowest sound intensity, a clogged or broken abrasive feed hose causes cavitation effects in the mixing head and so a higher sound level.
- Measuring the air flow rate sucked into the mixing head gives a good method to control the diameter of the focusing nozzle.
- Instead of measuring the air flow rate it seems to be useful to measure a pressure loss in a specific length of the transport hose because of easier handling. This loss characterises an air flow rate and so the diameter of the focus.
- The cutting result - cutting through or kerfing only - can't be controlled reliable by sound analysis. Sound intensity as well as sound frequency give no reproducable indication on the cutting result up to now.
- Up to now there was found no correlation between the changing of sound intensity and the geometry of the bottom of the kerf.
- Further investigations will be focused on the application of accelerometers to detect the reflected abrasive jet in case of kerfing.

5.0 Acknowledgements

The authors are thankful to the Deutsche Forschungsgemeinschaft (contract SFB 264) and to the Commission of the European Communities (contract FI2D-0009) for partly sponsoring the work.

6.0 References

/1/ Ebdon, R.W. and C.P. Ellinas:
"Decommissioning and Removal of Offshore Structures: A State of the Art"
In: Proc. of the 8. Intern. Conf. on Offshore Mechanics and Arctic Engineering (The Hague, Netherlands, March 1989) ASME, New York, USA, 1989

/2/ Louis, H. and G. Meier
"Process Control for Submerged Cutting by Abrasive water Jets"
In: Proceeding of the 3. Intern. Symposium on Underwater Technology, GKSS Forschungszentrum, Geesthacht, Germany, 1991

/3/ Haferkamp, H.; Louis, H. and G. Meier:
"Submerged cutting of contaminated material by abrasive water jets under the protection of water shield".
In: Proc. of the 9th International Symposium on Jet Cutting Technology (Sendai, Japan, Oct. 1988) BHRA, The Fluid Engineering Centre, Cranfield, U.K., 1988

/4/ Haferkamp, H.; Louis, H. and G. Meier:
"Submerged cutting of steel by abrasive water jets"
Decommissioning of Nuclear Installations
Ed.: Pflugrad, Bisci, Huber, Skupinski
Elsevier Science Publishers Ltd.; Essex, England, 1990

/5/ Haferkamp, H.; Louis, H. and G. Meier:
"Deep-sea Application of Abrasive Water Jets: Feasibility and Limitations"
In: Proc. of the 10th International Symposium on Jet Cutting Technology (Amsterdam, Netherlands, Nov. 1990) BHRA, The Fluid Engineering Centre, Cranfield, U.K., 1990

7.0 Figures

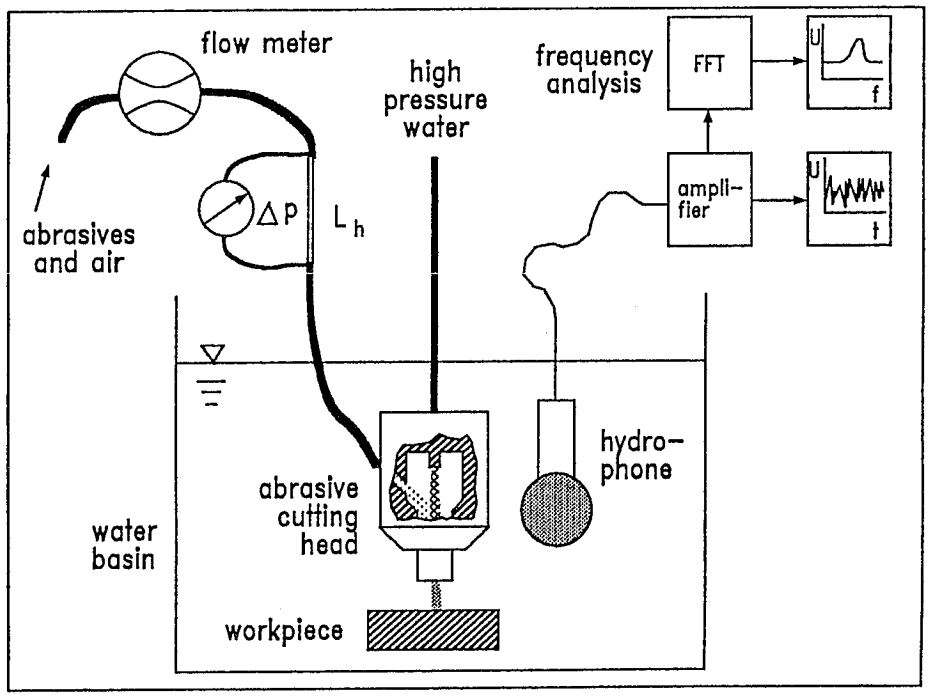

Figure 1 Experimental setup

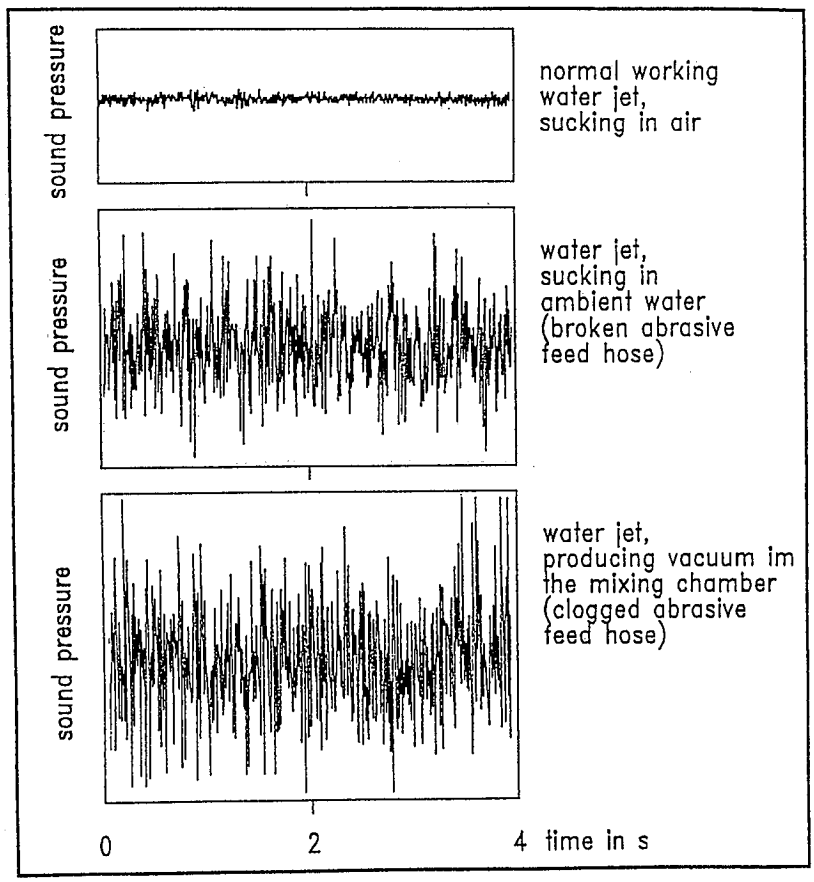

Figure 2 Comparison of sound intensity

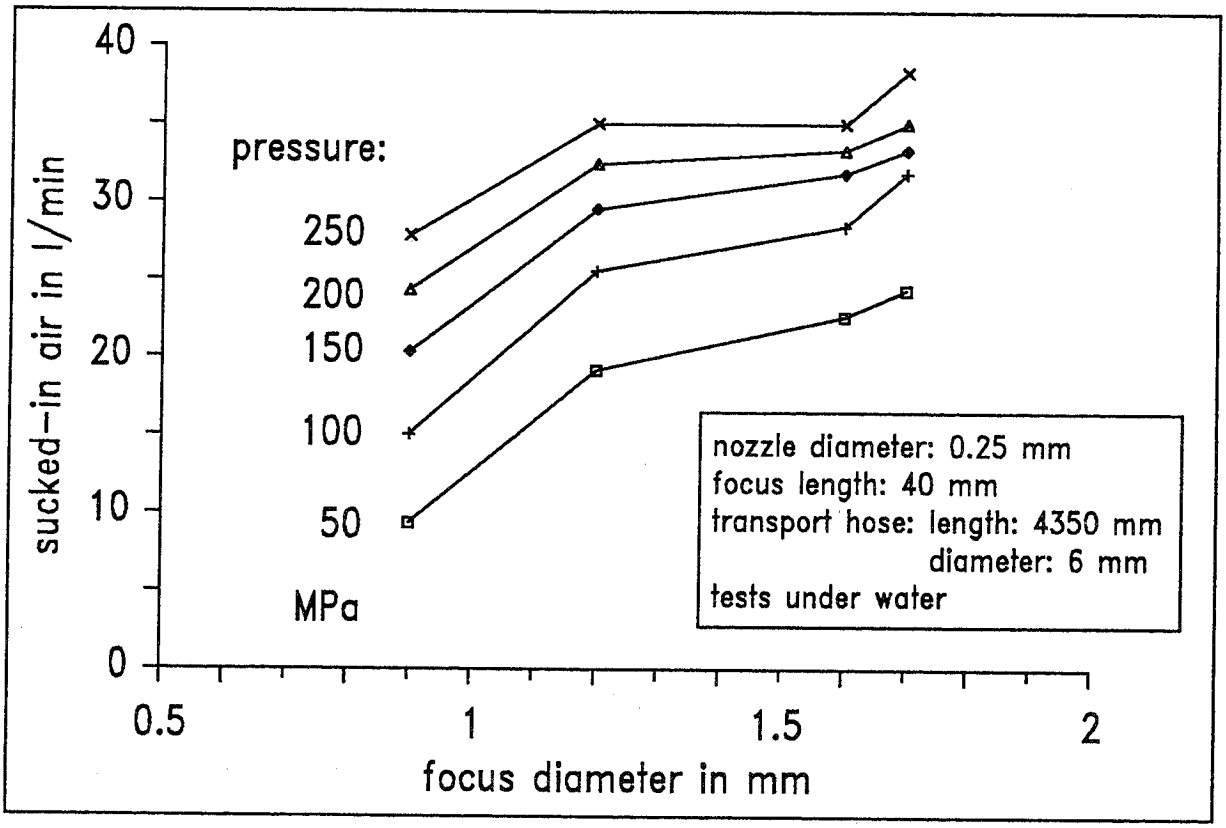

Figure 3 Effect of focus diameter on air flow rate

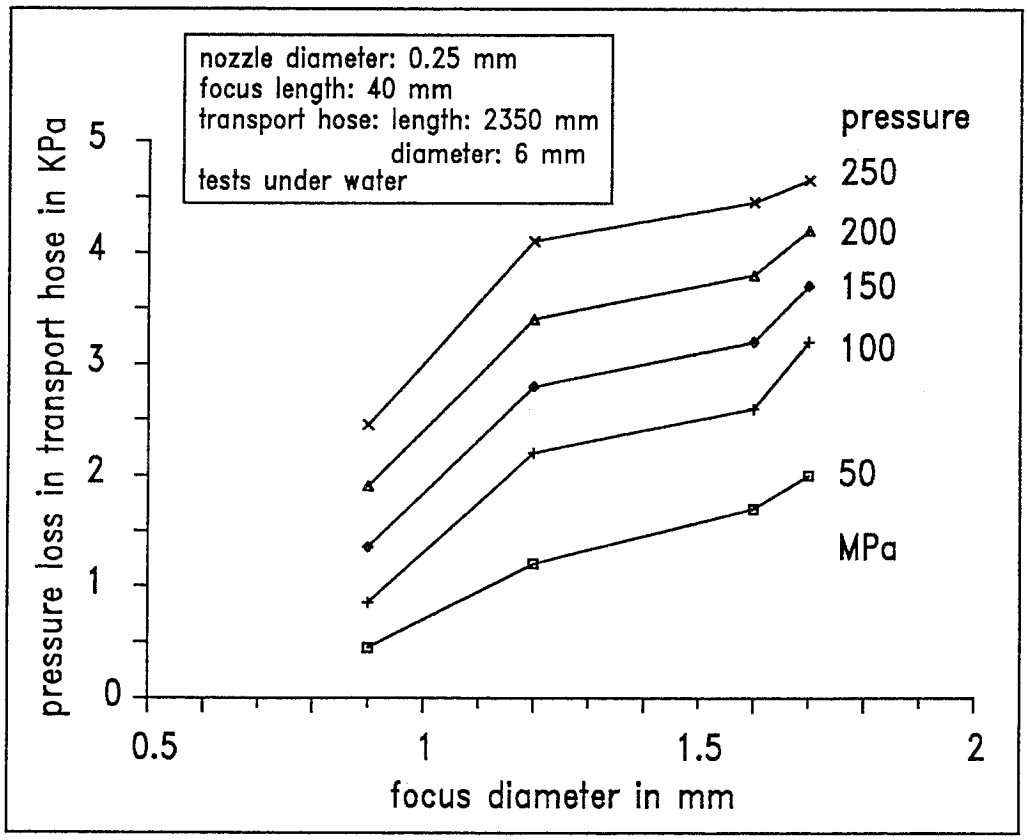

Figure 4 Effect of focus diameter on pressure loss

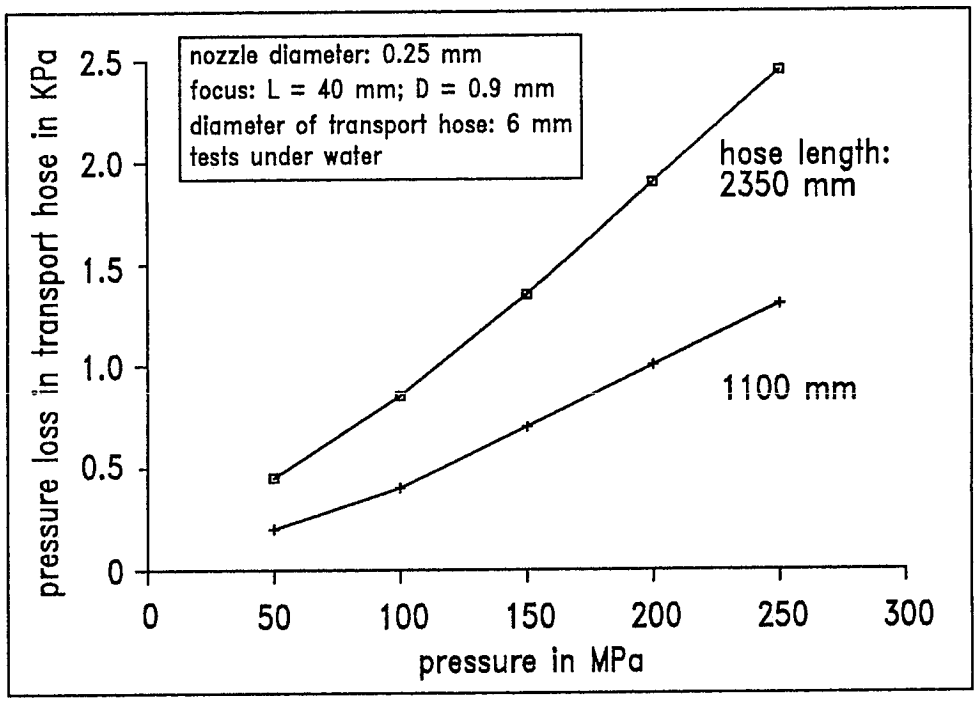

Figure 5 Effect of pressure on pressure loss

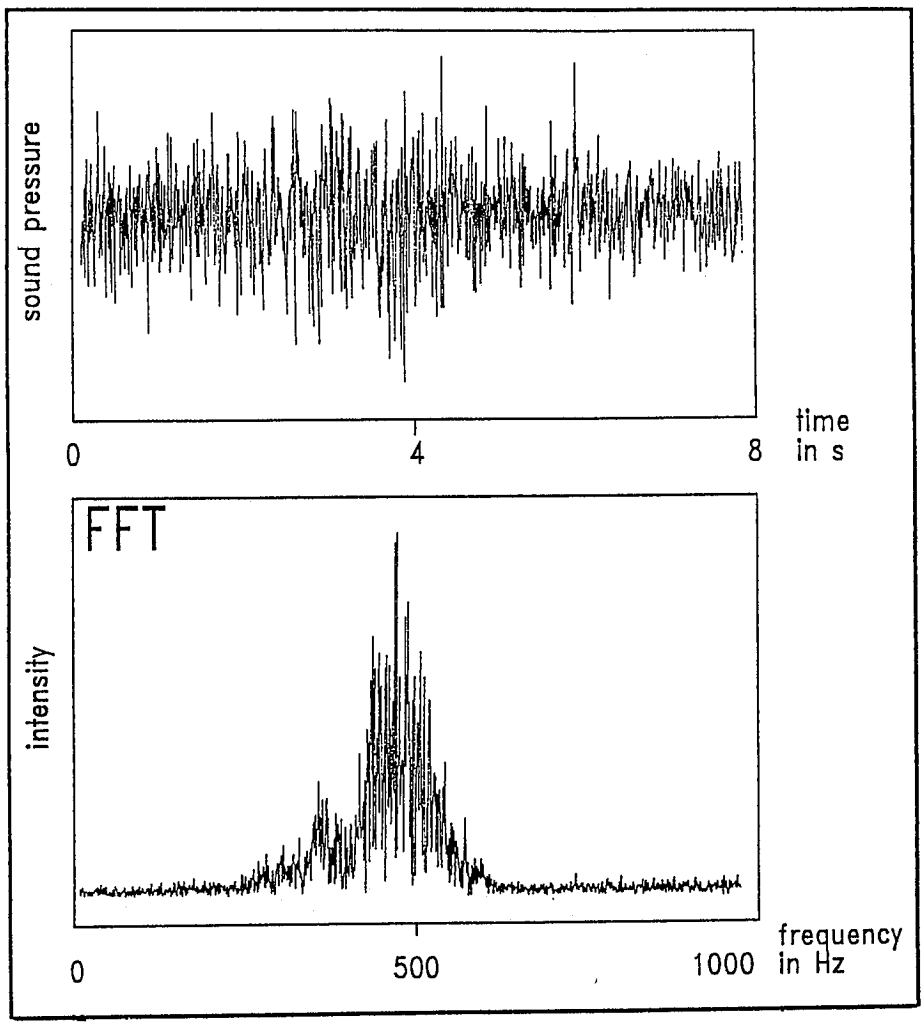

Figure 6 Sound analysis in case of cutting through

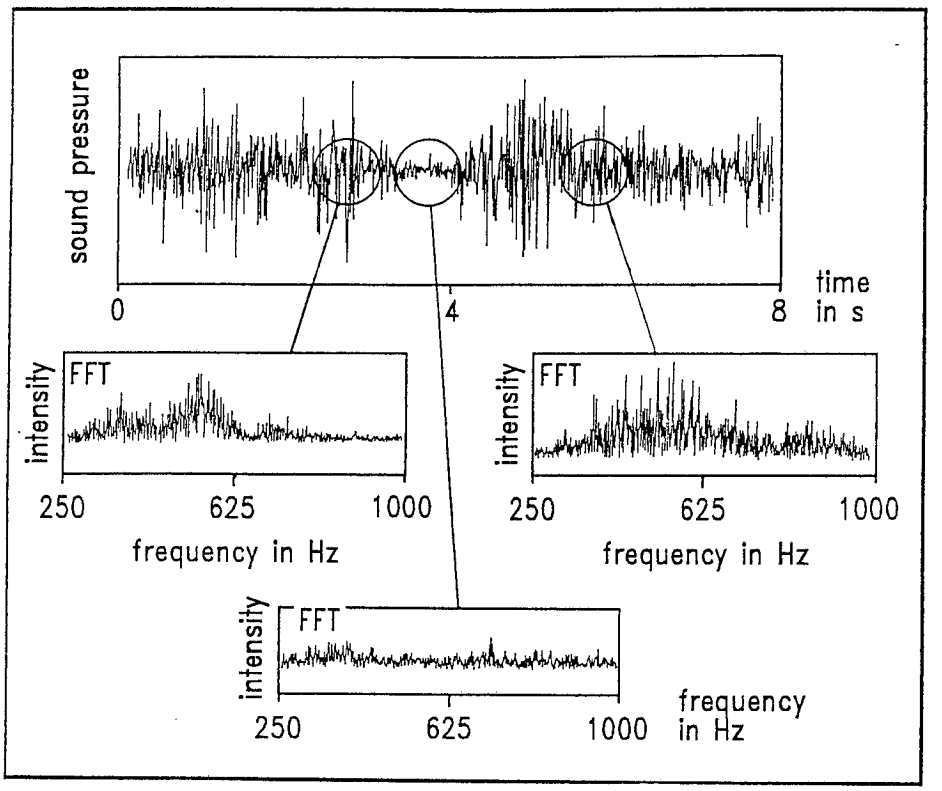

Figure 7 Sound analysis in case of kerfing

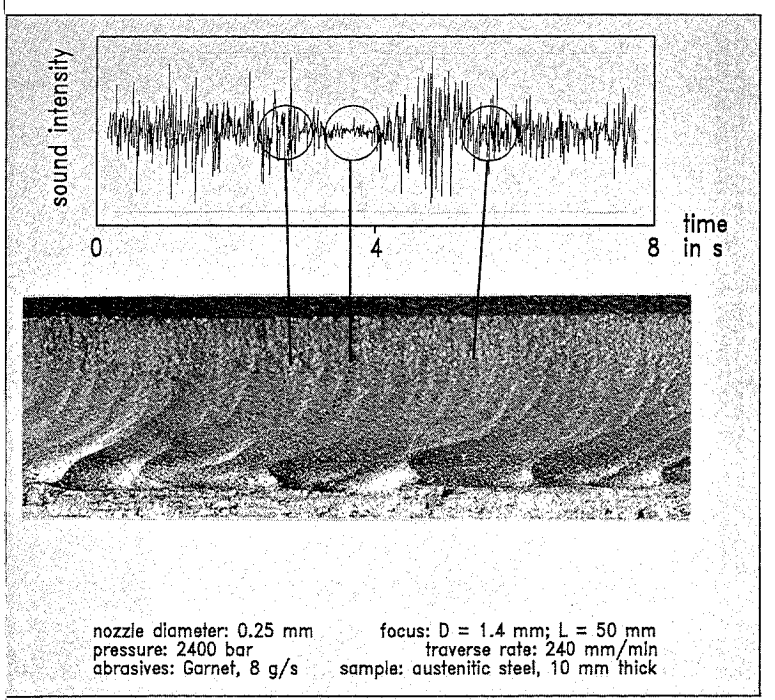

Figure 8 Kerf geometry and sound intensity

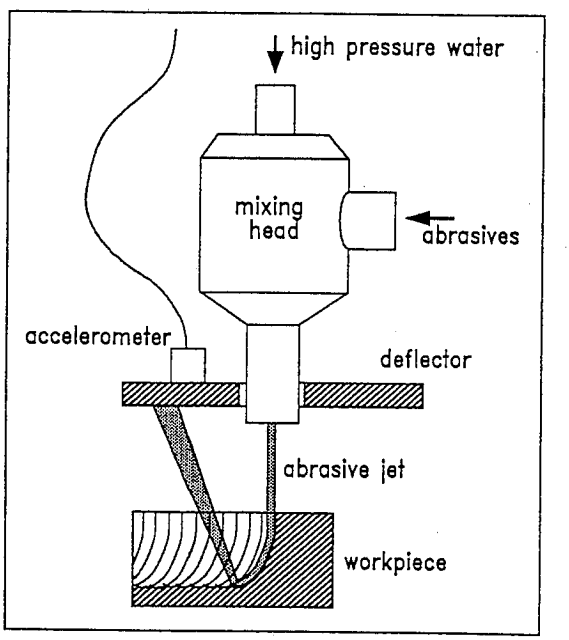

Figure 9 Detection of kerfing by an accelerometer

6th American Water Jet Conference
August 24 - 27, 1991: Houston, Texas Paper 33

CUTTING WITH HIGH-PRESSURE ABRASIVE SUSPENSION JETS

Mohamed Hashish
QUEST Integrated, Inc.
Kent, Washington

ABSTRACT

Parametric cutting results obtained with high-pressure abrasive suspension jets (ASJs) are presented in this paper. Pressures up to 345 MPa were used to directly pump premixed abrasive suspensions through a relatively small-diameter nozzle (0.229 mm) to form an ASJ. Although considerable wear was observed in critical system components, such as nozzles and valves, significant improvements in cutting performance were observed compared to the results of cutting with an abrasive-waterjet (AWJ). For example, the ASJ cuts were 2 to 5 times deeper than those of the AWJ. Furthermore, a preliminary cost analysis indicates that the running cost of a jet cutting system is dominated by the rate of abrasive consumption. Thus, the ASJ operating at elevated pressures and with a reduced abrasive flow rate appears to be more economical than an ASJ working at lower pressures.

1.0 INTRODUCTION

Abrasive-waterjet (AWJ) technology was introduced commercially in 1983. Since that time, substantial advances have been made in all facets of AWJ technology, including our basic understanding of the cutting process, hardware improvements, and software developments. New applications in drilling, turning, and milling are constantly emerging, and significant efforts are being made to develop the AWJ into a "machine tool" for the next generation of processing technologies. Despite these efforts, new jetting processes need to be developed to fill existing performance gaps and extend current machining capabilities.

The pumping of premixed abrasive suspensions is an alternative technique that improves upon and extends the capabilities of the AWJ. An AWJ is formed by entraining particles into a high-velocity waterjet, whereas an abrasive suspension jet (ASJ) is formed by directly pumping an abrasive suspension through a nozzle. This results in a thinner cutting jet and potentially more efficient machining performance (Hashish, 1990).

The idea of pumping solid suspensions for the purpose of cutting was first attempted in oil well drilling, where steel shot was added to the mud and pumped through the nozzles of drill bits (see Maurer, 1980, for details). Significant improvements in drilling rates were observed, but many hardware components quickly failed. Hashish (1982) reviewed the different methods of forming an AWJ, which included the direct pumping approach, and their advantages and disadvantages. Exploratory tests conducted at 138 MPa using an isolator-type batch system (Hashish, 1986) demonstrated the great potential of the direct

pumping of abrasive suspensions for cutting, but the sapphire nozzles lasted only a few minutes. To reduce the problems of both wear and suspension preparation associated with high-pressure systems, Fairhurst et al. (1986) developed a low-pressure (up to 69 MPa) batch-pumping system. The reduced pressure was compensated for by using relatively high abrasive flow rates (to 180 g/s). Bloomfield and Yeomans (1991) reported cutting data using this system that indicated its capability for metal cutting. Hollinger et al. (1989) conducted tests using an abrasive suspension jet at pressures up to 104 MPa to demonstrate the thin kerf cutting capability of the ASJ. They observed that the nozzle (d_n ~ 0.254 mm) plugs if the suspension concentration exceeds about 10%. Also, the ASJ at a pressure of 104 MPa resulted in cuts with less depth than those produced by a lower pressure (69 MPa) ASJ. This was attributed to the jet's loss of coherency at higher pressures.

This paper presents the results of a preliminary experimental study of abrasive suspension jets. The ranges of the cutting parameters explored in this paper differ considerably from those used by Hollinger et al. (1989) and Bloomfield and Yeomans (1991), as shown in Figure 1; additional parameters are listed in Table I.

2.0 ASJ PROCESS PARAMETERS

The process parameters of an ASJ are as follows:

- Pressure
- Nozzle Geometry
  - Exit diameter
  - Shape
- Suspension Parameters
  - Solid concentration
  - Abrasive material
  - Abrasive particle size
  - Abrasive flow rate
  - Rheological characteristics of suspension
- Cutting Parameters
  - Traverse rate
  - Standoff distance
  - Other

Depending on the direct pumping approach that is used, the abrasive flow rate may or may not be an independent parameter. For example, with the direct pumping system shown in Figure 2a, the abrasive flow rate will depend on other parameters, such as the pressure, nozzle geometry, and suspension characteristics. With the setup shown in Figure 2b, however, the abrasive flow rate can be controlled independently of other parameters, but the suspension concentration will vary according to selected

parameters. The approach shown in Figure 2a is used in this study because of its advantage in accurately controlling the suspension parameters.

When comparing the cutting performance of an ASJ and an AWJ, the pressure, abrasive flow rate, and hydraulic power must be the same. If the measured flow rate to the high-pressure pump is Q_t, then the abrasive flow rate, m_a, is

$$m_a = \frac{Q_t}{\rho_w} \cdot c_w \tag{1}$$

where c_w is the concentration by weight of the abrasives in the suspension. The equivalent waterjet orifice diameter to be used in an AWJ nozzle to yield the same power consumption would be

$$d_n = K\left(\frac{Q_t}{\sqrt{P}}\right)^{0.5} \tag{2}$$

where K is a numerical constant that depends on the units used. The use of the same abrasive material is also essential for an accurate comparison. However, the abrasive particle size does not need to be equal. For ASJs, the abrasive particle size is determined by the nozzle diameter, whereas in AWJs, the mixing tube diameter, not the waterjet orifice diameter, is the important factor to consider. The mixing tube diameter in an AWJ is typically 2 to 3 times greater than the waterjet orifice diameter, so larger abrasive particles can be used than with an ASJ, which may yield more efficient cutting. A meaningful comparison of these methods at the same pressure and power levels should use the optimum abrasive size for each method.

3.0 ADVANTAGES OF ABRASIVE SUSPENSION JETS

ASJs appear to have several advantages compared to AWJs. Hashish (1990) showed with a simple analysis that the direct pumping of abrasive suspensions is more efficient than the entrainment of abrasives if the hydraulic and suspension parameters are the same. For example, the energy transfer efficiency for an ASJ is estimated to be 20% greater than that for an AWJ at concentration ratios of 20%. At higher concentration ratios, the degree of improvement is higher.

Other advantages of the ASJ include the following:

- Small-diameter jets can be produced for thin kerf cutting.
- Jets with more power density (power per unit area of the nozzle) can be produced, thus reducing the required power levels.
- Relatively small nozzles can be made for operations in tight spaces, such as inside tubes.
- Abrasive feed is not limited by the jet pump concept of the AWJ nozzle, which allows higher abrasive flow rates to be pumped with the ASJ than with the AWJ.

The ratio of the energy transfer efficiencies for the ASJ and AWJ methods is termed α and can be expressed as (Hashish, 1990)

$$\alpha = \frac{C_{vs}^2}{\eta^2(1+c_w)} \tag{3}$$

The ratio of the particle velocities, β, is

$$\beta = \frac{C_{vs}}{\eta}\sqrt{\left[\frac{(s+c_w)(1+c_w)}{s}\right]} \tag{4}$$

The ratio for the energy density, γ, is

$$\gamma = \frac{C_{vs}^2}{\eta^2(1+c_w)}k\left[\frac{(s+c_w)(1+c_w)}{s}\right]^{3/2} \tag{5}$$

where k is a factor representing the ratio between the areas of the AWJ and ASJ nozzles. The above simplified equations indicate that higher values of α, β, and γ will be obtained at higher suspension concentrations, which correspondingly increases the operating cost and reliability of the equipment.

4.0 EXPERIMENTAL INVESTIGATION

The results of experimental tests with AWJs and ASJs are presented in this section. First, however, the experimental setup and parameters are described.

4.1 Experimental Setup and Parameters

To pump the abrasive suspensions to high pressures (up to 345 MPa), a high-pressure vessel was used as an isolator. Figure 3 shows a photograph of the setup. The abrasive suspension is prepared in an air-pressurized hopper (a paint tank was used) and then fed into the high-pressure vessel under air pressure (0.69 MPa), while allowing the water in the vessel to vent. The upper side of the vessel is attached to a high-pressure pump. By switching the valves above and below the high-pressure vessel, the suspension can be pumped into the vessel or discharged through the nozzle.

The abrasive suspension was prepared by adding abrasives to a mixture of water and Superwater,* a substance that contains a polymer. The Superwater was added to water in concentrations of up to 3% by weight. Then the abrasive particles were sieved to remove any larger size particles that could plug the nozzle. While the polymered water was agitated at a slow speed (100 rpm), the abrasives were added

*Superwater is a registered trademark of Berkeley Chemical Research, Inc.

into the vortex generated by the agitation device. Abrasive suspensions of 6%, 12%, 24%, and 48% were prepared using this method.

A number of settling tests were conducted to check the abrasive suspension capability of Superwater. The results indicated that the polymered water adequately suspended the abrasives during the duration of the test.

The following set of parameters was selected to conduct the cutting experiments:

- Pressure: 104, 138, 207, 276, and 345 MPa
- Concentration: 6%, 12%, 24%, and 48%
- Traverse rate: 17, 34, and 68 mm/s

Full factorial tests were completed using these parameters in different combinations while the following parameters were held constant:

- Nozzle diameter: 0.229 mm
- Abrasive material: Garnet
- Abrasive particle size: 220 mesh
- Suspension fluid: Water with 3% Superwater
- Standoff distance: 1.5 mm

The average flow rate of the suspension was determined by dividing the volume of the charged portion of the high-pressure vessel (under the isolator) by the time it takes to discharge that volume. The abrasive flow rate can be calculated from this average suspension flow rate using Equation (1). Figure 4 shows a plot of abrasive flow rate versus pressure for the different concentrations of suspensions. The flow characteristics of the suspension were observed to be similar to those of Newtonian fluids. The average coefficient of discharge was calculated to be between 0.65 and 0.80. No efforts were made in this study to alter the suspension's rheological characteristics for optimized ASJ structure and flow characteristics.

4.2 Cutting Results

The cutting tests were conducted on thick (25.4-mm) aluminum samples (6061-T6) to obtain different depths of cuts for comparison. Figure 5 shows the effect of pressure on the depth of cut, obtained at different traverse rates, for the case of a 48% suspension concentration. The same figure shows the specific kerfing area, expressed as the rate of kerf area ($h \cdot u$) generated per unit of hydraulic power input. The input power (E) is calculated from the pressure (P) and the measured flow rate (Q_t) as follows:

$$E \propto P \cdot Q_t \tag{6}$$

It can be seen from Figure 5 that the specific kerfing area peaks at a certain pressure (276 MPa) in the case of a high traverse rate (68 mm/s) while it decreases with pressure at slower traverse rates. This indicates that low pressures are sufficient for efficient cutting in aluminum. For harder-to-cut materials in which shallower cuts are obtained (similar to aluminum cutting at high traverse rates), optimal specific kerfing areas will occur at higher pressures. That is, the harder the material is to cut, the higher the pressure at which the specific kerfing area peaks.

The specific kerfing area should not be regarded as a term describing the effectiveness of the ASJ or the AWJ process, especially when comparing cuts of different thicknesses. This is because in shallow cutting (at reduced pressures or increased traverse speeds), the drag forces on the jet are less than those encountered in deep cutting. Accordingly, shallow cutting will often appear to reflect more efficient conditions. The appropriate term for effectiveness depends on the application. Probably a more versatile effectiveness term is the cost per unit productivity parameter (see Section 4.0).

Figure 6 shows the effect of suspension concentration in an ASJ on the depth of cut at different pressures. The trends shown here are generally similar to those of an AWJ. Note that the rate of increase for the depth of cut with increasing suspension concentration is higher for higher pressures (Hashish, 1990). However, a reduced abrasive suspension concentration should be used for low-pressure operation.

Observe that at lower pressures (the lower curves in Figure 6) increasing the suspension concentration results in less improvement in depth of cut than observed with higher pressures. This suggests that the use of abrasive particles to perform cutting is enhanced by increasing the pressure. To increase the abrasive flow rate, the water flow rate should correspondingly increase.

To compare the AWJ and the ASJ cutting performances, the same abrasive flow rate, pressure, and hydraulic power ranges were used as previously stated. The corresponding size of the waterjet orifice was calculated from Equation (2). The mixing tube diameter and abrasive size were selected to yield the best (i.e., deepest) cutting results. The following AWJ parameters were used to cut the same aluminum samples for comparison with ASJ cutting:

- Mixing tube diameter: 0.762 mm
- Mixing tube length: 75 mm
- Garnet mesh size: 120

Two suspension concentrations were selected to demonstrate the case of a typically optimum loading ratio (12%) in the AWJ and another case (24%) where the AWJ may be overloaded with abrasives. Figure 7 shows the depth of cut, using the above conditions, for both the AWJ and the ASJ. Observe that the cutting depth obtained with the AWJ at about 200 MPa is the same as the depth obtained with the ASJ at about 100 MPa due to the significantly increased power density, which is estimated at about 390%. Also, it is observed that the depth of cut ratio increases with increased pressure. This increase

implies that more advantages are obtained from the direct pumping approach at high pressures than at low pressures.

The data reported in this study for aluminum cutting were compared to those reported in Hollinger et al. (1989) and Bloomfield and Yeomans (1991) as shown in Figure 8. Observe that both the specific kerfing area and the erosion factors observed in this work are significantly higher than those reported in the other studies. One reason could be due to the higher pressure range used in this work. Also, the reported data are for through cutting, so deeper cuts or faster cutting speeds may have been obtained. However, even doubling or tripling the cutting speed or depth of cut would still result in a wide discrepancy in the data.

Figure 9 shows sample cuts made by an ASJ in aluminum. Although the cuts are thinner than those produced by an AWJ, all other kerf and surface characteristics are similar to those obtained by an AWJ.

4.0 COST

The performance of machining systems may not always be judged by economical factors. The capability of a machining process to produce the required quality may be more important than a reduced cost obtained with another process. However, for a single machining process where the required quality can be obtained at different combinations of parameters, the question of cost becomes important. Then the optimal set of parameters must be determined in order to minimize the cost.

The full economic optimization of AWJ or ASJ machining is beyond the scope of this paper. However, to shed some light on important cost elements, a simple estimate is presented here.

The initial cost of an ASJ pump can be estimated to be approximately $30,000 for a single intensifier pump, as was used for the experimental results presented in this paper. The additional cost for the abrasive suspension isolator system is conservatively projected to be approximately $4,000 per kW. These costs are approximations and do not include operating or maintenance costs. The costs of the manipulator, labor, physical facilities, supporting equipment, and training are not considered here.

The primary operating expenses are the costs for abrasives and nozzle wear. Conservatively, the abrasive cost is about $0.88 per kg, including sieving and suspension costs. The projected cost for nozzle wear is about $5/hour at a nominal condition of 207 MPa and 7.5 g/s. It is assumed that nozzle wear costs are linearly proportional to the pressure and abrasive flow rate. Other running costs include maintenance costs, which will be proportional to the power level used, the cost of power, and the cost of disposal.

Figure 10 shows a bar diagram of hourly costs, including initial, operating, and maintenance costs, combining different elements of an ASJ system at three pressure levels. Note that the abrasive cost is the most significant factor, amounting to more that 50% of the overall cost.

The specific costs, expressed as the cost per unit area generated, for the conditions presented in Figures 5 and 6 are presented in Figures 11 and 12, respectively. Observe that increasing the pressure reduces the specific cost. This fact supports the previous discussion that stated that the use of hydraulic power through the specific kerfing area (see Figure 5) is not a consistent judgement criterion, at least not with the added cost of cutting. The abrasive consumption rate, which dominates the hourly cost, should be used instead of the hydraulic power. Accordingly, the erosion factor, which is defined as the material removal per unit mass of abrasives, is a better criterion for determining the actual and practical process feasibility. The material removal rate may be expressed as the total weight or volume removed per unit width of cut. Figure 13 shows the erosion factor for the data presented in Figure 6, which matches the trends of costs shown in Figures 11 and 12.

5.0 CONCLUSIONS

The following conclusions can be drawn from this study:

- Using the same abrasive flow rate, pressure, and power, the depth of cut obtained with an ASJ is at least double that obtained with an AWJ.
- High-pressure (up to 345 MPa) ASJ systems are more effective using abrasives for material removal than low-pressure (up to 70 MPa) ASJ systems.
- A high-pressure (over 250 MPa) AWJ matches or exceeds the performance of a low-pressure (100 MPa) ASJ system.
- It is more economical to operate an ASJ system at higher pressures than at low pressures due to the improved utilization of abrasive particles in cutting.
- The abrasives are the major expense in AWJ and ASJ systems. The erosion factor, rather than the specific kerfing area, is a better criterion for comparing the performances of the ASJ and the AWJ, as it better reflects the economics of the ASJ process.

6.0 ACKNOWLEDGEMENTS

The author is grateful to the National Science Foundation for supporting the work presented in this paper under the SBIR program (Grant No. ISI-8961341).

7.0 REFERENCES

Bloomfield, E. J., and Yeomans, M. J., "DIAJET - A Review of Progress," *Proc. of the First Asian Conference on Recent Advances in Jetting Technology*, Singapore, 1991.

Fairhurst, R. M., Heron, R. A., and Saunders, D. H., "DIAJET - A New Abrasive Water Jet Cutting Technique," *Proc. of the 8th International Symposium on Jet Cutting Technology*, Durham, England, BHRA, The Fluid Engineering Centre,1986.

Hashish, M., "Steel Cutting with Abrasive Waterjets," *Proc. of the 6th International Symposium on Jet Cutting Technology*, University of Surrey, U.K., BHRA Fluid Engineering, 1982.

Hashish, M., "Experimental and Theoretical Investigation of the Abrasive-Waterjet Cutting Process," Final Report to the National Science Foundation under Grant No. MEA-82-12878; also Flow Research Report No. 363, February 1986.

Hashish, M., "Abrasive-Fluidjet Machining Systems: Entrainment Versus Direct Pumping," *Proc.of the 10th International Symposium on Jet Cutting Technology*, Amsterdam, BHR Group Ltd., 1990.

Hollinger, R. H., Perry, W. D., and Swanson, R. K., "Precision Cutting with a Low Pressure, Coherent Abrasive Suspension Jet," *Proc. of the 5th American Water Jet Conference*, Toronto, Canada, U.S. Water Jet Technology Association, 1989.

Maurer, W. C., *Advanced Drilling Techniques*, The Petroleum Publishing Co., Tulsa, Oklahoma, 1980.

NOMENCLATURE

C_v	velocity coefficient for liquid flow
C_{vs}	velocity coefficient for slurry flow
c_w	concentration by weight of abrasives in suspension
d_n	waterjet orifice diameter
E	input power
h	depth of cut
K	numerical constant
k	coefficient
m_a	abrasive flow rate
P	pressure
Q_t	total flow rate
s	ρ_a/ρ_w
sod	standoff distance
α	ratio of energy transfer efficiencies
β	ratio of particle velocities
γ	ratio for energy density
η	$\eta_m C_v$
η_m	mixing efficiency
ρ_a	abrasive particle density
ρ_w	liquid (water) density

Table I. Range of Parameters of Current and Published Work on Abrasive Suspension Jets

Parameters		Range		
		This Paper	Hollinger et al. (1989)	Bloomfield & Yeomans (1991)
Pressure	MPa	104-345	52-104	35-69
Nozzle Diameter	mm	0.229	0.254	0.3-2.8
Abrasive Flow Rate	g/s	0.98-11.3	1.2-1.7	2.8-173
Suspension Concentration		6%-48%	10%	12%
Hydraulic Power	kW	1-10	0.6-1.7	2-72

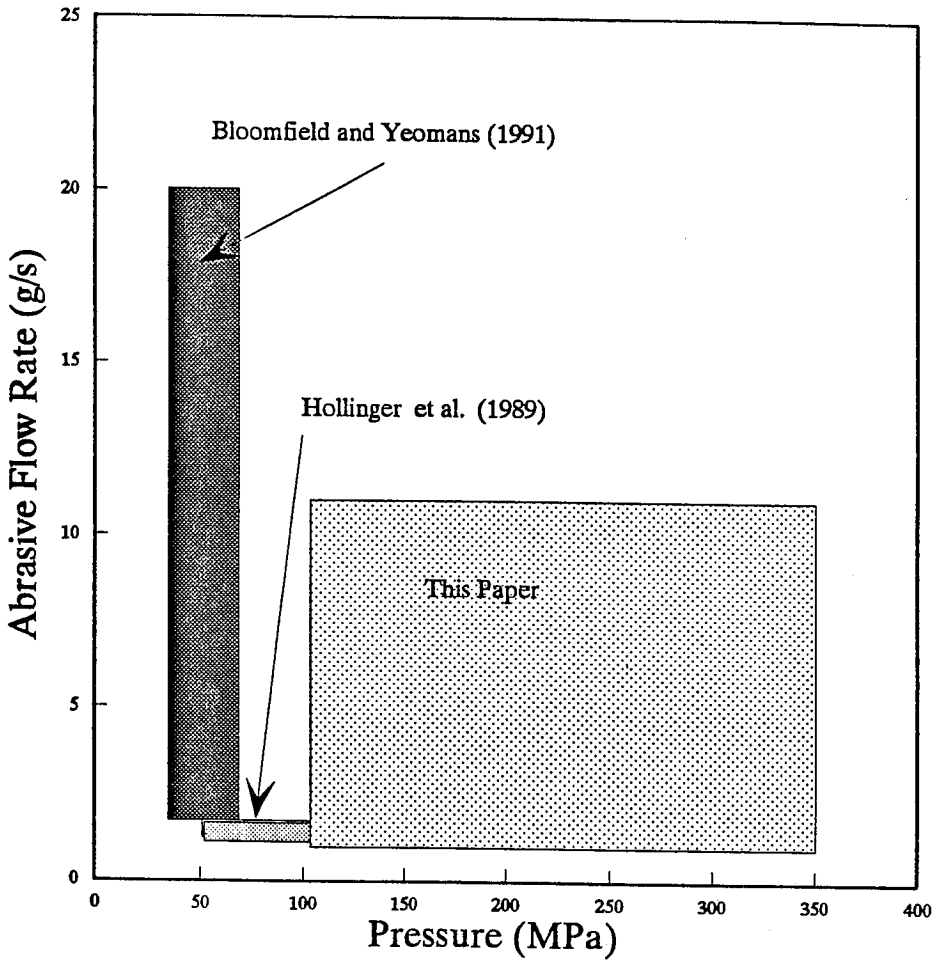

Figure 1. Ranges of Cutting Parameters Used in This Paper and in Other Comparable ASJ Studies

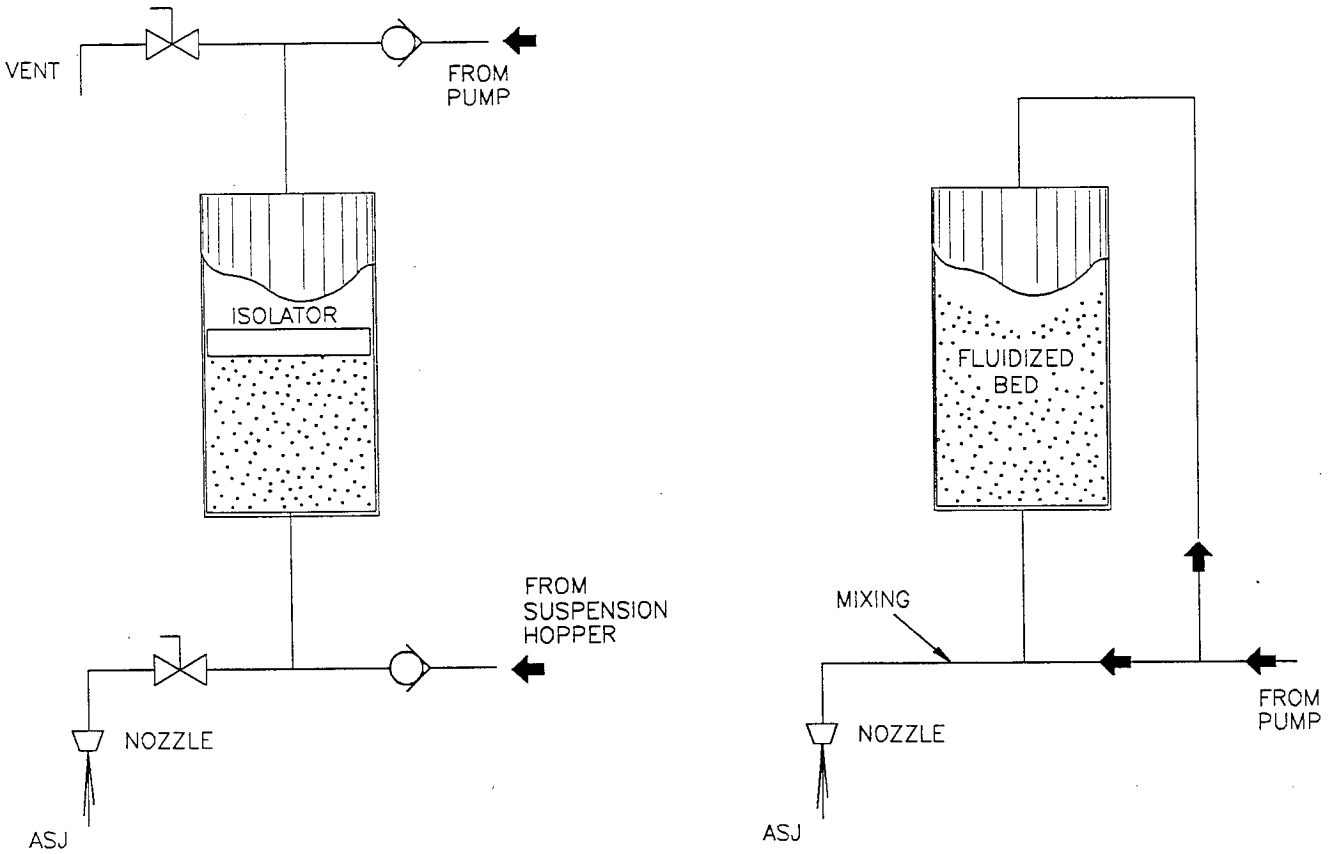

a. Direct pumping using an isolator

b. Direct pumping with downstream mixing

Figure 2. System Approaches for Pumping of Abrasive Suspensions

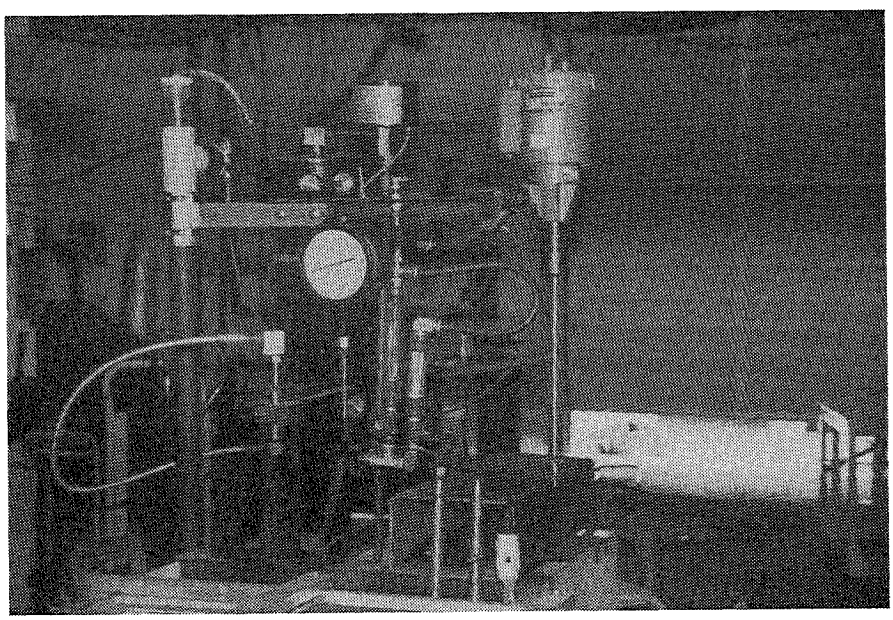

Figure 3. Experimental Setup

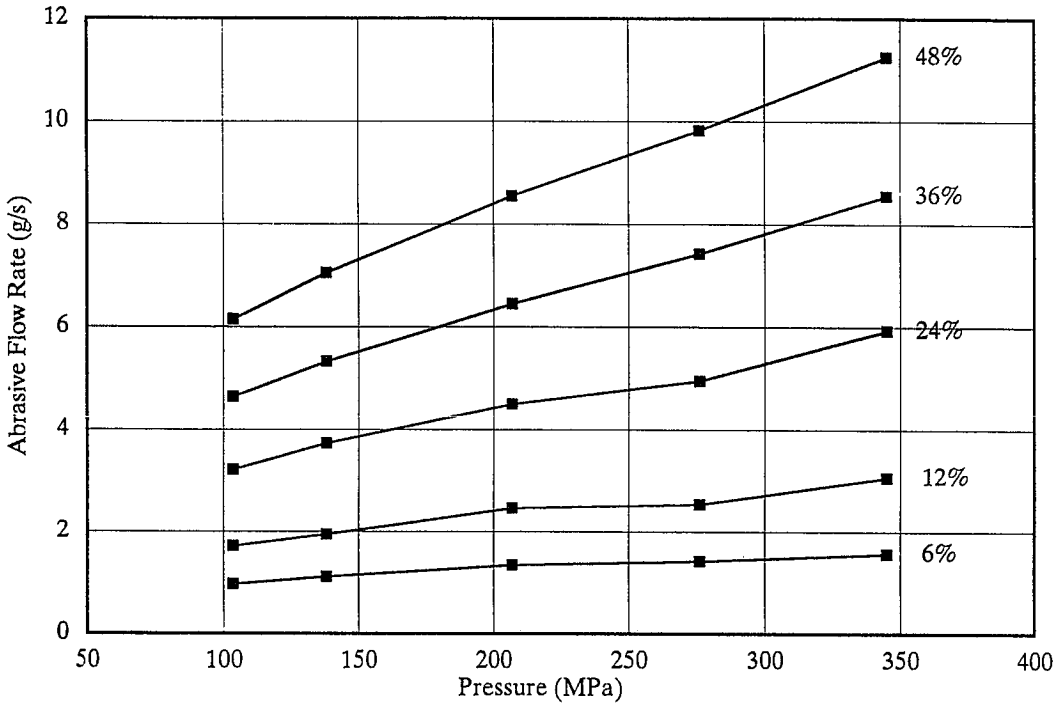

Figure 4. Measured Abrasive Flow Rate Through 0.229-mm-Diameter Nozzle at Different Pressures and Suspension Concentrations

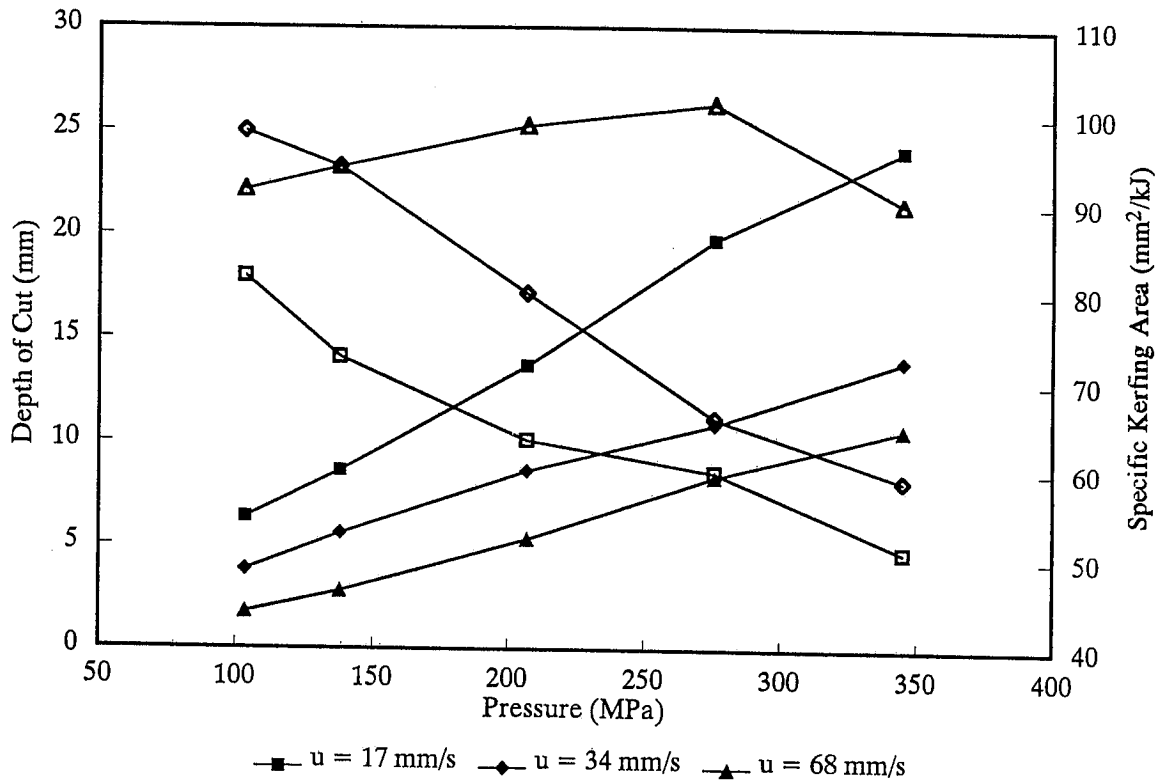

Figure 5. Effect of Pressure on Depth of Cut and Specific Kerfing Area in Aluminum Using an ASJ - Open symbols represent specific kerfing area; solid symbols represent depth of cut. Garnet mesh 80, d_n = 0.229 mm, sod = 1.5 mm, c_v = 48%.

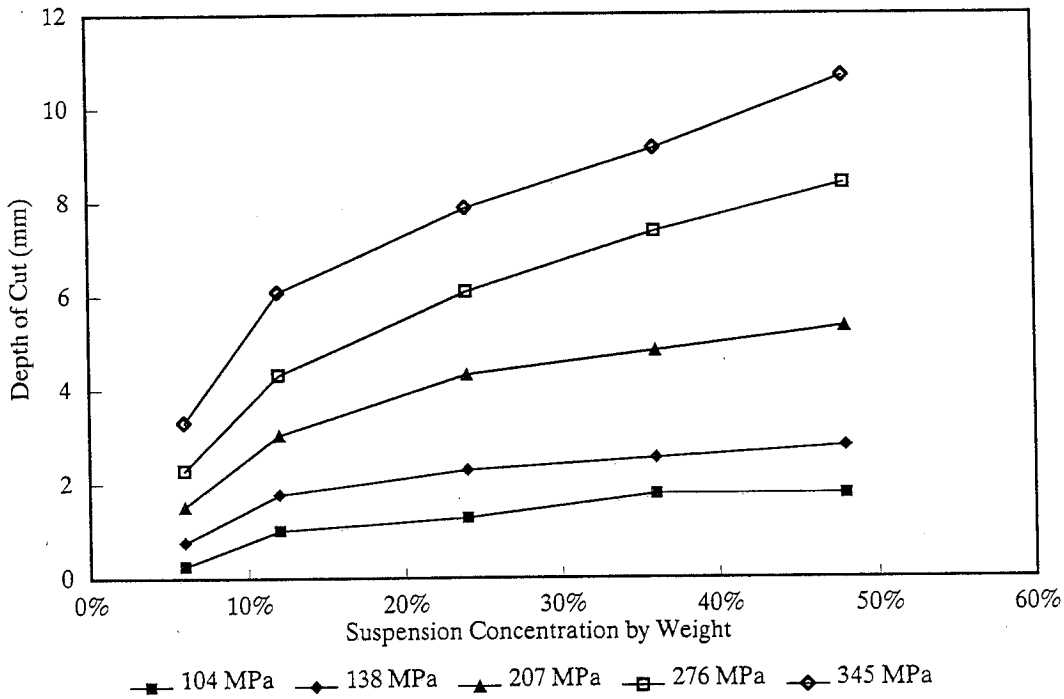

Figure 6. Effect of Suspension Concentration on Depth of Cut in Aluminum Using an ASJ - Garnet mesh 80, d_n = 0.229 mm, sod = 1.5 mm, u = 68 mm/s.

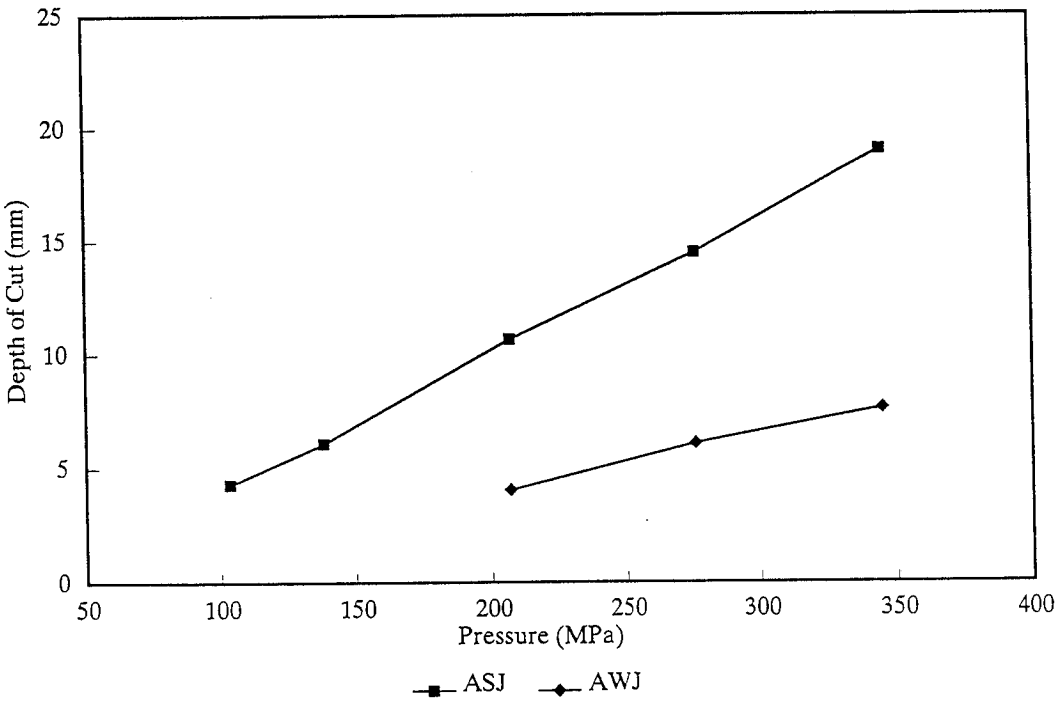

a. Suspension concentration of 24%

Figure 7. Comparison Between ASJ and AWJ for Aluminum Cutting - Garnet mesh 80, d_n = 0.229 mm, sod = 1.5 mm, u = 17 mm/s.

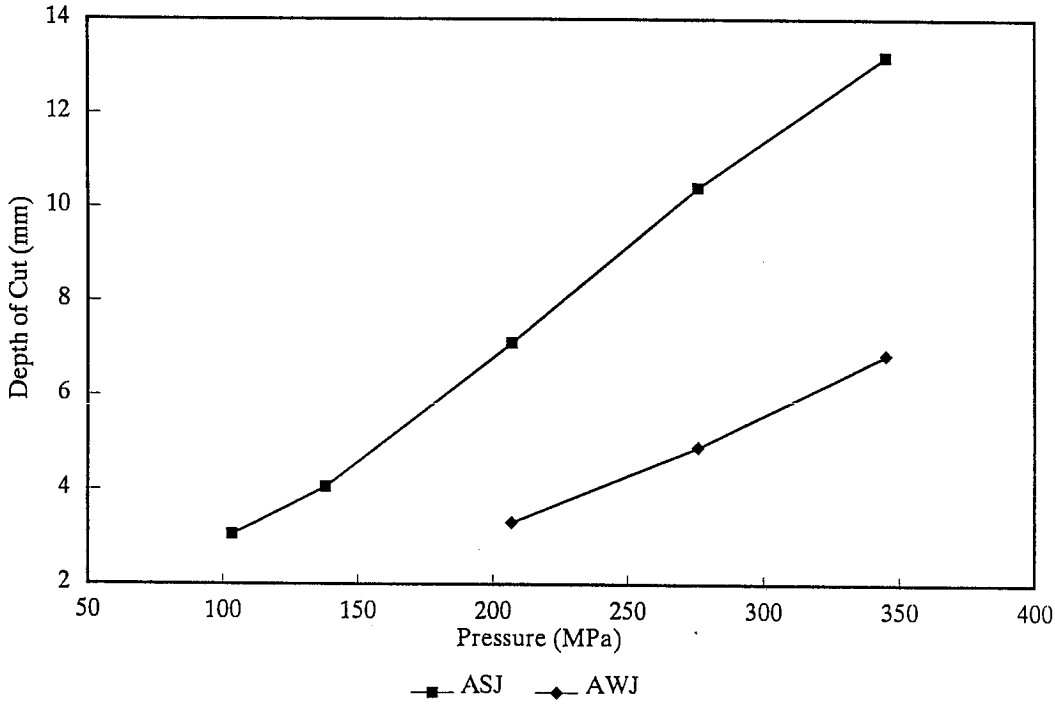

b. Suspension Concentration of 12%

Figure 7. Comparison Between ASJ and AWJ for Aluminum Cutting (Cont.) - Garnet mesh 80, d_n = 0.229 mm, sod = 1.5 mm, u = 17 mm/s.

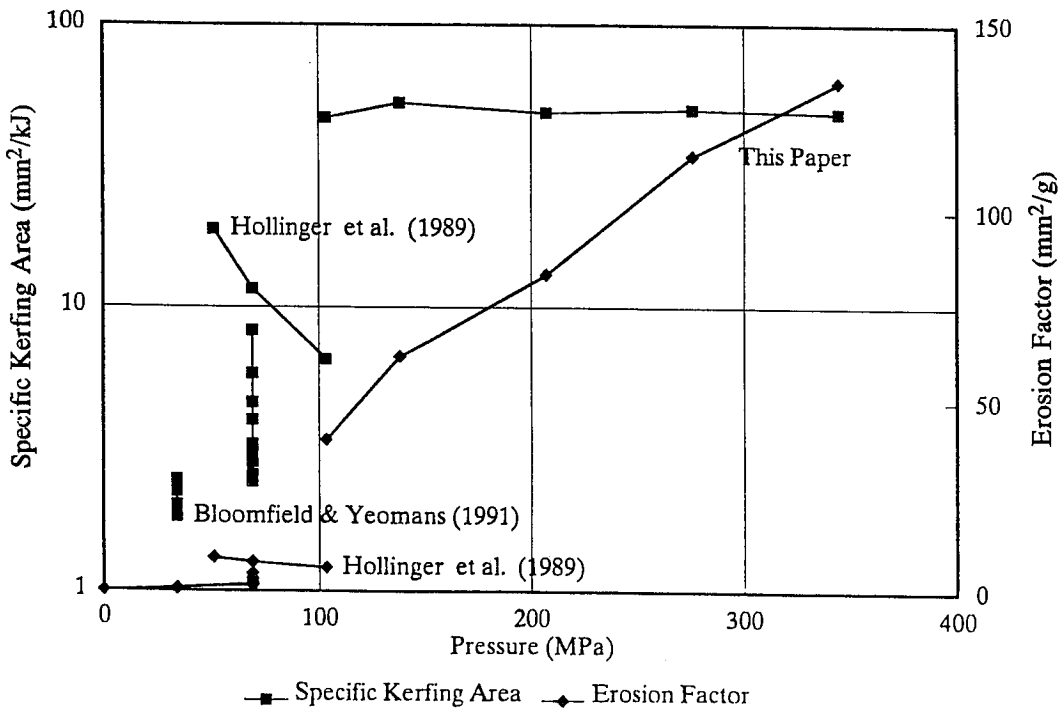

Figure 8. Present Data Compared to Other ASJ Studies

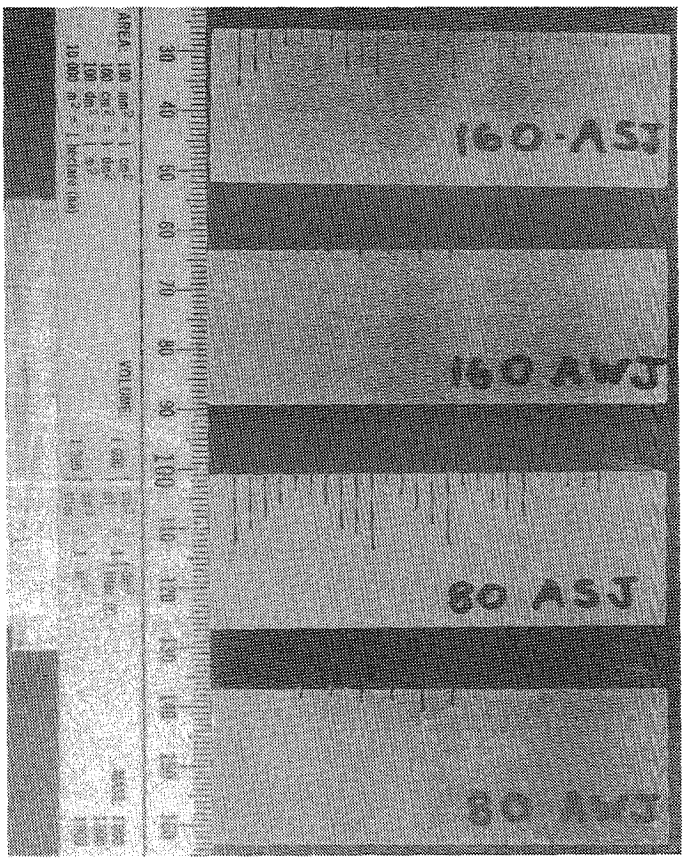

Figure 9. Sample Cuts Made in Aluminum

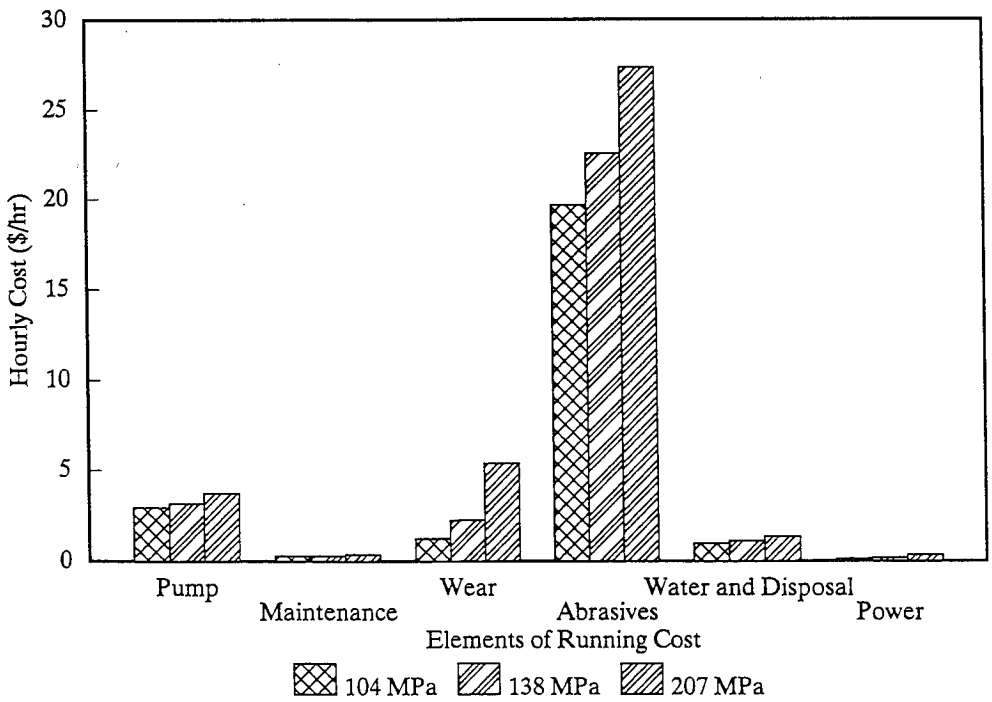

Figure 10. Cost Elements of ASJ Operation at Suspension Concentration of 48% and d_n = 0.229 mm

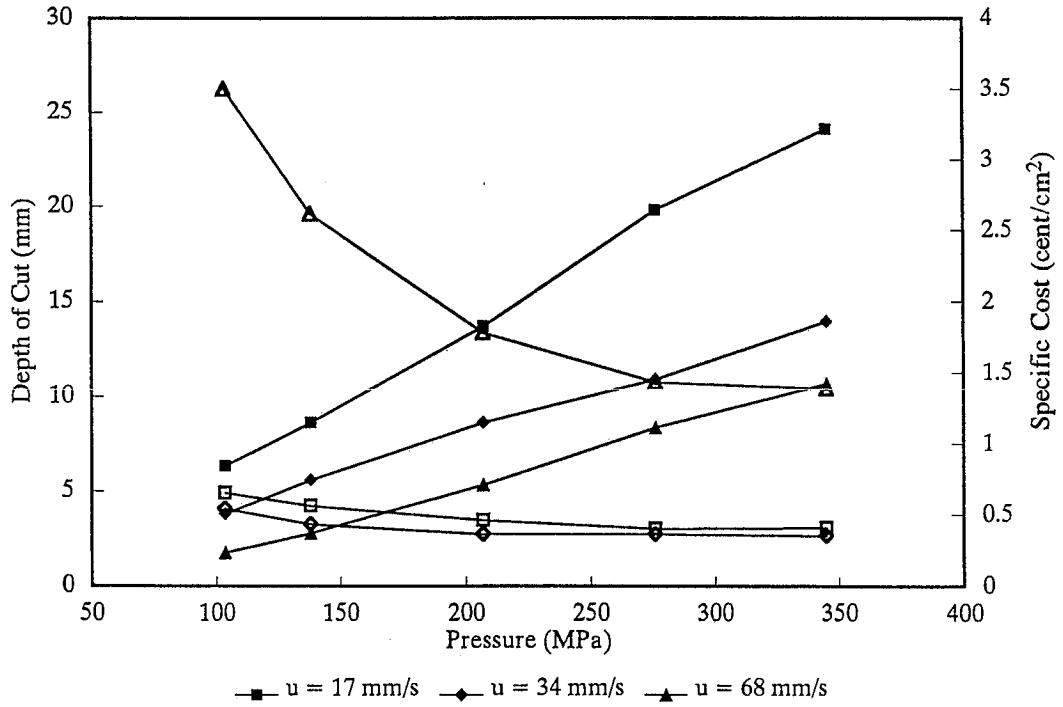

Figure 11. Effect of Pressure on Depth of Cut and Corresponding Specific Costs - Open symbols represent specific cost; solid symbols represent depth of cut. Garnet mesh 80, d_n = 0.229 mm, sod = 1.5 mm, c_v = 48%.

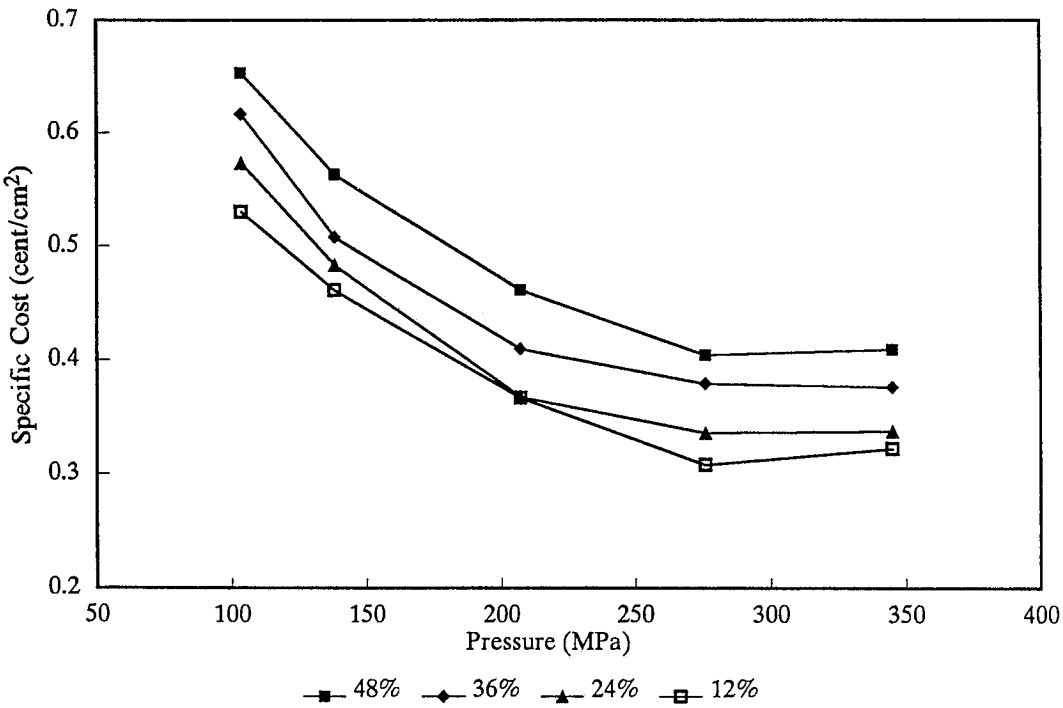

Figure 12. Effect of Pressure on Specific Cost at Different Suspension Concentrations

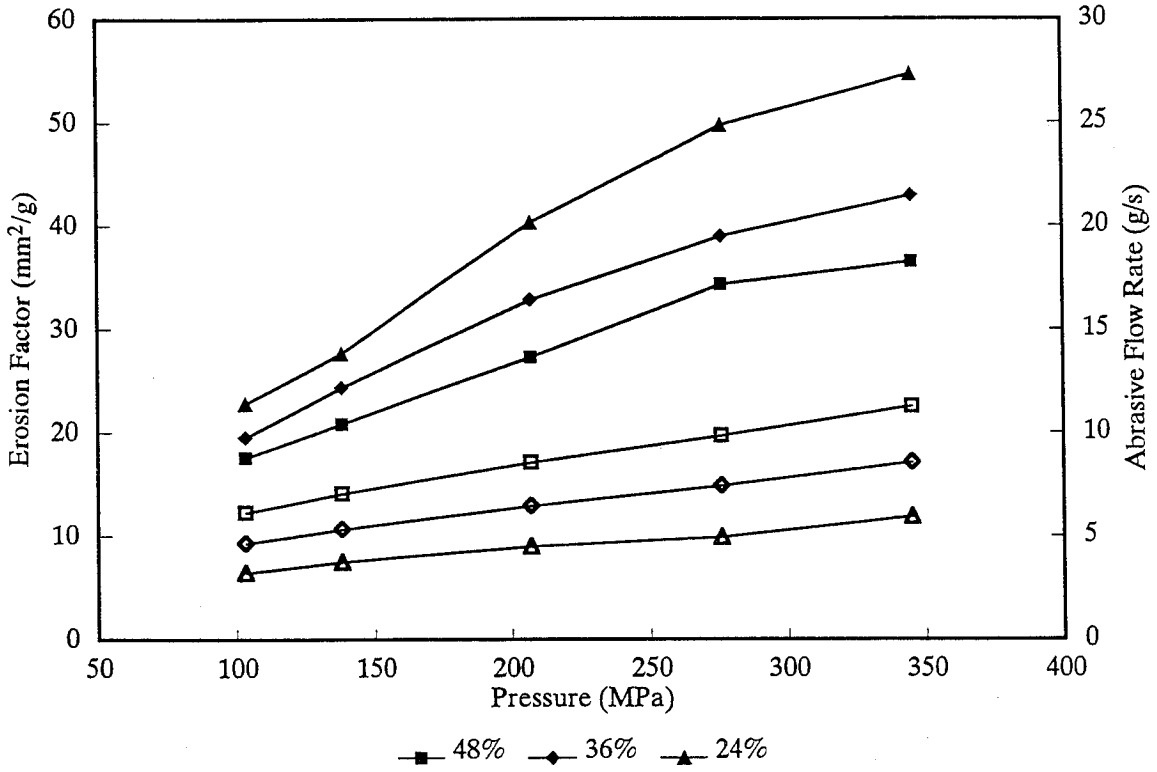

Figure 13. Effect of Pressure on Erosion Factor and Abrasive Flow Rate in Aluminum - Open symbols represent abrasive flow rate; solid symbols represent erosion factor. Garnet mesh 80, d_n = 0.229 mm, sod = 1.5 mm, u = 17 mm/s.

6th American Water Jet Conference
August 24 - 27, 1991: Houston, Texas Paper 34

A newly developed spiral nozzle for abrasive acceleration in jet cutting applications

K.Horii, Y.Matsumae
Shirayuri Women's College, JAPAN

X.M.Cheng, S.Kage, H.Shoda, B.Hashimoto
Waseda University, JAPAN

T.J.Kim
University of Rhode Island, USA

ABSTRACT

A spiral flow nozzle has been developed to improve the cutting efficiency in abrasive jet cutting applications. The abrasive water jet cutting is generally dependent on the efficiency of the abrasive acceleration and jet stream energy transfer to target material surface. The average abrasive velocity generated by the spiral nozzle is approximately 20% higher than that of the conventional nozzle. The spiral-flow jet stream erodes the target material surface more effectively, because it is self-focused and the azimuthal velocity component of spiral flow decreases the chance of collision between the direct and rebounded jets. The steeper axial velocity distribution and presence of an azimuthal component of the spiral flow jet contribute to the enhanced performance over a conventional jet.

Organized and Sponsored by the Water Jet Technology Association.

1.0 INTRODUCTION

The water jet cutting process has recently been introduced in many industrial applications. However, it has not been sufficiently developed to allow for the precision machining of high performance materials such as super alloys, ceramics, and composites. One of the essential approaches for achieving the high accuracy of AWJ machining is to increase the jet stream momentum as well as creating a stable jet stream at the exit of the mixing tube.

The jet diameter, the coherent jet stream length, and the collision between the direct and rebounded jets can be controlled up to a certain degree by adjusting several key water jet process parameters.

As a preliminary experiment, a nozzle with an annular slit connected to a conical cylinder has been developed. This nozzle creates a spiral-flow jet stream which is much more structured than a conventional turbulence jet resulting in an efficient cutting environment.

This paper presents the design analysis of a newly developed device from the perspective of fluid deformation.

2.0 EXPERIMENTS

2.1 SPIRAL JET APPARATUS

The development of new water jet mixing nozzle is based on the spiral flow theory as illustrated in Fig.1. To generate a spiral flow, a nozzle with an annular slit is connected to a conical cylinder, then pressurized water is fed through the sides of nozzle assembly into a buffer area through a slanted annular slit, and into the conical cylinder. The annular jet creates an abrasive-port suction which takes in additional flow through the nozzle entrance. Due to the Coanda effect of the annular jet attached to the nozzle walls, the flow-pattern at nozzle's downstream becomes a spiral flow that is much more structured than that of a typical turbulent jet at the same mass-flow rate. The spiral flow is more effective for abrasive capture and acceleration.

For the purpose of comparison, a conventional jet was also generated by using an ejector of the same nozzle diameter, 8mm at the tip.

2.2 FOCUSING AND STABILITY EXPERIMENTS

In order to compare the jet focusing characteristics of the spiral-flow and conventional jets, water was stored in the suction port of the nozzles. The water pressure of the spiral nozzle was $2.4\text{kgf}/\text{cm}^2$ at the section 4 shown in Fig.1, and that of the conventional nozzle was $2.3\text{kgf}/\text{cm}^2$. Both nozzles had a flow rate of $14.6l/\text{min}$, and the calculated velocity near the tip was $4.8\text{m}/\text{s}$ resulting in the Reynolds number of 4.5×10^4.

Measurements of the jet stream diameters near and at 34cm away from the nozzle tip show that the spiral-flow jet has a smaller radius than the conventional jet, as shown in Fig.2.

To study the pattern of azimuthal velocity component, the photographs using a light sheet method were taken as the spiral-flow jet was injected into water as shown in Fig.3. It was concluded that the spiral-flow jet has a steeper axial velocity distribution regardless of the existence of azimuthal component.

2.3 JET COLLISION

It has been known that the collision between the direct and rebounded jets greatly decreases the jet cutting efficiency. To study the jet collision phenomenon, photos were taken, using a light sheet method, from the opposite side of the glass as the jet impinges on the target materials as shown in Fig.4.

With the spiral-flow jet, very few air bubbles resulted from the collision with the rebounded jet was observed, while the turbulence jet produced a significant amount of air bubbles. These results indicate that the spiral-flow jet impinges on the target surface more effectively, having less chance of collision with the rebounded jet.

2.4 ABRASIVE ACCELERATION

The abrasive velocities of both air jets were measured using the stroboscope method. The air jet velocity was set to be $90\text{m}/\text{s}$ at the nozzle tip in accordance with the same Reynolds number 4.5×10^4 used for the water jet. The spiral-flow jet's abrasive acceleration rate was found to be $22\text{m}/\text{s}$ which is about 20% higher than $18\text{m}/\text{s}$ that of the conventional jet.

3.0 RESULTS AND DISCUSSION

3.1 SPIRAL JET FOCUSING

The experimental results, shown in Fig.5, reveal that the spiral-flow jet is tightly formed due to a higher focusing ability, while the conventional jet tends to disperse. The focusing ability of these two types of jets were measured quantitatively and the results were compared.

The velocity distribution of the air jet was measured using a fiberoptic laser anemometer (10W He-Ne Laser), and the results of the axial velocity measurements, v_z at z/d=1.25, 2.5, 3.75 and 5.0 from the nozzle tips are shown in Fig.6. It was found that, compared to the conventional jet, the spiral-flow jet attains the higher axial velocity and the steeper velocity distribution.

The focusing ability of the spiral nozzle assembly is described in terms of half width, potential core length and divergence angle of mixing layer, as shown in Fig.7. By using the spiral-flow jet, the divergence angle was reduced by 45%, from 14.3° to 7.8°, and the length of the potential core was increased by 25%, from 4.8cm to 6.0cm. This clearly indicates that the spiral flow has a much better focusing capability than that of the conventional jet flow.

Furthermore, this tightly formed jet stream tends to concentrate the energy for cutting in a narrower area resulting in a higher efficiency of energy transfer.

3.2 SPIRAL JET STABILITY

As shown in Fig.8, the spiral-flow jet has lower pulsation rate than a conventional jet. The axial turbulence-fluctuation of both air jets was measured with a fiberoptic laser anemometer as shown in Fig.9. At z/d = 1.25, a spiral-flow jet reduces pulsation rate by 55%, from 0.206 to 0.081.

This means that the spiral-flow can achieve a higher degree of radial stability enabling the abrasive concentrate in the center area of the jet.

3.3 AZIMUTHAL COMPONENT OF SPIRAL-FLOW JET AND COLLISION

The experimental results indicate that the spiral-flow jet also helps to decrease the collision between the direct and rebounded jets.

To confirm the relationship between the azimuthal component and collision, two types of nozzles were produced; a turbulence jet nozzle consisting of a series of straight 1mm bores parallel to the jet axis, and a spiral-flow jet nozzle consisting of a series of twisted 1mm bores.

As shown in Fig.10, the spiral-flow jet nozzle decreases the collision rate significantly. The azimuthal component of the spiral jet alters its rebounded jet angle resulting in highly efficient jet energy transfer.

4.0 THEORETICAL ANALYSIS

The spiral-flow jet flow applicable to a conical section of the nozzle body was analyzed using a single phase flow model. The generation of the azimuthal component will be deduced by applying the radial component due to the conical structure of nozzle.

4.1 GOVERNING EQUATIONS

Analysis is limited to the flow field in a conical section of the spiral nozzle as shown in Fig.11. The flow field is assumed to be axial symmetrical, steady and incompressible.

The Reynolds equation is expressed in the cylindrical coordinate system (r,θ,z) and analysis is carried out by applying the boundary layer approximation method. The Reynolds equation can be written as follows,

$$v_r\frac{\partial v_r}{\partial r} + v_z\frac{\partial v_r}{\partial z} - \frac{v_\theta^2}{r} = -\frac{1}{\rho}\frac{\partial p}{\partial r} + \nu\left(\frac{\partial^2 v_r}{\partial r^2} + \frac{1}{r}\frac{\partial v_r}{\partial r} - \frac{v_r}{r^2} + \frac{\partial^2 v_r}{\partial z^2}\right) - \left(\frac{\partial}{\partial r}\overline{v_r'^2} + \frac{\partial}{\partial z}\overline{v_r'v_z'} + \frac{\overline{v_r'^2}}{r} - \frac{\overline{v_\theta'^2}}{r}\right) \quad (1)$$

$$v_r\frac{\partial v_\theta}{\partial r} + v_z\frac{\partial v_\theta}{\partial z} + \frac{v_r v_\theta}{r} = \nu\left(\frac{\partial^2 v_\theta}{\partial r^2} + \frac{1}{r}\frac{\partial v_\theta}{\partial r} - \frac{v_\theta}{r^2} + \frac{\partial^2 v_\theta}{\partial z^2}\right) - \left(\frac{\partial}{\partial r}\overline{v_r'v_\theta'} + \frac{\partial}{\partial z}\overline{v_\theta'v_z'} + 2\frac{\overline{v_r'v_\theta'}}{r}\right) \quad (2)$$

$$v_r\frac{\partial v_z}{\partial r} + v_z\frac{\partial v_z}{\partial z} = -\frac{1}{\rho}\frac{\partial p}{\partial z} + \nu\left(\frac{\partial^2 v_z}{\partial r^2} + \frac{1}{r}\frac{\partial v_z}{\partial r} + \frac{\partial^2 v_z}{\partial z^2}\right) - \left(\frac{\partial}{\partial r}\overline{v_r' v_z'} + \frac{\partial}{\partial z}\overline{v_z'^2} + \frac{\overline{v_r' v_z'}}{r}\right) \tag{3}$$

$$\frac{\partial}{\partial r}(rv_r) + \frac{\partial}{\partial z}(rv_z) = 0 \tag{4}$$

4.2 ASSUMPTIONS

1. The analysis is carried out within the boundary surface formed by a revolving curve expressed by Eq.(5) as shown in Fig.11. This boundary surface has the same shape as that of the spiral nozzle.

$$z = \frac{\kappa}{R^2} \tag{5}$$

Here, $\kappa = \dfrac{R_H^2 R_L^2}{R_L^2 - R_H^2}$ in which

R: radius of nozzle, H: length of nozzle in z direction,
R_H: radius of nozzle outlet, R_L: radius of nozzle inlet.

2. Viscous stress is ignored, since it is very small compared to Reynolds stress.
3. $\partial/\partial z[\overline{v_z' v_\theta'}]$ is ignored due to $\partial/\partial r \gg \partial/\partial z$.
4. Axial velocity varies in proportion to r^2 in the radial direction according to the experimental result.

$$v_z = G(z) + Br^2 \tag{6}$$

$G(z)$ is determined as follows, assuming that the mass flow rate at every section of nozzle is constant.

$$Q = 2\pi\int_0^R v_z r dr = \pi G(z) z R^2 + \frac{\pi}{2} B R^4$$

This equation can be rewritten as,

$$G(z) = \frac{Q}{\pi\kappa}z - \frac{B\kappa}{2z}$$

5. Boussinesq approximation

$$\overline{v_r' v_\theta'} = -\nu_T\left[\frac{\partial v_\theta}{\partial r} + \frac{v_\theta}{r}\right] \tag{7}$$

4.3 ANALYSIS

(1) Point $A(r,\theta,z)$, located on the vortex tube, is arbitrarily chosen on the plane with nozzle radius R as shown in Fig.11.
Vortex tube is expressed using dimensionless number D for radius R and r of nozzle as,

$$z = \frac{D^2\kappa}{r^2} \tag{8}$$

Here, $D=\frac{r}{R}=\frac{r_H}{R_H}=\frac{r_L}{R_L}$.

Circulation Γ_A at point A is expressed as,

$$\Gamma_A = \int_0^{2\pi} v_\theta r d\theta = 2\pi r v_\theta$$

Circulation of every point on the vortex tube is the same value as,

$$\Gamma_A = \Gamma_{A'} = \Gamma$$

$$\frac{\partial\Gamma}{\partial z} = \int_0^{2\pi}\frac{\partial}{\partial z}(v_\theta r)d\theta = 0$$

$$\frac{\partial v_\theta}{\partial z} = -\frac{v_\theta}{r}\frac{\partial r}{\partial z} \tag{9}$$

Eq.(9) is rearranged by substituting Eq.(8) into Eq.(9) as,

$$\frac{\partial v_\theta}{\partial z} = \frac{v_\theta r^2}{2D^2\kappa} = \frac{\Gamma_A r}{4\pi D^2\kappa} = M(D)r \tag{10}$$

Here, $M(D) = \dfrac{\Gamma_A}{4\pi D^2 \kappa} = \dfrac{\Gamma_{A'}}{4\pi D^2 \kappa}$. Circulation $\Gamma_{A'}$ at point A' is expressed as,

$$\Gamma_{A'} = 2\pi r_H v_\theta(r,z)\big|_{r=r_H, z=z_H} \tag{10-1}$$

From Eqs.(9) and (10), one can obtain the v_θ vs. $M(D)r$ relationship as,

$$\frac{\partial v_\theta}{\partial z} = M(D)r \tag{11}$$

(2) From Eqs.(4) and (6), v_r can be obtained as,

$$v_r = -\frac{1}{2}K(z)r \tag{12}$$

Here, $K(z) = \dfrac{Q}{\pi\kappa} + \dfrac{B}{2}\dfrac{\kappa}{z^2}$.

(3) Combining Eqs.(2),(7),(11) and (12), v_θ is obtained as follows,

$$v_\theta = \frac{1}{r}\frac{2\nu_T C}{K(z)}\left[1 - \exp\left[-\frac{1}{2}S_{Re}\cdot\frac{r^2}{R^2}\right]\right] + M(D)zr - \frac{M(D)B}{K(z)}\left[\frac{4\nu_T}{K(z)} - r^2\right]r \tag{13}$$

Here, the radius Reynolds number is set as $S_{Re} = v_{rR}\cdot R/\nu_T$, v_{rR} being the velocity component in the r direction at $r=R$, and ν_T is kinematic viscosity. The numerical approximation of v_θ for various S_{Re} is shown in Fig.12.

Eq.(13) indicates that the spiral-flow jet would be generated when applying initial radial velocity. Since kinematic viscosity is assumed as a constant given by the method of successive approximation, Eq.(13) is an approximate solution. In order to report a complete solution, some correction is necessary.

The approximate solution shows that the forced vortex and the free vortex are generated in the vicinity of the axis and the neighborhood of $r=R$, respectively.

The maximum vorticity is found in the neighborhood of the central axis, which means the converging vortex is generated and leads to the focusing of the spiral-flow jet.

5.0 CONCLUSION

A new spiral flow nozzle has been developed to improve the cutting efficiency in abrasive jet cutting applications.

The jet stream produced by a spiral-flow nozzle deforms into a slender jet with high jet-energy concentration. It accelerates the abrasive approximately 20% faster than a conventional nozzle, and it reduces the chance of collision with the rebounded jet.

Substantially improved performance of the abrasive water jet can be achieved by utilizing the spiral flow, i.e., steeper axial velocity distribution leading to a tight jet with high stability increasing abrasive acceleration, and an azimuthal component resulting in the less collision.

ACKNOWLEDGMENTS

The authors wish to acknowledge the valuable assistance given by Prof. Yasuhiko Aihara of Tokyo University. The financial support of the Japan Development Corporation was greatly appreciated.

REFERENCES

1) Horii,K., 1990, "Using Spiral Flow for Optical Cord Passing", *Mechanical Engineering ASME*, Vol.112, No.8, pp.68-69.

2) Horii,K., Matsumae,Y., Cheng,X.M., Takei,M., Hashimoto,B. and T.J.Kim., 1990, "Development of a New Mixing Nozzle Assembly for High Pressure Abrasive Waterjet Application, *10th International Symposium on Jet Cutting Technology*,

3) Horii,K., Matsumae,Y., Cheng,X.M., Takei,M. and Ikeda,Y., 1989, "Spiral Flow and Its Industrial Applications – Optical Cord Passing Method", *Industrial and Agricultural Applications of Fluid Mechanics - ASME*, FED-Vol.86, pp.65-68.

4) Horii,K., 1988, US.PAT. No.4,721,126, UK.PAT. No.2,180,957.

5) Horii,K., Matsumae,Y., Cheng,X.M., Miyamoto,M. and Takei,M., 1988, "A Study of Spiral Flow (Part 2) – Vortex Phenomena in a Specially Shaped Bend", *Transactions of the Japan Society for Aeronautical and Space Science*, Vol.31, No.92, pp.71-78.

6) Horii,K., Matsumae,Y., Cheng,X.M., Takei,M. and Hashimoto,B., 1990, "A Study of Spiral Flow (Part 4) – The Effect of Radial Reynolds Number of Spiral Flow on Plasma Deposition of Pipe" *Transactions of the Japan Society for Aeronautical and Space Science*, Vol.32, No.98., pp.165-175.

7) Batchelor,G.K., 1967, "An Introduction to Fluid Dynamics", *Cambridge University Press*, pp.546-550.

8) Laufer,J., 1955, *NACA Tech. Rep.* No.1174.

9) Horii,K., Matsumae,Y., Cheng,X.M., Takei,M., Eiji,Y. and Hashimoto,B., 1991, "Focusing Phenomenon and Stability of Spiral-flow Jet", *Transactions of the Japan Society for Aeronautical and Space Science*, Vol.33, No.102., pp.141-153.

NOMENCLATURE

B	constant
C	constant
D	$\frac{r}{R} = \frac{r_H}{R_H} = \frac{r_L}{R_L}$
H	length of nozzle in z direction
p	pressure
Q	mass flow rate
r,θ,z	cylindrical polar coordinates
R	radius of nozzle
R_H	radius of nozzle outlet
R_L	radius of nozzle inlet
S_{Re}	$-R \cdot v_{rR}/\nu_T$ dimensionless number
v	velocity
v_r,v_θ,v_z	velocity component in r,θ and z directions, respectively
v_{rR}	velocity component in r direction at $r=R$
v_r',v_θ',v_z'	fluctuating velocity
κ	$\frac{R_H^2 R_L^2}{R_L^2 - R_H^2}$
ν_T	kinematic viscosity
Γ	circulation
Γ_A	circulation at point A
Z	distance from nozzle tip
d	nozzle diameter

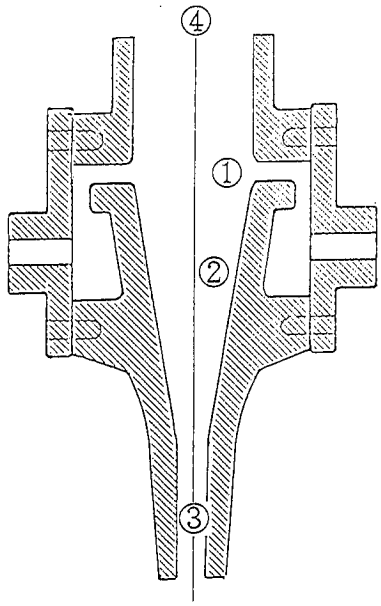

Fig.1 Spiral-flow nozzle

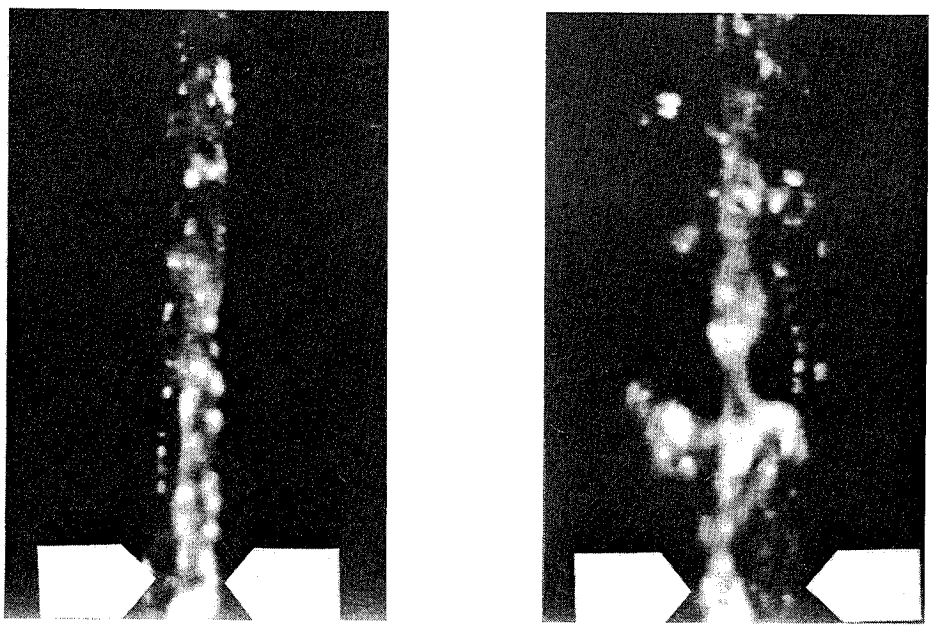

Spiral-flow jet Normal turbulence jet

Fig.2 Jet structure deformation for jet energy concentration

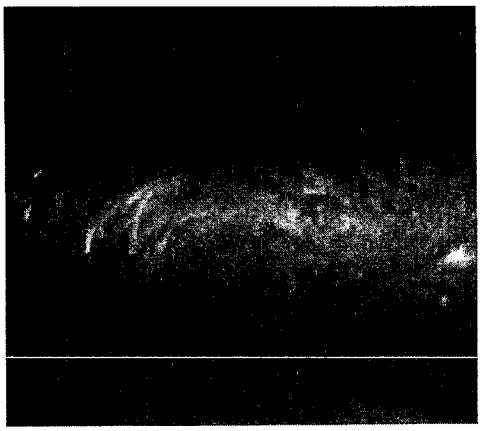

Spiral-flow jet

Normal turbulence jet

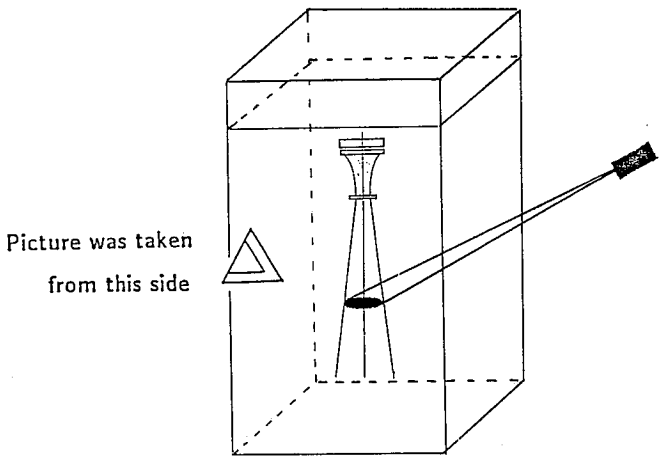

Fig.3 Pattern of azimuthal velocity component

Spiral-flow jet

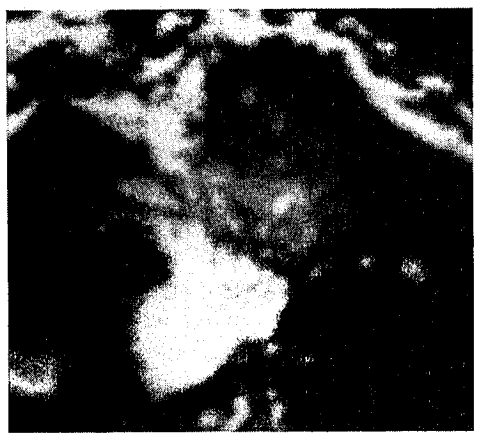

Normal turbulence jet

Fig.4 Jet collsion

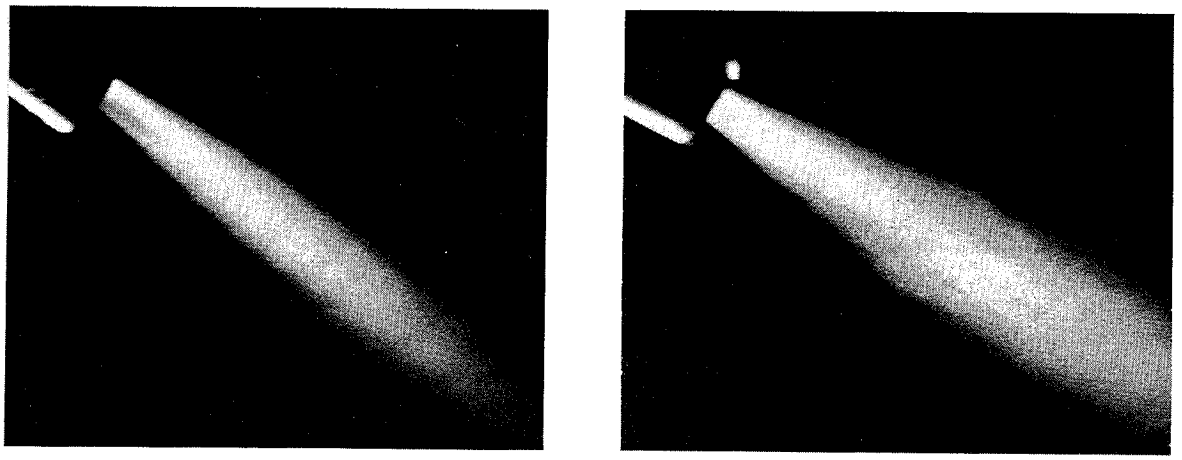

Spiral-flow jet　　Normal turbulence jet

Fig.5　Jet stream pattern

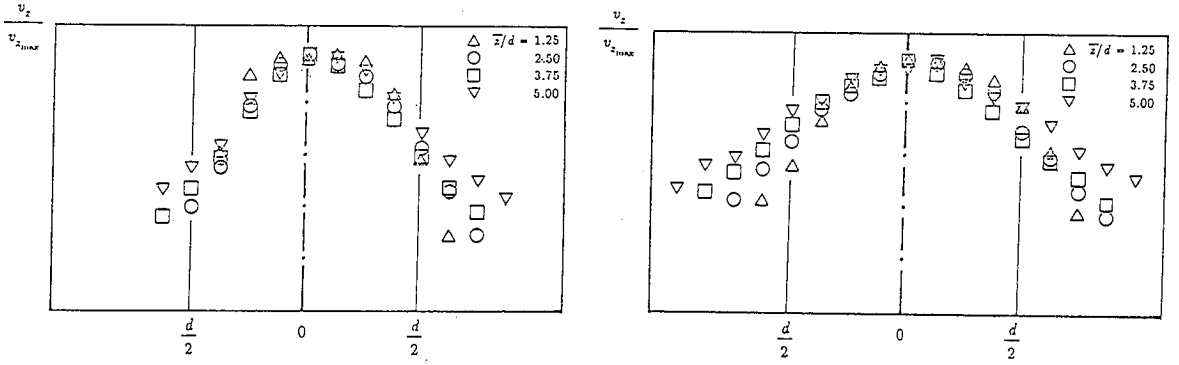

Spiral-flow jet　　Normal turbulence jet

Fig.6　Axial velocity profile

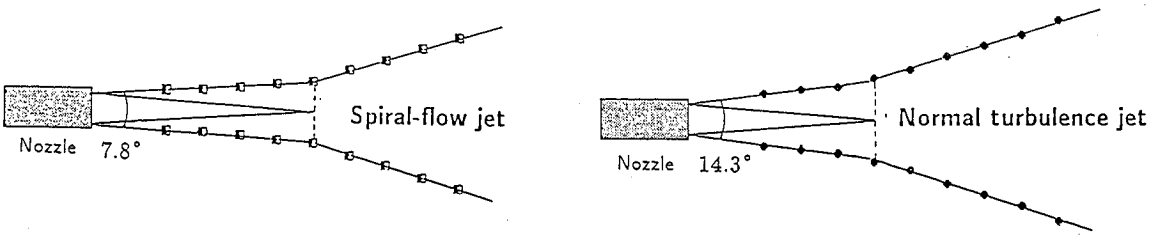

Fig.7　Half width

Normal turbulence jet

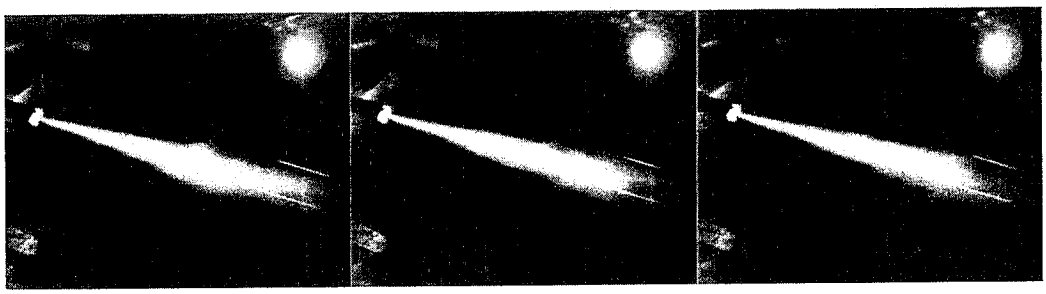

Spiral-flow jet

Fig.8 Picture sequence of jet flow

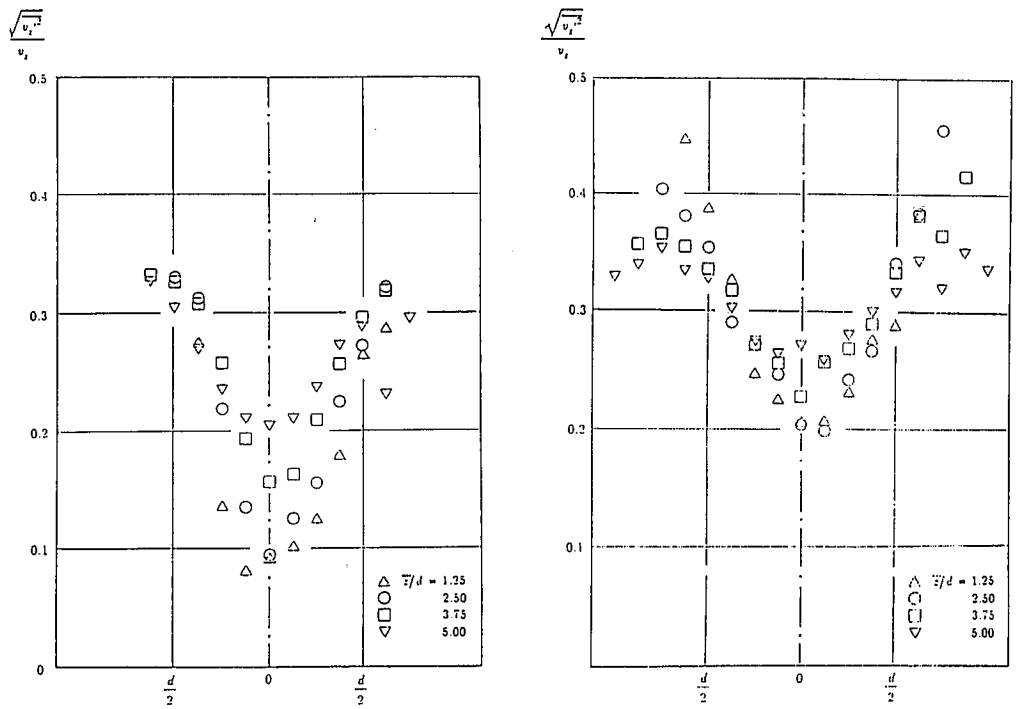

Spiral-flow jet

Normal turbulence jet

Fig.9 Axial turbulence level

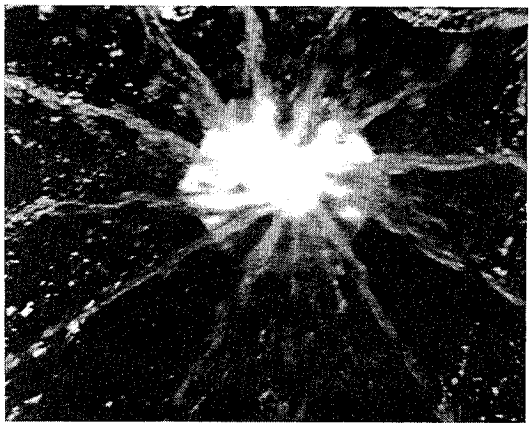

Spiral-flow jet

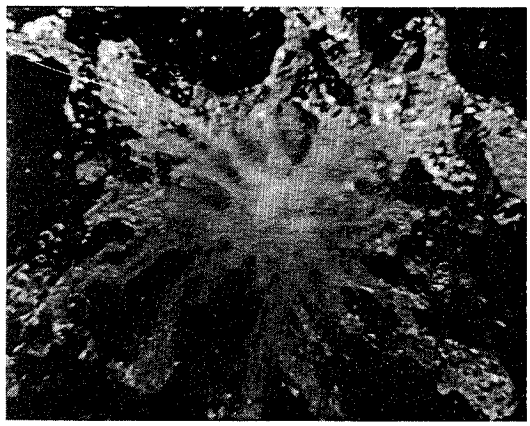

Normal turbulence jet

Fig.10 Relationship between azimuthal component and collision

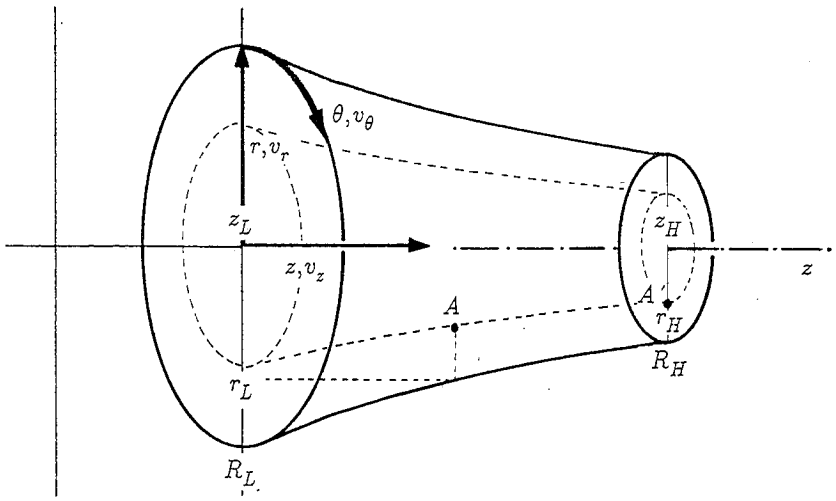

Fig.11 Flow field (axisymmetric flow)

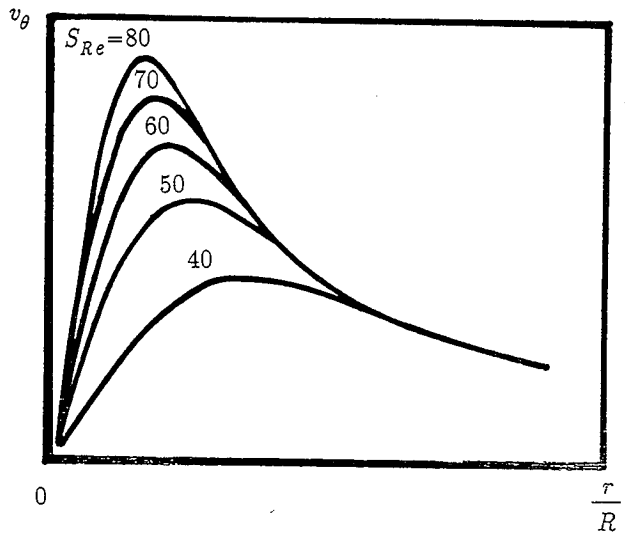

Fig.12 v_θ for various S_{Re}

6th American Water Jet Conference
August 24 - 27, 1991: Houston, Texas Paper 35

DEVELOPMENT OF A CRYOGENIC WATERJET TECHNIQUE FOR BIOMATERIAL PROCESSING APPLICATIONS

Patrick TRUCHOT, Pascal MELLINGER and Robert DUCHAMP
ENSAM, Paris France
Thomas J. KIM
University of Rhode Island,Kingston, RI, USA
R. OCAMPO
CNRS, Grenoble, France

ABSTRACT

A study was conducted to develop a cryogenic waterjet system for food processing and medical applications. The hard biomaterials such as bones are difficult to cut with a high pressure waterjet. However, by mixing the pellets of ice crystals with the stream of pure jet, the cutting efficiency can be drastically enhanced. Several different approaches for entraining the ice pellets in the jet stream were tested including a method of direct solidification during the discharge phase. A method of producing calibrated ice pellets as well as the mixing with the jet stream will be discussed in terms of the cutting efficiency.

Organized and Sponsored by the Water Jet Technology Association.

1.0 INTRODUCTION

The "new product design" department of ENSAM(*) has been equipped with a waterjet cutting platform since 1986. Our first activity was to dissemate this technology in the french industry. So, we have developed a new two axes table for abrasive cutting which led to create a company called "Aquarese Industries" This company is now one of the leading manufacturer of shape cutting systems in France.

Thus we have carried out a great number of experiments for companies and various industrial sectors. Very quickly, two areas of interest emerged where the technical feasibility was practically guaranteed, one centred around a pure waterjerjet and another around an abrasive waterjet. However a group of potential users found one or other technologies unsatifactory. The four insatisfactory points can be listed as follows :

- defficiency of the pure waterjet
- destructive power of the abrasive waterjet
- thermal pollution
- particulate pollution of abrasives

The cryogenic waterjet is an appropriate answer. The principle of cooled water loaded with ice particles totally meets these objectives. The food industry and medical field are the most obvious application areas. We have been working on this project since 1987.

2.0 PROBLEMATICS OF CRYOGENIC WATER JET

The ice crystal injection [1] into a gaseous stream is already in use. The ice crystals are either water based or compressed solid carbon dioxide. We know an another principle used to produce artificial snow. The ice microcrystals are obtained during the jet expansion. However transforming these technologies to suit the waterjet presents certains difficulties due to the watery medium, the temperature, the pressure and the speed. The references and experiments are scarce. We have founded a Soviet patent [2] about a cooling down the nozzle.

These investigations enabled us to define two research possibilities. The figures (1) and (2) show these two hypothesises on the water-ice diagram. For the moment we haven't included the carbon dioxide ice which involves other knowledge and equipment.

*** First hypothesis (fig 1)**

The water temperature was lowered at constant pressure down to its solidification limit. During the jet's pressure reduction in the atmosphere, there is an instantaneous formation of ice, when the expansion curve cuts the phase change curve. We can observe that this hypothesis could be better for pressures down to 200 Mpa.

*** Second Hypothesis (Fig 2)**

The calibrated ice crystals are fed in the jet stream by the venturi effect, as in the case of conventional abrasive jet. The feasability of this solution depends on thermic exhanges, firstly between ice and air, then between ice and waterjet. Computations show that a 0.1 mm diameter crystal at atmospheric pressure needs

-8×10^{-2} s in air at 20°C
-2×10^{-4} s in water at 40°C

to change its temperature from -194°C to 0°C.These value must be compared at the transfer time of ice crystal :

- in air from the hopper to the nozzle
- in the waterjet on a 0.1 mm distance (2×10^{-4} s)

We can see that we are within the same size rate. Therefore,theoretically it is possible to obtain ice in the jet. In practise, the crystals in the jet are subjected to special experimental conditions because of uncontrolled thermal

exchanges and mechanical effects. Fig. 2 illustrates the practical problematics of this hypothesis. It shows that we must determine the experimental zone of the presence of crystals. The zone's limit is fixed in the upper part by a set of curves , depending on the water's cooling temperature, the pressure and a set of experimental conditions and parameters to be determined. In the lower part it is fixed by the phase change curves involving freezing of the water in the pipelines. Of course the shape of the curves and numerical values can also be modified by other factors such as the presence of additives in the water.

3.0 PRESENTATION OF THE EXPERIMENTAL INSTALLATION

This installation has been designed to test the two hypotheses. It has two independent circuits joined at the cutting head.

*** Ice crystals production cicuit (Fig. 3)**

The 2.0 to 5.0 mm diameter crystals are made in a hydrous ice generator. Held at a constant temperature in atmospheric nitrogen, they are crushed and calibrated in a cryogrinder. The diameter is between 0.5 and 1.0 mm included. They are then transferred into the isothermal hopper from where they are drawn up by the jet.

*** Refrigerated water circuit (Fig 4)**

The water is fed under pressure by a 'Flow System 9X' pump. It is cooled down in a heat exchanger. The water circuit is made up of a coil of high pressure pipework. This arrangement is immerged in a bath of silicon oil cooled by bubbling through liquid nitrogen. Regulation of the temperature is obtained by adjusting the height of the coil in the bath.

4.0 RESULTS

We have made experiments in the two quoted principles. As of now we can just measure the temperatures of the two circuits and water pressure. We have no means to evaluate the ice water mix in the jet. We can just observe visually the crystals present on the table. The short-lived crystal requires instantaneous observance means, like an ultra speed camera.

*** The first principle**

We have conducted many expriments between 200 and 400 MPa. The best temperatures we can observe were :

* -35°C in the silicon oil bath
* -18°C water input a 0.08 mm diameter nozzle
* -10°C water input a 0.20 mm diameter nozzle

In the two cases we estimate that the waterjet temperature was positive near 0°C. Measuring the jet's temperature presents some incertainty and we still search an adaptated mean of measure.

We have also tried to replace silicon oil directly by a liquid nitrogen bath. But it is very difficult not to freeze the water in the pipe. We have also cooled down the crystals presence. It could be caused by the two main phenomena :

* the water heating trough the nozzle
* the ice crystallysation time

It would be possible perhaps to obtain some results with lower pressures. But it seems to be improbable enough to succeed in waterjet cutting technology. So we have to abandon this approach.

Nevertheless, we obtained some results and know-how in the jet cooling down. We modified the heat exchanger and we hope to obtain a temperature of -18°C input for any diameter nozzle and a negative temperature in the jet. We know that on average, the water temperature increases from 12 to 18°C trough the sapphire nozzle.

*** The second principle**

We have used the previous same conditions with silicon oil.
The ice crystals characteristics were in the hopper

* diameter 1.0 mm
* temperature - 80°C
* flow-rate 0.0166 Kg/s

We used an abrasive head with

* Sapphire nozzle diameter 0.2 mm
* Refocalization nozzle diameter 2.0 mm
* Refocalization nozzle length 30 mm

We visually observed the crystals presence. We know the method to repeat this experience, but we still don't know :

- effective quantity and dimensions of the crystals in the jet
- other experiment points

We have stabilized this process during a few seconds.
So we could conduct some comparative cutting experiments on a 4 mm thickness P.V.C sheet.
With the pure waterjet, we observed clean cutting.
With the cryogenic waterjet, we observed the ice crystals impact near the cut. But we still don't know the effective efficiency of the cryogenic waterjet.

5.0 CONCLUSIONS AND PERSPECTIVES

We have demonstrated the feasibility of the cryogenic abrasive waterjet. We are currently working on the qualitative and quantitative evaluation of the process.

As regards identification and quantification of the parameters, we group together the inherent difficulties of the waterjet and of the biphase behaviour of the water. So we are consulting with a specialist team in :

- waterjet (University of Rhodes Island)
- cryogenic (CNRS Grenoble).

Our objectives are :

* in one year to obtain significant scientific and industrial results to show the efficiency of this process. This work depends on the applications.

* in two years, to produce a demonstrative prototype of the cryogenic waterjet process.

ACKNOWLEDGEMENTS :

- The authors wish to thank Mrs . TONNELIER and BIONDAT of the research center of the company "AIR LIQUIDE" , Jouy en Josas, FRANCE for their help with the project. The financial support provided by ANVAR and NOVELECT is gratefully acknowledged.

REFERENCES :

[1] G. GALECKI and G.W VICKERS - "The development of ice-blasting for surface cleaning " - 6 th International Symposium on Jet Cutting Technology - 6-8 April 1982

[2] E.N. CHAPKINE -- "Nozzle to obtain a liquid cutting jet" - Soviet patent N° 3704998/23-05 - 22 february 1984 -

[3] W. B DURHAM, S.H. KIRBY, H.C. HEARD and L.A STERN - " Inelastic properties of several high pressure crystalline phases of H2O : Ices II, III and V - Journal de Physique - Colloque C1, supplément au N°3, Tome 48 , pages 221 - 226 - March 1987 -

NOMENCLATURE :

ENSAM : Ecole Nationale Supérieure d'Arts et Métiers

CNRS : Centre National de Recherche Scientifique

MPa : 10^6 Pa

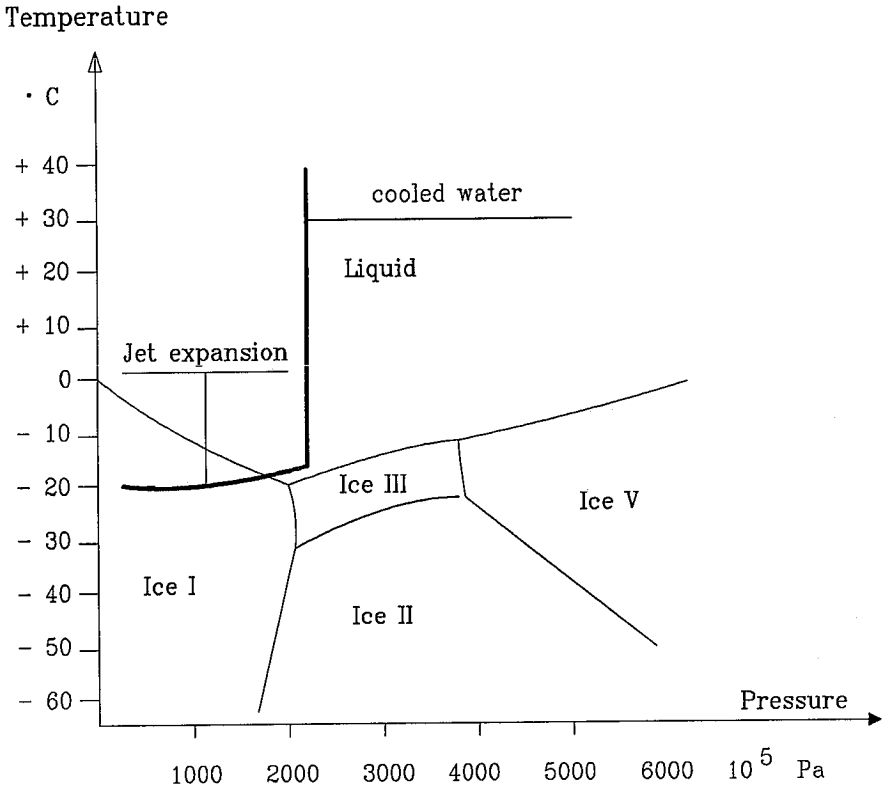

Figure 1 : Ice crystallization by expansion

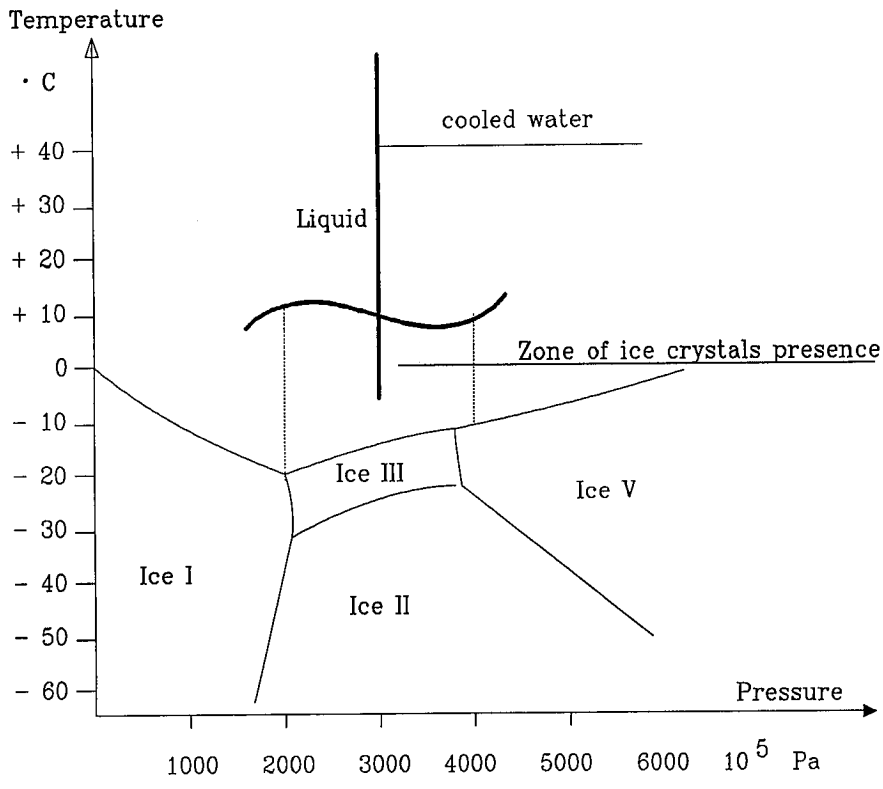

Figure 2 : Ice crystals injection

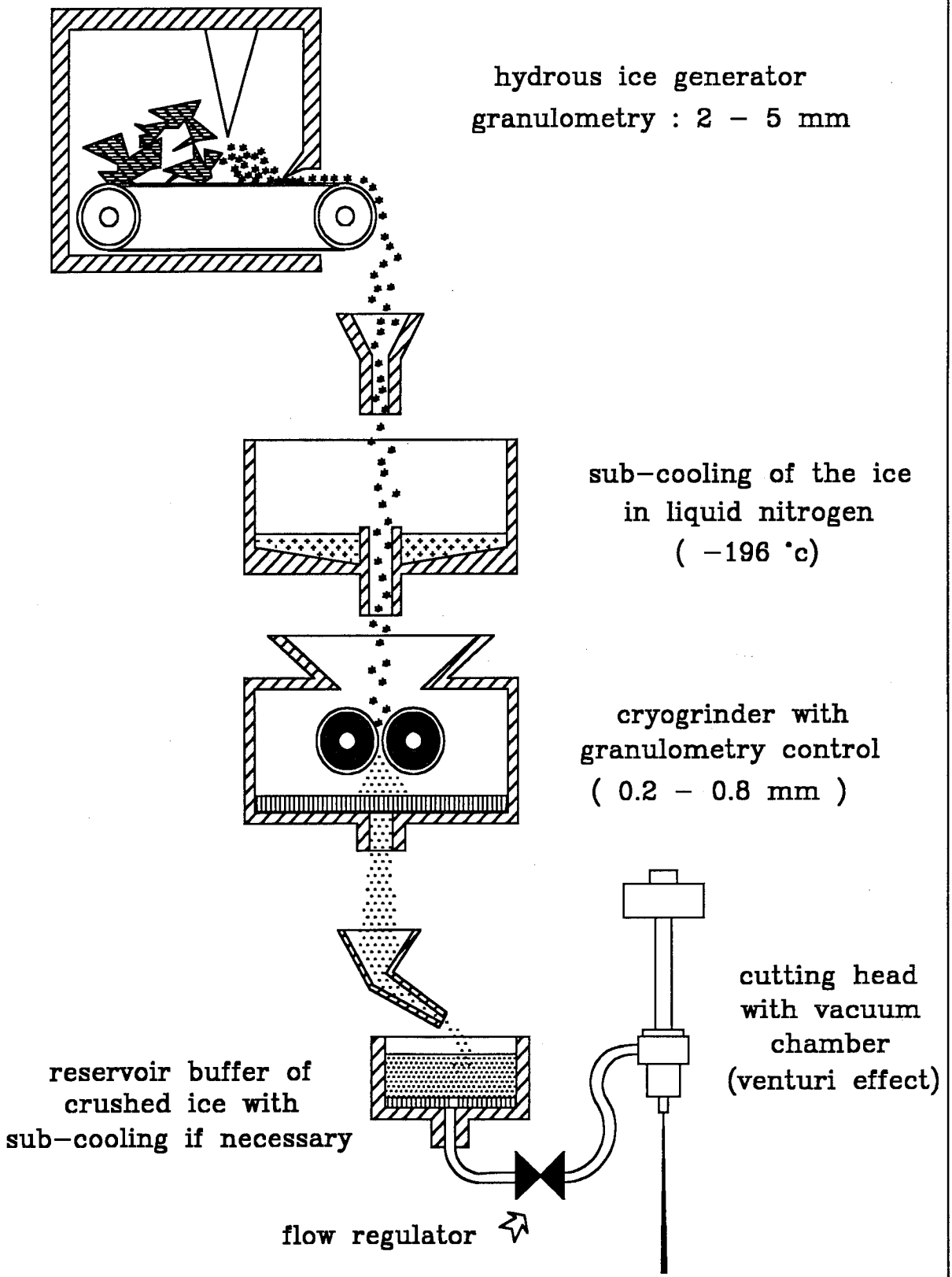

Fig 3
ICE CRYSTALS CIRCUIT

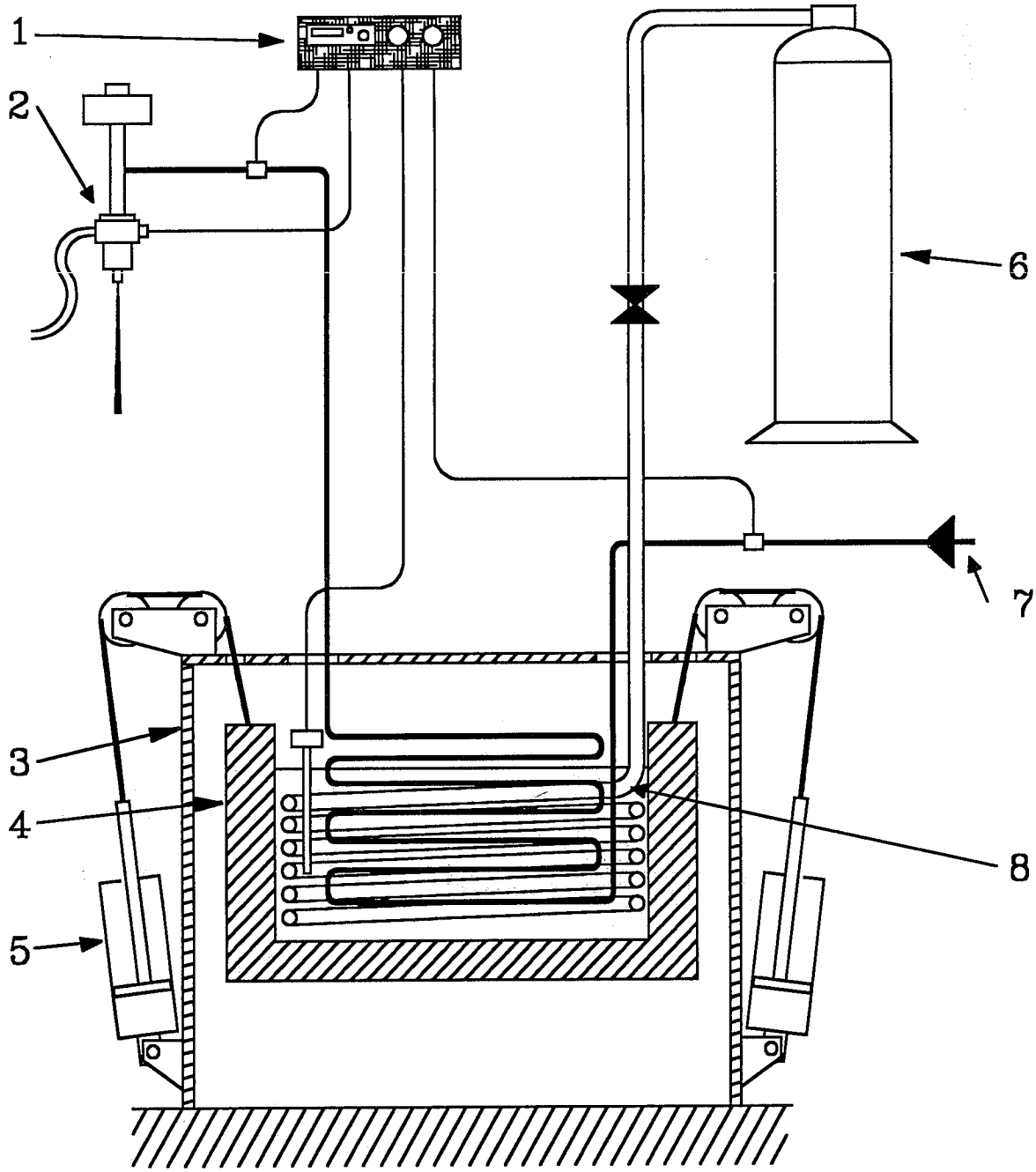

1 = Temperature controller
2 = Cutting nozzle
3 = Exchanger frame
4 = Insulating tank containing silicon oil
5 = Level adjustment system
6 = Liquid nitrogen cylinder
7 = Water pressure inlet
8 = Coil of liquid nitrogen pipework

Fig 4
REFRIGARATED WATER CIRCUIT

6th American Water Jet Conference
August 24 - 27, 1991: Houston, Texas Paper 36

HOLE PIERCING IN THIN METAL TARGETS USING WATER JETS

by

T.J. Labus
SCIRE Corporation
Fontana, Wisconsin, USA
and
K.F. Neusen
University of Wisconsin-Milwaukee
Milwaukee, Wisconsin, USA

ABSTRACT

Thin metal targets can be penetrated by water jets without the aid of abrasives in short time periods. These thin targets are characterized by ratios of target thickness to nozzle diameter ratios lying in the range of 1.33 to 3.33. A characteristic hole diameter versus pulse time curve results for all nozzle diameters. This curve exhibits a stable and unstable portion, which are determined by operating conditions and target geometry.

Hole quality is characterized by roundness and repeatability. An exit burr generally occurs, but it was found that this could be eliminated by careful control of the geometry of the impact surface directly below the back of the target. Hole geometry is significantly affected by restraints put on the target and motion of the jet caused by valve actuation. A timed, gate assembly eliminated the valve actuation problem, and provided precise control of the pulse duration.

Variations in hole geometry are related to pressure, nozzle size, and pulse duration, with nozzle size being the controlling variable for long pulses.

Organized and Sponsored by the Water Jet Technology Association.

1.0 INTRODUCTION

The geometry of holes produced by fluid jets depends on the type of the jet be used, target material properties, jet parameters and thickness of the target. As these parameters change the type of jet employed to produce the holes will affect the resulting hole geometry. The study reported in here investigates hole piercing for thin, ductile target materials using pure water jets. The goal was to establish the parameters which control the piercing process, and produce a stable, repeatable hole geometry.

With the use of thin specimens (i.e. thickness to nozzle diameter ratio of 3.33:1 to 1.33:1) and the fact that the holes produced were of the same order of magnitude as the nozzle diameter, pure water jets could be used as opposed to abrasive jets. Abrasive jets or very high pressure water jets (in the range of 700 MPa) are required for holes which are much larger than the nozzle diameter, since the jet must now be traversed around the perimeter of the hole. Since the thickness of the specimens varied over a narrow range, the diameter was used to characterize the resulting hole.

2.0 EXPERIMENTAL ARRANGEMENT

The high pressure water jet system located at the University of Wisconsin-Milwaukee was used to perform all the tests. This system is composed of a hydraulically powered intensifier capable of 413.9 MPa (60,000 psi) max pressure, and 4.55 l/min (1.0 GPM) max flow rate, coupled to a cylindrical robot. Fig. 1 shows a view of the high pressure pumping system, while fig. 2 shows the robot with a ON/OFF valve mounted on the end of the radial arm.

The ON/OFF valve response time was not fast enough to produce a pulse duration short enough so that penetration would not occur. Hence, a gate mechanism shown in fig. 3 was constructed. This mechanism is composed of a pneumatically driven cylinder equipped with a magnetic piston. Two (2) reed switches were mounted on the cylinder, and were actuated with passage of the piston. The signal from a simple battery circuit was passed through the reed switches (one wired normally OPEN, and the other wired normally CLOSED), and controlled the start/stop gate on a frequency meter. A schematic of the circuit is shown in fig. 4a and the complete gate system with the frequency meter is shown in fig. 4b. The frequency meter time base was set at 1000 Hz.

Attached to the rod of the cylinder was a blank plate of steel with a notch such that the only time the jet impacted the target was when it was over the notch. The notch is visible on the left-hand side of the plate shown in fig. 5. The reed switches on the cylinder were set apart the same distance as the length of the notch. Hence, the frequency meter display gave a direct readout (in milliseconds) of the pulse duration (i.e. the time the target was exposed to the jet).

The speed of the cylinder could be adjusted, hence the pulse range could be varied over a wide range of values. This range was such that the pulse duration could be shortened to the point where penetration of the target would not occur, or lengthened to produce a fully developed hole diameter. A manual trigger was used to activate the gate once the jet had been turned on. Fig. 5 also shows a close up of

the nozzle positioned over the blanking plate, and the specimen holders for the flat stock.

The resulting hole produced by the jet was measured by photographing the magnified hole on a shadowgraph. Then, a polar planimeter was used to measure the hole area. Three (3) measurements were taken on each hole and averaged for the reported area value. Min and max hole diameters were also noted, since the jet does not produce perfectly "round" holes. From these values the variation of hole diameter could be established. An equivalent "circular" hole diameter was computed from the measured area values.

3.0 TEST RESULTS

A total of over 290 tests were performed to determine the effects of pressure, nozzle size, and pulse duration on the resulting hole produced. Initial testing indicated that an exit burr would occur if the jet was allowed to freely pass through the target. This exit burr could be controlled by keeping the target material firmly pressed against an erosion resistant backing and controlling the duration of the pulse. Various backing materials were utilized, but the best results were obtained with a sapphire impact disc. Alumina ceramic, hardened tool steel, titanium, and tungsten carbide were all evaluated, but the sapphire disc proved the most durable in maintaining a flat backing surface. This flat surface directed the jet exiting the target back on itself and also laterally away from the impact area. This lateral and back flow removed the burr. Several spacings between the target material and the impact disc were tried, but the best results in terms of "burr free" hole were obtained when the impact disc was in contact with the exit side of the target.

Fig. 6 shows the quality of the resulting holes produced by the gated jet arrangement. The holes are not perfectly round, and there is are irregularities on the perimeter. The quality of the perimeter of the hole is dependent on jet coherence, relative movement of the nozzle to the target during the piercing process, and the pulse length to nozzle diameter ratio. A series of tests were performed for standoff distance to nozzle diameter ratios (S/Dn) in the range of 145-208. The results showed little variation in hole diameter over this range. Hence, for all subsequent tests the standoff distance was fixed and the nozzle sizes employed resulted in S/Dn ratios in the aforementioned range. Photographs of mechanically pierced holes are shown in fig. 7, and the variations on the perimeter are evident. The quality of water jet versus mechanically pierced holes in thin ductile targets is equivalent if care is taken to control nozzle movement and orifice quality.

Fig. 8 shows a plot of the hole diameter (Dh) to nozzle diameter (Dn) ratio versus the pulse length (L) to nozzle diameter ratio. Pulse length (L), is equal to the product of the jet velocity and pulse time. Both the nozzle diameter and jet pressure are constant for this series of tests, hence the variations are due to pulse length only. Note, there is a critical L/Dn ratio below which the target is not pierced. This corresponds to a minimum energy content of the pulse to affect penetration. This minimum is not a specific energy since it is dependent on the thickness of the sample. The variations in L/Dn at zero diameter ratio in fig. 8 are due to thickness differences in the

targets.

The second point to note about the curve is fig. 8 is that there are two areas of operation. For L/Dn ratios of between 1-1.3x10^6 a hole of approximately the size of the nozzle diameter can be produced, but small variations in L/Dn result in large changes in the hole diameter. For L/Dn <2.3x10^6 these large changes in diameter ratio with small changes in L/Dn make operation in this regime rather precarious, and hence this portion of the curve is termed "unstable". Beyond L/Dn> 2.3x10^6 the curve begins to flatten out, and the diameter ratio becomes less sensitive to variations in L/Dn. This portion of the curve is termed "stable", since the diameter ratio does not change radically with small variations in L/Dn.

The behavior of the diameter ratio as shown in fig. 8 is similar to the depth of cut versus exposure time for a continuous jet as reported by Kiyohashi, et al, in that the depth of cut exhibited similar dependence on the time the target was exposed to the jet.
Fig. 9 shows the effect of target thickness on the diameter ratio for various values of the L/Dn. These curves also exhibit stable and unstable operational areas similar to those observed in
fig. 8, but with normalized stock thickness and L/Dn determining the where the "knee" in the curve is. (Note, the parameter L/Dn on the curves is given in millions: 5.4E6=5,400,000 etc.) The variation in L/Dn shown in fig. 9 is due to pulse length changes only since pressure and nozzle size were held constant. Hence, longer pulse times will extend the stable portion of the curve to produce holes in thicker targets.

Fig. 10 shows a composite plot of diameter ratio versus L/Dn for three different nozzles sizes and targets of different thickness. The parameter for the different data sets is D/Dr (nozzle diameter to reference nozzle diameter ratio). The data for D/Dr=.666 exhibits the characteristic curve that was described in fig. 8, as does the data for D/Dr=1.0, although there is scatter at low values of L/Dn. The data for D/Dr=1.333 was not carried to short enough L/Dn for it to exhibit the characteristic curve.

4.0 CONCLUSIONS

For piercing of thin metal specimens using a pure water jet the following conclusions can be drawn.

1.) The resulting hole quality of a water jet pierced hole can be equivalent to mechanically pierced if the movement between the nozzle and target and orifice quality are controlled.

2.) A characteristic diameter ratio versus L/Dn curve results in which stable and unstable operation regimes are identified based on L/Dn ratio and target thickness. This is for target thickness to nozzle diameter ratios in the range of 1.33 to 3.33.

REFERENCES

Kiyohashi, H., Kyo, M. and Ishihama, W., "Water Jet Breaking of Imitation Hot Dry Rock", Proc. Fourth Int. Sym. on Jet Cutting Technology, Paper No. C2, BHRA Fluid Engineering, April 12-14, 1978, Canterbury, England.

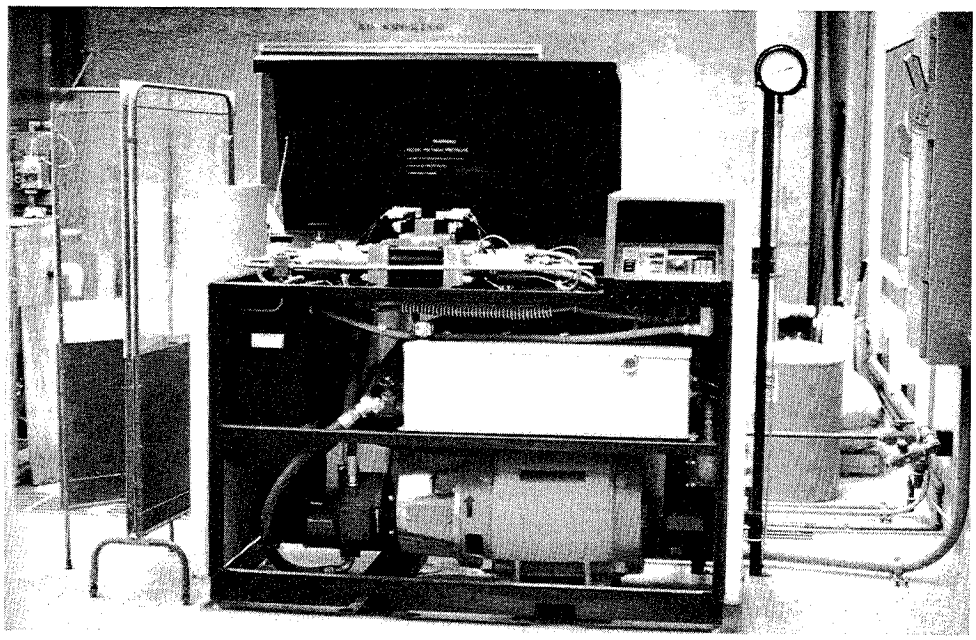

Fig. 1 High Pressure Pumping System

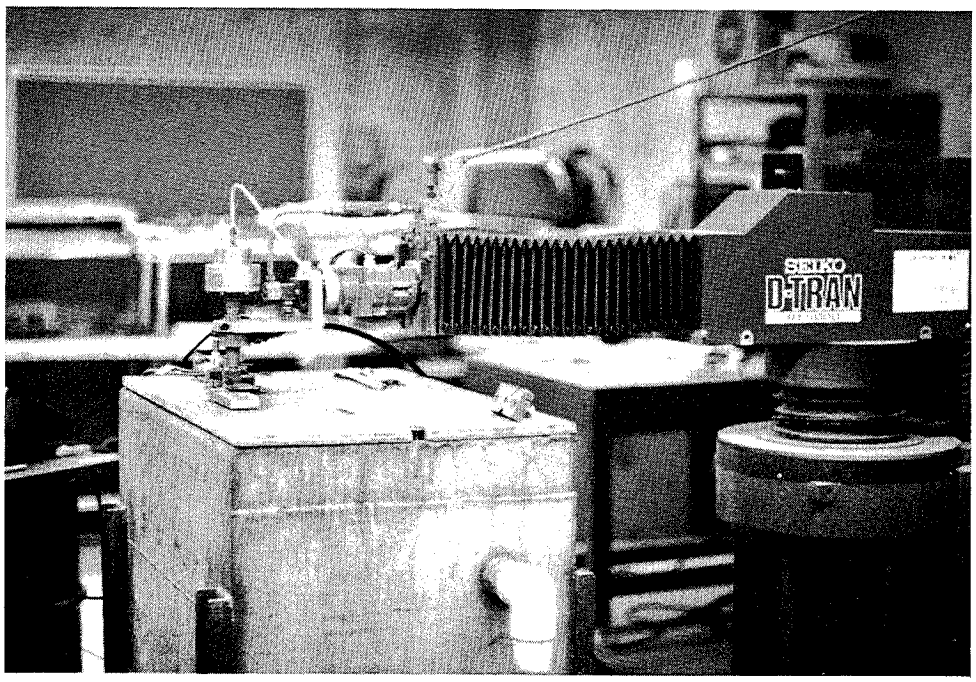

Fig. 2 ON/OFF Valve on Robot Arm

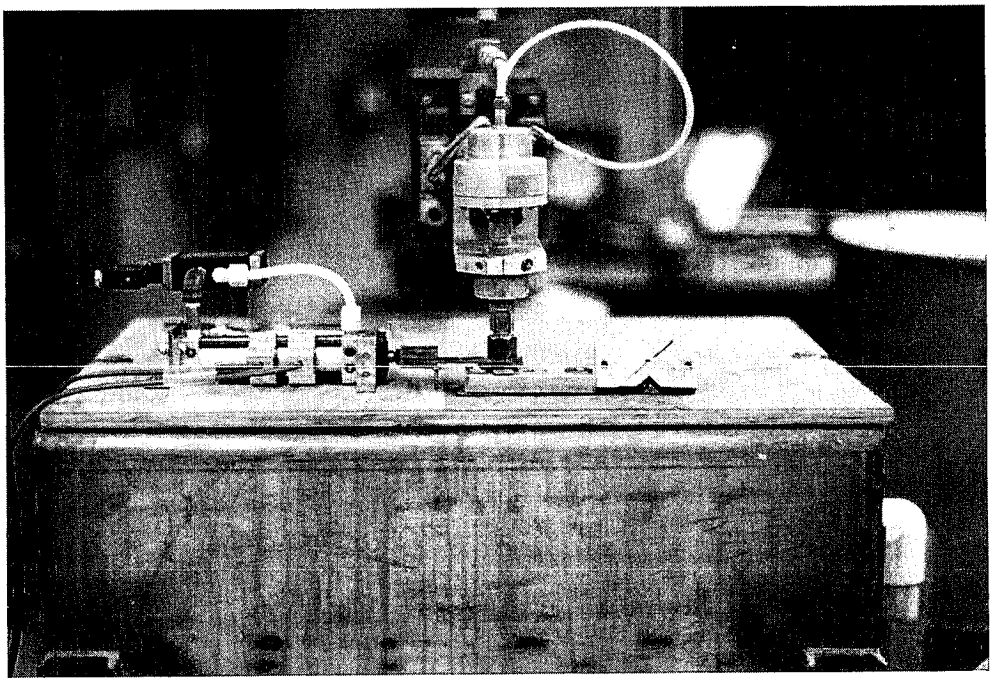

Fig. 3 Pneumatic Powered Gate Mechanism

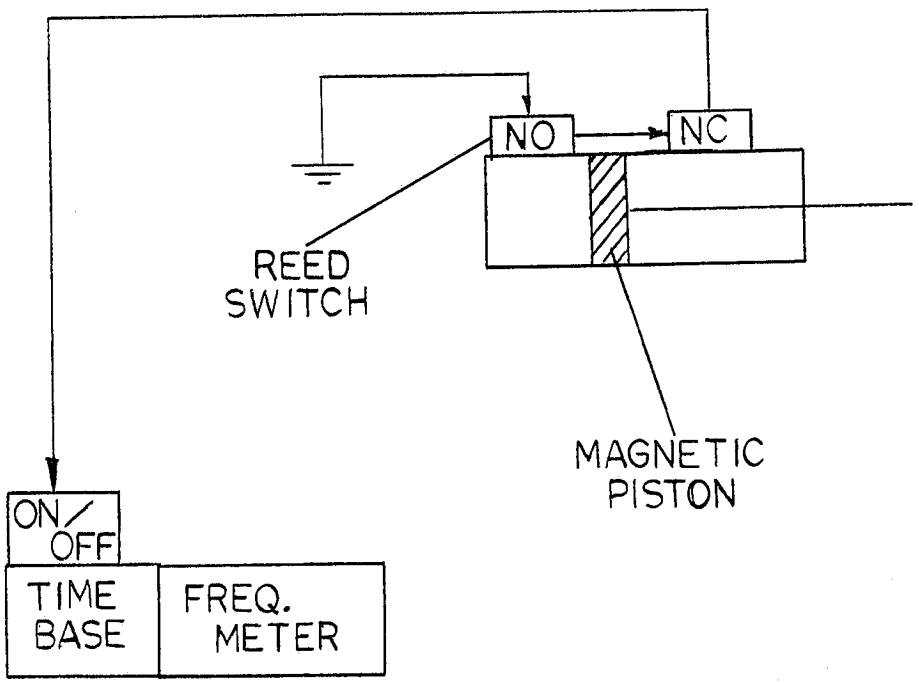

Fig. 4a Gated Pulse Circuit Schematic

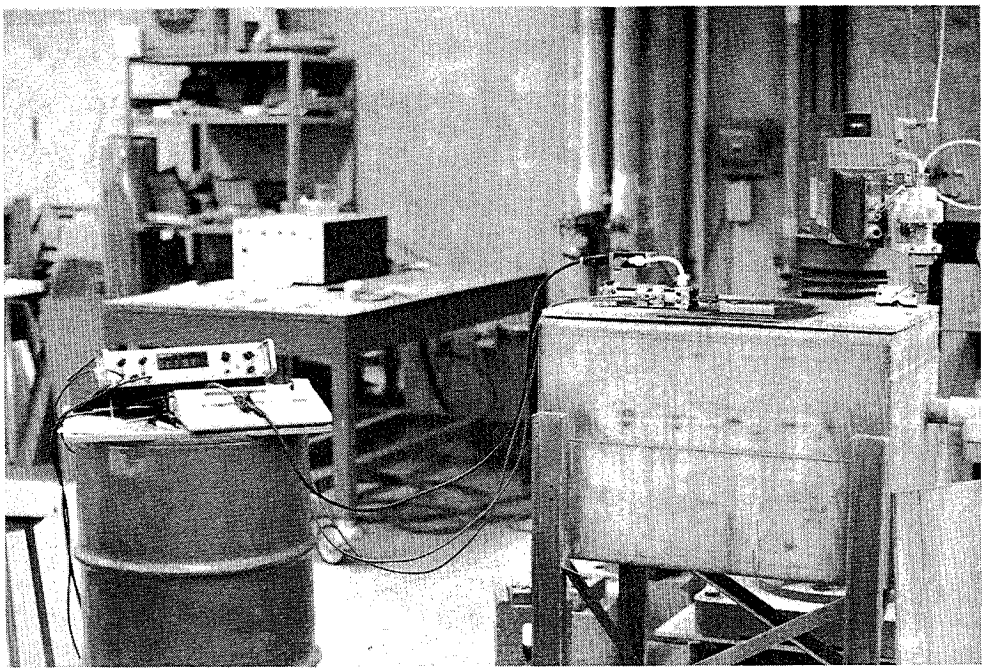

Fig. 4b Gate System and Frequency Meter

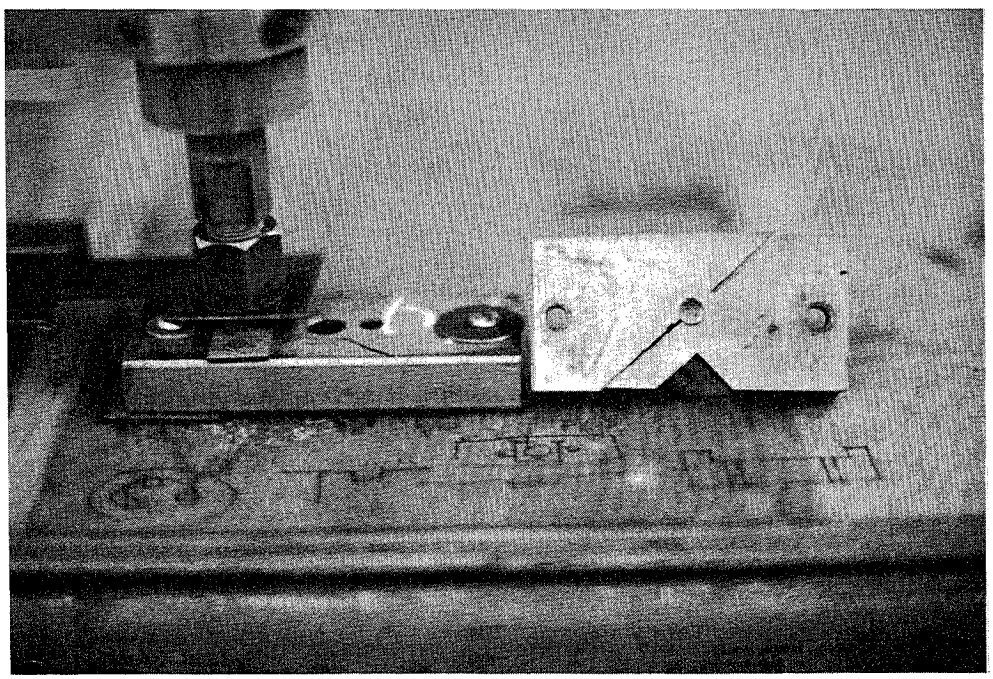

Fig. 5 Notched Blanking Plate and Target Holder

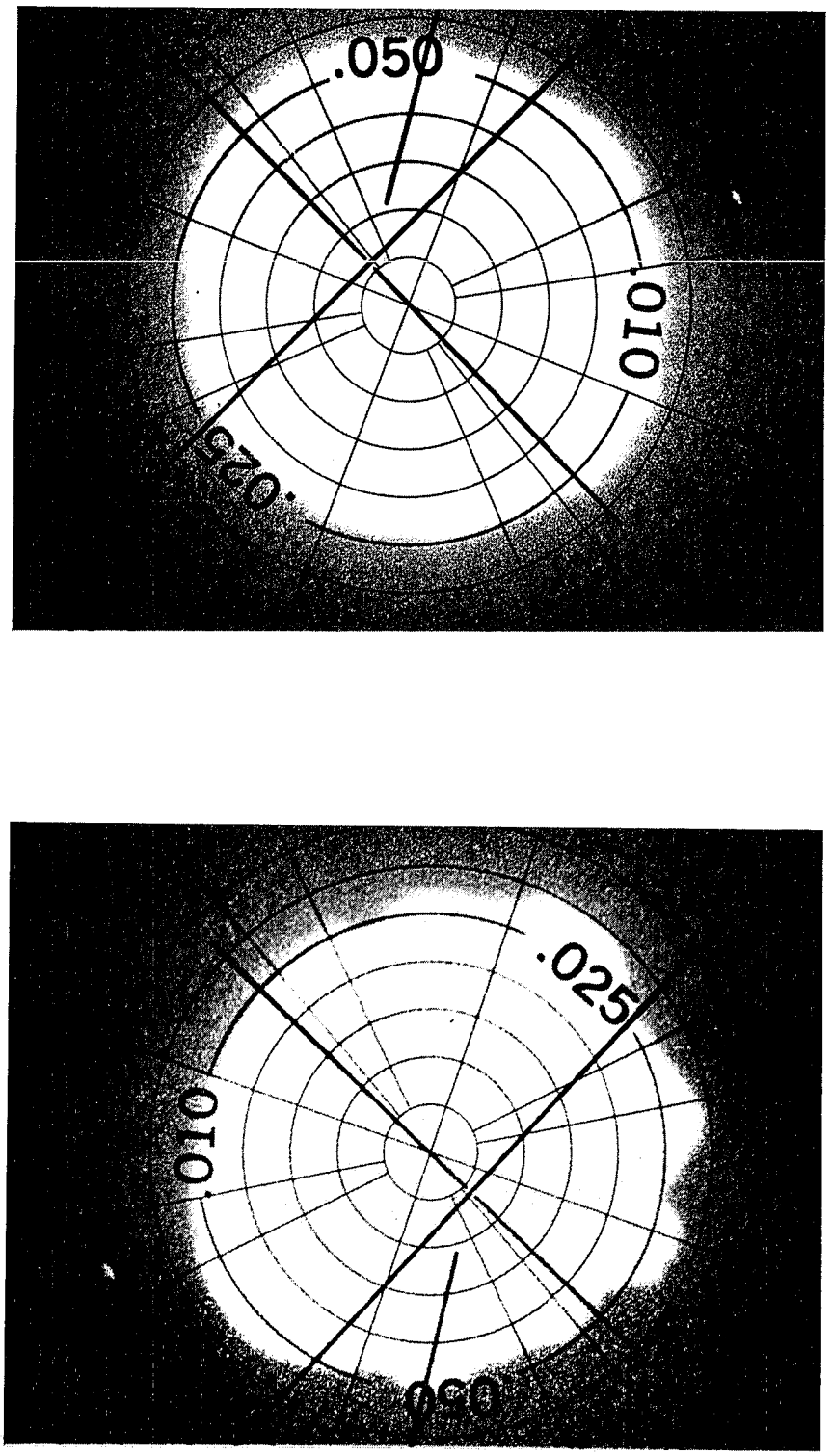

Fig. 6 Water Jet Pierced Holes
L/Dn=2.65E6, D/Dr=1.0, t/Dn=2.0

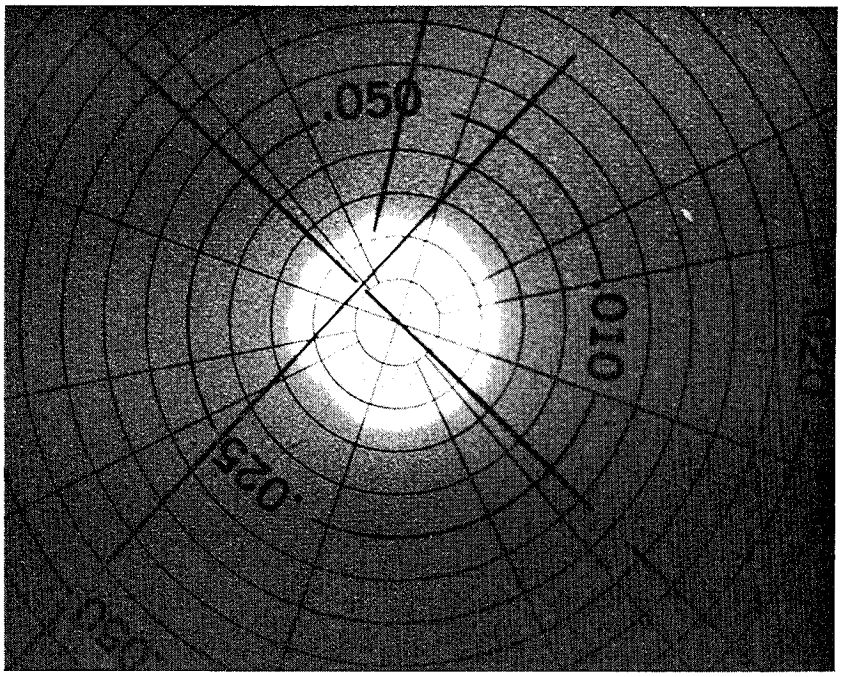

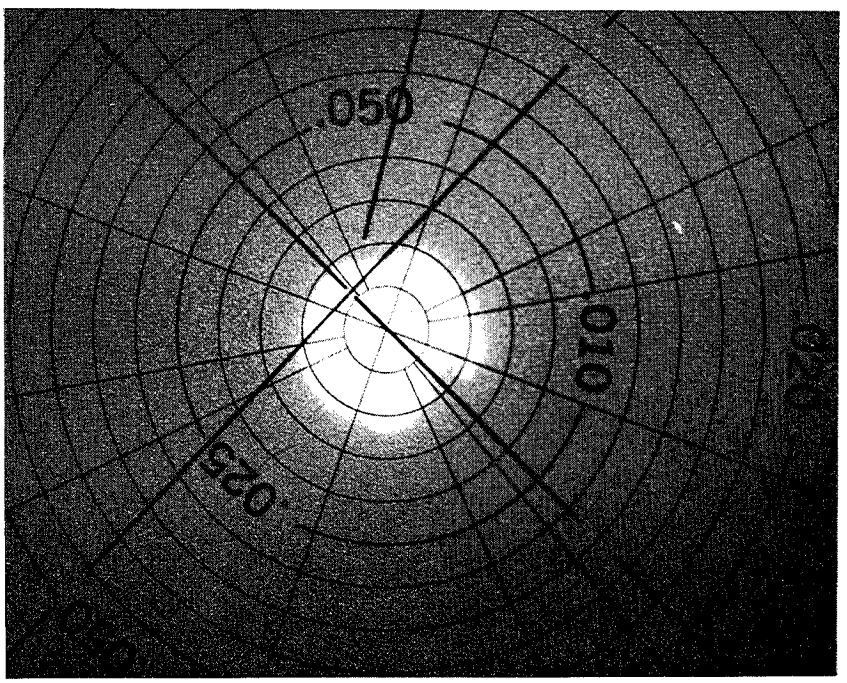

Fig. 7 Mechanically Pierced Holes

FIG. 8
Diameter Ratio (Dh/Dn) versus
Pulse Length to Diameter Ratio (L/Dn)

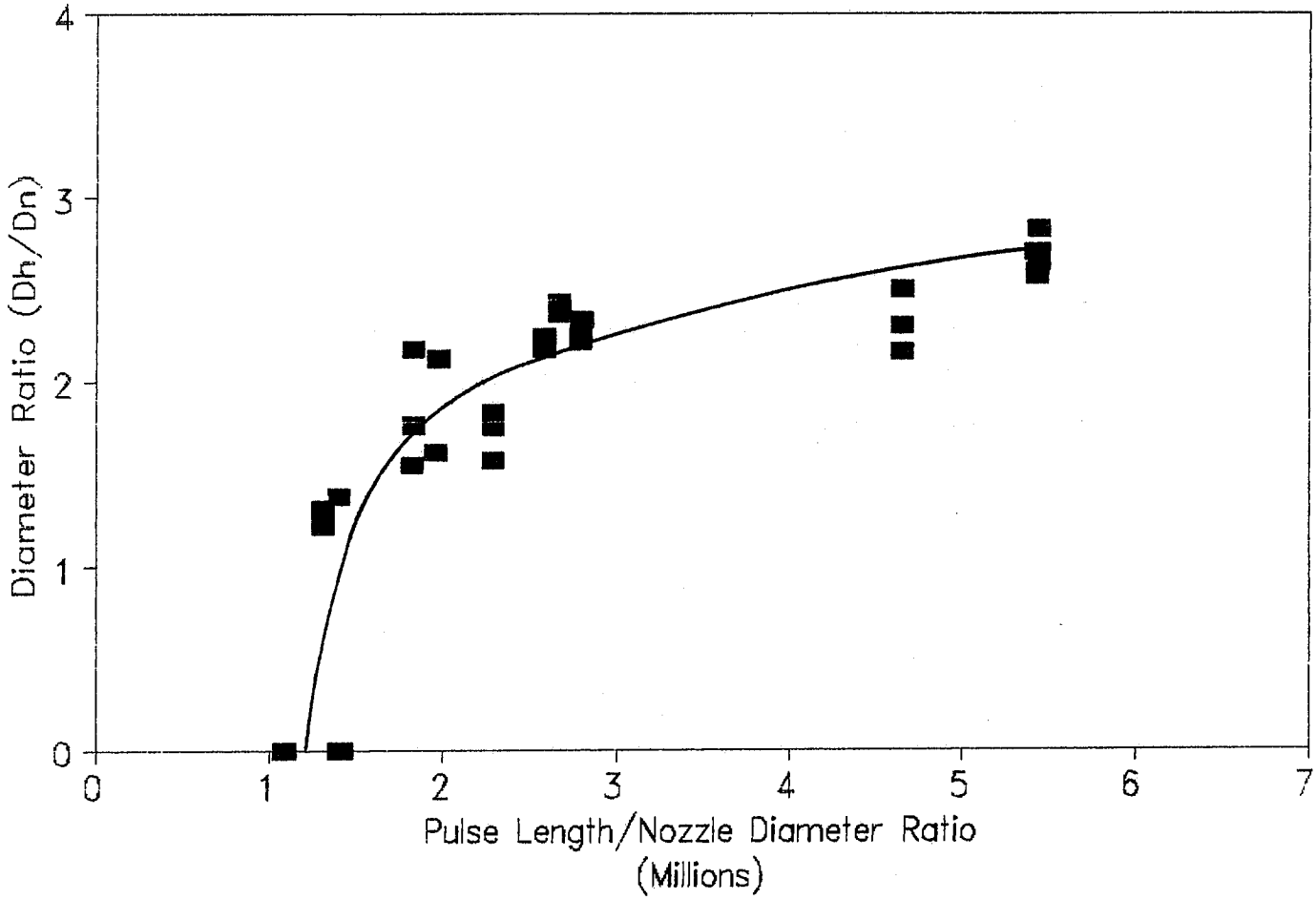

FIG.9
Diameter Ratio (Dh/Dn) versus
Stock Thickness/Nozzle Dia. Ratio

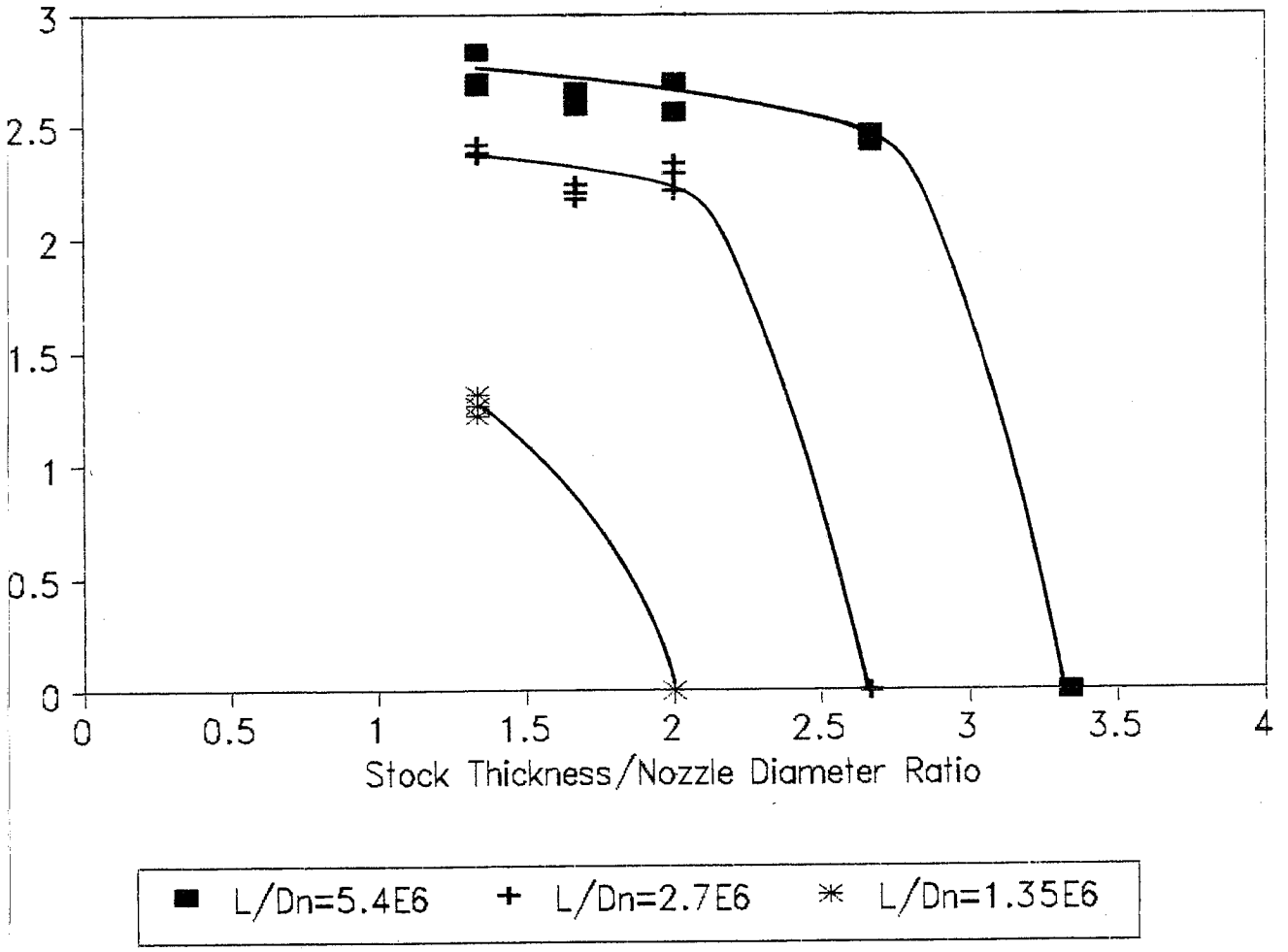

■ L/Dn=5.4E6 + L/Dn=2.7E6 ✳ L/Dn=1.35E6

FIG. 10

Diameter Ratio (Dh/Dn) versus
Slug Length to Diameter Ratio (L/Dn)

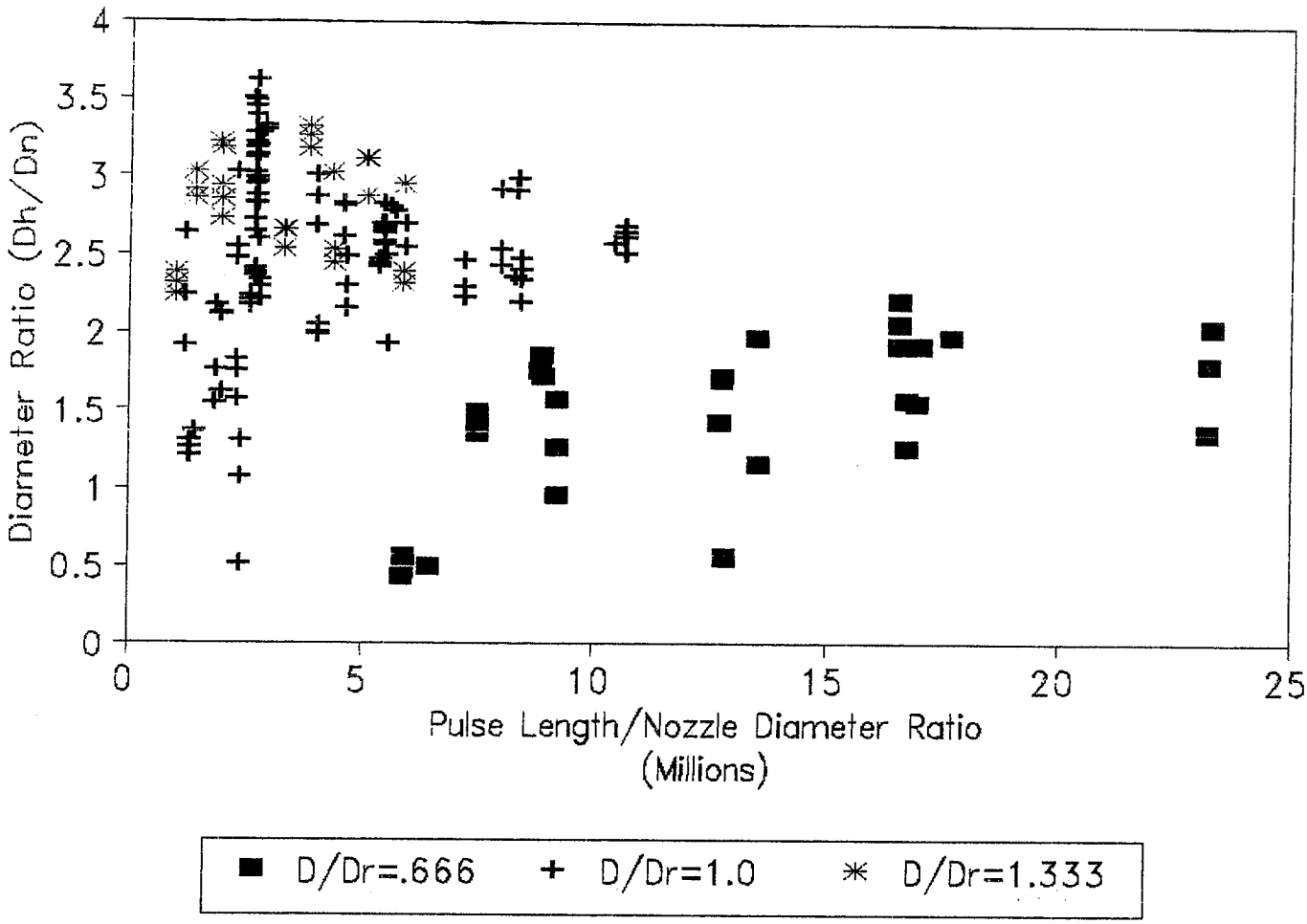

6th American Water Jet Conference
August 24 - 27, 1991: Houston, Texas

Paper **37**

HYPER PRESSURE WATERJET CUTTING OF THIN SHEET METAL

by

C. Raghavan
and
E. Ting

of

Flow International Corporation
Kent, Washington

ABSTRACT

An intensifier to continuously pump water at pressures up to 690 mPa (100,000 psi) was designed and built by Flow International Corporation to investigate waterjet and abrasive waterjet cutting at this pressure. The first area of investigation was the cutting of thin sheet metals in the range from 0.6mm (0.025 inch) to 3.2mm (0.128 inch) in thickness using a pure waterjet. The tests were conducted on Stainless Steel, Titanium and a variety of Aluminum alloys. It was found that a significant threshold exists for certain thin sheet metals that makes it possible to cut an order of magnitude faster at 100 Kpsi than at 55 Kpsi using the same nozzle size. The high cut speeds achieved appear to make hyper pressure waterjet cutting of thin sheet metals a commercial proposition. The test cut data is presented and discussed in this paper.

Organized and Sponsored by the Water Jet Technology Association.

1.0 INTRODUCTION

Waterjets at pressures up to 379 mPa (55,000 psi) are currently being used in industrial applications for cutting a variety of materials such as plastic, fiberglass, foam, paper, rubber and food products. They are not being used for cutting metal because of low cutting rates. To cut metal at commercially viable rates, it has been necessary to use abrasive waterjets. However an abrasive waterjet is a more complex system than a pure waterjet. There is also the problem of abrasive waste disposal in a society that is very sensitive to environmental impact. Therefore this study was undertaken to find out whether waterjets at pressures up to 690mPa (100,000 psi) can cut metal at substantially higher rates.

The existence of a threshold pressure in cutting rock and concrete with waterjets up to 413 mPa (60,000 psi) has been well documented in the literature [1]. This is the pressure above which the cutting speed increases rapidly with pressure. Below this pressure, cutting is caused by erosion and is slow. Various regimes exist in which the mechanism of cutting differs and there may be points at which a transition from one regime to another takes place [2]. This study is aimed at ascertaining whether these characteristics for three metals, Aluminum, Titanium and Steel can be defined by exploring the zone from 379 mPa (55,000 psi) to 690 mPa (100,000 psi).

2.0 EQUIPMENT

An intensifier converts low pressure high flow rate hydraulic power to high pressure low flow rate hydraulic power. The fluid on the low pressure side is hydraulic oil and the fluid on the high pressure side is water. The standard 379 mPa (55,000 psi) intensifier made by Flow International Corporation provided the starting point for the design of the 690 mPa (100,000 psi) intensifier. This intensifier has an intensification ratio of 20:1. With 19 mPa (2,750 psi) on the low pressure side, we can obtain 379 mPa (55,000 psi) on the high pressure side.

Two approaches were taken. The first was to modify this intensifier so that the low pressure side could be taken up to 34 mPa (5,000 psi). The second method was to retain the low pressure side at 19 mPa (2,750 psi) but change the intensification ratio to 33.3:1. Both systems were built and worked satisfactorily. They provided smooth and continuous flow at 690 mPa (100,000 psi).

The tests described in this paper were performed using one 20:1 intensifier by the first method. It could run a 0.2mm (0.008 inch) diameter orifice. At the operating pressure of 690 mPa (100,000 psi) this corresponds to a nozzle power of 19 kW (25 hp). A pressure spike lasting a few milli-seconds was observed on the high pressure side every time the intensifier shifted (ie. changed direction of motion). It was less than 20 mPa (3,000 psi) at the operating pressure of 690 mPa (100,000 psi).

3.0 EXPERIMENTAL METHOD

Three different metals were tested for cutting, Aluminum, Steel and Titanium. Within the Aluminum family, four types of Aluminum covering a range of properties were used. One steel and one titanium sample were test cut. The properties of each sample material and its thickness are listed in Table 1.

Each sample material was mounted on a computer controlled table. A catcher was mounted below the sample. The jet nozzle was kept stationary. The motion of the sample was programmed to step over a range of traverse speeds after every 1.2 cm (0.5 inch) of travel. This range was selected so that the speed at which the jet fails to consistently cut through the sample over the 1.2 cm (0.5 inch) travel could be identified. The speed below this is then the maximum cut speed. The maximum cut speed is therefore defined as the maximum speed at which the jet consistently cuts through the sample over a 1.2 cm (0.5 inch) distance. No uncut regions of metal should be found in this zone. No specification is made with regard to the surface finish in the cut zone. It was found that this method of identifying the maximum cut speed was objective, could be easily determined by an operator and was fairly repeatable.

The pressure of the waterjet was adjusted to a certain value. The values chosen were 241 mPa (35,000 psi), 310 mPa (45,000 psi), 379 mPa (55,000 psi), 448 mPa (65,000 psi), 517 mPa (75,000 psi), 620 mPa (90,000 psi) and 690 mPa (100,000 psi). The standoff from the nozzle to the sample was maintained at 2.5 mm (0.1 inch) for all tests. The maximum cut speed under these conditions was then determined.

4.0 EXPERIMENTAL RESULTS

4.1 Effect of Pressure

The first sample to be test cut was a 0.8mm (0.032 inch) thick Al 2024-T3 Alclad sheet. At 379 mPa (55,000 psi) the maximum cut speed was 30 mm/min (1.2 inch/min). If cut speed is assumed to be a linear function of pressure, an extrapolated cut speed of 56 mm/min (2.2 inch.min) can be calculated. However, actual data indicated a cut speed of 914 mm/min (36 inch/min)! Further tests at intermediate pressures revealed that there was a significant discontinuity in the maximum cut speed vs Pressure curve (Figure 1). This occurs at about 379 mPa (55,000 psi). The variation from 379 mPa (55,000 psi) to 690 mPa (100,000 psi) is quite linear. Multiple values for maximum cut speed at 517 mPa (75,000 psi), 620 mPa (90,000 psi) and 690 mPa (100,000 psi) were taken to see how repeatable the data was.

From Figure 1, for Al 2024-T3 (0.8mm), we may conclude that the variation of the maximum cut speed with pressure is highly linear above a pressure of 517 mPa (75,000 psi). A straight line has been fitted to this data.

Similar observations can be made from Figure 2 showing the results for Al 6061-T6 of the same thickness 0.8mm (0.032 inch). The threshold pressure is slightly lower and the slope of the straight line is less than that for Al 2024-T3 observed in Figure 1.

4.2 Effect of thickness

The next step was to examine the variation of the slope of the maximum cut speed vs Pressure curve and the threshold pressure as the thickness of the sample was changed.

Figure 3 shows the results for an Al 2024-T3 Alclad sample of thickness 0.64mm (0.025 inch). The threshold pressure is still 379 mPa (55,000 psi) but the slope varies inversely with thickness. At 690 mPa (100,000 psi) the maximum cut speed is 1143 mm/min (45 inch/min) compared to 889 mm/min (35 inch/min) for the same material with a thickness of 0.8mm (0.032 inch). Figure 4 shows the results for the same material with a thickness of 1.6mm (0.063 inch). At (100,000 psi), the maximum cut speed is 381 (15 inch/min).

The variation of maximum cut speed with thickness has been plotted for Al 2024-T3 Alclad in Figure 5. We observe that the slope of the curve for 690 mPa (100,000 psi) is steep while it is almost flat at 379 mPa (55,000 psi). Therefore, at hyper pressures, the effect of material thickness on the maximum cut speed is very pronounced. It is much less so at lower pressures.

The next set of results deal with Al 6061-T6. Figures 2, 6 and 7 show the results for samples of thickness 0.8mm (0.032 inch), 1.6mm (0.063 inch) and 3.2mm (0.128 inch) respectively. For this material, the transition is a bit more gradual. The maximum cut speed has been plotted against thickness in Figure 8 and is similar to Figure 5. Figures 9 and 10 show the results for two other Aluminum alloys Al 2024-O and Al 5052-H32 Alclad respectively. Both are of thickness 1.6mm (0.063 inch).

4.3 Effect of material change

In this section we examine the data obtained for Stainless Steel and Titanium. The material specifications for these two samples are listed in Table 1. Both samples were 0.8mm (0.032 inch) thick. The maximum cut speed vs pressure curves shown in Figures 11 and 12 are similar to each other and to the curve obtained for the "thick" Al 6061-T6 sample 3.2mm (0.128 inch) shown in Figure 7. There is first a region of zero or low cut speed up to around 300 mPa (44,000 psi). Next there is a non-linear region up to around 517 mPa (75,000 psi). Then the variation is a steep straight line similar to that obtained for the other Aluminum samples.

5.0 DISCUSSION

There is one common fact that can be observed from all this data. Above a certain pressure which we have found to be 517 mPa (75,000 psi), the variation of the maximum cut speed with pressure becomes linear. This is true for Aluminum, Steel and Titanium, covering a range of thicknesses from 0.64mm (0.025 inch) to 3.2mm (0.128 inch). We can therefore characterize all "thin" sheet metal cutting with "hyper pressure" waterjets with just two parameters, a slope and an intercept on the pressure axis where "thin" is defined as "up to 3.2mm (0.128 inch)" and "hyper pressure" is defined as "517 mPa (75,000 psi) and greater"

The data obtained for these tests has been presented along with the specifications for the material samples and their properties. Additional information regarding hardness of the samples has also been provided. A theoretical model to cover thin sheet metal cutting with hyperpressure waterjets will be presented at a later date.

6.0 CONCLUSIONS

1. There exists a threshold pressure for metal cutting with waterjets. Above this pressure, the cutting rate increases rapidly with pressure. Below this pressure the cutting rate is very low.

2. The cutting of certain "thin" sheet metal using a "hyper pressure" waterjet can be characterized with one straight line to represent the maximum cut speed as a function of pressure.

3. The effect of material thickness on the maximum cut speed is more pronounced at hyper pressures than at lower pressures.

7.0 REFERENCES

1. (Hashish) M. and Reichman J. M., "Analysis of Waterjet cutting at high traverse rates", Paper B2, Fifth International Symposium on Jet Cutting Technology, 1980.

2. (Olsen) J. H., "Jet slotting of concrete", Paper G1, Second International Symposium on Jet Cutting Technology, 1974.

Sl No	Material	Yield Kpsi	Ult Kpsi	Elong %	Measured Hardness Rockwell	Thickness mm (Inch)
1	A12024-0	10.9	26.8	20	RE 53	1.6 (0.063)
2	A12024-T3ALC	45	65.8	18	RE 94	0.64(0.025)
3	A12024-T3ALC	45	65.8	18	RE 94	1.6 (0.063)
4	A12024-T3ALC	45	65.8	18	RE 94	0.8 (0.032)
5	A15052-H32	31.2	37.7	10	RE 78	1.6 (0.063)
6	A16061-T6	39.9	45	12	RE 89	0.8 (0.032)
7	A16061-T6	39.9	45	12	RE 89	3.2 (0.128)
8	A16061-T6	39.9	45	12	RE 89	1.6 (0.062)
9	SS321AMS5510	35	90	45	RA 48	0.8 (0.032)
10	Ti-T9046JCP3	65	80	25	RA 55	0.8 (0.032)

Table 1: Typical mechanical properties of the sample materials

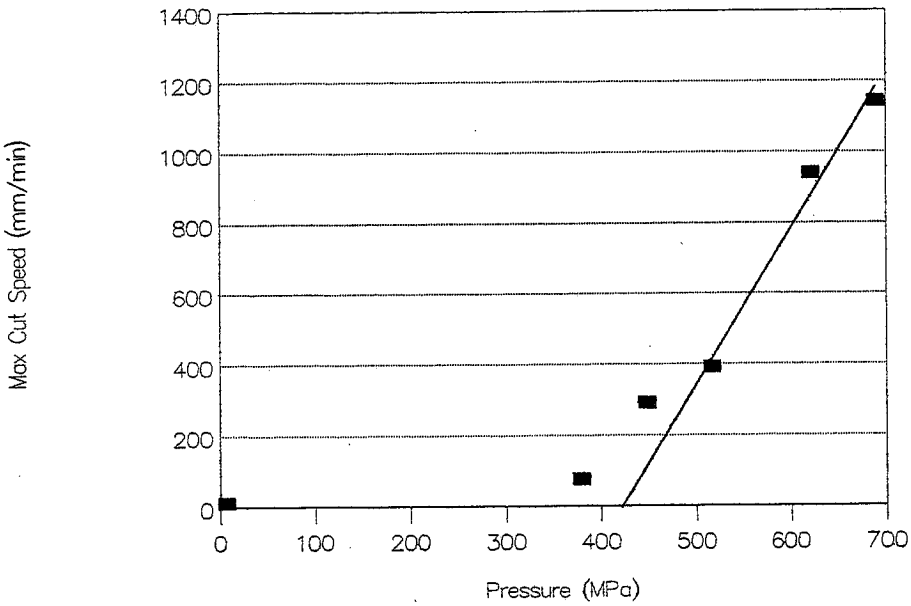

Fig. 3: Pressure vs. max. cut speed for Al 2024-T3 Alclad 0.64mm plate

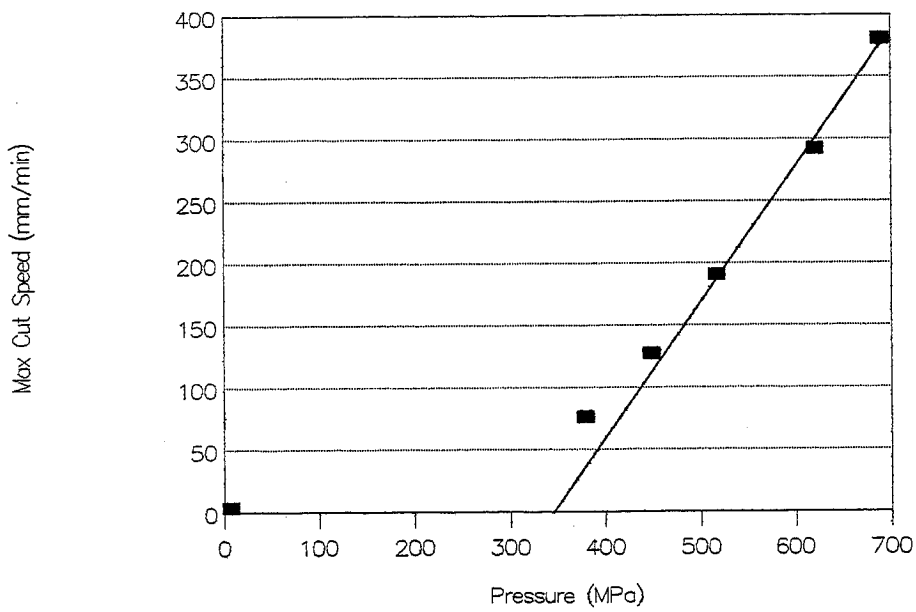

Fig. 4: Pressure vs. max. cut speed for Al 2024-T3 Alclad 1.6mm plate

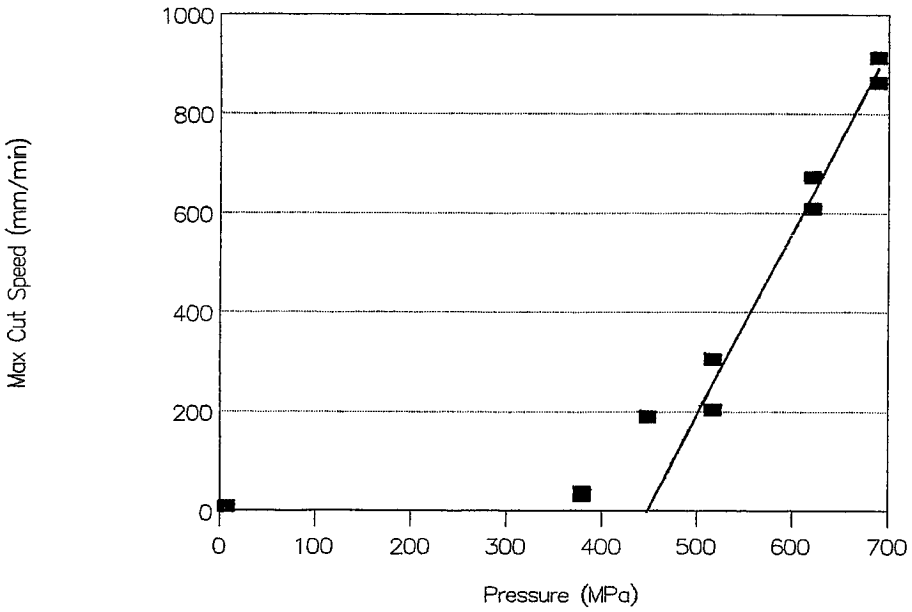

Fig. 1: Pressure vs. max. cut speed for Al 2024-T3 Alclad 0.8mm plate

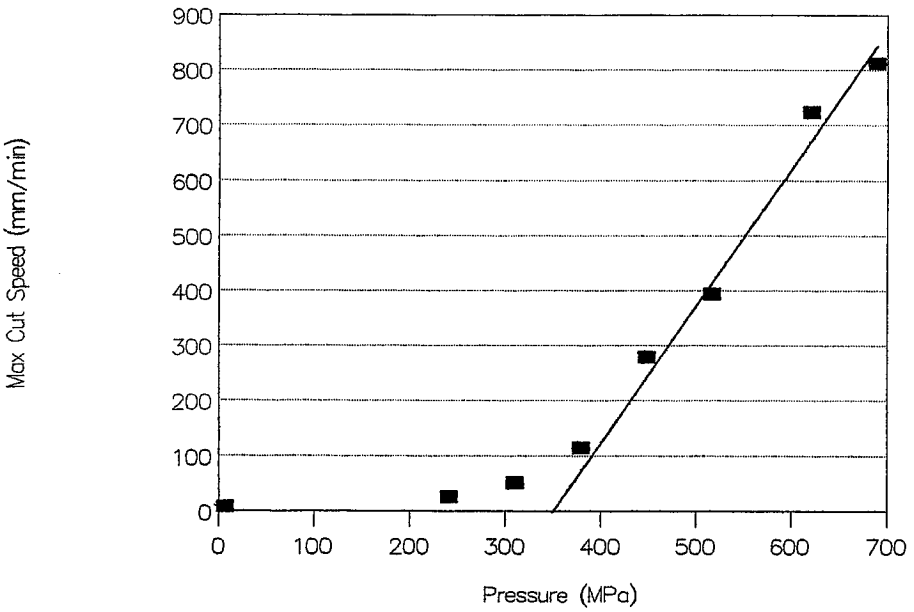

Fig. 2: Pressure vs. max. cut speed for Al 6061-T6 0.8mm plate

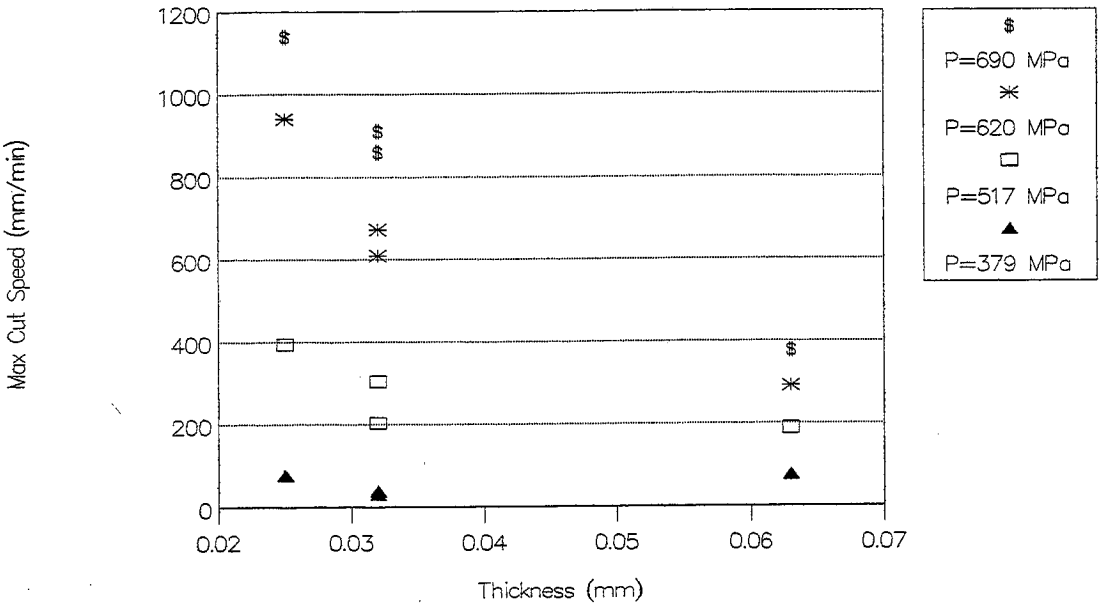

Fig. 5: Max cut speed vs. thickness for Al 2024-T3 Alclad

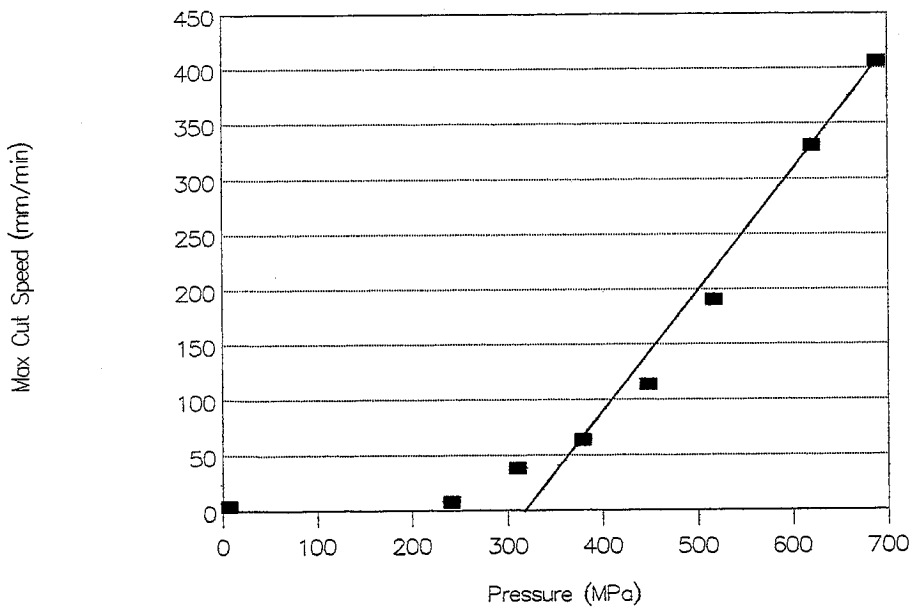

Fig. 6: Pressure vs. max. cut speed for Al 6061-T6 1.6mm plate

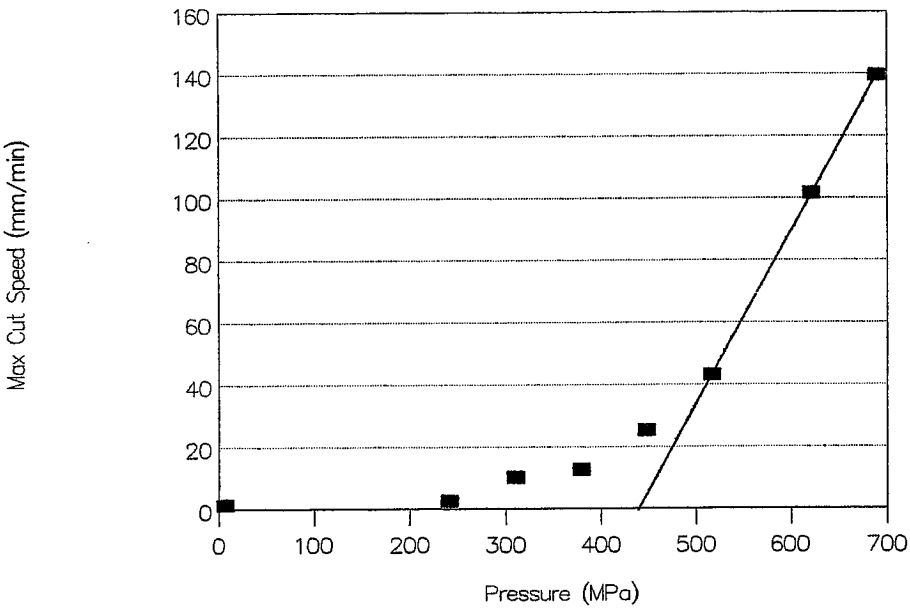

Fig. 7: Pressure vs. max. cut speed for Al 6061-T6 3.2mm plate

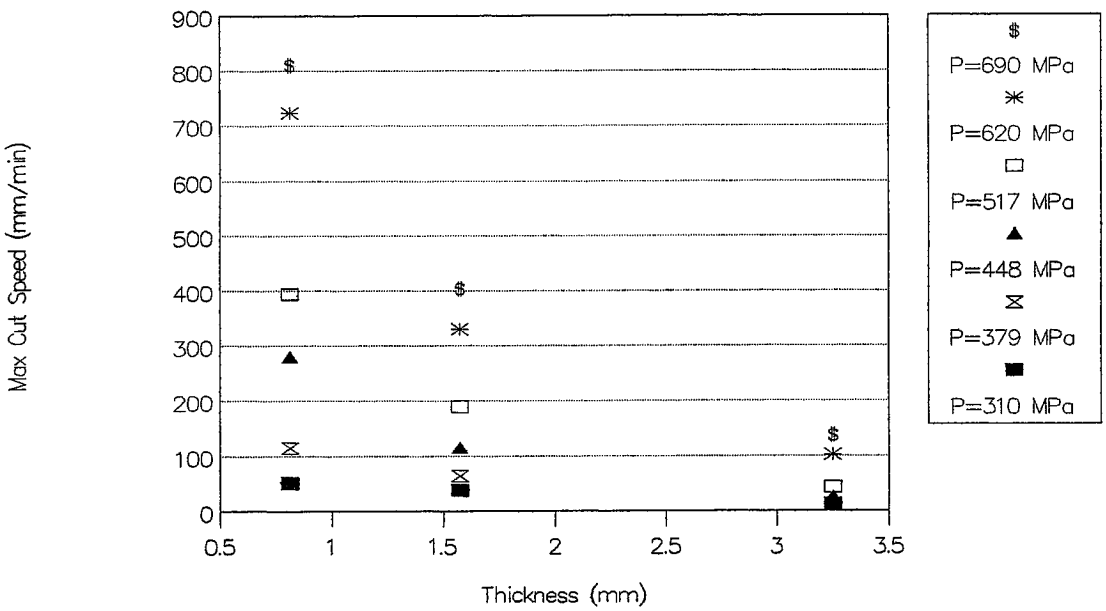

Fig. 8: Max cut speed vs. thickness for Al 6061-T6

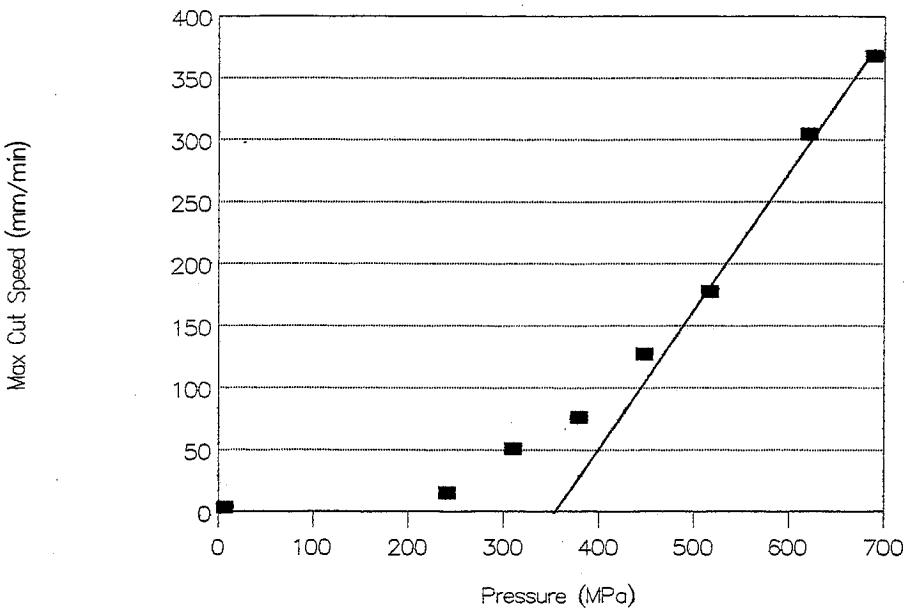

Fig. 9: Pressure vs. max. cut speed for Al 2024-O 1.6mm plate

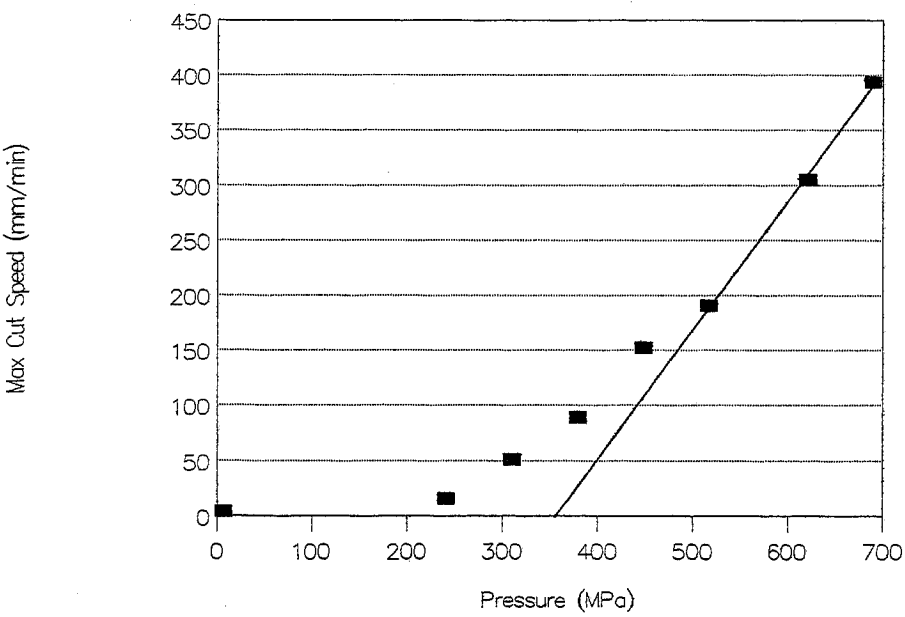

Fig. 10: Pressure vs max. cut speed for Al 5052-H32 Alclad 1.6mm plate

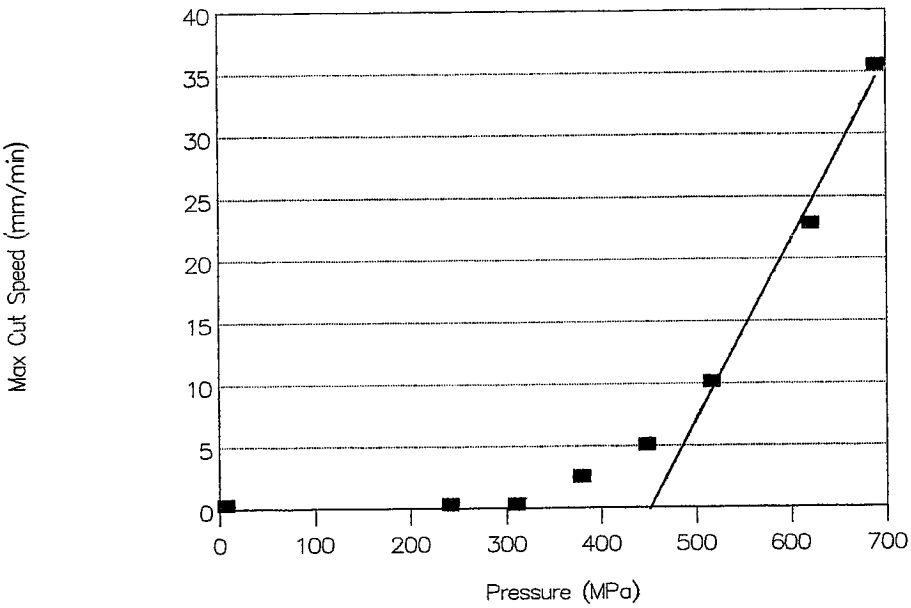

Fig. 11: Pressure vs. max. cut speed for stainless steel 321 AM55510 0.8mm plate

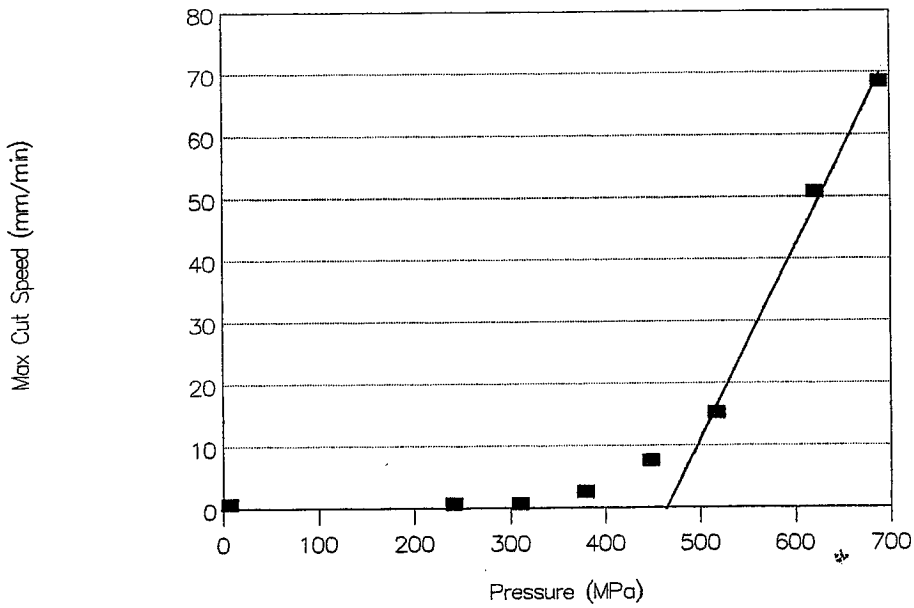

Fig. 12: Pressure vs. max. cut speed fot Titanium T9046JCP3 0.8mm plate

6th American Water Jet Conference
August 24 - 27, 1991: Houston, Texas

Paper **38**

Preparation Of Secondary Fiber Stock By High Pressure Waterjets

G. Galecki, M. Mazurkiewicz, D.A. Summers
University of Missouri-Rolla, USA
High Pressure Waterjet Laboratory
Rolla, MO 65401, USA

T. Nixon
Technology Development, Inc.
Rolla, MO 65401, USA

ABSTRACT

To reuse waste paper, current technology essentially launders the ink from the pulp using mechanical, chemical, and detergent action in flotation and washing processes. The objective of this study was to determine the feasibility of pulping and deinking newsprint using high pressure waterjets. In experimental studies with the proposed concept, all pulp samples met the criteria provided by industry contacts for secondary pulp except for test related to color, brightness, and tensile tests.

Organized and Sponsored by the Water Jet Technology Association.

1.0 INTRODUCTION

Newspapers make up an estimated 28% of recoverable household waste, and waste paper makes up about 70 million tons, or 40%, of the 180 million tons of solid waste generated annually. As of 1977, the United States recycled only about 25% of its waste paper as compared with Japan, which recycled 44%.

Currently, only 14% of the annual usage of newsprint is composed of recycled fibers, so most newsprint is being disposed of in landfills. Newsprint can take decades to decompose in landfills. Through legislation, politicians are trying to force newspaper publishers to use more recycled fiber. Both California and Connecticut have passed recycle-content bills addressing newsprint, and 20 other states have similar bills under consideration [Powell]. However, publishers have claimed inferior quality, and the cost of recycled newsprint has been approximately the same as new paper. As recently as August 1989, the market for newsprint collapsed because of oversupply: prices went from recyclers receiving $30 per ton of newsprint to recyclers paying $10 per ton to have newsprint hauled away.

Current technologies to pulp and deink newsprint use a secondary pulper and a deinking system. The deinking system uses chemicals and mechanical energy to dislodge the ink particles from the fibers and to disperse the particles in the aqueous medium. The ink particles are then separated from the stock, either by a washing or a flotation process or by a hybrid process combining the two elements [Smook]. The chemical surfactants commonly used include detergents, dispersants, and foaming agents. Other chemicals such as caustic soda, sodium silicate, and borax are also used to enhance the action of the surfactants.

In the washing process, dispersants are used with the detergents to disperse the ink constituents into very fine particles. The ink is then dispersed by a multistage washing sequence. Both the cleaning and dispersion operations are carried out in the pulper. A representative washing process is shown in Figure 1.

In the washing process, the separation of ink corresponds to a stock-thickening process, whether conventional washing equipment or screens are used. If the ink particles are extremely small ($<20\ \mu m$), the amount of ink removed is theoretically proportional to the amount of water removed. In practice, the fiber network acts as a filter to reduce the actual removal efficiency [Smook].

Flotation deinking systems attempt to keep ink particles within a range of particles sizes much larger than washing systems so that surface collection can be achieved using specific chemical systems. In the flotation process, the cleaning stage is carried out in the pulper. Chemicals are then added to promote foaming and flocculation of the ink particles. The stock is finally aerated in a series of flotation cells, causing the light flocs of ink particles to rise to the surface, where they are skimmed off. A representative flotation process is shown in Figure 2 [Smook].

The flotation process, which is widely used in Europe, has higher capital equipment costs and space requirements than the washing process but lower fiber losses. The flotation cell is the key to the process. Small air bubbles are blended with the stock suspension; and the bubbles attach to the ink and dirt particles, causing them to rise to the surface of the cell. The flotation process provides higher fiber yield, but removes less filler and fines than washing. The deinked stock from flotation requires little washing, and effluent treatment is generally simplified.

A recent study completed in England compares the flotation and washing processes for deinking [Read]. Most inks consist of a pigment, which provides the system's coloration, and a vehicle, which transports the pigment from the press to the paper and holds it there. In deinking, the vehicle largely determines the ease with which the ink may be removed and the eventual particle size distribution on repulping.

The Japanese have used cold nonpressurized dispersion of deinked furnishes, in conjunction with flotation and washing. This method improves deinking efficiency in converting non-impact-printed ledger to tissue and in recycling offset-printed newsprint to newsprint [Gilkey, et al]. Also in Japan, talc is being used to absorb inks and other materials and is separated from the usable fibers by flotation, screening, and cleaning [Hiraoka and Yamamoto]. In another Japanese process, phosphoric acids or their salts have been added to pulp dispersions in the washing process after deinking to prevent calcium carbonate-based deposits [Kiuchi and Hashimoto].

Papelera Peninsular of Spain is using a deinking system based on the principle of measuring and controlling the ink particle size distribution with a dedicated chemical and incorporating highly efficient ink-removal stages. The raw material was 100% newsprint and the ink was removed by flotation only [Zabala and McCool].

In Germany, a study of producing printing paper with a large share of deinked waste paper indicates that ink particles display the same size distribution before and after flotation. This refutes the opinion that preferential separation is feasible or that the flotation of a specific particle size is more difficult. More significant is the completeness with which the ink particles are detached from the fiber. The average particle size is 5 to 8 μm in conventional inks, compared with 25 to 30 μm in UV curing inks [Blechschmidt, et al].

One Canadian firm, has done recent work on deinking; their proprietary technology uses rapidly expanding steam to separate the fibers. Also in Canada, the Pulp and Paper Research Center at the University of Quebec has examined the relationship between operating variables and the particle size distribution of deanchored ink in flotation deinking and between the demension of ink particles and brightness and cleanliness of the pulp obtained [Marchildon]. In Canada, another system for deinking waste newspaper uses a new low-foaming surfactant to eliminate foaming problems during deinking. Deinking of newsprint stored longer than six months has been examined. Ink removal could be improved by increasing chemical levels and by pH, by temperature, or by mechanical refibering [Mah].

In Sweden, recyclers have used flotation deinking and Fibreflow fiberizing methods. Wastepaper is wetted to 15% to 20% consistency and then successively dropped on a hard surface. The resulting shearing forces fiberize the paper without disintegrating the contaminants. The Fibreflow drum claims automatic sorting of contaminants, savings in deinking chemicals from high-consistency treatment, and power savings by eliminating a power-consuming waste-paper-cutting operation [Rutqvist, et al].

The Chinese have used ultrasonic deinking and have evaluated the effects of consistency of slurry, irradiation time, temperature, and pH on the purity of deinked pulps [Chem, et al]. They noted fewer carbon impurities in the ultrasonically deinked pulp than in chemically and mechanically deinked pulp.

In Poland, the Pulp and Paper Institute is studying neutral pH deinking using only synthetic surfactants [Gonera].

2.0 DESCRIPTION OF THE CONCEPT

In previous work [Galecki and Mazurkiewicz] in wood pulping and coal comminution, waterjets have demonstrated a tendency for preferential separation at microcracks and grain boundaries. This observed characteristic leads us to believe that the high-pressure liquid jet could be effective in separating contaminants such as ink from secondary fibers.

In a preliminary test, we pulped newsprint samples. Inspection of the pulped material indicates evidence of deinking. This deinking was also noted by the U.S. Forest Products Laboratory. To determine the feasibility of using a high pressure waterjet to pulp and deink newsprint, we evaluated the system's ability to separate ink particles and common contaminants from secondary fibers.

Five pulp samples were run by Integrated Paper Service, Wisconsin. All samples were made from the same newsprint from a local newspaper. The printer uses an oil-based ink. The objective of the tests were to determine waterjet parameters that provided the best test results. The supplier of the newsprint, Newsprint South, provided the following starting values:

Elmendorf Tear	33.5
MD Tear	22 to 23
Tensile properties	
Cross	3.6
MD	13
Color, Hunter L	81.6
a	-0.3
b	4.9
ISO Brightness %	58.5

Based on conversations with the paper industry references, the following tests were requested be run on samples provided to Integrated Paper Services, Inc.:

Canadian Standard Freeness
ISO Brightness
Color, Hunter L
a
b
Elmendorf Tear, g
Tensile Properties:
Tensile Strength, lb f/in

Stretch, %
Tensile Energy
Absorption, J/sq m
Breaking Length, km

Fiber Index, %
Fiber Classification
Scattering Coefficient

The image analysis could not be done because it required an 200mm x 200mm sheet and the standard British hand sheets were too small (British hand sheets were made from the pulp samples). The freeness was run after the pulp was disintegrated for 2.5 minutes using standard laboratory equipment.

More specific information is available upon written request to:

Dr. Grzegorz Galecki
University of Missouri-Rolla
High Pressure Waterjet Laboratory
Rock Mechanics Facility
1006 Kingshighway
Rolla, MO 65401
tel. (314) 341-4938
fax (314) 341-4368

Mr. Terry Nixon
Technology Development, Inc.
Twitty Park Research Drive
Route 4, Box 519
Rolla, MO 65401
tel. (314) 341-3614
fax (314) 364-9589

3.0 DISCUSSION OF RESULTS

Table 1 summarizes all preliminary test results. All of the tests appear to have met the criteria provided by industry sources, except for the test results related to color, brightness, and tensile strength. Because the pulp was not washed and no dispersants were added to

prevent redeposition of ink particles in the fibers, the color and brightness values were considered acceptable.

Lower than the original value of the tensile strength indicates some failure in fibers. This is a problem difficult to avoid in contact between the fibers and the high pressure waterjet.

4.0 CONCLUSIONS

To date, we have shown that using high pressure waterjet to deink newsprint is feasible. However, several key considerations still need to be addressed. Based on data from FSC Paper Company, Illinois, where they used a 225 kW motor to process 8.5 ton charge of newsprint for 5 minutes, energy usage in the waterjet deinking process is several hundreds times higher. This is our main concern. Probably in such a situation, Shakespeare would say, "To waterjet it or not to waterjet it". An additional factor is the fiber loses. It is very important to know how much, by volume, of fibers has been shortened during the process.

The proposed technology is not intended to replace the entire pulping/deinking process. The results need to be compared with washing and flotation systems at an equivalent processing stage.

5.0 ACKNOWLEDGEMENTS

This process has been developed under University of Missouri-Rolla Patent Disclosure 88-UMR-033. Financial support by the U.S. Department of Energy is greatly appreciated.

6.0 REFERENCES

1. Blechschmidt, J., H.J. Naujock, A. Opherden, and M. Schlegel, 1982. "Production of Printing Paper with a Large Shar of Deinked Waste Paper in the German Democratic Republic." European Liaison Committee for Cellulose and Paper Conf. (Budapest) Proc., 20th Paper I/4: 24p.

2. Chem, M., G. Tan, and G. Cao. 1988. "Deinking of Waste Newspaper Under Ultrasonic Irradiation." Northwest Institute of Light Industry, Dept. of Paper Making, Xianyang, China, Xibei Qinggongye Xueyuan Xuebao 6(4): 77-85. [Chinese].

3. Galecki, G., M. Mazurkiewicz, 1989. "Effectiveness of Coal Comminution by High Pressure Waterjet". Proceedings of 5th American Waterjet Conference, Toronto, Canada.

4. Gilkey, M., H. Shinohara, and H. Yoshida. 1988. "Cold dispersion Unit Boosts Deinking Efficiency at Japanese Tissue Mills." Pulp Paper 62(11): 100-103.

5. Gonera, H. 1989. "Use of Deinked Waste-Paper Pulp in the Manufacture of Newsprint and Wood-Containing Printing Papers." Pulp and Paper Institute [Polish], Papermaking Department, Przeglad Papier. 44(1): 16-17.

6. Hiraoka, M., and T. Yamamoto. 1975. "Removal of Inks for Regeneration of Paper." Patent Assignees: Hokuetsu Paper Mfg., Co. Ltd., Japanese Patnet Kokai 20005/75.

7. Kiuchi, K., and A. Hashimoto. 1989. "Prevention of Deposition in Washing of Deinked Waste paper." Patent Assignees: Kurita Water Industries, Ltd., Japanese Patent Kokaii 77,693/89.

8. Mah, T. 1983. "Deinking of Waste Newspaper." Tappi Journal 66(10): 81-83.

9. Marchildon, L., M. LaPointe, and B. Chabot. 1989. "Influence of Particulate Size in Flotation Deinking of Newsprint." Pulp and Paper Can. 90 (4): 90-95.

10. Powell, J. March 1990. "The Further Development of the Deinked Newsprint Market." Resource Recycling 9(3):30.

11. Read, B.R. 1986. "Deinking Chemicals and Their Effects." IChE/PITA Symp. Chemicals in Pmkg. Manchester 2nd, No. 7, p. 16.

12. Rutqvist, S., F. Sundman, and J. Venho. 1977. "Fibreflow-High-Consistency Defibering System for Waste Paper." Pulp Paper 51(8):54-55.

13. Smook, G.A. 1987. Handbook for Pulp and Paper Technologists. Chapter 14, Joint Textbook Committee of the Paper Industry.

14. Zabala, J.M., and M.A. McCool. 1987. "Deinking at Papelera Peninsular (Madrid Spain)." TAPPI Pulping Conference, Washington, D.C., Proc. (Book 1), pp. 143-149.

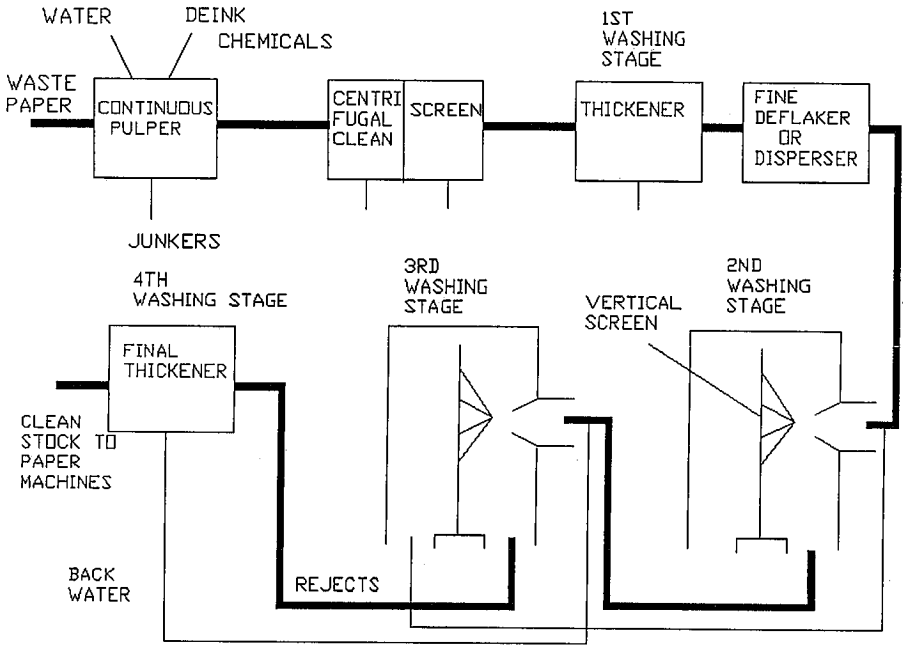

Figure 1. Washing Deinking Process

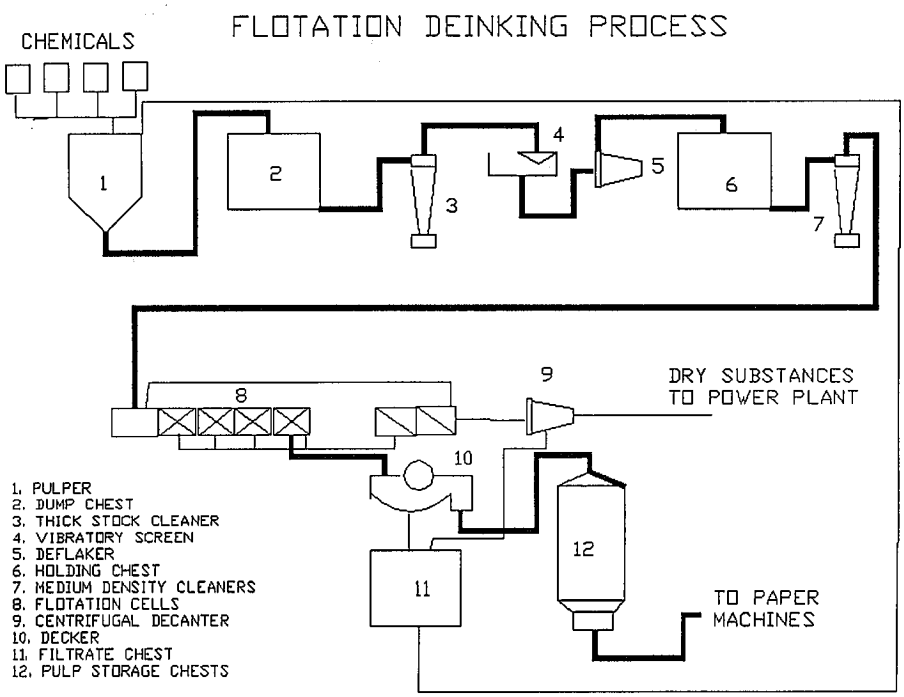

Figure 2. Flotation Deinking Process

TABLE 1. Test Results

Parameter	Sample 1	2	3	4	5
Canadian Std. Freeness	135	130	130	130	150
ISO Brightness	52.6	52.9	52.6	54	51.76
Color, Hunter L	74.4	74	74.1	75.1	73.84
a	-0.068	-0.6	-0.63	-0.67	-0.78
b	2.87	2.51	2.48	2.51	3.23
Elmendorf Tear, g	56	55.5	54.4	54.1	58.2
Tensile Properties					
Tensile Strength, lbf/in	9.8	10	10.6	10.9	10.9
Stretch, %	1.6	1.5	1.5	1.4	1.67
Tensile Energy Absorption, J/sq m	18.7				22.4
Breaking Length, km	2.7				2.87
Fiber Index				0.14%	
TAPPI Opacity		99.6	99.2	98.9	
Scattering Coefficient		642.3	634.1	618.7	
Fiber Classification Average					
Retain on 14 Mesh				13.43%	17.10%
Through 14 on 28				16.86%	16.77%
Through 28 on 48				16.57%	15.77%
Through 48 on 100				13.04%	14.33%
Through 100				40.10%	36.63%

6th American Water Jet Conference
August 24 - 27, 1991: Houston, Texas Paper 39

RHEOLOGICAL INVESTIGATION OF THE ABRASIVE SUSPENSION JET

R. H. Hollinger and R. J. Mannheimer
Southwest Research Institute
San Antonio, Texas, USA

ABSTRACT

A suspension of abrasive particles in polymer-thickened water gives a jet of impressive penetrating power when the jet impacts upon a substrate material such as steel or aluminum. Judging from the width and depth of cuts produced by such jets, some polymeric thickening agents produce deeper, narrower cuts than do others, even though all other conditions remain the same. It was reasoned that the rheological properties of the polymer solution must have a controlling effect on jet behavior. Consequently, this work was undertaken to determine the degree to which rheological properties affect the formation of coherent, high velocity jets.

The appearance of the free jets of different polymer solutions was studied using stroboscopic flash photographs of the jet.

High speed photographs indicated that, if the shear viscosity of the jet fluid was high enough to be used to create an abrasive suspension, the jet cores did not show sufficient divergence differences to explain the difference in cutting ability. The outer cone was considerably affected by the solution viscosity since the shear layer turbulence in the jet is reduced at higher viscosities. The effect is most pronounced when the solution has a high viscoelastic component which results in a near absence of the outer cone.

The viscoelastic component of the jet fluid was found to control jet penetration and cut width. A jet of viscoelastic fluid does not break up immediately on impact and more energy is transferred to the impact point. This was demonstrated in cutting experiments in which tripling the concentration of viscoelastic polymer approximately doubled the jet penetrating power.

Organized and Sponsored by the Water Jet Technology Association.

1.0 INTRODUCTION

Conventional water/abrasive jets have been used in the cutting of metals, ceramics, masonry, and composite materials for over ten years. More recently, investigations have shown that the abrasive suspension jet can achieve cuts in the same materials using lower pressures.

The conventional water/abrasive jet head is shown in the functional diagram of Figure 1A. A sapphire orifice is used to create a primary jet of water at velocities above 6.4 x 10^2m/sec. Typical driving pressures for the jet range from 207 to 380 MPa (30,000 to 55,000 psi). The abrasive, usually garnet sand, is aspirated into the mixing chamber by the action of the jet, mixed with the jet, and the whole is reformed into a secondary, lower velocity jet by means of a focusing cone and focusing tube. The velocity of the collimated, secondary jet may be increased by increasing the water flow in the primary jet. This may be done by using a larger diameter orifice, a higher driving pressure, or both together. A smaller diameter focusing tube may also be used. At some point,depending on the primary jet flow and focusing tube diameter, water will enter the abrasive feed line and stop the abrasive flow. Accurate alignment of the focusing tube with the center line of the primary jet is required in order to obtain a well collimated secondary jet and to decrease tube wear. Inefficiencies in momentum exchange between the primary jet and the abrasive particles reduces the cutting efficiency of the collimated jet, while the focusing tube, being of larger diameter than the orifice, allows jet divergence and reduction of jet velocity.

In order to impart as much as possible of the primary jet velocity to the abrasive particles, Southwest Research Institute devised an abrasive suspension jet. The abrasive particles are suspended in polymer-thickened water and the suspension is pumped directly through a diamond jet forming orifice. A functional diagram of the jet head for the abrasive suspension jet is shown in Figure 1B. Work with the abrasive suspension jet has shown it to have better cutting efficiency than the conventional jet while using less abrasive, lower power, and lower pressure. A part of the abrasive suspension jet's higher efficiency comes from the higher abrasive particle velocity, but a large part comes from the coherence of the jet which allows the energy of the jet to be brought to bear on a small area of the target. This is done without the necessity of collimation as with the conventional jet, and makes the set-up and aiming of the suspension jet at the work piece much easier.

The abrasive suspension jet has advantages over the conventional water/abrasive jet so long as the jet remains coherent. Loss of coherence produces cuts similar to those of the conventional system with regard to the width of the cut and depth of penetration. In experiments (Hollinger), pressures exceeding 69 MPa (10,000 psi) produced degradation of jet quality as evidenced by wider cuts and reduced penetration.

The problem posed by the foregoing observation is one of understanding to what extent the rheological properties of the suspending media affect the formation of coherent, high pressure, high velocity jets, and this program was undertaken to develop information leading, at least, to a preliminary understanding of the interactions involved. If the operating pressure of the jet can be increased without loss of coherence, higher cutting rates can be achieved on thicker and harder materials.

2.0 BACKGROUND

Very little literature is concerned with fluid jets at near sonic velocities. However, Koziol and Glowacki studied turbulent jets of dilute polymer solutions impinging on a surface. The study, together with their discussion of previous studies, appears to have a bearing on this investigation. The impinging jet is divided into three regions: the potential core or free jet region; the impingement region; and the wall jet region or region of flow spreading after impact. Polymer additives increased the coherence length of the free turbulent jet while attenuating small scale turbulence. In the case of viscoelastic fluids at high jet velocities, a sufficiently high viscoelasticity causes a solid-like response on impact. Mannheimer, while working with solutions of polymers in organic solvents instead of in water, was able to link the antimisting properties of dilute polymer solutions to the viscoelasticity of the solutions as measured by a packed tube viscometer.

In order to explain the findings reported for the abrasive suspension jet (Hollinger), it was noted that the jet in free flight was coherent and therefore concentrated the abrasive jet impact on a small area of the substrate. The indications from Koziol and Glowacki would seem to indicate that free flight coherence may not, of itself, explain the abrasive jet's ability to penetrate a substrate, but that the viscoelastic properties of the polymer solution may play a large role in the impact behavior of the jet. The work reported by Mannheimer gives a relatively easy method of determining the viscoelastic properties of the polymer solution.

3.0 APPROACH AND RESULTS

The experimental approach to the work was divided into the characterization of the free jets of polymer solutions by high speed photography, and the determination of the rheological properties of the polymer solutions by rotational viscometer for shear viscosity and packed tube viscometer for extensional viscosity or viscoelastic properties. When it became obvious that the free flight coherence of all the polymer solutions was nearly the same, a third experiment involving actual abrasive suspension jet cutting using three polymer solutions was added to show cutting differences.

3.1 Photographic Characterization

3.1.1 Experimental

A technique was developed to document free jet behavior photographically. In this technique, a stroboscopic flash unit was placed at 90° to the camera, thus utilizing both scattered and reflected light from the jet. Using white light, the turbulent, divergent mixing zone surrounding the jet core was visible, while use of a red filter (Wratten "A") over the flash unit allowed the central core of the jet to be seen without the interference of the fine droplets in the mixing zone. Both white light and red light photographs are necessary to characterize a jet. Measurements were made on enlargements of the photographs to determine the jet diameter at points 25, 50, and 100 orifice diameters from the orifice holder. The polymer solutions were pumped through the jet orifice using a floating piston pumping unit. Except as noted, all tests were conducted using a .0254 cm (0.01-inch) diameter diamond orifice. Tests were conducted at pressures of 52, 69, 103, 138, and 207 MPa (7.5, 10, 15, 20, and 30 kpsi).

3.1.2 Results

Figure 2 shows red and white light photographs of a waterjet at 69 MPa (10 kpsi). A considerable diffuse cone is visible in both cases. Large droplets are being sheared from the surface of the jet as indicated by the red light photograph. Figure 3 shows a jet of Xanvis®, 1 percent by weight, at pressures of 52 and 207 MPa (7.5 and 30 kpsi). The outer diffuse cone is not visible in the red light core photograph at 52 MPa (7.5 kpsi), but the core at 207 MPa (30 kpsi) is more divergent and shows a slight outer cone. Figure 4 shows a jet of Xanvis®, 2.5 weight percent, at 52 and 207 MPa (7.5 and 30 kpsi). No outer cone is visible under red light at either pressure. Figure 5 shows a jet of Superwater®, 1.3 weight percent, at 52 and 207 MPa (7.5 and 30 kpsi). The outer cone in white light is considerably reduced at 52 MPa (7.5 kpsi), but is clearly visible at 207 MPa (30 kpsi). The jet cores are not divergent. Figure 6 shows a jet of Superwater®, 3.9 weight percent, at 52 and 207 MPa (7.5 and 30 kpsi). The white light outer cone is reduced even at 207 MPa (30 kpsi) and the core at 52 MPa (7.5 kpsi) is extremely narrow. Figure 7 shows a jet of methyl cellulose, 2.0 weight percent, at 52 and 207 MPa (7.5 and 30 kpsi). Its behavior is similar to Xanvis®, but the jet cores are narrower.

3.2 Rheological Measurements

3.2.1 Experimental

Measurements of shear viscosity were made using a Chan-35 rotational viscometer at shear rates ranging from 1 to over 1,000 reciprocal seconds. A packed tube viscometer, described by Mannheimer, was used with a packing of 840 micrometer (.033 in) diameter beads to determine the viscoelastic component of the test solutions of polymers. Consistency parameters, suggested by Savins, were used to analyze the viscosity-shear rate data for the packed tube which had a cross-sectional area of 0.177 cm^2, a porosity of 0.4, and a length to bead diameter ratio of 11.9. Solutions of three different polymers were used. These were the same polymers and polymer concentrations used in the photographic measurement previously described. The solution concentrations were selected for closeness of match of shear viscosity at 1000 sec^{-1} shear rate, and for a low shear rate viscosity high enough to form a suspension of abrasives. An exception was methyl cellulose solution where a very high shear viscosity at 1000 sec^{-1} had to be accepted if a suspension was to be formed. The shear viscosities at 1000 sec^{-1} shear rate are shown in Table I.

3.2.2 Results

Apparent viscosities as a function of rate of shear are shown in the log/log plots of Figures 8 through 10. All the solutions show a shear viscosity which decreases with increasing shear rate and are, therefore, shear thinning. The Xanvis® and Superwater® solutions follow the power law formula. The packed tube viscosities show the same decrease in viscosity with increasing shear rate except in the case of Superwater® which is a solution of partially hydrolyzed polyacrylamide. The polyacrylamides are known to exhibit viscoelasticity and the solutions stopped decreasing in apparent viscosity with increasing shear rate when a critical shear rate was reached. The critical shear rate appears to be a function of polymer concentration with the critical shear rate decreasing with increasing concentration.

3.3 Cutting Experiments

3.3.1 Experimental

The photographic examination of the free jets showed only slight differences in the jet cores, and it was questionable whether these differences were sufficient to explain the differences in cutting ability observed with different polymer solutions. Koziol and Glowacki mentioned the more nearly solid-like impact obtained with jets of viscoelastic jets. A solid-like impact would lead to more energy exchange with the substrate before impact break-up of the jet occurred. It was, therefore, possible that two factors were acting instead of only the in-flight coherence of the free jet. The second factor would be the ability of the jet to resist impact break-up.

Since viscoelastic polymer solutions exhibit a relaxation time which increases with increasing polymer concentration, increasing relaxation time would inhibit jet impact break-up. The internal stresses built up in the impacting jet cause the jet to break up, and the break-up is resisted by the viscoelastic forces which relax in a time period dependent upon the viscoelasticity. A jet of a polymer solution having a short relaxation time would then break up at a lower impact energy or velocity than a jet having a longer relaxation time. A series of cutting experiments using three polymer solutions was performed to test jet penetration ability as a function of viscoelasticity or relaxation time. The experiments were carried out on 0.75-inch thick aluminum substrates at pressures of 52, 69, 103, 138, and 207 MPa (7.5, 10, 15, 20, and 30 kpsi) using a .0254 cm (0.01-inch) diameter diamond orifice. A traverse speed of the jet across the substrate was set at 15.9 cm/min (6.25 in/min), and an abrasive concentration of 105.6 grams/liter was used with the polymer solution to give a suspension.

3.3.2 Results

Figure 11 shows the effectiveness of a jet of 2 weight percent methyl cellulose solution. The methyl cellulose solution gave little or no sign of a viscoelastic component in rheological tests and jet penetration is low even at 207 MPa (30 kpsi).

Figure 12 shows the cuts made by a jet of 1.3 weight percent Superwater® solution. Full penetration occurred at 207 MPa (30 kpsi) but jet form at impact was lost at about 69 MPa (10 kpsi) as shown by widening of the cuts above that pressure level.

Figure 13 shows the cuts made by a jet of 3.9 weight percent Superwater® solution. Full penetration occurred at 69 MPa (15 kpsi) and jet form at impact persisted to about 138 MPa (20 kpsi). Even at 207 MPa (30 kpsi) the cut width was narrower than the 1.3 weight percent Superwater® solution.

4.0 CONCLUSIONS

The free-flight characteristics of jet cores are not appreciably different with various viscous materials. As long as the low shear rate viscosity is sufficiently high to produce a stable suspension, jet core diameter is not divergent in the normal abrasive suspension jet working range from 25 to 50 orifice diameters. While coherence of the jet is necessary to allow the jet core to impact in the smallest possible area, it does not explain why with some polymer solutions, abrasive suspension jets penetrate a substrate more deeply and with narrower kerf widths than do others under identical conditions.

Polymer solutions which show viscoelastic properties allow deeper and narrower cuts to be made in a substrate with the abrasive suspension jet. The depth and narrowness of the cut improves with increasing viscoelasticity. The viscoelasticity, hence the potential for use as a suspending medium, can be determined by packed tube viscometer measurements of viscosity as a function of rate of shear.

ACKNOWLEDGEMENTS

The authors acknowledge the contributions of Mr. Pierre Guiterrez who obtained the rheological data, Mr. Pat Chenault who operated the high pressure equipment in obtaining photographs and cutting data, Ms. Kim Barclay who typed the manuscript, and the Committee for Internal Research of Southwest Research Institute who furnished the funding to carry out this program.

REFERENCES

Hollinger, R.H., Perry, W.D., and Swanson, R.K., Proceedings of the 5th American Water Jet Conference, Toronto, Canada, pp. 245-252, August 1989 .

Koziol, K., and Glowacki, P., Journal of Non-Newtonian Fluid Mechanics, Vol. 32, No. 3, pp. 311-328, July 1989.

Mannheimer, R.J., Chemical Engineering Communications, Vol. 48, pp. .57-77, 1986.

Mannheimer, R.J., Proceeding of the Fourth International Conference on Coal Slurry Technology, pp. 155-166, 1989.

Savins, J.G., Industrial and Engineering Chemistry, 61, No. 10, pp. 18-47, 1969.

TABLE I. SHEAR VISCOSITIES	
Solution	**Apparent Viscosity @ 1000 sec^{-1}**
Xanvis®, 1 weight percent	38 cP
Xanvis®, 2.51 weight percent	92 cP
Superwater®, 1.3 weight percent	40 cP
Superwater®, 3.81 weight percent	90 cP
Methyl Cellulose, 2 weight percent	260 cP

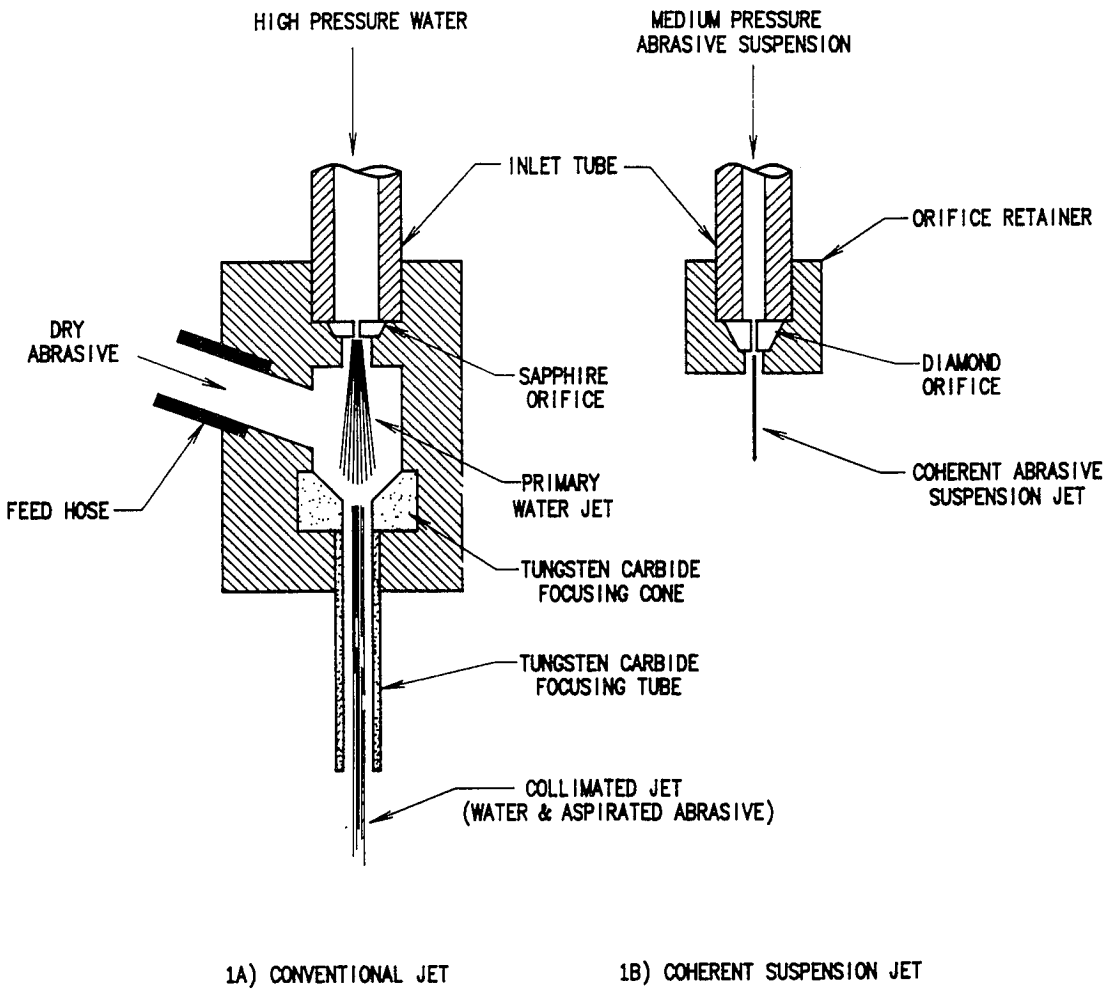

FIGURE 1. JET HEAD FUNCTIONAL DIAGRAMS

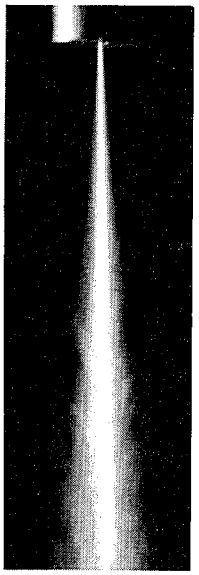

Outer Cone

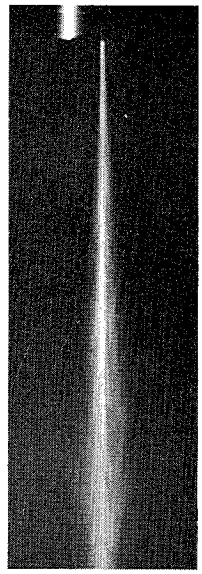

Core

FIGURE 2. WATER JET AND JET CORE AT 69 MPa

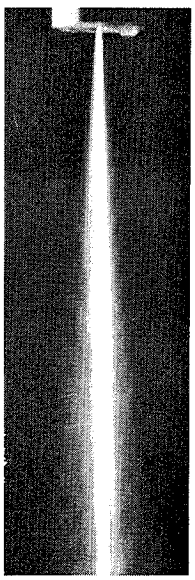

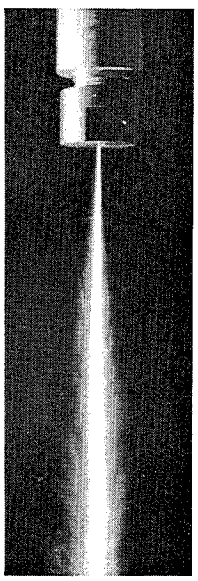

52 MPa 207 MPa

Outer Cone

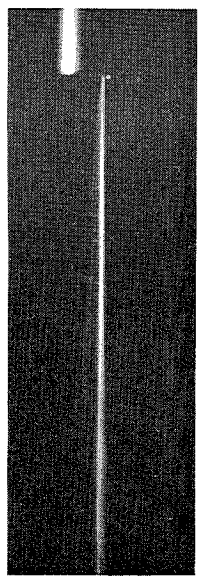

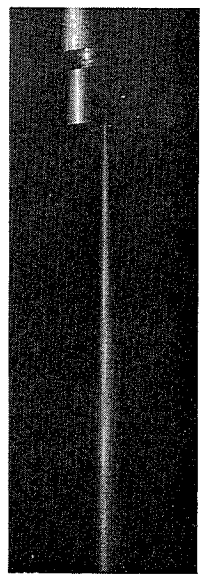

52 MPa 207 MPa

Core

FIGURE 3. 1.0 WEIGHT PERCENT XANVIS® JET AND CORE AT 52 MPa AND 207 MPa

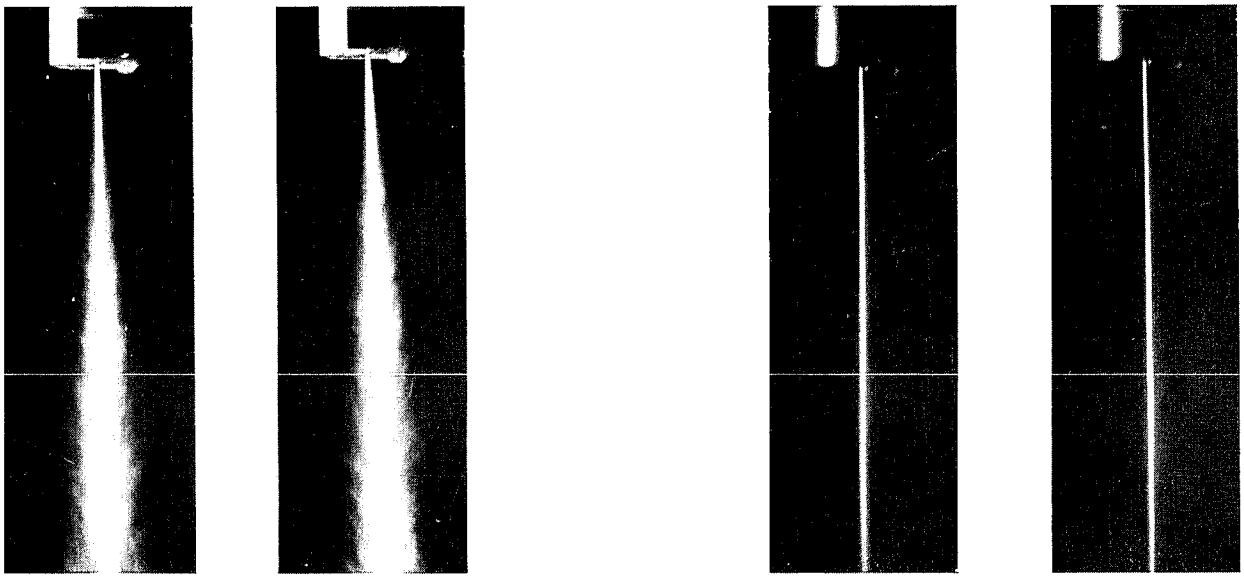

52 MPa 207 MPa 52 MPa 207 MPa

Outer Cone Core

FIGURE 4. 2.5 WEIGHT PERCENT XANVIS® JET AND CORE AT 52 MPa AND 207 MPa KPSI

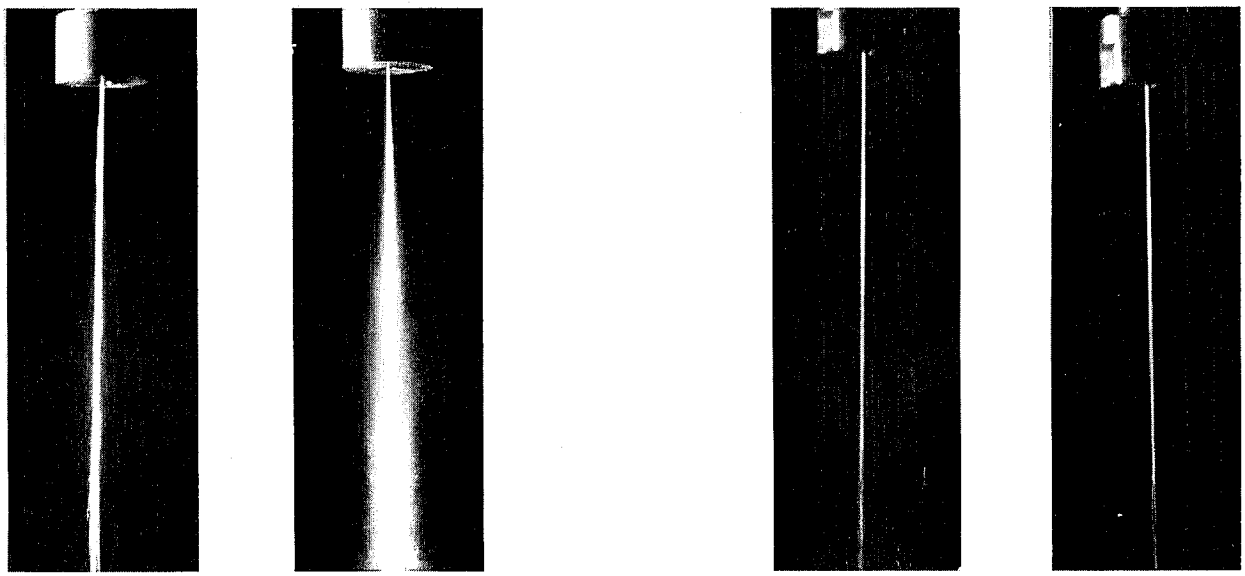

52 MPa 207 MPa 52 MPa 207 MPa

Outer Cone Core

FIGURE 5. 1.3 WEIGHT PERCENT SUPERWATER® JET AND CORE AT 52 MPa AND 207 MPa

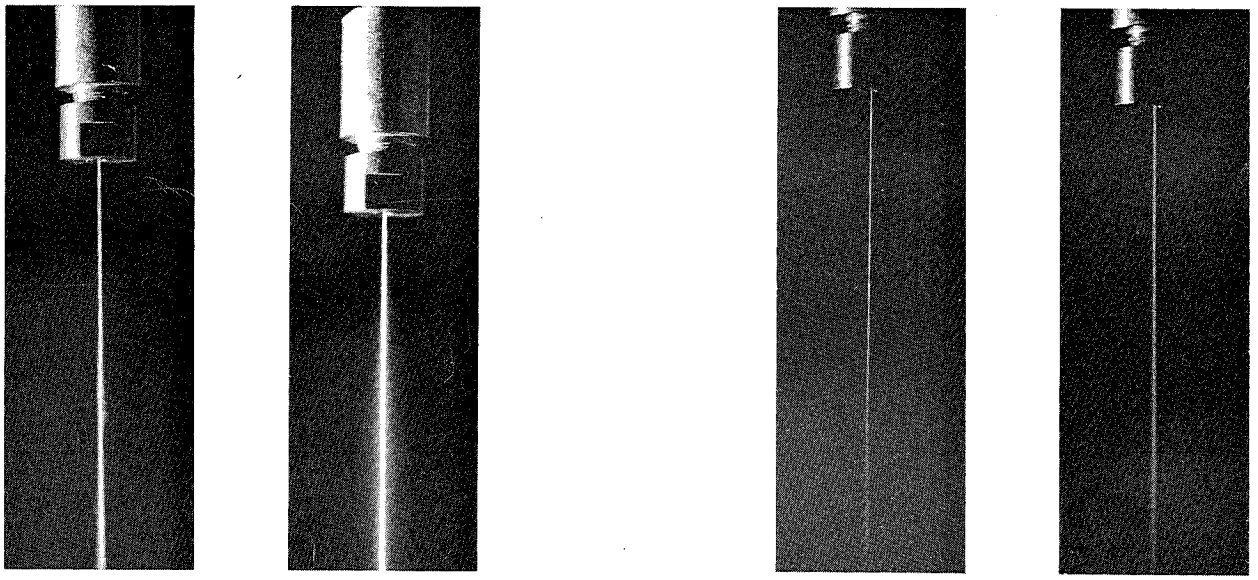

52 MPa 207 MPa 52 MPa 207 MPa

Outer Cone Core

FIGURE 6. 3.9 WEIGHT PERCENT SUPERWATER® JET AND CORE AT 52 MPa AND 207 MPa

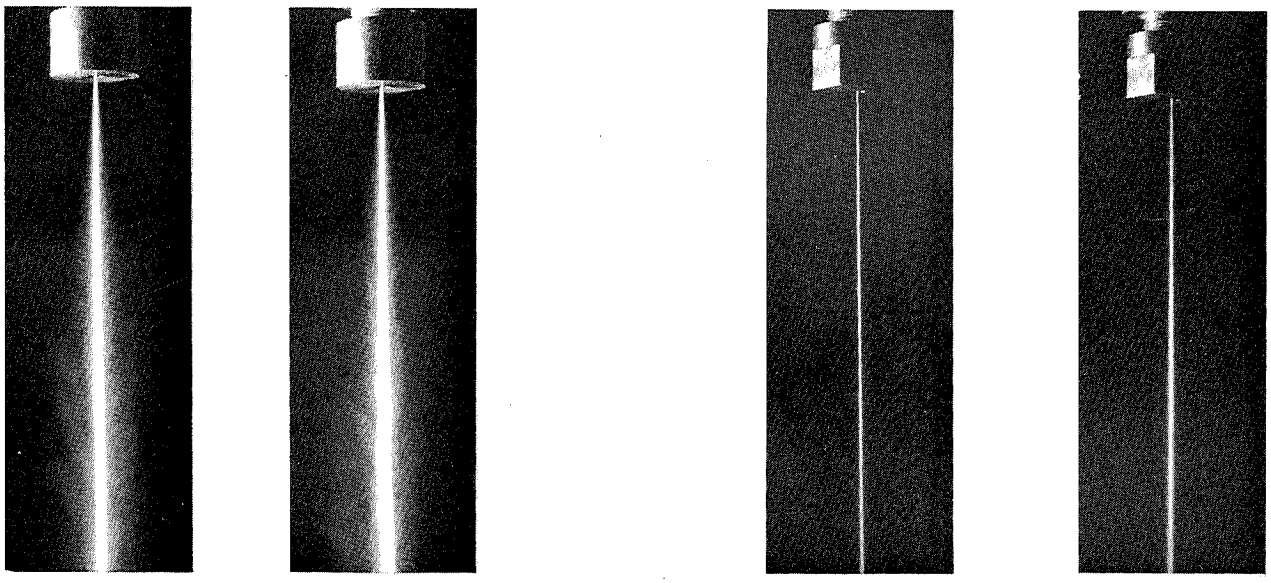

52 MPa 207 MPa 52 MPa 207 MPa

Outer Cone Core

FIGURE 7. 2.0 WEIGHT PERCENT METHYL CELLULOSE JET AND CORE AT 52 MPa AND 207 MPa

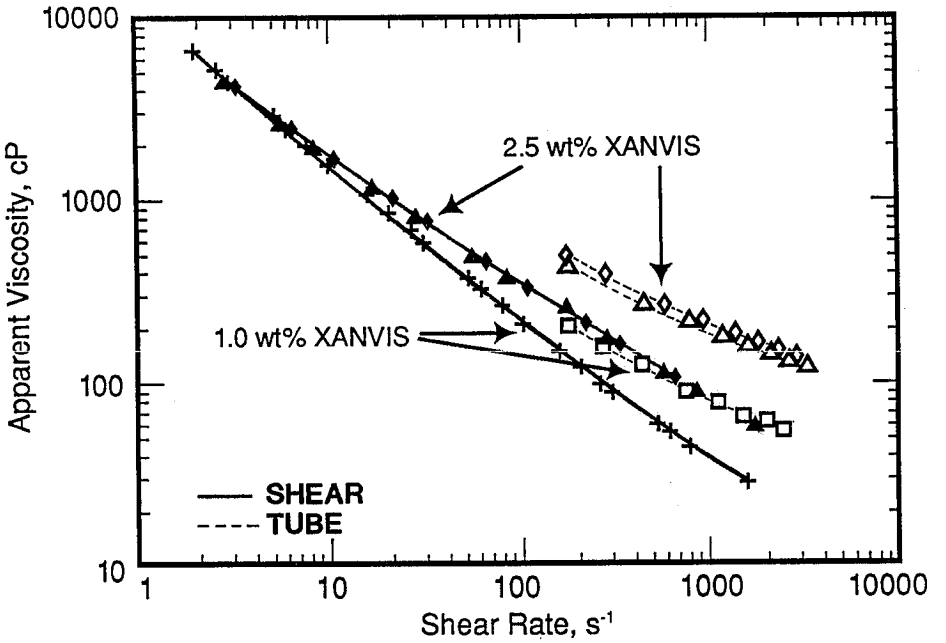

FIGURE 8. VISCOSITY VS SHEAR RATE, 1% AND 2.5% XANVIS®

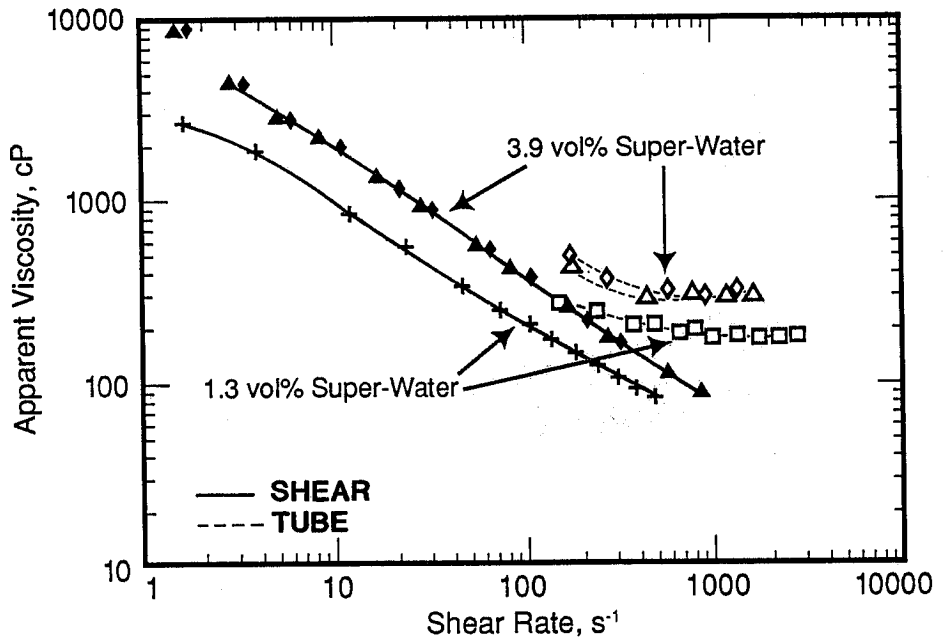

FIGURE 9. VISCOSITY VS SHEAR RATE, 1.3% AND 3.9% SUPERWATER®

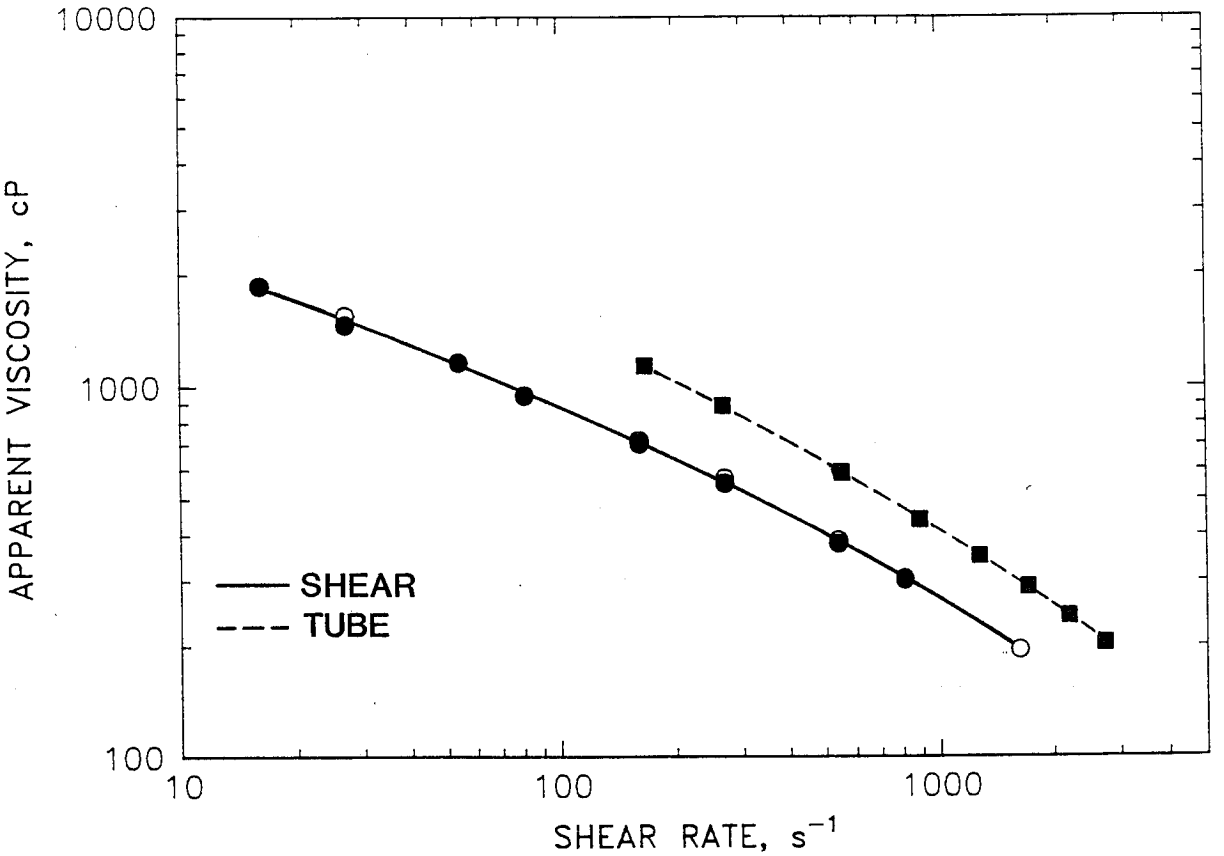

FIGURE 10. VISCOSITY VS SHEAR RATE, 2% METHYL CELLULOSE

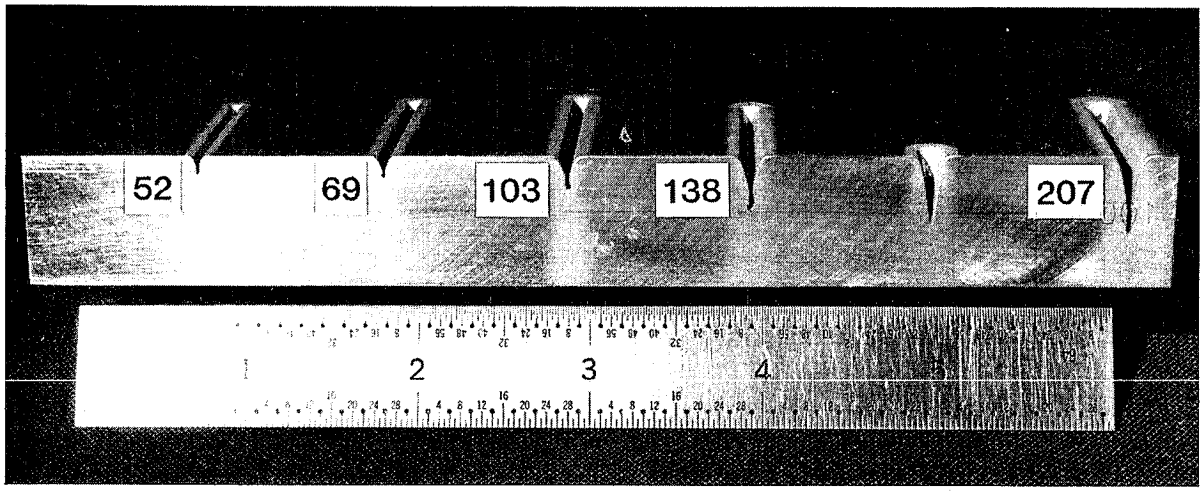

FIGURE 11. PENETRATION WITH 2% METHYL CELLULOSE SUSPENSION JET

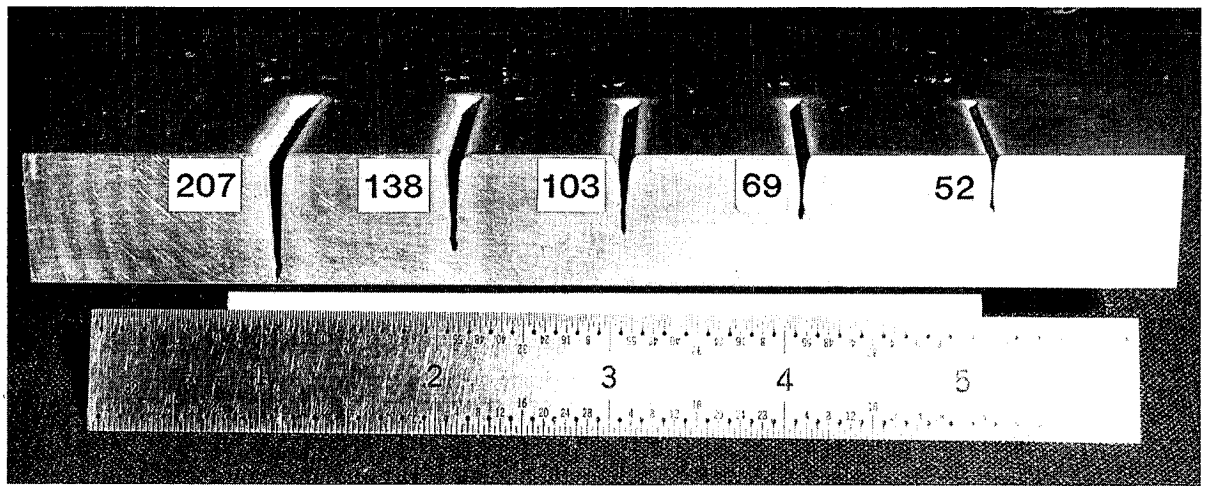

FIGURE 12. PENETRATION WITH 1.3% SUPERWATER® SUSPENSION JET

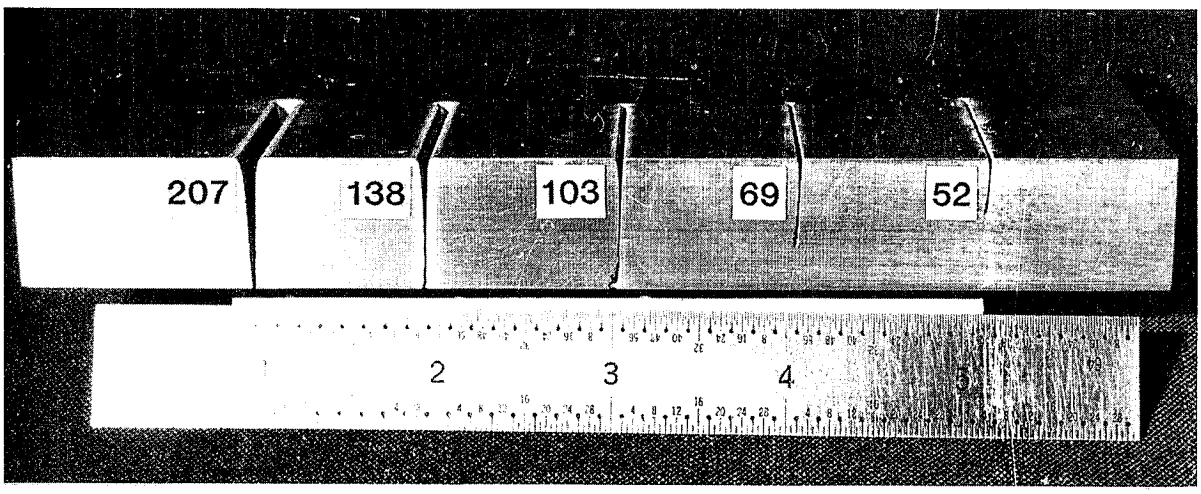

FIGURE 13. PENETRATION WITH 3.9% SUPERWATER® SUSPENSION JET

6th American Water Jet Conference
August 24 - 27, 1991: Houston, Texas Paper 40

DIAjet Cutting of Dolomite & Chert— A Case Study at the St. Louis Arch

Mr. J. Yao, Dr. D.A. Summers and Dr. G. Galecki
University of Missouri-Rolla
High Pressure Waterjet Laboratory
Rolla, Missouri 65401 USA

ABSTRACT

In order to add a second theater to the St. Louis Jefferson National Expansion Memorial Museum, located under the Gateway Arch in St. Louis, it was necessary to lower the floor of an existing 18 m by 24 m room by an average of approximately 3 m. To maximize seating in the theater, the walls of the excavation had to be cut as close to flush under the existing footings as could be achieved.

Waterjet use was planned for two aspects of the excavation, to assist in bulk rock removal, and in the linear cutting of the edges of the excavation. After several experiments it was found that the use of waterjets in assisting the rock removal were unnecessary. On the other hand the use of a dual nozzle DIAjet unit for cutting the final surface on the edge of the opening proved effective.

An economic comparison was made between the use of garnet, sand and steel shot, as a result of which the sand was used for the majority of the cutting. This conclusion was based, in part, on the difficulty in collecting all the spent abrasive after a cut. The DIAjet system cut between 4 and 28 cm deep, depending on the rock being cut. The rock to the free side of the cut could then be removed down to the succeeding bedding plane of the rock, using a mechanical breaking technique. A simple mechanism was built to move the lances. This was sufficiently light that it could be suspended from a cable and moved along the concrete wall to expedite the cutting process.

During the cutting operation, the jet occasionally generated an intense blue light while cutting. The light was most prominent when the abrasive jets were cutting in the thick layers of chert and when cutting in concrete.

A major problem arose in the disposal of the water from the cutting process. The excavation took place in a closed room with the exit corridor, for rock removal, from 4 to 10 m above the floor of the excavation. Entrained mud in the water made recirculation and disposal difficult. Various filtration attempts were unsuccessful. The problem was resolved by pumping, once the excavation reached the water table.

1.0 INTRODUCTION

The Jefferson National Expansion Memorial (JNEM) Museum has been created as an underground facility beneath a grass and lake covered park surrounding the 189 meter high, and wide, Gateway Arch in St. Louis. The museum complex (Figure 1) includes an entrance foyer, a museum chronicling the development of the land west of the Mississippi River, and a theater where normally a movie is shown describing the construction of the Arch some twenty-five years ago. The Foyer also providess access, down two sloping ramps, to the legs of the Arch where visitors may board a small tram which will carry them to an observation gallery located in the top sections at the center of the Arch.

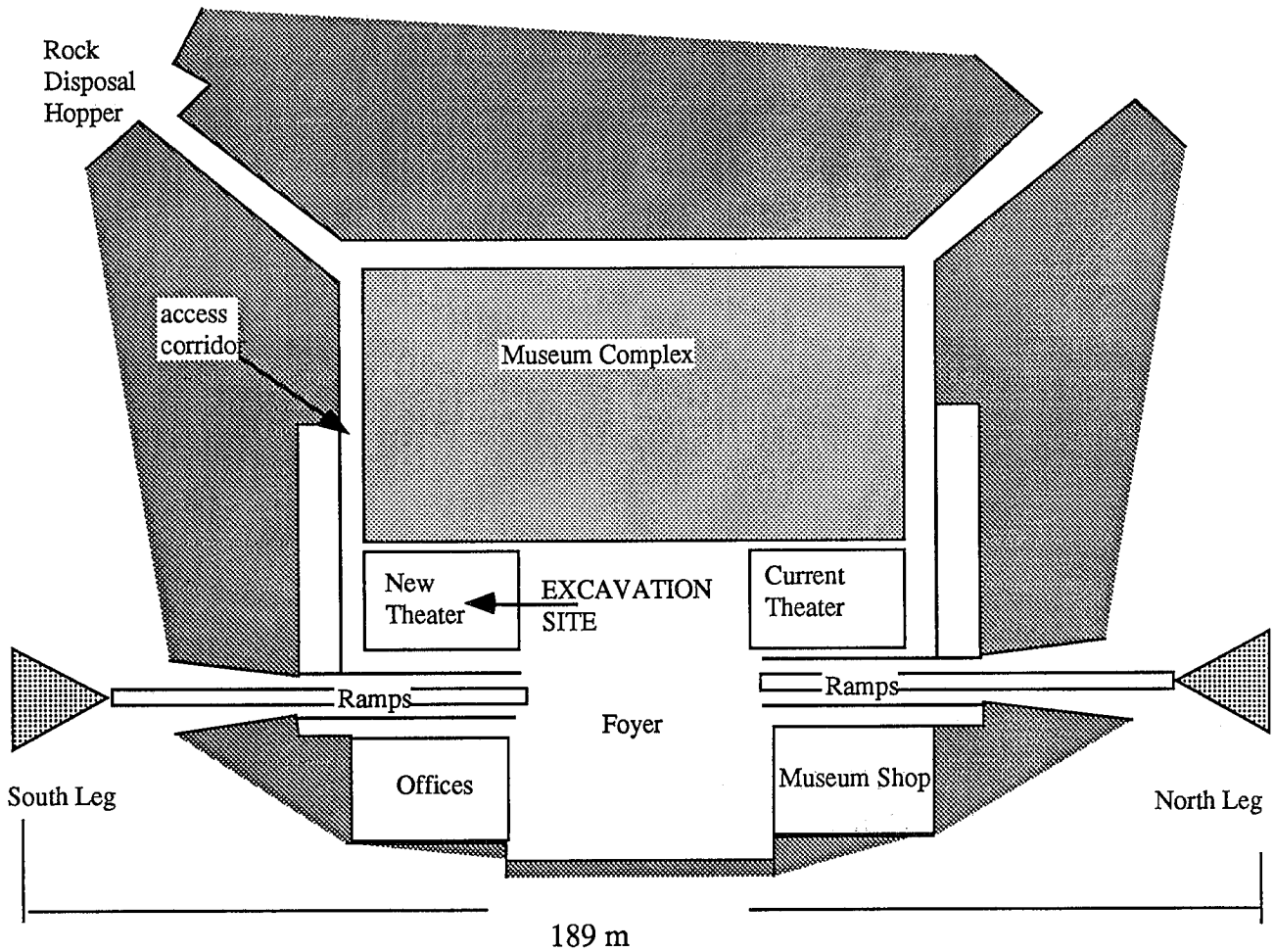

Figure 1. Plan view of the underground layout of the JNEM facility.

When the Arch was originally constructed, the space on the opposite side of the Foyer to the first theater was left undeveloped as a future site for an undesignated facility. In 1988, it was decided that this facility would comprise a large-screen theater of the Imax type. This projection system requires that the screen fill virtually the entire face area of the viewing wall and that the audience are seated on a relatively steeply dipping incline before the screen.

At the time that this decision was made, this second theater was defined by four concrete walls and an overlying concrete roof. The floor itself (Figure 2) was a sloping, dirt covered, natural rock surface. The top layers of rock had been partially blasted as part of the excavation process for the installation of the Arch. In the original design for this theater, some 1200 cubic meters of material needed to be removed. In order to provide the maximum number of seats for the theater, it was required that the walls of the excavation continue downward along the plane of the existing concrete walls (Figure 3).

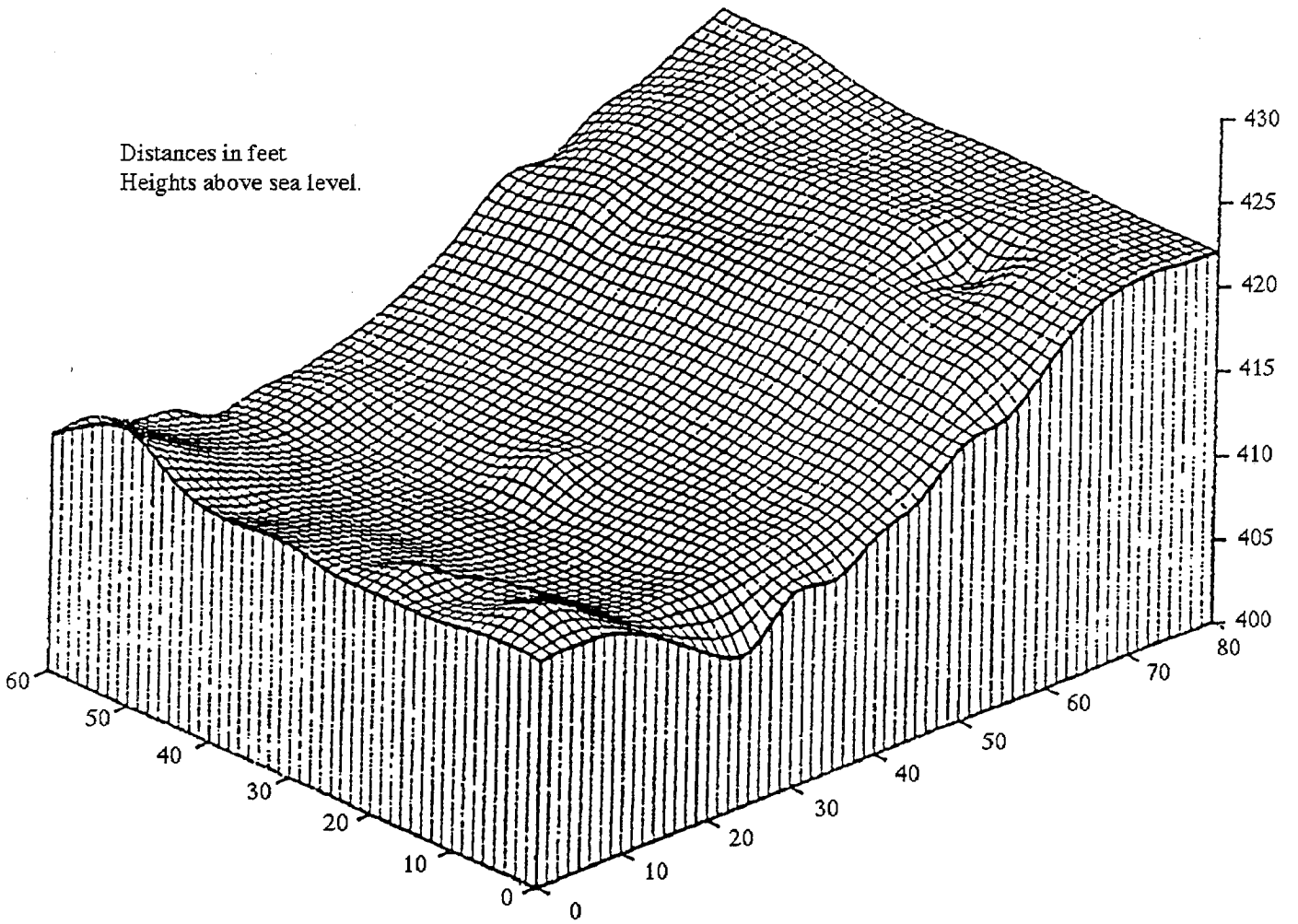

Figure 2. Original ground contour within the second theater.

The problem was complicated by several critical requirements for breaking and removal.

- The excavation process could not use blasting or any process which would weaken the rock wall of the opening or the foundation of the Arch itself.

- Access to and egress from the site could only be through a back corridor located in the south wall of the room. The floor of this corridor was, at the start of the excavation, some 3.6 meters above the floor of the room. At the end of the excavation, it would be up to 10 meters above the floor.

- All the material excavated must be removed along a sloping back corridor with a minimum dimension of approximately 2.4 meters by 2.4 meters. The size of this corridor and its location, together with the final geometry, required made it difficult to foresee the use of any large pieces of excavation equipment.

- The presence of some 2 million visitors a year to the facility, particularly adjacent to the room, made the requirements for a minimal amount of dust, noise, and other adverse impacts mandatory.

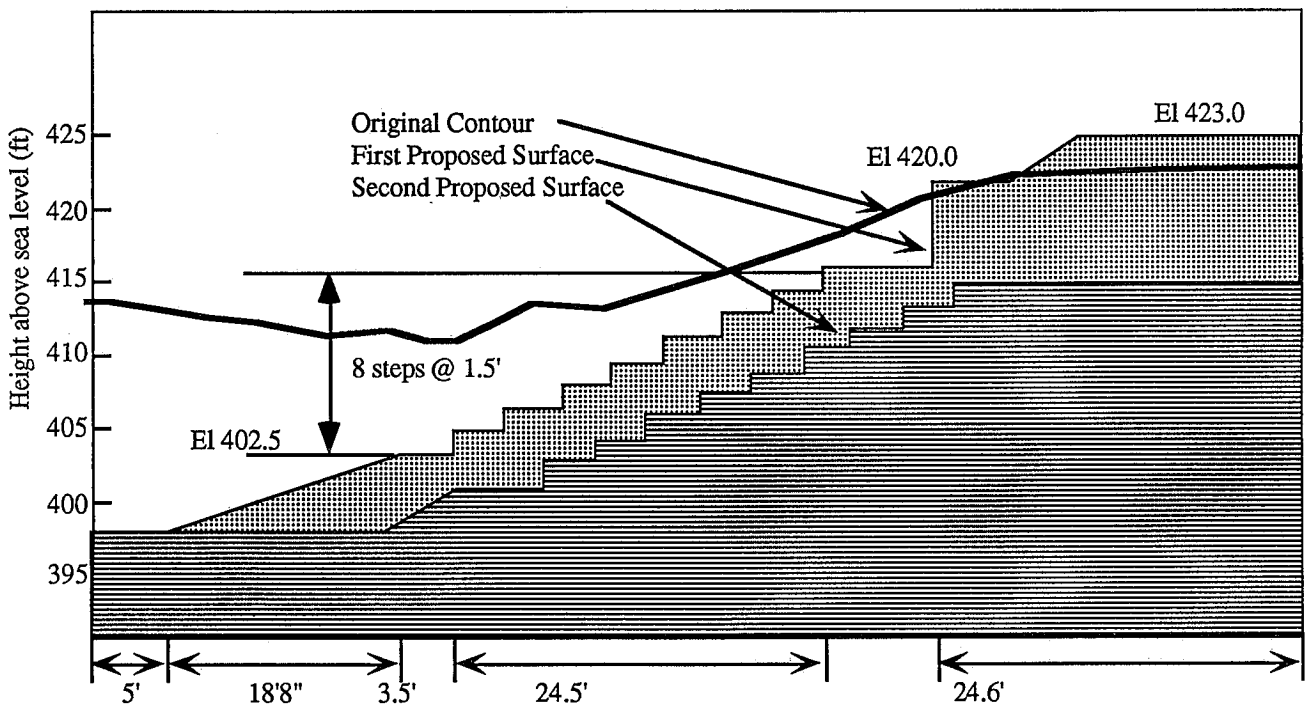

Figure 3. Original design for the excavated space.

These limiting conditions significantly reduced the choices of conventional technology which could economically and practically be used. The University of Missouri-Rolla, accordingly, suggested that the site would provide a unique opportunity for researching and developing a method of high pressure waterjet abrasive cutting and rock splitting previously conceived as the CUSP (CUt and SPlit) method of excavation (Reference 1). After negotiation and considerable discussion, an agreement was entered into by the National Park Service and the University to carry out such a program.

2.0 THE CUSP METHOD OF EXTRACTION

The trend in the development of mining excavation equipment has been toward the development of larger, more complex, and more functionally comprehensive machines. In-

creasingly these units incorporate some degree of computer control increasing the levels of complexity and requiring increasingly sophisticated maintenance procedures. These developments have raised the cost of the equipment such that it requires a relatively large program of excavation to justify the purchase, while the use of the computer control limits use of the equipment to a relatively narrow band of variation in the excavation pattern, without continuously adjusting the controlling programs.

Many excavation sites, however, are relatively small. Access for equipment is limited and the down-time and delays required for maintenance and repair of a single complex machine carrying out all the excavation tasks, is an unacceptable burden to the economic operation of the facility.

In order to overcome these problems, the approach taken has been to develop a relatively simple, inexpensive method of excavation built around the use of a limited number of simple tools. The basic principle underlying this development has been one of minimizing the amount of energy required to remove the rock. With most mining equipment and excavation processes the procedure is to break the rock from the solid in small pieces which are then collected and removed. If the rock can be broken out in significantly larger fragments then the amount of energy expended in both breaking the rock and in its removal could be much reduced. (As a simple analogy, one can remove a slice of cake by making two single cuts along the edges of the wedge desired and then lifting out the piece defined. Alternately, one can chop the segment of cake into small fragments before trying to remove it. In the latter case, not only is more energy required to excavate the cake, but, significantly more time and effort is also required to pick up the pieces.)

There are two aspects to the method developed. That of bulk material removal within the body of the excavation; and, that of the trimming of the edges. In this program the need for accurate edge-trimming is critical, from two aspects. Firstly, a clean cut along the edges of the wall would increase the available space for seating. Secondly, if this cut were made before the bulk of the rock were to be removed, it would limit any damage from the bulk excavation method. For example, El-Saie (Reference 2) and McGroarty (Reference 3) have both shown that even when blasting, a pre-existing slot around the edge of the excavation significantly limits damage to the rock wall. For this reason, it was proposed to use a directly injected abrasive laden waterjet (DIAjet) at a pressure of 35 MPa to cut a slot in the wall of the excavation around the perimeter. To demonstrate the ability of such a jet and its advantages, a slot 1/2 meter deep was cut through a sample of dolomite on a single pass, and a second slot cut through a 2.5 cm thick glass plate, during the initial discussions. These demonstrated both the range of the equipment and the very limited damage to the edges of the cut which occur with the use of an abrasive laden waterjet.

The abrasive waterjet would, thus, provide a free surface to which the rest of the rock could be broken. The remaining rock would be removed by a process of drilling and splitting. It was anticipated that boreholes would be placed approximately 1/2 meter apart and 1/2 meter from the free surface (Figure 4). Once these boreholes were drilled, a vibrating splitter (Reference 4) would be placed in these holes to break the defined rock volume and separate it from the solid.

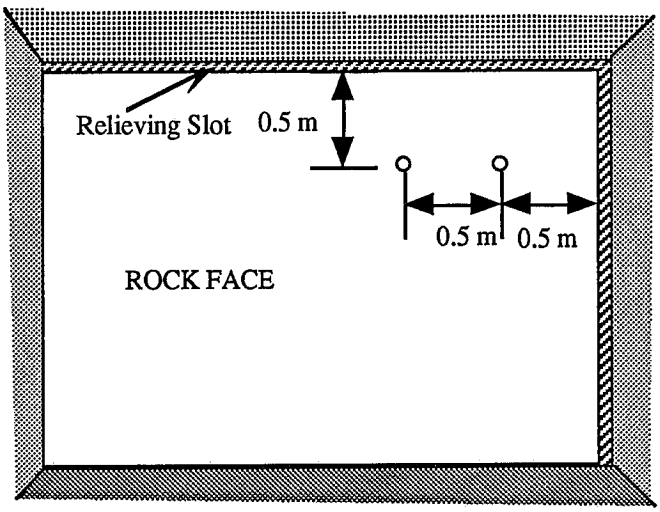

Figure 4. Splitter hole location for block definition and removal.

The separated blocks would then be slid onto a roller conveyor which would move them under a hoist. The hoist, suspended from a monorail which was to be mounted from the beams of the overlying roof, would raise each block and carry it to the corridor where it would be transferred to a forklift which would carry it through the corridor and out to a storage container which would be periodically emptied.

3.0 DEVELOPMENT OF THE BLOCK REMOVAL PROCESS

The monorail was installed without any problem and a small front-end loader (Bobcat, Model #743, 27 kw.) was brought into the excavation to remove the initial overlying soil which was loaded into small, self-dumping hoppers of approximately 0.4 cu. m. capacity. These could be readily handled by the transportation system. Experience with these showed that they would also handle blocks up to the maximum size designed for the monorail (500 kg) and, would carry the mud and small rock fragments which were created throughout the excavation. The loader could pick up individual blocks without problem, and the hoppers provided a better means of safely lifting the blocks than the original concept proposed. Accordingly, this method of material handling was adopted for the entire excavation.

As the excavation progressed, the material being excavated changed from loose rock to blast-fractured, but otherwise intact, rock layers. Initially, this could be easily loosened by utilizing an impact breaker (up to 1,000 blows/min at 407 J - (300 ft.lbs)) instead of the bucket on the front-end loader. This worked well in the relatively loose material, but did not have sufficient power once solid rock was reached. The breaker had available only 10.2 kw. The main body of the rock in the room was a dolomite of up to 160 MPa uniaxial compressive strength. It was inter-lain with layers of chert up to 10 cm thick. Excavation rates with the impact breaker were less than 0.4 cu. m./ hr. At this point a change was made to make use of the CUSP rock removal system.

The first splitters to be used in the program were an inflatable cylinder marketed as the RexRock™ device. In the laboratory, these proved readily capable of splitting blocks, particularly where the DIAjet had been used to pre-notch the borehole in the required direction of fracture. This device required a relatively smooth-walled hole, and the original intent to drill this hole with a waterjet drill could not be implemented because of the rough wall which this latter system created (Reference 5). The initial alternative to this was to substitute a diamond core drilling tool, however, the slow penetration rate achieved with this system, the difficulty in accurately aligning and holding it in position during the drilling of a 70 cm hole, the high wear rate, and thus, cost, made this an unacceptable choice. A pneumatic drill was, therefore, substituted and was able to achieve a penetration rate which averaged between 30 and 60 cm./min. in drilling holes for the splitter.

At this point in the development of the process, the design of the theater was modified, significantly increasing the volume of material which had to be removed (Figure 5). It had originally been anticipated that a second DIAjet system would be used to develop slots in the drillhole walls to control the direction of fracture. The increase in the volume led to a decision to dedicate the second DIAjet system to the linear cutting program. An alternative method, had to be found to notch the boreholes. Two small compressed air-driven, high pressure waterjet pumps, were obtained and manifolded together. These produced sufficient water that would create a jet of 210 MPa when directed through a 0.17 mm orifice. This jet nozzle was mounted on a flexible tube and used to notch several holes. The notch created was quite small, often only several millimeters, but was sufficient to initiate the rock fractures.

The procedure was only partially successful. The splitter was found to have insufficient power to handle blocks of the initial dimensions planned, particularly where the bed thickness of the dolomite and chert increased above 25 cm. A specialized splitter was loaned to the project by the U.S. Bureau of Mines (Reference 6) and was effective in breaking out a layer from the solid, but again was of insufficient power in dealing with the more massive layers of rock found in the lower levels of the excavation.

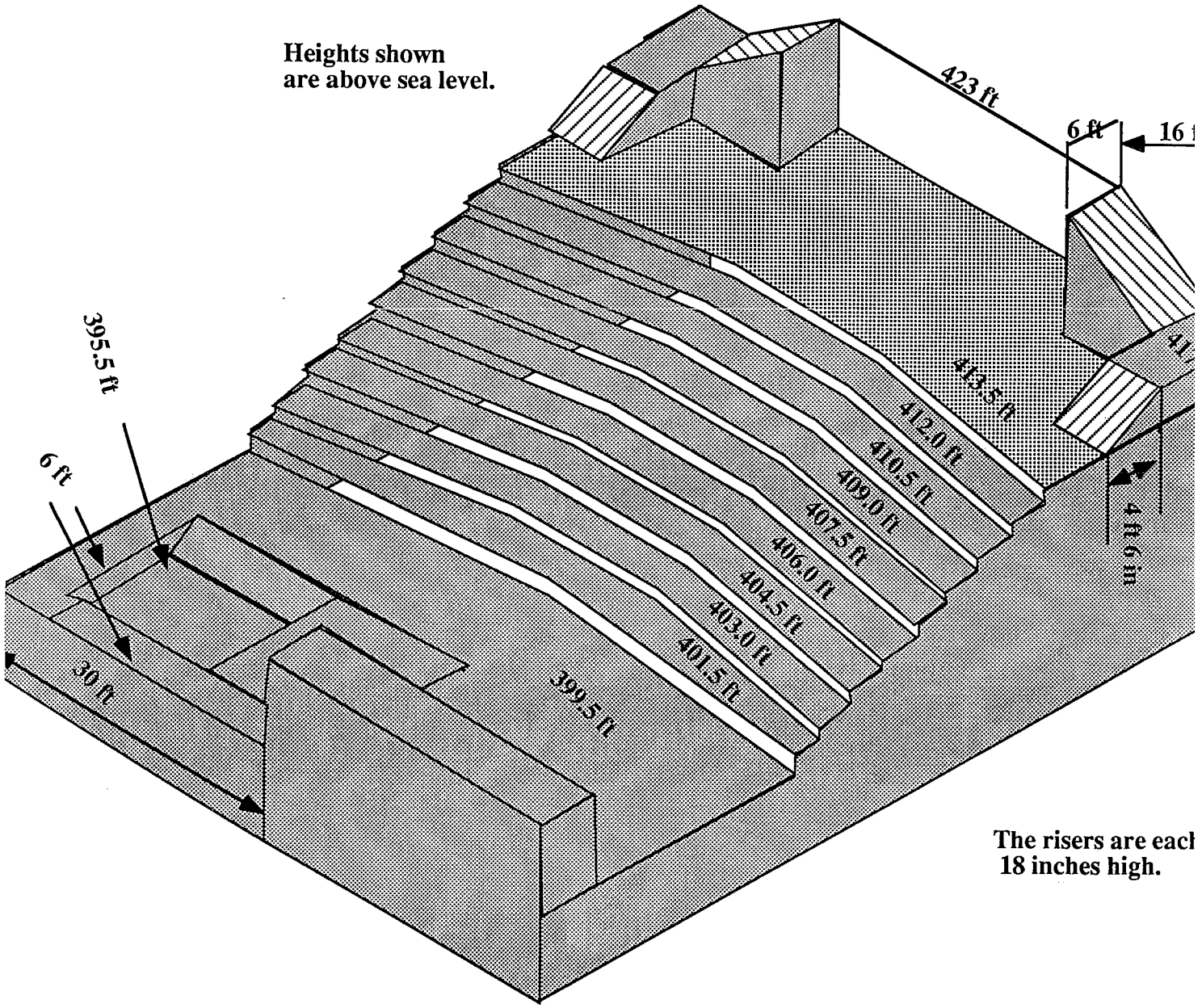

Figure 5. Final shape of theater excavation.

A third splitter (Darda Model #5/5802/5) worked on a feather and plug principle similar to that first proposed, but without the vibrating component, was then introduced. This tool had sufficient power that it was not necessary to pre-notch the holes before using the splitter. The rock, in general, broke perpendicular to the orientation of the feathers. The initial fracture was, however, often quite short and did not liberate the block from the solid. To overcome this problem, the tip of the impact breaker was inserted into the drillhole and the device activated (Figure 6). The vibration of the tool not only extended the crack, but also liberated the block along the underlying joint plane (Figure 7).

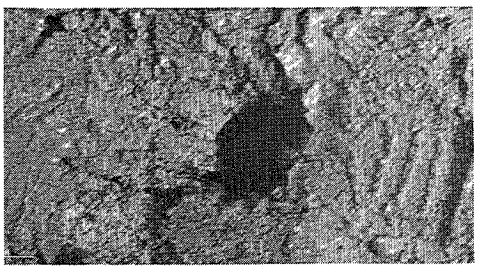

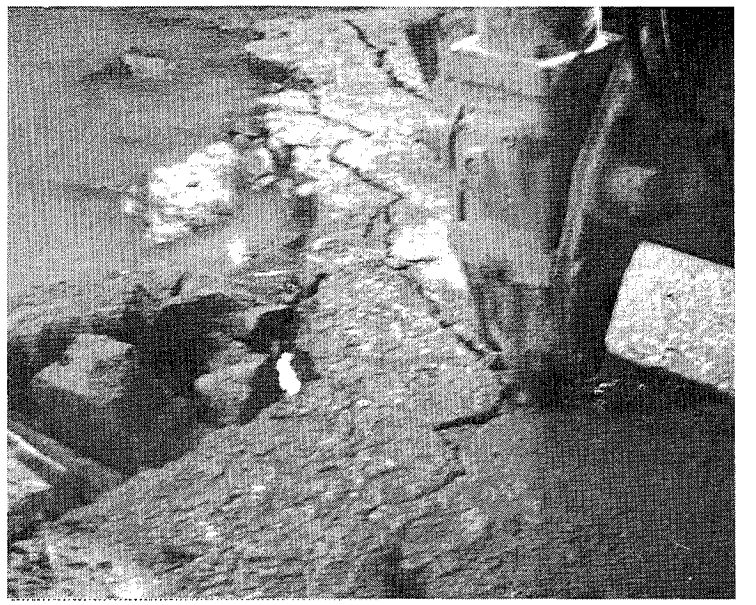

Figure 6 Stages in the Break-out of a Block. The picture above shows the crack started by the splitter, that to the right the growth after 15 - 30 seconds of applying the impact breaker

This method proved to be quite effective in removing the majority of the rock from the excavation. Blocks could quite easily be developed to the maximum size (500 kg) which the system could handle (Figure 7).

Figure 7. Pattern of blocks broken out in the floor of the excavation.

Drilling each hole took approximately 1.5 minutes, running the splitter would usually fracture the block within 2 minutes, and the use of the impact breaker to separate the blocks could be typically achieved within less than a minute. (The length of time which the splitter required included a pause to lubricate the tongue.) Rock removal rates achieved were in excess of 3 cu. m./hr. by the three-man crew. As a point of reference, (Reference 7), a mining version of the impact breaker will break up to 3.8 cu. m./hr. in rock of this strength, but has required a machine power of up to 90 kw. In underground production, (Reference 8), such a machine averaged 5 cu. m./man shift. By comparison,

the productivity here, if continued for a shift would have reached 7 cu. m./man shift of seven hours. The restricted working area and the need to remove the rock broken did not, however, make that possible. This process proved significantly faster than the use of the impact breaker alone, and appeared to match its performance, with 10 kw, to that of competing systems which required 90 kw without the splitting addition..

4.0 SLOT CUTTING

In the initial design, it had been anticipated that the DIAjet system would be used extensively within the excavation to provide free surfaces to which the rock could break. However, this did not prove necessary since the judicious use of the Bureau of Mines Splitter and the fortuitous presence of a vertical clay seam in the opening, provided sufficient free surfaces to break the central volume of rock.

In order to increase the speed of slotting, the output from two DIAjet units were combined to feed two cutting nozzles on a traversing framework. This framework was built around a section of radio antenna mast, chosen for its lightness and strength. A support carriage held the two lances and was drawn down the lance by a bicycle chain, in turn, pulled through a gear reduction by an electric motor (Figure 8).

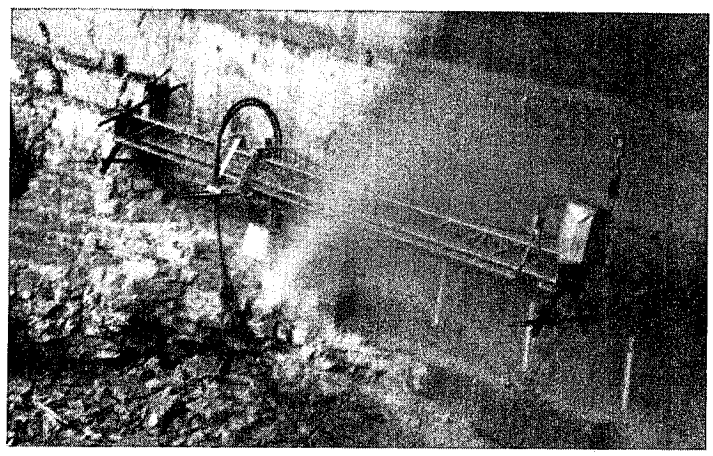

Figure 8. Traverse mechanism .(Note the intensity of the light in the jetstream)

The design had both lances feeding separate nozzles, thus one cut over the rock should be equivalent to two passes of a single jet over the surface. In addition, it was expected that the system could be used to make multiple passes over the rock surface, using the optimum cutting parameters of the system. It had previously been determined by Yazici, (Reference 9), that a traverse velocity of approximately 50 cm./min. would provide the most efficient cutting rate (Figure 9) even though this only cut a few cm.

The original plan had also been to collect both the water and the abrasive from the cutting process and to recirculate them in a closed loop system. Preliminary experiments at Rolla had shown (Reference 10) that steel shot would cut twice as deeply as other abrasives in this rock (Figure 10) and thus, would provide the best choice of abrasive.

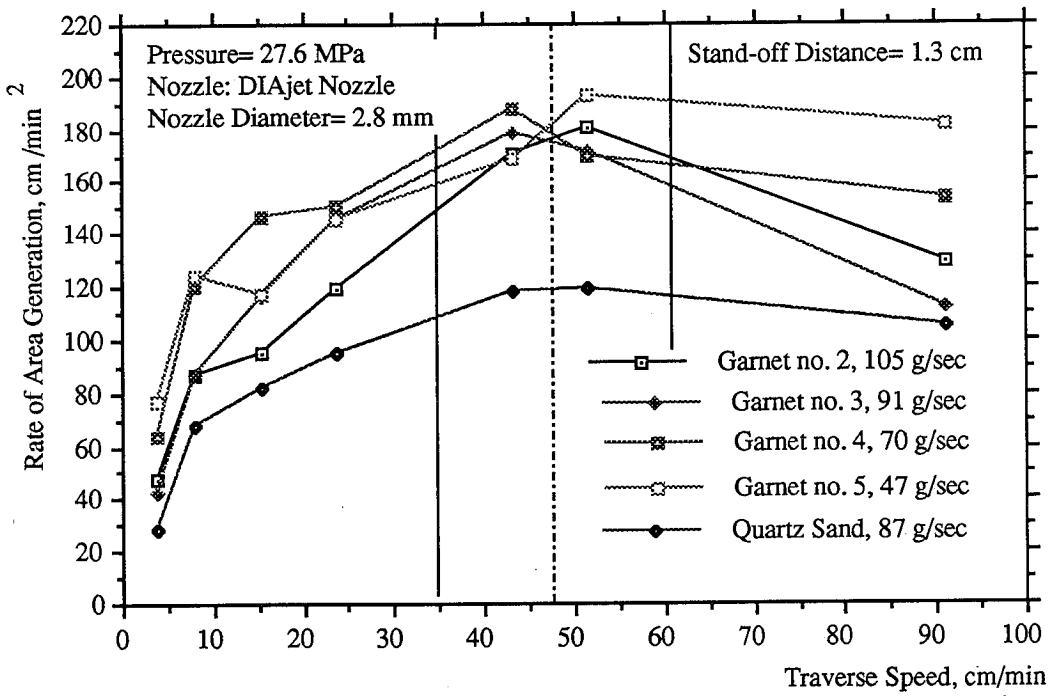

Figure 9. Rate of curve area generated as a function of traverse speed. (Reference 9)

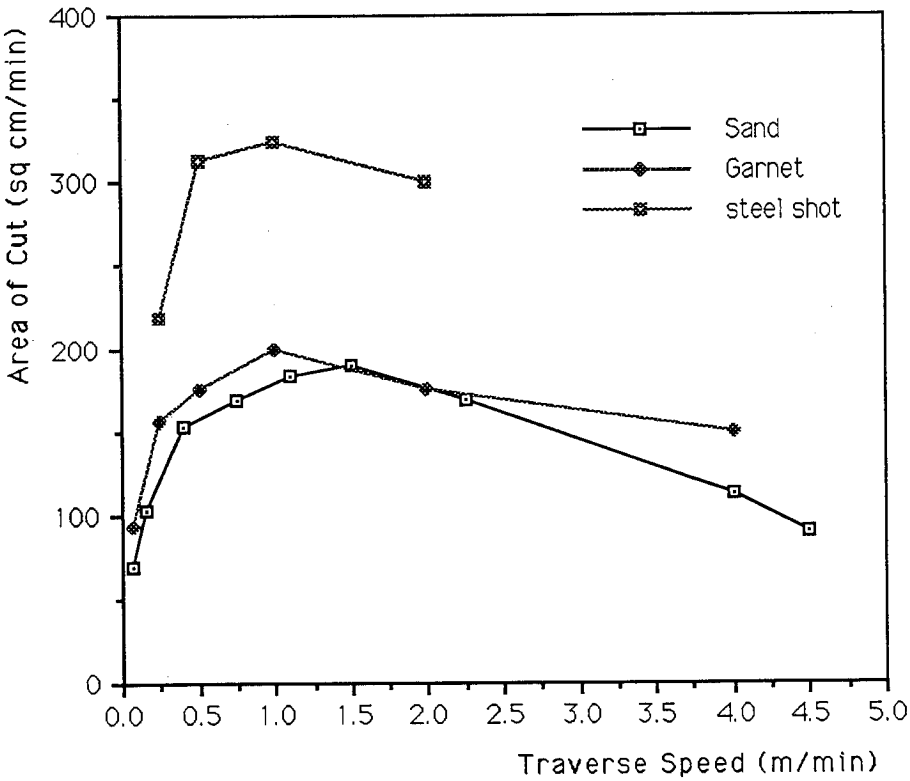

Figure 10. Depth of cut as a function of abrasive type. (Reference 10)

When work began at the site slotting was delayed while the blast-damaged rock was removed. This was to insure that large quantities of abrasive would not be lost into open fractures. An apparently minor problem, ultimately led to a complete revision of the plan for the DIAjet cutting. As the top layer of rock was removed, a major vertical clay seam was found, which crossed the room on a diagonal from one corner to the other. As the

excavation progressed, other clay seams were also encountered, measuring up to 45 cm. thick. The quantity of mud which was generated by the water flowing over these seams, swamped the filtration system initially proposed. Significant changes in the capacity and method of treatment of the water prior to recycling did not prove adequate. The residual fines in the water led to a rapid destruction of the valving of the initial pump used for the program. Fortunately, due to the generosity of Halliburton, Inc., a pump capable of delivering water with a heavy concentration of mud particles at 35 MPa was made available to the project. The progress of the excavation down through the water table (with a continuing in flow of water from that point) and the appearance of more clay layers, led, however, to a change in plan.

It proved more effective economically and practically to merely collect the water and pump it away from the site. Fresh water was then used for the cutting system without the need for recirculation. This change made it impractical to recirculate the abrasive. This had already proved to be difficult to accomplish since the rough surface of the rock and the uneven nature of the terrain combined with the rebounding force of the jets to distributed the abrasive over a relatively large area.While the abrasive could be contained during the central cutting of the rock within the room, it proved much more difficult once the wall cutting began.

One of the reasons for this was the change in the way the traverse mechanism was supported. Initially the antenna mast had been supported on four legs which each could be adjusted to hold the lance at the required position above the surface. This mechanism became cumbersome and difficult to manipulate once the wall cutting began. It proved more effective to run cables along the wall from which the mechanism could be suspended during both movement and for the cutting process. The reaction force from the jets could easily be balanced to allow this. This change allowed the jet to cut very close to the concrete wall, but meant that it was difficult to retain a collecting shroud around the nozzles to catch the abrasive. As a result, it was decided that such a process would be economic and that the abrasive would only be used once. An economic analysis of the performance of the three possible abrasives (Reference 10) then indicated that the use of locally available quartz sand was by far the cheapest option for the abrasive to be used. The economic advantages of either steel shot or garnet only accrue when these materials can be recirculated, a process which the use of the DIAjet system would otherwise allow.

The quartz sand did not cut as deeply as the steel shot, but in some of the rock types encountered, it did cut almost as well. It was interesting to note, that when this abrasive is used, an unexpected physical phenomenon was occasionally encountered. Where the jet cut through the edges of the concrete wall, or in chert, a relatively intense blue light was generated along the line of contact between the jet and the cutting surface. This light did not appear, at least at the same level of intensity, when the jet was cutting the

dolomite. It is suggested that the light might be a piezoelectric effect caused by the impact pressure generated in the sand particles when they hit a resistant target material. This has been a remarkably difficult phenomenon to photograph (Figure 8).

This system proved effective in cutting down through ridges of concrete which had protruded from the rock wall, and in cutting through both the dolomite and chert layers encountered as the excavation deepened (Figure 11).

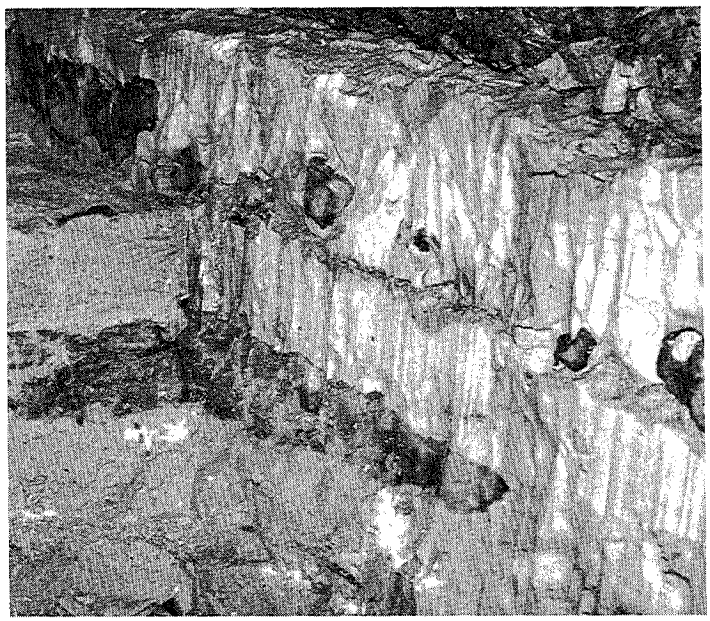

Figure 11. Wall cut by the DIAjet through dolomite and chert.

Because the nozzle assembly travelled across the surface cut in a previous pass, the cut became rougher as the wall deepened. At the same time, the independent motion of the two nozzles meant that they did not satisfactorily track along the same cutting path. Thus, instead of achieving a single slot of twice the depth, two shallower cuts were often made with an intervening rib of material. Further, the less rigid support system did not always insure that the jets passed over the same path when the direction of motion was reversed.

To overcome the problem of tracking over multiple passes, it was decided to try and cut through the individual layers of the rock in a single pass, recognizing that this made the cutting process slightly less efficient. Concurrently, the jet orifices were all combined in a single holder to resolve the problem with the jet tracking mechanism. In order to insure that the jets cut a quasi-vertical wall, the lance just above the nozzle was slightly bent inward (at a 1 in 12 inclination) so that subsequent jet cuts would lie vertically aligned. With these changes, it proved possible to run the cutting lance slightly away from the surface of the previous cut reducing the amount of roughness generated in the process.

5.0 CONCLUDING REMARKS

As this paper is being prepared, in April 1991, the project is entering its closing phases. The main volume of rock down to the main floor of the theater has been excavated, and the walls are currently being cut back to their final position (Figure 12). The progress of this work is constrained by the need to install long rock bolts in the walls, as they are exposed, in order to insure the stability of the structure for future generations.

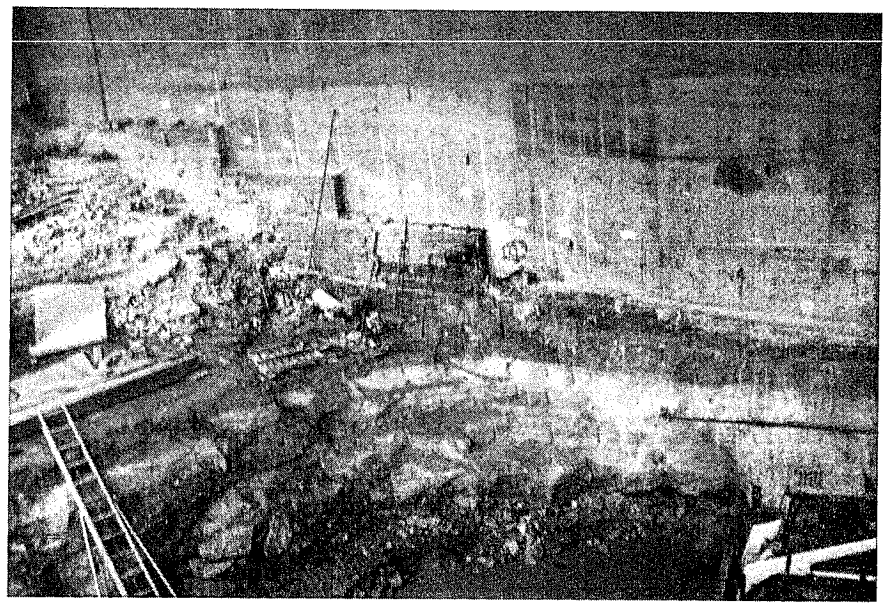

Figure 12. Status of the excavation site, April, 1991 (Note that the original surface was at the top of the concrete footing)..

6.0 ACKNOWLEDGEMENTS

This work would not have been undertaken without the considerable interest, enthusiasm, and encouragement which we have received from the National Park Service personnel at the Jefferson National Expansion Memorial; from the Superintendent, Mr. Schober, and Assistant Superintendent, Mr. Easton, through the day to day cooperation with Mr. Patterson, and Mr. Caselli, and the cooperation of the Park Rangers. This made the whole program possible. We gratefully acknowledge the assistance we have received from Ms. J. Nixon of the Bi-State Development Agency; Mr. Anderson of the U.S. Bureau of Mines was a considerable help in arranging the loan of the Bureau of Mines splitter; Mr. Lehman and personnel at Halliburton provided considerable assistance in providing, modifying, and maintaining the pumping equipment.

As with virtually every program in the Research Center, this work could not have been carried out without the considerable help and advice of Mr. James Blaine, Mr. L. John Tyler, and Mr. Robert Fossey of the RMERC staff, we are grateful to them and to Mrs. Jo Blaine, who prepared this paper.

7.0 REFERENCES

1. Summers, D.A., "High Speed Quarrying Techniques Applied to the Tunnelling Industry (The CUSP Miner)," Proceedings of the Third International Conference on Innovative Mining Systems, University of Missouri-Rolla, November 2-4, 1987, pp. 253-259.

2. El-Saie, A.A., "Investigation of Rock Slotting by High Pressure Water Jet for Use in Tunneling", Ph.D. Thesis, University of Missouri-Rolla,1977.

3. McGroarty, S.,An Evaluation of the Fracture Control Blasting Technique for Drift Round Blasts in Dolomitic Rock, M.S. Thesis, University of Missouri-Rolla, 1984.

4. Clark, G.B., Maleki, H., "Basic Operational Parameters of an Automated Plug and Feather Rock Splitter," Annual Report on NSF Grant APR73-07846-A02, July, 1978, Colorado School of Mines, pp. 178.

5. Yao, J, Summers, D.A., Blaine, J.G., Tyler, L.J., Galecki, G., "Field Trials and De velopments of the DIAdrill Concept," 6th American Water Jet Technology Confer ence, Houston, Texas, August 24-27, 1991.

6. Anderson, S.J., "Drill Split Mining with Radial-Axial Loading Splitters," Proceed ings of the 31st Rock Mechanics Symposium, Colorado School of Mines, June 18-20, 1990.

7. Morris, A.H., Moore, K., Rodford, I.G., "Impact-Ripping—A Survey of Experience to Date," The Mining Engineer, Number 157, November, 1973, pp. 93-104.

8. Ashurt, J., "Successful Impact Ripping Trials in West Germany," World Coal, December, 1976, Volume 2, Number 12, pp. 12-14.

9. Yazici, S., "Abrasive Jet Cutting and Drilling of Rock," Ph.D. Thesis, Department of Mining Engineering, University of Missouri-Rolla, 1989.

10. Yao, J., "High Pressure Water Jets in Rock Excavation," Ph.D. Thesis, Department of Mining Engineering,University of Missouri-Rolla, 1991.

6th American Water Jet Conference
August 24 - 27, 1991: Houston, Texas Paper 41

Field Trials and Developments of the DIAdrill Concept

Mr. J. Yao, Dr. D.A. Summers, Mr. J.G. Blaine, and Mr. L.J. Tyler
University of Missouri-Rolla
High Pressure Waterjet Laboratory
Rolla, MO. 65401 U.S.A.

ABSTRACT

The use of a waterjet drilling device has considerable advantage in the long straight hole drilling of rock. However, the range of rock which can be effectively cut by waterjets alone is somewhat restricted. To overcome this limitation the use of abrasives, introduced into the jet using the DIAjet process, has been found to be very effective.

This paper reviews the development of an abrasive waterjet drilling device, outlining the considerations which are necessary to develop an effective tool. This includes the changes in operational parameters whch are required when the system changes from plain waterjet drilling to drilling with an abrasive laden waterjet.

Initial experiments had shown that such a tool could be used for drilling a vertical hole to a depth of over 18.3 m (60'). In the current paper, the problems and advantages of this new drill in drilling holes up to 7.62 cm in diameter, into rock to a depth of 4.57 m (15') but at an angle close to the horizontal, are described.

1.0 INTRODUCTION

The mining industry relies extensively on the use of mechanical drills to help in removing material. Many of the holes which must be drilled are relatively short and it is generally straightforward to maintain the accuracy required in their location. A number of mining techniques, however, rely on the accurate location of much longer holes in order to make it economic to mine the deposit. The problem that then arises with mechanical drilling is that the penetration rate is controlled by the amount of force applied through the drill bit to the cutting faces of the head. As hole length increases, it becomes more difficult to keep the drill string straight under this applied load. In addition, changes in the angles at which different rock layers are intersected will have an effect on positional accuracy. Ultimate accuracies of one to two percent are thus, often the norm in this type of operation. This restricts the hole length and thus, the size of the mining operation. A more accurate drilling method would, therefore, be of advantage.

2.0 BACKGROUND

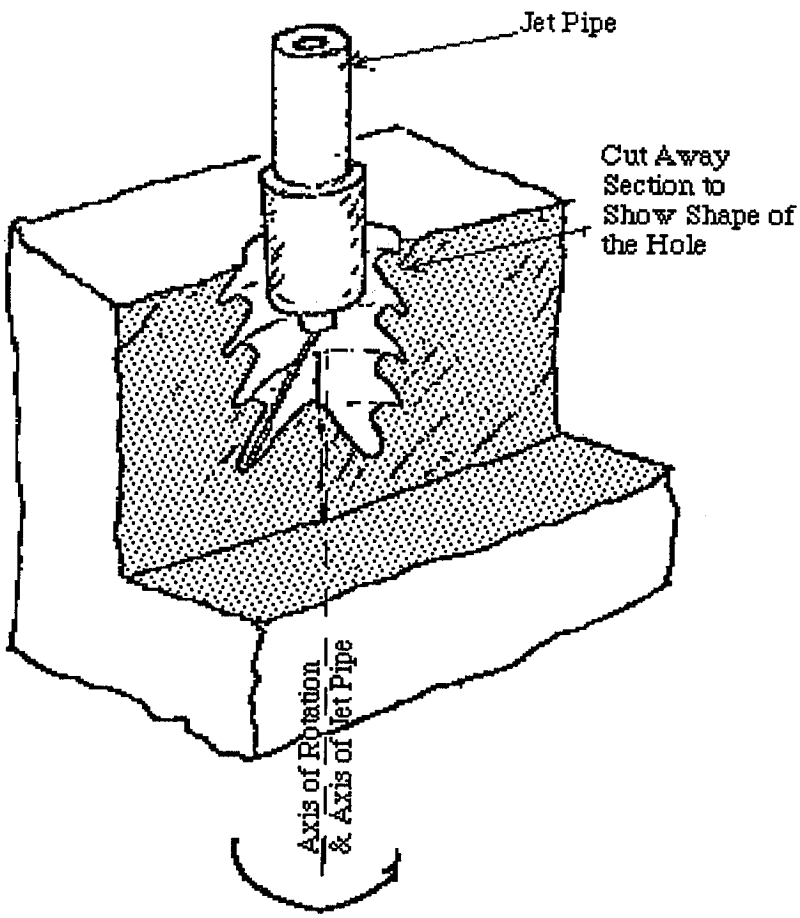

Figure 1. Jet slightly inclined outward to produce larger diameter hole for nozzle advancement (Ref. 1).

In early studies of waterjet use (Ref. 1), it rapidly became clear that the continued penetration of a jet into rock was diminished by a rebounding flow of spent water from the impact point. In order to overcome this problem, two approaches were proposed. One was to interrupt the water flow, allowing time for the spent water to escape before the subsequent pulse hit the surface. The other was to rotate the jet slightly off axis thereby allowing a passage for the spent water to leave the hole. When this jet was then slightly inclined at an outward angle, the rotating action cut a hole large enough in diameter to allow the nozzle to advance (Figure 1), and the first "pure" waterjet drill was born. Further the rotation of the jet gave an improved performance over the condition where the jet was pulsed, to allow the jet to escape (Figure 2).

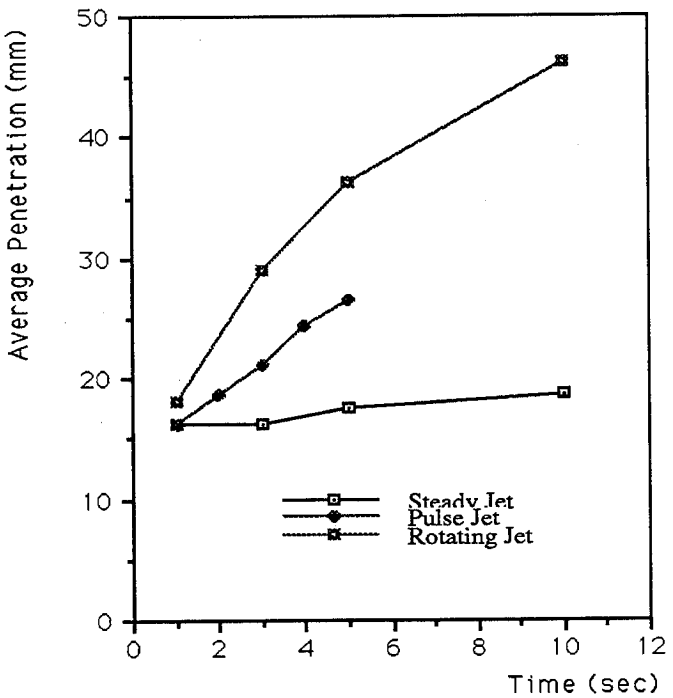

Figure 2. Relative Penetration of Rock with Steady, Pulsating and Rotating Jets (Ref. 1).

The development of the waterjet drilling concept proceeded relatively slowly since advance rates achieved were quite slow. Early in the 1970's, however, the drill design was modified (Figure 3) to include a second axial orifice, half the diameter of the original "reaming" jet. The presence of this secondary nozzle had two initial advantages, the first was that it removed material directly ahead of the center of the bit. The second, resulting benefit, was that this allowed the reaming jet orifice to be moved outward toward the gage of the hole. The resulting improvement in performance was quite dramatic since by the addition of only 25% more water to the nozzle, advance rates were increased by two orders of magnitude (Figure 4). This design, therefore, formed the basis for the development of a waterjet drilling concept. The design was demonstrated for drilling a wide variety of different materials and provided the hole diameter was less than approximately

10 cm, this design performed quite well (Ref. 2). Penetration rates in coal of up to 4 m per minute were achieved (Ref. 3). At larger hole diameters, however, the unbalanced nature of the nozzle design caused it to wobble in the hole and some accuracy in positioning was, therefore, lost. The drill was further restricted in application since plain waterjet cutting is not an effective tool in penetrating through very hard rock and other material.

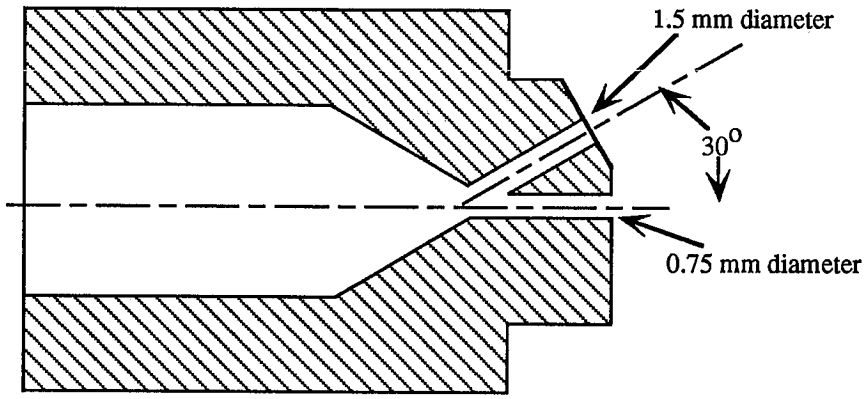

Figure 3. Modified Waterjet Drill design showing secondary nozzle (Ref. 2).

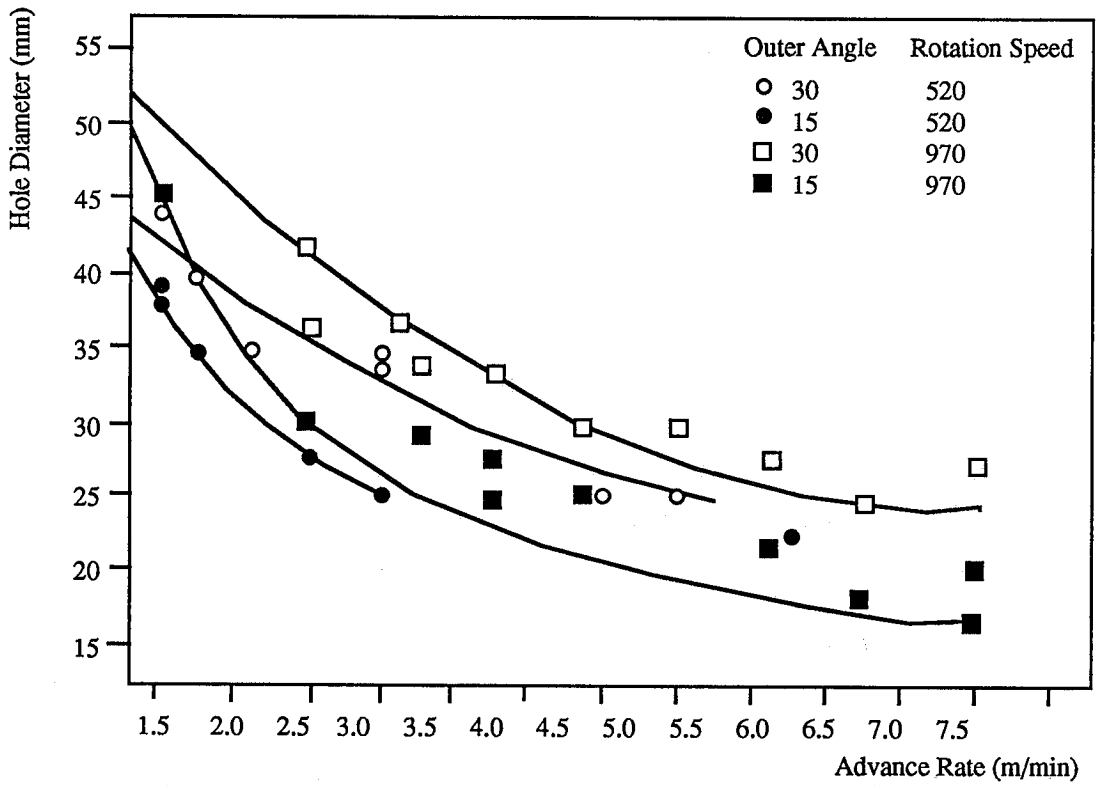

Figure 4. Improvement in drilling performance with the improved design (Ref. 2).

3.0 ABRASIVE DEVELOPMENT

Although the addition of abrasive to waterjet streams is not, in itself, a novel idea—the technique having been used as an aid to cleaning surfaces - it was not until the early 1980's that abrasive was first commercially entrained in a high velocity jet stream for industrial cutting use. Following the initial introduction of the tool, it rapidly demonstrated that it had an economic application for cutting conventionally difficult materials such as titanium, Inconel, and advanced composite materials. It also had the ability to cut through glass and ceramic materials with relatively little damage to the walls of the cut. Experiments have shown (Ref. 4), that the addition of the abrasive did not significantly increase the reaction force from the jets and this remained at a relatively low level.

The conventional method for abrasive injection had, however, one significant disadvantage as it related to the development of a waterjet drilling device. In conventional injection, the abrasive is mixed with the high velocity water after this has been accelerated to its maximum velocity. This occurs right at the cutting end of the tool and thus, requires that two separate feed lines must supply the drill head. While this is relatively easy to accomplish in a linear cutting operation, it provides a logistical problem where the two feed lines must supply a drill. This is because the drill generally makes a relatively small diameter hole through the rotation of the drilling mechanism. The development of separate feed lines and concentric swivels to supply the fluids, while not impossible, is an expensive requirement--both in development and maintainability.

The introduction of the DIAjet concept in 1986 (Ref. 5) provided a supply of abrasive-laden water through a single hose to the cutting head. This overcame the primary difficulty in the development of an abrasive drilling system requiring only the development of a rotating swivel capable of feeding an abrasive-laden stream. Such a swivel was, therefore, developed.

The first experiments with this new tool, which will be referred to as the DIAdrill showed that it could be used to drill a suite of rocks oriented unfavorably to the borehole axis without deviation. The drill was also used to drill vertical holes down through dolomite to depths of up to 18 m (Ref. 6).

4.0 DESIGN CONSIDERATIONS

The first trials of the DIAdrill used the same design that had been developed for plain waterjet cutting. This proved to be a relatively inefficient design and a number of other designs were tried (Table 1, Ref. 7), before one was found sufficiently practical to drill the 18 m hole (Figure 5). The suite of nozzles which were examined looked at both the method of accelerating the abrasive and the collimation of the flow into the orifices.

Design #	Inner Angle	Outer Angle	Pressure (MPa)	RPM	Drilled Rate mm/min	Specific Energy (KJ/mm3)	Hole Dia mm	Erosion (cc/gm)	Result
6	5	30	25	475	76	0.016	50.8	0.015	drilled OK
6	5	30	25	475	102	0.015	45.7	0.016	drilled OK
6	5	30	25	475	127	0.013	44.5	0.020	jammed
6	5	30	25	475	152	0.011	44.4	0.024	jammed
3	20	30	25	475	102	0.016	44.4	0.016	jammed
6	5	30	25	475	127	0.013	44.4	0.020	hit bottom
6	5	30	25	120	102	0.014	47.5	0.018	wobbling
7	3	10 deg	35	475	127	0.005	46.7	0.063	jammed
5	0	30	35	475	127	0.021	40.6	0.016	drilled OK
6	5	30	35	475	94	0.022	46.0	0.016	drilled OK
10	7	30	37	150	127	0.012	43.7	0.027	jammed
10	7	30	37	220	127	0.011	49.0	0.028	jammed
10	7	30	37	300	127	0.013	42.4	0.023	jammed
10	7	30	37	475	127	0.015	40.9	0.021	jammed
3	20	30	37	475	138	0.013	44.5	0.028	jammed
3	20	30	37	475	162	0.013	40.0	0.027	jammed
8B	0	30	35	200	149	0.013	49.0	0.026	drilled OK
8C	-5	30	35	200	171	0.011	45.5	0.031	hit bottom
8D	0	30	35	200	164	0.012	42.9	0.028	hit bottom
8B	0	30	35	200	172	0.013	44.5	0.027	jammed
8B	0	30	35	200	166	0.012	45.2	0.028	jammed
8B	0	30	37	200	182	0.010	45.7	0.029	jammed
8B	0	30	37	200	155	0.022	45.2	0.027	drilled OK
8E	5	30	37	200	144	0.014	46.0	0.025	jammed
8F	5	30	35	200	150	0.014	41.4	0.025	jammed
8F	5	30	35	100	143	0.013	41.1	0.026	jammed
8G	10	30	35	100	155	0.010	50.8	0.033	hit bottom
8H	single	26 deg	35	100	126	0.012	38.6	0.027	jammed
8H	25	26	35	100	161	0.014	41.1	0.025	jammed
8H	25	26	35	100	158	0.014	39.5	0.025	jammed
8A	5	30	35	50	170	0.014	39.4	0.028	jammed
8A	5	30	35	100	162	0.014	39.0	0.024	jammed
8A	5	30	35	100	143	0.014	38.6	0.024	jammed

Table 1. Drilling Configuration Tests (Ref. 7).

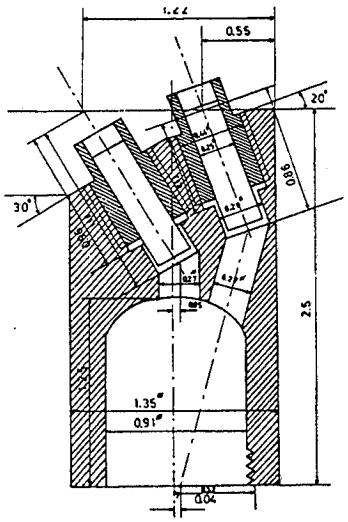

Dimensions are given in inch
. Nozzle Holder # 3, 20° - 30°

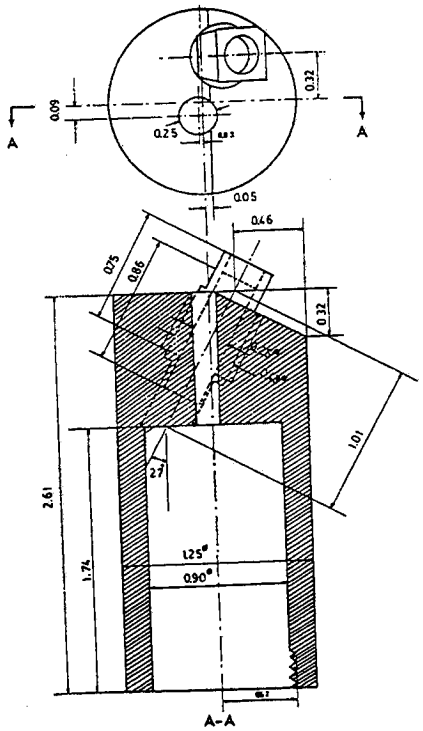

Dimensions are given in inch
. Nozzle Holder # 5, with a Straight and 27° Insert

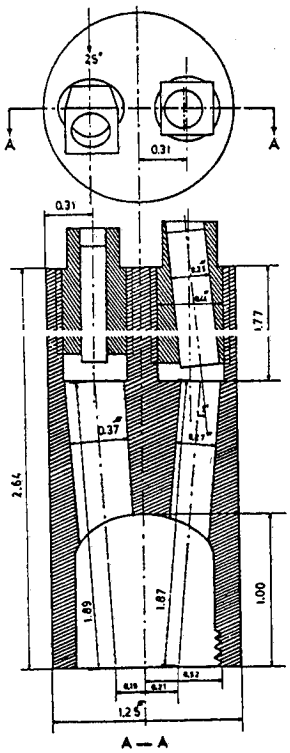

Dimensions are given in inch
Nozzle Holder # 6 with Two Inclined Inserts

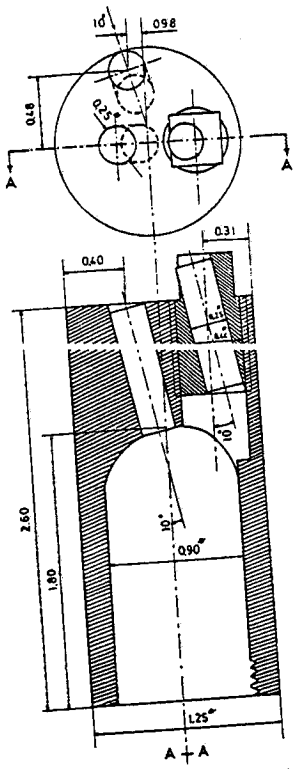

Dimensions are given in inch
Nozzle Holder # 7 with Three Inclined Inserts

Figure 5a Nozzle Designs Evaluated (Ref. 7).

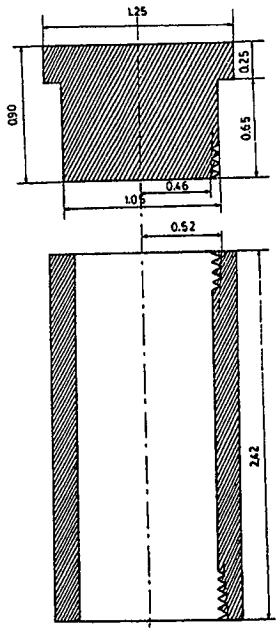

Dimensions are given in inch
Nozzle Holder # 8

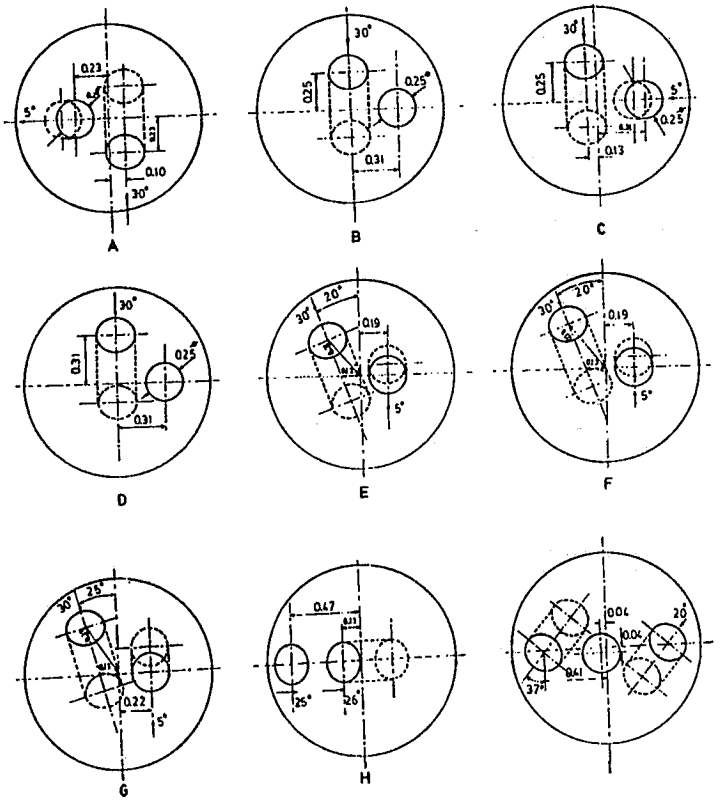

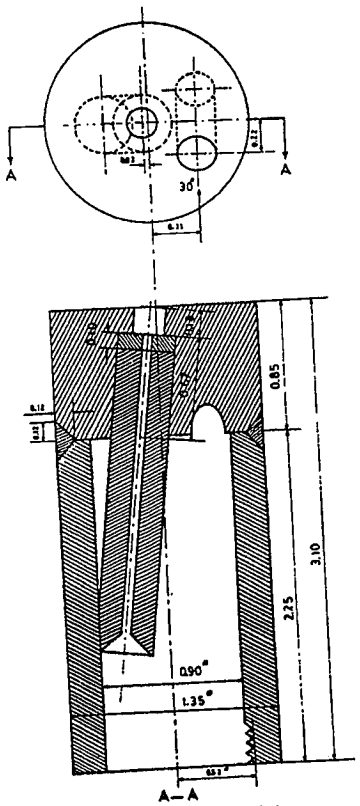

Nozzle Holder # 10, for 2.18 mm Carbide Inserts and Slurry Nozzles

Figure 5b. Nozzle Designs with a Front Loaded Insert Holder (Ref . 7).

For this reason both long and short nozzle inserts were used. The results obtained did not indicate, to a first examination, that, for this purpose, longer inserts were any better than the shorter ones. In fact, since the shorter ones were more easy to insert, and could be turned to a greater angle to the axis of the drill, these proved preferable for this application.

An early problem in the development of the drill was a lack of sufficient awareness of the differences now established between plain waterjet cutting of rock and abrasive jet cutting. Many of these changes have now been identified (Ref. 8) and it is clear that a different approach to the design of the DIAdrill is required.

Perhaps the most important change relates to the effect of nozzle diameter. With conventional jet cutting, nozzle diameter is a critical parameter in controlling the depth to which the jet will cut. In abrasive jet cutting, where the abrasive is added between the pump and the nozzle, it has virtually no effect as an independent parameter. Thus, increasing the diameter of the outer reaming jet to provide the cutting depth to reach the required hole gage, is not an effective strategy. Further, the abrasive jet appears a little more sensitive to the angle of impact with the rock wall than is the case with plain waterjet cutting.

The series of experiments given in table 1 show that where the outermost jet is inclined at an angle of less than 25 degrees, that the hole will cone inward as the drill advances, ultimately, binding the drill head against the parameter of the hole.

This creates a peculiar problem because with the existing drill bit design the jet is cutting to gage at some distance ahead of the drill. Thus, in order to remove the obstructing rock the drill body must be withdrawn back up the hole several cm. In practice it is difficult to effectively work this into the operating cycle and an alternate procedure is required.

With plain jet drilling this difficulty can be overcome by affixing a collar to the front of the drill head which establishes the gage of the hole at the point where the jet will cut to this diameter (Figure 6). This has been found to work well in practice, particularly when it is used in conjunction with a spring-loaded drive mechanism. Under that circumstance, the binding of the collar against the parameter of the hole stops the drill advance. The jet then will cut against the obstructing rock until it is removed freeing the drill to continue to move forward.

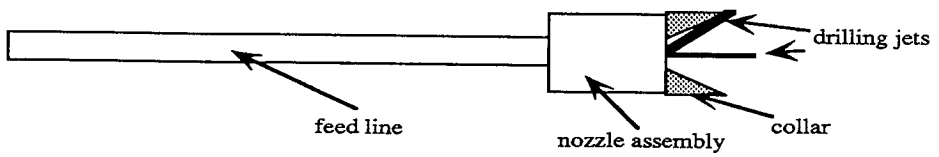

Figure 6. Plain jet with hole gaging collar attached to the drill head.

With an abrasive cutting system, however, this is not a practical option since the cutting abrasive will just as effectively cut the gaging collar as it will the rock ahead of it. An alternative solution, however, is now available because of the difference in the performance parameters of the abrasive jet. There is no advantage in this system to concentrating the flow in a small number of orifices, rather, performance is improved where a greater number of orifices of smaller size can be used.

As a result it is advantageous to redesign the configuration of the nozzles toward three goals. Firstly, an orifice can now be directed to place a jet of abrasive-laden fluid to cut the gage of the hole at the face of the bit. This removes the requirement for a collar, and, by leaving a suitable space around the jet impact point, also removes the concern in regard to erosion of the cutting head. The second objective is to insure that the hole does not cone in as the drill advances. This objective can be achieved by using an outward inclined angle of 28 degrees or greater for this gage cutter. The remaining nozzles can then be oriented to remove the material in the central block of rock ahead of the bit.

The jets should be oriented and spaced so as to minimize the fragment size of the particles removed by the jets. This is important since the relatively large size of the nozzle bodies inserted into the bit head fill a significant volume of the borehole behind the cutting plane. Thus, the gap available between the body of the bit and the hole will be quite small. Large fragments catching in this annulus can jam the drill, stopping progress. The exact orientation of the jets has yet to be optimized. However, it is of significant importance that the orientation and diameter of the different jets be such that the reaction forces across the nozzle body are balanced. This requires that the angle of each jet be considered in assessing the relative diameter of the orifice at that location.

5.0 FIELD TRIALS

The high pressure waterjet group at the University of Missouri-Rolla are currently engaged in removing rock from under the Gateway Arch, in downtown St. Louis (Ref. 9). During the course of the excavation of the cavity for the new theater being installed, abrasive waterjets have been used to cut vertical walls down up to 4.5 m. below the existing concrete support walls. In order to ensure that these rock walls do not fail under either static loads or the dynamic loads associated with earthquake ground shocks the structural engineering consultants to the National Park Service, Woodward Clyde, recommended that a series of 3 to 4.5 m long, Dywidag - 2.5 cm in diameter bolts be installed and encapsulated in resin at 1.2 m centers along the rock wall exposed (Figure 7). The spacing of the bolts within each column was to begin 0.3 m. below the base of the concrete footing. A second bolt would then be inserted some 0.9 m. below the first bolt, and a third bolt, where sufficient exposure existed, would be located 1.2 m. below the second. The bolts were to be installed at a grade of 1 in 10, sloping downward into the face.

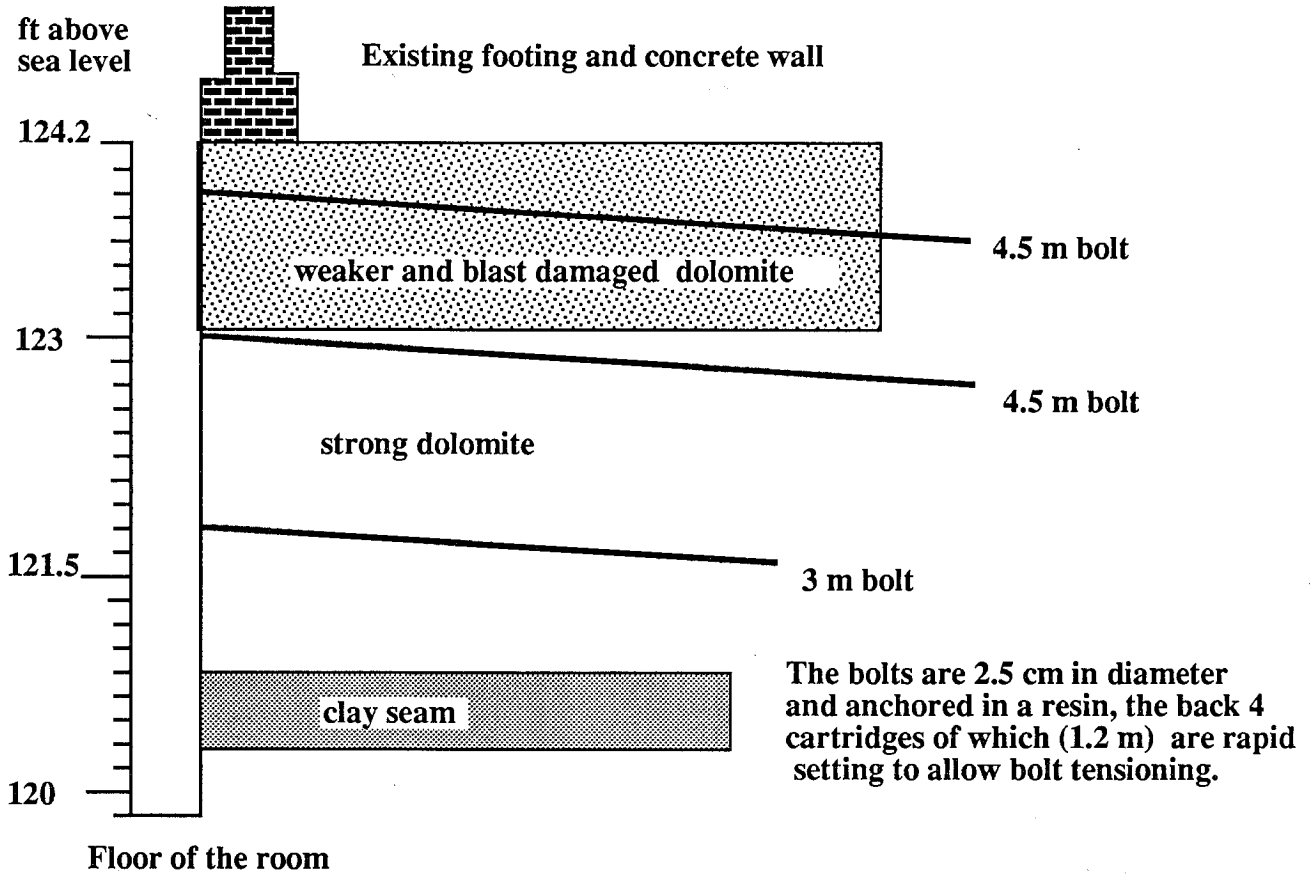

Figure 7. Schematic of a typical section showing the rock bolting plan.

Although the majority of the rock is a relatively competent dolomite inter-layered with relatively thick layers of chert, the upper surfaces of the rock had been fractured by blast damage during the initial Arch excavation and there were in addition, vertical and horizontal clay seams exposed by the current excavation. To insure wall stability, therefore, the consultants recommended that once the bolts had been installed, that they be placed under a compressive loading in conformity with recommended practice (Ref. 10).

In order to insure the accuracy of the anchorage in this procedure, applied loads in excess of 40,000 kg would be applied through the bolt to the back 1.2 m of the walls of the drilled hole. This requirement provided an opportunity to compare the behavior of waterjet drill and conventional drilled holes for use with such a system of rock bolting. The first holes to be drilled were in the upper sections of the excavation where the holes were drilled using the abrasive waterjet DIAdrill. This rock had been blast-damaged and fragmented rock frequently poses some problems for conventional rock drilling. In addition, quite thick clay seams were encountered along the axis of several of the holes drilled. In all cases, however, the holes were successfully drilled, and with one exception where the hole ended within the clay seam, the bolts were satisfactorily installed (Figures 8 & 9) and tested to proof pressure (Table 2).

Table 2. A Typical Bolt Test History (waterjet drilled hole).

Time	Applied Pressure (psi)	Bolt Load (lb)	Displacement
12:31:10	500	8925	0.366 re-zeroed
12:S33:20	1000	17850	0.060
12:34:44	1900	33915	0.217
12:37:37	1000	17850	0.165
12:38:33	500	8925	0.145
12:39:19	1000	17850	0.168
12:39:29	1900	33915	0.228
12:40:50	3200	57120	0.363
12:44:53	3200	57120	0.363
12:45:16	1900	33915	0.315
12:46:05	1000	17850	0.236
12:46:50	500	8925	0.197
12:47:04	1000	17850	0.212
12:47:30	1900	33915	0.286
12:49:16	3200	57120	0.376
12:52:58	4200	74970	0.486
13:07:53	3200	57120	0.461
13:08:10	1900	33915	0.369
13:08:35	1000	17850	0.287
13:08:47	500	8925	0.249
13:09:15	1000	17850	0.258
13:09:35	1900	33915	0.330
13:12:s50	4200	74970	0.503
13:15:15	4200	74970	0.503
13:18:32	4700	83895	0.558
13:21:48	4700	83895	0.560
13:24:36	1900	33915	0.402

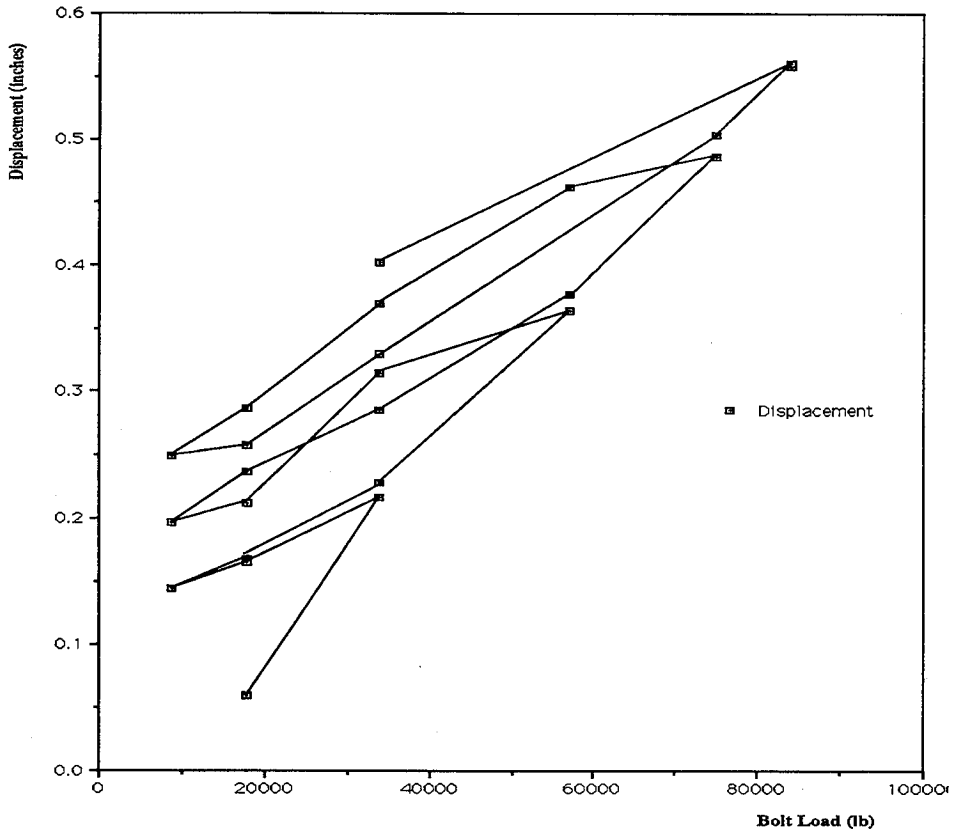

Figure 8. Bolt Stressing Graph taken from Table 2 figures.

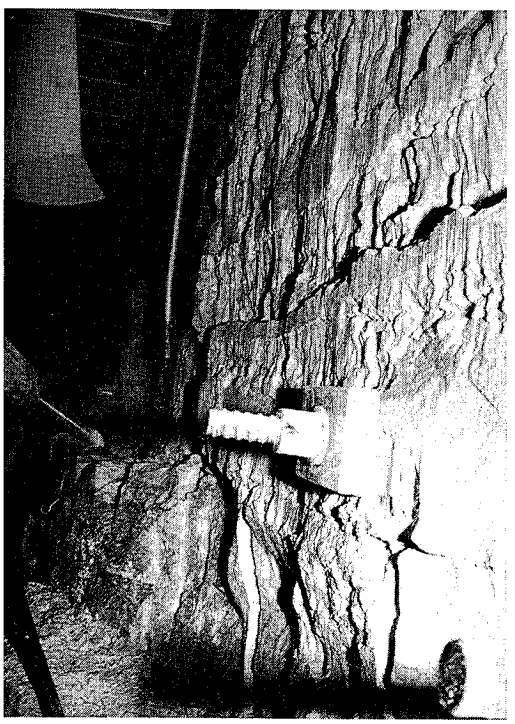

Figure 9. Bolt Installation in a Waterjet Cut Wall.

The holes drilled were not smooth and in order to easily slide the cartridges to the back of the hole an extensible metal tape was stretched along the bottom of the hole to provide a passage for the cartridges. Unfortunately, it was not possible to determine the full dimensions of the hole since only the narrowest dimensions could be gaged from its mouth. The holes were irregular and the largest dimensions could only be guessed at, yet nevertheless no problems were encountered with the anchor strengths achieved. No problem was in addition encountered in drilling through the broken rock or clay. Penetration rates for the drill were, however, somewhat disappointing, averaging 10 cm/minute or less. Part of this problem related to the obstruction of the drill head where the drill did not have a gage cutter.

In contrast, in the mechanically drilled holes, higher penetration rates were achieved and under normal circumstances a competent anchorage was also established. The mechanical drill, however, was not tried in the broken rock because of the risks of jamming the bit. Where it was used to drill through a thick clay lens it was difficult to re-collar the bit on the other side of the clay and this led to failure of a drill component. In addition, the support structure for the mechanical drill had to be quite significantly stronger than the waterjet drill and this greater weight took a longer time to move into position. Further comparative testing of the two designs is still continuing. As part of this evaluation a simpler and lighter carriage for the DIAdrill is being fabricated, and the drill will be tested to determine if the angle of the hole has any bearing on the drill performance. In addition a provision for recirculating abrasive will be developed.

6.0 ACKNOWLEDGEMENTS

This work could not have been undertaken without the considerable interest, enthusiasm, and encouragement which we have received from the National Park Service personnel at the Jefferson National Expansion Memorial. From the Superintendent, Mr. Jerry Schober, and his assistant, Mr. Gary Easton, through the day to day cooperation with Mr. John Patterson, and Mr. David Caselli, and the cooperation of the Park Rangers, this program has been considerable advanced by their willingness to help.

We also gratefully acknowledge the assistance provided by the U.S. Bureau of Mines, through the Generic Mineral Technology Center for Mine Systems Design and Ground Control at Virginia Polytechnic Institute and State University at Blacksburg, Virginia. This program is providing funding support toward the design and testing of the DIAdrill tool.

REFERENCES

1. Summers, D.A., Disintegration of Rocks by High Pressure Jets, Ph.D. Thesis, Department of Applied Mineral Sciences, University of Leeds, UK, 1968.

2. Summers, D.A., Yazici, Sina, "Progressing Rock Drilling", Article for Mechanical Engineering, December, 1989.

3. Summers, D.A., Peters, J., "Preliminary Experimentation of Coal Cutting in the Pressure Range 500-2000 Atmospheres", Second International Symposium on Jet Cutting Technology, Cambridge, U.K., paper H2, April, 1974.

4. Summers, D.A., Wu, W-Z, and Yao, J. "A Further Investigation of DIAjet Cutting", Proc. 10th Int. Symp. Jet Cutting Tech., Amsterdam, October, 1990.

5. Fairhurst, R.M., Heron, R.A., and Saunders, D.H., "Diajet" - a new abrasive waterjet cutting technique", 8th International Symposium on Jet Cutting Technology, Durham, England, September, 1986.

6. Yazici, S., Summers, D.A., "Abrasive Jet Drilling - A New Technology", Proc. 30th Rock Mech. Symp., Morgantown, W. Va, June 18-22, 1989.

7. Yazici, Sina, "Abrasive Jet Cutting and Drilling of Rock", Ph.D. Thesis, University of Missouri-Rolla, Rolla, MO., 1989.

8. Summers, D.A., "Keynote Address", 1st Asian Recent Advances in Jetting Technology Conference, Singapore, May, 1991.

9. Yao, J., Summers, D.A., Galecki, G., "DIAjet Cutting of Dolomite & Chert—A Case Study at the St. Louis Arch", 6th Waterjet Technology Conference, Houston, TX., August, 1991.

10. Recommendations for Prestressed Rock and Soil Anchors, Post-Tensioning Institute, Phoenix, AZ., 1st edition, 2nd printing, 1980.

6th American Water Jet Conference
August 24 - 27, 1991: Houston, Texas Paper 42

THE FUTURE FOR ABRASIVE JET CUTTING

BY

D S MILLER
BHR Group Ltd, Cranfield, Bedford, UK

E J BLOOMFIELD
Fluid Developments Ltd, Cranfield, Bedford, UK

ABSTRACT

The paper sets out the reasons for the remarkably rapid commercial exploitation of abrasive water jet (AWJ) cutting. It outlines why direct abrasive AWJ systems are preferred by contractors for on-site and sub-sea cutting and why, at present, only abrasive entrainment AWJ systems are used in manufacturing applications.

The future developments are discussed in relation to industrial needs, equipment capital and operating costs, technical and commercial risks.

Research and development needs are described which are aimed at:

1. Providing the detailed performance and component reliability information to build a new generation of precision CNC controlled AWJ machine tools.

2. Developing AWJ systems that will operate to any depth sub-sea and down hole in oil and gas wells.

3. Building up data and knowledge bases for linear and contour cutting that will enable AWJ systems to be fully exploited in manufacturing and for site and sub-sea operations.

Organized and Sponsored by the Water Jet Technology Association.

1.0 INTRODUCTION

In mechanical engineering, few new technologies can rival the speed at which AWJ cutting has been commercialised at such a small cost in R & D. Within a decade abrasive water jet cutting has advanced from exploratory laboratory studies to commercial application in many industries and countries.

There are a number of reasons for the rapid application of AWJ cutting, which include:

1. Strong market pull because of the need for effective ways of cutting difficult to machine materials - metal matrix composites, ceramic matrix composites, titanium, super alloys, etc.

2. The need by contractors for a powerful, flexible and safe, cold cutting tool for demolition and repair of process, chemical and other plants, civil engineering structures, sub-sea installations, mine installations, etc.

3. Relatively low financial, technical and commercial risks because many of the major components for AWJ systems were already proven in the industries who have the greatest need to use AWJ cutting. In the case of abrasive entrainment systems for manufacturing industries, the entrainment head and its abrasive feed was a relatively low cost edition to water jet cutting systems. In the case of direct abrasive injection systems, contractors already used suitable pump sets for water jet cleaning.

Initially AWJ systems for contracting and manufacturing industries were based on abrasive entrainment cutting heads. To give acceptable cutting performance, entrainment AWJs require the ultra high pressures (>2000 bar) produced by intensifiers. They also need to operate with a dry abrasive in an air feed system. Operating environments for intensifiers require a high level of cleanliness and operator support. This support is readily provided in manufacturing plants but is difficult to achieve for on-site operations. The difficulties of operating intensifiers on-site, combined with problems of keeping abrasives dry have severely restricted the application of entrainment AWJs for site operations. There were also perceived safety problems of having ultra high pressure equipment in a site environment and difficulties in handling the two hoses needed for entrainment cutting heads.

To overcome problems with entrainment systems for site operations, BHR Group developed the DIAJET direct injection system. In DIAJET a water-abrasive slurry is delivered in a single hose to the cutting head. Direct injection is inherently more effective than entrainment (typically five times at the same pressure and power input) but against this has to be set greater flow circuit complexity and cost; abrasive slurry having to be generated at high pressure and passed through components and hoses to the cutting head.

By adopting an operating pressure of under 350 bar the first generation DIAJET systems could:

1. Use the water pumping sets and pressures contractors were familiar with from their water jet cleaning activities.

2. Employ standard pressure vessels, hoses and components for the flow circuit and achieve adequate nozzle life without the use of exotic materials.

3. Out-perform entrainment systems in the thickness of concrete, steel and other materials that could be easily cut.

4. Achieve certification for cutting in inflammable environments.

The development of infactory and site AWJ systems has followed a route that minimized financial and technical risks by using, as far as possible, proven technology. For the future the financial and commercial risks of developing and using AWJs will increase because of:

1. Competition as more companies enter the CNC cutting market with similar AWJ systems coupled to X-Y cutting tables and robotic systems.

2. The cost of R & D to achieve product differentiation as companies try to maintain and grow their market share.

3. Extensive developments to achieve the reliability necessary for 16 to 24 hours per day operation, which is becoming the norm in many companies.

4. AWJ systems being built as an integral part of production systems with high consequential losses when they fail.

5. Contractors needing to operate their machines under extreme conditions for de-commissioning reactors, off-shore structures, etc.

2.0 BACKGROUND EXPERIENCE

In this section a number of developments at the author's organisations are outlined to provide background and credence to a discussion on AWJ limitations and R & D requirements outlined in subsequent sections.

BHR Group Limited and its subsidiary Fluid Developments Limited, have been at the forefront of the development and exploitation of AWJ technology. Since 1970 BHR Group has been an international centre for jetting research and since 1972 has organised the bi-yearly International Symposium on Jet Cutting Technology. The links with the international jetting community has allowed BHR to build up an extensive knowledge base on AWJ technology.

The first containerised AWJ system for off-shore use (Fig 1) had a twin hose system to feed an entrainment cutting head. On the latest direct injection DIAJET systems (Figs 2 and 7) only a single hose is required

making deployment much easier. This hose can be up to 1000m long and deployed vertically as well as horizontally. Currently work is in progress to use DIAJET technology for de-scaling of oil field tubulars on-site at depths of 3500m and slotting of casings to improve oil production.

A barometric vessel (Fig 3) has been used for cutting trials down to the equivalent of 3500m. Typical cuts at 3500m on different compressive strength rocks (Fig 4) are similar to those at atmospheric pressure. Direct injection systems operate reliably on pipeline and platform repairs sub-sea (Fig 5).

Operating direct injection AWJ systems with sea water is practical. A 2000 bar sea water intensifier for operation on a remote operated vehicle (ROV) or in a suspended cage, has been developed for cleaning and AWJ applications (Fig 6). This compact unit limits pressure fluctuations, compared to conventional intensifiers, by innovative control over two independent, floating pistons. As a result the fatigue life of components in the high pressure circuit is extended.

AWJs are non-contact cutting tools that are ideal for operations on batches of components that vary in size. The fettling of castings (removal of runners, risers, flash, etc) is a particular application which is difficult to automate using conventional cutting tools but practical with an AWJ (Fig 7).

Profiling of difficult to machine materials is relatively easy on a CNC profiler (Fig 8) using a DIAJET system. Materials such as titanium (Fig 9) and Metal Matrix Composites (MMC) can readily be cut with a good edge shape and finish (Figs 10 and 11). Edge shape and finish can be further improved by angling the jet.

3.0 AWJ LIMITATIONS

Currently AWJ systems are only capable of meeting a small part of the ultimate market for such systems. By machine tool standards current systems are mechanically and electronically crude but they work. Their use in the diverse applications outlined in section 2 is providing the feedback to drive R & D for the next generation of AWJ systems.

Deficiencies with current cutting systems include:

1. Entrainment systems are inherently inefficient because of energy dissipation in the entrainment process and the destruction of abrasive before it leaves the cutting head. The longer term use of entrainment systems is questionable for many machining applications.

2. Direct injection systems currently operate at low pressures (300 to 700 bar) and as a consequence need high water and abrasive flow rates to achieve acceptable cutting speeds. High abrasive use is not a serious problem in contracting applications but is important in manufacturing industries. An increase in operating pressure is called for to reduce running costs but without significant increase in capital costs or reduction in reliability.

3. There is no positive control over or monitoring of abrasive at the cutting head. Feedback between the abrasive flow and manipulation systems is called for. The technology exists to develop on-line monitoring of abrasive flow rate and feeding this to the manipulator control.

4. Cut surface finishes and related fatigue performance are often poor, necessitating extensive and costly secondary machining operations. The reasons for poor surface finish needs to be established together with corrective measures.

5. As material thickness increases there is a tendency for jets to wander and create wavy cuts that require additional material tolerances and difficult corrective machining. The reasons for jet wander and corrective strategies are needed.

6. Set-up times are excessive and often involve expensive trial and error cuts to determine how manipulators should be programmed. Reliable off-line programming of manipulators is required.

7. When cutting curves or changing direction, jets deviate within the material in ways which cannot at present be predicted. Data is needed to develop predictive models.

8. There are no predictive models for where and how jets leave a workpiece and how to position catchers to safely dissipate jet energy. (Failure to catch a jet when using a jet following catcher can be very dangerous, resulting in resistance to the technology, particularly by machine operators). Predictive models and new catcher designs are required.

9. The use of expensive jigs and fixtures to hold workpieces could be avoided by minimising workpiece forces. An understanding of strategies to minimise work forces is required.

Very little is known about the physical process involved when an abrasive jet interacts with a workpiece. Mathematical and experimentally based models are needed to be able to efficiently program abrasive jet cutting machines to cut a wide range of materials and shapes. Until these models are available, manufacturing companies will continue to have to invest in extensive R & D to understand how to use and to adapt machines to their needs.

The rest of this paper considers the R & D necessary to develop the technology of AWJs and in the process overcome many of its current limitations.

4.0 ABRASIVE JET GENERATION, INTERACTION WITH WORKPIECES AND ENERGY DISSIPATION

Abrasive jets can be visualised as a rod of water 400m long, 1mm in diameter with particles half the rod diameter every 2mm along the rod. Imagine this 400m long rod passing over the cut surface in one second causing 200,000 multiple interactions between particles and workpiece.

In reality the jet is far from rod like; particles move slower than the mean water velocity; turbulence and air entrainment disrupts the jet; the distribution of particles is very uneven in time and space. Also with entrainment systems over half the particles are likely to be reduced to fragments before exiting the nozzle.

To gain a better understanding of abrasive jets research programmes in Europe are being directed to:

1. Determine the characteristics abrasive jets need to be more effective.

2. Establish how abrasive jets interact with a workpiece and how to change interactions to improve machining capabilities, particularly speed and finish.

3. Determine how to move jets/workpieces to achieve desired cut edge shapes with a quality finish and size tolerance.

4. Understand how to catch and destroy the energy in jets after they leave a workpiece; higher powered, more coherent jets are more difficult to deal with.

Events from the cutting head inlet to the dissipation of a jets energy in a catcher cannot be directly measured. This means events have to be inferred from observations and measurements which are open to wide interpretation. A framework is being put into place to guide how experiments are carried out and cut surfaces analysed. The aim being to help researchers identify and control important variables and to report measurements in a consistent manner.

Particular areas of study are:

1. The effect of time dependent variations in abrasive flow on surface finish of both entrainment and direct injection systems.

2. Investigating how to overcome the problem of striations on cut surfaces which are characteristic of not only pure water and abrasive jets but also laser and plasma beam cutting systems.

3. A data base of cutting performance that includes edge shape, roughness, fatigue properties along with operating parameters, abrasive used, etc. The data base will be supported with prediction software that recommends cutting strategies to achieve particular objectives of edge finish, fatigue strength, etc.

4. Mathematical models for contour cutting which will use the output of CAD systems as input to manipulation programmes. This will allow for off-line programming of CNC-AWJ cutting systems so as to achieve high machine utilisation.

5. The design of compact jet catchers that utilise hydrodynamic effects to minimise the energy to be dissipated against wear elements.

5.0 MACHINING SYSTEMS

The development of the AWJ cutting machine market is likely to follow that of laser systems.

1. Many companies will enter the market with profiling systems (this is currently happening).

2. Companies who manufacture total systems (intensifiers + table or robot) or have strategic alliances to provide systems, will begin to dominate the market.

3. Japanese and far Eastern companies will then enter the market with machines that undercut Western products.

4. Product differentiation will grow to enable Western producers to remain in niche markets.

Product differentiation will require improvements in performance. This will involve factors such as speed, depth of cut, drilling capabilities, re-use of abrasives, specialised manipulation equipment, compact cutting heads and catchers for operation in confined spaces.

To achieve high performance and product differentiation manufacturers of AWJ systems will have to adopt direct abrasive injection technology. This will happen because:

1. Direct injection systems offer a five fold increase in cutting performance at the same operating pressure and power input compared to entrainment systems.

2. Narrower kerf widths, greater cutting depths, better edge shapes and surface finishes are possible.

3. The greater coherence of direct injection jets enables operation at large stand-offs, relative to jets from entrainment heads.

4. Re-cycling of abrasive is much easier with direct injection because the abrasive is handled in the wet state.

R & D is in progress to develop the DIAJET direct injection system to operate at pressures in excess of 2000 bar. Because of the large number of potential applications of DIAJET technology, international collaboration is being developed to carry out the necessary R & D.

To fully exploit AWJ it is essential to continuously monitor cutting performance. As an AWJ is a non-contact cutting tool, small disturbances that cause a deviation in a jet can be amplified in the jet/workpiece interaction. This can result in very poor surface shape and finish. Methods are required to detect that material removal is deviating from the ideal so that corrective action can be taken. Correcting for deviations is particularly important for deep cutting,

selective removal of surface material, turning and milling. The potential exists for on-line, three dimensional surface visualisation to better the 10 microns using a single camera vision system. Such a system could be the basis for a sensing and control system for AWJ machine tools.

The use of vision systems will also be important for operational safety in automatic shut-down if a jet enters no go areas or has undesirable characteristics due to nozzle wear etc. For processes like de-burring of machined components and fettling of castings (removal of flash, runners, gates, etc) vision systems are potentially the best form of monitoring and control. The Commission of the European Communities is currently supporting a study into the automation of fettling processes which is co-ordinated by BHR Group.

The cost of disposal of spent abrasive and water is likely to rise above their initial cost. Disposal costs are driving activities to reduce abrasive and water use and to develop the technology for re-circulation of abrasive and water. As the number of AWJs increases it is likely that it will become economic for abrasives to be re-cycled to the abrasive manufacturers for use in other products.

6.0 CONCLUSIONS

The commercial benefits of AWJs have been demonstrated. New manufacturing methods that exploit AWJs are being developed. To maintain market share, manufacturers of AWJ products will increasingly have to specialise in order to satisfy market needs. A new generation of predictive control and monitoring systems will be developed to compensate for and exploit the lack of a direct force connection between the workpiece and the tool manipulation system.

AWJ systems for use by contractors will continue to operate at low pressures, relative to systems in manufacturing industries. The exceptions will be in nuclear de-commissioning and similar critical applications. The operating pressure of direct injection systems will be increased to that of intensifier driven entrainment systems. The benefits will be higher cutting speeds and precision than can be achieved with current AWJ technology.

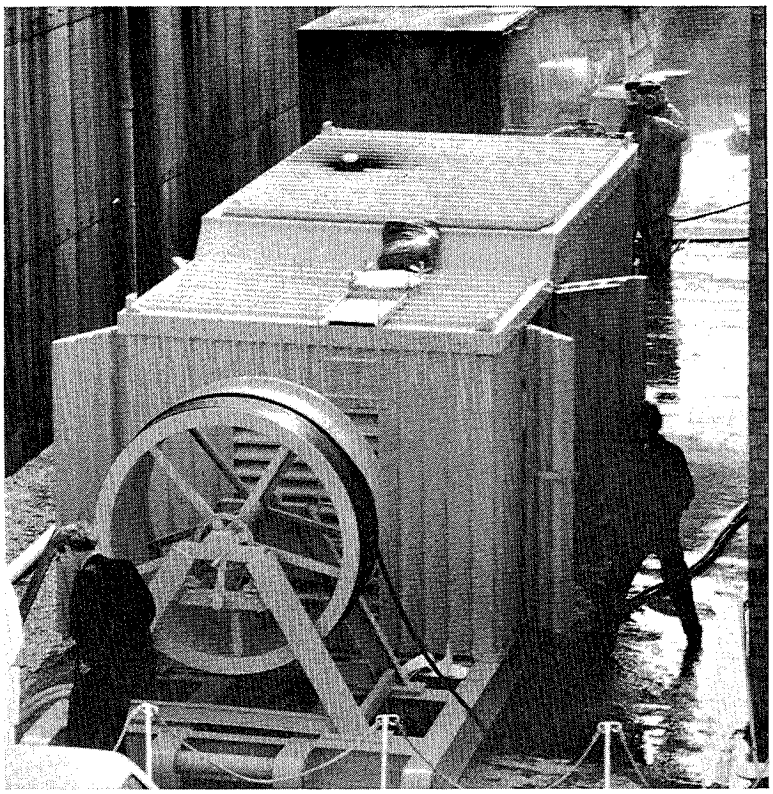

Fig 1 A containerised, entrainment AWJ system for off-shore operation undergoing trials at BHR Group in 1984

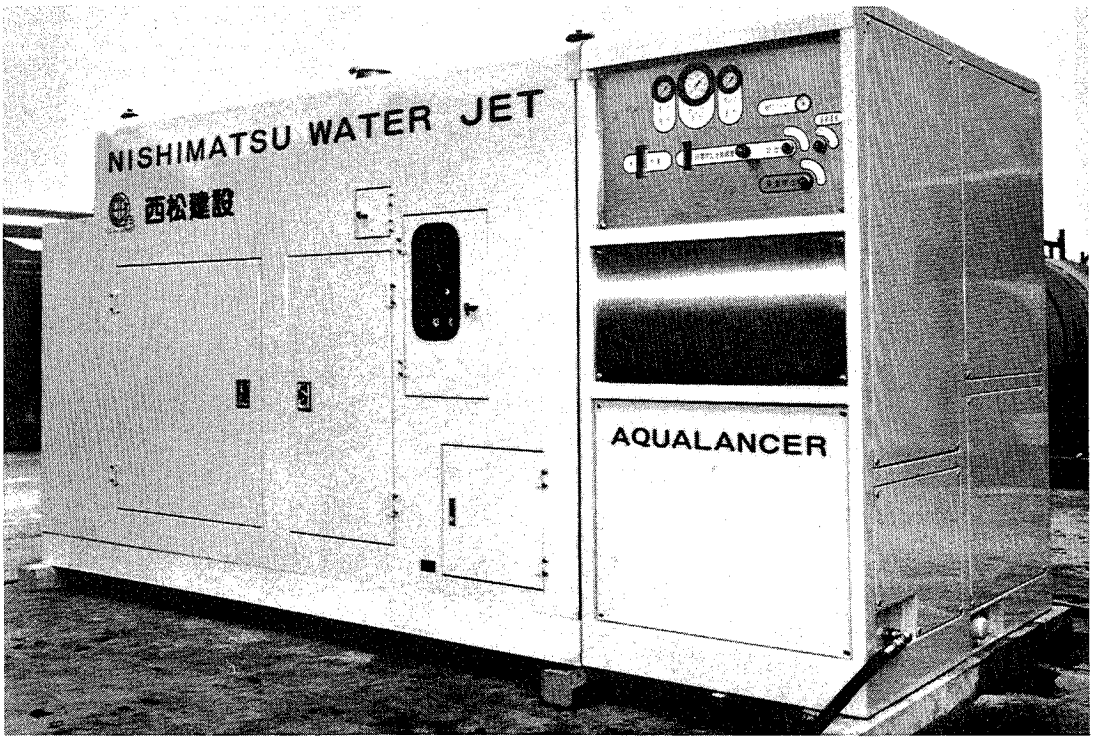

Fig 2 DIAJET containerised system built under licence by Iseki Poly-tech Inc, Tokyo, Japan, for the construction company NISHIMATSU

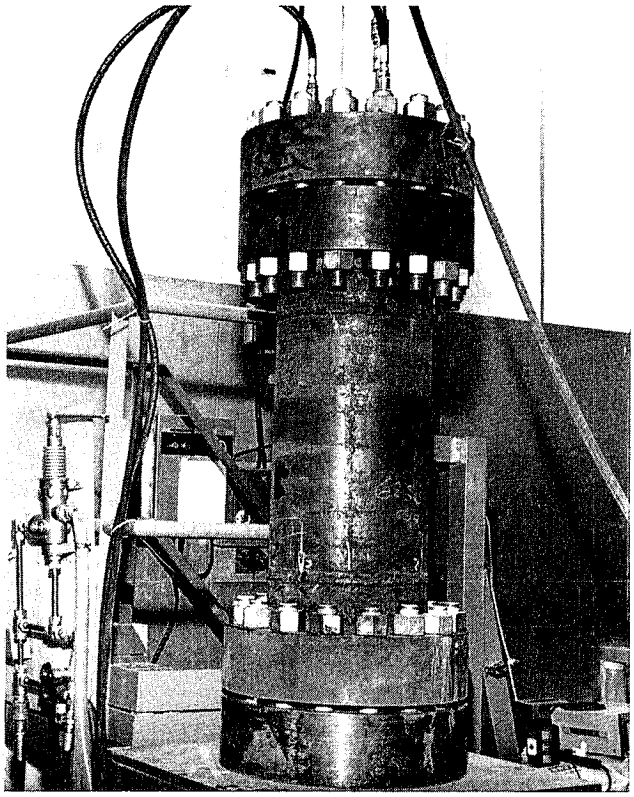

Fig 3 Barometric vessel with a rotating table for trials at 350 bar (equivalent to 3500m sub-sea)

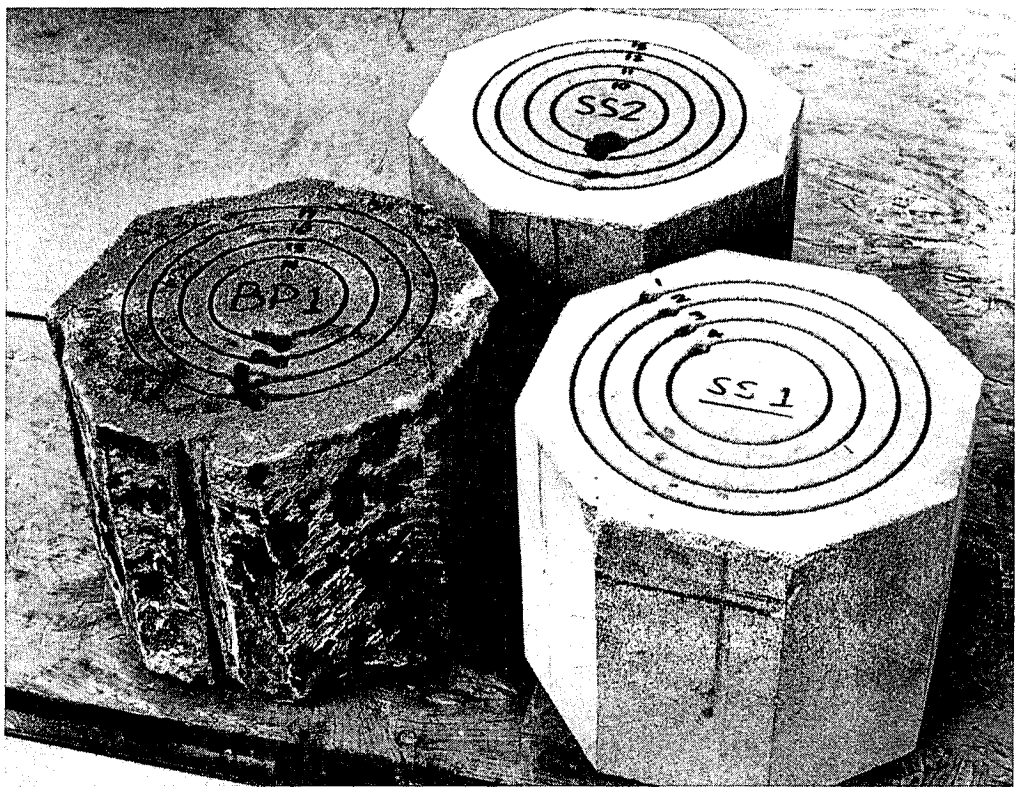

Fig 4 Cuts in three rock samples at the equivalent of 3500m water depth with a nozzle differential pressure of 350 bar

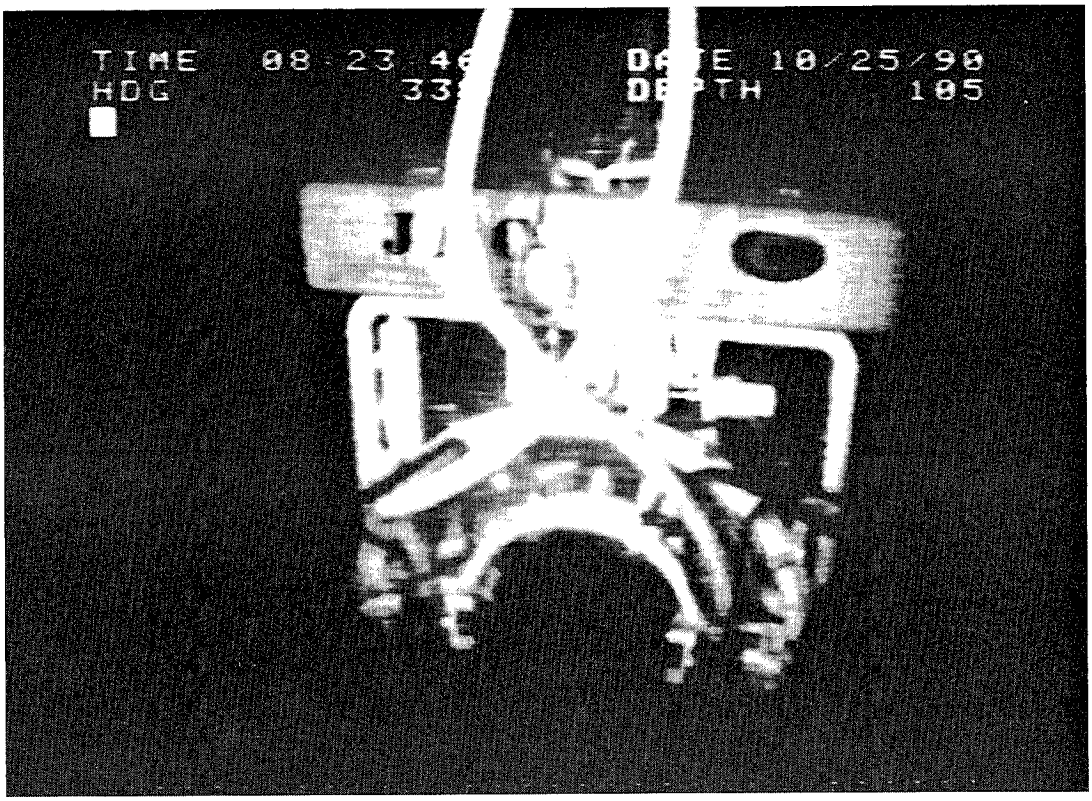

Fig 5 Comex Jet Abrasive Clamp operating 105m sub-sea off Norway cutting a pipeline with two DIAJET nozzles

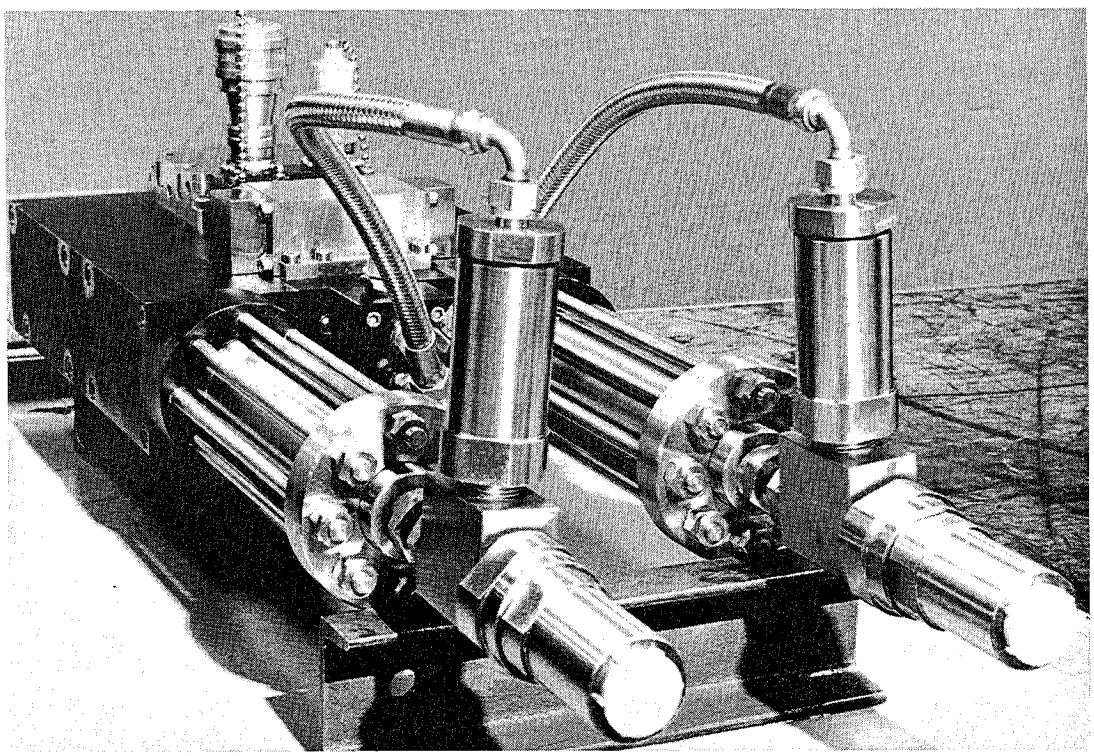

Fig 6 Low pressure ripple sea water intensifier for 2000 to 3000 bar operation on a ROV

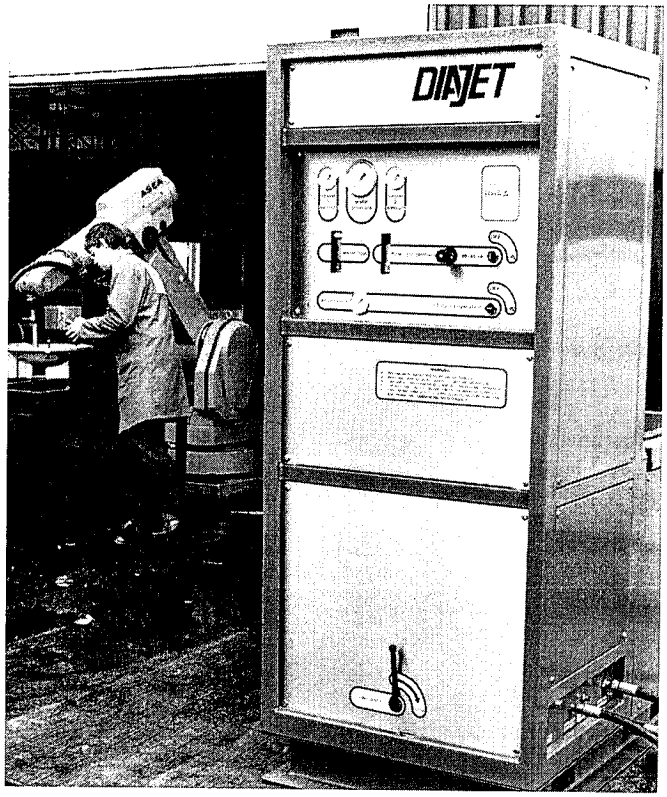

Fig 7 DIAJET site module used for trials of robot automated fettling of castings

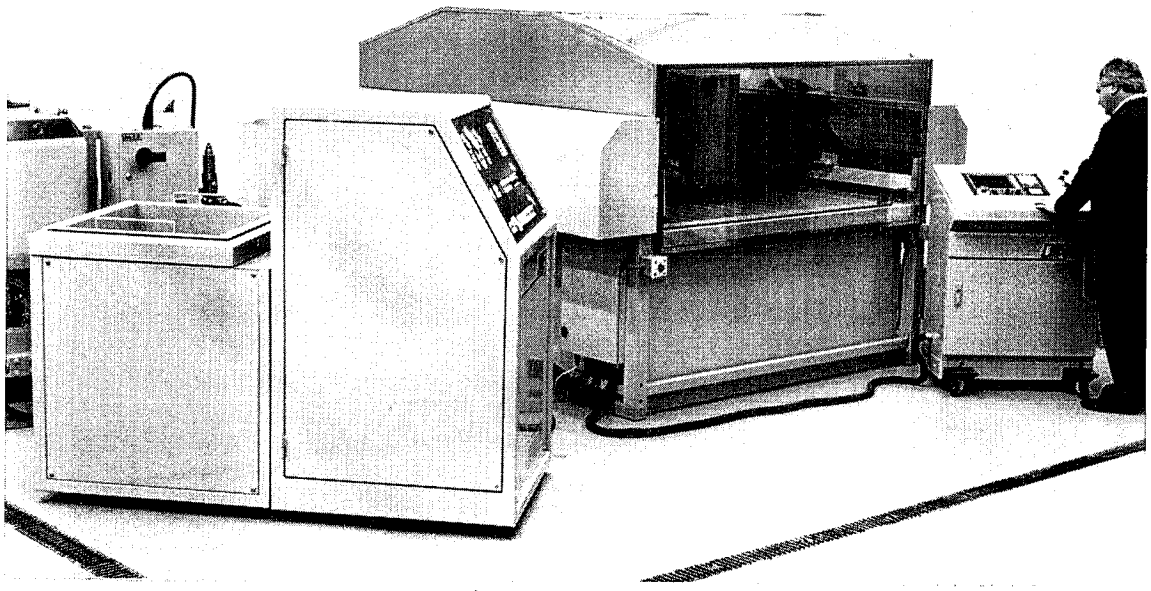

Fig 8 CNC profiler using a DIAJET abrasive feed system

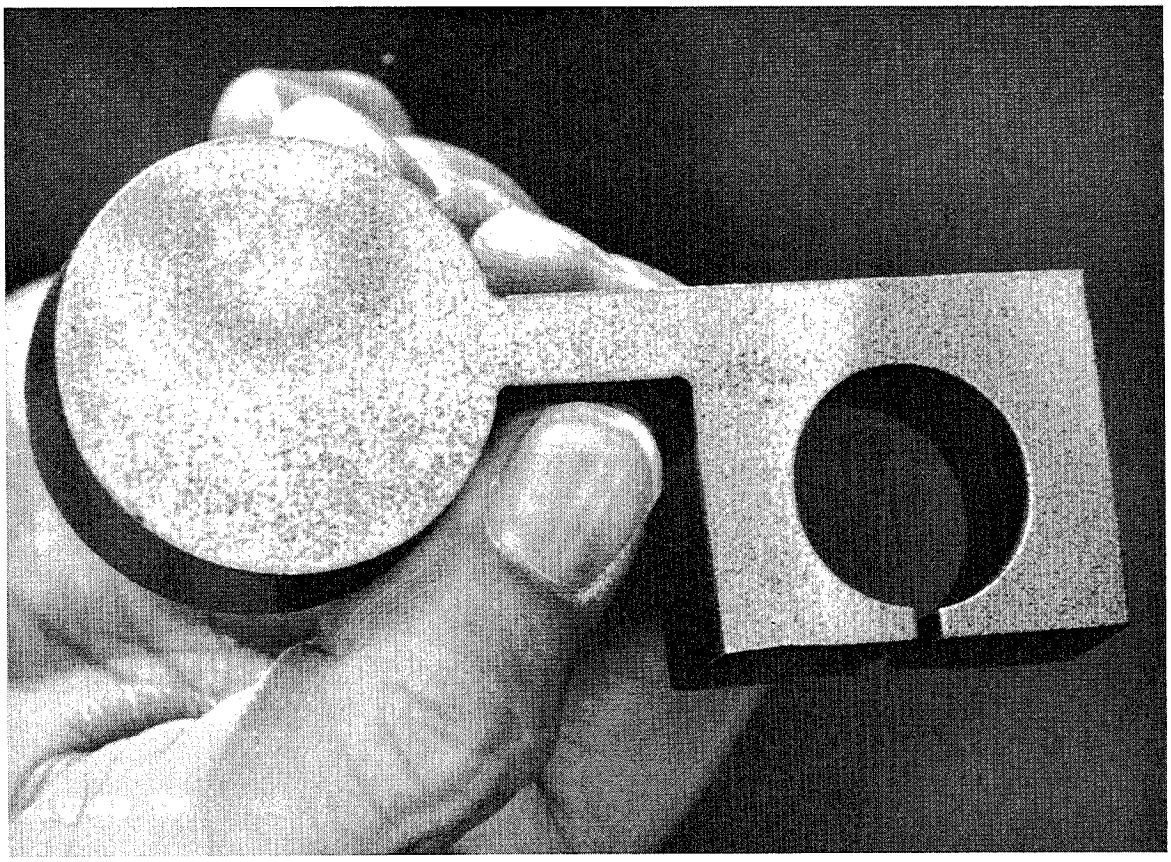

Fig 9 16mm Titanium profiled at 50mm/min with 345 bar nozzle pressure

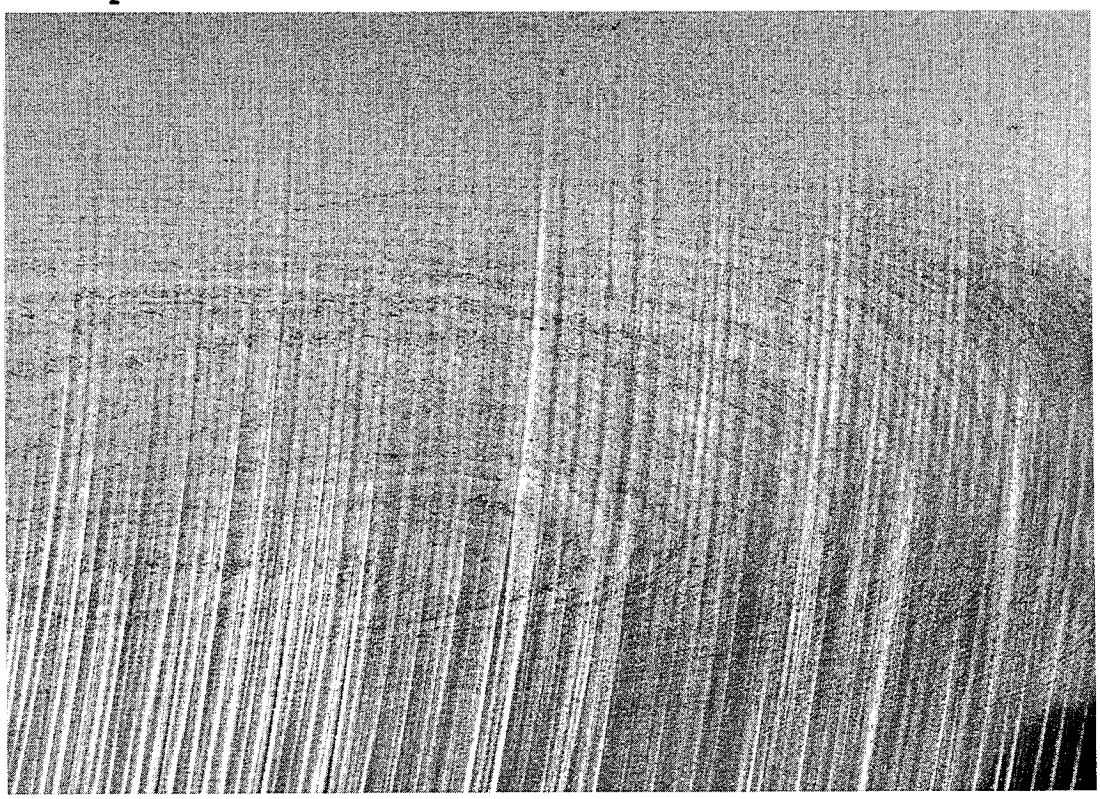

Fig 10 Cut through MMC aluminium with 20% SiC (Note striations due to forging process and to cutting process)

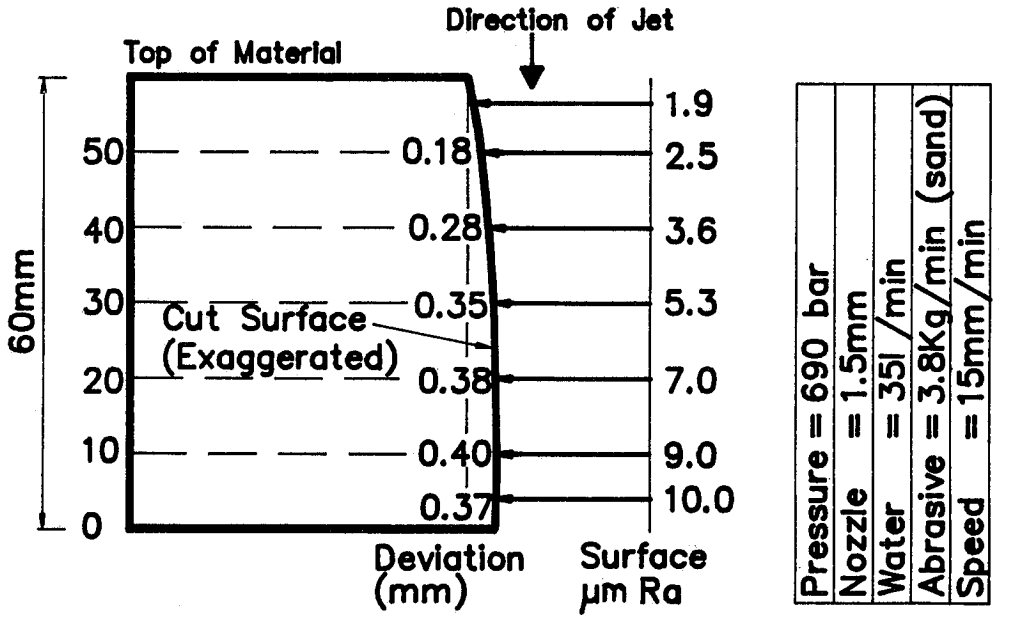

Fig 11 Sample of cut edge shape and finish for MMC sample of Fig 10

6th American Water Jet Conference
August 24 - 27, 1991: Houston, Texas

Paper **43**

HIGH PRESSURE FLOW CONTROL VALVES

Gene G. Yie
Fluidyne Corporation
Auburn, Washington U.S.A.

ABSTRACT

Flow control valves are indispensable components in any fluid systems. Waterjet systems are no exceptions; both powered and manually operated flow control valves are critical system components and are in common use today. At low fluid pressures, existing valves perform well and many are available for various tasks. At high fluid pressures, however, the selection of suitable valves is significantly limited, particularly in instant on-off type. At present, both closure valves and dump valves are employed in handheld waterjet lancing operations; both types are known to have serious shortcomings regarding their pressure capability, ease of operation, reliability and safety. Powered on-off valves available today for waterjet operations are also known to have shortcomings in reliability at high cycling rates. This paper discusses the novel design of a group of flow control valves developed recently by Fluidyne Corporation. These valves have basically circumvented the shortcomings of conventional on-off valves in both powered and manual versions. The manually-operated versions are made in both closure and dump types; they have pressure capability in excess of 207 MPa (30,000 psi)and yet without significant problems in component reliability, fluid pressure drop, leakage, or operator fatigue. The powered versions can be advantageously used as on-off valves or as pressure- or flow-regulating valves.

Organized and Sponsored by the Water Jet Technology Association.

1.0 INTRODUCTION

High pressure waterjet is rapidly becoming an accepted tool in many industrial applications. In these applications, there are needs to control the flow of high-pressure water in different ways. The most common need is to turn on or off the water flow instantly by means of an on-off valve. Others involve the relief or reduction of fluid pressure or diversion of flow direction. At low fluid pressures, these tasks are easy to accomplish and many valves are currently available. At fluid pressure above 69 MPa (10,000 psi), the availability of suitable valves is drastically reduced, particularly in fast-actuating types. Further, currently available high-pressure valves have well-known shortcomings in various applications. For example, available manually-operated dump valves are known to develop leaksprematurely and require powerful hand grip to operate. Available manually-operated closure valves are known to have limited pressure capability and problems in component reliability. Even powered on-off valves have reliability problem in the useful life of valve stem and valve seat. Pressure regulators currently in use with water jetting systems are also known to have performance and reliability problems. Fluidyne Corporation recognized the importance of flow control valves in waterjetting operations and undertook the task of developing improved valves. The result of this effort is the development of a group of instant valves that can serve multiple functions in waterjetting operations with much improved performance. These valves are discussed here on the basis of their function.

2.0 MANUALLY-OPERATED DUMP VALVES

A dump valve is a device that is used to relieve the pressure of a fluid system through quick opening of a relatively large outlet port. Powered versions are provided with either pneumatic or hydraulic actuators and are reasonably reliable if they are not cycled at high frequency. The manually-operated dump valves are commonly used in waterjetting operations in conjunction with crankshaft pumps at water pressures up to 138 MPa (20,000 psi). Although some are foot operated these dump valves are very similar in design; they function on the opening and closing of a large outlet port in the valve. The general design of conventional manually-operated dump valves used in waterjetting systems is illustrated in Figure 1. They consist of a few components such as valve body, handle, trigger lever, valve cover, inlet tube, outlet tube, valve seat, valve plunger, bias spring, and seals. In operation, the operator pulls the trigger lever against the handle to close the dump port, thus directing the water from the pump to the nozzle, which is situated at the far end of the outlet tube and is sized to maintain the desired system pressure. When the operator needs a break, the hand grip on the trigger lever is released and the valve plunger is retracted by the bias spring, thus opening the dump port, drastically reducing the water pressure inside the valve cavity, and rendering the waterjet from the nozzle harmless. The key to the proper function of these manually-operated dump valves is the mating of the valve plunger and the dump port. The closure of the dump port by the tip of the valve plunger must be perfect for the dump valve to function properly. It must not produce high water-induced downward force (in reference to Figure 1) on the plunger to cause hand fatigue to the operator. Yet it also must not produce

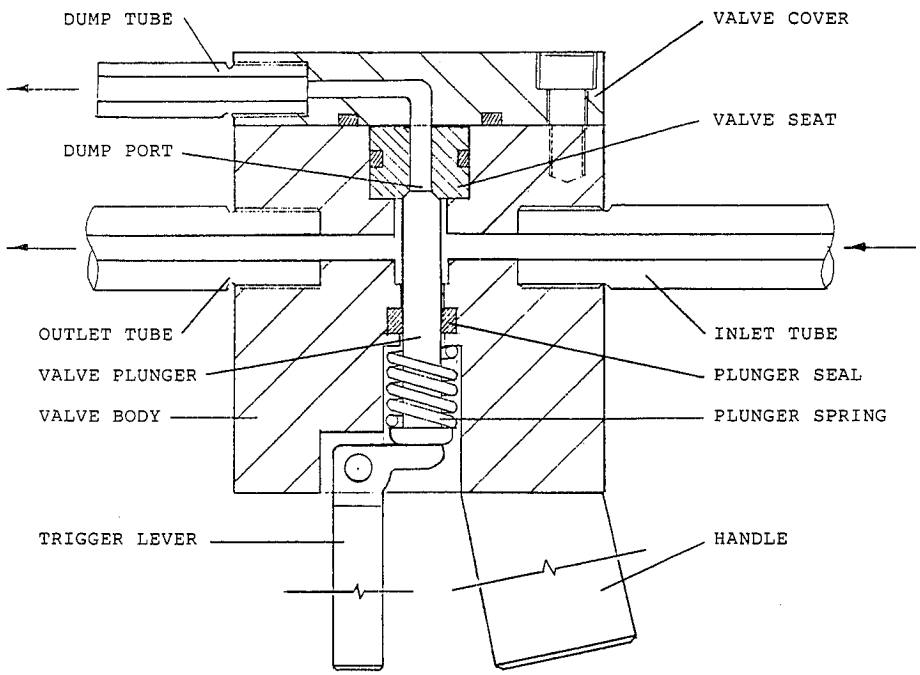

Fig.1 A Conventional Hand-Operated Dump Valve For Waterjetting Applications

high valve-closure force on the plunger such that the plunger spring will not retract the plunger promptly to open the dump port when the trigger lever is released. There is very little room between the two conflicting conditions for the valve designer to work with. As a result, the valve plunger and the valve seat are prone to developing leaks quickly even if they are made of very hard metals. Once fluid leakage occurs, the operator must apply even stronger hand grip to operate the valve as high-pressure water gets into the interface of valve plunger and valve seat to generate high downward force along the valve plunger. The result is operator fatigue and the loss of useful power.

Fluidyne's solution to this dump valve problem is to devise a pilot-operated scheme through which the high-pressure fluid inside the valve is utilized to operate the valve plunger while the operator's hand is merely for controlling the pilot operation. This patent-pending scheme is illustrated in Figure 2, which shows a complete assembly of a hand-operated high-pressure dump valve configured for waterjet lancing operations. The scheme involves the creation of two separate fluid chambers along a valve plunger having a central fluid passage such that fluid-induced force of two different levels are generated at the ends to move the valve plunger and to open/close a dump port. A hand-operated trigger lever is employed to move a small valve stem to open and close a pilot passage. The valve plunger is shaped like a piston, having a shoulder and shoulder seal. The plunger is situated inside a valve cavity while the plunger shoulder is situated inside a larger, separate cavity connected to the valve cavity through a small fluid passage. Between the plunger seal and the plunger shoulder is a compression spring that constantly

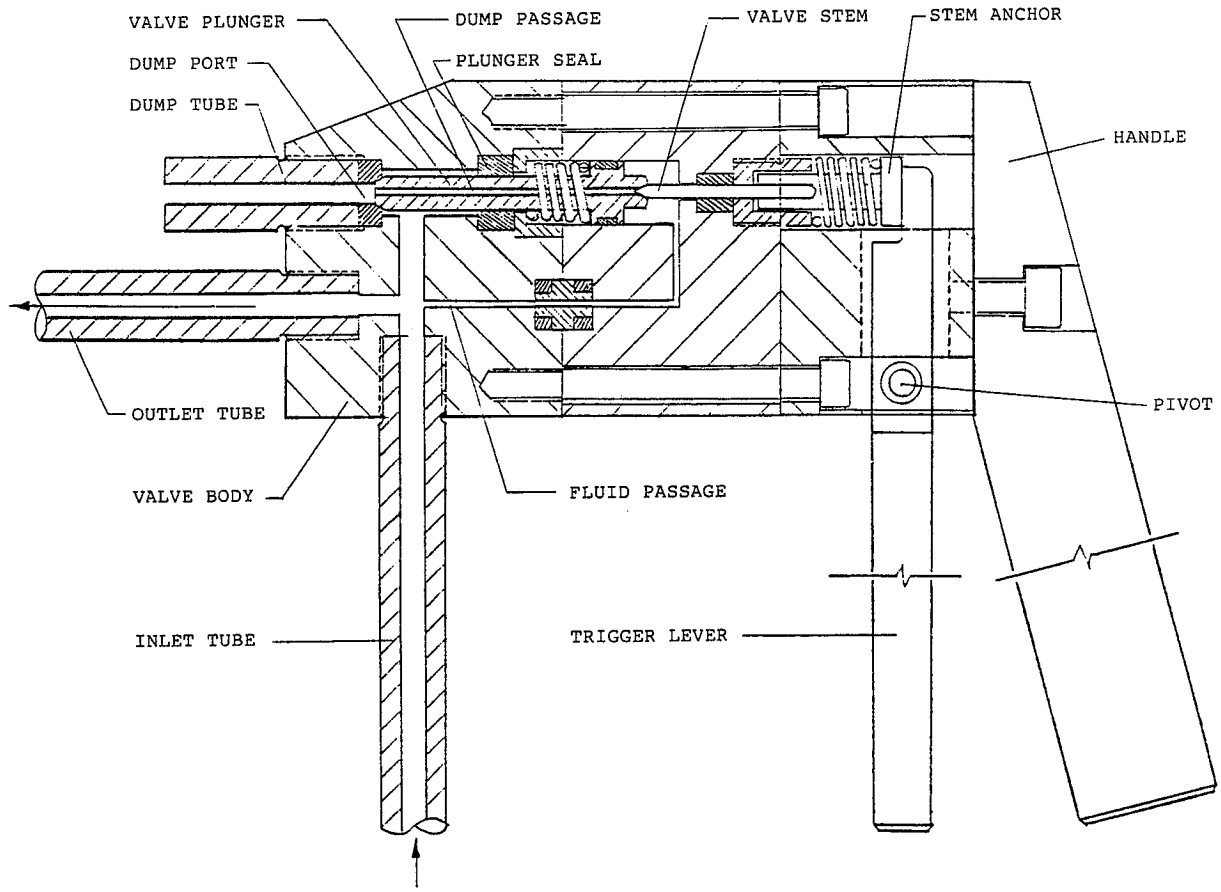

Fig. 2 Fluidyne's Pilot-Operated Dump Valve For Waterjet Lancing Operations

exerts force to unseat the valve plunger from the dump port and is situated in a space that is connected to the ambient. The plunger has a central through passage that is controlled by a manually-operated, needle-shaped valve stem. In operation, the operator pulls the trigger lever against the handle to close the dump port and releases the trigger lever to open the dump port, just like operating conventional dump valves. The difference is in the forces involved in operating the valves. When the trigger lever of Fluidyne's dump valve is pulled toward the handle, the needle-shaped valve stem is pushed from right to left, which in turn pushes the valve plunger from right to left to close the dump port. Thus the fluid pressure inside the valve cavity builds up quickly; so is the pressure inside the plunger shoulder cavity. Because of the shape of the plunger, a very large force is generated inside the valve plunger shoulder cavity pushing against the plunger shoulder in the direction of closing the dump port. At the same time, the fluid-induced force inside the plunger cavity in pushing the plunger from left to right in the direction of unseating the plunger is much smaller because of the area differential involved. The force differential can be as large as 456 kg (1,000 lb) at fluid pressure of 138 MPa (20,000 psi) in the case of a valve plunger having a diameter of 8 MM (0.31 inches) and a plunger shoulder of 11 MM (0.44 in). Because of the small diameter of the needle-shaped valve

stem, a very small hand force is required to keep the central dump passage of the valve plunger closed. Further, a small leakage through this dump passage will not affect the overall performance of the dump valve.

When the hand grip on the trigger lever is released, the central dump passage of the valve plunger is opened, thus quickly reducing the fluid pressure inside the plunger shoulder cavity while the fluid pressure inside the valve cavity is still high. Therefore, the valve plunger will be moved by fluid from left to right to fully open the dump port. Due to the fact that valve plunger is deliberately made to be slightly larger than the dump port, there will be fluid-induced force of significant magnitude to push the valve plunger and to quickly open the dump port. The presence of two compression springs further assures that dump port will stay fully open when the fluid pressure inside the valve cavity is reduced to a low level. Failure to open the dump port fully has been cited as one of the shortcomings of conventional dump valves as there is no fluid-induced force available for opening the dump port.

Because of the fact that valve seating force in Fluidyne's dump valves is so high, fluid leakage through the valve seat is basically eliminated. Therefore the useful life of both valve plunger and valve seat is significantly improved. The basic design of Fluidyne's dump valves is not pressure sensitive - it works at 0.2 MPa (30 psi) or 207 MPa (30,000 psi) without having to change any parts, providing the unit is made to handle the fluid pressures involved. It is obvious that this valve design can be applied for powered operations as well, requiring only a very small pneumatic, hydraulic or electric actuator to move the small valve stem.

3.0 POWERED CLOSURE VALVES

Remotely operated on-off valves are indispensable components in automated waterjet or abrasive waterjet systems. Currently, several pneumatic models are commercially available for pressures up to 414 MPa (60,000 psi). Hydraulically operated on-off valves are also available but are not as common. Although serving the purpose, these valves have shortcomings in the reliability of their valve stem and valve seat in high-cycling applications due to the constant pounding between the two components. These valves are supplied generally in two forms depending on the construction of the actuator. One is the so-called normally-closed type in which the valve port is closed by the valve stem through spring force exerting on the actuator piston, as shown in Figure 3. To open the outlet port of such valves, compressed air is introduced into the actuator chamber below the piston to lift the piston against the spring, thus releasing the downward force acting on the valve stem. Venting the compressed air will again close the outlet port. Since the spring force is directly transmitted to the valve seat through the valve stem, a striking force of significant magnitude is produced everytime the outlet port is opened and closed. The exact magnitude of this force is a function of the spring involved and the fluid-induced force on the valve stem. It can be very high if the fluid pressure is very high as the spring force must be greater than the fluid force acting on the valve stem and seal to assure positive closure of the outlet port.

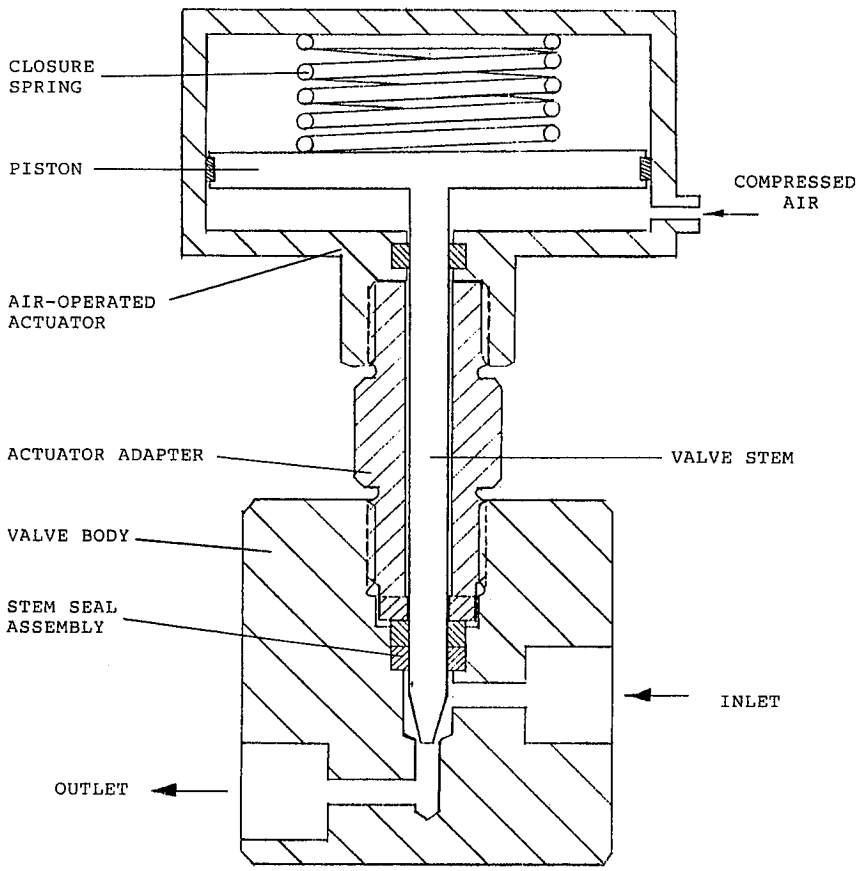

Fig. 3 Conventional Air-Operated On-Off Valve of the Air-to-Open Type

Another version of available air-operated remote on-off valve is the so-called normally-open type in which compressed air is employed to push down the actuator piston that in turn pushes down the valve stem against the valve seat to close the outlet port. To open the valve, the compressed air is vented off and the fluid-induced force acting on the valve stem will lift the valve stem to open the outlet port. This type of on-off valves is simpler than the normally-closed version due to the absence of closure spring or springs. However, they are not as safe because of the fact that valve will open inadventently if the supply of compressed air should fail or should develop leak. Similar to the normally-closed versions, the force from the compressed air in these valves will also be transmitted to the valve stem and to the valve seat, resulting in repeated pounding of these two components. To avoid breakage of the valve stem, stout valve stem is employed in some valves. As a result, very large and bulky air actuators must be employed in order to handle very high fluid pressures.

Fluidyne's solution to these problems is to design a unique poppet-valve stem arrangement such that the forces from an actuator will not be allowed to be transmitted to the valve poppet and the seating of valve poppet against the valve seat is accomplished by the action

of the high-pressure fluid, as shown in Figure 4. With this patent-pending arrangement, the poppet will engage the valve seat "softly" and the valve stem will not be subject to bending stresses induced by the function of the actuator. As a result, very slim valve stems can be used without the fear of breakage and actuators of small size can be used to handle very high fluid pressures. Fluidyne also made the valve seat reversible and readily replaceable and the valve poppet readily replceable as well. With a round valve poppet, a waterjet nozzle can be placed directly below the valve poppet and inside the valve seat if desired without appreciable fluid disturbance. This basic valve design can be readily incorporated to make on-off valves of all three types - normally-closed, normally-open, and fluid-to-closed-and-to-open. Needless to say both compressed air and hydraulic fluid can be used to operate the valve actuator.

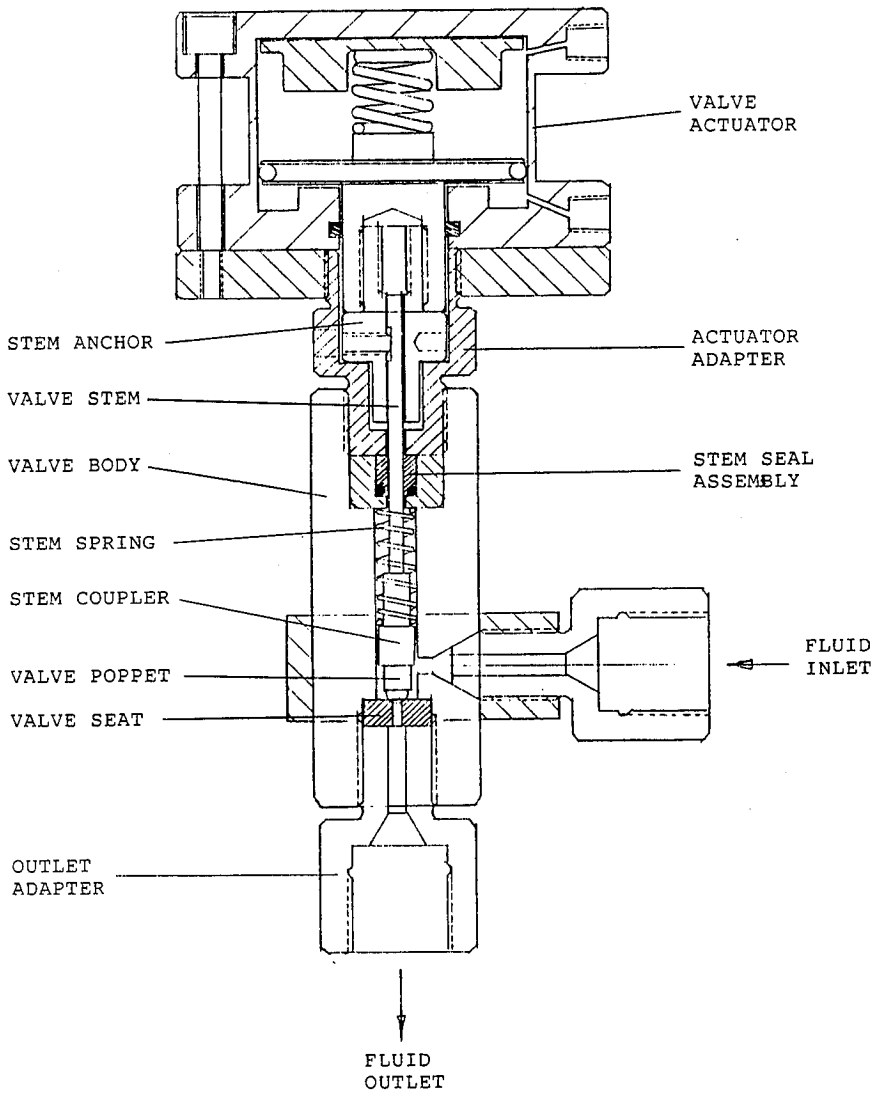

Fig. 4 Fluidyne's Air-Operated On-Off Valve

4.0 MANUALLY OPERATED CLOSURE VALVES

Another type of flow-control valves commonly used in manually-operated waterjet lances is the so-called closure valves or dead-end valves. They are basically manually-operated instant on-off valves. This type of valves are particularly popular with pump systems that are based on hydraulically-driven pressure intensifiers but are also used today in increasing numbers with crankshaft pump systems. Some of them are used to handle fluid pressures up to 241 MPa (35,000 psi). The basic construction of available valves of this type is quite simple, involving a valve stem, a valve seat, a powerful closure spring, a trigger lever, and a spring-actuating mechanism, as shown in Figure 5. These valves are all normally-closed in which the outlet port is closed by the valve poppet (the end of valve stem) from the force supplied by the compression of the closure spring. To open the valve, the operator pulls the valve trigger lever against the handle to compress the closure spring through various actuating arrangements. As a result, the valve stem is pushed from left to right either by the action of the pressurized fluid alone or with the aid of trigger lever actuating mechanism as well to open the outlet port. The high-pressure fluid inside the valve cavity exerts full force on the valve stem once the outlet port is open. To assure positive valve closure, the closure spring must provide force greater than the fluid induced force on the valve stem. And this spring force must be dealt with by the operator's hand grip as well. Therefore, the valve designer is facing a problem of balancing the force requirements and still achieving a working valve. In order to minimize operator's hand fatigue, the valve stem is made deliberately small so that a practical compression spring can be employed. For example, at fluid pressure of 207 MPa (30,000 psi), a 3.2 mm (1/8-inch-diameter) valve stem will be subject to a force of 167 kg (368 lbs), which is beyond the capability of small die springs. However, reducing the diameter of the valve stem to 1.6 mm (0.063 inches), this fluid-induced force is reduced to 42.5 kg (94 lbs), which can be provided by available springs. However, the result of using such small valve stems in valves of conventional design is breakage problem even if they are made of very strong metals. Further, using small valve stems requires that valve's outlet port be made small as well; otherwise, the valve may not open. Thus, there can be a significant pressure drop across the outlet port if the valve is used to handle high flow.

Fluidyne developed closure valves that eliminated the cited problems. There are several versions. One is for use at relatively low flow rates and is labeled as "Ultra-Light" units; others are used at higher flow rates and are called High-Flow types. The ultra-light waterjet lances use valves that have internal valve poppet-valve stem arrangement very similar to that employed in Fluidyne's air-operated on-off valves discussed earlier. By virtue of separating the valve poppet from the valve stem, Fluidyne is able to use small valve stems without breakage problem. This patent-pending design also allows precise determination and arrangement of the magnitude of fluid-induced forces acting on the valve poppet to close the outlet port and on the valve stem to open the outlet port. This condition is advantageous in the design of valve parts and the valve's operation. With it Fluidyne is able to produce closure valves capable of handling fluid pressure in excess of 241 MPa (35,000 psi) and yet the

whole waterjet lance equipped with this closure valve weighs only 3.6 kg (eight pounds). The internal layout of the closure valve is shown in Figure 6 and a photograph of this ultra-light waterjet lance is presented in Figure 8.

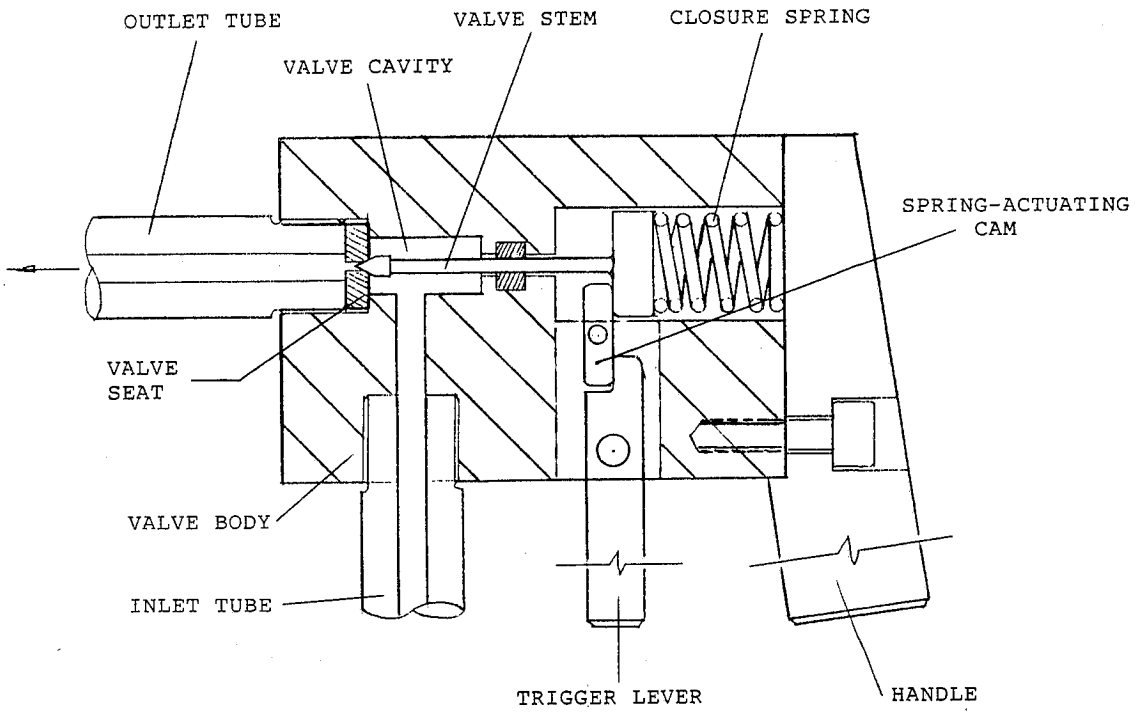

Fig. 5 A Manually-Operated Closure Valve of Conventional Design

Fluidyne's ultra-light manual closure valves have an outlet port of 1.8 to 2.0 mm (0.070 to 0.080 inches) in diameter and therefore are more suited for low-flow operations. For high-flow operations, Fluidyne developed another family of valves in which a pilot passage was added into the valve body to aid the valve operation in a way similar to that of Fluidyne's manually-operated dump valve. These valves are still under development but the prototypes have shown that such pilot-operated high-pressure closure valves will be reliable and easy to use, and will have high flow and pressure capabilities without hand fatigue problems. One version of these valves has been incorporated into a dual-valve waterjet lance that requires both hands from the operator in order to function, which can be a desirable safety feature.

5.0 PRESSURE REGULATORS

A fluid pressure regulator is a device commonly used in fluid systems to avoid over pressurization and to maintain a desired system pressure. Although there are many types, a fluid pressure regulator functions basically as a fast-actuating on-off valve capable of sensing the occurrence of over pressurization and letting out a certain portion of fluid to restore the desired system pressure.

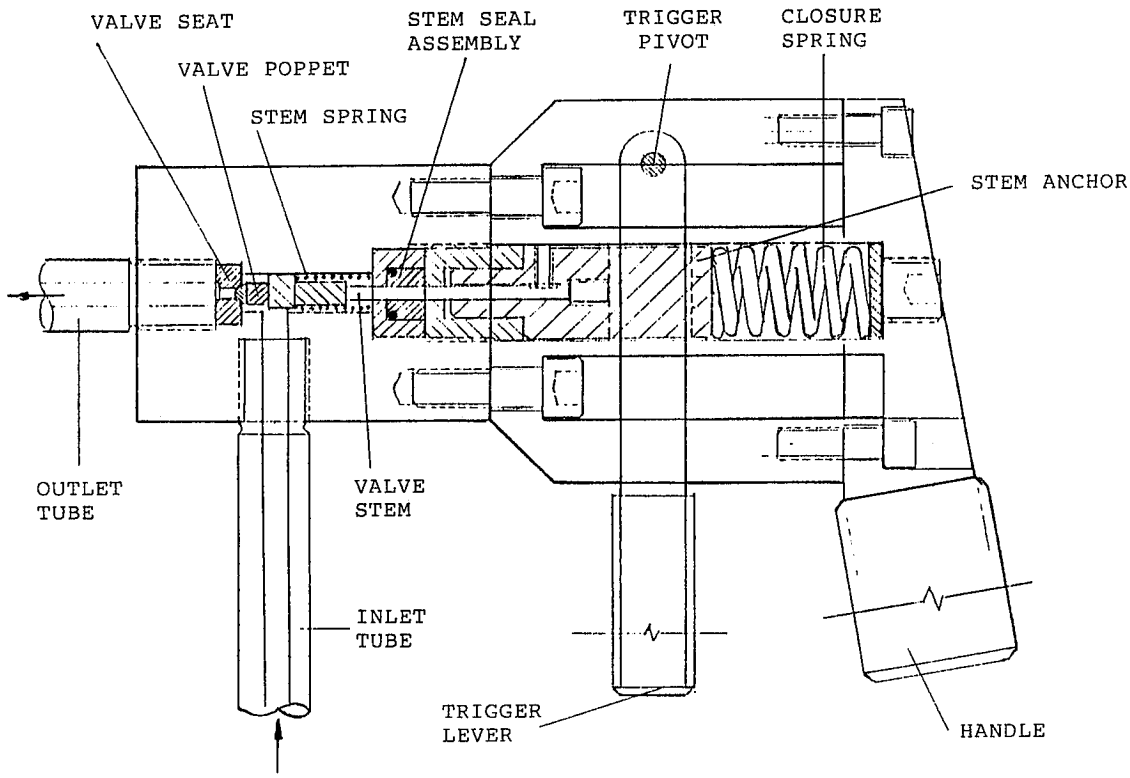

Fig. 6 Fluidyne's Manually-Operated Closure Valve

The selection of suitable pressure regulators is significantly limited when the system fluid is incompressible, such as water and oil, and is at very high pressures. The reason is that partial opening of an outlet port, commonly applied in pressure regulators for gases, cannot be applied easily due to severe erosion problems.

In waterjetting operations, pressure regulating valves are generally used in conjunction with crankshaft pumps. These valves are mostly spring operated involving a spring-loaded plunger moving up and down in accordance with the fluid pressure fluctuations inside the valve cavity to open and to close a dump port. Very stout springs are used in high-pressure systems and therefore such pressure regulators are not capable of sensing small pressure changes. When waterjet lances are deployed downstream from a conventional pressure regulator, the valve plunger is subject to constant pounding against the valve seat. Thus, both valve plunger and valve seat of such pressure regulators have reliability problem as well. Replacing the plunger spring with a gas cylinder will improve the regulator's sensitivity somewhat but will not solve the reliability problem.

Fluidyne recognized the unique nature of incompressible fluids at high pressures such that a pressure-regulating outlet port must be either fully open or fully closed; partial opening of an outlet port will not work. Fluidyne proceeded to develop pressure regulators that have improved pressure-sensing capabilities and component reliability. The basic design of these pressure regulators is very similar to that of Fluidyne's air-operated on-off valves, having a

unique valve poppet-valve stem arrangement that separates the two components to provide independent fluid actions and yet connects the two to perform the valving task in unison. In Fluidyne's on-off valves, the valve stem is deliberately made small to minimize the force required from an actuator. In pressure regulators, the valve stem is desirably to be larger so as to increase its pressure-sensing capability. In most cases, a single outlet port is sufficient as the ball poppet can handle high-frequency operations, particularly when the valve seat is equipped with a durable orifice of precise size. In other cases, Fluidyne elected to provide multiple outlet ports and multiple corresponding valve poppets that are strung together axially to provide an orderly, sequential operation. A sketch of this patent-pending design is presented in Figure 7, which does not show the pneumatic cylinder situated on the top to serve as a sensitive spring. As shown in this sketch, the up or down movement of the valve stem will result in opening or closing of one or more outlet ports of different sizes, thus letting out different amount of system fluid depending on the extent of over pressurization inside the system. Therefore, a pressure regulator of this design will have high sensitivity and wide range of pressure capability.

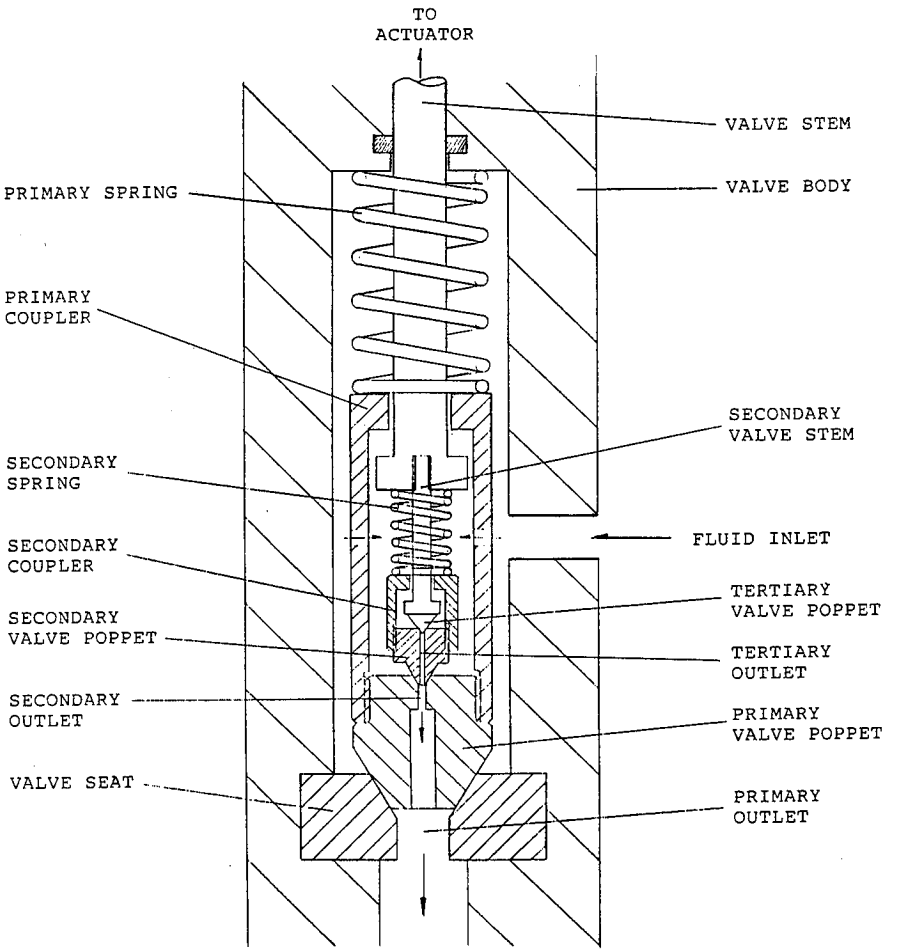

Fig. 7 Fluidyne's Multiple-Outlet Fluid Pressure Regulator

6.0 UNLOADING, FLOW-DIVERSION AND OTHER VALVES

The internal valving mechanisms developed by Fluidyne can be employed in valves to serve some other purposes, such as fast unloading of pressurized fluids or diversion of fluid flow in a system. Such tasks are commonly involved in waterjetting operations. For example, unloading valves are needed when multiple jet lances equipped with closure valve are used in conjunction with a crankshaft pump system. Flow restricting valves are highly desired when multiple jet lances equipped with dump valve are used with a crankshaft pump. Flow diversion valves are needed when pressurized fluid must be routed instantly and remotely from one outlet to another. Fluidyne's newly developed valve design can be applied to all these valve functions. Further, Fluidyne's multiple-port valve design can be used to provide instant on-off valves for handling incompressible fluids at high pressure and/or high flow rates. The ability of such valves to let out or shut off pressurized fluids slowly and in a controlled manner will greatly lessen the shock and "water hammer" effect that are commonly associated with the operation of conventional one-stage on-off valves. Such fluid-induced shocks are known to cause damage to system components situated both upstream and downstream of an on-off valve. In waterjetting systems, high-pressure hoses and pump parts have been known to be damaged by the operation of closure valves.

Fluidyne is in the process of bringing out these valves to the users. Some of them are already being used on job sites; others are being tested in the field. Still others are not yet out of laboratory. Figure 8 presents a photograph of Fluidyne's ultra-light waterjet lance equipped with a manual closure valve. Figure 9 presents a photograph of a waterjet lance equipped with a manual dump valve. Figure 10 presents a photograph of Fluidyne's air-operated instant on-off valve. And Figure 11 presents a photograph of Fluidyne's air-operated pressure regulator for waterjetting operations.

7.0 CONCLUSION

Flow control valves are vital to the growth of high-pressure waterjet technology. It is the hope of the author that some progress has been made in providing waterjet system users with valves of improved performance and reliability. This effort will be continued in order to bring out even better valves in the future.

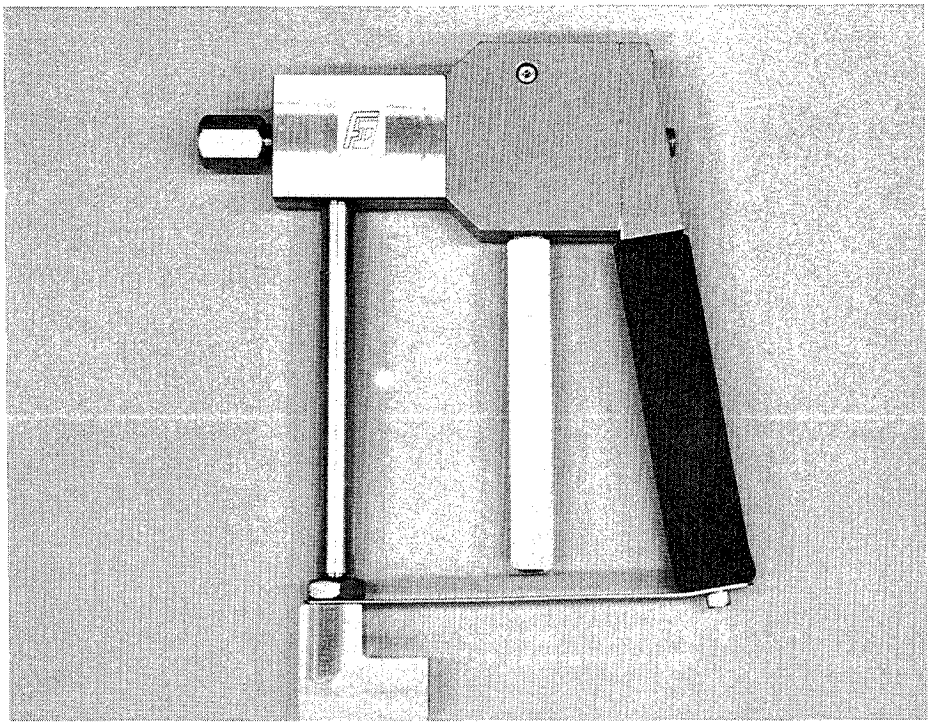

Fig. 8 Fluidyne's Hand-Operated Closure Valve for Waterjetting Applications at Pressures up to 35,000 psi

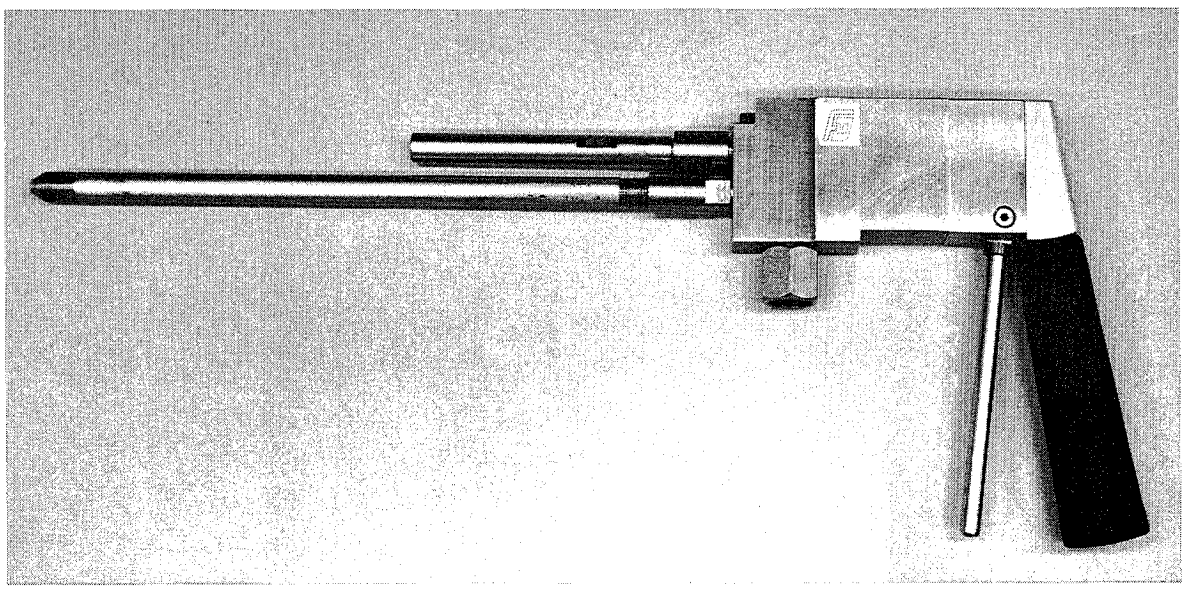

Fig. 9 Fluidyne's Hand-Operated Dump Valve for Waterjetting Applications at Pressures up to 30,000 psi

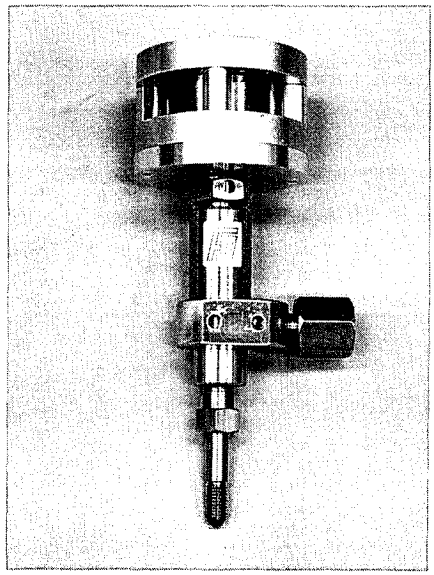

Fig. 10 Fluidyne's Air-Operated On-Off Valve for Waterjetting Applications at Pressures up to 60,000 psi

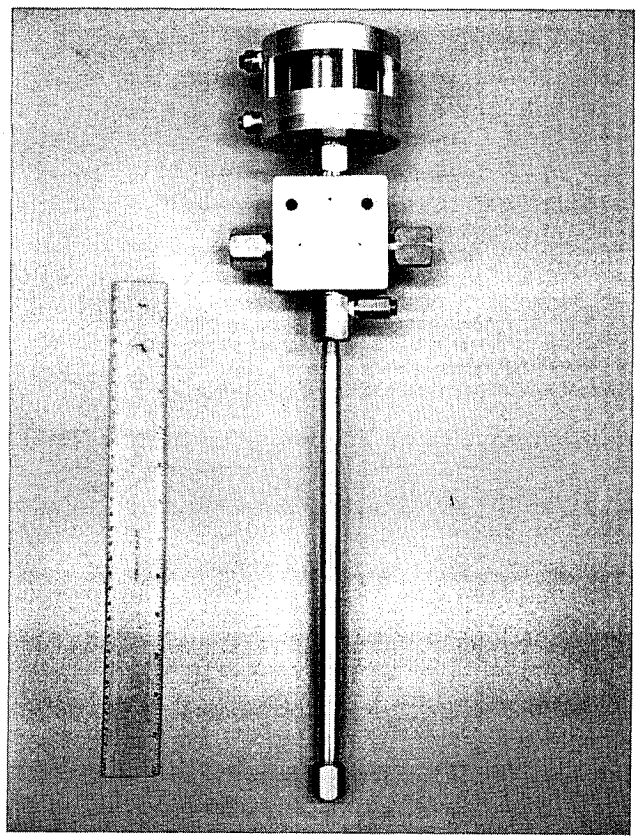

Fig. 11 Fluidyne's Air-Operated Pressure Regulator for Waterjetting Applications

6th American Water Jet Conference
August 24 - 27, 1991: Houston, Texas

Paper 44

Application of New Rotary Water Jet Concrete Demolition Method (CALM JET METHOD)

T. Sakamoto, T. Isobe, M. Arai
Kajima Corporation
Tokyo, Japan

ABSTRACT

Rotary water jet technology has been widely used for the demolition of concrete structures. As reported at the 5th AWJTC, the authors have commercialized highly efficient rotary water jet technology which used a new type of nozzle and swivel. Moreover, a new system for reviewing buildings and other structures was developed based on this technology. This report outlines the favorable results which were obtained by applying the system to several structures.

Organized and Sponsored by the Water Jet Technology Association.

6th American Water Jet Conference
August 24 - 27, 1991: Houston, Texas

HYDRODEMOLITION SYSTEM USING 600 HP AT 20,000 PSI

SUBMITTED BY

JOHN A. TURNBULL
NLB CORPORATION
WIXOM, MICHIGAN USA

ABSTRACT

The infrastructure of the United States is deteriorating so rapidly, that this may require a major national program to correct. The nation's bridges and parking structures are in serious need of repair. The water jetting industry is participating in this program through hydrodemolition of the existing deteriorated concrete, prior to reconstruction. This paper will review the technical requirements of this industry and illustrate the techniques with a review of state-of-the-art equipment, systems using 600 HP at 20,000 psi water pressure.

Organized and Sponsored by the Water Jet Technology Association.

1.0 INTRODUCTION

Presently 220,000 bridges or 38% of our nation's bridges are considered substandard, not to mention the thousands of parking decks in need of rehabilitation. As a result of this crisis, the owners of these structures are searching for more effective replacement materials and removal methods that do not create additional structural damage, or remove excessive amounts of sound concrete.

More and more of these owners are utilizing hydrodemolition as the proven method for removing deteriorated concrete on a high production basis.

Hydrodemolition also creates an excellent bonding surface and washes away entrained chlorides from contaminated concrete.

2.0 HYDRODEMOLITION

Concrete, as a construction material, is a relatively porous product. Hydrodemolition (Hydro-Blasting, Hydro-Jetting) uses concrete's porous property to its advantage during removal operations. High pressure water jets remove concrete by two separate mechanisms:

1. Direct Impact on Surface

2. Pressurization of Cracks

The hydrodemolition process can provide selective removal of concrete by its flexibility to control the amount of released energy. The equipment is designed to remove concrete to a prescribed and controlled depth.

Deteriorated Concrete Removal:

With deteriorated, delaminated, or spalled concrete, the high pressure water stream takes the path of least resistance. In other words, the water stream finds a greater resistance with sound concrete and a lesser resistance to debonded, unsound concrete.

Sound Concrete Removal:

In sound concrete the high pressure water stream enters the concrete through pours and cracks and starts breaking up any component in the concrete that has the least resistance to the water stream. Generally, the concrete components with the least resistance to the water jet stream, are the cement and sand (mortar paste).

In the typical concrete deck that has been hydrodemolished you will find:

1. The rebar intact and descaled - the water jet cleans the embedded rebar removing the surrounding concrete and weakly bonded corrosion scale

2. Aggregate intact and washed due to concrete mortar paste removal

As you can see, resistance or the lack of resistance in concrete, is the key to success of hydrodemolition. But, not all concrete offers the same resistance. So how do we size and calibrate a hydrodemolition system for maximum productivity?

First, a ratio of 3.5 psi water pressure for every 1 psi compressive strength of concrete is used which is based on the results of many hydrodemolition projects. So if the concrete core testing indicates nominal compressive strength of the concrete to be hydrodemolished is 5,000 psi, a water pressure of 17,500 psi would be selected. After water pressure selection, the traversing speed of the nozzle jet is set for minimum duration of the water stream, but still achieving the desired depth of concrete removal.

Once the water pressure and nozzle jet traversing speed has been established, experience has proven, to maximize production is to reduce water stream duration time. The most efficient way to reduce duration time is to increase the water stream thrust. Increasing thrust is achieved by increasing the gallons per minute of the pressure of the hydrodemolition system. When the thrust is increased, the duration time can be reduced proportionally, thus increasing production.

Perhaps the most profound effect that hydrodemolition has is the superior bonding surface created by the process.[1,2,3] Numerous "bond tests" have proven that overlay materials placed on a hydrodemolished surface regardless of removal depth or reinforcing bar exposure either meet or exceed standard bond strength regulations.

References

1. "Bond Tests on Reinforcement Exposed by Hydrodemolishing"
   Michigan Department of Transportation - Lansing MI
   Research Project 87TI-1269

2. "In-Place Bond Testing & Surface Preparation of Concrete"
   Kal Hindo - NTH Consultants - Farmington Hills, MI
   ACI - Concrete International April 1990

3. "New Bond Testing Method Developed"
   Claus G. Peterson - Germann Instruments Inc - Chicago IL
   IACRS Concrete Repair Bulletin - September 1990

3.0 SUMMARY

Owners of suspended structures are quickly realizing that hydrodemolition is the only method available today that can guarantee removal of deteriorated concrete, while at the same time minimizing sound concrete removal, not to mention the superior bond surface, and elimination of entrained chlorides in the remaining surface area.

These are all benefits that mechanical impact methods cannot provide. Additional cost savings are also realized with hydrodemolition in the forms of low replacement volumes of overlay material, reduced manpower and virtual elimination of secondary damage created by mechanical impact equipment.

Considering the overwhelming number of suspended structures in need of major repair, possibly the biggest benefit of hydrodemolition is the drastic reduction in the time it takes to remove concrete with high pressure water,in comparison to mechanical methods. Hydrodemolition can fractionalize the time it takes to rehabilitate a structure, enabling greater numbers of structures to be rehabed in any given construction season. Additionally, reduced reconstruction time assures owners of suspended structures, minimum inconvenience to their users and in certain cases a rapid return to maximum revenues.

The above mentioned features and benefits are being realized with every project that specifies the use of hydrodemolition. As a result of this, hydrodemolition is an industry that has a lasting place in a constantly growing market.

HYDRODEMOLITION ROBOT

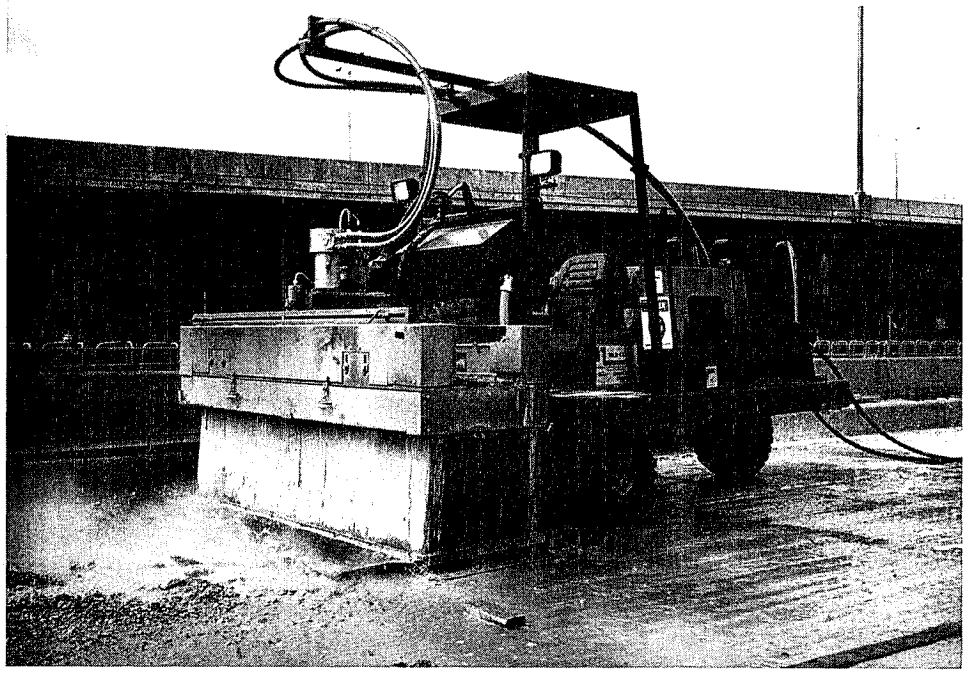

HIGH PRESSURE WATER JET TRAVERSES IN THE LONGITUDINAL DIRECTION UNTIL DESIRED DEPTH IS ACHIEVED. WHEN DESIRED REMOVAL DEPTH IS FOUND, THE ROBOT MOVES THE LATITUDINAL DIRECTION TO START THE PROCESS OVER AGAIN. DURATION TIME OF THE WATER JET AT A PRESET PSI AND GPM WILL DETERMINE THE VOLUME OF CONCRETE REMOVED.

Picture Courtesy of NLB Corp.

HIGH PRESSURE PUMP

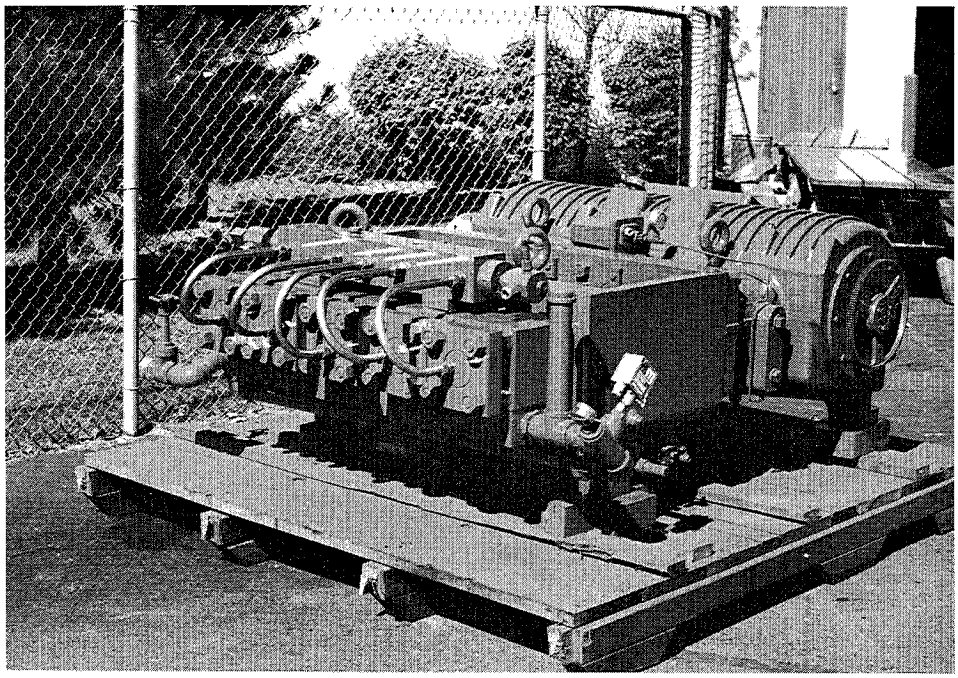

DELIVERS NECESSARY WATER PRESSURE AND GALLONS PER MINUTE TO THE ROBOT'S WATERJET NOZZLE.

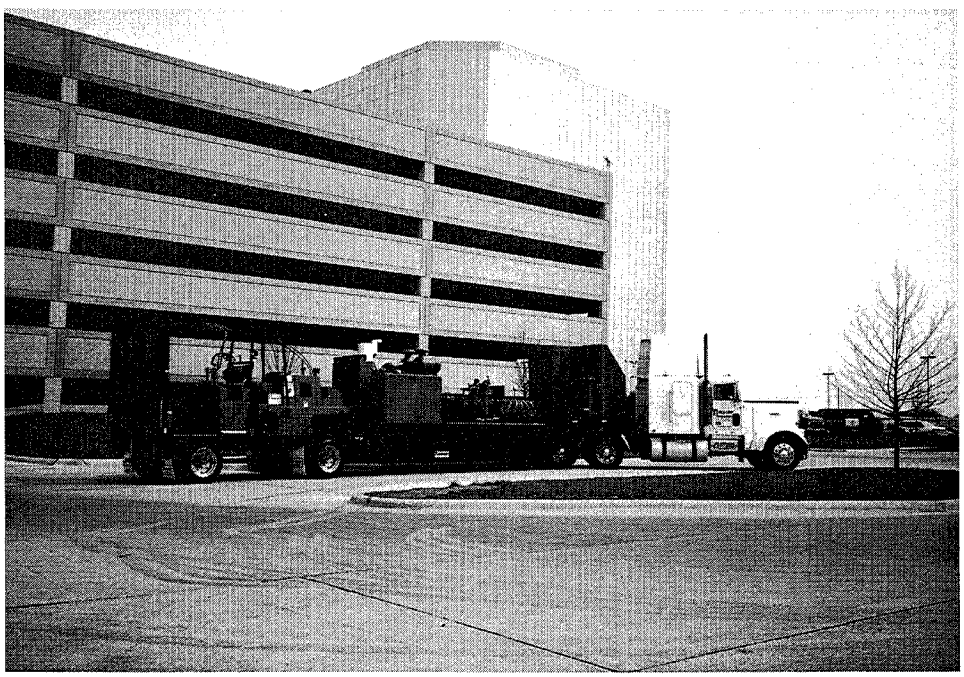

SINGLE OR MULTIPLE PUMPS CAN BE CONNECTED TO 1 ROBOT TO INCREASE THE GALLONS PER MINUTE. ONCE THE PSI OF WATER NECESSARY TO CUT CONCRETE IS REACHED, THE MORE GPM OF WATER PUMPED, THE MORE PRODUCTIVE THE SYSTEM BECOMES.

Pictures Courtesy of NLB Corp.

SPIN JETS®

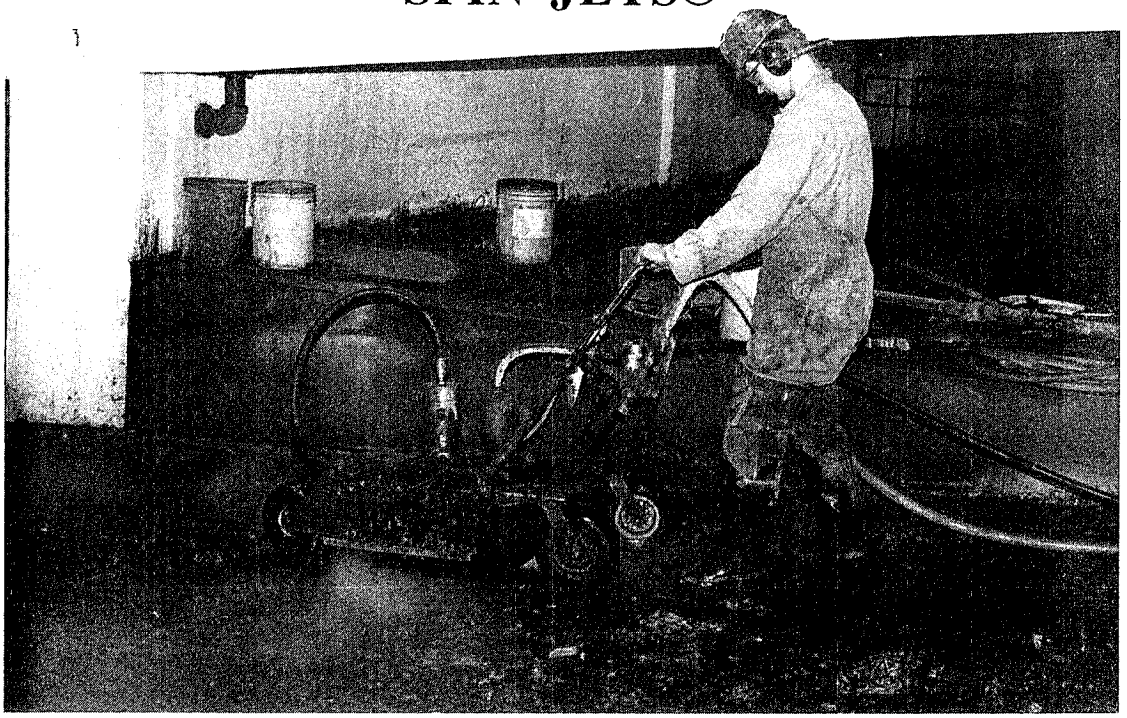

COLD TAR MEMBRANE IS REMOVED WITH 15,000 PSI AT 18 GPM AT A PRODUCTION RATE OF 480 SQUARE FEET PER HOUR, USING A SPIN JET®.

URATHANE MEMBRANE REMOVED WITH 18,000 PSI AT 14 GPM AT A RATE OF 900 SQUARE FEET PER HOUR, USING A SPIN JET®.

PAINT STRIPES, GREASE, AND NUMEROUS OTHER COATINGS ARE REMOVED WITH HIGH PRESSURE WATER AND ROTATIONAL JETS.

Pictures Courtesy of NLB Corp.
SPIN JET® is a registered trade mark of NLB Corp.

HAND LANCE

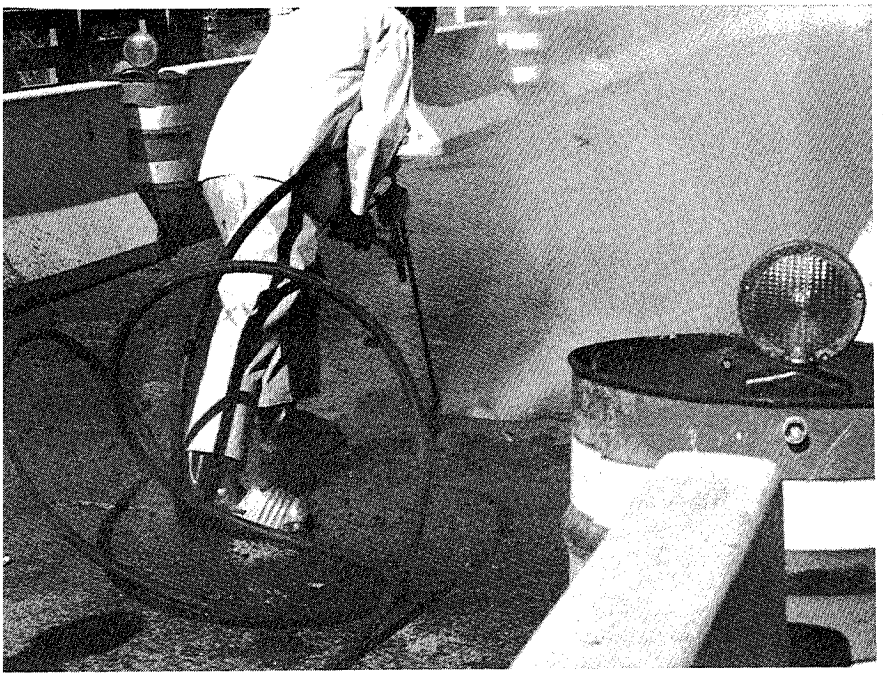

HAND LANCES CAN BE USED FOR A VARIETY OF CONSTRUCTION TASKS SUCH AS GENERAL CLEAN-UP, PAINT REMOVAL, MEMBRANE REMOVAL, EXPANSION JOINT COMPOSITE REMOVAL AND CONCRETE AND GUNITE REMOVAL.

CONCRETE BEING REMOVED AT 20,000 PSI

HAND LANCES CAN BE OPERATED AT VARIED PRESSURES WHILE INCORPORATING VERSATILITY TO THE CONTRACTOR'S NEEDS.

DESCALING OF REBAR AT 10,000 PSI

Pictures Courtesy of NLB Corp.

6th American Water Jet Conference
August 24 - 27, 1991: Houston, Texas Paper 46

PRACTICAL APPLICATION OF PORTABLE ULTRA HIGH WATER PRESSURE JET CUTTING AND JET BLASTING EQUIPMENT AND TECHNOLOGY

W. Hall Jr.
Jet Edge, Inc.
Minneapolis, Minnesota

ABSTRACT

Many factors influence the growing acceptance of ultra high pressure (UHP) portable water jetting equipment and technology as a practical, cost effective method to solve many problems in a wide variety of applications.

These influences include:

1. evolution of rehabilitation and repair specifications and criteria allowing the practical application of new technology
2. improved reliability of equipment
3. improved equipment availability
4. enhanced equipment design, resulting in simplified operation and maintenance
5. development of new attachments to address a growing number of applications
6. acceptance of UHP technology as a practical, cost effective tool and method for industry and contractors

The focus of the paper is to review existing accepted mobile UHP applications, discuss established trends in acceptance of applications, and project what applications are expected to be successfully addressed in the near future. A model will be constructed defining mobile UHP applications in four categories:

1. coating removal and surface preparation
2. portable abrasivejet cutting
3. industrial cleaning
4. hydrodemolition

Each category will be described and discussed, and the application and UHP technology will be compared to:

1. conventional, "accepted" methods of process
2. "low pressure" waterjet methods
3. other new, novel technologies

Organized and Sponsored by the Water Jet Technology Association.

6th American Water Jet Conference
August 24 - 27, 1991: Houston, Texas

Paper 47

SELF-ROTATING NOZZLE HEADS

John E. Wolgamott and Gerald P. Zink
StoneAge, Inc.
Durango, Colorado U.S.A.

ABSTRACT

Industrial waterblast cleaning is being increasingly done with rotary jets. Their use has eliminated many difficult and dangerous operations. They are effective on hard deposits and efficient for wide coverage. Self-powered nozzle heads are the tool of choice in a variety of applications. Many of these tools are recent developments and some are now capable of 140 MPa (20,000 psi) operation. Their adaptability to mechanized cleaning results in safe, productive operations. This paper describes the operating principles and types of designs currently available. Several successful applications are described.

Organized and Sponsored by the Water Jet Technology Association.

1.0 INTRODUCTION

Self-rotating nozzle heads are a relatively new development. The earliest designs were low pressure tank cleaners. They used large volumes of water and were primarily rinsing tools. As rotary seals were improved, the operating pressures increased, making them useful for tougher jobs and they became widely accepted tools. Currently, models are available that operate at 140 MPa (20,000 psi) capable of cutting very hard deposits.

Waterblast cleaning is faster and easier with rotary jets. They use hard hitting needle type nozzles instead of the fan type nozzles. Needle type nozzles focus the jets power in a small area. This enables them to penetrate tough materials and be effective at large standoff distances. Uniform, full surface coverage is quickly achieved by rotating the jets. The pump is better utilized because the jets are always covering new area.

This can make a dramatic difference. A good example is in pipeline cleaning. A pair of rotating jets can achieve more complete coverage and less streaking than a non-rotating mole head with a dozen jets. The two rotating jets will be larger and more powerful than the dozen smaller jets. For a given pump size the more jets used, the smaller and weaker each jet becomes. Two nozzles of six gpm each will have more penetrating power than twelve nozzles of one gpm each.

The distinction between powered and self-rotating nozzle heads is significant. They each have their advantages and disadvantages. In general, the self-powered tools are simpler, more compact, lighter weight and less expensive. They require no separate power source or extra supply hoses to operate. However, they are more limited in nozzle head design and have less control over rotation speed.

Manual waterblasting methods are increasingly being replaced by mechanically assisted tools. Rotating nozzle heads have made much of this possible. With further improvements in speed control technology the self-rotating heads will play an even larger part. In many applications, their usefulness is just being discovered.

2.0 DESCRIPTION

There are two major types of rotary nozzle heads; single axis rotation (2D or two-dimensional) and dual axis rotation (three dimensional or 3D). Most self-rotating nozzle heads use the jet reaction force to power rotation. Many also employ a mechanism for limiting the rotation speed. A critical element in all designs is the high pressure seal.

The 2D tools are the simplest type and the most widely used. They have one axis of rotation so only one high pressure seal is required. There are many styles and capacities available from several manufactures. They are used in a variety of applications, over a wide range of operating pressures and flow rates.

The 3D has two axes of rotation and usually some means of gearing between them. A

certain number of rotations on one axis will result in a set number of rotations of the other axis. This results in omnidirectional coverage, with the jet paths spaced over an entire volume. This is especially useful in tank or vessel cleaning. The heads may be used on rigid lances, telescopic arms or suspended on flexible hoses. The majority of these tools are designed for low to medium pressure, and high flow applications.

2.1 Reaction Force

Jet reaction is used to propel rotation because it is simple. There are a minimum of mechanical components to deal with. It is only necessary to design the nozzle head so that the reaction force will cause the head to turn. The force available is proportional to the operating pressure and the flow rate. The resulting torque is also dependent on the jet nozzle location and angle from the axis of rotation. **Figure 1** is a drawing of a self-rotating nozzle head showing these components. These relationships are accurately described by the following equations:

METRIC: (1) **Thrust** (N) = 0.738 * Sqrt **P** (MPa) * **Q** (liters/min)
(2) **Torque** (N-m) = Thrust (N) * **R** (meters) * sin **Ø**

ENGLISH: (1') **Thrust** (lbf) = 0.0522 * Sqrt **P** (psi) * **Q** (gpm)
(2') **Torque** (in-lbf) = Thrust (lbf) * **R** (in) * sin **Ø**

Where: **P** = the pressure at the nozzle
Q = the discharge flow rate
R = the distance the jet is offset from the axis of rotation
Ø = the angle of the jet measured from the axis

Depending on the swivel design, the amount of torque required can be from less than 1N-m (9 in-lb) to more than 11 N-m (100 in-lb).

Only a very small amount of the jet's velocity is used to provide rotary power. Typically this is less than 75 Watts (0.1 Hp). This power is available regardless of what the jet encounters after it leaves the nozzle. It can strike a surface or shoot into the air without affecting the torque.

2.2 Speed Control

Most self-rotating tools use some means of speed control. Without this the nozzles would spin to extremely high speeds and be less effective. Jet penetration and cleaning effectiveness are dependent on the traverse velocity of the jet. Slower speeds will result in more dwell time and greater penetration. Higher speeds provide fast and uniform surface coverage. Too fast however, and the jet deteriorates due to sideways movement through the air. It is important therefore to choose the correct rotation speed for the application.

In all swivels there is some inherent drag or braking due to seal and bearing friction. This is a fixed amount however and is not proportional to speed. Therefore this drag is not capable of providing speed control. It simply determines the minimum torque required to start rotation. If any additional torque is applied the swivel will "run away". A true governor mechanism must develop increased resistance with greater speed.

Again, all swivels have this to some degree due to air friction. A spinning nozzle head will develop air resistance proportional to the cube of it's speed. However, depending on the head's shape and size, this will be extremely weak until very high speeds are reached.

Maximum control is obtained with an additional governor mechanism. Three types of governors currently used are: hydraulic pump, magnetic braking, and viscous shear. Each type has advantages for certain applications.

Hydraulic pumping through an orifice is very effective at low speed ranges (2 to 50 rpm). This design is most often used in slow turning, high volume cleaning. Several designs provide speed control by using an adjustable orifice size.

Braking action by viscous shear is useful in the mid-range speeds (25 to 800 rpm). A thick fluid fills the gap between rotating and stationary cylinders. The gap is very narrow and the fluid must shear to allow the cylinders to slip past each other. The mechanism can be quite compact and functional over a wide speed range.

Magnetic braking is effective in the higher speed ranges (1000 to 3000 rpm). This is probably the simplest design and easiest to maintain. It can be used directly or with reduction gearing for control at slow nozzle speeds.

A special design of self-rotating nozzle head is the turbine drive type. It does not use jet reaction force for rotation power. Instead it takes some of the pressure out of the flow to drive the turbine. Gear reduction is employed to achieve the necessary torque and speed.

2.3 High Pressure Seal

The two types of seals are; controlled leak and positive seal. The leak type is a close fitting bushing style. It is simple, economical and requires no maintenance. It is almost frictionless and therefore takes little power to rotate. The design does waste some power due to leakage however and is expensive to repair when worn. Current technology is limited to about 140 MPa (20 ksi), since the leak becomes excessive at higher pressures.

The positive seal type is more complicated. It uses a soft seal material with a close fitting backup support. This results in higher seal drag and requires more power to rotate. The seals are generally easy to replace and inexpensive. The design is more tolerant of dirty water but wears quickly at high rotation speeds. Practically any flow capacity can be accommodated.

3.0 APPLICATIONS

Self-rotating nozzle heads are used in a variety of waterblast applications. This includes manual as well as mechanized cleaning. The tool size and waterblast power used for manual applications is limited to what can be safely handled. Typically this limit is about 7 kg (15 lb) of mass and less than 75 kW (100 Hp). Mechanized cleaning

systems have no such limitations and can apply waterjet power in excess of 750 kW (1000 Hp). There are self-rotating nozzle heads successfully meeting all these needs.

3.1 Manual Shotgunning

For handheld waterblasting applications the tool must be small and lightweight. An example is shown in **Figures 2** and **3**. Typically these tools operate at 35 to 140 MPa (5 to 20 ksi) and 20 to 60 l/min (5 to 15 gpm). They use two or more forward pointing jets offset from the axis. The jets have small angles (5 to 15°) from straight ahead which creates the torque. A fast rotation is often preferred, 1000 rpm and above. This provides quick coverage and reduces streaking.

These rotary tools are replacing fan spray nozzles and straight jet cleaning in many applications. Developed in only the last few years, these are now probably the most common self-rotating tool.

3.2 Line Moleing

This category covers a wide range of applications. It can include 5 cm (2 in.) diameter process lines up to 1.5 m (5 ft) diameter sewer lines. The standard historic method was to build a nozzle head with several jets, 6 to 10 or more, depending on the pipe diameter. This would be run back-and -forth a few times and perhaps manually oscillated with great effort. Self-rotating nozzle heads have improved many of these operations. With fewer and harder hitting jets the cleaning is more effective. And with rotation the coverage is complete with just one pass. For maximum efficiency, the rotary tools are often used with centralizer skids to hold the nozzle head in the center of the line. Heads designed with back jets can also self-propel themselves through the line. Pulling rings can be attached for pulling the self-rotating tools when back jets are not practical.

One type of project is the cleaning of **underground pipelines**. Often these lines need to have internal corrosion and failed lining removed prior to rehabilitation. On a recent project self-rotating tools were used to remove the cement lining from a system of gas lines. These lines were 10 cm to 20 cm (4 in. to 8 in.) diameter and several miles in length. The heavy walled steel pipe had a cement lining approximately 1 cm (.4 in.) thick that needed to be removed so that a new plastic lining could be installed. Sections up to 400 meters (1200 ft) in length were cleaned in one pass. A cleaning rate of 1 m/min was obtained using 200 l/min (50 gpm) at up to 100 MPa (15 ksi).

Another application suited for self-rotating tools is **downhole well** cleaning. It can be used for opening up to the formation after cementing or for removing paraffin in producing wells. These rotating tools are used with coil tubing rigs for quick access and fast results. The tools work submerged, often at depths of several thousand feet. There are tools that can operate at 70 MPa (10 ksi) and handle 400 l/min (100 gpm).

The cleaning of **coke lines** (or coker tubes) in fossil fuel processing is a very common and difficult task. The buildup can be quite hard, the lines are often difficult to access and have lots of elbows. Concentrating the waterblast power of 80 l/min at 100 MPa (20 gpm at 15 ksi) into two slow rotating jets can be very effective. A typical tool is shown in **Figure 4**.

Another application for self-powered rotary nozzles is to clean commercial and agricultural **water wells**. The submerged well screens become clogged over time with scale and corrosion. Traditional methods of cleaning have relied on using a large quantity of acid to dissolve the buildup. It is a less than perfect method and is increasingly expensive. Slow turning jets can open up the screen mesh and unclog the gravel pack around the screens. Successful cleaning operations have used pressures of 35 to 70 MPa (5 to 10 ksi) and flow rates of 80 to 160 l/min (20 to 80 gpm). The jetting technique is effective both in horizontal (radial) and vertical wells. Inflow is improved and production capacity greatly increased.

3.3 Tanks and Vessels

The most common application for **3D nozzles** (two axis) is to clean the inside of large enclosures. These are storage tanks, reactor vessels, autoclaves, mixing vessels, distillation towers, etc. They often have agitator blades, mixing vanes or other obstructions inside. The 3D nozzles are most effective with high flows at medium pressures. They are usually left in one position for a period of time to allow the jets to work at their many angles. Two or three positions can clean a very complicated tank interior, and an accurate location of the 3D nozzle is not required. **Figure 6** shows a commonly used two axis rotating head.

In open vessels the **2D nozzle** (single axis) can be utilized effectively. By slowly traversing the nozzle along the tank centerline, the jets can be directed at the wall at all times. No waterblast power is wasted shooting in unnecessary directions. Nozzle extensions can be used to place the jets close to the tank wall and improve jet quality. By using angled jets and moving the tool, a 2D nozzle head can simulate the action of a 3D nozzle. This only works in more open vessels where the geometry allows it. **Figure 5** shows a 2D nozzle capable of 600 l/min and 70 MPa (150 gpm and 10 ksi).

3.4 Mechanized Cleaning

There are several reasons for mechanizing the waterblast cleaning process. It can be to allow for better control, improve safety, or apply greater amounts of power. The most common mechanized tool is the floor or **grate cleaner**. They eliminate the fatigue and tediousness associated with cleaning these surfaces by hand. Most of these are powered by air or hydraulics. The self-powered versions are simpler, less expensive, compact and easy to maneuver. An example is shown in **Figure 7**. Many custom cleaning applications can benefit from these same features.

4.0 CONCLUSIONS

Self-rotating nozzle heads are being applied successfully in a variety of waterblast cleaning applications. Improved safety and productivity are the primary results. Although not the answer for every job, they do offer significant advantages and can be used in many standard operations. A general lack of precise speed control and sensitivity to throughput power are the major drawbacks. There are several styles available with new types and improvements being made all the time. As the interest in mechanization intensifies the use of self-rotating nozzle heads will increase.

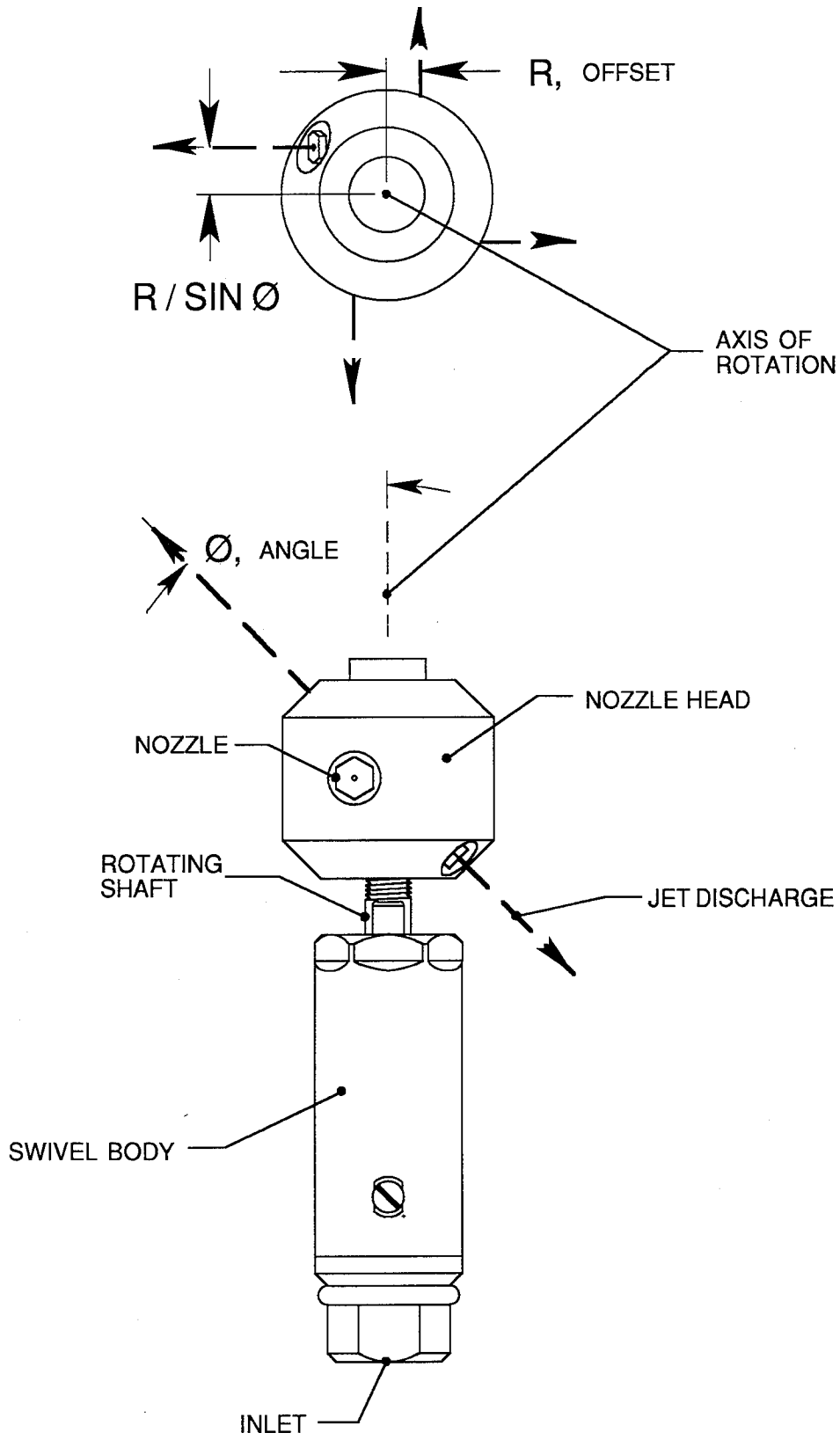

Figure 1. SELF - ROTATING NOZZLE HEAD

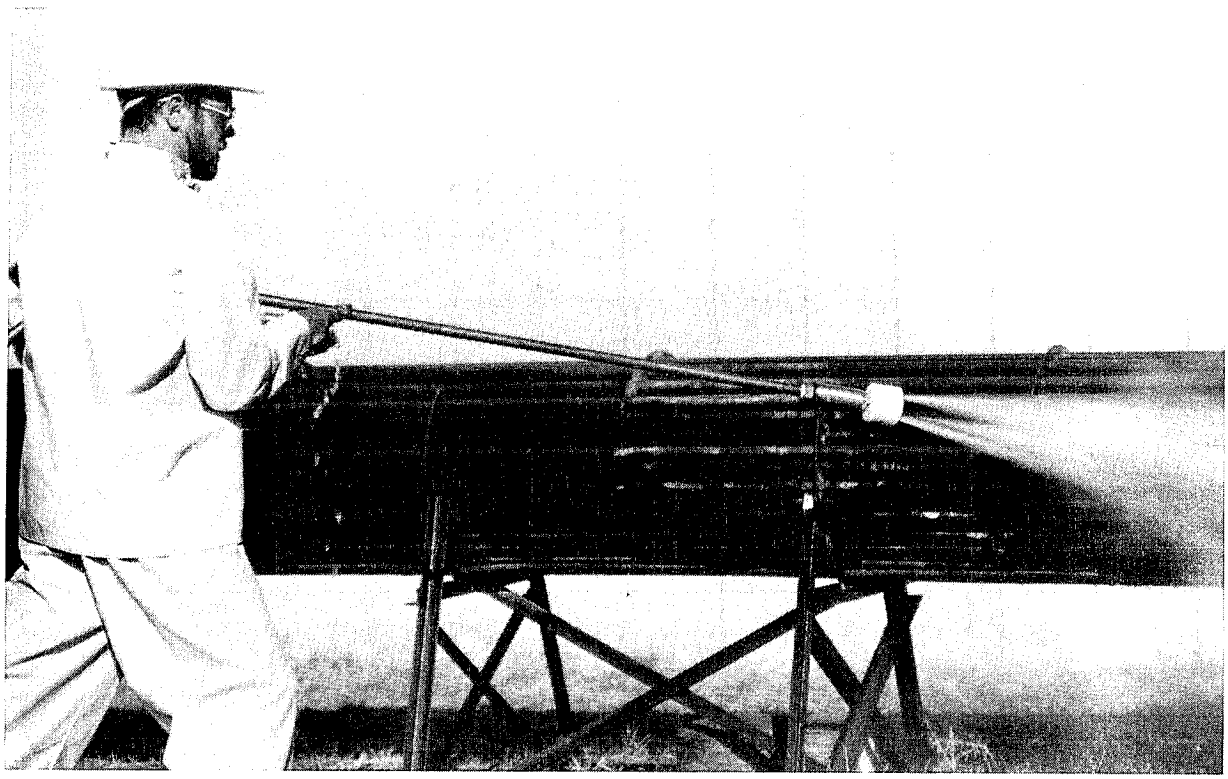

Figure 2. MANUAL SHOTGUN CLEANING

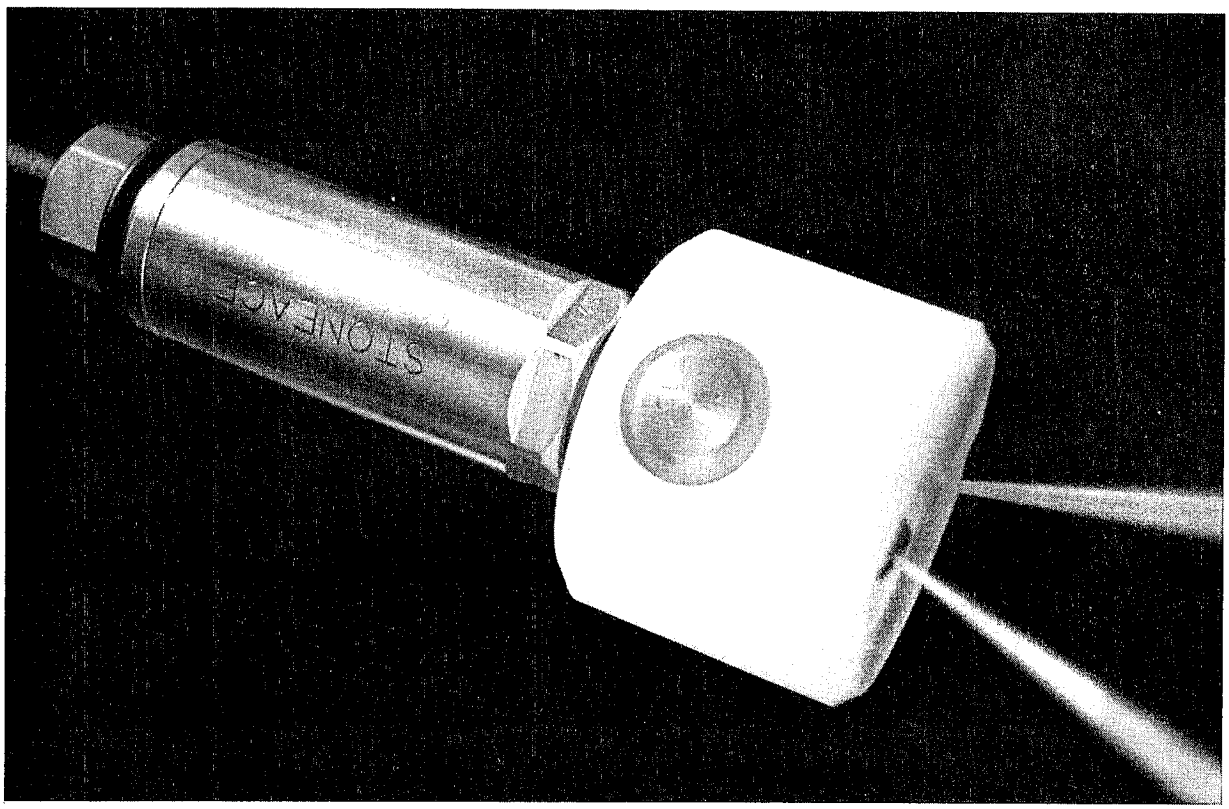

Figure 3. SELF-ROTATED NOZZLE HEAD

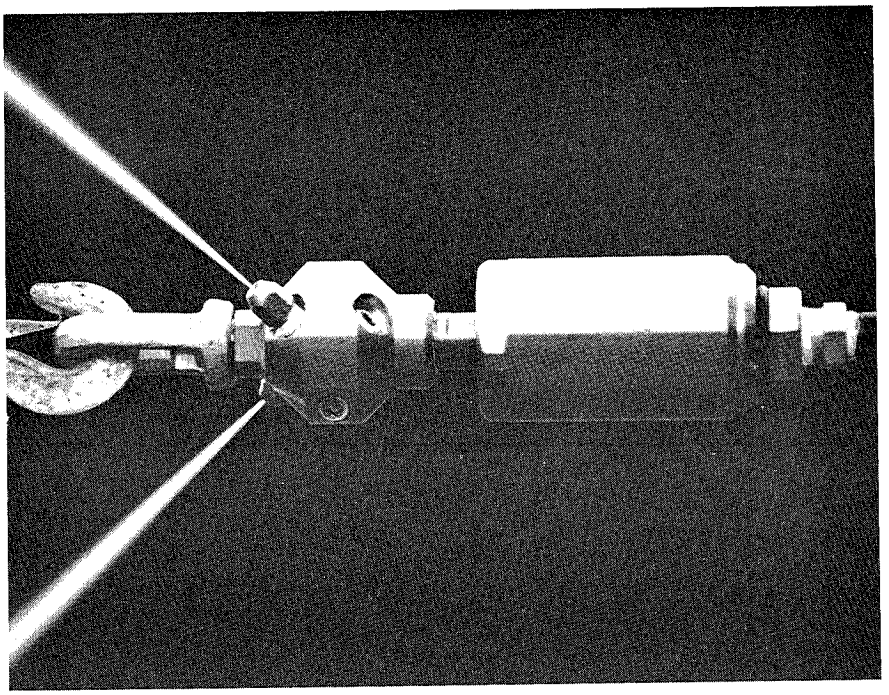

Figure 4. ROTARY NOZZLE FOR PIPE CLEANING

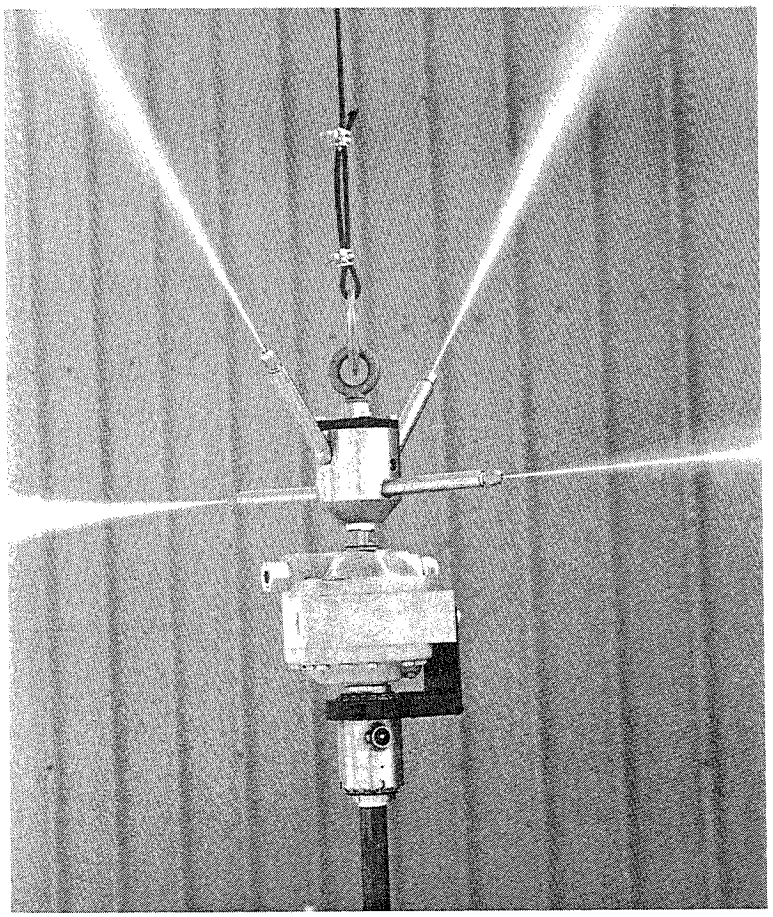

Figure 5. HIGH VOLUME NOZZLE FOR TANK CLEANING

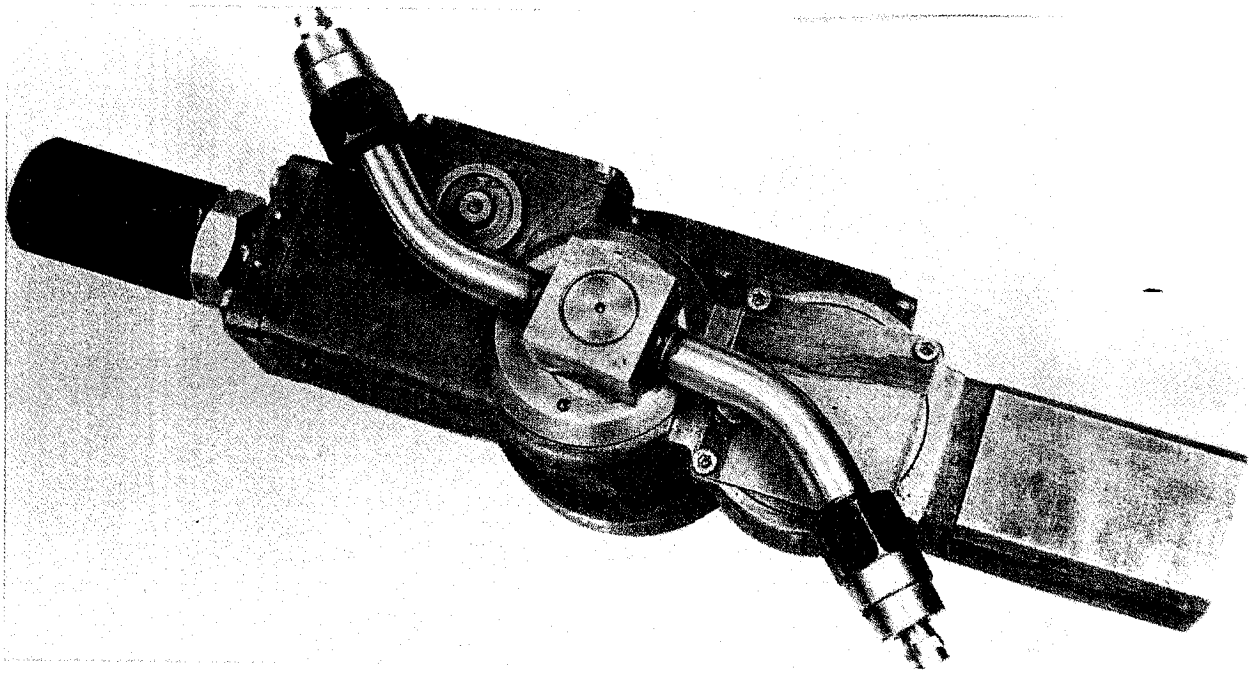

Figure 6. TWO AXIS ROTARY NOZZLE HEAD

Figure 7. SELF-ROTATING FLOOR CLEANER

6th American Water Jet Conference
August 24 - 27, 1991: Houston, Texas

Paper 48

6th American Water Jet Conference
August 24-27, 1991 Houston, Texas

RECENT DEVELOPMENTS IN THE HIGH PRESSURE WATERBLAST GUN

Michael T. Gracey
Hydro-Services
Missouri City, Texas

ABSTRACT

The high pressure waterblast gun and much of the water jetting equipment, came from services related to the Oil Industry. This paper traces some of the history of the hand held waterblast gun and discusses recent operational and safety developments. Future innovations are discussed that may include even higher pressures, safer guns, and space age technology.

Organized and Sponsored by the Water Jet Technology Association.

1.0 INTRODUCTION

Sometime in the 1950's, operators of water flood trucks used in the oil industry had the idea to wash their trucks with the 500 to 1500 psi produced by the positive displacement pumps onboard. The end of a piece of pipe could be flattened to form a fan spray for washdown operations. Later in the 1950's, brine trucks and kill trucks, with their triplex pumps capable of 2000 to 3000 psi, were used to blast away mud and salt after deliveries into remote areas of the oil patch. It was reported that a piece of pipe with a plug drilled for a nozzle, was used as a cleaning wand, therefore, the first waterblast gun was invented and looked something like FIGURE 1.

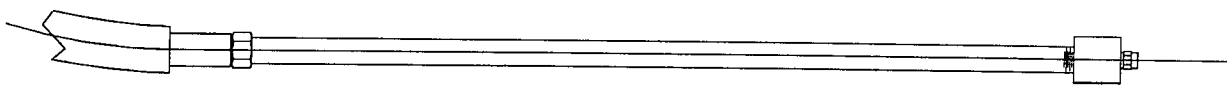

FIGURE 1
EARLY WASH WAND

The gunman would hold the piece of pipe and signal the operator to engage or disengage the pump for the washdown operation. Maybe the next improvement to the wand, was a handle welded to the pipe which helped the gunman control the gun as indicated in FIGURE 2.

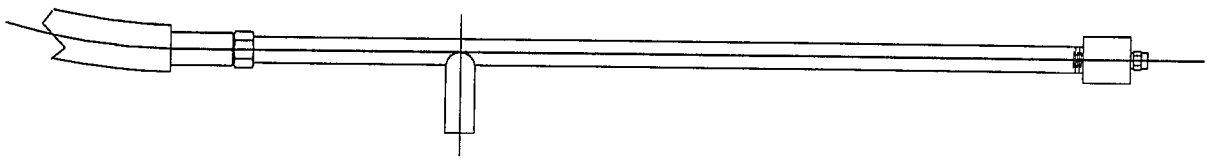

FIGURE 2
WASH WAND WITH HANDLE

The next known addition around 1963, was a needle valve to provide a measure of safety because now the control of the pressure was in the hands of the gunman, as shown in FIGURE 3.

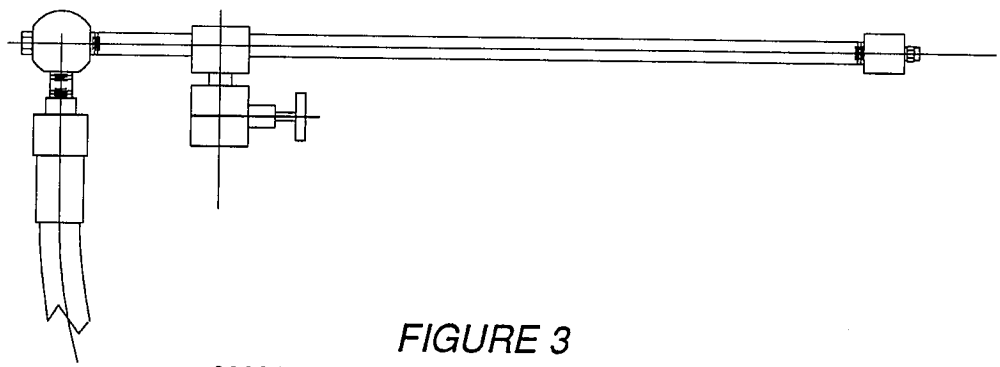

FIGURE 3
WAND WITH CONTROL VALVE

By 1966, the valve was protected somewhat as shown in FIGURE 4.

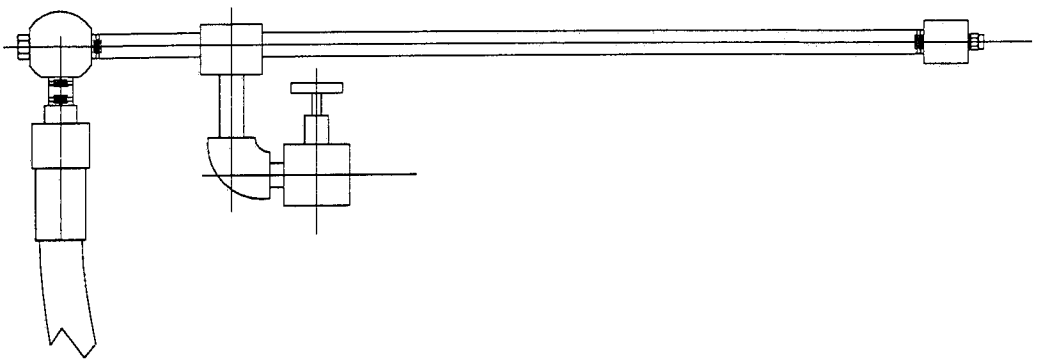

FIGURE 4
WAND WITH PROTECTED CONTROL VALVE

Meanwhile, KACY Manufacturing Co. Inc. probably had one of the earliest 10,000 psi dump style waterblast guns on the market, but it was very hard to hold the trigger. Some people even welded extensions on the trigger to help make it work. C.C.I. Pumps Inc. also had a version of the dump gun that reportedly did not work well. In 1967, Mr. Clem Mondy devised a dump style gun because there didn't seem to be one suitable for marketing with waterblast equipment. This gun proved to be lighter weight, more reliable, easier to hold and was undoubtedly the model for several companies in the evolving waterblast industry. In 1968, Mr. Jack Hinrichs patented an air control system as shown in FIGURE 5.

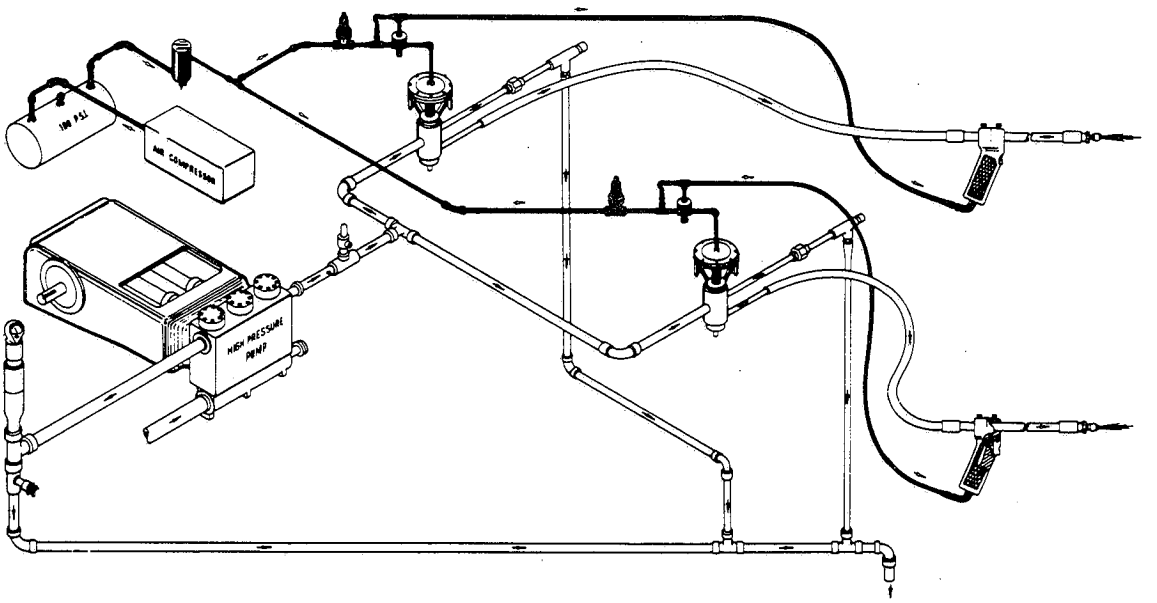

FIGURE 5
AIR CONTROL SYSTEM FOR MULTIPLE GUNS

An improvement to the dump gun was also patented in 1972 which added a double cam action for the trigger to make the trigger easier to hold. These ideas slowly developed into a number of gun styles and innovations such as shut-off style guns, unloader valves, remote control type systems, and eventually into ultra high pressure guns. This paper will explore a few of the many recent developments in the high pressure waterblast gun.

2.0 TYPE OF GUNS

High pressure waterblast guns have several categories that include "dump style guns", "shut-off style guns" and "air control guns". An example of each, respectively, are shown in FIGURE 6, FIGURE 7, and FIGURE 8.

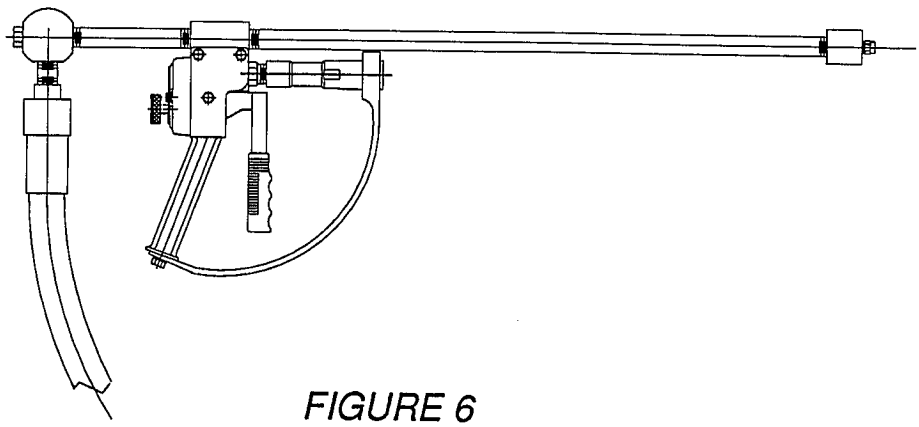

FIGURE 6
DUMP STYLE GUN

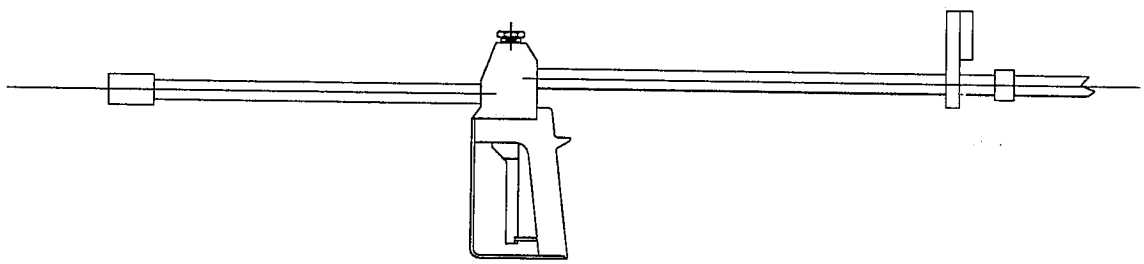

FIGURE 7
SHUT-OFF STYLE GUN

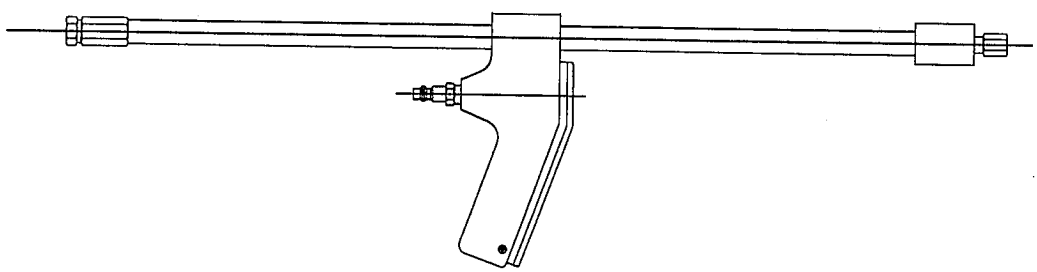

FIGURE 8
AIR CONTROL STYLE GUN

The dump style gun relieves the pressure in the system until the trigger is operated and is sometimes called a deadman valve. The shut-off gun normally holds pressure in the system and requires an unloader or pressure regulator at the pump to by-pass the flow from the pump. The air control gun has an air valve at the gun which operates a poppet valve and a by-pass valve (in some systems) so that the water is usually not furnished to the gun until the trigger is operated. The variations of the air control system include multiple gun operations and multiple stations as seen earlier in FIGURE 5.

In a discussion of waterblast guns, the foot operated version should be mentioned. Usually, the foot gun is similar to its companion hand gun. If a dump style hand gun is being used, it could follow that a dump style foot gun would be used also. An example of the various foot operated styles are shown in FIGURE 9, 10 and 11.

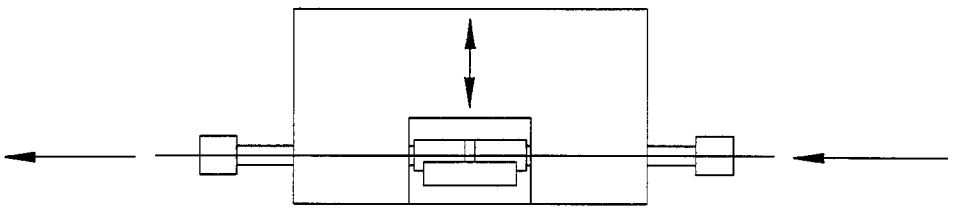

FIGURE 9
FOOT OPERATED SHUT-OFF STYLE GUN

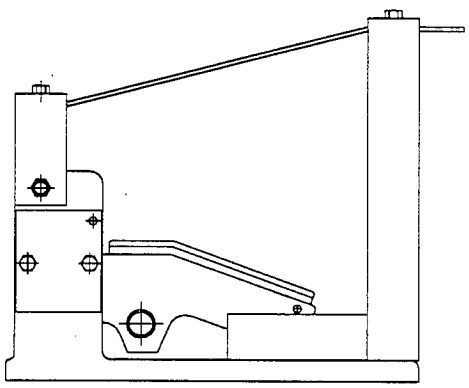

FIGURE 10
FOOT OPERATED AIR CONTROL GUN

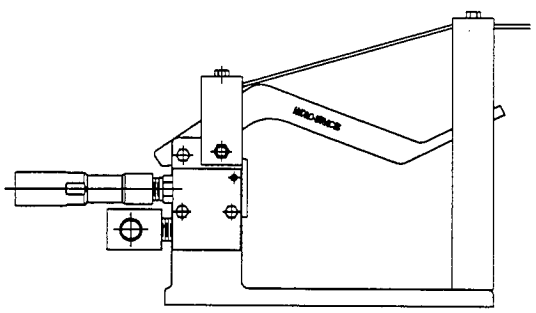

FIGURE 11
FOOT OPERATED DUMP GUN

Much of the waterblasting equipment is designed to operate at pressures up to 10,000 psi and a general rule has been that a gunman can hold about 10,000 psi at 10 gpm. This, of course, varies greatly with the size of the gunman. TABLE 1 shows the recommended maximum operating pressure by body weight and nozzle diameter. The formula used in this table is:

$$\text{PRESSURE} = \frac{\text{BODY WEIGHT}}{4.71 \times \text{DIAMETER SQUARED}}$$

The nozzle diameter relates to the flow produced at a given pressure, so therefore is proportional to the thrust that the gunman experiences. The major component in the thrust formula is the flow as indicated in:

$$\text{THRUST} = .05260 \times \text{FLOW} \times \text{SQUARE ROOT OF PRESSURE}$$

Table 1
Recommended Maximum Operating Pressure
(By Body Weight And Nozzle Diameter)

DIAMETER (Inches)

BODY WEIGHT (lbs)	1/32" 0.031	0.038	0.041	3/64" 0.047	0.054	1/16" 0.063	5/64" 0.078	3/32" 0.094	7/64" 0.109	1/8" 0.125
160	35,349	23,525	20,208	15,378	11,650	8,559	5,584	3,845	2,859	2,174
165	36,454	24,260	20,840	15,859	12,014	8,826	5,758	3,965	2,949	2,242
170	37,558	24,995	21,471	16,339	12,378	9,094	5,933	4,085	3,038	2,310
175	38,663	25,731	22,103	16,820	12,742	9,361	6,107	4,205	3,127	2,378
180	39,767	26,466	22,734	17,300	13,106	9,629	6,281	4,325	3,217	2,446
185	40,872	27,201	23,366	17,781	13,470	9,896	6,456	4,445	3,306	2,514
190	41,977	27,936	23,997	18,262	13,834	10,164	6,630	4,565	3,395	2,582
195	43,081	28,671	24,629	18,742	14,198	10,431	6,805	4,686	3,485	2,650
200	44,186	29,406	25,260	19,223	14,562	10,699	6,979	4,806	3,574	2,718
205	45,291	30,142	25,892	19,703	14,926	10,966	7,154	4,926	3,663	2,786
210	46,395	30,877	26,523	20,184	15,290	11,234	7,328	5,046	3,753	2,854
215	47,500	31,612	27,155	20,664	15,654	11,501	7,503	5,166	3,842	2,921
220	48,605	32,347	27,787	21,145	16,018	11,768	7,677	5,286	3,931	2,989
225	49,709	33,082	28,418	21,625	16,382	12,036	7,852	5,406	4,021	3,057
230	50,814	33,817	29,050	22,106	16,746	12,303	8,026	5,527	4,110	3,125
235	51,919	34,553	29,681	22,587	17,110	12,571	8,201	5,647	4,199	3,193
240	53,023	35,288	30,313	23,067	17,474	12,838	8,375	5,767	4,289	3,261
245	54,128	36,023	30,944	23,548	17,838	13,106	8,550	5,887	4,378	3,329
250	55,233	36,758	31,576	24,028	18,203	13,373	8,724	6,007	4,468	3,397
255	56,337	37,493	32,207	24,509	18,567	13,641	8,899	6,127	4,557	3,465
260	57,442	38,228	32,839	24,989	18,931	13,908	9,073	6,247	4,646	3,533
265	58,547	38,963	33,470	25,470	19,295	14,176	9,248	6,368	4,736	3,601

3.0 RECENT IMPROVEMENTS

Some of the waterblast guns in use today have not changed much in the last twenty years, but the most notable additions are trigger guards, safety catches, safety hose shrouds and secondary dumps. One of the first safety features to appear on the waterblast gun was the guard around the trigger as shown in FIGURE 12.

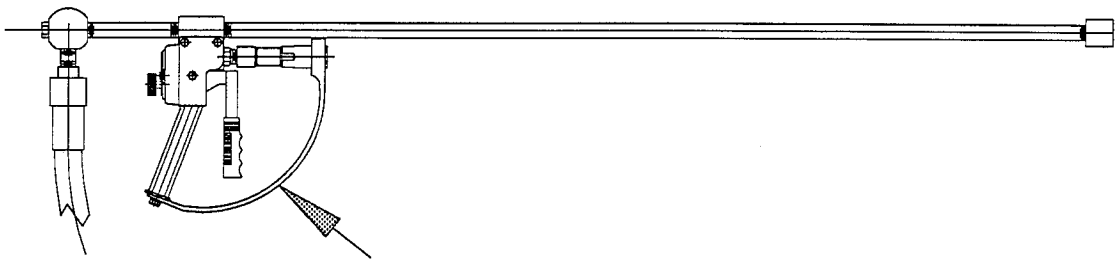

FIGURE 12
TRIGGER GUARD ON HAND GUN

More recently, safety catches were added to many of the guns on the market, but they didn't appear on the high pressure guns until the 1980's. An example of safety catches is shown in FIGURE 13.

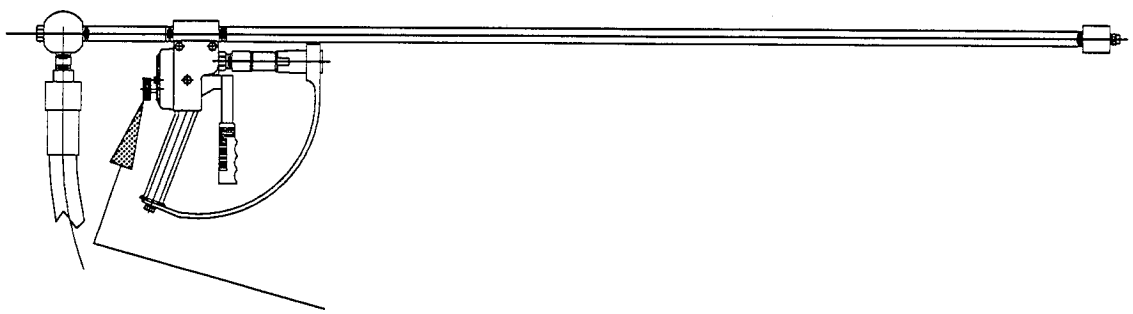

FIGURE 13
SAFETY CATCH TO KEEP TRIGGER FROM OPERATING

Some guns have exposed high pressure hose near the gunman, so the safety shroud, usually including a short whip hose, was developed in the 1970's and has been improved in many ways over the years. The most recent improvement to the safety shroud may be the use of Kevlar covered with a slick coating as indicated in FIGURE 14 to shield the gunman from a leak or rupture in the high pressure hose.

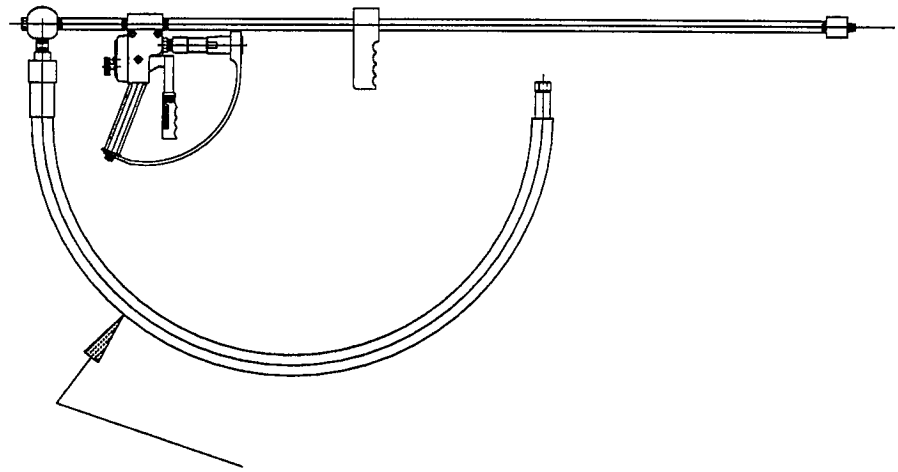

FIGURE 14
SAFETY SHROUD AND WHIP HOSE

The secondary dump and the two hand waterblast gun are not a new concept, but have become mandatory in some Petro-Chemical plants. The first known way to meet the requirement was to connect two dump style guns together; in case one gun did not dump, the other one was expected to operate correctly. This is illustrated in FIGURE 15.

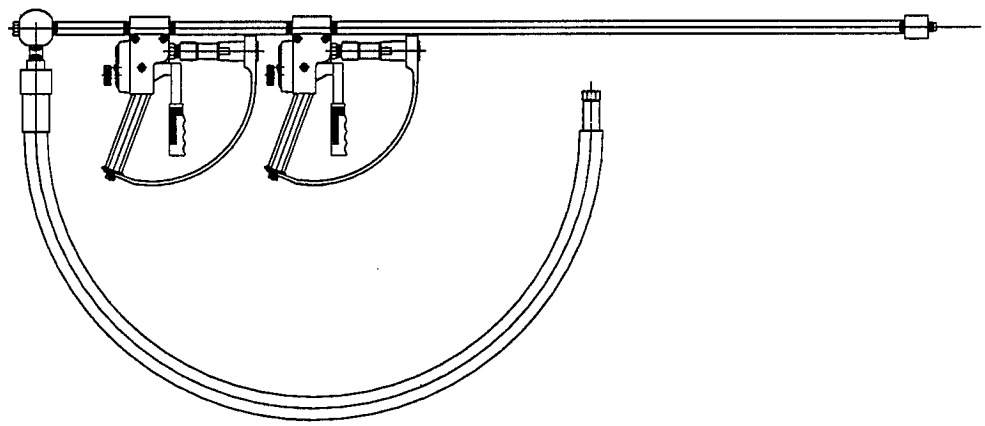

FIGURE 15
DOUBLE DUMP STYLE GUN

Maybe it should be noted that any type of high pressure gun can malfunction in some way. The malfunction could be caused by dirt, worn parts, some sort of jam or obstruction, or in the case of remote control systems, a mechanical problem can arise. An example of a secondary dump is shown in FIGURE 16 and can range from the addition of a hand valve that will not allow the system to pressure-up, to a second type of gun to backup the primary waterblast gun.

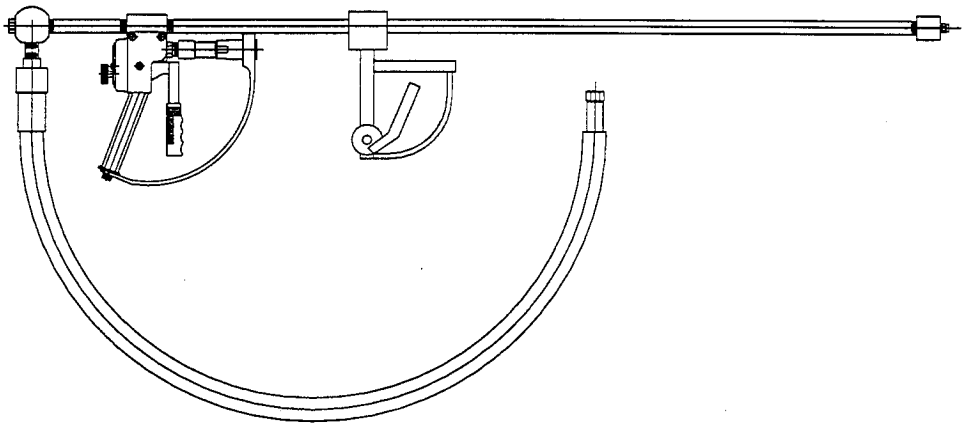

FIGURE 16
GUN WITH SECONDARY DUMP

There have also been improvements within the gun types such as the replaceable valve cartridge introduced by JETSTREAM in late 1982, as well as continuing improvements in seals and seal materials. Internal gun parts have been under continual scrutiny as well as refinements in their operation. The research is usually aimed at making the gun easier to trigger and eliminating the occasional malfunction. If a customer complains, the problem is reviewed. If many customers complain, the problem is vigorously investigated. As a safety tip, Mr. Charles Mondy of JOB-MASTER suggests that users be cautioned to buy only the proper brand repair parts for servicing guns. Manufacturers and users are very interested in a safe water blasting operation because no one wants accidents. The personal, legal and insurance costs are too high to take a chance with safety. In Section 4.0 of Reference 1, the safe operation of jetting guns is discussed.

4.0 GUNS OF THE FUTURE

One type of gun not discussed previously in this paper is the ultra high pressure water jetting guns. The concepts of the high pressure waterblast guns have been carefully adapted to pressures in the 36,000 psi range. The JETEDGE GYRAJET includes hydraulically operated nozzle rotation and the LITELANCE features electrical actuation of a remote control valve to do 36,000 psi blasting. The ultra high pressure equipment is sure to be part of future developments in the waterblast industry.

Many other ideas have been investigated to varying degrees. These include radio control guns, light control guns and even laser guns. SERVOJET guns may become more widely used in the future along with CAVIJET and STRATOJET guns. These patented nozzle technologies are discussed in Reference 2 and Reference 3 and have shown to increase cleaning effectiveness in hand held and automated operations. Possible innovations for future guns may make more use of hydraulics, servo motors, pilot valves, and electronics to increase reliability, decrease fatigue, and decrease weight.

Some of the items presently being developed, are better secondary dumps and dual guns. The future gun will have more safety features and should be lighter with some way to reduce back thrust experienced by the gunman. Space age plastics and composites may replace the stainless steel and aluminum used in most of the high pressure guns of today.

5.0 CONCLUSIONS

Manually operated high pressure water blasting guns are still the tool needed to do much of the work in the field today. They are used underwater, in vessels, in tanks, on surfaces and to supply water to mechanical cleaning devices such as lance machines, cabinets or fixtures. Guns have experienced improvements in safety and reliable operation, but the search should continue to increase the gunman's comfort and personal safety.

6.0 ACKNOWLEDGMENTS

The author wants to thank the companies such as JOB-MASTER, JETEDGE, BUTTERWORTH, JETSTREAM and HYDRO-SERVICES for helping with history and information about waterblast guns. Also thanks to Mr. John Dillard for the CAD illustrations.

7.0 REFERENCES

1. Savanick Dr. G., "Recommended Practices for the Use of Manually Operated High Pressure Water Jetting Equipment", Approved at the annual meeting of The U.S. Water Jet Technology Association, Berkeley, California, August 1987
2. March P.A., "Cavitating Jet Facility For Cavitation Erosion Research", Proceedings of the ASME International Symposium on Cavitation Research Facilities and Techniques, Boston, Massachusetts, December 13-18, 1987
3. Gracey M.T., "Industrial Applications For Rotating Nozzle Technology", 5th American Water Jet Conference, Toronto, Canada, August 29-31, 1989.

6th American Water Jet Conference
August 24 - 27, 1991: Houston, Texas

Paper 49

NEGLIGENCE AND THE BUSINESS COMMUNITY

M. Rankin

Attorney at Law, Houston, Texas U.S.A.

ABSTRACT

A basic introduction to the laws covering the topic of negligence is provided. These laws influence the current business environment and should be considered when conducting business and implementing operations. Once a basic knowledge of the laws is gained, people involved in business can work to conduct their operations in a manner which is aware of negligence laws. It should be noted that advice from corporate counsel should be acquired before implementing any programs or procedures which concern the law.

Organized and Sponsored by the Water Jet Technology Association.

NEGLIGENCE AND THE BUSINESS COMMUNITY

1.0 INTRODUCTION

Many people consider the climate of American society at this time to be extremely litigious. Currently, more lawsuits are filed in the courts than ever before in our history. The American legal system provides a forum readily available where disputes can be decided under consistent rules. As a consequence, there is a high probability that businesses will be subjected to a lawsuit.

A basic understanding of the law is important to persons when they may be directly or indirectly involved with any aspect of the law. All interested persons should be at least familiar with some fundamental concepts of the law to function more efficiently in today's business climate.

The purpose of this paper is to introduce the basic foundations of negligence theories in American tort law. Since many recent lawsuits asserted against businesses have been based on negligence law, the elements and concepts of negligence law are important to parties involved in business.

2.0 NEGLIGENCE AND THE BUSINESS COMMUNITY

Lawyers, Lawsuit, Litigation. These words have been known to strike chords of fear and hatred in the minds of many business operators. Regardless of the emotions conjured by these words and the concepts they represent, the legal system in the United States of America was put in place to provide a neutral forum where parties who had a legitimate dispute could appear before the forum and present disputes for solution. Disputes, in the form of lawsuits are presented before a judge who sits as a

neutral decision maker to adjudicate the disputes and render judgments on issues of law. At times, a jury is involved to hear and decide matters based on fact. The judge and jury then assimilate the facts and law to deliver a verdict under the ensuing situations. This system and working process is a basic foundation of American society and provides some sense of continuity and order in situations which are at times volatile.

As long as humans have lived in groups, they have created rules to govern and guide behavior. Behaviors have been classified as acceptable and unacceptable under those rules and laws which have developed to reflect society's requirements. In the British Empire, after the Dark Ages, decisions of courts were not formally recorded as rules, but decisions were made and later followed to develop precedent. Today, this body of precedent is referred to as the "Common Law." Common law rules have been redrafted as various codes of conduct to form a large part of today's body of law. During the colonial times, the Colonies, and later the United States of America, adopted the English common law system of rules. Through the years, the American courts and legislatures have codified and interpreted the common law to form the codes and regulations which govern American society today.

Civil law developed two types of actions, actions against contracts - where parties agreed to impose specific behavior on themselves and create a related duty to that behavior; and tort laws where society imposed a duty on parties to act within the boundaries set by the society.

3.0 THE HISTORY OF TORT LAWS

Many groups and topics of law have been created to control diverse types of behaviors. There are laws to control actions concerning contracts, property, and business operations, to name a few. Especially in today's business environment, individuals should be aware of basic legal theories, elements and requirements of the law so as to be able to operate efficiently.

One group of laws, called "Torts" covers behavior which when acted by a party can cause injury to other parties or their belongings. The word tort has evolved from the latin word "tortum", translated as "twisted or distorted" and from the word "torquere", from the Old French language, which meant to "twist." Tortious actions involve behavior twisted from that which is considered normal and accepted by society.

Tort actions are state law based actions, are not criminal in nature, but are classified as civil actions. A party complaining of a tortious act committed against him by another party can bring a lawsuit in the proper civil court and assert the actions available under modern tort laws. These laws which are drafted by each state's legislature set forth the requirements and elements of tortious conduct which, when present, gives rise to a tort action.

A source of tort law information is the Hornbook Series volume titled "Prosser and Keeton on Torts." During his lifetime, Mr. Prosser was a law professor at various law schools. His

theories and explanations of tort laws and concepts are continuously updated and remain a credible reference standard.

4.0 MODERN NEGLIGENCE LAWS

A subsection of tort law involves a group of laws titled "Negligence". Negligence laws fall under the heading of torts and involve laws which control conduct involving a breach of a legal duty which causes an injury to another party. Although negligence is not a tort in and of itself, if four elements occur simultaneously, a negligence cause of action under tort law can arise.

The standard definition of the elements required for a negligence cause of action stated by Prosser is:

> 1. A duty, or obligation, recognized by law, requiring the actor to conform to a certain standard of conduct, for the protection of others against unreasonable risks.
>
> 2. A failure on his part to conform to the standard required...
>
> 3. A reasonable close causal connection between the conduct and the resulting injury...
>
> 4. Actual loss or damage resulting to the interests of another [Prosser, Law of Torts, Section 30 (4th Ed. 1971)].

Thus, a cause of action based on negligence must assert: 1) a duty, 2) a breach of the duty, 3) causation, and 4) damage, because mere negligent conduct does not give rise to a negligence cause of action. Just as a baker must have all of the basic ingredients to mix and bake a cake, a negligence cause of action must cumulatively assert and prove all four of the elements

constituting negligence. Negligence has also been defined as the failure to do that which a person of ordinary prudence would have done under the same or similar circumstances, or the doing of that which a person of ordinary prudence would not have done under similar circumstances. These definitions and elements work together to define that conduct which can be classified as negligent conduct.

A. THE DUTY OWED UNDER NEGLIGENCE LAWS

A negligence cause of action cannot arise unless there is a duty owed to the injured person; where no duty is owed to that person, no legal liability may arise on account of negligence. A duty can be imposed by action (malfeasance or misfeasance) and inaction (omission or nonfeasance), but not all undertakings can be considered so as to activate a duty of care. A duty owed by a party to others is related to the degree of care that one party owes to another. The degree of care that a person is generally required to observe in the performance of his or her common-law duty to avoid injury to others is ordinary or reasonable care.

In most situations, the law applies a standard referred to as the "reasonable man" standard and compares conduct complained of to the objectively examined conduct of a reasonable man. This fictitious reasonable man, acting with reasonable prudence in like or similar circumstances, then owes a duty of ordinary care to others around him who share in the common experiences of mankind.

The standard for the duty of care must be related to the nature of the act performed, the place where the act occurred and

the extent of danger or risk of injury the act placed on others. Caution, care and concern all factor in to determine whether or not a duty is owed to a party in a particular situation's circumstances.

A higher standard of care is owed in some situations. Where a higher standard is imposed, the reasonable man standard is extended to include care applicable in specific situations. For example, common carriers are required to care for parties in the manner which a reasonable common carrier should deliver care. Professionals and tradesmen are required to deliver care comparable to the special skills possessed by a reasonable man having similarly special knowledge and ability. Any special situations generally applicable to a type of activity can be subject to a higher standard of care than that of the ordinary standard of care.

Applicable comparison standards derive from various sources. The legislative laws drafted and enacted in the various states provide standards within the statutes and laws. Also, the custom and usage in specific situations can provide a standard for comparison.

A party involved in any business operation should be aware of the standards generally applied in that profession. Any act undertaken by a business should be executed with a concerned eye focused on special standards which are applicable to the situation at hand.

B. BREACH OF A DUTY OWED BY A PARTY

The second element in a negligence cause of action is the breach of a duty owed to a party by another party. Once the existence of a duty is determined, and the standard is examined; the party against whom a negligence cause of action is asserted must be shown to have breached the duty. A breach of the duty occurs when a party acts, or does not act and that action is considered to be negligent conduct. This placement of the injured party in peril or danger is considered the breach of the duty as owed by the offending party.

C. THE CAUSAL CONNECTION BETWEEN THE ACT AND THE INJURY

The third element involved in negligence law is that of proximate causation. Two elements together define proximate causation. First, there must be a cause in fact; and second the cause in fact must be foreseeable. The party bringing the lawsuit, referred to as the plaintiff, must prove proximate cause by the legal standard called "a preponderance of the evidence" to establish a cause of action. Proximate cause may be proven by direct and circumstantial evidence, and may not be proven by presumption, mere conjecture or guess. Proof that the complained of conduct - the conduct of the defendant - was the proximate cause of the injury suffered by the plaintiff is an absolute prerequisite to recovery. It should be remembered, however, that not every act of negligence is the proximate cause of an injury, and not every negligent act gives rise to a cause of action.

To establish that an act is the proximate cause of an injury, a plaintiff must prove that the negligent act was a substantial factor of the injury. There must be a chain of events forming a link between the injury and the act alleged to be negligent, but a proximate cause must not be too remote. Also, the plaintiff must show that without the negligence, no injury would have taken place. This logical connection between the injury and the act is referred to as the proximate cause of the injury - where the defendant's act is a substantial factor in bringing about the plaintiff's injury.

The negligent act complained of need not be the only act which caused the injury, because many acts can combine together to cumulatively cause an injury. But in the case where the injury causing event or occurrence would have resulted regardless of the negligent acts of the defendant, there can be no proximate cause.

The second element of proximate causation is foreseeability and the following quotation has been applied over the years to describe it:

> "Human beings in their common dealings with each other in society should be required to exercise some degree of deliberation or forethought. It would be unreasonable to require them, before doing or refraining from doing a particular act, to exhaust the field of speculation concerning every possible or conceivable consequence which might result from their conduct. It is just that one should be charged with the duty to anticipate those consequences which in the ordinary course of human experience might reasonably be expected to result therefrom, and therefore that he should be held legally responsible for those consequences."

To apply the test of foreseeability, legal liability will not attach to an act or omission unless the alleged wrongdoer could have reasonably anticipated probable harm from his or her conduct. In foreseeability, the reasonable man standard is again applied, and the conduct under examination is compared against the conduct of a reasonable man where a person of ordinary intelligence should have anticipated the danger to others which was caused by his negligent act. Thus, an act must have been reasonably foreseeable to cause injury to be deemed negligent.

The law has extended the issue of foreseeability to include other situations where parties should or could have reasonably foreseen that an injury would have resulted from the acts undertaken. Doctrines have developed so that an injured party can find recovery and redress when other parties are deemed responsible for his injury, or where the circumstances display the necessary elements to infer negligence.

"Res Ipsa Loquitur", a doctrine which is derived from the Latin phrase meaning "the thing speaks for itself" is applied in actions which, in certain limited types of cases, the circumstances surrounding an accident may constitute sufficient circumstantial evidence to support a finding of the defendant's negligence. These circumstances are those where the mere occurrence of an accident supports a reasonable inference that there was negligence involved and that the defendant was the negligent party.

Especially of interest to businesses is the doctrine of imputed negligence, also referred to as vicarious liability. In

these types of cases, the negligence of one party is charged to another party - in other words, the party who is determined to be responsible for the party who caused the injury is held responsible for the damages incurred. The fault of one party is attributed to another party. This occurs in the relationship between an employer and his employees under agency, the doctrine of respondeat superior.

The doctrine of respondeat superior shifts the incidence of negligence from one to another and simply means "look to the higher up." When an employee causes injury to another, the plaintiff will look to the party higher up. The party who controls the actions of the employee is then held responsible for the injury. Any business relationship where an employer exerts control over another can invoke the principles of vicarious liability. Only in situations where completely independent contractors are involved and where no control over the job tasks is extended by the employer is vicarious liability not imposed. Businesses should examine all relationships between the business and employees and any independent contractors to determine whether or not vicarious liability could be imposed. Corporate counsel should be consulted in situations where relationships exist between various parties and actions should be taken to protect the parties with consideration given to vicarious liability.

All of the issues discussed above factor into the examination of the causal connections between the act complained of and the resulting injury. The causal connection showing the

proximate cause of an injury as between an act and an injury constitutes the third necessary element of negligence.

D. THE DAMAGE CAUSED BY A NEGLIGENT ACT

The fourth and final element required for a negligence cause of action is that of a damage. The damage must be tangible and actual for the loss to combine with the other three elements and constitute a complete negligence cause of action. General claims of damage can be made for damages suffered because of a particular injury, such as pretrial pain and suffering pertaining to a serious injury. Specific damages occur as medical expenses, lost earning capacity and future pain and suffering. These damages also referred to as compensatory damages must be fully defined, described and proven by the plaintiff.

Furthermore, a plaintiff has a general duty to mitigate the damages; that is, to avoid increasing the amount of damage by either taking additional actions, or failing to take action. The plaintiff is not entitled to recover damages that could have been avoided by caring and treating the injury as an ordinary and prudent person would have undertaken in similar circumstances. The duty to mitigate is not effectuated before the wrong and arises after the wrong has been committed.

Another type of damage claim available to plaintiffs is that of an exemplary damages. Also referred to as punitive damages, exemplary damages are available only if there is a wrong actuated or accompanied by some special type of aggravating circumstance, such as malice, fraud, gross negligence, or the like.

Exemplary damages can only be assessed in addition to the actual or compensatory damages which are asserted and proven to the court.

5.0 ADDITIONAL CONCERNS BEYOND THE BASIC ELEMENTS OF NEGLIGENCE

Other concepts and laws act in concert with the four elements of negligence and negligence cannot be discussed without mentioning these issues. The date that a cause of action "accrues" or occurs is important. Generally, a cause of action sounding in tort accrues on the date on which the tort was committed, absent fraudulent concealment or a contrary statute.

The date of the occurrence of the tort is crucial because in tort law, there are applicable statutes of limitations which expressly state the dates available for a plaintiff to bring the cause of action. The statute of limitations is a tort action's biological clock, where if the date has passed, the tort action has lapsed and cannot be asserted.

The concepts and rules of contributory negligence and comparative responsibility are also important in an examination of negligence laws. Contributory negligence occurs where a plaintiff's injury is partially caused by his own negligence. In the few jurisdictions where contributory negligence remains as the law, if a plaintiff is in any way responsible for his injury, he is completely prohibited from asserting a cause of action.

Since contributory negligence is harsh, the doctrine of comparative responsibility has developed in the majority of jurisdictions. Where the negligence of the plaintiff and the defendant combine to cause the injury to the plaintiff, the

plaintiff's recovery is reduced by the percentage of the total negligence which is attributed to him. This is a situation where the jury, as the fact finder determines the percentages of negligence attributable to each party and apportions the liability accordingly.

6.0 CONCLUSION

Negligence laws have been enacted to provide a recovery for parties tortiously injured by the actions of another. Business operators and employees should have a basic understanding of these laws so that they can engage in business activities aware of applicable legal principles. Negligence laws can work for and against businesses and with proper exposure to the fundamental concepts of these laws, businesses can use the laws to their most favorable advantage.

6th American Water Jet Conference
August 24 - 27, 1991: Houston, Texas

Paper 50

Surface Strengthening of Metals by Water—Jet

LUO Xiaoling
Beijing Aeronautical Manufacturing
Technology Research Institute
Beijing 100024, P. R. China

ABSTRACT

The possibilities and advantages of using high pressure water—jet to strengthen the surface of metal materials are investigated in this paper.
Various factors such as metal properties, target distance (i. e. standoff distance), feedrate and pressure of the water—jet used are experimently tested and the strengthened results are quantitatively analyzed.

Organized and Sponsored by the Water Jet Technology Association.

1. 0 INTRODUCTION

Water—jet cutting has been widely used and followed with interest day by day on the world, but it is really a new subject to strengthen surface of metal by means of high pressure water—jet in order to improve the status of stress on the surface while not worsening the surface rate.

To strengthen surface of metals by shot — ball peening usually roughens the strengthened surface and invokes more surface stress concentration which would partially cancel the improvement of fatigue characteristics. Therefore we tried to strengthen the surface by using continous water—jet while avoiding the surface roughening and surface stress concentration.

2. 0 EXPERIMENTAL CONSIDERATIONS AND IMPLEMENTAIONS

To study the possibilities and effects of water—jet strengthening, three metal materials——carbon steel, titanium alloy and stainless steel are preferred and various technological parameters such as target distance, feedrate and pressure of water — jet are tested. The tests were organized with normal multiparameter test method and then parameters concerned are optimized.

Factors and levels used in those tests are listed in Table 1, test organization and results are listed in Table 2 and data processing is shown in Table 3.

Hardness and surface stress of the strengthened specimens are considerated for evaluating the strengthened results. For each specimen, hardness and surface stress at three points should be measured and their mean values are calculated.

In Table 2, sign" —" refers to pressing stress and sign " +" refers to tension stress. In Table 3, "I"is a summation of the values under label "1" of each column in Table 2, "II" is a summation of the values under label "2" of each column inTable 2 and "III" is a summation of the values under label "3" of each

column in Table 2. $\bar{K}_1$, $\bar{K}_2$ and $\bar{K}_3$ are the mean values of the data under label "1","2" and "3" of each column. R is the variance.

From the data in Table 3, it can be known that factor M possesses the maximum variance (R=26. 27), it means that material M is the chief factor which has influence on the strengthened result concerning the hardness. Concerning the values of $\bar{K}$, $\bar{K}_{2M}$, $\bar{K}_{3L}$, $\bar{K}_{2V}$ and $\bar{K}_{3P}$ are the maximum one in each column, it means that level "2" of material, level "3" of target distance, level"2" of feedrate and level "3" of water jet pressure possess the most powerful influence on the stregthencd results.

As for surface stress, factor M still possesses the maximum variance (R=215. 6), it means that material M is the chief factor too. Concerning the values of $\bar{K}$, $\bar{K}_{3M}$, $\bar{K}_{1L}$, $\bar{K}_{1V}$ and $\bar{K}_{3P}$ are the maximum one in each column, it means that level "3" of material, level "1" of target distance, level "1" of feedrate and level "3" of water—jet pressure possess the most powerful influence on strengthened results.

3. 0 THE STRENGTHENED RESULTS

Because the data produced from normal multi—parameter test are comprehensively comparable with each other, the function relations of strengthened results against the levels of material, target distance, feedrate and water—jet pressure are shown in Figures 1,2,3 and 4.

From those figures, it can be known that the hardness is insensitive to the levels of factors (M,L,V,P), but the surface stress is rather sensitive to the levels. Tension stress has changed into pressing one, this is due to that the water—jet extends the surface area of specimen and invokes the next internal layer elastically tensile. But material is a whole entirety, the elastical tension residual on the internal layer makes pressing stress residual on the jetted surface(see Fig. 5).

4. 0 ADDITIONAL DISCOVERING

We have made an additional test on a specimen of carbon steel. It verifies again that the hardness of jetted material almost remains unchanged, but the surface stress changes obviously. When factors L, V and P vary, the cardinal levels are P, L and V too, the sequence is P, L, V, their variance is 23. 7 (R = 23. 7).

In addition, we found that water—jet strengthening had never worsened surface quality. There are neither roughness nor stress concentration invoked on the strengthened specimens of the three materials used. We also found that water—jet strengthening can delete the rust from the specimen of carbon steel.

5. 0 CONCLUSIONS

From the tests and analyses mentioned above, we can come to the conclusions listed below.

5. 1 Water — jet strengthening achieves good results. Water — jet strengthening makes pressing stress appear on the strengthened surface, it would improve the fatigue strength and immunize the material from stress corrosion.

5. 2 Water — jet strengthening is superior to shot — ball peening, it has never worsened surface rating because water—jet is a continous, uniform and thin (with diameter about 0. 2—0. 3mm. only) stream.

5. 3 Water—jet strengthening hardly changes the surface hardness. The variation of Rockwell hardness (HR15N)invoked by the water—jet is less than 1%.

5. 4 With suitable target distance, feedrate and scanning course, water—jet can cover all the surface, but shot—ball peening usually cover only 50—80% area of surface.

5. 5 Concerning the corelation between strengthened results and the three factors (target distance, feedrate and water — jet pressure), the pressure exerts the biggest influence upon strengthened results, higher the pressure, better the strengthened results. From the test data, it can be known that less target distance, slower feedrate make better results.

5. 6 The values of technological parameters should vary according to material properties. For example, water — jet pressure should be as high as 240 MPa or greater for strengthening stainless steel, but it should be less than 160MPa for strengthening aluminium.

5. 7 Because the jet velocity of the water can be as high as 900 meters/sec. , water — jet is able to strengthen parts with high productivity. In addition, water — jet does not pollute environment and water — jet can strengthen deep hole even its diameter is as small as 3 mm or less.

ACKNOWLEDGEMENTS

Taking this opportunity, the author of this paper would like to express her gratitude to Mr. G. Zhou and his Beijing High Pressure Service Centre for the experimental conditions and hospitable support they have offered.

REFERENCES

1. "Cutting with high — pressure water jets", Plastics Machinery and Equipment, March 1980.

2. "Strengthening Materials by High Pressure Waterjet", Aeronautical Manufacturing Technolgy, Beijing P. R. China, Page 20, March 1990.

3. "Shot Peening", Engineer, July 1976.

TABLES AND FIGURES

Table 1 Factors and Levels

LEVEL / FACTOR	1	2	3
Material:M	M1:carbon steel	M2:titanium alloy	M3:stainless steel
Target distance:L	L1:20mm.	L2:40mm.	L3:80mm.
Feedrate:V	V1:1 m./min	V2:2 m./min	V3:4 m./min.
Water—jet pressure:P	P1:70 MPa	P2:160 MPa	P3:240 MPa

Table 2 Test Results

Test No.	Factor				Test Results			
	M	L	V	P				
	Level				Evaluation of Streng. Effect: (I)Hardness (II)Surface Stress			
	1, 2, 3,				(I)HR15N	(II)MPa	Score X	
1#	1	1	1	1	43.0 42.4 42.0	−188.0 −190.0 −196.0	X1	(I)42.4 (II) −190.0
2#	1	2	2	2	44.0 44.3 44.5	−130.0 −152.0 −158.0	X2	(I)44.3 (II) −152.0
3#	1	3	3	3	44.9 45.4 45.0	−141.0 −158.0 −163.0	X3	(I)45 (II) −158.0
4#	2	1	2	3	71.0 70.6 70.0	−283.0 −328.0 −351.0	X4	(I)70.6 (II) −328.0
5#	2	2	3	1	69.4 70.0 71.0	−11.3 −37.7 −52.8	X5	(I)70.0 (II) −37.7
6#	2	3	1	2	71.6 70.2 69.8	−237.5 −245.0 −245.1	x6	(I)70.2 (I) −245.1
7#	3	1	3	2	53.5 54.3 54.3	-370.0 -390.0 -422.0	X7	(I)54.3 (II) −390.0
8#	3	2	1	3	55.0 54.0 55.8	−508.0 −550.0 −573.0	X8	(I)55.0 (II) −550.0
9#	3	3	2	1	56.0 55.0 55.0	−190.0 −207.0 −248.0	X9	(I)55.0 (II) −207.0
Virgin materials	—	—	—	—	M1:(I) 44.0, (II) −116.0 M2:(I)69.4, (II)+3.8 M3: (I)54.0, (II)+76.0			

Table 3 Data Processing

Data Processing \ Factor		M	L	V	P
Hardness	I	131.7	167.3	167.6	167.4
	II	210.8	169.3	169.9	168.8
	III	164.3	170.2	169.3	170.6
	$\overline{K}1$	49.3	55.77	55.87	55.80
	$\overline{K}2$	70.27	56.43	56.63	56.27
	$\overline{K}3$	54.77	56.73	56.43	56.87
	R	26.37	0.96	0.76	1.07
	Superior	M2	L3	V2	P3
	Sequence	M, P, L, V			
Surface stress	I	−500	−908.	−985.1	−434.7
	II	−610.8	−739.7	−687.	−787.1
	III	−1147	−610.1	585.7	−1036
	$\overline{K}1$	−166.7	−302.7	−328.4	−144.9
	$\overline{K}2$	−203.6	−246.6	−229	−262.4
	$\overline{K}3$	−382.3	−203.4	195.2	345.3
	R	−215.6	99.3	133.2	200.4
	Superior	M3	L1	V1	P3
	Sequence	M, P, V, L			

Note: The diameter of nozzle is of 0.35mm.

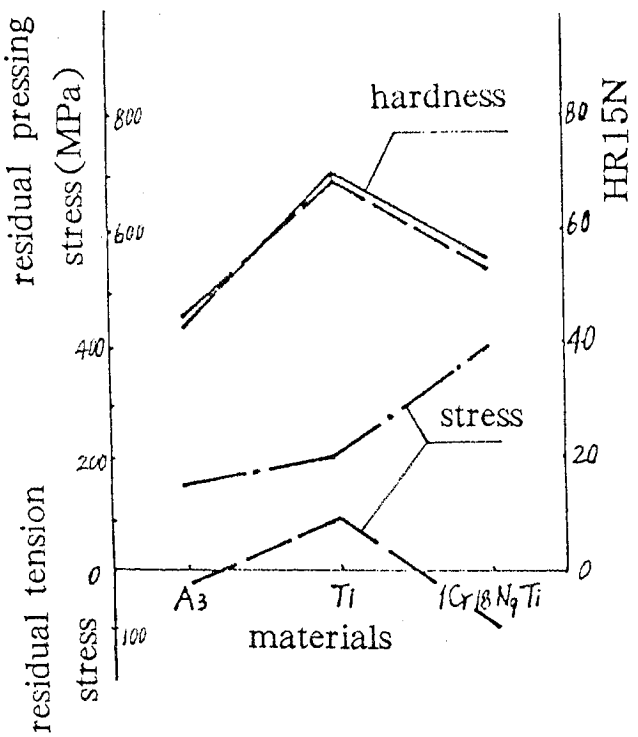

Fig. 1 Strengthened Results Against Materials (dotted lines refer to Virgin materials)

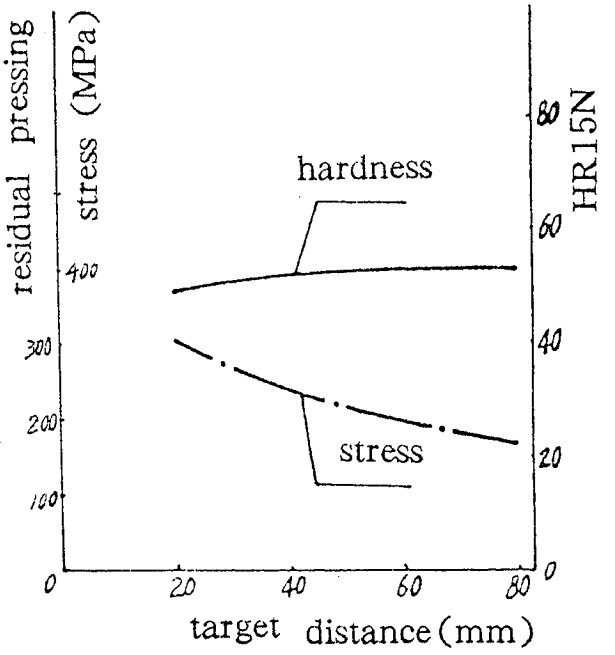

Fig. 2 Strengthened Results Against Target Distance

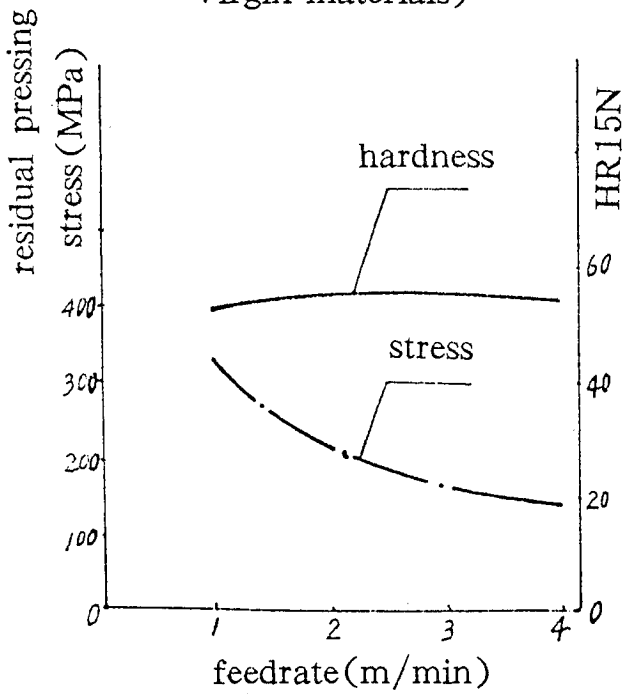

Fig. 3 Strengthened Results Against Feedrate

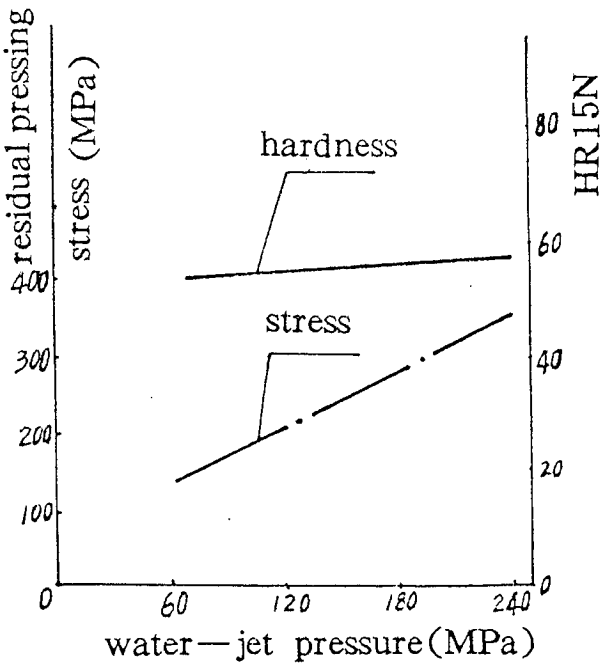

Fig. 4 Strengthened Results Against Water—Jet Pressure

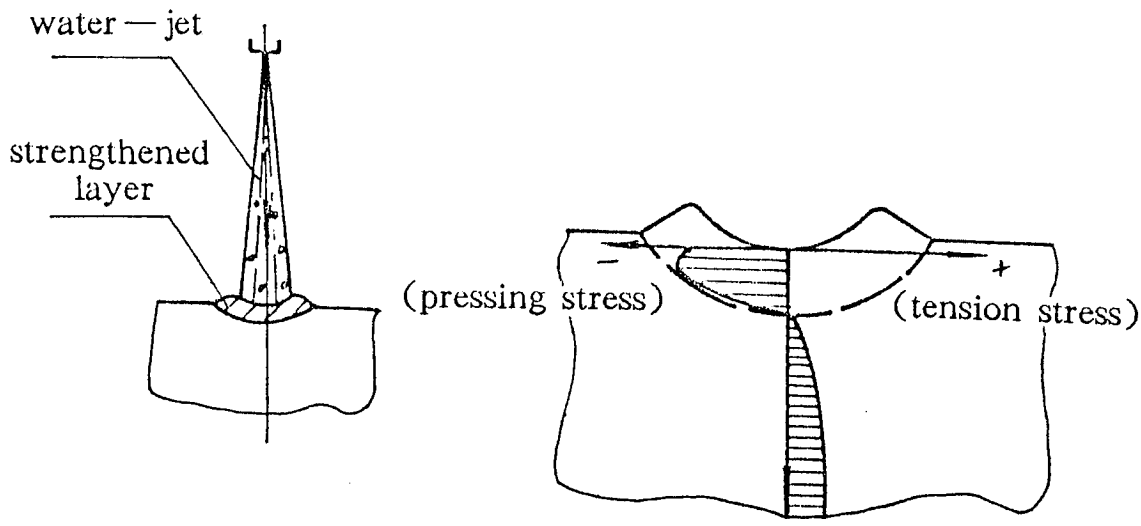

a. Effect Imposed On Surface By Water Jet

b. Residual Stress On The Strengthend Layer

Fig. 5 Stress Distribution In Strengthened Layer

Index of Authors